New Mono and Binuclear Ru(II) Complexes of O, N, S Donor Ligands: Catalytic Applications to C-C, C-N and C-O Coupling Reactions

Thesis submitted to Bharathidasan University

for the award of the degree of

DOCTOR OF PHILOSOPHY
IN
CHEMISTRY

By

V. TAMILTHENDRAL, M.Sc.,
(Reg. No. 16683)

Research Supervisor

Dr. R. RAMESH
Professor and Chair
Coordinator (COMC)

Centre for Organometallic Chemistry
School of Chemistry
Bharathidasan University
Tiruchirappalli - 620 024
Tamilnadu, India

August 2022

BHARATHIDASAN UNIVERSITY

Dr. R. Ramesh, Ph.D.,
Professor and Chair
Coordinator (COMC)

Centre for Organometallic Chemistry
School of Chemistry
Bharathidasan University
Tiruchirappalli − 620 024
Tamil Nadu, India.

Date:

CERTIFICATE

This is to certify that the thesis entitled "**New Mono and Binuclear Ru(II) Complexes of O, N, S Donor Ligands: Catalytic Applications to C-C, C-N and C-O Coupling Reactions**" is a bonafide work done by **Mr. V. TAMILTHENDRAL** (Reg. No. **16683**) under my guidance in the Centre for Organometallic Chemistry, School of Chemistry, Bharathidasan University, Tiruchirappalli – 620 024 and has not been included in any other thesis submitted previously for the award of any degree.

R. RAMESH

(Research Supervisor)

Fax: 0091-431-2407045; Tel: 0431- 2407053; E-mail: ramesh_bdu@yahoo.com; rramesh@bdu.ac.in

BHARATHIDASAN UNIVERSITY

V. Tamilthendral
Doctoral Student

Centre for Organometallic Chemistry
School of Chemistry
Bharathidasan University
Tiruchirappalli – 620 024
Tamil Nadu, India.

Date:

DECLARATION

I, hereby declare that the thesis entitled "**New Mono and Binuclear Ru(II) Complexes of O, N, S Donor Ligands: Catalytic Applications to C-C, C-N and C-O Coupling Reactions**" is based on the original and independent research work done by me under the guidance **Dr. R. RAMESH**, Professor and Chair, Coordinator, Centre for Organometallic Chemistry, School of Chemistry, Bharathidasan University, Tiruchirappalli - 620 024 and this work has not been submitted in a whole or in a part for any other degree or diploma to this or any other University.

(V. TAMILTHENDRAL)

Ouriginal by Turnitin

Document Information

Analyzed document	Thesis for plagiarism - Tamil.pdf (D143125289)
Submitted	8/21/2022 6:57:00 PM
Submitted by	S ARUMUGAM
Submitter email	sarumugam1963@gmail.com
Similarity	1%
Analysis address	profsarumugam1963.bdu@analysis.urkund.com

Sources included in the report

W	URL: https://www.science.gov/topicpages/c/ch3cl+ch2cl2+chcl3 Fetched: 11/19/2021 11:45:03 AM	1
W	URL: https://link.springer.com/article/10.1007/s41061-021-00342-w Fetched: 1/19/2022 12:33:36 PM	2
W	URL: https://www.ncbi.nlm.nih.gov/pmc/articles/PMC6682138/ Fetched: 8/3/2020 9:46:27 PM	2
W	URL: https://www.scielo.br/j/jbchs/a/FRQyPTtdkCCTWQrrHq3YyWp/?format=pdf Fetched: 8/8/2022 12:45:00 PM	2

Entire Document

The research work described in this Ph.D. thesis themes on mono and binuclear ruthenium(II) complexes catalyzed C-C, C-N and C-O bond forming reactions via dehydrogenative coupling of alcohols. The present thesis comprises six chapters. The first chapter is the introduction about the chelating ligands including thiourea, aroylhydrazone and aroylhydrazine ligands along with their structural features and their coordination ability in metal complexes. Further, a detailed literature survey on recent advancements in the mono and binuclear ruthenium(II) complexes catalyzed alcohol dehydrogenation and its importance in C- C, C-N and C-O bond formation reactions towards organic synthesis. Chapters 2-5 mainly focused on the synthesis and characterization of new mono and binuclear Ru(II) complexes featuring thiourea, aroylhydrazone and aroylhydrazine ligands. In addition, special attention has been focused on the synthesis of some biologically important compounds such as imines, E-olefins, 2-amino-4H-chromenes and pyrazoles via oxidative dehydrogenation / acceptorless dehydrogenation coupling of readily available alcohols with the suitable coupling partners. All the reactions operate under mild conditions with the liberation of hydrogen gas and water as the only by-products. Chapter 6 describes the summary of all the five chapters. Organometallic chemistry concerns with the compounds encompassing atleast one direct bond between the carbon atom of the organic compound and metal centre such as alkaline, alkaline earth, transition metal and other cases. 1 In addition, several other compounds such as transition metal hydrides or metal phosphine complexes are also included in organometallic research. Organometallic chemistry combines the chemical characteristics of

Dedicated to My Beloved Family

and

My Guide

ACKNOWLEDGMENT

The work done in this thesis would not have been possible without the help provided by many persons in different ways.

I avail this opportunity with great pleasure to express my unfathomable gratitude and wholehearted thanks to my respected research supervisor and guide, **Dr. R. Ramesh,** Professor & Chair, Coordinator (COMC), School of Chemistry, Bharathidasan University, Tiruchirappalli – 620 024, for providing me an opportunity to do research in the frontier area of organometallics and bioinorganic chemistry under his supervision and strong leadership. I have been inspired by his meticulousness, his attention to detail and energetic application to any problem. It is significant to say that he has been a source of inspiration from the right beginning and for what I am today. His forensic scrutiny of my technical writing has been invaluable. He has been a keen observer, invaluable guidance, truly encourager, broad knowledge and rational thinking in organometallic chemistry and perpetual inspiration always act as motivating factors to my research work. I am extremely thankful to him for his immense training, provoking discussions, constructive criticism and constant support provided at all times during the course of work. It has been a pleasure working in his group and his suggestions in a friendly manner have helped me to achieve my research target successfully.

I express my sincere thanks to Doctoral Committee Members; **Dr. K. Nehru**, Assistant Professor, Department of Chemistry, Anna University, BIT Campus, Tiruchirappalli and **Dr. L. Nagarajan**, UGC-Assistant Professor, School of Chemistry, Bharathidasan University, Tiruchirappalli, for their support, extensive discussion and insightful comments during my research work.

I express my special thanks to **Head of the Department** and all other **faculty members**, School of Chemistry, Bharathidasan University, Tiruchirappalli, for having provided the necessary facilities to carry out this work. I am also grateful to all the **Non-Teaching staffs** of School of Chemistry for their help and support.

I owe my special thanks and cooperation extended to me by my lab super seniors, seniors and lab members **Dr. T. Sathya kamatchi (PDF), Dr. M. Mohamed Subarkhan, Dr. R. Rajkumar, Dr. S. Muthumari, Dr. N. Mohan, Dr. T.S. Manikandan, Dr. G. Balamurugan, Dr. S. Saranya, Dr. S. Balaji, Mrs. P. Ramya,**

Mr. P. Anandaraj, Mr. S. Clinton, Ms. A. Abirami, Ms. S. Monika and **Mr. S. Pranesh Kavin** for their help at different stages of my research.

I am heavily indebted to the **Science and Engineering Research Board (SERB)**, New Delhi, India, for providing me the financial assistance in the form of JRF which buttressed me to perform my work effectively.

DST-FIST, UGC-SAP, are gratefully acknowledged for providing instrumental facilities like NMR spectrometer, UV-Vis spectrophotometer and FT-IR spectrometer available in the School of Chemistry, Bharathidasan University.

I owe a great deal of appreciation and gratitude to my research collaborator, **Dr. Jan Grzegorz Malecki,** Department of Crystallography, Institute of Chemistry, University of Silesia, Katowice, Poland for crystal characterization studies.

It is my pleasure to express my gratitude to my friends and well-wishers, **Dr. K. Manikandan, Dr. M. Manikandan, Dr. S. Prabhu Kumar, Dr. G. Paulraj, Dr. P. Perumalsamy, Dr. T. Rajkumar, T. Ajay Kamal, R. Naveen** and **S. Thangamalar** who helped me towards this successful academic carrier.

I owe my warmest thanks to my parents **Mr. P. Pappusamy, Mrs. P. Chinnathai, Mr. P. Veerappan, Mrs. V. Ramulakshmi**, **Mr. R. Raja and Mrs. R. Kavitha** and **Mr. P. Venkatesan, Mr. V. Prabakaran,** my brothers who moulded me into the present position and their love, affection, moral support, tireless efforts and constant inspiration for me in shaping my carrier.

Also, I am thankful to **Dr. P. Kalapagasuganthi Ramesh** for her wishes and encouragement.

I extend my special thanks to all **my friends** for their love and support.

Nothing would be possible without the mercy of Almighty; I wish to record my thanks to **GOD** for having given me both physical and mental strength to carry out my research successfully.

- V. Tamilthendral

CONTENTS

Chapter 1

INTRODUCTION

The research work described in this Ph.D. thesis themes on new mono and binuclear ruthenium(II) complexes catalyzed C-C, C-N and C-O bond forming reactions towards the synthesis of important heterocycles *via* dehydrogenative coupling of alcohols. The present thesis comprises six chapters. The first chapter is the introduction about the chelating ligands including thiourea, aroylhydrazone and aroylhydrazine ligands along with their structural features and their coordination ability in forming metal complexes. Further, a detailed literature survey on recent advancements in the mono and binuclear ruthenium(II) complexes catalyzed alcohol dehydrogenation and its importance in C-C, C-N and C-O bond formation reactions towards sustainable organic synthesis is portrayed. Chapters 2-5 mainly focused on the synthesis and characterization of new mono and binuclear Ru(II) complexes featuring thiourea, aroylhydrazone and aroylhydrazine ligands. In addition, special attention has been focused on sustainable synthesis of some biologically important compounds such as imines, E-olefins, 2-amino-4H-chromenes and pyrazoles using the newly synthesized ruthenium complexes as efficient catalysts *via* oxidative / acceptorless dehydrogenation coupling of readily available alcohols with the suitable coupling partners. All the reactions operate under mild conditions with the liberation of hydrogen gas and water as the only by-products. Chapter 6 describes the summary of all the five chapters.

Organometallic chemistry concerns with the compounds encompassing atleast one direct bond between the carbon atom of the organic compound and metal centre such as alkaline, alkaline earth, transition metal and other cases.[1] In addition, several other compounds such as transition metal hydrides or metal phosphine complexes are also

included in organometallic research. Organometallic chemistry combines the chemical characteristics of classic inorganic and organic compounds.[2] Chemistry of such compounds provides solutions to the challenges faced by researchers in catalytic, synthetic organic and material chemistry. They have wide applications as catalysts in stereoselective organic synthesis and industrially important homogeneous catalysts.[3] Further, the synthesized metal complexes have attracted great interest in cancer metallotherapeutics due to the structural diversity in ancillary ligands and easy accessibility to the hydrophobic nature of substitutions.[4]

In recent years, there has been extensive interest in the chemistry of transition metal complexes mainly due to the fact that they offer opportunities for tuning the electronic factor of the metal centre, including substrate chirality, enhancing the stability of homogeneous or heterogeneous catalysts.[5] Particularly, ruthenium complexes are effectively exploited in diverse fields such as catalysis, biology and material chemistry due to the ability of ruthenium to exist in various oxidation states (-2 to +8), geometries, coordination numbers, ligand exchange kinetics and iron-mimicking capability etc.[6] More specifically, organoruthenium complexes were exploited as catalysts in various organic reactions, such as imine synthesis,[7] asymmetric catalysis,[8] amidation reactions,[9] transfer hydrogenation,[10] olefin metathesis,[11] alkylation reaction,[12] hydroformylation,[13] tandem reactions,[14] hydrosilylation.[15] Recently, many ruthenium complexes appended arene moiety were reported as potent anticancer agents.[16] Intense investigations were focused on ligands such as arene, phosphine, and other multidentate ligands containing oxygen, nitrogen, and sulfur.[17]

1.1. Thiourea ligands

Thiourea is a significant compound with the common structure $(R_1R_2N)(R_3R_4N)C=S$ and commonly attained by the reaction of isothiocyanate with

hydrazides/amines. Particularly, aroylthiourea ligands have received immense importance because of their flexible coordination ability with numerous transition metal ions.[18] Due to their soft (C=S) and hard (C=O) donor groups, thiourea ligands exhibit a very high binding probability and serve as possible O, S donors (Scheme 1). The thiocarbonyl group which is connected with N-H group substituents have an impact on the coordination behaviour and also the chemical and physical properties of the complexes.[19]

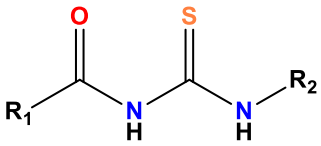

Core unit

Scheme 1. General formula of thiourea ligands

Thiourea ligands with O, N, or S donor atoms show several coordination modes and bind to the metal ion in monobasic, dibasic, or neutral forms (Scheme 2). Typically, they coordinate in a monoanionic bidentate way with the transition metal ion (**I**). They also bind with the metal ions in neutral monodentate mode *via* sulphur atom (**II**). By the use of O and N atoms, they can coordinate with the metal ion (**III**) in a neutral bidentate form as well. It was also found that O and S atoms were bound to one metal ion in a monobasic bridging ligand, whereas N was linked to another metal ion (**IV**). It can also coordinates to metal as neutral N and S donor atoms forming a four-membered chelate ring (**V**).[20]

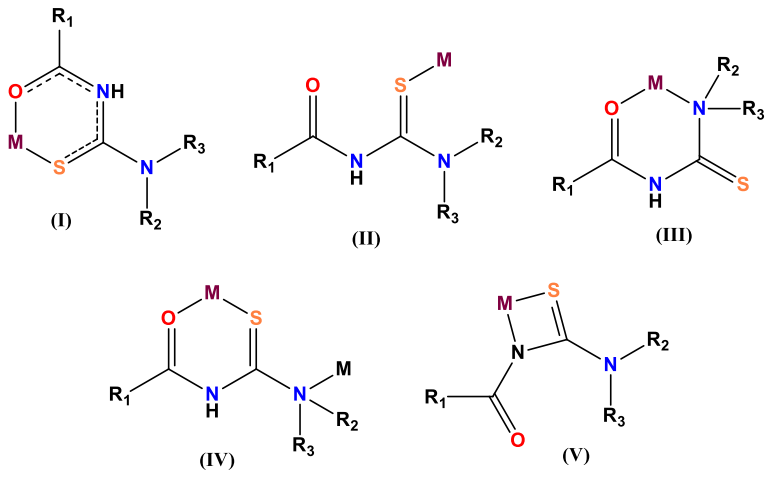

Scheme 2. Various modes of coordination of aroylthiourea ligands

Among the various coordination modes, the monoanionic bidentate (O, S) coordination mode has been found to be very common and leads to stable transition metal complexes.[21] Thiourea has many catalytic applications in organic synthesis and also provided many applications in the field of analytical chemistry, agriculture and biology. In addition, they treated as antioxidant, anti-bacterial, anti-cancer, anti-inflammatory agents and for urease inhibition.[22] Thiourea-based metal complexes have received favourable attention in recent years due to their chemical and biological characteristics. The ability to coordinate metal ions through a variety of coordination modes results in a structural variety of their metal complexes, which attracts momentous scientific investigation.[23]

1.2. Aroylhydrazone ligands

Aroylhydrazones are analogues of Schiff's base ligands with nitrogen and oxygen donor atoms. They are synthesized under smooth conditions by reacting aldehydes or ketones with hydrazides (Scheme 3).[24]

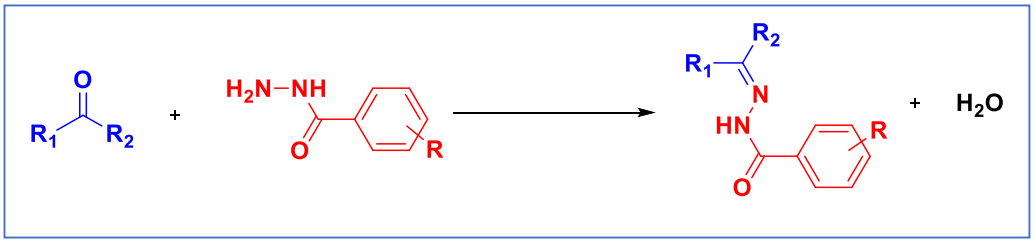

Scheme 3. General preparation of hydrazone ligands

Hydrazones are extremely important because they are responsible for the formation of active species with various oxidation states and for forming a stable chelate ring with transition metals, which catalyse the corresponding chemical processes. This is due to their ability of complex formation with metal ions and their active involvement in a variety of catalytic and biological processes.[25] In addition, hydrazone derivatives have been extensively utilised as anti-HIV agents, anti-bacterial agents, and anti-microbials agents. In particular, hydrazone containing azomethine -NHN=CH protons constitutes a crucial class of compounds for the development of new drug molecules (Figure 1).[26]

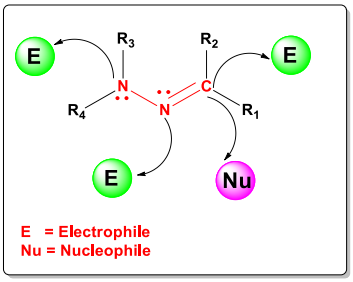

Figure 1. The general formula of hydrazone ligands

Hydrazones have a strong coordinating ability to transition metals using phenolate-O or enolate-O, imine-N and deprotonated amide-O atoms and form stable complexes with transition metals. The competition between binding and chelating coordination modes is an important fact in producing mono, di, and polynuclear metal complexes (Scheme 4).[27] When compared to free ligands, these metal complexes exhibit a wide range of stereochemical, electrochemical, catalytic and biological properties.[28]

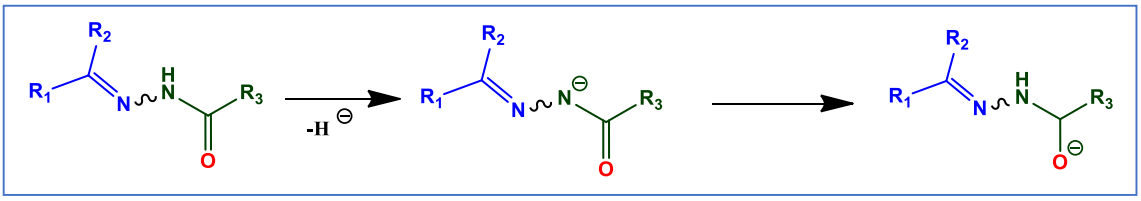

Scheme 4. The general formula of acyl/ aryl-hydrazone and mesomerism of the anion obtained by deprotonation

Hydrazones are yet another class of versatile ligands that exhibit amido-imidol tautomerism in solution and exhibit unique coordination modes (Scheme 5). Changes in the parent aryl or acid benzhydrazides with different aldehyde or ketone were used for the enhancement of electronic properties of the ligands.

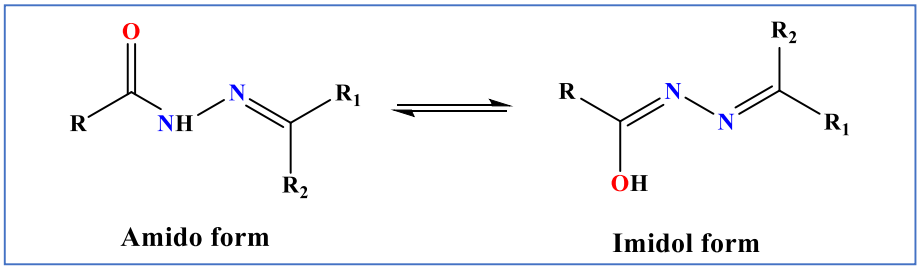

Scheme 5. Amido and imidol forms of hydrazones

Generally, hydrazones behave as O^N bidentate donor ligand.[29] Tri and tetradentate ligands may also be attained if R_2 and/ or R_3 residues are moieties such as –PR_2, -NR_2, -OH, -SH, etc. (Scheme 6).[30]

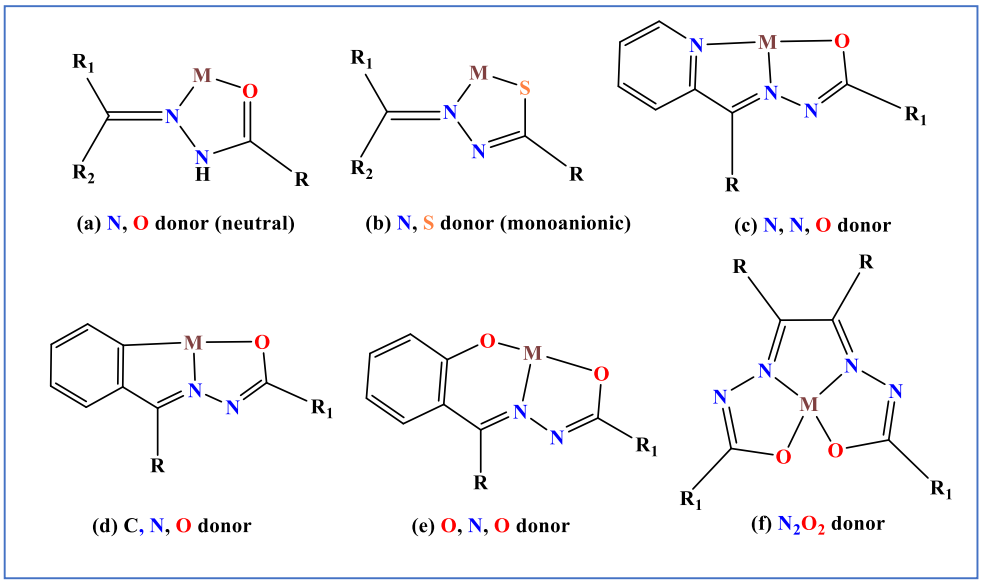

Scheme 6. Different bonding modes of hydrazone derivatives

The stability of the metal complexes increases the mechanism of electron delocalization and the size of the chelate rings produced. Exclusively, metal complexes containing ligands with tridentate donor sites, have a unique shape, structural diversity and chemical sensitivity.[31] Moreover, several hydrazone ligand containing metal complexes have been reported to have potential applications as catalysts, anticancer agents,[32] analytical reagents for spectrophotometric and sensitive spectrofluorimetric titrations,[33] ultra-trace determination of metals,[34] conversions, storage and photo-sensitizers in redox reactions.[35]

1.3. Aroylhydrazine Ligands

Aroylhydrazine ligands bearing nitrogen and oxygen donor atoms are generally produced from the reaction of acid chloride with acid hydrazide. They are characterized by the presence of >C(O)-NH-NH-C(O) functional group and have a strong tendency to bind the transition metals. These ligands can be easily modified by variation of the parent acid hydrazides (Scheme 7).

Aroylhydrazine have a broad range of biological activity due to the presence of an electron-rich hydrazine group *via* hydrogen bonding with biological enzymes. They possess several biological activities such as insecticidal, herbicidal, fungicidal, enzyme inhibition, antiviral and antitumor activities.[36] There has been considerable attention to the synthesis of aroylhydrazines and their metal complexes because of their applications in the synthesis of several heterocyclic compounds including oxadiazoles, triazoles, thiadiazoles and tetrazines.[37]

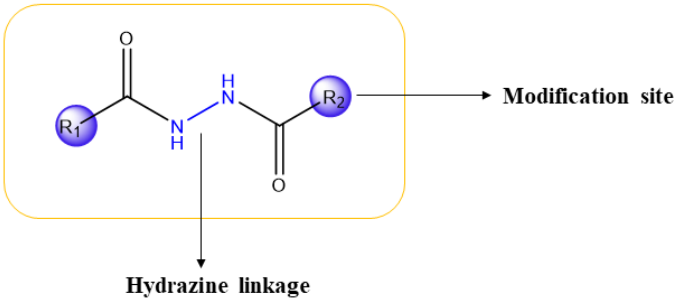

Scheme 7. The framework of arylhydrazine ligand

These ligands can coordinate to the metal ions in different modes such as bidentate and tetradentate manner.

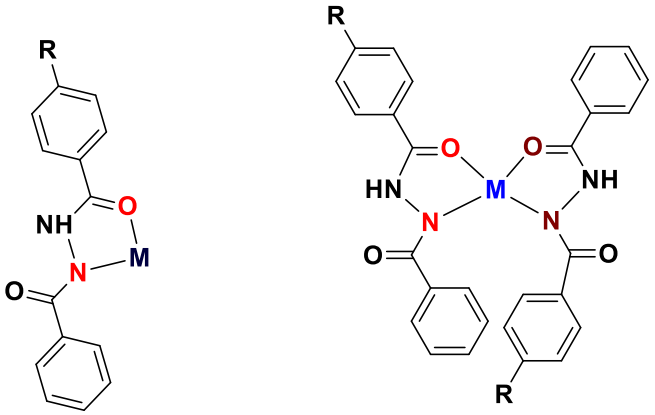

1.4. Metal complexes of half-sandwich arene ligands

Half-sandwich complexes are considered as one of the significant classes of organometallic compounds. Among them, arene ruthenium complexes represent one of the most important organometallic compounds due to their potential applications in various areas.[38] The synthesis of ruthenium(II) arene complexes requires mild reaction conditions and furnishes greater yields, excellent stability and water solubility that have allowed them to a reputable place in the field of organometallics.[39] Further, it has been demonstrated that the nature of the arene, the chelating moieties and the leaving group in these complexes exhibit structure-activity relationship and significantly influence their chemical and biological activity.[40] The half-sandwich complexes encapsulating a (η^n-arene)Ru-moiety have emerged as tunable intermediates in organic synthesis due to facile functionalization of the arene moiety.[41] Further, the arene ring enhances the electrophilic character by coordination with a metal centre. Therefore, reactions such as nucleophilic addition or substitution, arene and benzylic deprotonation become more facile (Scheme 8). The coordinated η^n-bonded hydrocarbon ligands such as (η^6-arene)Ru- and (η^5-cyclopentadienyl)- Ru-moieties in the complexes are relatively inert towards substitution and behave as spectator ligands. These arene fragment stabilizes and prevents rapid oxidation of metal centre.[42]

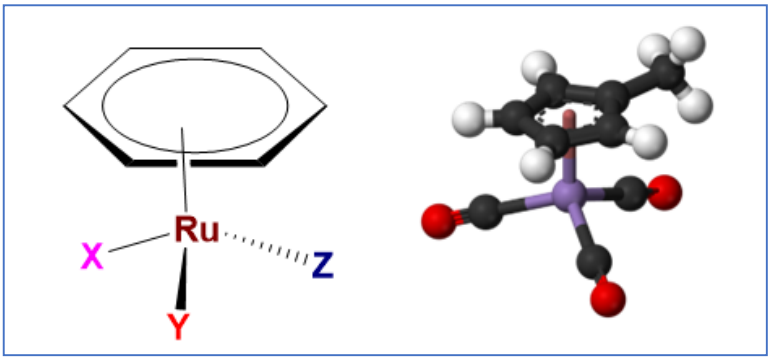

Scheme 8. A general structure of half sandwich metal complexes

(X = halide or N, S, O, P etc. and Y, Z = chelating group with NN, NO, NS, NP etc., donor atoms; X, Y, Z = mono or bi or tridentate ligand)

A huge number of catalytic reactions were carried out by half-sandwich complexes including hydration reaction in alkynes,[43] organonitriles,[44] olefin metathesis,[45] Diels-Alder reactions,[46] hydrogenation of alkenes,[47] transfer hydrogenation of imines/ketones[48] and oxidation of alcohol.[49] The chiral half sandwich-based metal complexes have given important contribution to the synthesis of chiral intermediates.[50]

1.5. Transition metal-catalyzed C-C, C-N and C-O cross-coupling reactions towards the synthesis of heterocycles

Heterocycles are found the largest and most diverse family of organic compounds. They play a vital role in the development of organic synthesis and medicinal chemistry.[51] The heterocyclic compounds containing nitrogen, oxygen and sulphur atoms have a key role in many biological processes and as therapeutic agents.[52] A huge number of heterocyclic derivatives have been found and display physiological and pharmacological properties such as anti-inflammatory, anti-bacterial, analgesic and antioxidant agents.[53] Considering the importance of these useful compounds in modern science, the synthesis of heterocycles and their derivatives has always been an emerging topic in organic synthesis. Over the past few decades, great research efforts have been made to develop novel, flexible, and efficient synthetic methods for the construction of heterocycles through cross-coupling reactions.[54]

Generally, the carbon-carbon (C-C) and carbon-heteroatom (C-X, X = N, O) bond-forming reactions are central importance and constitute the backbone of synthetic organic chemistry.[55] These reactions have a prodigious contribution towards the synthesis of natural products, agrochemicals and important synthetic compounds. Further, these bond formation reactions towards the synthesis of heterocyclic frameworks are immense importance in drug discovery and development of the compounds with novel or selective pharmacologic targets.

The traditional protocol involves a C-C bond formation reaction from aryl or vinyl halides with terminal alkyne.[56] The C-N bond formation takes place from amines with organic halides and C-O bond formation reactions between aryl bromides or iodides with phenols.[57] These reactions are associated with the use of harsh chemicals and the generation of a large amount of toxic waste which affects the environment and sustainability.

During the past decade, transition metal-catalyzed cross-coupling reactions played a remarkable role in the construction of bioactive compounds because of their extended scope and practicability.[58] Here, a coupling reaction has occurred between two organic fragments with the help of transition metal catalyst by the formation of a new carbon-carbon (C-C) or carbon-heteroatom bond.[59] The general mechanism for cross-coupling reactions has been demonstrated in scheme 9. The reaction starts with a rate-determining step in the catalytic cycle to activate the carbon-substituent bond (R-X) by oxidative addition to a transition metal complex followed by a transmetallation step with organic substituent. Further, the reductive elimination step of metal complex forms the desired cross-coupled product (R'-R) with the regeneration of the active metal catalyst.[60]

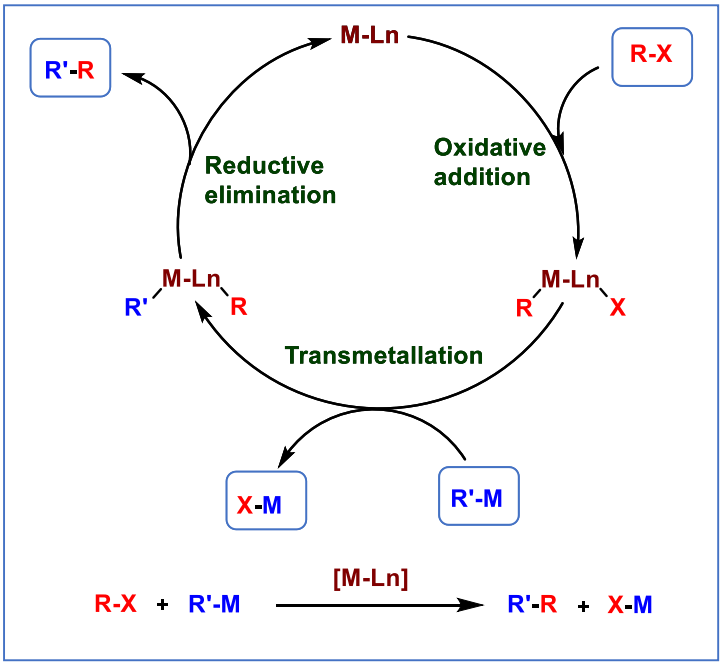

Scheme 9. A general mechanism for transition metal-catalyzed cross-coupling reaction

The transition metal-catalyzed cross-coupling between aryl halide with organometallic reagents, such as the Heck, Suzuki and Negishi reactions are well established for the construction of C-C and carbon-heteroatom bond formation.[61] However, these methods suffer with some limitations such as the heteroaryl organometallic reagents and pseudohalides are not readily accessible and may also ineffectively contribute to the coupling reaction. Moreover, heteroaryl-heteroaryl bond formation is irregular, because of the reactivity and selectivity of coupling partners in the coupling reaction. As a result, the replacement of traditional methods with another effective approach is highly appealing, which helps to overcome these limitations to a great extent.

There is continuous growth in developing new methodologies for the coupling reaction by applying new innovative solutions to overcome the problems. Recent reports revealed the ongoing growth and innovation in metal catalyzed coupling reactions towards the synthesis of heterocycles through the dehydrogenative coupling of alcohols.

1.6. Dehydrogenative coupling of alcohols

Alcohols are significant building blocks for synthetic organic and pharmaceutical chemistry to build advanced organic structures.[62] They are greener starting materials, economical, highly abundant, and utilized as important precursors for the synthesis of numerous fine chemicals with the aid of metal catalysts.[63]

Acceptorless dehydrogenative coupling of alcohol reaction has developed as one of the proficient methods in synthetic organic chemistry to construct carbon-carbon and carbon-heteroatom bonds in an environmentally benign and sustainable way. The transition-metal catalyzed acceptorless dehydrogenative coupling (ADC) strategy have attracted much attention in recent trend. [64] The traditional dehydrogenation reactions have been performed using oxidants/additives, cocatalysts, and ended with the formation of toxic waste. When compared to conventional protocols, acceptorless dehydrogenative strategies are more sustainable, and act as an alternative and practical technique for the synthesis of bioactive heterocycles.[65] Moreover, ADC process involves initial dehydrogenation of alcohols without use of oxidants or sacrificial acceptors followed by a coupling reaction with suitable coupling partners to afford the desired final product. Similarly, dehydrogenation of alcohols performed in open atmospheric condition leads to oxidative dehydrogenation. The overall process involves the liberation of hydrogen gas and water as by-products.

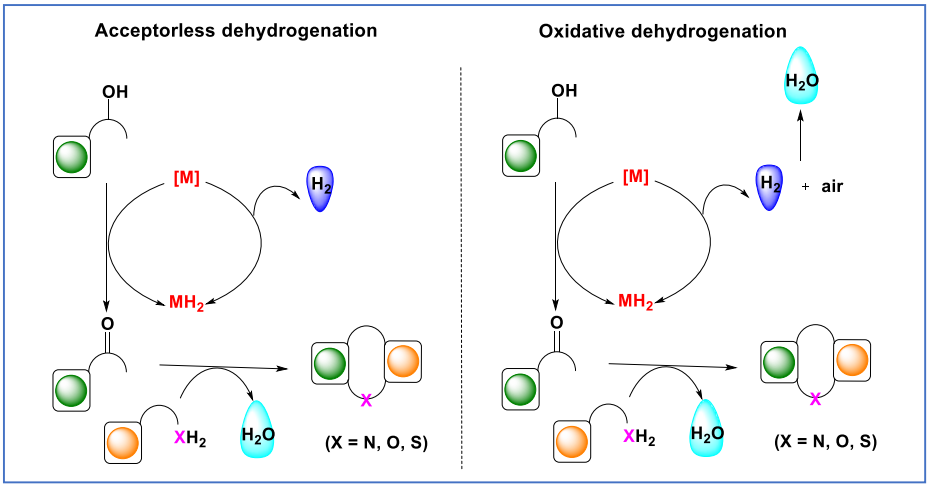

Scheme 10. Transition metal mediated acceptorless / oxidative dehydrogenative coupling of alcohols

Therefore, significant progress has been achieved in the sustainable synthesis of heterocyclic compounds employing C-C or C-X (X = N, O) bond-forming reactions *via* acceptorless dehydrogenative coupling of readily available alcohols with suitable reactant partner.[66] Recently, various transition metal-based catalyst systems have been used for the dehydrogenative synthesis of various heterocycles using the ADC reaction. However, those reported methods have some disadvantages such as harsh reaction conditions, high catalyst loading, higher temperature and limited substrate scope etc.[67] Among them, Ru-catalyzed ADC reactions have gained major interest because of their widespread applications in organic synthesis.[68] For example, Madsen *et al.* used ruthenium-catalyzed acceptorless dehydrogenative coupling reactions of primary alcohols to obtain functional ester derivatives.[69] Beller and co-workers described an efficient dehydrogenative coupling reaction towards pyrroles synthesis from 1,4-diols and amines.[70] Milstein *et al.* reported an ADC protocol for synthesis of peptides and pyrazines from *β*-amino alcohols.[71]

However, ruthenium-catalyzed sustainable synthesis of heterocycles from alcohols following an acceptorless dehydrogenative coupling protocol is not explored well. Hence, this thesis focuses on the new mono and binuclear ruthenium(II) complexes mediated construction of various heterocycles *via* C-C, C-N and C-O bond formation reactions using acceptorless dehydrogenative coupling of alcohols.

1.5.1. Synthesis of imines

Imines are one of the most imperative compounds which have led to significant applications in variety of organic synthesis reactions, pharmaceuticals, agricultural and also in various industries.[72] In traditional routes, synthesis of imines was accomplished by condensation of ketones/aldehydes with amines in presence of acid or base. After that, numerous approaches were developed for synthesis of imines such as self-condensation of

amines, the reaction of nitroarenes with primary alcohols, oxidative dehydrogenation of amines using various oxidants such as quinine, TEMPO, iodosylbenzene.[73] However, these methods have lead to the formation of stoichiometric amount of toxic waste.[74] Hence, the development of an efficient method for the synthesis of imines is highly desirable due to their potential versatility and wide scope.

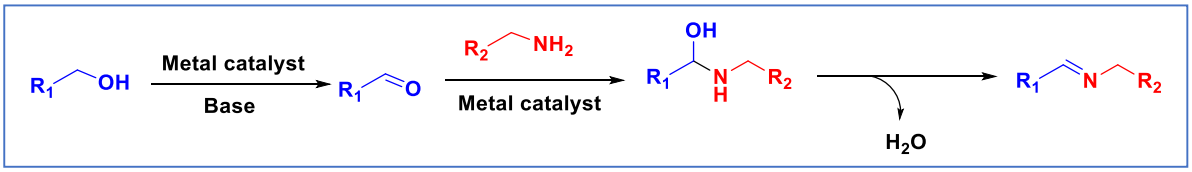

Scheme 11. General reaction of transition metal-catalyzed imine synthesis from alcohols

Based on recent reports,[75] a plausible mechanism for the direct synthesis of imine from alcohols and amines has been depicted (Scheme 12).

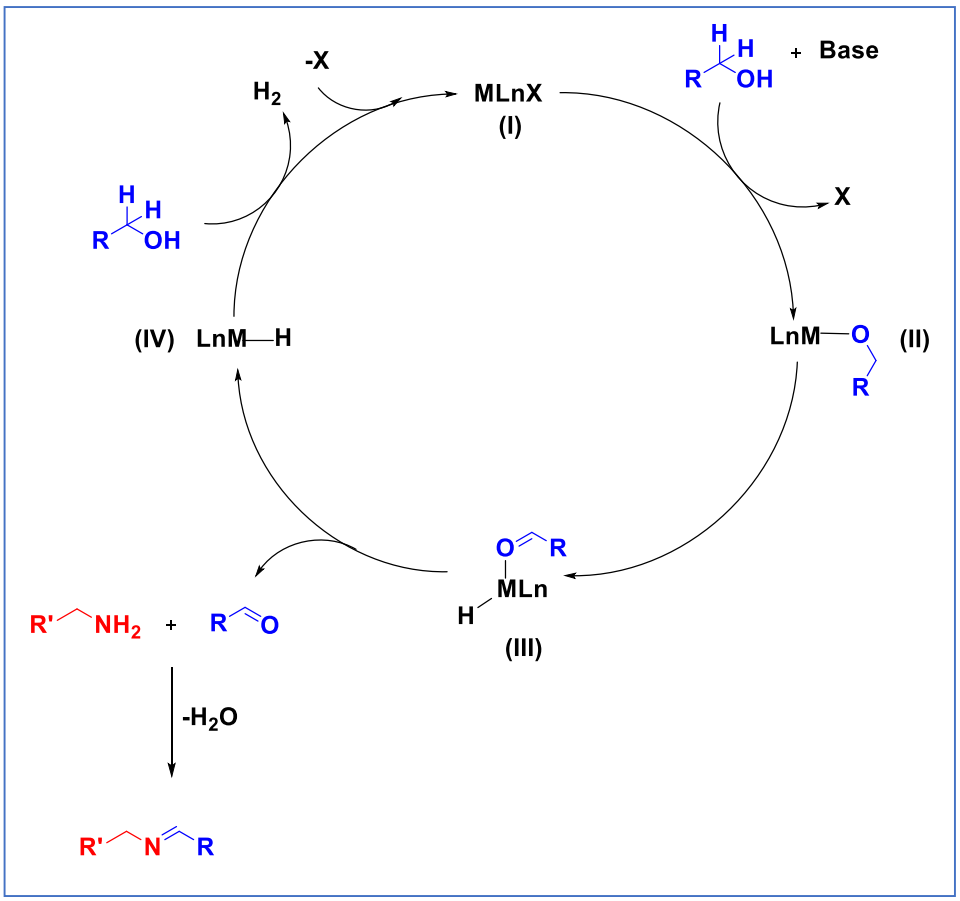

Scheme 12. General catalytic cycle for the imine synthesis from alcohol and amine

The reaction involves the formation of metal alkoxide species (**II**) from the catalyst through deprotonation of the alcohol followed by *β*-hydride elimination (**III**) to form aldehyde. This aldehyde intermediate further reacts with amines to produce imines and water is eliminated as a by-product. Further, the metal hydride (**IV**) reacts with alcohol to form the next catalytic cycle with the release of water.

1.5.2 Olefination of methyl-N-heteroarenes

E-Selective conjugated olefins are found to be an important intermediates in most synthetic organic transformations.[76] They are indispensable building blocks for the construction of important heterocyclic frameworks including natural products and pharmaceuticals.[77] Particularly, most drug molecules and agrochemicals containing heteroarene units were proved to have promising biological applications. A large number of olefin synthetic routes were developed such as Wittig reaction, Peterson olefination and Julia olefination.[78] The Heck, Suzuki, and olefin metathesis reactions are found to be most useful synthetic strategies for olefins as well.[79]

The recent reports available on the synthesis of conjugated olefins were performed by the condensation of aldehydes with N-heteroarenes in the presence of a strong acid or base.[80] However, these methods often suffer from, multistep reaction sequence, use of oxidant, generation of stoichiometric waste, poor selectivity and poor atom economy. Thus, the development of new methodologies for the construction of olefins conjugated with N-heteroarenes is a highly demanding goal.

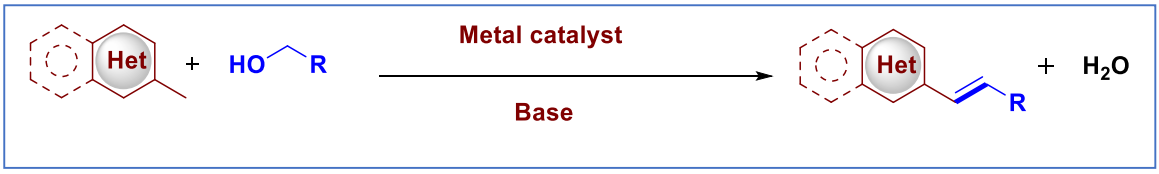

Scheme 13. General reaction of metal-catalyzed olefination of methyl-N-heteroarenes

Following recent reports,[81] a plausible reaction mechanism for olefination of methyl-N-heteroarenes is depicted (Scheme 14). Initially, the metal catalyst (**I**) reacts with alcohols in the presence of a base to form metal alkoxide (**II**). After that, **II** underwent *β*-hydride elimination (**III**) to release aldehyde and M-H species (**IV**). Further, alcohol reacts with metal hydride species (**IV**) to generate metal alkoxide species (**II)** with the liberation of H_2 and thereby catalyst enters into the next catalytic cycle. Afterwards, the liberated aldehyde reacts with 2-methylheteroarenes in the presence of a base to afford desired olefinated product.

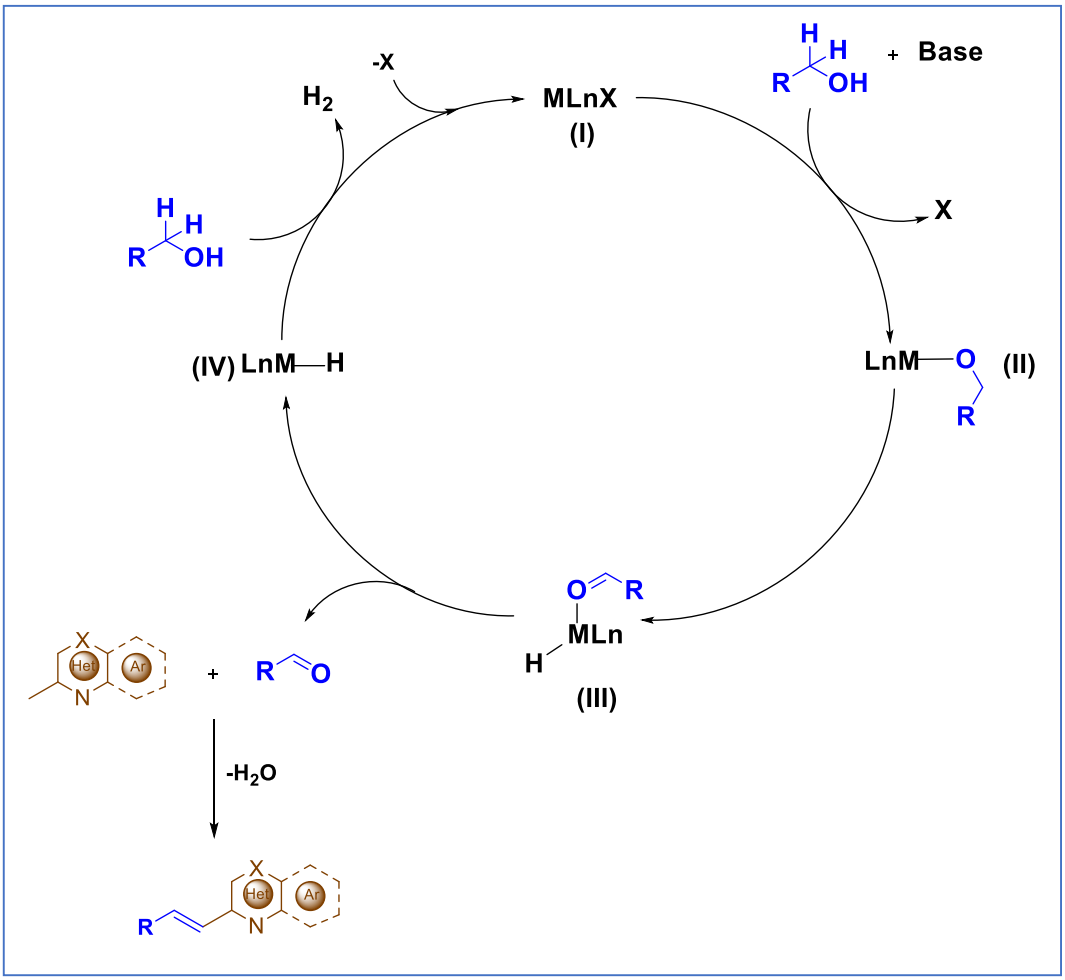

Scheme 14. General catalytic cycle for metal-catalyzed olefination of methyl-N-heteroarenes

1.5.3 Synthesis of 2-amino-4H-chromenes

2-Amino-4H-chromenes and their derivatives are of significant importance due to their wide range of biological activities such as antimicrobial, antiproliferative and antitumor activity.[82] They are used as a drugs for Alzheimer's disease, Huntington's disease and anticancer therapeutic agents etc.[83]

Multi-component reactions (MCRs) have gained significant attention for constructing a broad range of bioactive molecules in highly efficient, rapid, low-cost, and eco-friendly manner.[84] Several multicomponent protocols have been reported for the synthesis of 2-amino-4H-chromenes and their derivatives using malononitrile, resorcinol and aldehyde with various catalysts such as piperidine, triethyl amine, aqueous K_2CO_3 etc.[85] Most of these reported protocols require a long reaction time, harsh condition, high temperature and possess poor recyclability of catalysts. To make the reaction simple and green, it is important to use the environmentally friendly medium for the synthesis of 2-amino-4H-chromenes.

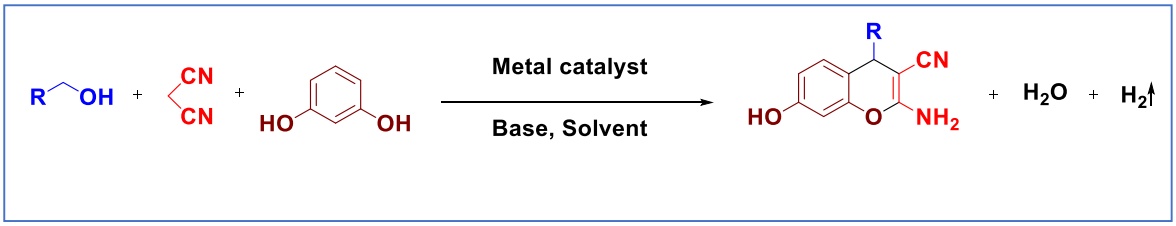

Scheme 15. General reaction of metal-catalyzed synthesis of 2-amino-4H-chromenes from alcohols

In accord with the previous reports,[86] a plausible mechanism for metal catalysed synthesis of 2-amino-4H-chromene has been proposed (Scheme 16). At first, the catalyst (**I**) reacts with alcohol with the aid of base to give metal-alkoxide species (**II**). Further, **II** undergoes *β*-hydride elimination (**III**) to discharge aldehyde along with the generation of metal-hydride species (**IV**). Further, the *in-situ* generated aldehyde underwent Knoevenagel

condensation with malononitrile to form benzylidenemalononitrile intermediate. Later, Michael addition[87] of benzylidenemalononitrile and resorcinol followed by intramolecular cyclization to result the 2-amino-4H-chromene. Finally, metal-hydride species (**IV**) reacts with another molecule of alcohol to regenerate the catalyst with the liberation of hydrogen gas.

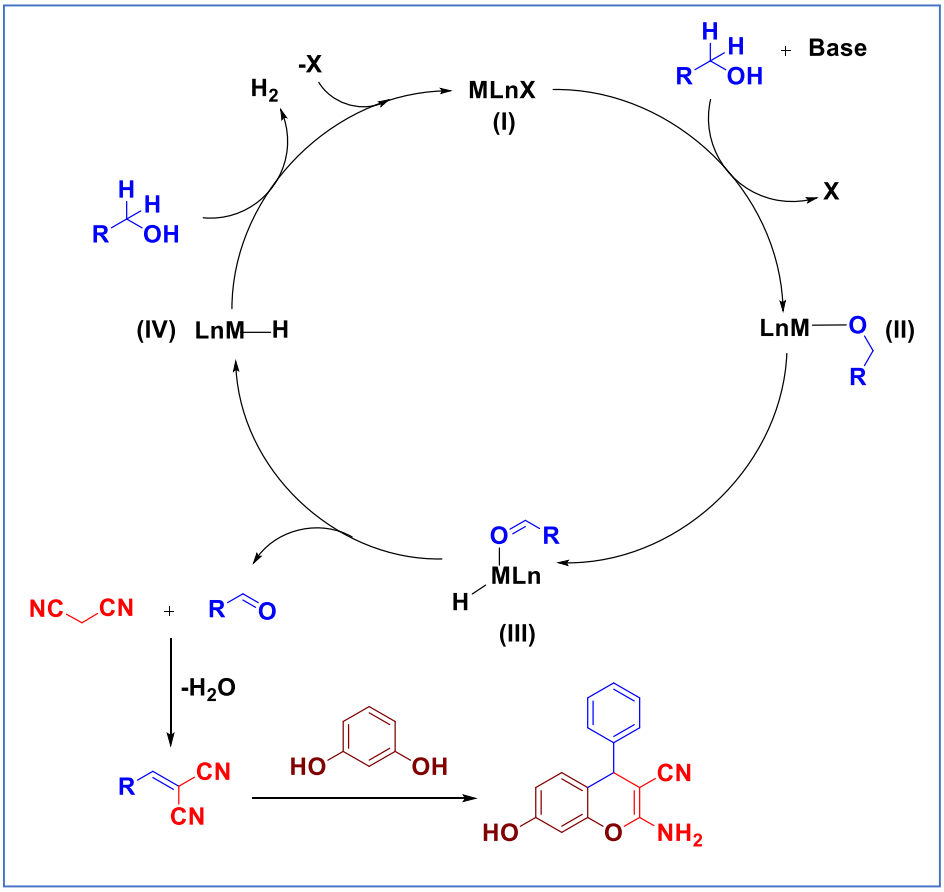

Scheme 16. General catalytic cycle for the metal mediated synthesis of 2-amino-4H-chromenes from alcohols

1.5.4 Synthesis of pyrazoles

Pyrazole and its derivatives have tremendous application in pharmaceutical and agrochemical industries.[88] These compounds are known to exhibit antimalarial, antitumor, antifungal and antimicrobial[89] and insecticidal activities.[90] Several methods have been reported for pyrazole syntheses such as 1,3-dicarbonyl compounds with hydrazines and 1,3-

dipolar cycloaddition of dipolarophiles.[91] These methods have drawbacks such as the need of expensive catalyst, long reaction time and tedious work-up process. Consequently, great efforts have been made to find efficient synthesis of pyrazoles *via* dehydrogenation of alcohols.

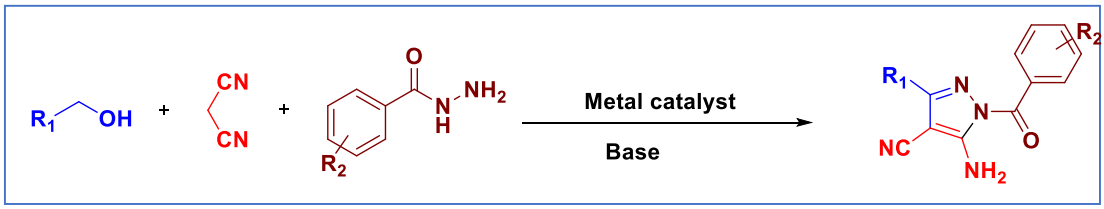

Scheme 17. General reaction of metal-catalyzed synthesis of pyrazole derivatives

Based on the previous reports,[92] a plausible mechanism for metal-catalysed synthesis of pyrazole has been demonstrated (Scheme 18). Initially, the catalyst (**I**) reacts with alcohol with the help of base to give metal-alkoxide species (**II**). Further, **II** undergoes *β*-hydride elimination (**III**) to discharge aldehyde. Further, the *in-situ* generated aldehyde reacts with malononitrile to form benzylidene malononitrile intermediate. Later, reaction of benzylidenemalononitrile with benzohydrazide followed by intramolecular cyclization to result the pyrazole products. Further, metal-hydride species (**IV**) react with another molecule of alcohol to regenerate the catalyst with the liberation of hydrogen gas.

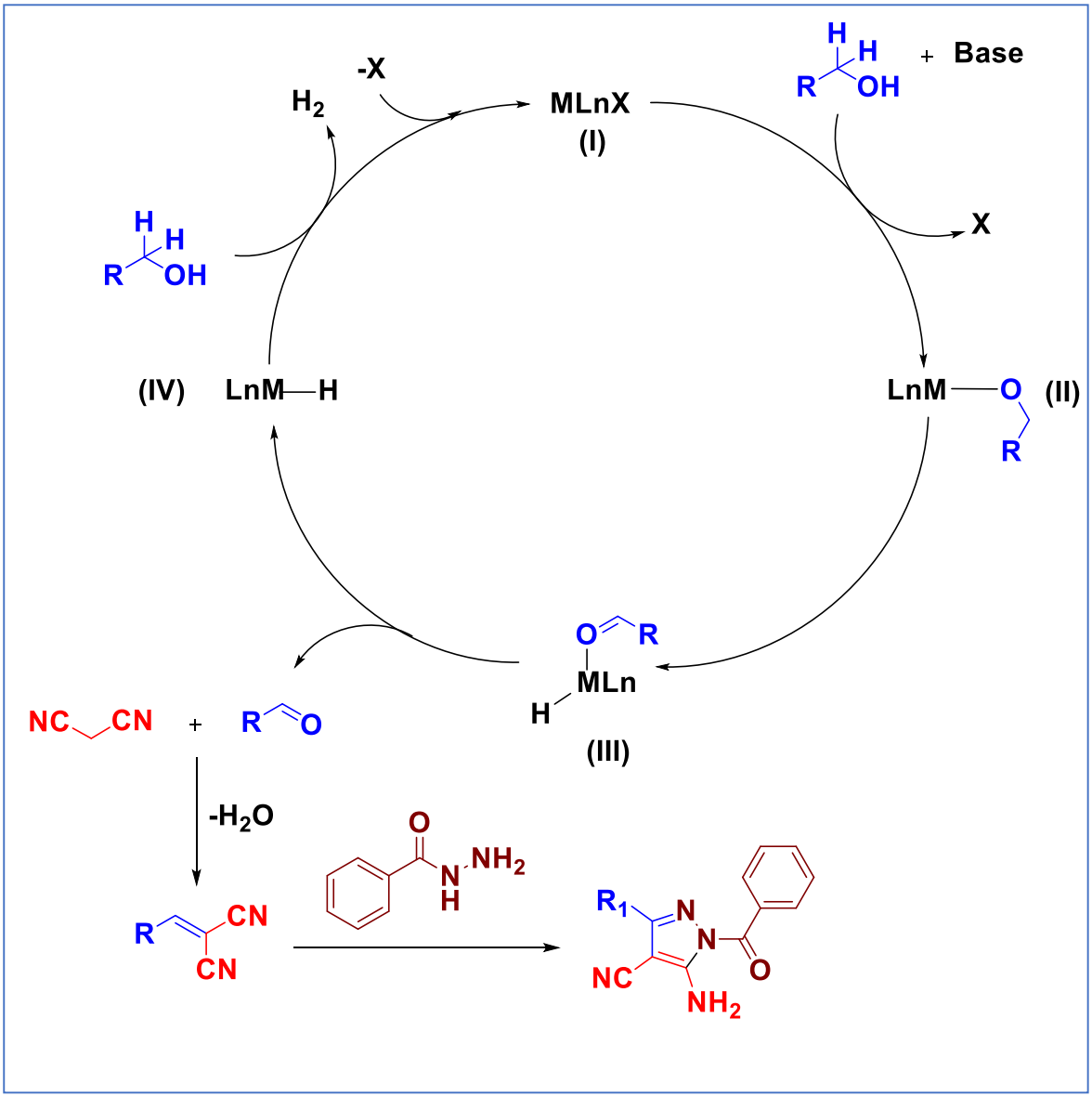

Scheme 18. General catalytic cycle for the synthesis of pyrazole derivatives from alcohols

1.6 Literature survey

A detailed literature survey on the mono and binuclear ruthenium complexes featuring thiourea, aroylhydrazone and aroylhydrazine ligands has been described.

1.6.1 Arene ruthenium(II) thiourea complexes

Sheeba *et al.* have reported six new arene ruthenium(II) complexes containing chiral acyl thiourea ligands. Single-crystal X-ray investigations on three of the complexes verified

their molecular structures. For the first time, the monodentate coordination of the ligands with the ruthenium ion through sulphur atom was reported. The synthesized complexes act as efficient catalysts for the asymmetric transfer hydrogenation of aromatic ketones in the presence of 2-propanol and KOH to produce chiral alcohols. All of the catalysts showed excellent conversions of up to 99% and enantiomeric excesses of up to 99%.[93]

Rao and co-workers have described two cationic arene ruthenium(II) complexes containing 1-benzoyl-3-(pyridine-2-yl)thiourea ligands. All the complexes have been characterized by FT-IR, UV-vis and NMR methods. Single crystal X-ray crystallographic studies of the complexes established the coordination of the ligand to the metal atoms in bidentate mode and reveals a pseudo-octahedral geometry [94]

The reactions of chiral thiourea ligands with ruthenium benzene dimer gave chiral half-sandwich arene Ru(II) complexes as described by Sheeba *et al*. The solid-state molecular structures of ligand and complexes were confirmed by single crystal X-ray diffraction study. Further, synthesized complexes were successfully screened as catalysts for the asymmetric transfer hydrogenation of ketones using 2-propanol as the hydrogen source in the presence of KOH. These catalytic reactions proceeded with excellent yields (up to 99%) and very good enantioselectivity (up to 99% ee).[95]

A series of ruthenium(II) arene complexes were synthesized from acyl/aroyl thiourea ligands ruthenium(II) starting precursors. The solid-state structural studies of the complexes revealed that the ligands coordinated to the metal *via* neutral monodentate fashion through sulphur atom. Furthermore, the newly synthesized complexes were treated with NaN_3, which resulted in the formation of highly strained four-membered azido complexes. The reaction of azido complexes with diethylacetylene dicarboxylate (DEAD) and dimethylacetylene dicarboxylate (DMAD) directed to the formation of triazolato complexes and the results were documented by Kollipara and co-workers.[96]

Our research group has reported two ruthenium complexes encompassing aroyl thiourea ligands. Notably, the catalytic efficiencies of six- and four-membered N, S chelated ruthenium complexes were evaluated in synthesis of azines from alcohols and hydrazines *via* acceptorless dehydrogenative pathway. A diverse range of azines was synthesized in good to high yields using a catalyst loading of 0.5 mol %, in marked contrast to the previous reports.[97]

Next, a series of arene Ru(II) complexes comprising acylthiourea ligands were synthesized. All Ru(II) complexes were well characterized by analytical and spectral (UV-Vis, FT-IR and NMR) methods. The molecular structures of two of the complexes were confirmed by single crystal X-ray diffraction technique. The catalytic ability of the Ru complexes was evaluated in the synthesis of quinoxaline compounds from various 2-nitroaniline and hydroxy ketone derivatives *via* transfer hydrogenation approach.[98]

Recently, Gumus's research group has disclosed ruthenium(II) complexes supported acylthiourea ligands. The synthesized complexes used as homogeneous catalysts for the direct oxidation of the *α*-methylene group in amine. The catalytic activity of all the complexes for the *α*-oxygenation reactions of primary benzylic amines to amides was investigated. Overall, all catalysts exhibited excellent activity and selectivity towards the formation of amide production under mild reaction conditions.[99]

1.6.2. Ruthenium(II) aroylhydrazone complexes

Our group has explored the convenient synthesis of Ru(II) carbonyl complexes comprising thiophene-based benzhydrazone ligands. The synthesized Ru(II) complexes were employed as catalysts in one-pot conversion of aldehydes to corresponding amides in presence of $NH_2OH.HCl$. Moreover, the screening of solvents, bases, temperatures, and catalyst loading were also evaluated in the catalytic reaction.[100]

In 2016, Jia's research group reported a set of ruthenium(II)-*p*-cymene complexes featuring hydrazone ligands. The molecular structures of ruthenium complexes were further confirmed by single-crystal X-ray diffraction methods. Further, these half-sandwich ruthenium complexes are developed as active catalysts for the mild hydrogenation of nitroarenes to aromatic anilines in the presence of sodium tetrahydroborate reducing agent in water medium.[101]

Ruthenium(II) complexes were synthesized from pyridine-2-carboxaldimine ligands with ruthenium(II) precursors. The complexes were confirmed by spectral and analytical methods. The X-ray diffraction studies showed that complexes possess pseudo-octahedral geometry. Further, synthesized complexes were used as effective catalysts in transfer hydrogenation reaction of ketones into alcohols.[102]

A series of Ru(II) arene complexes encompassing Schiff-base ligands have been synthesized and characterized by IR, NMR and mass studies. The exact molecular structures of Ru(II) complexes were further authenticated by single-crystal X-ray diffraction analysis. Additionally, these complexes were employed as catalysts for the hydrogenation of nitroarenes to aromatic anilines in aqueous medium in the presence of a reducing agent sodium tetrahydroborate.[103]

Manikandan *et al.* has described the synthesis of new air-stable octahedral ruthenium(II) carbonyl complexes bearing O, and N-bidentate benzhydrazone ligands. Further, complexes were characterized by elemental analysis, spectral and single crystal X-ray diffraction methods. The synthesised complexes were exploited as a catalyst for the transfer hydrogenation process of different ketones using isopropanol medium and KOH base, and the maximal conversion is reached up to 100%.[104]

Viswanathamurthi and co-workers has documented a new series of ruthenium(II) 2-oxo-1,2-dihydroquinoline-3-carbaldehyde hydrazone complexes. Further, the solid-state molecular structure of complexes was confirmed by the single-crystal X-ray diffraction method. In addition, the catalytic efficiency of the synthesized complexes has been investigated in direct amidation of alcohols with amines. The catalytic parameters like base, temperature and catalyst loading in the amidation reaction were also evaluated.[105]

Mohan *et al.* have reported a panel of *p*-cymene Ru(II) benzhydrazone complexes synthesized from the reaction of acetophenone benzoyl hydrazone ligands with [Ru(η^6-*p*-cymene)(μ-Cl)Cl]$_2$ starting precursor. The solid-state molecular structures of the few of the complexes were confirmed by single crystal X-ray diffraction studies. All the ruthenium(II) arene complexes were explored as catalysts for transfer hydrogenation of a wide range ketones with 2-propanol using 0.1 mol% catalyst loading, and conversions of up to 100% were obtained. Further, the influence of other variables on the transfer hydrogenation reaction, such as base, temperature, catalyst loading and substrate scope, was also investigated.[106]

Half-sandwich η^6-*p*-cymene ruthenium(II) complexes containing pyrrole-2-hydrazones have been synthesized and characterized by various spectral and analytical techniques. All the complexes exhibit exceptional catalytic activity towards the synthesis of quinoline derivatives from 2-aminobenzyl alcohol and ketones or secondary alcohols. The maximum yield of the quinolines obtained was up to 97%.[107]

Our group has reported a series of neutral ruthenium(II) complexes containing methyl-2-pyrrole ketone hydrazone ligands. The single crystal X-ray study of the complexes reveals the bidentate coordination mode of the ligand to ruthenium ion *via* azomethine nitrogen and imidazolate oxygen. These complexes were established as selective catalysts for the direct synthesis of imine from alcohol and amine in toluene medium. Further, the

model catalyst shows maximum yield using 1 mol% catalyst loading under aerobic conditions.[108]

In 2018, Ramachandran *et al.* disclosed new ruthenium(II) complexes with PNO/PNS donor ligands. The single crystal X-ray study of the synthesized complexes revealed the distorted octahedral geometry around the ruthenium(II) ion. The catalytic study of complexes was carried out towards the regioselective *N*-alkylation of a wide range of heterocyclic amines with alcohols.[109]

Three new half-sandwich η^6-*p*-cymene ruthenium(II) complexes bearing benzothiazole hydrazone ligands were synthesized. The solid-state molecular structure of the complexes reveals that the hydrazone ligand coordinated to Ru(II) ion *via* monobasic bidentate fashion. The complexes were used as active catalysts for transamidation of primary amide and the findings were documented by Viswanathamurthi group.[110]

A panel of Ru(II) complexes containing hydroxyquinoline hydrazone ligands were synthesized. Further, solid-state molecular structures of two of the complexes were resolved by single crystal X-ray diffraction method which revealed a pseudo-octahedral geometry around the ruthenium ion. All the new complexes have been employed as efficient catalysts in N-alkylation reactions for the synthesis of tertiary amines by the coupling of secondary amines with aromatic primary alcohols at low catalyst loading and resulted maximum yields.[111]

1.6.3 Arene ruthenium(II) aroylhydrazine complexes

Dinuclear arene ruthenium(II) complexes of dipropionylhydrazine, dibutanoylhydrazine and dipentanoylhydrazine ligands were synthesized and characterized by analytical and spectral methods. The solid-state molecular structures of all ruthenium(II)

complexes were corroborated with aid of single crystal X-ray studies. The geometry of the complexes was found to be pseudo-octahedral geometry.[112]

Our research group has reported diruthenium(II) complexes encompassing 1,2-diacylhydrazine ligands. The solid-state molecular structure of complex was authenticated with the help of single-crystal X-ray diffraction method. Further, the complexes were employed as catalysts for the synthesis of imine derivatives from alcohols and amines and the catalytic system produced water as the only by-product. The oxidative imination reaction operated under environmentally benign condition with low catalyst loading. The catalytic protocol tolerates a wide range of imine derivatives in good to excellent yields.[113]

The new dinuclear *p*-cymene Ru(II) complexes have been synthesized and characterized by spectral and analytical methods. The resulted complexes performed as efficient catalysts for the synthesis of 2,4,5-trisubstituted imidazoles from easily accessible primary alcohols. A variety of imidazoles products was achieved with a yield up to 95% by using 0.25 mol% of catalyst loading. The catalytic protocol is environmentally benign, performed under mild conditions and discharges water as the only by-product.[114]

1.7. REFERENCES

1. H. Carbtree, *The Organometallic Chemistry of Transition Metals*, 5th ed. New York, NY: John Wiley and Sons. pp. 2560.

2. (a) B. khera, A. K. Sharma and N. K. Kaushik, *Polyhedron*, 1983, **2**, 1177-1180; (b) S. Woodward, *Curr. Sci.*, 2000, **78**, 1314-1317.

3. (a) C. Ruppin and P. H. Dixneuf, *Tetrahedron. Lett.*, 1986, **27**, 6323-6324; (b) D. Devanne, C. Ruppin and P. H. J. Dixneuf, *Org. Chem.*, 1988, **53**, 952-926; (c) T. Opstal, K. Couchez and F. Verpoort, *Adv. Synth. Catal.*, 2003, **345**, 393-401; (d) H. Brunner, T. Zaack, M. Zabel, W. Beck and A. Bohm, *Organometallics.*, 2003, **22**, 1741-1750; (e) N. A. Owston, A. J. Parker and J. M. J. Williams, *Org. Lett.*, 2007, **9**, 3599-3601; (f) J. W. W. Chang and P. W. H. Chan, *Angew. Chem. Int. Ed.*, 2008, **47**, 1138-1140; (g) D. Gnanamgari and R. Crabtree, *Organometallics.*, 2009, **28**, 922-924.

4. (a) R. E. Morris, R. E. Aird, P. del Socorro Murdoch, H. Chen, J. Cummings, N. D. Hughes, S. Parsons, A. Parkin, G. Boyd, D. I. Jodrell and P. J. Sadler, *J. Med. Chem.*, 2001, **44**, 3616-3621; (b) Z. Adhireksan, G. E. Davey, P. Campomanes, M. Groessl, C. M. Clavel, H. Yu, A. A. Nazarov, C. H. Yeo, W. H. Ang, P Droge, U. Rothlisberger, P. J. Dyson and C. A. Davey, *Nat. Commun.*, 2014, **5**, 3462; (c) B. S. Murray, M. V. Babak, C. G. Hartinger and P. J. Dyson, *Coord. Chem. Rev.*, 2016, **306**, 86-114; (d) L. Zeng, P. Gupta, Y. Chen, E. Wang, L. Ji, H. Chao and Z. S. Chen, *Chem. Soc. Rev.*, 2017, **46**, 5771-5804; (e) P. Zhang and P. J. Sadler, *J. Organomet. Chem.*, 2017, **839**, 5-14; (f) R. H. Berndsen, A. Weiss, U. K. Abdul, T. J. Wong, P. Meraldi, A. W. Griffioen, P. J. Dyson and P. Nowak-Sliwinska, *Sci. Rep.*, 2017, **7**, 43005.

5. (a) K. S. Murray, *Aust. J. Chem.*, 1978, **31**, 203-207; (b) H. Doine, *Bull. Chem, Soc, Jpn.*, 1985, **58**, 1327-1328; (c) K. Nagajima, Y. Ando, H. Mano and M. Kojima, *Inorg. Chim. Acta.*, 1998, **274**, 184-191; (d) S. N. Pal and S. Pal, *Inorg. Chem.*, 2001, **40**, 4807-4810; (e) B. Declercq and F. Verpoort, *Macromolecules.*, 2002, **35**, 8943-8947; (f) T. Opstal and F. Verpoort, *Synlett.*, 2002, **6**, 935-941; (g) T. Opstal and F. Verpoort, *Angew. Chem. Int. Ed.*, 2002, **42**, 2876-2879.

6. (a) J. P. Sauvage, J. P. Collin, J. C. Cambron, S. Guillerez, C. Coudret, V. Balzani, F. Barigelletti, L. D. Cola and L. Flamingni, *Chem. Rev.*, 1994, **94**, 911-937; (b) V. Balzani, A. Juris, M. Venturi, S. Campagna and S. Serroni, *Chem. Rev.*, 1996, **96**, 759-833; (c) P. D. *Beer, Acc. Chem. Res.*, 1998, **31**, 71-80; (d) N. Chitrapriya, V. Mahalingam, L. C. Channels, M. Zeller, F. R. Fronczek and K. Natarajan, *Inorg. Chim. Acta.*, 2008, **361**, 2841-2850; (e) A. Bacchi, P. Pelagatti, C. Pelizzi and D. Rogolino, *J. Organomet. Chem.*, 2009, **694**, 3200-3211; (f) N. P. Priya, S.

Arunachalam, A. Manimaran, D. Muthupriya and C. Jayabalakrishnan, *Spectrochim. Acta A.*, 2009, **72**, 670-676; (g) M. U. Raja, N. Gowri and R. Ramesh, *polyhedron.*, 2010, 1175-1181; (h) M. Aydemir, A. Bayasal, S. Ozkar and L. T. Yildrim, *Inorg. Chim. Acta.*, 2011, **367**, 166-172; (i) F. O. N. Silva, M. C. L. Candido, A. K. M. Holanda, I. C. N. Diogenes, E. H. S. Sousa and L. G. F. Lopes, *J. Inorg. Biochem.*, 2011, **105**, 624-625; (j) Z. Travnicek, M. M. Malarova, R. Novotna, J. Vanco, K. Stepankova and P. Suchy, *J. Inorg. Biochem.*, 2011, **105**, 937-948.

7. (a) B. Gnanaprakasam, J. Zhang and D. Milstein, *Angew. Chem. Int. Ed.*, 2010, **49**, 1468-1471; (b) A. Maggi and R. Madsen, *Organometallics.*, 2012, **31**, 451-455.

8. L. Gong, M. Wenzel, and E. Meggers, *Acc. Chem. Res.*, 2013, **46**, 2635-2644.

9. (a) C. Gunanathan, Y. Ben-David and D. Milstein, *Science.*, 2007, **317**, 790-792; (b) B. Gnanaprakasam and D. Milestein, *J. Am. Chem. Soc.*, 2011, **133**, 1682-1685; (c) D. Cho, K. C. Ko and J. Y. Lee, *Organometallics.*, 2013, **32**, 4571-4576.

10. (a) T. Ohkuma, H. Ooka, S. Hashiguchi, T. Ikariya and R. Noyori, *J. Am. Chem. Soc.*, 1995, **117**, 2675-2676; (b) W. Baratta, G. Chelucci, S. Gladiali, K. Siega, M. Toniutti, M. Zanette, E. Zangrando and P. Rigo, *Angew. Chem. Int. Ed.*, 2005, **44**, 6214-6219; (c) W. Baratta, M. Bosco, G. Chelucci, A. Del Zotto, K. Siega, M. Toniutti, E. Zangrando and P. Rigo, *Organometallics.*, 2006, **25**, 4611-4620; (d) W. Baratta, K. Siega and P. Rigo, *Adv. Synth. Catal.*, 2007, 349, 1633-1636; (e) F. Zeng and Z. Yu, *Organometallics.*, 2008, **27**, 6025-6028; (f) W. Baratta and P. Rigo, *Eur. J. Inorg. Chem.*, 2008, 4041-4053; (g) B. J. Sarmah and D. K. Dutta. *J. Organomet. Chem.*, 2010, **695**, 781-785; (h) F. E. Fernandez, M. C. Puerta and P. Valerga, *Organometallics.*, 2011, **30**, 5793-5802; (i) H. Turkmen, I. Kani and B. Cetinkaya, *Eur. J. Inorg. Chem.*, 2012, 4494-4499.

11. R. H. Grubbs and A. G. Wenzel, *Handbook of metathesis*, Wiley-VCH, Volume 1, page 61-80.

12. (a) R. Hermatschweiler, I. Fernandez, F. Breher. P. S. Pregosin, L. F. Veiros and M. J. Calhorda, *Andew. Chem. Int. Ed.*, 2005, **44**, 4397-4400; (b) C. Schlepphorst, B. Maji and F. Glorious, *ACS. Catal.*, 2016, **6**, 4184-4188.

13. L. Wu, I. Fleischer, R. Jackstell, I. Profier, R. Franke and M. Beller, *J. Am. Chem. Soc.*, 2013, **135**, 14306-14312.

14. (a) C. W. Bielawski, J. Louie and R. H. Grubbs, *J. Am. Chem. Soc.*, 2000, **122**, 12872-12873; (b) B. A. Siegal, C. Fajardo and Marc L. Snapper, *J. Am. Chem. Soc.*, 2005, **127**, 16329-16332; (c) S. Burling, B. M. Paine, D. Nama, V. S. Brown, M. F. Mahon, T. J. Prior, P. S. Pregosin, M. K. Whittlesey and J. M. J. Williams, *J. Am. Chem. Soc.*, 2007, **129**, 1987-1995.

15. (a) B. M. Trost and Z. T. Ball, *J. Am. Chem. Soc.*, 2005, **127**, 17644-17655; (b) A. Hayashi, T. Yoshitomi, K. Umeda, M. Okazaki and F. Ozawa, *Organometallics.*, 2008, **27**, 2321-2327.

16. (a) F. Martínez-Peña, S. Infante-Tadeo, A. Habtemariam and A. M. Pizarro, *Inorg. Chem.*, 2018, **57**, 5657-5668; (b) J. Zhao, D. Zhang, W. Hua, W. Li, G. Xu and S. Gou, *Organometallics.,* 2018, **37**, 441-447; (c) F. Chen, I Romero-Canelon, J. J. Soldevila-́ Barreda, J I. Song, J. P. C. Coverdale, G. J. Clarkson, J. Kasparkova, A. Habtemariam, M. Wills, V. Brabec and P. J. Sadler, *Organometallics.,* 2018, **37**, 1555-1566; (d) J. J. Li, Z. Tian, X. Ge, Z. Xu, Y. Feng, Z. Liu, *Eur. J. Med. Chem.*, 2019, **163**, 830-839; (e) W. Ma, L. Guo, Z. Tian, S. Zhang, X. He, J. Li, Y. Yang and Z. Liu, *Dalton Trans.*, 2019, **48**, 4788-4793.

17. (a) S. Grguric-Ś ˇ ipka, I. Ivanovic, G. Rakić, N. Todorović, N. Gligorijevic, S. Radulovic, V. B. Arion, B. K. Keppler and Ź . L. Teś ič, *Eur. J. Med. Chem.,* 2010, **45**, 1051-1058; (b) F. Martínez-Peña, S. Infante-Tadeo, A. Habtemariam, and A. Pizarro, *Inorg. Chem.*, 2018, **57**, 5657-5668; (c) R. Pettinari, F. Marchetti, C. Di Nicola, C. Pettinari, A. Galindo, R. Petrelli, L. Cappellacci, M. Cuccioloni, L. Bonfili, A. M. Eleuteri, M. F. C. Guedes da Silva and A. J. L. Pombeiro, *Inorg. Chem.*, 2018, **57**, 14123-14133; (d) F. U. Rahman, M. Z. Bhatti, A. Ali, H. Q. Duong, Y. Zhang, X. Ji, Y. Lin, H. Wang, Z. T. Li and D. W. Zhang, *Eur. J. Med. Chem.*, 2018, **157**, 1480-1490.

18. (a) G. fitzl, L. Beyer, J. Sieler, R. Richter, J. Kaiser and E. Hoyer, *Z. Anorg. Allg. Chem.*, 1977, **433**, 237-241; (b) R. Richter, L. Beyer and J. Kaiser, *Z. Anorg. Allg. Chem.*, 1980, **461**, 67-73; (c) W. Bensch and M. Schuster, *Z. Anorg. Allg. Chem.*, 1992, **615**, 93-96; (d) C. Sacht, M. S. Datt, S. Otto and A. Roodt, *J. Chem. Soc. Dalton Trans.,* 2000, 727-733; (e) H. Arslan, N. Kulcu and U. Florke, *Tansition Metal. Chem.,* 2003, **28**, 816-819. (f) R. D. Campo, J. J. Criado, R. Gheorghe, F. J. Gonzalez, M. R. Hermosa, F. Sanz, J. L. Manzano, E. Monte and E. Rodriguez-Fernandez, *J. Inorg. Biochem.*, 2004, **98**, 1307-1314.

19. (a) V. Lachkova, S. Varbanov, G. Hagele, H. Keck and T. Tosheva, *Phosphorus. Sulfur Silicon Relat. Elem.*, 2002, **177**, 1303 - 1313; (b) M. D'hooghe, A. Waterinckx and N. De Kimpe, *J. Org. Chem.*, 2005, **70**, 227-232; (c) M. Eweis, S. S. Elkholy and M. Z. Elsabee, *Int. J. Biol. Macromol.,* 2006, **38**, 1-8; (d) S. Saeed, N. Rashid, R. Hussain, M. Ali and P. G Jones, *Eur. J. Med. Chem.*, 2010, **45**, 1323 - 1331; (e) S. Saeed, N. Rashid, P. G. Jones, R. Hussain and M. H. Bhatti, *Cent. Eur. J. Chem.*, 2010, **8**, 550 - 558; (f) S. Saeed, N. Rashid, P. G. Jones and U. Yunus, *J. Heterocycl. Chem.*, 2010, **47**, 908 -912.

20. (a) G. De Munno, B. Gabriele and G. Salerno, *Inorg. Chimi. Acta.*, 1995, **234**, 181-183; (b) A. C. Moro, A. E. Mauro, A. V. G. Netto, S. R. Ananias, M. B. Quilles, I.

Z. Carlos, F. R. Pavan, C. Q. F. Leite and M. Horner, *Eur. J. Med. Chem.*, 2009, **44**, 4611-4615; (c) K. Jeyalakshmi, J. Haribabu, N. S. P. Bhuvanesh, and R. Karvembu, *Dalton Trans.*, 2016, **45**, 12518-12531; (d) J. P. Barolli, I. S. Maiab, L. C. Vegasa, *Polyhedron.*, 2017, **126**, 33-41.

21. (a) M. Hanif, M. Azhar and M. V. Babak, *Molecules.*, 2014, **19**, 8080-8092; (b) M. Kalidasan, R. Nagarajaprakash and K. M. Rao, *Z. Anorg. Allg. Chem.*, 2015, **641**, 715-723; (c) S, Rakhshani, A. Rezvani, M. Dušek and V. Eigner, *Appl. Organometal. Chem.*, 2018, **32**, e4342; (d) L. Shadap, S. Diamai and M. R. Kollipara, *J. Organomet. Chem.*, 2019, **884**, 44-54.

22. S. Adhikari, O. Hussian, R. M. Phillips, W. Kaminsky and M. R. Kollipara, *Appl. Organomet. Chem.*, 2018, **32**, 4362-4365.

23. (a) A. C. Moro, A. E. Mauro and S. R. Ananias, *Ecletica Quim.*, 2004, **29**, 57-61; (b) A. C. Moro, F. W. Watanabe, S. R. Ananias, A. E. Mauro, A. V. G. Netto, A. P. R. Lima, J. G. Ferreira and R. H. A. Santos, *Inorg. Chem. Commun.*, 2006, **9**, 493-496; (c) A. C. Moro, A. E. Mauro, A. V. Netto, S. R. Ananias M. B. Quilles, I. Z. Carlos, F. R. Pavan, C. Q. Leite, and M. Hörner, *Eur. J. Med. Chem.*, 2009, **44**, 4611-4615.

24. (a) M. Carcelli, C. Pelizzi, G. Pelizzi, P. Mazza and F. Zani, *J. Organomet. Chem.*, 1995, **488**, 55-61; (b) P. K. Singh and D. N. Kumar, *Spectrochim. Acta Part A Mol. Biomol. Spectrosc.* 2006, **64**, 853-858.

25. (a) Y. X. Ma, Z. Q. Ma, G. Zhao, Y. Ma and M. Yan, *Polyhedron*, 1989, **8**, 2105-2108; (b) X. Su and I. Aprahamin, *Chem. Soc. Rev.*, 2014, **43,** 1963-1981.

26. (a) P. Vicini, M. Incerti, P. La Colla and R. Loddo, *Eur. J. Med. Chem*. 2009, **44**, 1801-1807. (b) N. G. Kandile, I. M. Mohamed, H. Zaky and H. M. Mohamed, *Eur. J. Med. Chem.* 2009, **44**, 1989-1996. (c) O. O. Ajani, C. A. Obafemi, O. C. Nwinyi and D. A. Akinpelu, *Bioorg.Med. Chem*. 2010, **18**, 214-221.

27. (a) J. Hou, W. H. Sun, D. Zhang, L. Chem, W. Li, D. Zhao and H. Song, *J. Mol. Catal. A*, 2005, **231**, 221-233. (b) B. D. Wang, Z. Y. Yang and T. R. Li, *Bioorg. Med. Chem*., 2006, **14**, 6012- 6021. (c) A. M. Stadler and A. Harrowfield, *Inorg. Chem. Acta*., 2009, **362**, 4298-4314.

28. D. R. Richardson, *Crit. Rev. Oncol. Hemat*, 2002, **42**, 267-281.

29. (a) H. Taube, *Surv. Prog. Chem.*, 1973, **6**, 1. (b) P.C. Ford, *Coord. Chem. Rev*., 1970, **5**, 75-99.

30. R. Raveendran and S. Pal, *Inorg.Chim. Acta*, 2006, **359**, 3212-3220.

31. R. Dinda, P. Sengupta, S. Ghosh and W. S. Sheldrick, Oxotransferases. *Eur. J. Inorg. Chem.* **2003**, 363-369.

32. (a) K. Shanker, R. Rohini, V. Ravinder, P. M. Reddy and Y. P. Ho, *Spectrochim. Acta A*, 2009, **73**, 205-211; (b) M. Shebl, S. M. E. Khalil, S. A. Ahmed and H. A. A. Medien, *J. Mol. Struc.*2010, **980**, 39-50.

33. H. D. Yin and S.W. Chen, *Inorg.Chim. Acta.,* 2006, **359**, 3330-3338.

34. Schiff, H. *Ann. Suppl*., 1864, **3**, 343-343.

35. O. Nashwan, Tapabashi, Kirkuk University *Journal- Scientific Studies*, Vol **8**, No.3, 2013.

36. (a) Z. H. Sui, J. H. Guan, M. P. Ferro, K. Mccoy, M. P. Watcher, W. V. Murray, M. Singer, M. Steber, D. M. Ritchie and D. C. Argentieri, *Bioorg. Med. Chem. Lett.*, 2000, **10**, 601-604; (b) H. A. Seow, P. G. Penketh. K. Shyam, S. Rochwell and A. C. Sartorelli, *Proc. Natl. Acad. Sci. U. S. A.* 2005, **102**, 9282-9287; (c) C. Boss, O. Corminboeuf, C. Grisostomi and T. Weller, *Expert. Opin. Ther. Pat.*, 2006, **16**, 295-317; (d) C. X. Tan, D. L. Shen, J. Q. Weng, N. B. Sun and X. M. Ou, *Chin. J. Pestic. Sci.,* 2006, **8**, 63-366; (e) P. Caboni, G. Sarais, A. Angioni, S. Vargiu, D. Pagnozzi, P. Cabras and E. J. Casida, *J. Agric. Food. Chem.,* 2008, **56**, 7696-7699; (f) Q. C. Xia, Q. Z. He, D. F. Xu, X. Y. Li and D. Z. Sun, *Acta. Chim. Sinica.*, 2010, **68**, 775; (g) Y.Y. Zhou, Q. Feng, F. J. Di, Q. X. Liu, D. Y. Wang, Y. W. Chen, L. X. Xiong, H. B. Song, Y. X. Li and Z. M. Li, *Bioorg. Med. Chem.*, 2013, **21**, 4968-4975.

37. (a) Z. N. Cui, L. Yang, X. C. Li, Z. Wang and X. L. Yang, *Chin. J. Org. Chem.*, 2006, **26**, 1647-1656; (b) E. Sagot, A. Le Roux, C. Soulivet, E. Pasquinet, D. Poullain, E. Girard and P. Palmas, *Tetrahedron.,* 2007, **63**, 11189-11194; (c) A. Moulin, M. Bibian, A. L. Blayo, S. El. Habnouni, J. Martinez and J. A. Fehrentz, *Chem. Rev.,* 2010, **110**, 1809-1827; (d) G. Nagendra, R. S. Lamani, N. Narendra and V. V. Sureshbabu, *Tetrahedron. Lett.,* 2010, **51**, 6338-6341; (e) Z. N. Cui, Y. X. Shi, L Zhang, Y. Ling, B. J. Li, Y. Nishida and X. L. Yang, *J. Agric. Food. Chem.,* 2012, **60**, 11649-11656.

38. (a) E. Ferrer Flegeau, C. Bruneau, P. H. Dixneuf and A. Jutand, *J. Am. Chem. Soc.*, 2011, **133**, 10161-10170; (b) S. Mirtschin, A. Slabon-Turski, R. Scopelliti, A. H. Velders and K. Severin, *J. Am. Chem. Soc.,* 2010, **132**, 14004-14005; (c) G. S. Smith and B. Therrien, *Dalton Trans.,* 2011, **40**, 10793–10800; (d) N. J. Farrer and P. J. Sadler, in *Bioinorganic Medicinal Chemistry,* ed. E. Alessio, Wiley-VCH, 2011, vol. 1, pp. 1-47.

39. (a) J. Canivet and G. Sss-Fink, *Green Chem.*, 2007, **9**, 391-397; (b) S. K. Singh, S. Joshi, A. R. Singh, J. K. Saxena and D. S. Pandey, *Inorg. Chem.*, 2007, **46**, 10869-10876.

40. A. Habtemariam, M. Melchart, R. Fernandez, S. Parsons, I. D. H. Oswald, A. Parkin, F. P. A. Fabbiani, J. E. Davidson, A. Dawson, R. E. Aird, D. I. Jodrell and P. J. Sadler, *J. Med. Chem.*, 2006, **49**, 6858-6868.

41. R. D. Pike and D. A. Sweigart, *Coord. Chem. Rev.*, 1999, **187**, 183-222.

42. A. F. A. Peacock and P. J. Sadler, *Chem. Asian J.*, 2008, **3**, 1890-1899.

43. (a) M. A. Bennet and A. K. Smith, *J. Chem. Soc. Dalton. Trans.*, 1974, 233-241; (b) R. A. Zelonka and M. C. Baird, *Can. J. Chem.*, 1972, **50**, 3063-3072.

44. M. Nirmala, M. Adinarayana, K. Ramesh, M. Maruthupandi, M. Vaddamanu, G. Raju and G. Prabusankar, *New. J. Chem.*, 2018, **42**, 15221-15230.

45. D. F. Schreiber, Y. Ortin, H. Muller-Bunz and A. D. Phillips, *Organometallics.*, 2011, **30**, 5381-5395.

46. (a) D. L. Davies, J. Fawcett, S. A. Garrat and D. R. Russell, *Organometallics.*, 2001, **20**, 3029-3034; (b) J. W. Faller and P. P. Fontaine, *Organometallics.*, 2005, **24**, 4132-4138.

47. M. Tokunaga, T. Suzuki, N. Koga, T. Fukushima, A. Horiuchi and Y. Wakatsuki, *J. Am. Chem. Soc.*, 2001, **123**, 11917-11924.

48. (a) M. Bassetti. F. Centola, D. Semeril, C. Bruneau and P. H. Dixneuf, *Organometallics.*, 2003, **22**, 4459-4466; (b) Y. Borguet, X. Sauvage, G. Zaragoza, A. Demonceau and L.Delaude, *Organometallics.*, 2010, **29**, 6675-6686.

49. C. Daguenet, R. Scopelliti and P. J. Dyson, *Oragnometallics.*, 2004, **23**, 4849-4857.

50. (a) R. Noyori and S. Hashiguchi, *Acc. Chem. Res.*, 1997, **30**, 97-102; (b) Y. Ma, H. Liu, L.Chen, X. Cui, J. Zhu and J. Deng, *Org. Lett.*, 2003, **5**, 2103-2106.

51. (a) A. R. Katritzky, *Chem. Rev.* 2004, **104**, 2125-2126; (b) T. Eicher, and S. Hauptmann, The Chemistry of Heterocycles: Structure, Reactions, Syntheses, and Applications, 2003, 2nd edn, Wiley-VCH Verlag GmbH, Weinheim.

52. (a) A. Gursoy, S. Demirayak, G. Capan, K. Erol and K. Vural, *Eur. J. Med. Chem.*, 2000, **35**, 359; (b) M. Amir and S. Kumar *Indian J. Chem.*, 2005, **44**, 2532; (c) Md. Amir, H. Kumar and S. A. Khan. *Bio.Med.Chem.Lett.*, 2008, **18**, 918-922; (d) H. Iqbal, V. Prabhakar, A. Sangitha, B. Chandrika and R. Balasubramanian. *Med. Chem. Res.*, 2014, **23**, 4383-4394;.

53. (a) G. Roma, G. C. Grossi, M. Di Bruccio, M. Ghia, and F. Mattioli. *Eur. J. Med. Chem.*, 1991, **26**, 489-496; (b) S. Kankala, R. K. Kankala, P.Gundepaka, N. Thota, S. Nerella, M. R. Gangula, H. Guguloth, M. Kagga, R. Vadde and O. Chandra. *Med. Chem. Lett.*, 2013, **23**,1306-130; (c) S. C. Karad, V. B. Purohit, P. Thakur, V. R. Thakkar, D. K. Raval, *Eur. J. Med. Chem.*, 2016, **112**, 270-279.

54. (a) D. M. D'Souza and T. J. J. Müller, *Chem. Soc. Rev.* 2007, **36**, 1095-1108; (b) X.-F. Wu, H. Neumann and M. Beller, *Chem. Rev.,* 2013, **113**, 1-35; (c) A. L. Odom and T. J. McDaniel, *Acc. Chem. Res.* 2015, **48**, 2822-2833; (d) J.- J. Feng and J. Zhang, *ACS Catal.*, 2016, **6**, 6651-6661; (e) X. F. Wu, Transition metal-catalyzed heterocycle synthesis via C-H activation, Wiley-VCH, Weinheim, 2016; (f) J. Liu, J. Zou, J. Yao and G. Chen, *Adv. Synth. Catal.* 2018, **360**, 659-663; (g) R. Sreedevi, S. Saranya and G. Anilkumar, *Adv. Synth. Catal.* 2019, **361**, 4625-4644; h) Y. Xiang, C. Wang, Q. Ding, and Y. Peng, *Adv. Synth. Catal.* 2019, **361**, 919-944; (i) W. Chen, X. Zhu, F. Wang, Y. Yang, G. Deng and Y. Liang, *J. Org. Chem.* 2020, **85**, 3349-3357; (j) J. S. S. Neto and G. Zeni, *Tetrahedron.,* 2020, **76**, 130876-130995.

55. (a) Corey, E., Cheng, X. M.; The Logic of Chemical Synthesis. Wiley, New York: 1989. (b) C. S. Yeung, V. Dong, *Chem. Rev.*, 2011, **111**, 1215-1292; (c) Y. Yang, J. Lan and J. You, *Chem. Rev.*, 2017, **117**, 8787-8863.

56. (a) H. A. Dieck and F. R. Heck, *J. Organomet. Chem.*, 1975, **93**, 259-263; (b) K. Okuro, M. Furuune, M. Miura and M. Nomura, *Tetrahedron Lett.,* 1992, **33**, 5363-5364; (c) K. Okuro, M. Furuune, M. Enna, M. Miura and M. Nomura, *J. Org. Chem.*, 1993, **58**, 4716-4721.

57. F. Ullmann and P. Sponagel, *Ber. Dtsch. Chem. Ges.,* 1905, **38**, 2211-2212.

58. B. M. Trost, *In Transition Metals for Organic Synthesis;* Wiley-VCH Verlag GmbH, 2008.

59. (a) T. Colacot, *New Trends in Cross-Coupling: Theory and Applications*, Ed.; 2015, RSC Catalysis Series, Royal Society of Chemistry, Cambridge, UK, p 864; (b) Snieckus, V. Johnson Matthey *Technol. Rev.*, 2016, **60**, 99-105.

60. P. Fitton and E. A. Rick, *J. Organomet. Chem.*, 1971, **28**, 287-291.

61. (a) N. Miyaura, A. Suzuki, *Chem. Rev.,* 1995, **95**, 2457-2483; (b) N. Miyaura and S. L. Buchwald, Cross-Coupling Reactions: A Practical Guide. Springer: 2002; Vol. 219. (c) A. Suzuki, *Angewandte Chemie International Edition.,* 2011, **50**, 6722-6737.

62. (a) D. M. Alonso, J. Q. Bond and J. A. Dumesic, *Green Chem.,* 2010, **12**,1493-1513; (b) T. P. Vispute, H. Zhang, A. Sanna, R. Xiao and G. W. Huber, *Science*, 2010, **330**, 1222-1227.

63. (a) M. Besson, P. Gallezot and C. Pinel, *Chem. Rev.*, 2014, **114**, 1827-1870; (b) H. T. Luk, C. Mondelli, D. C. Ferré, J. A. Stewart and J. Pérez-Ramírez, *Chem. Soc. Rev.*, 2017, **46**, 1358-1426.

64. (a) G. E. Dobereiner and R. H. Crabtree,*Chem. Rev.*, 2010, **110**, 681–703; (b)G. Guillena, D. J. Ramón and M. Yus, *Chem. Rev.*, 2010, **110**, 1611–1641; (c) C. Gunanathan and D. Milstein, *Science.*, 2013, **341**, 1229712; (d) R. H. Crabtree, *Chem. Rev.*, 2017, **117**, 9228-9246; (e) G. Chelucci, *Coord. Chem. Rev.*, 2017, **331**, 37–53; (f) Q. Yang, Q. Wang and Z. Yu, *Chem. Soc. Rev.*, 2015, **44**, 2305-2329; (g) X. Cui, Z. Huang, A.P. van Muyden, Z. Fei, T. Wang, and P.J. Dyson, *Science advances.*, 2020, **6**, e3831; (h) M. Maji, D. Pania, I. Borthakur and S. Kundu, *Org. Chem. Front.*, 2021, **8**, 2673-2709.

65. (a) S. Michlik and R. Kempe, *Angew. Chem., Int. Ed.*, 2013, **52**, 6326-6329; (b) G. Chelucci, *Coord. Chem. Rev.*, 2017, **331**, 37–53; (c) H. Valdés, M. A. García-Eleno, D. Canseco-Gonzalez and D. Morales-Morales, *ChemCatChem.*, 2018, **10**, 3136–3172; (d) P. Daw, Y. Ben-David and D. Milstein, *J. Am. Chem. Soc.*, 2018, **140**, 11931–11934.

66. (a) A. J. Watson, A. C. Maxwell, and J.M. Williams, *Org. Biomol. Chem.*, 2012, **10**, 240-243; (b) A. K. Nezhad and F. Panahi, *ACS Catal.*, 2014, **4**, 1686-1692; (c) P. Daw, Y. Ben-David and D. Milstein, *J. Am. Chem. Soc.*, 2018, **140**, 11931-11934; (d) Y. Zheng, X. Nie, Y. Long, L. Ji, H. Fu, X. Zheng, H. Chen, and R. Li, *Chem. Commun.*, 2019, **55**, 12384-12387; (e) M. Pan, X. Wang, Y. Tong, X. Qiu, X. Zeng, and B. Xiong, *Chem. Commun.*, 2022, **58**, 2379-2382.

67. (a) D. Srimani, E. Balaraman, B. Gnanaprakasam, Y. Ben-David and D. Milstein, *Adv. Synth. Catal.*, 2012, **354**, 2403–2406; (b) S. Musa, L. Ackermann and D. Gelman, *Adv. Synth. Catal.*, 2013, **355**, 3077–3080; (c) K. Paudel, B. Pandey, S. Xu, D. K. Taylor, D. L. Tyer, C. L. Torres, S. Gallagher, L. Kong and K. Ding, *Org. Lett.*, 2018, **20**, 4478–4481; (d) R. G. Alabau, M. A. Esteruelas, A. Martı́nez, M. Olivaán and E. Oñate, *Organometallics*, 2018, **37**, 2732–2740; (e) X. He, Y. Li, H. Fu, X. Zheng, H. Chen, R. Li and X. Yu, *Organometallics*, 2019, **38**, 1750–1760; (f) X. Jiang, J. Zhang, D. Zhao and Y. Li, *Chem. Commun.*, 2019, **55**, 2797–2800; (g) U. K. Das, Y. Ben-David, G. Leitus, Y. Diskin- Posner and D. Milstein, *ACS Catal.*, 2019, **9**, 479–484.

68. A. Khalafi-Nezhad and F. Panahi, *ACS Catal.*, 2014, **4**, 1686−1692.

69. A. Sølvhøj and R. Madsen, *Organometallics*, 2011, **30**, 6044–6048.

70. M. Zhang, H. Neumann and M. Beller, *Angew. Chem., Int. Ed*. 2013, **52**, 597−601.

71. B. Gnanaprakasam, E. Balaraman, Y. Ben-David and D. Milstein, *Angew. Chem., Int. Ed.,* 2011, **50**, 12240−12244.

72. (a) J. P Adams, *J. Chem. Soc. Perkin Trans.,* 2000, 125-139; (b) J. Gawronski, N. Wascinska and J. Gajeway, *Chem Rev.,* 2008, **118**, 5227-5252.

73. (a) L. Blackburn and R. J. Taylor, *Org. Lett.,* 2001, **3**, 1637-1639; (b) L. Jiang, L. Jin, H.Tian, X. Yuan, X. Yu and Q, Xu, *Chem. Commun.,* 2011, **47**, 10833-10835; (c) J. Xu. R. Zhuang, L. Bao, G. Tang and Y. Zhao, *Green Chem.,* 2012, **14**, 2384-2387; (d) Q. Kang and Y. G. Zhang, *Green Chem.,* 2012, **14**, 1016-1019; (e) E.L. Zhang, H.W.Tian, S. D. Xu, X.C. Yu and Q. Xu, Org. Lett., 2013, **15**, 2704-2707; (f) J. F. Soule, H. Miyamura and S. Kobayashi, *Chem. Commun.,* 2013, **49**, 355-357; (g) T. Zhang, L. Zhang, W. Wang, A. Q. Wang, Y. T. Cui, X. Yang, Y. Huang, X. Liu, W. Liu and J. Y. Son, *Green Chem.,* 2013, **15**, 2680-2684; (h) L. Han, P. Xing and B. Jiang, *Org. Lett.,* 2014, **16**, 3428-3431.

74. L Blackburn and R. J. K. Taylor, *Org. Lett.,* 2001, **3**, 1637-1639.

75. B. Ganaprakasam, J. Zhang and D. Milstein, *Angew. Chem.,* 2010, **122**, 1510-1513.

76. (a) N. Chatani, T. Asaumi, S. Yorimitsu, T. Ikeda, F. Kakiuchi and S. Murai, *J. Am. Chem. Soc.* 2001, **123**, 10935; (b) F. S. Chang, W. Chen, C. Wang, C. C. Tzeng and Y. L. Chen, *Bioorg. Med. Chem.* 2010, **18**, 124.

77. A. Mrozek-Wilczkiewicz, M. Kuczak, K. Malarz, W. Cieslik, E. Spaczynska, R. Musiol, *Eur. J. Med. Chem.,* 2019, **177**, 338.

78. (a) L. Horner, H. Hoffmann, H. G. Wippel and G. Klahre, *Chem. Ber.,* 1959, **92**, 2499; (b) D. J. Peterson, *J. Org. Chem.,* 1968, **33**, 780; (c) M. Julia and J. M. Paris, *Tetrahedron Lett.,* 1973, **14**, 4833; (d) K. C. Nicolaou, M. W. Harter, J. L. Gunzner and A. Nadin, *Liebigs Ann./Recl.* 1997, **1997**, 1283-1301; (e) B. E. Maryanoff and A. B. Reitz, *Chem. Rev.,* 1989, **89**, 863;

79. (a) R. F. Heck and J. P. Nolley, *J. Org. Chem.,* 1972, **37**, 2320; (b) A. V. Cheprakov and I. P. Beletskaya, *Chem. Rev.,* 2000, **100**, 3009; (c) O. M. Ogba, N. C. Warner, D. J. O'Leary and R. H. Grubbs, *Chem. Soc. Rev.,* 2018, **47**, 4510.

80. Y. Yan, K. Xu, Y. Fang and Z. A Wang, *J. Org. Chem.,* 2011, **76**, 6849.

81. (a) J. Das, M. Vellakkaran and D. Banerjee, *Chem. Commun.,* 2019, **55**, 7530-7533; (b) J. Das, M. S. M. Vellakkaran and D. Banerjee, *Org. Lett.,* 2019, **21**, 7514-7518.

82. (a) M. M. Khafagy, A. El-Wahas, F. A. Eid and A. M. El-Agrody, *Farmaco.,* 2002, **57**, 715; (b) P. R. Sebahar and R. M. Williams, *J. Am. Chem. Soc.,* 2002, **122**, 5666; (c) S. Kasibhatla, H. Gourdeau, K. Meerovitch, J. Drewe, S. Reddy, L. Qiu, H.

Zhang, F. Bergeron, D. Bouffard, Q. Yang, and J. Herich, *Mol. Cancer Ther.*, 2004, **3**, 1365-1374.

83. (a) W. Kemnitzer, S. Kasibhatla, S. Jiang, H. Zhang, J. Zhao, S. Jia, L. Xu, C. Crogan-Grundy Denis, N. Barriault and L. Vaillancourt, *Bioorgan. Med. Chem. Lett.*, 2005, **15**, 4745-4751; (b) M. Boominathan, M. Nagaraj, S. Muthusubramanian, and R. V. Krishnakumar, *Tetrahedron.,* 2011, **67**, 6057-6064; (c) P. Slobbe, E. Ruijter and R. Orru, *MedChemCom.,* 2012, **3**, 1189-1218.

84. (a) J. E. Biggs-Houck, A. Younai and J. T. Shaw, *Curr. Opin. Chem. Biol.,* 2010, **14**, 371-382; (b) N. Isambert, M. D. M. S. Duque, J. C. Plaquevent, Y. Genisson, J. Rodriguez, and T. Constantieux, *Chem. Soc. Rev.,* 2011, **40**, 1347-1357; (c) N. Azizi, M. Mariami and M. Edrisi, *Dyes Pigm.,* 2014, **100**, 215-221; (d) B. H. Rotstein, S. Zaretsky, V. Rai and A. K. Yudin, *Chem. Rev.,* 2014, **114**, 8323-8359; (e) V. Estevez, M. Villacampa, and J. C. Menendez, *Chem. Soc. Rev.*, 2014, **43**, 4633-4657;

85. (a) A. M. Shestopalov, Y. M. Emelianova and V. N. Nesterovb, *Russ. Chem. Bull.*, 2002, **51**, 2238-2243; (b) J. Tong-Shou, J. C. Xiao, S. J. Wang and T. S. Li, *Ultrason. Sonochem.,* 2004, **11**, 393-397; (c) M. Kidwai, S. Saxena, R. K. M. Khalilur and S. S. Thukral, *Bioorg. Med. Chem. Lett.,* 2005, **15**, 4292-4295; (d) R. Poddar and M. Kidwai, *Catal. Lett.,* 2008, **124**, 311-317; (e) M. P. Surpur, S. Kshirsagar and S. D. Samant, *Tetrahedron. Lett.,* 2009, **50**, 719-722; (f) Gong, H. L. Wang, J. Luo and Z. L. Liu, *J. Heterocycl. Chem.,* 2009, **46**, 1145-1150; (g) D. S. Raghuwanshi and K. N. Singh, *ARKIVOC,* 2010, **10**, 305-317; (h) S. R. Kolla and Y. R. Lee, *Tetrahedron.,* 2011, **67**, 8271-8275.

86. (a) W. Chen, Y. Cai, X. Fu, X. Liu L. Lin, and X. Feng, *Org. Lett.,* 2011, **13**, 4910-4913; (b) A. H. F. Abd El-Wahab, H. M. Mohamed, A.M. El-Agrody and A. H. Bedair, *Chem. Eur. J.,* 2013, **4**, 467-483; (c) N. Thomas, S. M. Zachariah and P. Ramani, *J. Heterocycl. Chem.,* 2016, **53**, 1778-1782; (d) A. Aminkhani, M. Talati, R. Sharifi, F. Chalabian and F. Katouzian, *J. Heterocycl. Chem.,* 2019, **5**, 1812-1819.

87. S. I. Murahashi, T. Naota, H. Taki, M. Mizuno, H. Takaya, S. Komiya, Y. Mizuho, N. Oyasato and M. Hiraoka, *J. Am. Chem. Soc.,* 1995, **117**, 12436-12451.

88. (a) H. Bienayme, C. Hulme, G. Oddon and P. Schmitt, *Chem. Eur. J.,* 2000, **6**, 3321; (b) A. Hasaninejad, A. Zare and M. Shekouhy, *Green Chem.,* 2011, **13**, 958-964.

89. (a) D. Nauduri and G. B. Reddy, *Chem. Pharm. Bull.,* 1998, **46**, 1254-1260; (b) G. Daidone, B. Maggio, S. Plescia, D. Raffa, C. Musiu, C. Milia, G. Perra and M. E. Marongiu, *Eur. J. Med. Chem.,* 1998, **33**, 375-382; (c) Y. Hiyama, K. M. Suzuki and J. Yamagishi, *J. Med. Chem.,* 2004, **47**, 3693-3696; (d) S. B. Katiyar, K. Srivastava, S. K. Purib and P. M. S. Chauhana, *Bioorg. Med. Chem. Lett.,* 2005, **15**, 4957-4960; (e) F. Q. He, X. H. Liu, B. L. Wang and Z. M. Li, *Hetero. Chem.,* 2008, **19**, 21-27.

90. (a) J. J. Parlow, *J. Heterocycl. Chem.,* 1998, **35**, 1493-1499; (b) G. Varvounis, Y. Fiamegos and G. Pilidis, *Adv. Heterocycl. Chem.,* 2004, **87**, 141-272.

91. V. Polshettiwar and R. S. Varma, *Green Chem.,* 2010, **12**, 743-754.

92. (a) S. Gupta, L. M. Rodrigues, A. P. Esteves, A. M. Oliveira-Campos, M. S. J. Nascimento, N. Nazareth, H. Cidade, M. P. Neves, E. Fernandes, M. Pinto and N. M. Cerqueira, *Eur. J. Med. Chem.,* 2008, **43**, 771-780; (b) H. T. Nguyen, T. Van Le and P. H. Tran, *J. Environ. Chem. Eng.,* 2021, **9**, 105228; (c) H. T. Nguyen, M. N. H. Truong, T. V. Le, N. T. Vo, H. D. Nguyen, and P. H. Tran, *ACS Omega.,* 2022, **7**, 17432-17443.

93. M. M. Sheeba, M. Muthu Tamizh, L. J. Farrugia, A. Endo and R. Karvembu, *Organometallics.,* 2014, **33**, 540-550.

94. M. Kalidasan, R. Nagarajaprakash, S. Forbes, Y. Mozharivskyj and K. M. Rao, *Z. Anorg. Allg. Chem.,* 2015, **641**, 715-723.

95. M. Mary Sheeba, S. Preethi, A. Nijamudheen, M. Muthu Tamizh, A. Datta, L. J. Farrugia and R. Karvembu, *Catal. Sci. Technol.,* 2015, **5,** 4790-4799.

96. I. L. Mawnai, S. Adhikari, W. Kaminsky and M. R. Kollipara, *J. Organomet. Chem.,* 2018, **869**, 26-36.

97. S. Saranya, R. Ramesh and D. Sémeril, *Organometallics.,* 2020, **39**, 194-3201.

98. D. Sindhuja, M. Gopiraman, P. Vasanthakumar, N. Bhuvanesh and R. Karvembu, *J. Organomet. Chem.,* 2021, **949**, 121933.

99. I. Gumus, and M. Aslan, *Polyhedron*, 2021, **210**, 115496.

100. R. N. Prabu and R. Ramesh, *RSC Advances.,* 2012, **2**, 4515-4524.

101. W. G. Jia, H. Zhang, T. Zhang, D. Xie, S. Ling and E. H. Sheng, *Organometallics.,* 2016, **35**, 503-512.

102. J. M. Gichumbi, *J. Mol. Catal. A: Chem.,* 2016, **416**, 29-38.

103. W. G. Jia, H. Zhang, T. Zhang, D. Xie, S. Ling, and E. H. Sheng, *Organometallics.,* 2016, **35**, 503-512.

104. T. S. Manikandan, S. Saranya and R. Ramesh, *Tetrahedron Lett.,* 2016, **57**, 3764-3769.

105. S. Selvamurugan, R. Ramachandran, G. Prakash, P. Viswanathamurthi, J. G. Malecki and A. Endo, *J. Organomet. Chem.,* 2016, **803**, 119-127.

106. N. Mohan and R. Ramesh, *Appl. Organomet. Chem.*, 2017, **31**, e3648.

107. M. Subramaniyan, S. Sundar and R. Rengan, *Appl. Organomet. Chem.,* 2018, **32**, e4582.

108. T. S. Manikandan, R. Ramesh, N. Shivalingegowda and L. N. krishnappagowda, *ChemistrySelect.,* 2018, **3**, 1561-1568.

109. R. Ramachandran, G. Prakash, P. Viswanathamurthi and J. G. Malecki, *Inorganica Chimi. Acta.,* 2018, **477**, 122-129.

110. S. Vijayapritha and P. Viswanathamoorthi, *J. Organomet. Chem.,* 2020, **929**, 121555.

111. K. Murugan, S. Vijayapritha, M. Nirmala, P. Viswanathamurthi and K. Natarajan, *J. Organomet. Chem.,* 2020, **923**, 121411.

112. S. Nikolic, I. Ciric, A. Roller, V. Lukes, V. B. Arion and S. Grguric-Sipka, *New. J. Chem.,* 2017, **41**, 6857-6865.

113. S. Saranya, R. Ramesh, and J.G. Małecki, *Eur. J. Org. Chem.*, 2017, **2017**, 6726-6733.

114. S. Sundar and R. Rengan, *Org. Biomol. Chem.,* 2019, **17**, 1402-1409.

Chapter 2

Arene Diruthenium(II) Mediated Synthesis of Imines from Alcohols and Amines Under Aerobic Condition

Abstract

The utility and selectivity of the newly synthesized dinuclear arene Ru(II) complexes were demonstrated towards the synthesis of imines from coupling of alcohols and amines in aerobic condition. Analytical and various spectral methods have been used to establish the unprecedented formation of the new thiolato bridged dinuclear ruthenium complexes. The molecular structure of the titled complexes was evidenced with aid of X-ray crystallographic technique. A wide range of imines were obtained in good to excellent yields upto 98% and water as the by-product through dehydrogenative coupling of alcohols with amines. The catalytic reaction operated a concise atom economical without any oxidant with 1 mol% of the catalyst load. Further, the role of base, solvent and catalyst loading of the coupling reaction has been investigated. A plausible mechanism has been described and was found to proceed *via* the formation of an aldehyde intermediate. Short synthesis of antibacterial drug N-(salicylidene)-2-hydroxyaniline illustrated the utility of the present protocol.

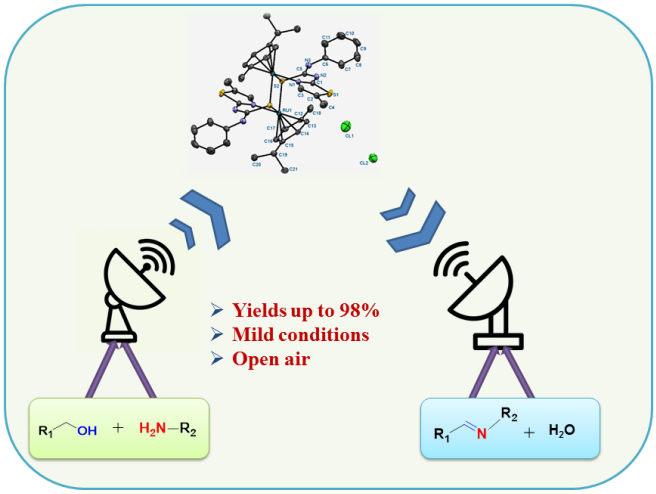

Pub.: *Appl. Organomet. Chem.*, 2021, **35**, e6122

2.1. INTRODUCTION

Imines are profound important class of nitrogen compounds due to their high reactivity.[1] They are ubiquitous intermediates in many organic reactions such as cyclization, cycloaddition, multicomponent reactions and condensation.[2] They are adaptable nitrogen sources which find applications in pharmaceuticals, industrial and agriculture.[3] Further, many nitrogen containing bioactive compounds such as amines, amides and pyrrolines can be constructed from imine functional group (Figure 1).[4] Hence, synthesis and applications of imines are essentially ever-appealing topics in synthetic organic chemistry.

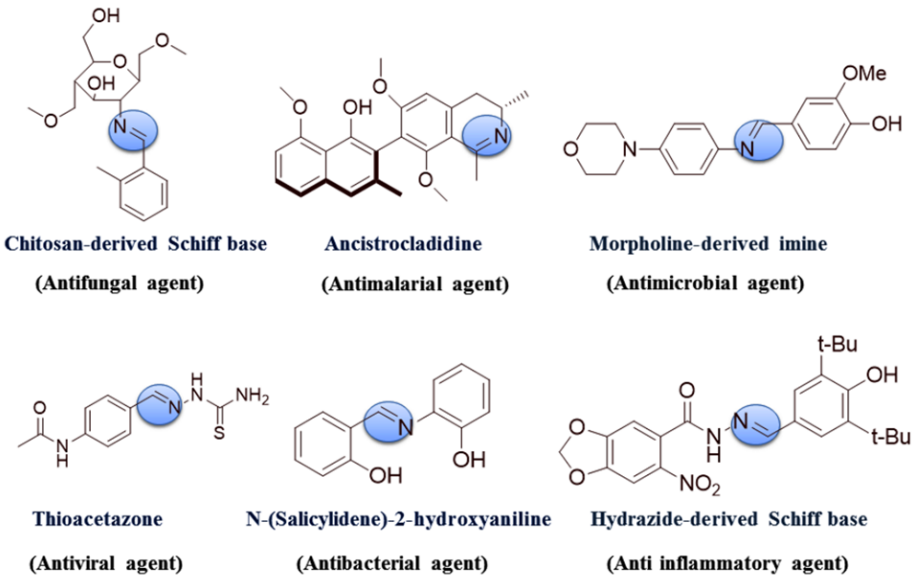

Figure 1. Examples for bioactive imine analogues

The conventional approach for imine synthesis involves the direct coupling of amines with aldehydes or ketones with lewis acid or dehydrating agents and higher reaction time are required in many situations.[5] Imines have been also synthesized in different circumstances includes Schmidt reaction, Aza-Wittig reaction[6] and oxidation of secondary amines using oxidizing agents (Scheme 1).[7]

Though a number of methods are known for imine synthesis in the literature, largely suffer from drawbacks like use of toxic reagents, poor atom economy, harsh synthetic process, and low level of selectivity.[8]

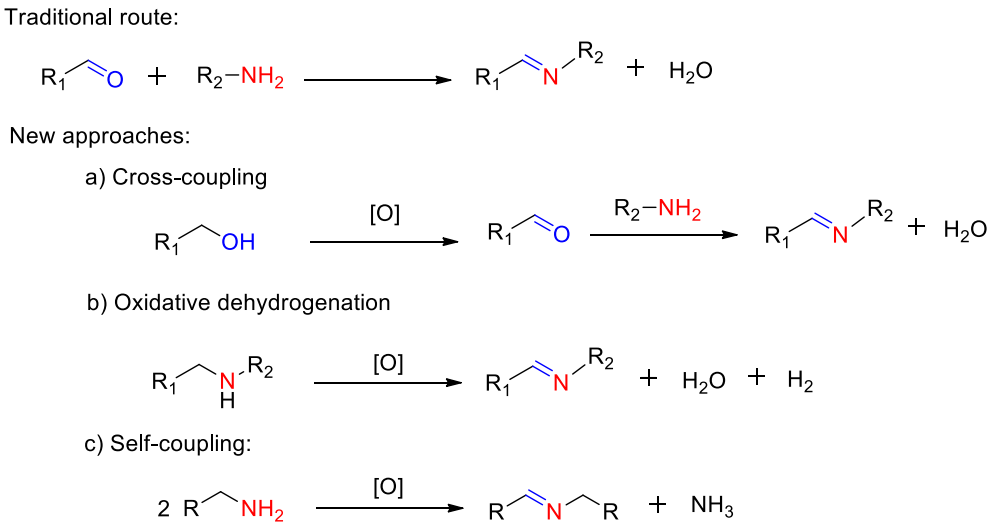

Scheme 1. Imine formation *via* traditional method and new approaches by aerobic oxidation of alcohols and amines (a, b, and c)

To overcome the aforementioned limitations, the metal-catalyzed direct synthesis of imines from alcohols with amines through dehydrogenation coupling mechanism is an alternative approach. The strategy consists of two steps: (i) aerobic oxidation of alcohol in the presence of a transition metal catalyst and (ii) generation of imine. More advantageously, the dehydrogenative methodology is a greener protocol for the coupling of alcohol and amine to desired imine with the water as the by-product.

Milstein and co-workers reported Ru-PNP type pincer complex promoted synthesis of imines from alcohols and amines under nitrogen atmosphere.[9] This significant breakthrough methodology has much attention to the researchers towards imine synthesis. Several wide transition metal complexes such as Ru, Os, Pd, Pt and Au have been reported as catalysts for imine synthesis under high temperature, inert atmosphere, special condition and long reaction time.[10-14] Shiraishi and co-workers employed Pt/TiO_2 heterogeneous

catalyst for the imine synthesis with UV-radiation and used nitrogen atmosphere protection.[13] Kobayashi and co-workers have reported synthesis of imines by gold/palladium alloy nanoparticles (1.5 mol%) in the presence of oxidant.[15] Donthiri *et al.* have described synthesis of imines by using NaOH (10 mol%) as a catalyst at high temperature.[16] Haiwen research group explored imine formation by employing CuI/bipyridine/TEMPO under neat conditions.[17] Later, the Zhang group reported mild one-pot synthesis of imines using $Fe(NO_3)_3$/TEMPO system as a catalyst in presence of additives.[18] Maggi *et al.* demonstrated the catalytic performance of Ru-NHC complex (5 mol%) in imine synthesis using DABCO ligand in the presence of molecular sieves for 24 h.[10b] The catalytic activity of Co(II)-NNN pincer complex has been explored for imines synthesis and the reaction was carried out with *n*-octane as a solvent at high temperature[19] (Scheme 2).

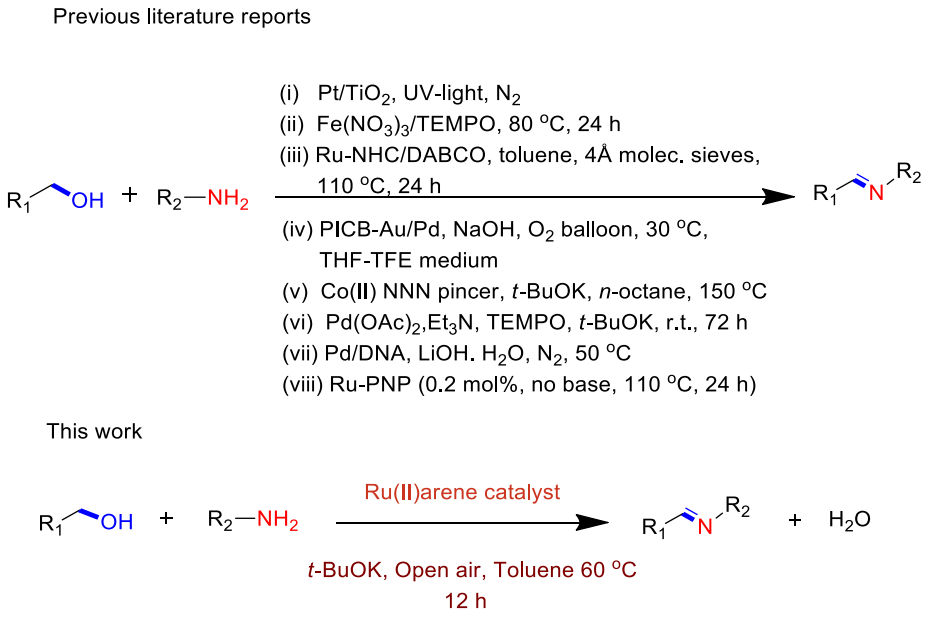

Scheme 2. Synthetic strategies of imine reaction

Overall, a large number of metal complexes with different ligand systems have been explored as catalysts for this reaction. In particular, metal-based catalysts for the synthesis of imines with phosphine labile ligands have been well explored. However, the catalytic

condition showed some draw backs such as higher temperature, higher catalyst load and inert atmosphere. To overcome the above issues, we are interested to execute the imine synthesis protocol using metal complexes with phosphine free ligands. Generally, metal complex containing phosphorus-free ligands has salient features like ease of synthesis, air stability, easy separation and efficient catalyst recovery.

In the present art of research, we have described the synthesis and characterization of new binuclear Ru(II) complexes of thiourea ligand and used as a catalyst for imine synthesis under aerobic catalytic condition. Catalysts featuring two closely associated metal active sites is one of the emerging areas in homogeneous catalysis. This bimetallic catalytic system complements the traditional focus on parameters in order to optimize catalytic behavior in a better way. Change of the steric and electronic properties of the ligands can fine-tune the performance of the bimetallic system. Such catalysts introduce new optimization parameters such as catalyst nuclearity and synergistic cooperation between the two metal active sites and the bridging ligands.[20] Hence, controlling selectivity and activity of the catalytic transformations will be offered by the suitable design of bimetallic catalysts. Exquisite levels of activities of these catalysts could be achieved by careful design of two metal active sites (Figure 2).

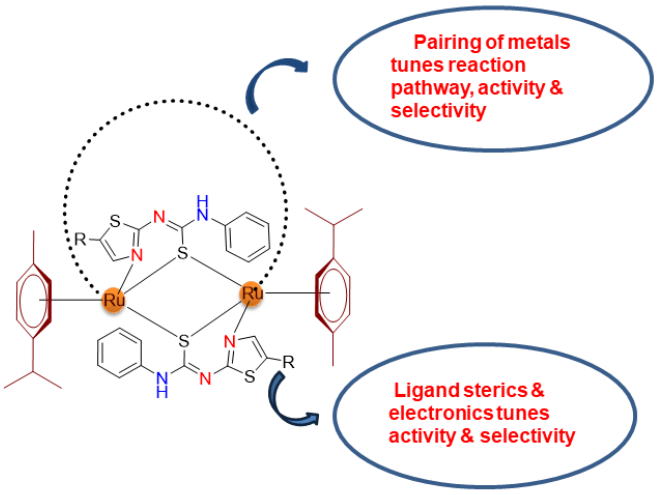

Figure 2. Structure-function relationship available in bimetallic catalysis

2.2. EXPERIMENTAL SECTION

2.2.1. Reagents and materials

All the reagents used were chemically pure and analytical grade. Phenyl isothiocyanate and 2-aminothiazole derivatives were purchased from Sigma Aldrich chemicals. The solvents were freshly distilled before use by following the standard procedures.[21]

2.2.2. Physical measurements and instrumentation

The elemental analysis of carbon, hydrogen, nitrogen and sulphur were performed at Sophisticated Test and Instrumentation Centre (STIC), Cochin University of Science and Technology, Kochi. Infrared spectra of complexes were recorded in KBr pellets with a Perkin Elmer 597 spectrophotometer in the range of 4000-400 cm^{-1}. The ^{1}H and ^{13}C NMR spectra were recorded in $CDCl_3$ with Bruker 400 MHz instrument using TMS as internal reference.

2.2.3. Preparation of 1-(5-methylthiazol-2-yl)-3-phenylthiourea ligands

1-(5-methylthiazol-2-yl)-3-phenylthiourea ligands (HL) ligands were prepared from the literature procedure.[22] To a stirred DMF solution (10 mL) of phenyl isothiocyanate (1 mmol), 2- and 2-amino thiazole derivatives (1 mmol) were added and the reaction mixture was stirred for 24 h. At the end of the reaction the solution was concentrated to 5 mL and poured into cold water 10 mL. The white solid was obtained, filtered and dried in vacuum (Scheme 3). Yield: 80-90%.

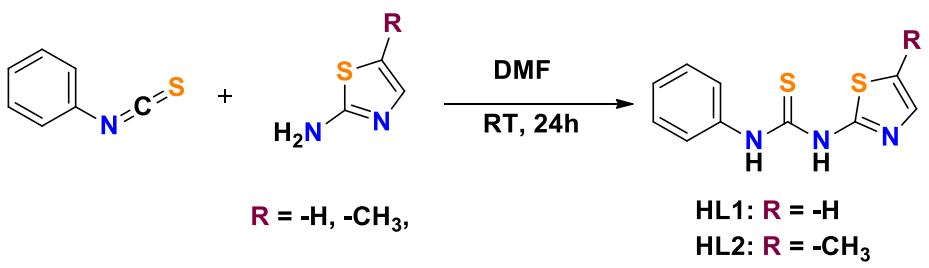

Scheme 3. Preparation of thiourea ligands

2.2.4. Synthesis of new arene diruthenium(II) thiourea complexes

The synthesis of cationic arene diruthenium(II) thiourea complexes can be accomplished in good yield from complexation of ruthenium starting precursor [(η^6-*p*-cymene)$RuCl_2$]$_2$ (1.0 mmol) with thiourea ligand in 1:2 molar respectively in benzene under open air condition. The complexes were yellow in color and air-stable. They were easily soluble in solvents like CH_2Cl_2, $CHCl_3$, CH_3CN, DMSO, THF etc. The resulting complexes were crystallized from the mixture of dichloromethane and methanol (1:1) (Scheme 4) and X-ray quality crystals were obtained only for complex **4**.

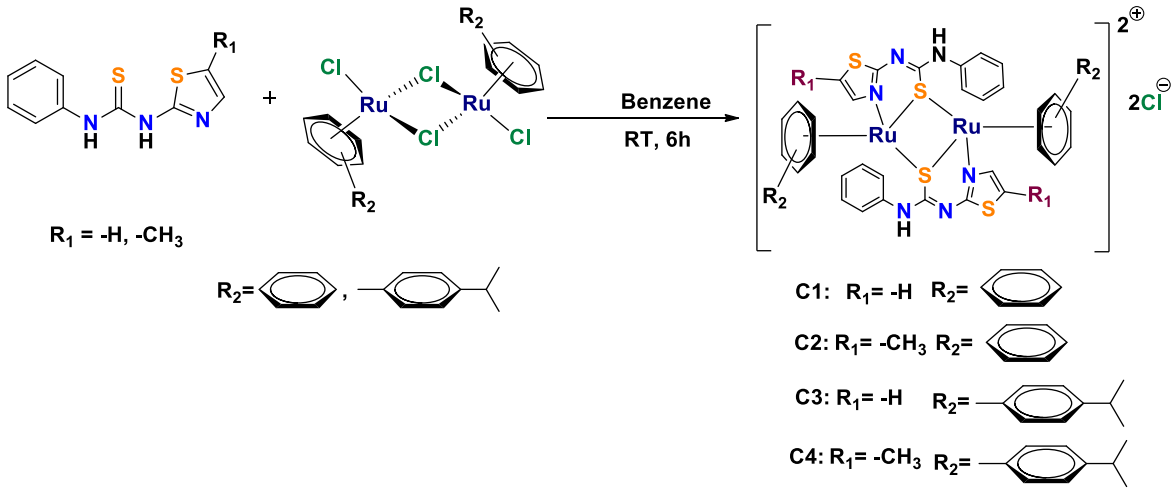

Scheme 4. Synthesis new arene Ru(II) thiourea complexes

Spectral characterization of arene Ru(II) thiourea complexes (1-4)

[Ru(η^6-benzene)(HL1)]$_2Cl_2$ (1): Yellow solid. Yield: 90%: Anal. Calcd. For $C_{32}H_{32}Cl_2N_6Ru_2S_4$: C, 42.80; H, 3.14; N, 9.36. Found: C, 42.62; H, 3.10; N, 9.26. ^{1}H NMR (400 MHz, $CDCl_3$): δ (ppm) = 11.42 (b, 2H, aromatic N-H), 7.59-7.36 (m, 7H, ArH), 7.26-7.05 (m, 7H, ArH), 5.74-5.67 (m, 12H). $^{13}C\{^1H\}$ NMR (100MHz, $CDCl_3$): δ (ppm) = 174.64, 170.18, 159.04, 143.91, 140.72, 139.79, 137.85, 129.30, 128.52, 128.29, 124.32, 121.15, 111.81, 111.20, 87.60. FT-IR (cm^{-1}): 2923 (N-H), 1620 (C=N), 1592 (C=C), 1267 (N-C=S), 1159 & 876 (C=S). UV-vis ($CHCl_3$): λ_{max} (nm) 254, 320, 456.

[Ru(η^6-benzene)(HL2)]$_2$Cl$_2$ (2): Yellow solid. Yield: 89%: Anal. Calcd. For $C_{34}H_{32}Cl_2N_6Ru_2S_4$: C, 44.10; H, 3.48; N, 9.08. Found: C, 43.90; H, 3.45; N, 8.91. ^{1}H NMR (400 MHz, $CDCl_3$): δ (ppm) = 11.24 (b, aromatic N-H), 7.83-7.73 (m, 4H, ArH), 7.59-7.52 (m, 6H, ArH), 7.43-7.33 (m, 2H, ArH), 5.88-5.52 (m, 12H, CH benzene), 2.42 (s, 6H, CH_3). ^{13}C{^{1}H} NMR (100MHz, $CDCl_3$): δ (ppm) = 175.43, 170.98, 159.83, 144.71, 141.52, 140.58, 138.64, 130.10, 129.31, 129.08, 125.12, 121.94, 112.61, 112.0, 88.40, 19.20. FT-IR (cm^{-1}): 2922 (N-H), 1640 (C=N), 1597 (C=C), 1265 (N-C=S), 1164 & 900 (C=S). UV-vis ($CHCl_3$): λ_{max} (nm) 269, 303, 452.

[Ru(η^6-*p*-cymene)(HL1)]$_2$Cl$_2$ (3): Yellow solid. Yield: 85%: Anal. Calcd. For $C_{40}H_{44}Cl_2N_6Ru_2S_4$: C, 47.56; H, 4.39; N, 8.32. Found: C, 47.37; H, 4.35; N, 8.25. ^{1}H NMR (400 MHz, $CDCl_3$): δ (ppm) = 11.38 (b, 2H, aromatic N-H), 7.59-7.68 (m, 7H, ArH), 7.44-7.27 (m, 7H, ArH), 5.55 (s, 4H, arene), 5.44 (m, 4H, arene), 2.82 (sept, 2H, $CH(CH_3)_2$), 2.06 (s, 6H, CH_3), 1.24 (s, 12H, $CH(CH_3)_2$). ^{13}C{^{1}H} NMR (100MHz, $CDCl_3$): δ (ppm) = 175.04, 143.85, 136.54, 129.52, 129.20, 127.64, 125.00, 114.76, 106.68, 100.04, 86.28, 84.87, 84.80, 84.47, 30.79, 22.50, 22.23, 18.55. FT-IR (cm^{-1}): 2922 (N-H), 1640 (C=N), 1591 (C=C), 1274 (N-C=S), 1159 & 874 (C=S). UV-vis ($CHCl_3$): λ_{max} (nm) 276, 331, 464.

[Ru(η^6-*p*-cymene)(HL2)]$_2$Cl$_2$ (4): Yellow solid. Yield: 92%: Anal. Calcd. For $C_{42}H_{48}Cl_2N_6Ru_2S_4$: C, 48.59; H, 4.66; N, 8.09. Found: C, 48.62; H, 4.60; N, 8.01. ^{1}H NMR (400 MHz, $CDCl_3$): δ (ppm) = 11.55 (s, 2H, N-H), 7.60-7.58 (m, 4H, ArH), 7.47-7.43 (m, 4H, ArH), 7.38-7.36 (m, 4H, ArH), 5.57-5.43 (m, 2H, CH), 5.38-5.30 (m, 6H, CH), 2.80 (sept, 2H, $CH(CH_3)_2$), 2.43 (s, 6H, CH_3), 2.08 (s, 6H, CH_3), 1.26-1.21 (m, 12H, $CH(CH_3)_{2(p\text{-cymene})}$). ^{13}C{^{1}H} NMR (100MHz, $CDCl_3$): δ (ppm) = 175.35, 158.22, 140.52, 136.32, 129.19, 128.95, 127.89, 125.28, 106.66, 100.06, 86.29, 84.89, 84.73, 84.24, 30.78, 22.52, 22.17, 18.54, 12.53. FT-IR (cm^{-1}): 2925 (N-H), 1642 (C=N), 1594 (C=C), 1261 (N-C=S), 1149 & 910 (C=S). UV-vis ($CHCl_3$): λ_{max} (nm) 280, 340, 463.

2.2.5. X-ray crystallographic data collection

Single crystals of complex were grown by slow evaporation of a dichloromethane – methanol solution at room temperature. The data collection was carried out using a Bruker AXS Kappa APEX II single crystal X-ray diffractometer using monochromated Mo–Kα radiation (λ = 0.71073 Å). Data was collected at 296 K. The absorption corrections were performed by the multi-scan method using SADABS software.[23] Corrections were made for Lorentz and polarization effects. The structures were solved by direct methods (SHELXS 97) and refined by full-matrix least squares on F^2 using SHELXL 97.[24] All non-hydrogen atoms were refined anisotropically and the hydrogen atoms in these structures were located from the difference Fourier map and constrained to the ideal positions in the refinement procedure. The unit cell parameters were determined by the method of difference vectors using reflections scanned from three different zones of the reciprocal lattice. The intensity data were measured using ω and φ scan with a frame width of 0.5° Frame integration and data reduction were performed using the Bruker SAINT-Plus (Version 7.06a) software.[25] Figure 11 was drawn with ORTEP and the structural data have been deposited at the Cambridge Crystallographic Data Centre: CCDC 1879184.

2.2.6. General Protocol for synthesis of imines

Alcohols (1 mmol), amine (1 mmol), *t*-BuOK (0.5 mmol), catalyst (1 mol%), was heated at 60 ^{o}C for 12 h under open air atmosphere in 5 mL toluene and the reaction was monitored by TLC until completion. Then, the reaction mixture was cooled and diluted with ethyl acetate (10 mL). For calculation of isolated yield, the layers were formed upon the addition of water (5 mL) and organic layer was separated. The organic phase was dried over Na_2SO_4 and concentrated in vacuum. The resulting residue was purified by column chromatography using EtOAc: hexane to afford imine products.

2.3. Results and Discussion

Thiourea ligands were easily prepared from the reaction of phenyl isothiocyanate and 2-amino thiazole derivatives in DMF. Complexation was accomplished by reacting these ligands with the Ru(II) precursor [Ru(η^6-arene)Cl_2] in a 1:1 molar ratio in the presence of benzene solvent. The resulted complexes are yellow in color. All the complexes are stable in air and readily dissolved in most organic solvents. The newly formed arene diruthenium(II) complexes were authenticated with the help of analytical and different spectral techniques.

2.3.1. FT-IR Spectra

In the IR spectra, thiazole N-H and phenyl group N-H in the ligands showed bands in the regions 3362-3161 cm^{-1} and 3162-3006 cm^{-1} respectively. Also, free ligands displayed the thiocarbonyl ($\nu_{C=S}$) stretching frequencies at 1254 cm^{-1}. On complexation, thiazole attached N-H stretching vibration was not observed in the complexes indicating that the ligands underwent enolization and decrease in $\nu_{C=S}$ (1150-1120 cm^{-1}). The shift in these bands revealed that coordination of ligands to the metal *via* thiazole nitrogen and thiocarbonyl sulphur.

2.3.2. NMR spectra

In the ^{1}H NMR spectra, the free ligands showed signals at 12.45-12.30 and 10.45-10.23 ppm due to N-H protons. Upon complexation, the thiazole connected –NH protons were disappeared in the complexes, further supporting enolization and coordination through thiocarbonyl sulphur to the Ru(II) ion. All aromatic protons of the complexes were appeared as multiplet in the region of 7.05-7.83 ppm. The arene protons of the complexes were observed at 5.37-5.80 ppm. The methyl protons of isopropyl group in *p*-cymene moiety exhibited as singlet in the region 1.21-1.26 ppm. A septet was appeared in the range of 2.82-2.81 ppm due to methine proton of the isopropyl group. Further, signals due to the methyl protons of the *p*-cymene were observed at 2.44 ppm as singlet.

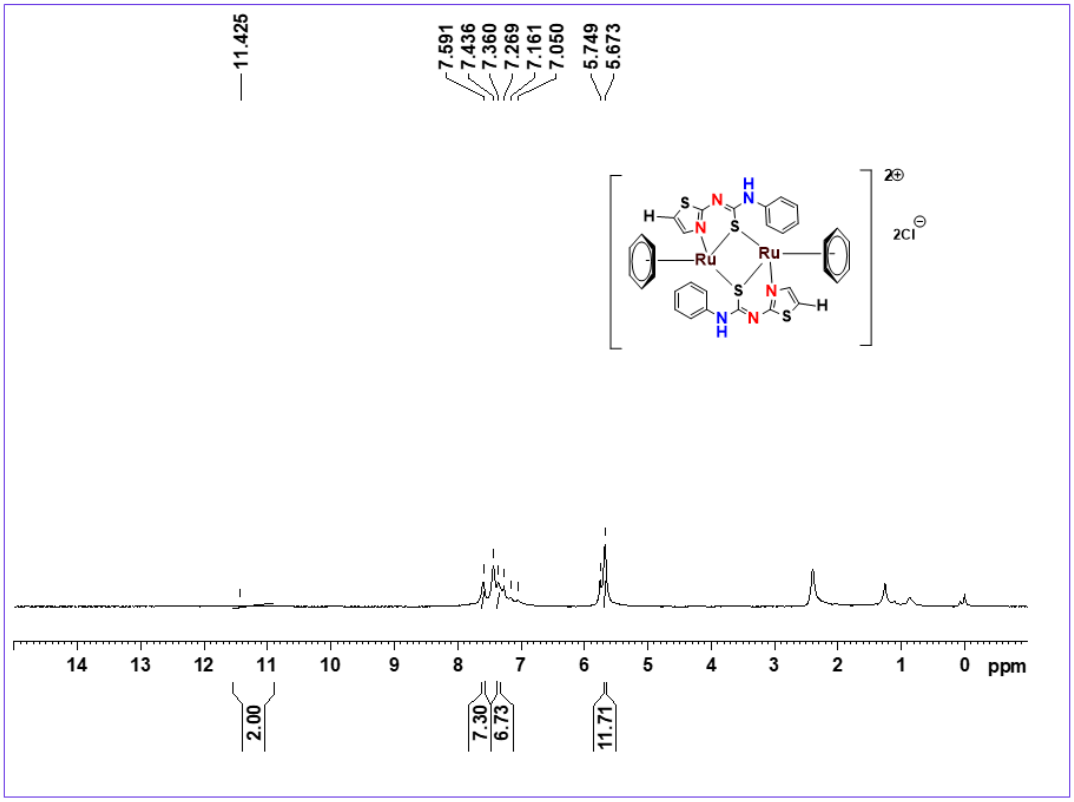

Figure 3. ^{1}H NMR spectrum of complex **1** in $CDCl_3$ (400 MHz, 293 K).

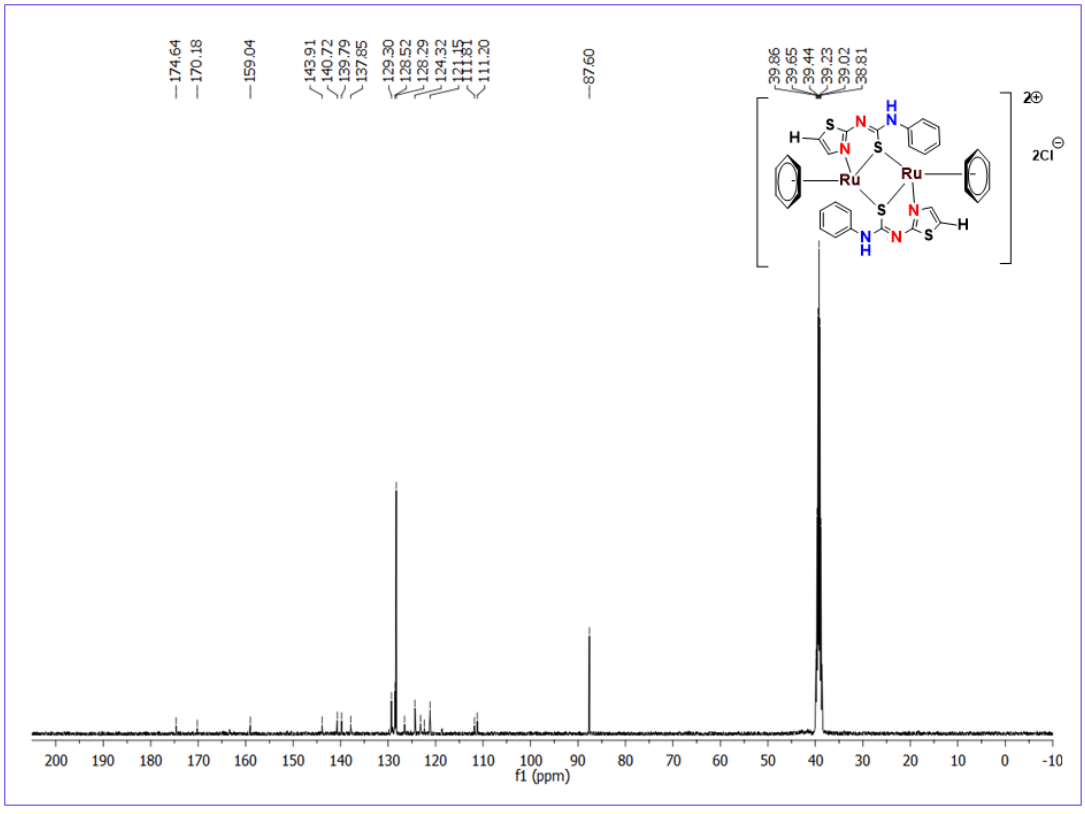

Figure 4. ^{13}C NMR spectrum of complex **1** in $CDCl_3$ (100 MHz, 293 K).

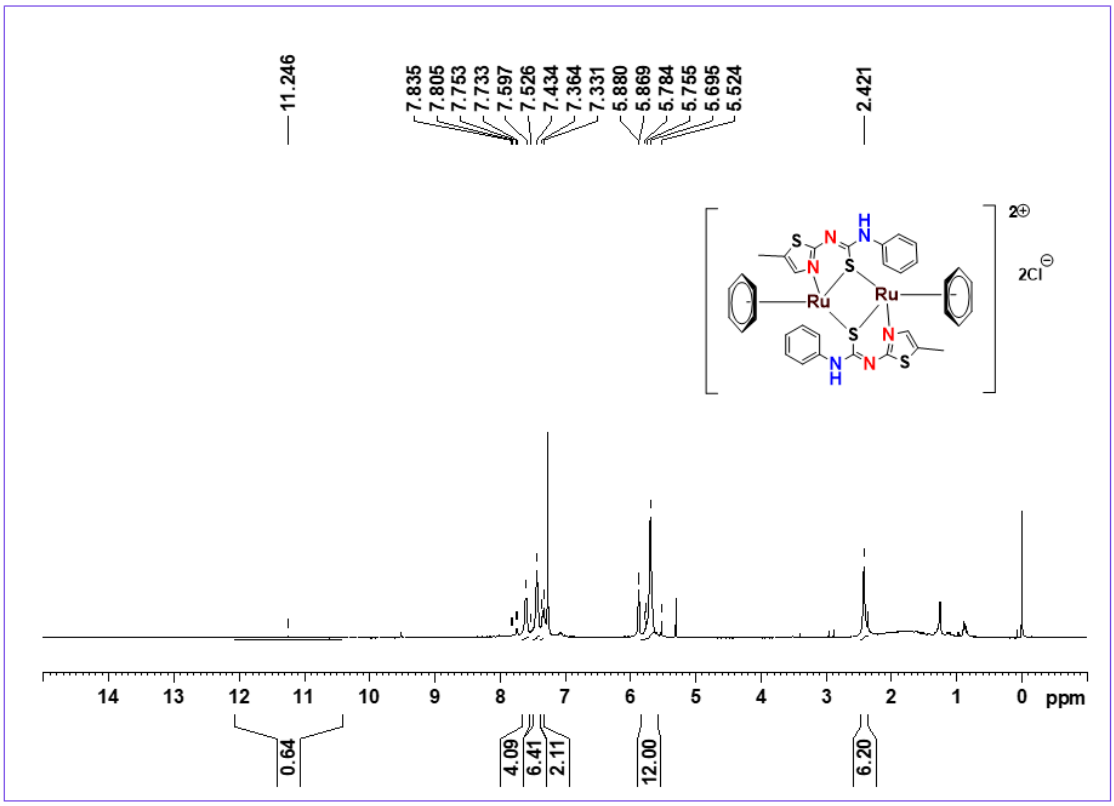

Figure 5. ^{1}H NMR spectrum of complex **2** in $CDCl_3$ (400 MHz, 293 K).

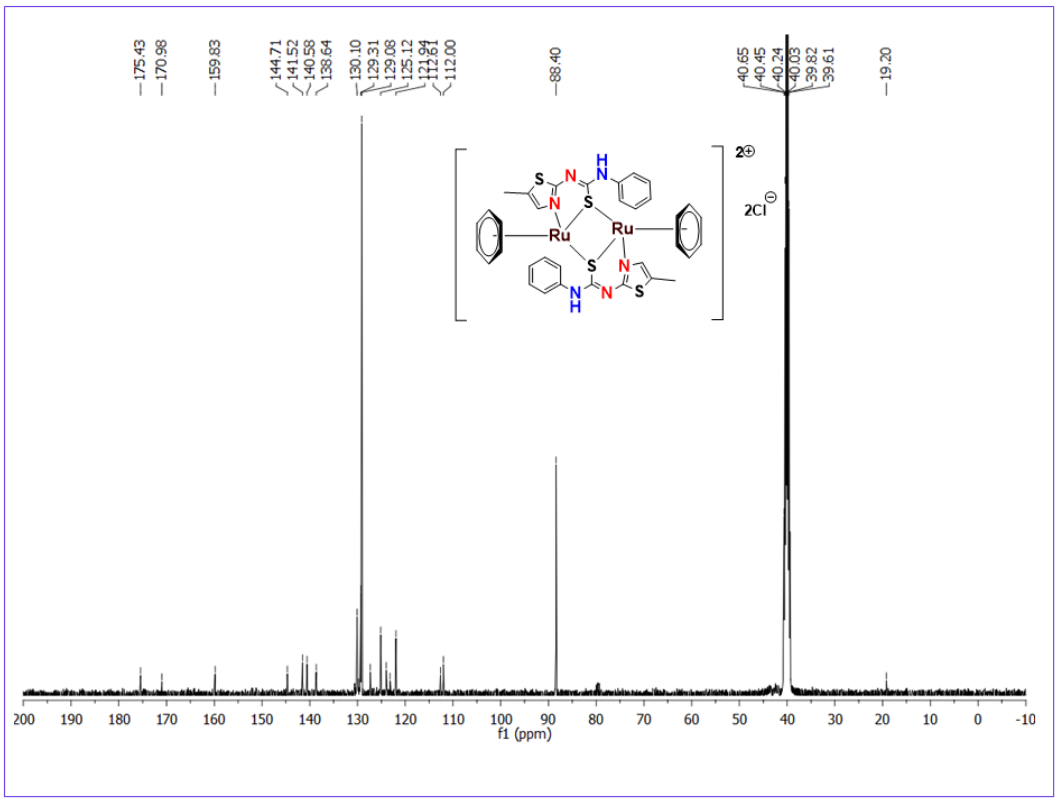

Figure 6. ^{13}C NMR spectrum of complex **2** in $CDCl_3$(100 MHz, 293 K).

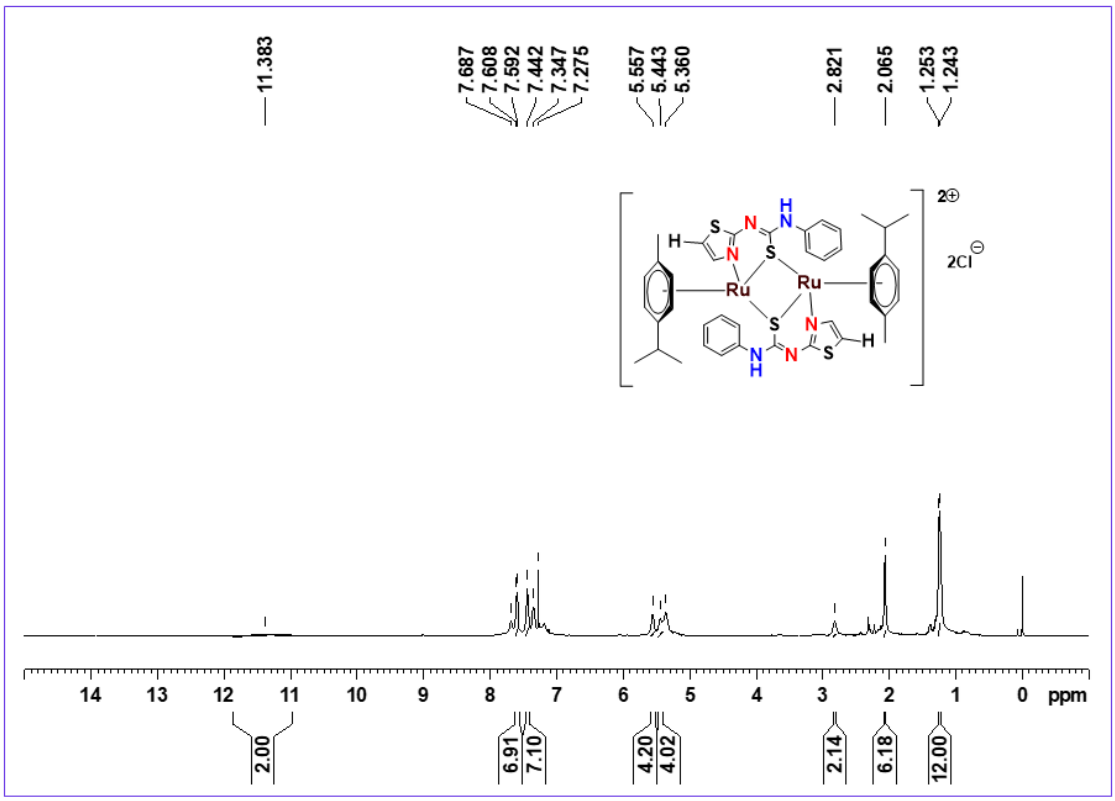

Figure 7. ^{1}H NMR spectrum of complex **3** in $CDCl_3$ (100 MHz, 293 K).

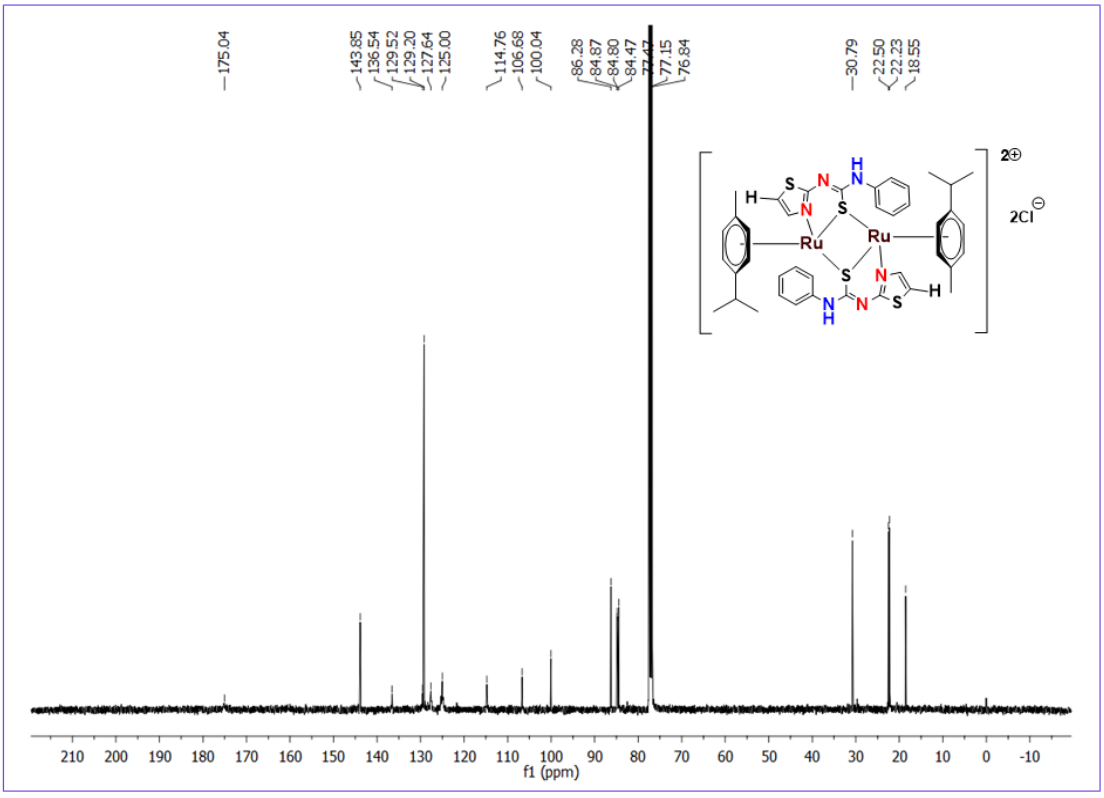

Figure 8. ^{13}C NMR spectrum of complex **3** in $CDCl_3$ (100 MHz, 293 K).

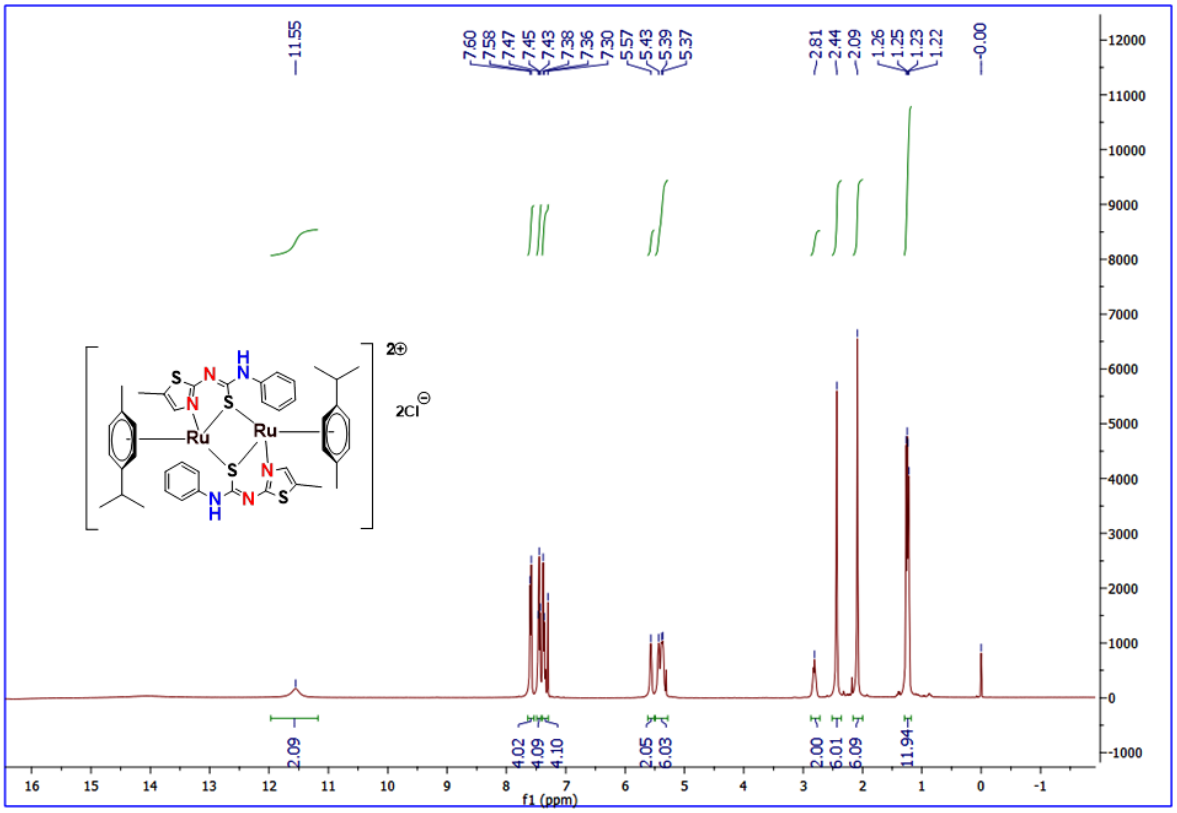

Figure 9. ^{1}H NMR spectrum of complex **4** in $CDCl_3$ (100 MHz, 293 K).

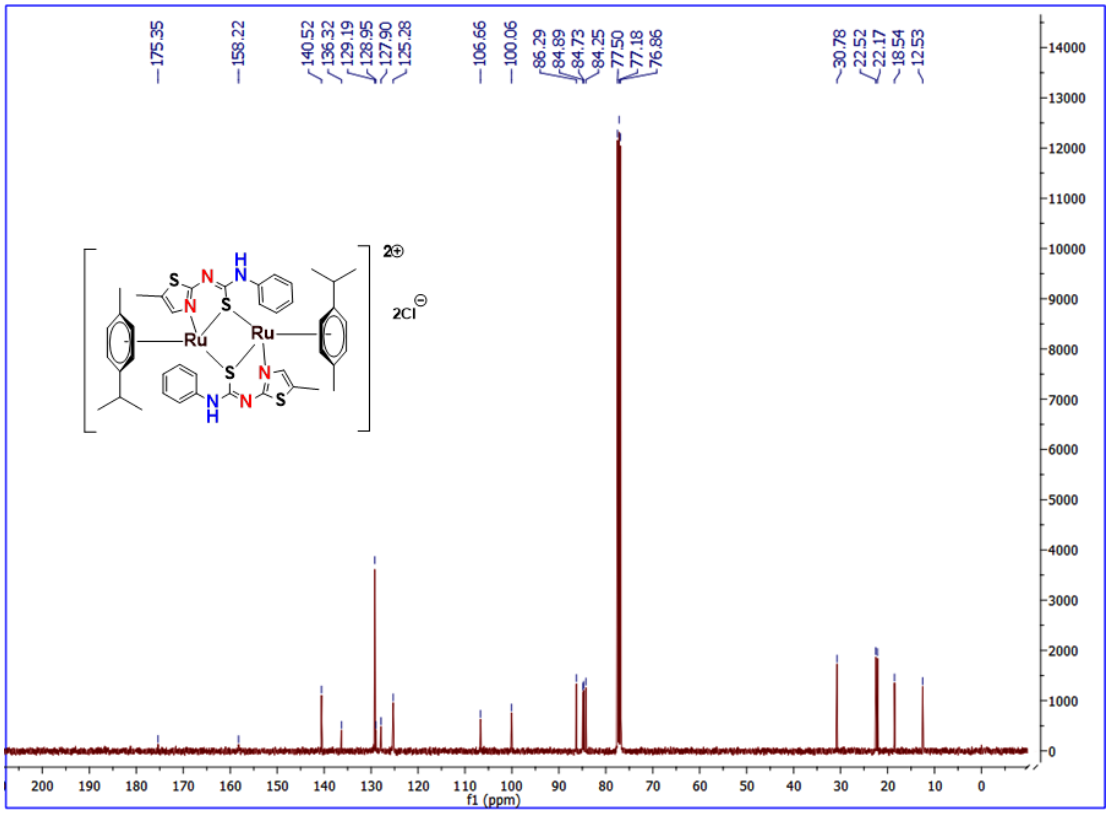

Figure 10. ^{13}C NMR spectrum of complex **4** in $CDCl_3$ (100 MHz, 293 K).

2.3.4. X-ray molecular structure determination

The solid state structure of the complex **4** [Ru(η^6-*p*-cymene)(HL2)]$_2$Cl$_2$ has been studied by X-ray crystallographic technique. Crystals of suitable size were obtained from mixed solvents of dichloromethane and methanol (1:1). The ORTEP view of the complex is shown in Figure 11. The crystal is belong to the monoclinic space group "*C 2/c*" with *Z* = 4. The thiourea chelates to Ru(II) ion through the two thiolato sulphur ions and thiazole nitrogen and the remaining position is occupied by arene moiety forming a pseudo octahedral geometry. A four-membered Ru-S-Ru-S ring system is formed due to the bridging position of sulphur atoms between the two Ru ions. The unprecedented formation of bridging system is due to pushing of electron density by the thiazole group through the amino nitrogen atom. This enabled the sulphur atom to make the new Ru-S bond, resulting in dimer formation. The observed dimeric structure is similar to the related compound contain a [Rh-N-C-S]$_2$ sulfur bridged dinuclear unit.[26] The Ru_2S_2 core is essentially planar which indicated the cymene ligands adopted *cis* arrangement in the complex, the similar to the arrangement observed in [(η^6-$C_6H_3Me_3$)Ru{$SCMe_2CH$-(CO_2H)NH_2}$_2$]$_2$.[27] All of the Ru-S distances of complex are basically equal length [range 2.3765(15)-2.4204(16)Å], indicating symmetrical sulphur atoms. It has been observed that the Ru-S-Ru bond angle [99.25 (6)^o] is slightly larger than the corresponding chloride bridging Ru-Cl-Ru [98.22^o] bond angle.[28] Hence, the single crystal X-ray diffraction studies confirmed the structure proposed with the aid of other spectroscopic techniques.

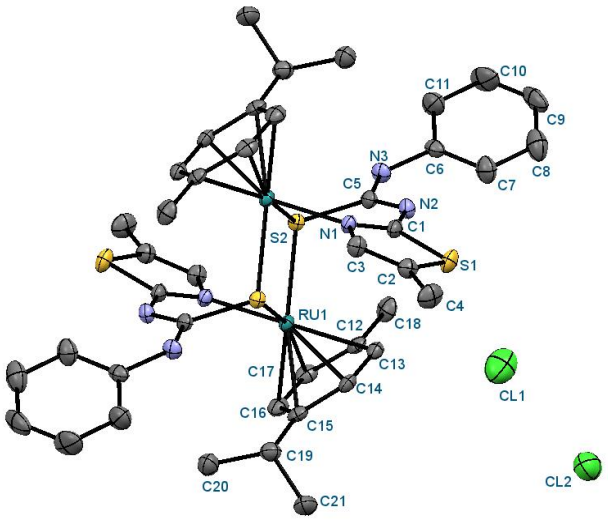

Figure 11. ORTEP diagram of the complex **4** with 30% probability. All the hydrogen atoms were omitted for clarity.

Table 1. Crystal data and structure refinement for complex **4** [Ru(η^6-*p*-cymene)(HL)]$_2$Cl$_2$

CCDC	1879184
Empirical formula	$C_{42}H_{48}Cl_4N_6Ru_2S_4$
Formula weight	1109.04
Temperature/K	295(2)
Crystal system	Monoclinic
Space group	*'C 2/c'*
a/Å, *b*/Å, *c*/Å	15.3174(10), 14.6942(9), 20.4178(14)
α/°, β/°, γ/°	90, 103.282(7), 90
Volume/Å^3	4472.7(5)
Z	4
ρ_{calc}mg/mm^3	1.647
m/mm^{-1}	1.140
F(000)	2248
Crystal size/mm^3	0.12 × 0.07 × 0.05
Theta range for data collection	3.364 to 29.345°
Index ranges	$-15 \leq h \leq 21$, $-17 \leq k \leq 19$, $-27 \leq l \leq 27$
Reflections collected	10472
Independent reflections	5282[R(int) = 0.0357]
Data/restraints/parameters	5282/0/270
Goodness-of-fit on F^2	1.099
Final *R* indexes [I>2σ (I)]	R_1 = 0.0710, wR_2 = 0.1440
Final *R* indexes [all data]	R_1 = 0.0934, wR_2 = 0.1527
Largest diff. peak/hole / e Å^{-3}	0.719/-0.986

Table 2. Selected bond lengths (Å) and angles (°) for the complex **4** [Ru(η^6-*p*-cymene)(HL)]$_2$Cl$_2$

Bond lengths (Å)	
Ru1-S2	2.3765 (15)
Ru2-S2	2.4204 (16)
Ru1-N1	2.120 (5)
Ru1-C12	2.261 (6)
Ru1-C13	2.189 (6)
Ru1-C14	2.189 (6)
Ru1-C15	2.230 (6)
Ru1-C16	2.178 (7)
Ru1-C17	2.225 (6)
S1-C1	1.722 (6)
S1-C2	1.727 (7)
S2-C5	1.800 (6)
N1-C1	1.321 (8)
N1-C3	1.393 (8)
N2-C1	1.346 (9)
N2-C5	1.306 (8)
N3-C5	1.329 (8)
N3-C6	1.433 (9)

Bond angles (°)	
Ru1-S2-Ru2	99.25 (6)
S2-Ru1-S1	80.75 (6)
N1-Ru1-S2	86.99 (14)
N1-Ru1-C12	122.3 (2)
N1-Ru1-C13	159.7 (2)
N1-Ru1-C14	153.9 (2)
N1-Ru1-C15	116.6 (2)
N1-Ru1-C16	93.3 (2)
N1-Ru1-C17	95.8 (2)
N1-C1-S1	112.2 (5)
N1-C1-N2	131.0 (6)
N2-C1-S1	116.5 (5)
N2-C5-S2	125.6 (5)
N2-C5-N3	122.5 (6)
N3-C5-S2	111.9 (5)
C5-S2-Ru1	103.4 (2)
C12-Ru1-S2	97.35 (17)
C12-C1-Ru1	74.0 (3)

2.3.5. Catalytic application to synthesis of imines

The remarkable applications of ruthenium catalysts to an extensive variety of coupling reactions motivated us to tune the present arene dinuclear Ru(II) complexes as catalysts in the direct synthesis of imines *via* dehydrogenative coupling substituted benzyl alcohols and amine derivatives under aerobic condition.

2.3.5.1. Optimization of bases, solvents and temperature

To initiate the test reaction between the equimolar amounts of 4-methylbenzyl alcohol and aniline with complex (1 mol%) as a catalyst with various solvents and KOH as a base to optimize the reaction condition (Table 3). When toluene was used as solvent, the corresponding imine product **3a** was obtained 83% yield in 12 h (Table 3, entry 1). Switching the solvent to xylene and benzene is also effective, furnishing imines up to 80% and 72% yield respectively (Table 3, entries 2 and 3). Moderate yields of imines were obtained when the reaction was performed in various polar solvents like dioxane, THF, acetonitrile, DMF and methanol (Table 3, entries 4-8). These results indicated that non-polar solvents outperformed polar solvents in the test reaction. No further the reaction was proceeded in the absence of base or catalyst (Table 3, entries 9-11). Furthermore, good product yields are observed in the presence of NaOH and NaOMe (Table 3, entries 12 and 13). In addition, upto 80% yield of imines were noted when K_2CO_3 and Cs_2CO_3 are present (Table 3, entries 14 and 15) in the catalytic synthesis. Further, it has been observed that *t*-BuOK outperformed other bases, which afforded **3a** in 90% yield of imine (Table 3, entries 16 and 17). Notably, the cationic dinuclear ruthenium complex catalyzed effectively the coupling of alcohol and amine, and yielded 98% of selective imine under the optimized condition of toluene/ *t*-BuOK at 60^{o}C (Table 3, entry 18).

Table 3. Screening of solvents, bases, and temperatures[a]

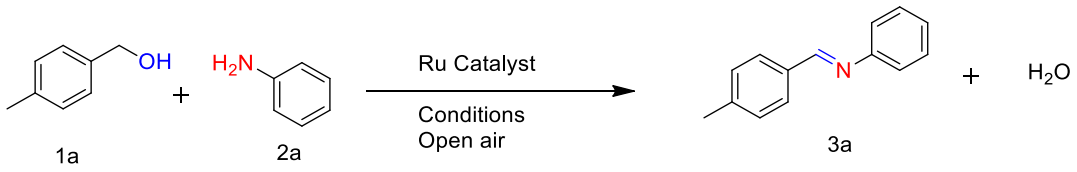

Entry	Solvent	Base	Temp. (°C)	Yield(%)[b]
1	Toluene	KOH	110	83
2	Xylene	KOH	140	80
3	Benzene	KOH	80	72
4	1,4 Dioxane	KOH	100	65
5	THF	KOH	66	78
6	Acetonitrile	KOH	82	60
7	DMF	KOH	150	52
8	Methanol	KOH	65	70
9[c]	Toluene	--	r.t	NR
10[c]	Toluene	--	80	NR
11[d]	Toluene	*t*-BuOK	110	10
12	Toluene	NaOH	110	82
13	Toluene	NaOMe	110	85
14	Toluene	K_2CO_3	110	79
15	Toluene	CS_2CO_3	110	80
16	Toluene	*t*-BuOK	110	88
17	Toluene	*t*-BuOK	80	90
18	**Toluene**	***t*-BuOK**	**60**	**98**
19[e]	Toluene	*t*-BuOK	r.t	70

[a]**Reaction conditions**: 4-methyl benzyl alcohol (1 mmol), aniline (1 mmol), catalyst (1.0 mol%), base (0.5 mmol) in presence of solvent (5 mL) at 60 °C for 12 h. [b] Isolated Yield. [c] absence of base. [d] absence of catalyst. [e] time 24 h.

2.3.5.2. Optimization of effect of substituent

Once the various catalytic parameters were optimized, the effect of substituents of all the complexes on the catalytic reaction has been investigated. At most, all the complexes (**1-4**) showed good catalytic activity in the formation of imine product with appreciable yields. However, based on experimental results, the complex **4** relatively provided a better yield than complexes (**1-3**) due to the presence of electron donating methyl group (Table 2, entries 1-3). Hence, the complex **4** was kept as a representative catalyst to explore the broad substrate scope using a diverse range of alcohols.

Table 4. Effect of the substituent of catalyst[a]

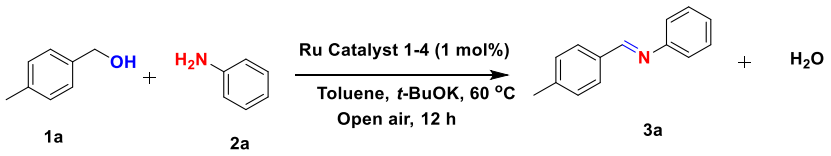

Entry	Ru complex	Yield(%)[b]
1	Complex 1	82
2	Complex 2	86
3	Complex 3	91
4	**Complex 4**	**98**

[a]**Reaction conditions**: 4-methyl benzyl alcohol (1 mmol), aniline (1 mmol), catalyst, (1.0 mol%), base (0.5 mmol) in presence of solvent (5 mL) at 60 °C for 12 h. [b] Isolated yield.

2.3.5.3. Optimization of catalyst loading

Further, the effectiveness of our catalyst was examined with different catalyst loadings for the test reaction (Table 5). Upon reducing the catalyst loading from 1 mol% to 0.25 mol%, there was a substantial decrease in yields (Table 5, entries 1 - 4). Therefore 1 mol% catalyst loading is the best choice for optimization.

Table 5: Effect of catalyst loading[a]

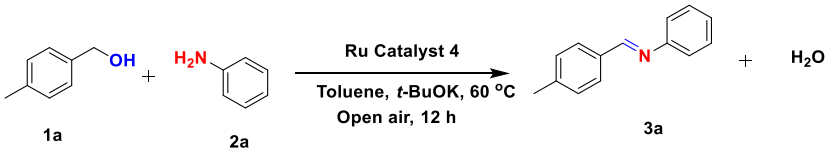

Entry	Catalyst 4 (mol %)	Yield(%)[b]
1	**1.0**	**98**
2	0.5	80
3	0.3	61
4	0.1	39

[a]**Reaction conditions**: 4-methyl benzyl alcohol (1 mmol), aniline (1 mmol), base (0.5 mmol) in presence of solvent (5 mL) at 60 °C for 12 h. [b] Isolated yield.

2.3.5.4. Scope of the reaction

The substrate scope of the reaction with respect to various types of alcohols and amines under the optimized catalytic conditions was displayed in Table 6. Fabulously, electron-rich functionalities of benzyl alcohols (-CH_3, -OCH_3) are efficiently reacted with aniline to yield the respective imines **3a-3c** in 83-95% of isolated yields. Further, electron-withdrawing substituents (-Cl, -F) on benzyl alcohols were tolerated well with aniline acquired desired imines **3d** and **3e** in the yields of 88-78%. In addition, the coupling reactions between different benzyl alcohols and 4-ethoxy and 4-methoxy anilines afforded the corresponding imines **3f** and **3g** in 80-83% of isolated yields. More interestingly, the complex catalyzed well in the coupling of sterically hindered 2-bromobenzyl alcohol with 4-methoxy aniline to afford the respective imine **3h** in 75% of yield. However, the electron-withdrawing substituent of 4-chlorobenzyl alcohol with 4-methoxy aniline showed a better result in the formation of respective imine **3i** in 79% of yield. The high yield of 82% for **3j** was obtained by the reaction of 4-methoxybenzyl alcohol and 4-methoxy aniline. Coupling

of benzyl alcohol bearing electron-donating and withdrawing substituents (4-methyl and 4-chloro) with 4-bromoaniline gave respective imines **3k** and **3l** in 98% and 90% of yields. Importantly, piperonyl based imine moieties were found to be effective in pharmaceutically active ingredients. But, the synthesis of piperonyl derived imines are less covered in previous literature.[29] Hence, we interested to couple the piperonyl alcohol with various amines. More significantly, we attained the piperonyl derived imines **3m-3o** up to 94% of yields. Gratifyingly, the catalytic efficiency of present complex proved in the synthesis of bis-imine product **3p** with the appreciable yield of 75% under optimized condition. Deliberately, a chiral imine **3q** was achieved from the coupling of 4-methylbenzyl alcohol with (*R*)-(+)-α-methylbenzylamine with 84% yield. Notably, the complex efficiently promoted the synthesis of imines from heterocyclic alcohols and amines and resulted in good yields of imine products **3r** and **3s** with 70% and 87% respectively. Attempt taken for coupling of alcohol and aliphatic amine to provide the expected product **3t** was successful. Further, the catalytic condition was found to be ineffective for the coupling of aliphatic alcohols with amines.

It is crucial at this point to compare the catalytic efficiency and scope of our catalytic system with other reported ruthenium(II) catalysts. Maggi *et al.* demonstrated the catalytic performance of Ru-NHC complex (5 mol%) in imine synthesis using DABCO ligand in presence of molecular sieves for 24 h.[10b] Gelman *et al.* have reported the catalytic activity of bifunctional Ru(II) PCP pincer complexes towards synthesis of imine from alcohols and amines in *p*-xylene medium with 2 mol% catalyst loading for 24 h under Argon atmosphere.[30] The binuclear Ru catalyst has documented to catalyzed an imine formation reaction with 5 mol% DABCO ligand and molecular sieves for 24 h.[31] In addition, Kazushi Mashima and co-workers reported the ruthenium complex catalyzed imination reaction with $Zn(OCOCF_3)_2$ (1 mol%) and KO^{t}Bu (20 mol%) as a base in dioxane medium.[32] The present dinuclear arene Ru(II) complex has considerable benefits over than other reported catalyst.

In contrast, the salient features of titled catalysts are insensitive towards air, simple, and convenient catalytic method for the synthesis of imines. Further, in the bimetallic catalytic system, cooperative effect between the two metal centers enhances the strong metal-metal interaction which interact with the substrates and increases the rate of the reaction than the monometallic system. We speculated that the catalytic performance may be from two active metal centers of the complex working independently, or only an active metal center under the electronic influence of the second one. Hence, the catalyst loading is 1 mol% sufficient to catalyze the reaction with good to excellent yields.[33]

Table 6. Synthesis of Imines from Alcohols and Amine[a]

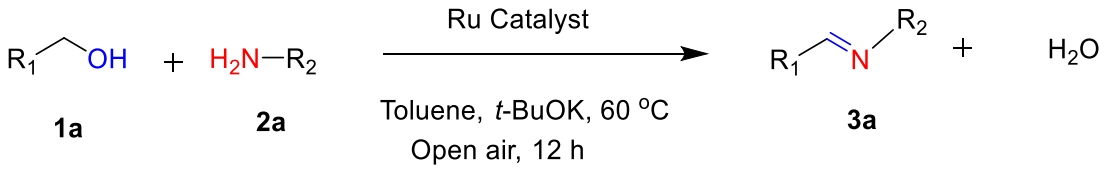

Entry	1	2	3		Yield[b] %
1	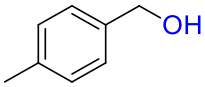	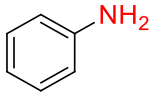	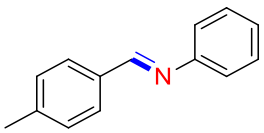	**(3a)**	95
2	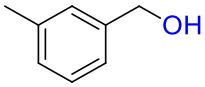	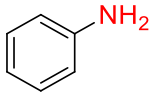	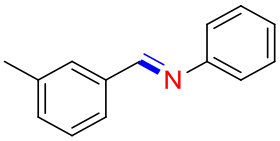	**(3b)**	80
3	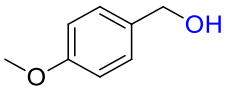	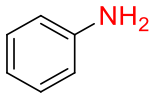	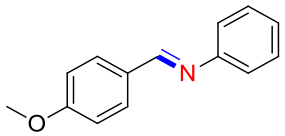	**(3c)**	83
4	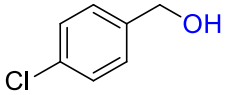	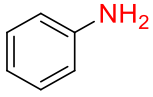	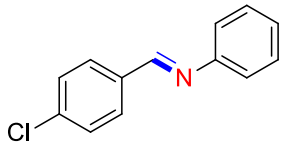	**(3d)**	88
5	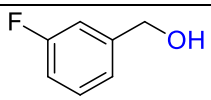	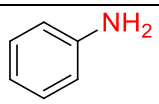	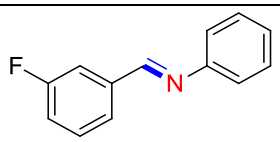	**(3e)**	78
6	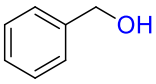	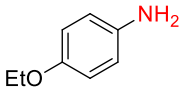	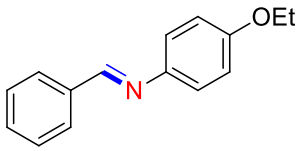	**(3f)**	80
7	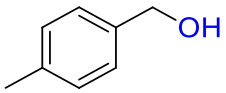	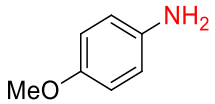	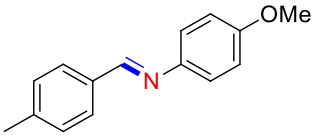	**(3g)**	83
8	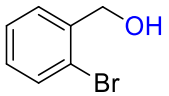	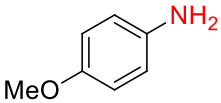	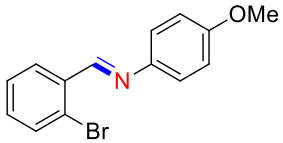	**(3h)**	75
9	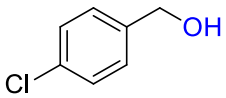	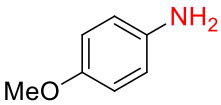	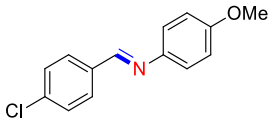	**(3i)**	79
10	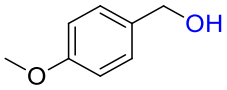	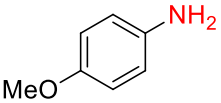	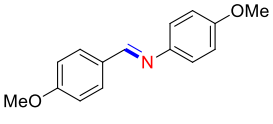	**(3j)**	82

Entry	1	2	3		Yield[b] %
11	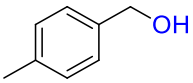	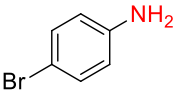	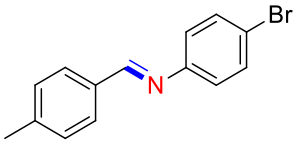	(**3k**)	98
12	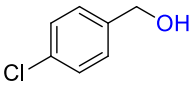	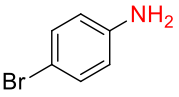	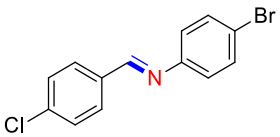	(**3l**)	90
13	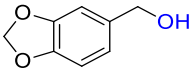	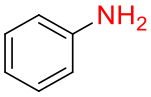	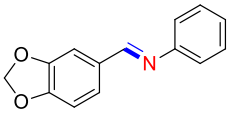	(**3m**)	70
14	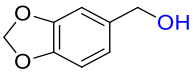	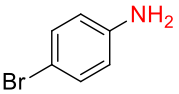	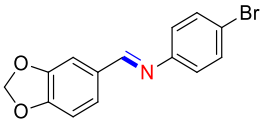	(**3n**)	94
15	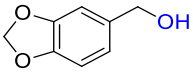	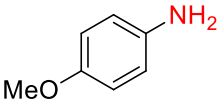	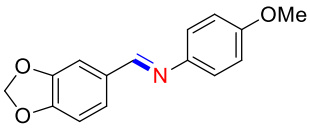	(**3o**)	82
16[c]	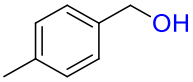	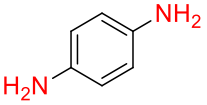	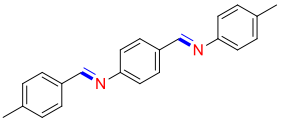	(**3p**)	75
17	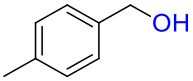	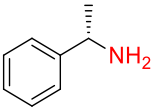	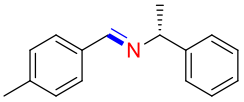	(**3q**)	84
18	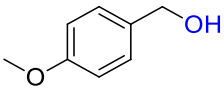	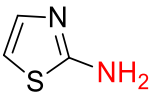	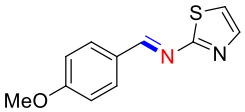	(**3r**)	70
19	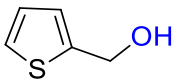	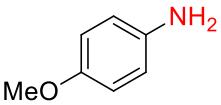	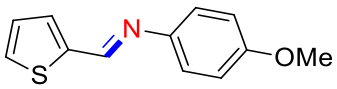	(**3s**)	87
20	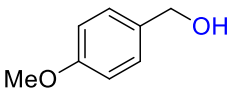	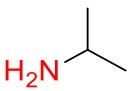	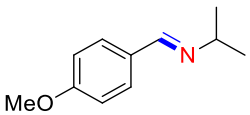	(**3t**)	60

[a]**Reaction conditions**: 1a (1 mmol), 2a (1 mmol), catalyst (1 mol %), *t*-BuOK (0.5 mmol) and Toluene (5 mL) stirred for 12 h in open air. [b] Isolated yields. [c] Reaction for 24 h.

It is worth to note that one of the antibacterial drugs namely N-(salicylidene)-2-hydroxyaniline was synthesized from 2-hydroxybenzyl alcohol and 2-amino phenol using our present protocol (Scheme 5) and an excellent yield of 95% was obtained.

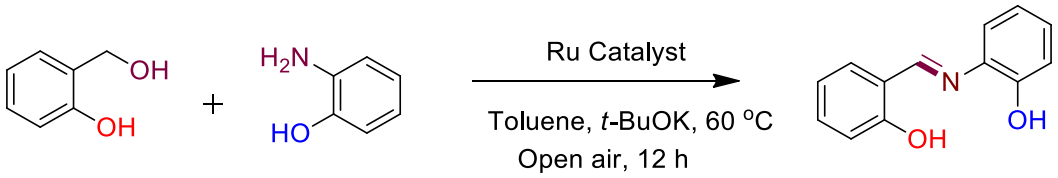

Scheme 5. Preparation of N-(salicylidene)-2-hydroxyaniline using our protocol

2.3.5.5. Control experiments

Control experiments were performed under standard conditions in order to examine the mechanism of the imination (Scheme 6). Initially, oxidation of alcohol lead to the formation of aldehyde. Further, mixture of products aldehyde and imine were obtained when the reaction was conducted in the presence of amine for 8 h. Complete imine product was obtained only after 12 h of the reaction. Hence, the formation of aldehyde clearly indicates that the reaction proceeds *via* oxidation of alcohol as an initial step.

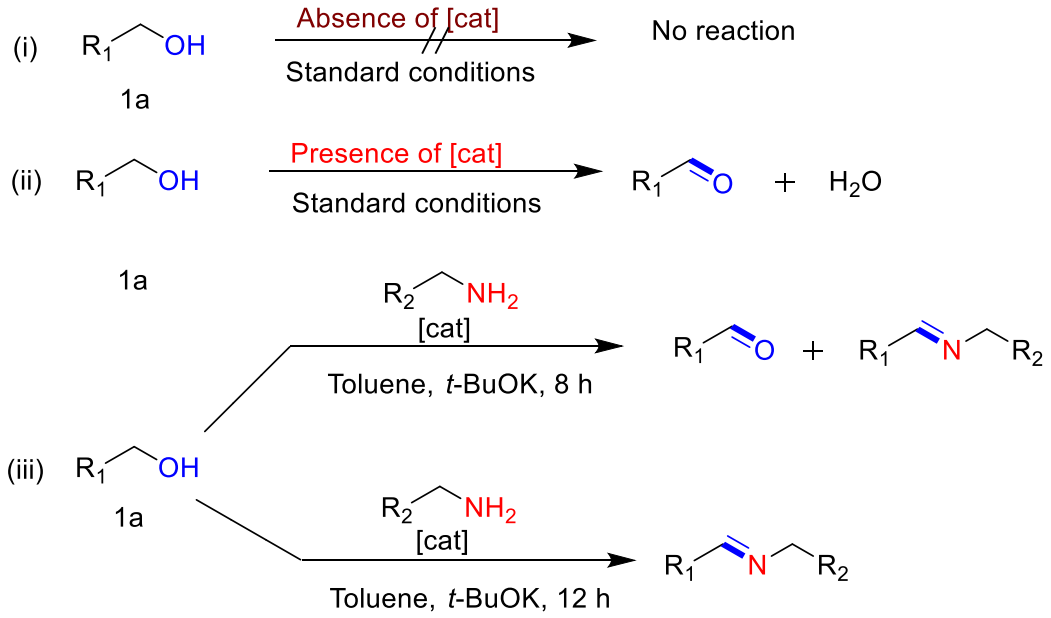

Scheme 6. Control experiments for mechanistic studies

2.3.5.6. Mechanism for the synthesis of imines

A plausible mechanism has been proposed based on the results from the control experiments and on the previously reported literature (Scheme 7). The reaction involves the formation of ruthenium alkoxide species (**B**) from the catalyst (**A**) through deprotonation of the alcohol followed by β-hydride elimination to form aldehyde. This aldehyde intermediate further reacts with amines to produce imines and water is eliminated as a by-product. Further, the ruthenium hydride[10b,34] intermediate (**C**) reacts with alcohol to form to the next catalytic cycle with the release of two molecules of water. The detailed studies on the mechanism for imine synthesis is under investigation.

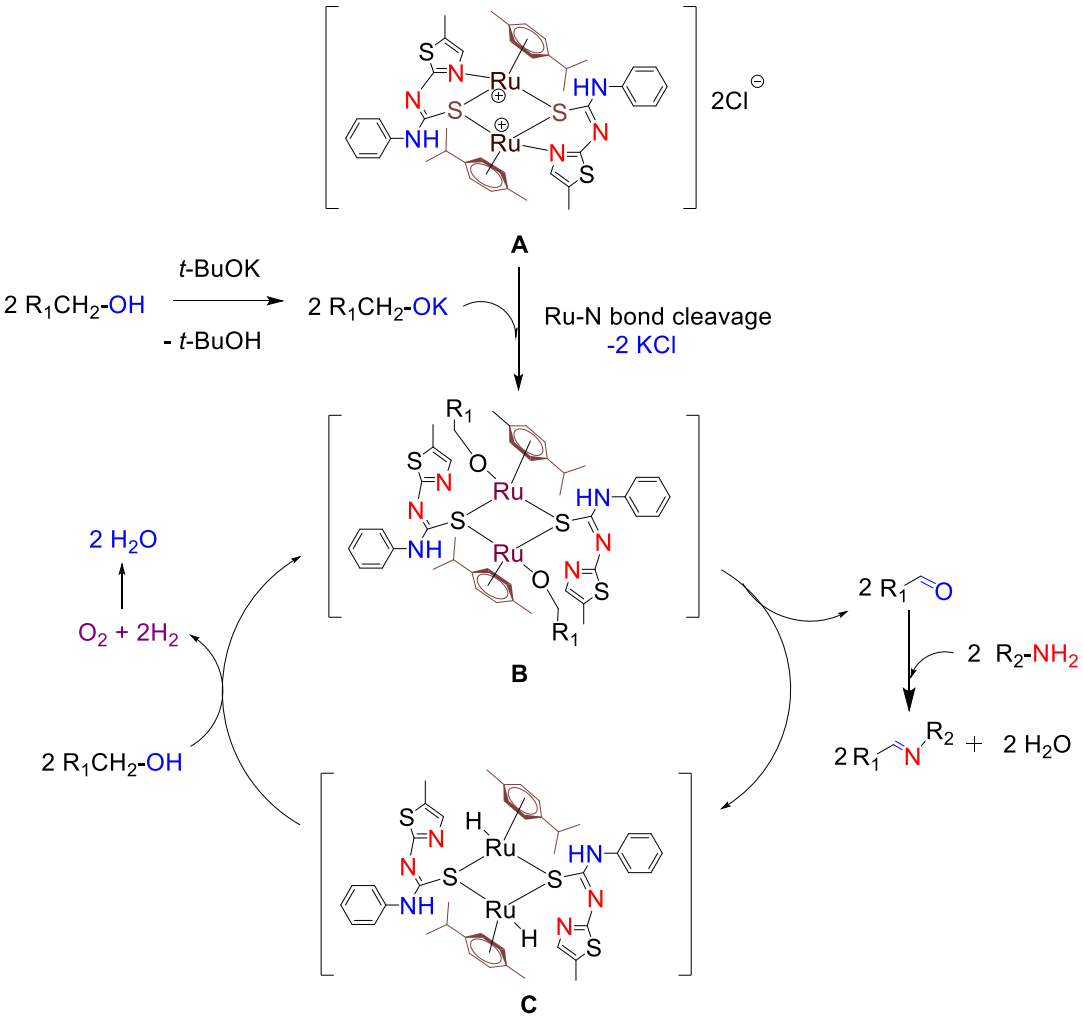

Scheme 7. Plausible mechanism for imine formation

Spectral data of aldehyde products

(1a) 4-methoxybenzaldehyde[34]. ^{1}H NMR (400 MHz, $CDCl_3$): δ (ppm) 9.78 (s, 1H, CH=O), 7.72-7.74 (d, J = 8 Hz, 2H), 6.89-6.91 (d, J = 8 Hz, 2H), 3.78 (s, 3H). ^{13}C NMR (100 MHz, $CDCl_3$): δ (ppm) 189.86, 163.59, 130.96, 128.87, 113.28, 54.53.

(1b) benzo[d][1,3]dioxole-5-carbaldehyde[35]. ^{1}H NMR (400 MHz, $CDCl_3$): δ (ppm) 9.69 (s, 1H, CH=O), 7.29 (dd, J = 7.9, 14 Hz, 1H), 7.20 (s, 1H), 6.81 (d, J = 7.9 Hz, 1H) 5.96 (s, 2H). ^{13}C NMR (100 MHz, $CDCl_3$): δ (ppm) 189.32, 152.07, 147.64, 130.76, 127.69, 107.29, 105.74, 101.12.

Spectral data of catalytic isolated imine products

(3a) (E)-N-(4-methylbenzylidene)aniline[35]. ^{1}H NMR (400 MHz, $CDCl_3$): δ (ppm) 8.40 (s, 1H, CH=N), 7.78 (d, J = 8 Hz, 2H), 7.37 (t, J = 7.7 Hz, 3H), 7.26 (m, 3H), 7.20 (d, J = 8 Hz, 1H), 2.40 (s, 3H). ^{13}C NMR (100 MHz, $CDCl_3$): δ (ppm) 160.43, 152.32, 141.93, 133.73, 129.59, 129.19, 128.89, 125.82, 120.96, 21.72.

(3b) (E)-N-(3-methylbenzylidene)aniline[35]. ^{1}H NMR (400 MHz, $CDCl_3$): δ (ppm) 8.28 (s, 1H, CH=N), 7.71 (s, 1H), 7.64 (d, J = 7.6 Hz, 1H), 7.53 (d, *J* = 7.2 Hz, 1H), 7.25 (m, 3H), 7.16 (m, 2H), 7.10 (m, 2H), 2.28 (s, 3H). ^{13}C NMR (100 MHz, $CDCl_3$): δ (ppm) 159.57, 151.04, 137.42, 135.06, 131.17, 128.06, 127.89, 127.57, 125.35, 124.81, 119.80, 20.22.

(3c) (E)-N-(4-methoxybenzylidene)aniline[36]. ^{1}H NMR (400 MHz, $CDCl_3$): δ (ppm) 8.37 (s, 1H, CH=N), 7.84 (d, J = 8.7 Hz, 2H), 7.38 (t, *J* = 7.7 Hz, 2H), 7.20 (t, *J* = 8.5 Hz, 3H), 6.98 (d, *J* = 8.7 Hz, 2H), 3.86 (s, 3H). ^{13}C NMR (100 MHz, $CDCl_3$): δ (ppm) 161.14, 158.62, 151.21, 129.45, 128.15, 128.12, 128.04, 124.51, 119.83, 117.28, 113.97, 113.08, 54.23.

(3d) (E)-N-(4-chlorobenzylidene)aniline[35]. ^{1}H NMR (400 MHz, $CDCl_3$): δ (ppm) 8.40 (s, 1H, CH=N), 7.82 (d, J = 8.4 Hz, 2H), 7.42 (m, 4H), 7.21 (m, 3H). ^{13}C NMR (100 MHz, $CDCl_3$): δ (ppm) 158.87, 151.71, 137.41, 134.74, 130.01, 129.26, 129.12, 126.26, 120.92.

(3e) (E)-N-(3-fluorobenzylidene)aniline[37]. ^{1}H NMR (400 MHz, $CDCl_3$): δ (ppm) 8.48 (s, 1H, CH=N), 7.73 (dd, J = 21.8, 8.5 Hz, 2H), 7.49 (m, 4H), 7.38-7.20 (m, 3H). ^{13}C NMR (100 MHz, $CDCl_3$): δ (ppm) 163.20, 160.75, 157.86, 157.83, 150.31, 137.31, 129.19, 128.14, 125.29, 123.94, 119.83, 117.11, 113.47.

(3f) (E)-N-benzylidene-4-ethoxyaniline. ^{1}H NMR (400 MHz, $CDCl_3$): δ (ppm) 8.48 (s, 1H), 7.88 (m, 2H), 7.49 – 7.39 (m, 3H), 7.23 (d, *J* = 8.8 Hz, 2H), 6.92 (d, *J* = 8.8 Hz, 2H), 4.05 (q, *J* = 7.0 Hz, 2H), 1.43 (t, *J* = 7.0 Hz, 3H). ^{13}C NMR (100 MHz, $CDCl_3$): δ (ppm) 158.37, 157.70, 144.78, 136.50, 131.05, 128.77, 128.61, 122.23, 114.99, 63.72, 14.92. Anal. Calcd. For $C_{11}H_{15}NO$: C, 79.97; H, 6.71; N, 6.22. Found: C, 79.87; H, 6.69; N, 6.16.

(3g) (E)-4-methoxy-N-(4-methylbenzylidene)aniline[34]. ^{1}H NMR (400 MHz, $CDCl_3$): δ (ppm) 8.44 (s, 1H), 7.77 (d, *J* = 8.0 Hz, 2H), 7.24 (dd, *J* = 16.8, 8.7 Hz, 4H), 6.92 (d, *J* = 8.8 Hz, 2H), 3.82 (s, 3H), 2.41 (s, 3H). ^{13}C NMR (100 MHz, $CDCl_3$): δ (ppm) 158.52, 158.14, 145.15, 141.51, 133.91, 129.52, 128.62, 122.18, 114.38, 55.55, 21.67.

(3h) (E)-N-(2-bromobenzylidene)-4-methoxyaniline[34]. ^{1}H NMR (400 MHz, $CDCl_3$): δ (ppm) 8.41 (s, 1H, CH=N), 8.08 (t, *J* = 1.6 Hz, 1H), 7.77 (d, *J* = 7.7 Hz, 1H), 7.57 (ddd, *J* = 7.9, 1.9, 1.0 Hz, 1H), 7.32 (t, *J* = 7.8 Hz, 1H), 7.24 (d, *J* = 8.9 Hz, 2H), 6.94 (d, *J* = 8.9 Hz, 2H), 3.83 (s, 3H).^{13}C NMR (100 MHz, $CDCl_3$): δ (ppm) 158.66, 156.35, 144.24, 138.49, 133.82, 131.08, 130.27, 127.39, 123.07, 122.35, 114.47, 55.54.

(3i) (E)-N-(4-chlorobenzylidene)-4-methoxyaniline[34]. ^{1}H NMR (400 MHz, $CDCl_3$): δ (ppm) 8.43 (s, 1H), 7.82 (d, *J* = 8.4 Hz, 2H), 7.43 (d, *J* = 8.4 Hz, 2H), 7.23 (d, *J* = 8.8 Hz, 2H), 6.93 (d, *J* = 8.8 Hz, 2H), 3.83 (s, 3H). ^{13}C NMR (100 MHz, $CDCl_3$): δ (ppm) 158.51, 156.75, 144.48, 136.97, 134.98, 129.75, 129.06, 122.28, 114.45, 55.53.

(3j) (E)-4-methoxy-N-(4-methoxybenzylidene)aniline[34]. ^{1}H NMR (400 MHz, $CDCl_3$): δ (ppm) 8.40 (s, 1H, CH=N), 7.83 (d, J = 8.7 Hz, 2H), 7.28 -7.15 (m, 2H), 6.94 (dd, J = 20.5,

8.8 Hz, 4H), 3.86 (s, 3H), 3.82 (s, 3H). ^{13}C NMR (100 MHz, $CDCl_3$): δ (ppm) 162.03, 158.01, 145.27, 130.30, 122.11, 114.39, 114.19, 55.52, 55.44.

(3k) (E)-4-bromo-N-(4-methylbenzylidene)aniline[34]. ^{1}H NMR (400 MHz, $CDCl_3$): δ (ppm) 8.37 (s, 1H, CH=N), 7.77 (d, J = 8.1 Hz, 2H), 7.48 (d, J = 8.7 Hz, 2H), 7.27 (d, J = 7.9 Hz, 2H), 7.07 (d, J = 8.6 Hz, 2H), 2.41 (s, 3H). ^{13}C NMR (100 MHz, $CDCl_3$): δ (ppm) 159.57, 149.99, 141.07, 131.03, 128.43, 127.82, 121.55, 117.99, 115.56, 20.57.

(3l) (E)-4-bromo-N-(4-chlorobenzylidene)aniline[38]. ^{1}H NMR (400 MHz, $CDCl_3$): δ (ppm) 8.39 (s, 1H, CH=N), 7.83 (d, J = 8.5 Hz, 2H), 7.48 (dd, J = 22.0, 8.6 Hz, 4H), 7.09 (d, J = 8.6 Hz, 2H). ^{13}C NMR (100 MHz, $CDCl_3$): δ (ppm) 158.03, 149.39, 136.53, 133.29, 131.15, 128.95, 128.03, 121.52, 118.54, 115.60.

(3m) (E)-N-(benzo[d][1,3]dioxol-5-ylmethylene)aniline[34]. ^{1}H NMR (400 MHz, $CDCl_3$): δ (ppm) 8.15 (s, 1H, CH=N), 7.39 (d, J = 1.4 Hz, 1H), 7.22 (d, J = 7.7 Hz, 2H), 7.06 (dd, J = 10.1, 9.0 Hz, 4H), 5.82 (s, 2H). ^{13}C NMR (100 MHz, $CDCl_3$): δ (ppm) 158.33, 150.90, 149.41, 147.32, 130.05, 128.05, 124.67, 124.63, 119.82, 117.33, 113.97, 107.08, 105.72, 100.51.

(3n) (E)-N-(benzo[d][1,3]dioxol-5-ylmethylene)-4-bromoaniline. ^{1}H NMR (400 MHz, $CDCl_3$): δ (ppm) 8.11 (s, 1H, CH=N), 7.36 – 7.30 (m, 3H), 7.07 (t, J = 8.6 Hz, 2H), 6.90 (d, J = 8.5 Hz, 2H), 5.86 (s, 2H). ^{13}C NMR (100 MHz, $CDCl_3$): δ (ppm) 158.61, 149.79, 149.63, 147.36, 131.04, 130.86, 129.77, 124.93, 121.55, 117.92, 115.57, 107.13, 105.70, 100.59. Anal. Calcd. For $C_{14}H_{10}BrNO_2$: C, 55.29; H, 3.31; N, 4.61. Found: C, 55.23; H, 3.27; N, 4.55.

(3o) (E)-N-(benzo[d][1,3]dioxol-5-ylmethylene)-4-methoxylaniline[34]. ^{1}H NMR (400 MHz, $CDCl_3$): δ (ppm) 8.34 (s, 1H, CH=N), 7.51 (s, 1H), 7.27 – 7.15 (m, 3H), 6.94 – 6.78 (m, 3H), 6.01 (s, 2H), 3.81 (s, 3H). ^{13}C NMR (100 MHz, $CDCl_3$): δ (ppm) 13C NMR (101

MHz, CDCl3) δ 158.10, 157.57, 150.27, 148.44, 144.94, 131.48, 125.37, 122.15, 114.40, 108.23, 106.75, 101.59, 55.52.

(3p) (E)-4-methyl-N-(4-((E)-(4-methylbenzylidene)amino)benzylidene)aniline. ^{1}H NMR (400 MHz, $CDCl_3$): δ (ppm) 8.46 (s, 2H, CH=N), 7.80 (d, *J* = 7.9 Hz, 4H), 7.27 (d, *J* = 8.5 Hz, 8H), 2.41 (s, 6H). ^{13}C NMR (100 MHz, $CDCl_3$): δ (ppm) 159.69, 150.02, 141.87, 133.77, 129.58, 128.84, 121.85, 21.68. Anal. Calcd. For $C_{22}H_{20}N_2$: C, 84.58; H, 6.45; N, 8.97. Found: C, 84.53; H, 6.38; N, 8.90.

(3q) (R,E)-N-(4-methylbenzylidene)-1-phenylethanamine. ^{1}H NMR (400 MHz, $CDCl_3$): δ (ppm) 8.32 (s, 1H, CH=N), 7.66 (d, *J* = 7.8 Hz, 2H), 7.42 (d, *J* = 7.4 Hz, 2H), 7.33 (t, *J* = 7.5 Hz, 2H), 7.21 (m, 3H), 4.51 (q, *J* = 6.5 Hz, 1H), 2.36 (s, 3H), 1.59 (s, 3H). ^{13}C NMR (100 MHz, $CDCl_3$): δ (ppm) 159.47, 145.38, 140.86, 133.87, 129.31, 128.45, 128.30, 126.83, 126.70, 69.73, 24.91, 21.56. Anal. Calcd. For $C_{16}H_{17}N$: C, 86.05; H, 7.67; N, 6.27. Found: C, 85.90; H, 6.61; N, 6.19.

(3r) (E)-N-(4-methoxybenzylidene)thiazol-2-amine. ^{1}H NMR (400 MHz, DMSO-d_6): δ (ppm) 9.00 (s, 1H, CH=N), 7.99 (d, J = 8.6 Hz, 1H), 7.70 (d, J = 3.2 Hz, 2H), 7.58 (d, *J* = 3.4 Hz, 1H), 7.11 (d, *J* = 8.6 Hz, 1H), 3.86 (s, 1H). ^{13}C NMR (100 MHz, DMSO-d_6): δ (ppm) 172.68, 168.77, 163.23, 141.27, 138.58, 131.71, 127.49, 118.69, 114.60, 106.46, 55.55. Anal. Calcd. For $C_{11}H_{10}N_2OS$: C, 60.53; H, 4.62; N, 12.83. Found: C, 60.47; H, 4.59; N, 12.75.

(3s) (E)-4-methoxy-N-(thiophen-2-ylmethylene)aniline[34]. ^{1}H NMR (400 MHz, $CDCl_3$): δ (ppm) 8.58 (s, 1H, CH=N), 7.46 (dd, J = 10.9, 4.3 Hz, 2H), 7.22 (d, J = 8.9 Hz, 2H), 7.12 (dd, J = 4.9, 3.7 Hz, 1H), 6.92 (d, J = 8.9 Hz, 2H), 3.83 (s, 3H). ^{13}C NMR (100 MHz, $CDCl_3$): δ (ppm) 158.37, 151.27, 144.24, 143.12, 131.93, 129.91, 127.87, 122.43, 116.57, 114.85, 114.48, 55.49.

(3t) (E)-N-(4-methoxybenzylidene)propan-2-amine. ^{1}H NMR (400 MHz, $CDCl_3$): δ (ppm) 8.09 (s, 1H), 7.70 (s, 1H), 7.48 (s, 1H), 7.54 (d, *J* = 8.7 Hz, 2H), 3.72 (s, 3H), 3.37 (sept, 1H), 1.13 (d, 6H). ^{13}C NMR (100 MHz, $CDCl_3$): δ (ppm) 163.55, 160.37, 130.90, 128.59, 127.47, 113.24, 112.84, 60.48, 54.46, 23.15. Anal. Calcd. For $C_{11}H_{15}NO$: C, 74.54; H, 8.53; N, 7.90. Found: C, 74.50; H, 8.51; N, 7.82.

N-(Salicylidene)-2-hydroxyaniline[39]. ^{1}H NMR (400 MHz, $CDCl_3$): δ (ppm) 12.29 (s, 1H, OH) 8.69 (s, 1H, CH=N), 7.43 (t, *J* = 8.7 Hz, 2H), 7.22 (t, *J* = 7.2 Hz, 1H), 7.15 (d, *J* = 7.8 Hz, 1H), 7.05 – 6.90 (m, 4H), 5.86 (s, 1H). ^{13}C NMR (100 MHz, $CDCl_3$): δ (ppm) 164.02, 149.90, 135.84, 133.79,132.76, 128.81, 121.08, 119.64, 118.36, 117.31, 115.92.

NMR spectra of the aldehyde intermediates

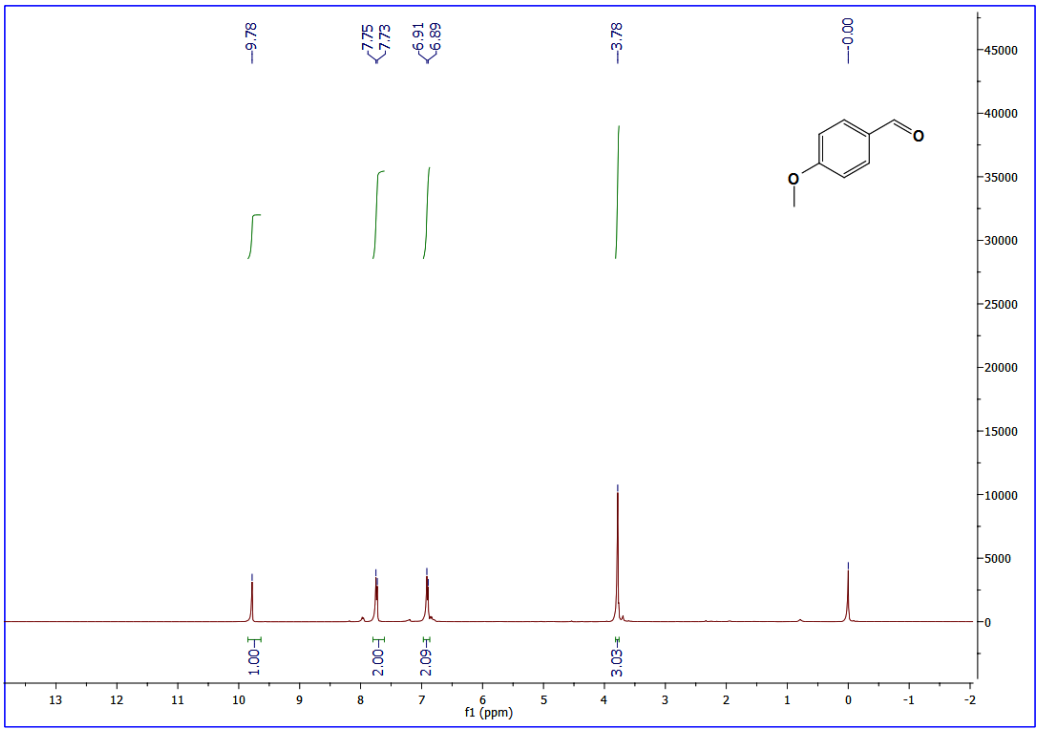

Figure 12. ^{1}H NMR spectrum for 4-methoxybenzaldehyde in $CDCl_3$ (400MHz, 300K).

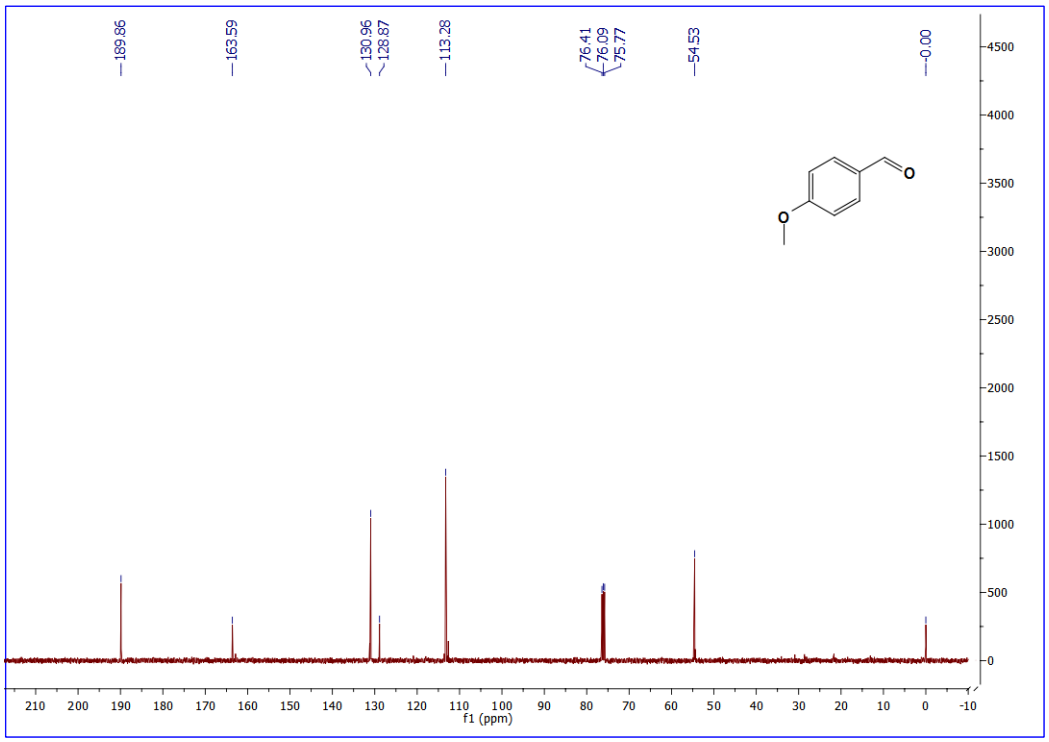

Figure 13. ^{13}C NMR spectrum for 4-methoxybenzaldehyde in $CDCl_3$ (100MHz, 300K).

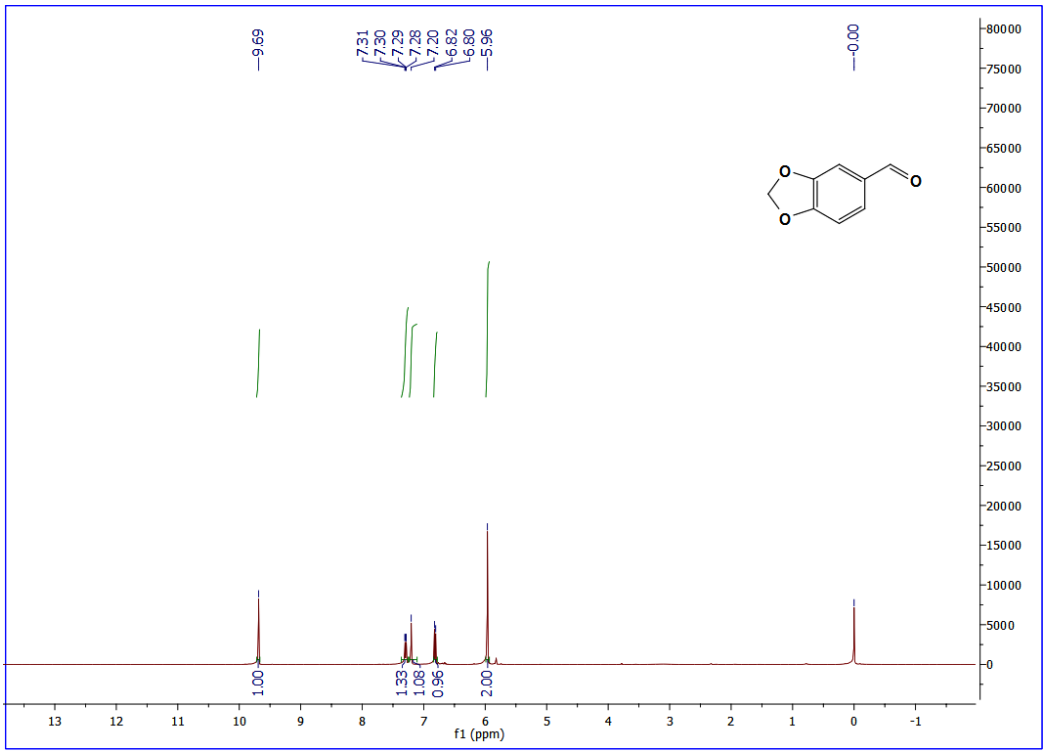

Figure 14. ^{1}H NMR spectrum for benzo[d][1,3]dioxole-5-carbaldehyde in $CDCl_3$ (400MHz, 300K).

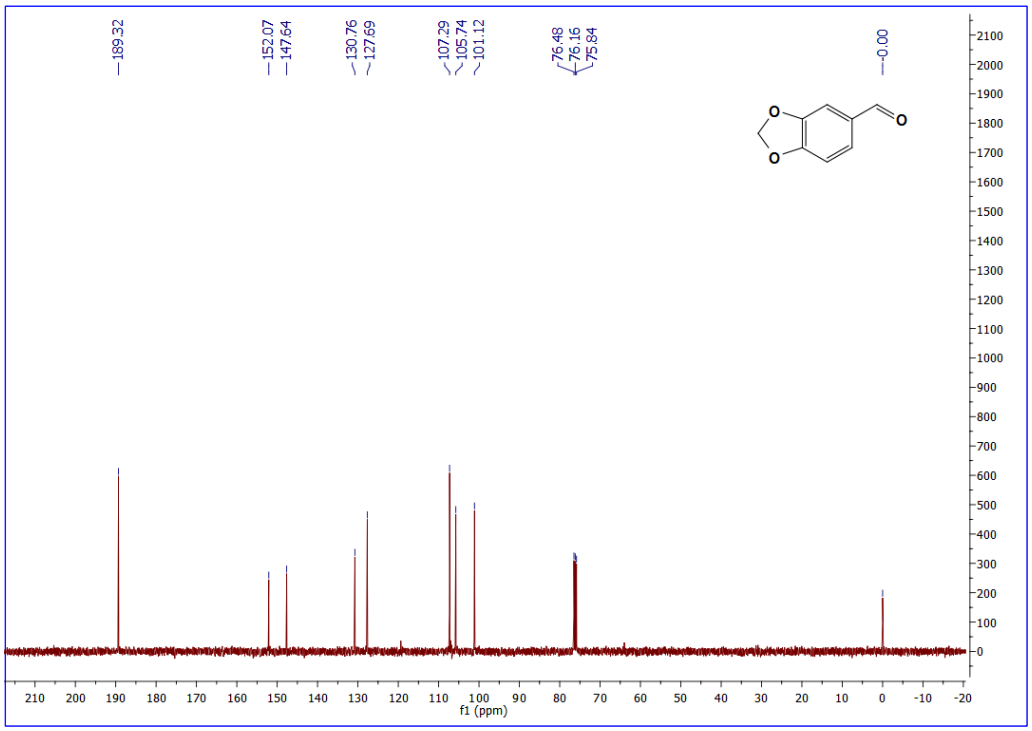

Figure 15. ^{13}C NMR spectrum for benzo[d][1,3]dioxole-5-carbaldehyde in $CDCl_3$ (100MHz, 300K).

NMR spectra of imine products

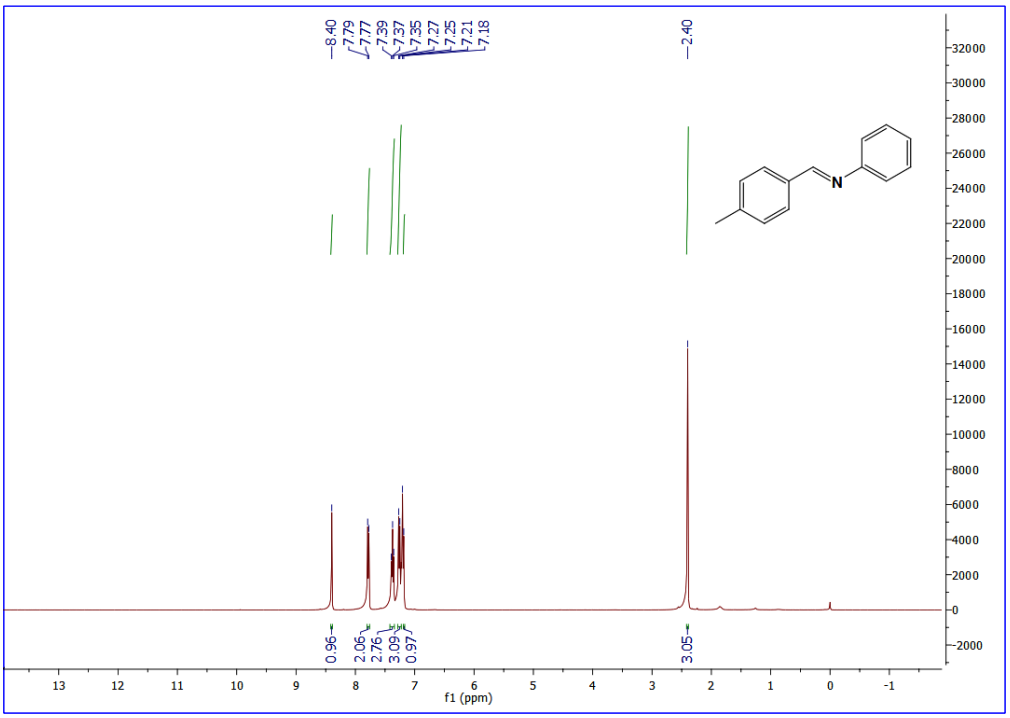

Figure 16. ^{1}H NMR spectrum for (**3a**) in $CDCl_3$ (400MHz, 300K).

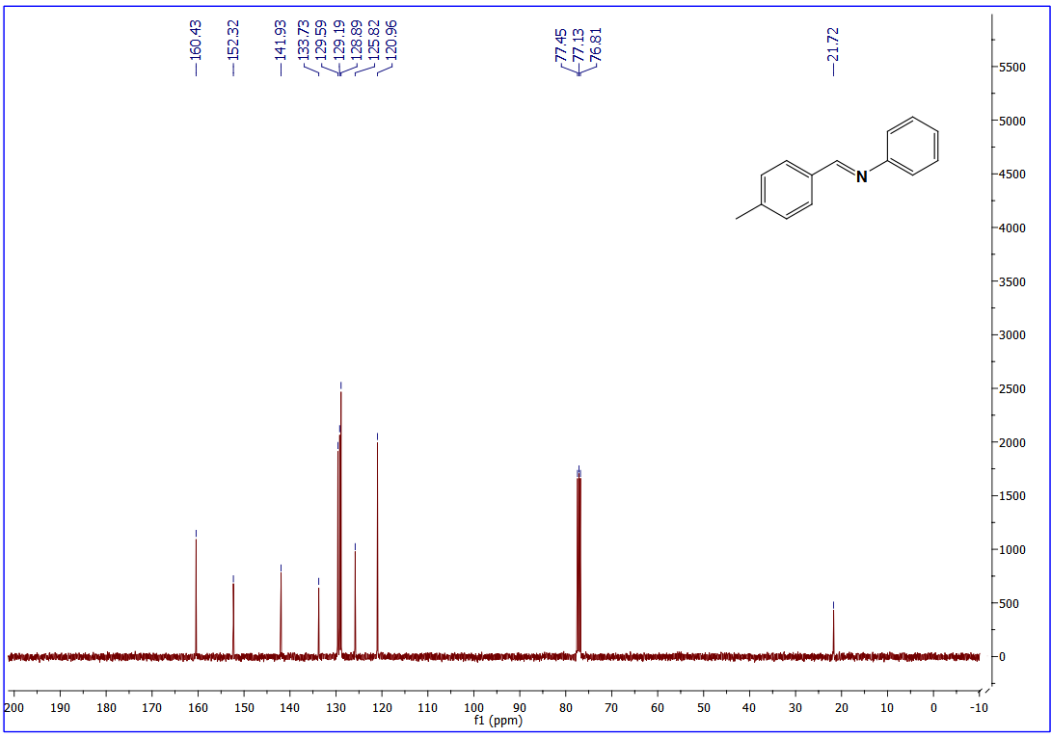

Figure 17. ^{13}C NMR spectrum for (**3a**) in $CDCl_3$ (100MHz, 300K).

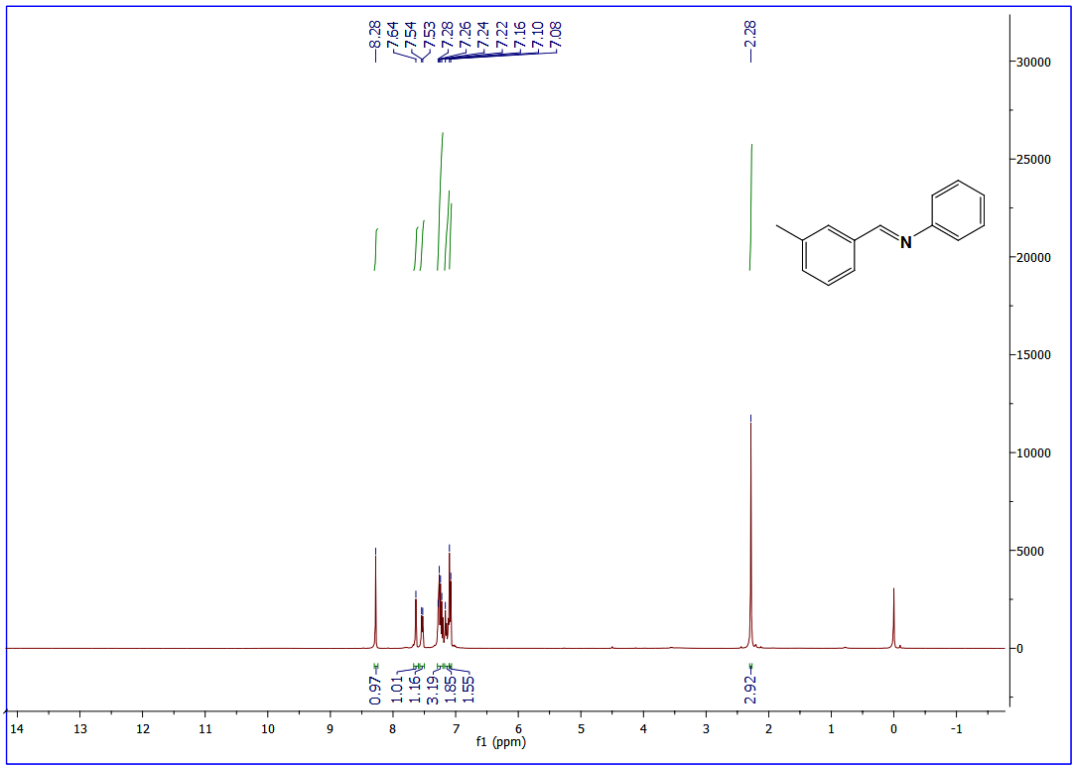

Figure 18. ^{1}H NMR spectrum for (**3b**) in $CDCl_3$ (400MHz, 300K).

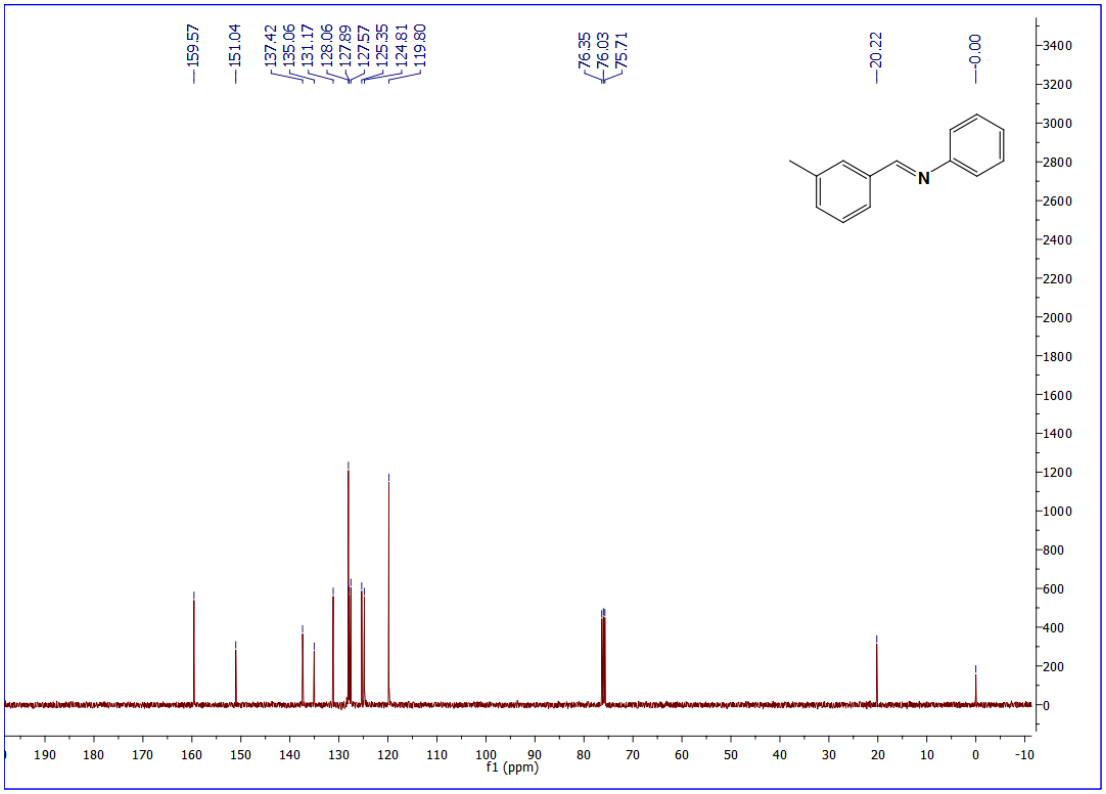

Figure 19. ^{13}C NMR spectrum for (**3b**) in $CDCl_3$ (100MHz, 300K).

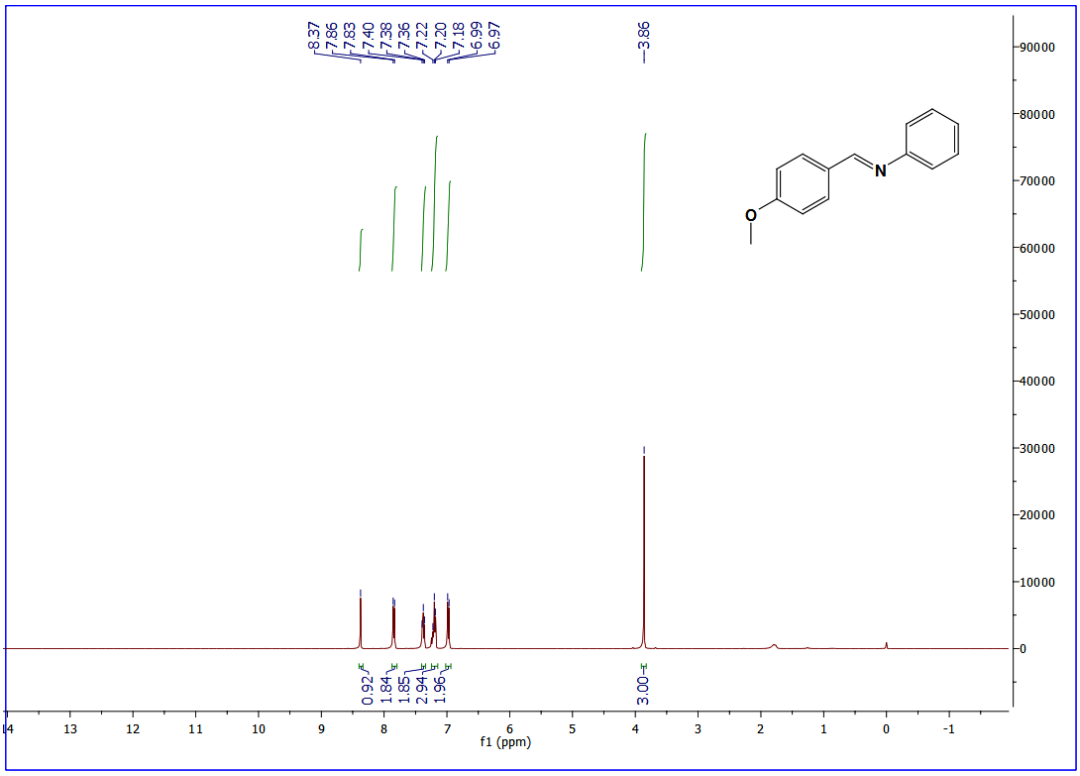

Figure 20. ^{1}H NMR spectrum for (**3c**) in $CDCl_3$ (400MHz, 300K).

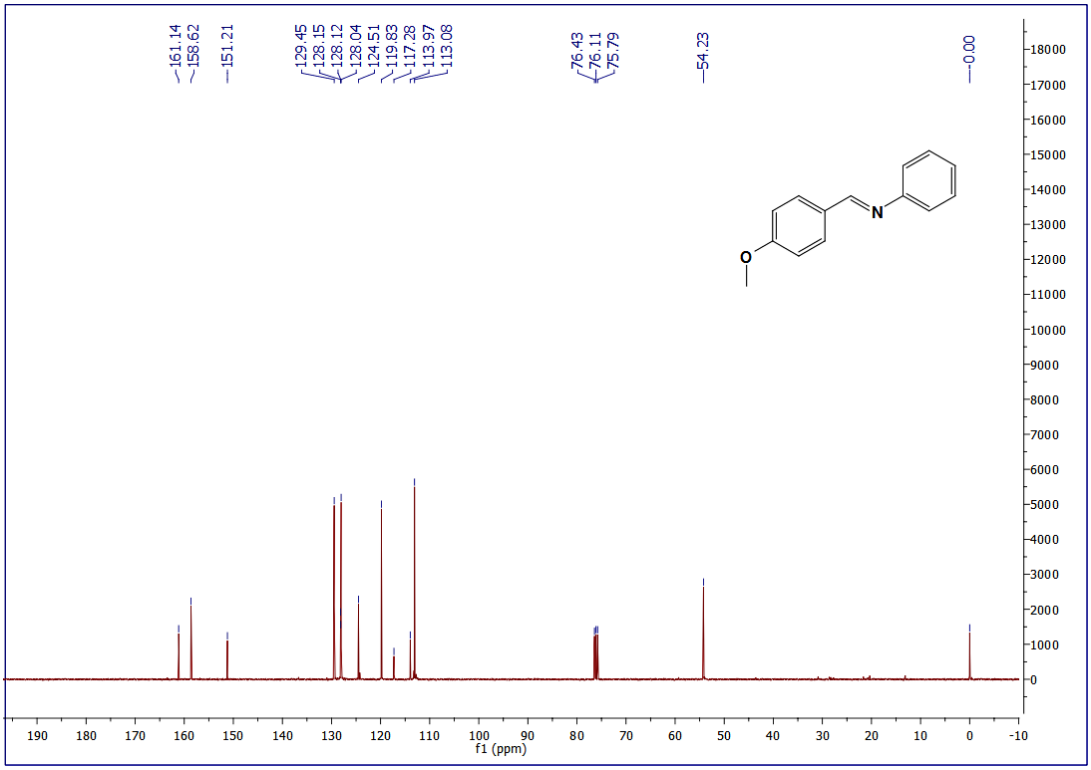

Figure 21. ^{13}C NMR spectrum for (**3c**) in $CDCl_3$ (100MHz, 300K).

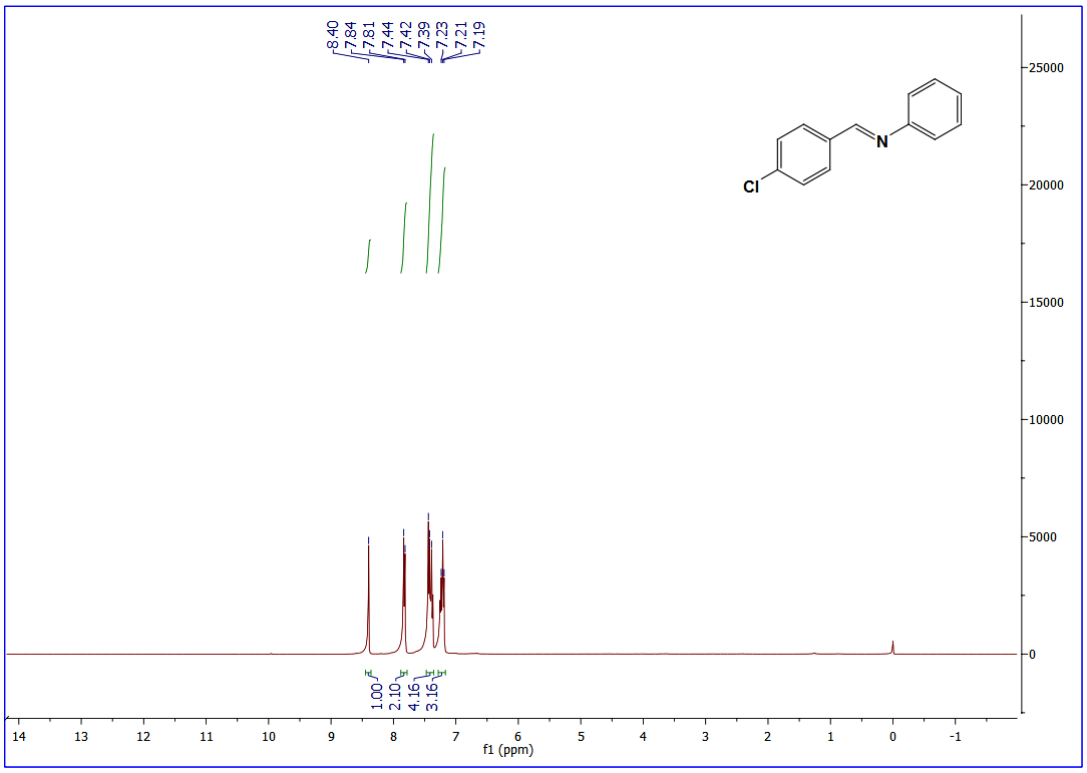

Figure 22. ^{1}H NMR spectrum for (**3d**) in $CDCl_3$ (400MHz, 300K).

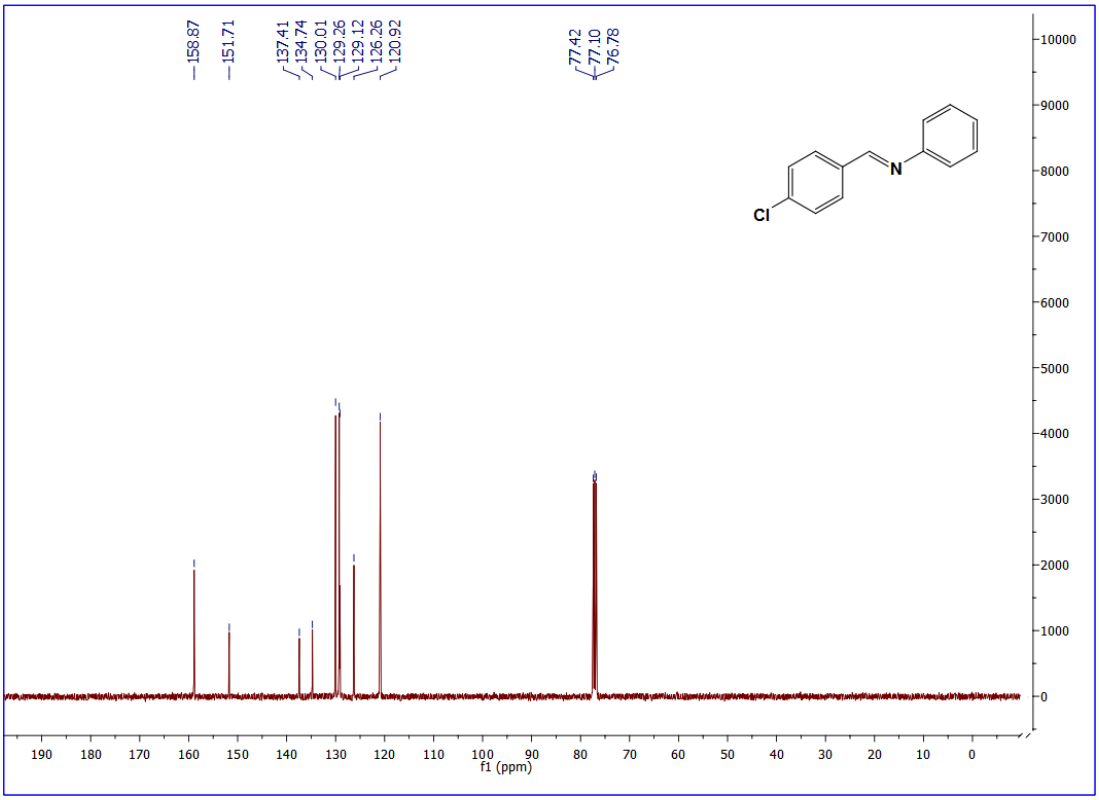

Figure 23. ^{13}C NMR spectrum for (**3d**) in $CDCl_3$ (100MHz, 300K).

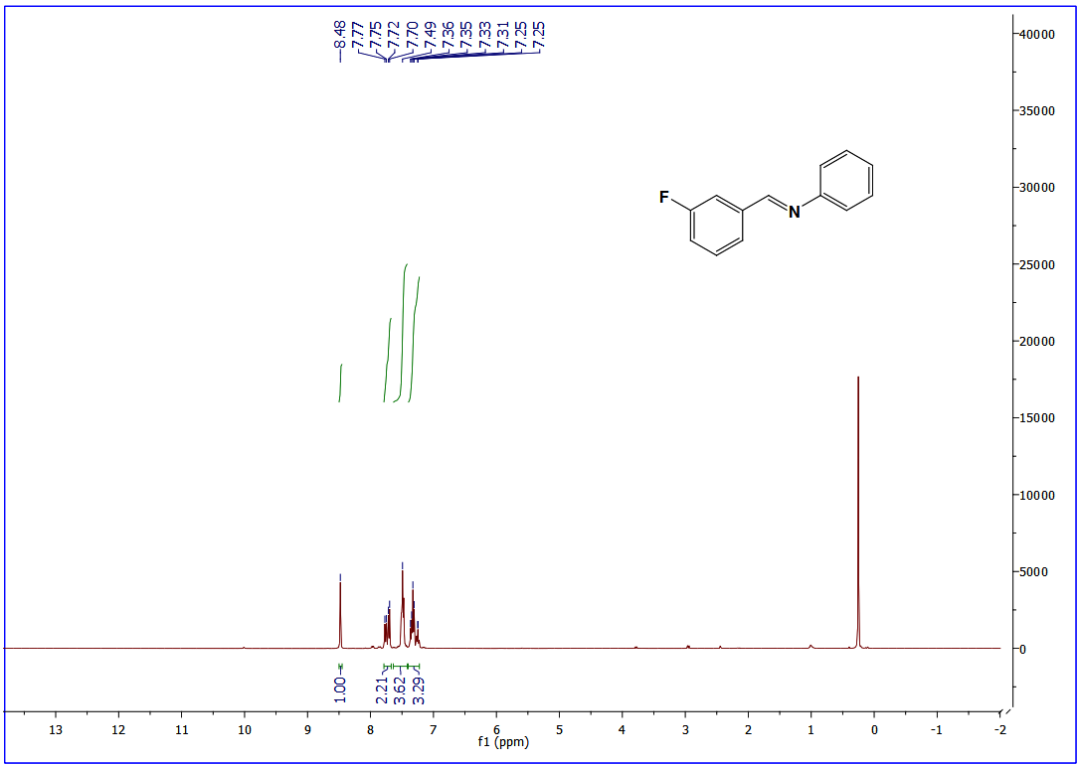

Figure 24. ^{1}H NMR spectrum for (**3e**) in $CDCl_3$ (400MHz, 300K).

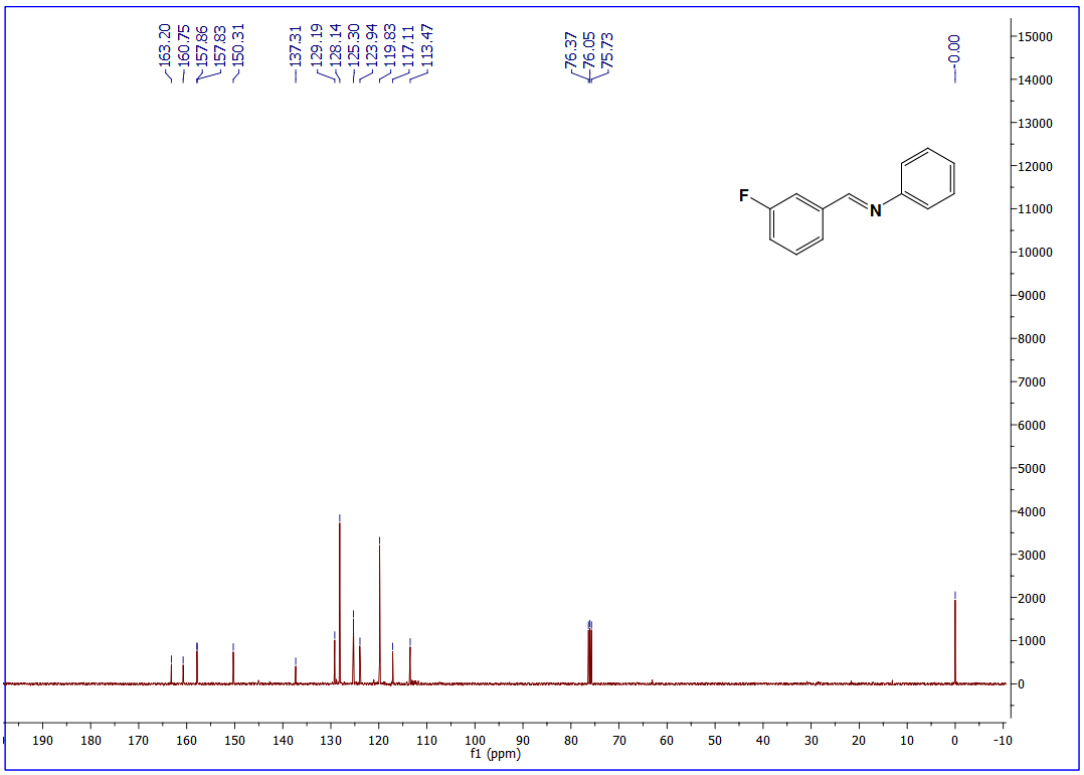

Figure 25. ^{13}C NMR spectrum for (**3e**) in $CDCl_3$ (100MHz, 300K).

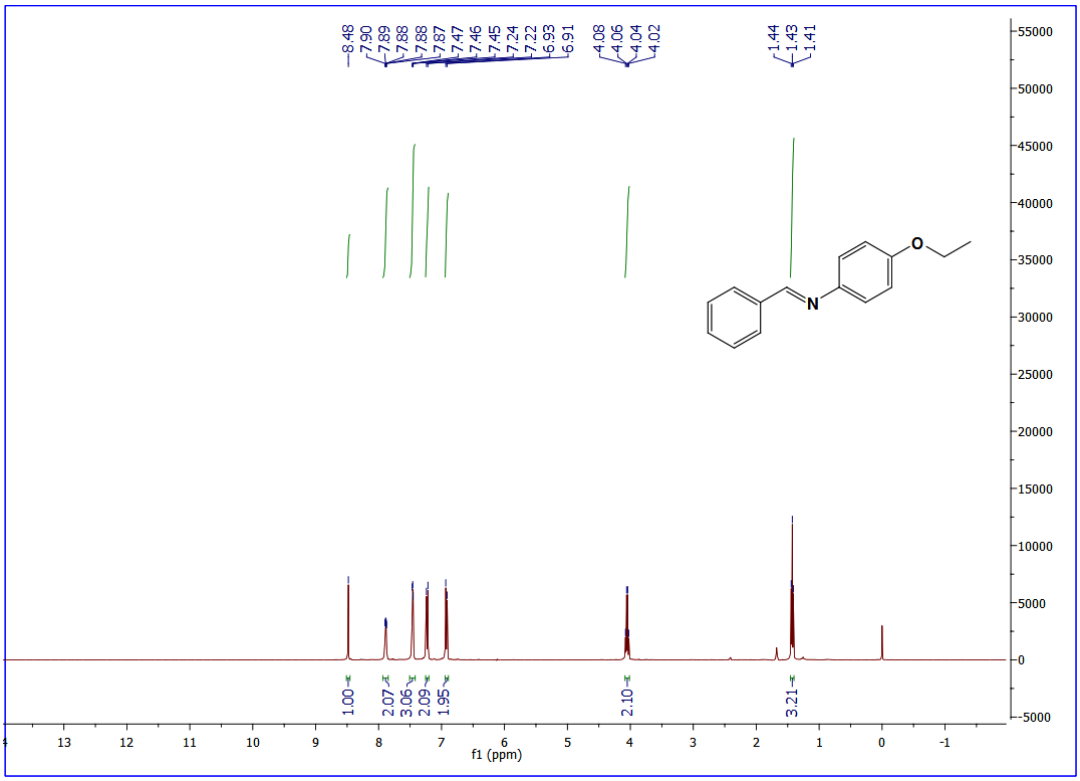

Figure 26. ^{1}H NMR spectrum for (**3f**) in $CDCl_3$ (400MHz, 300K).

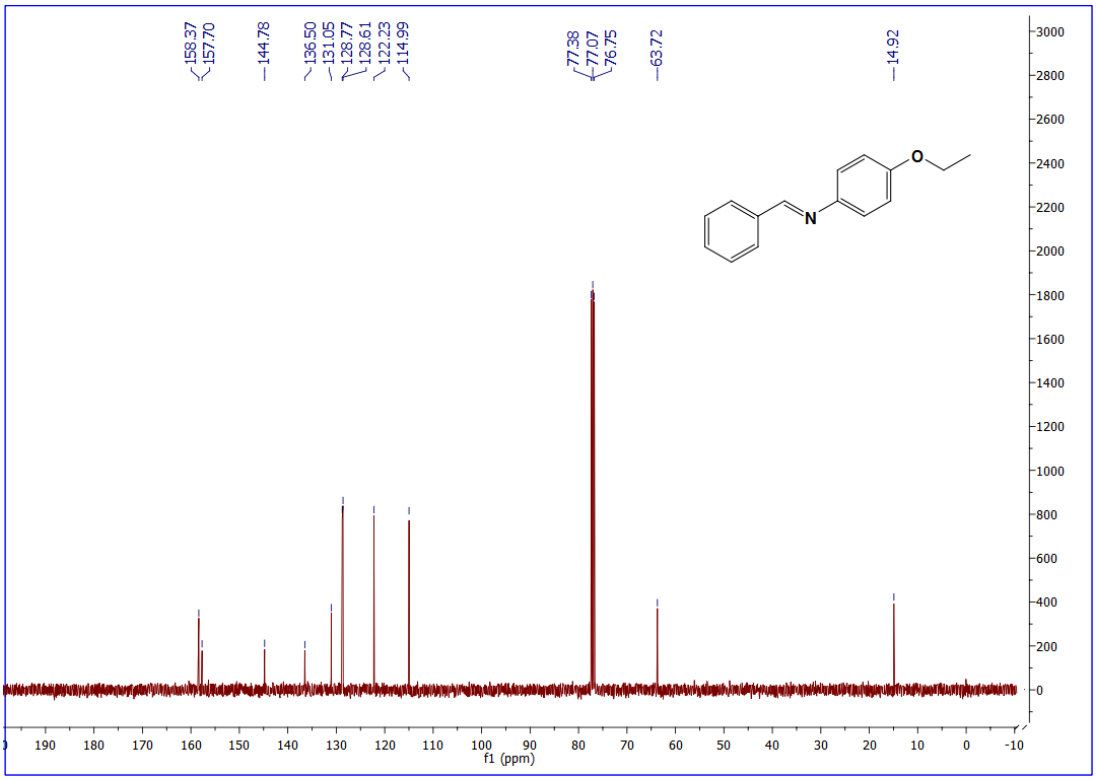

Figure 27. ^{13}C NMR spectrum for (**3f**) in $CDCl_3$ (100MHz, 300K).

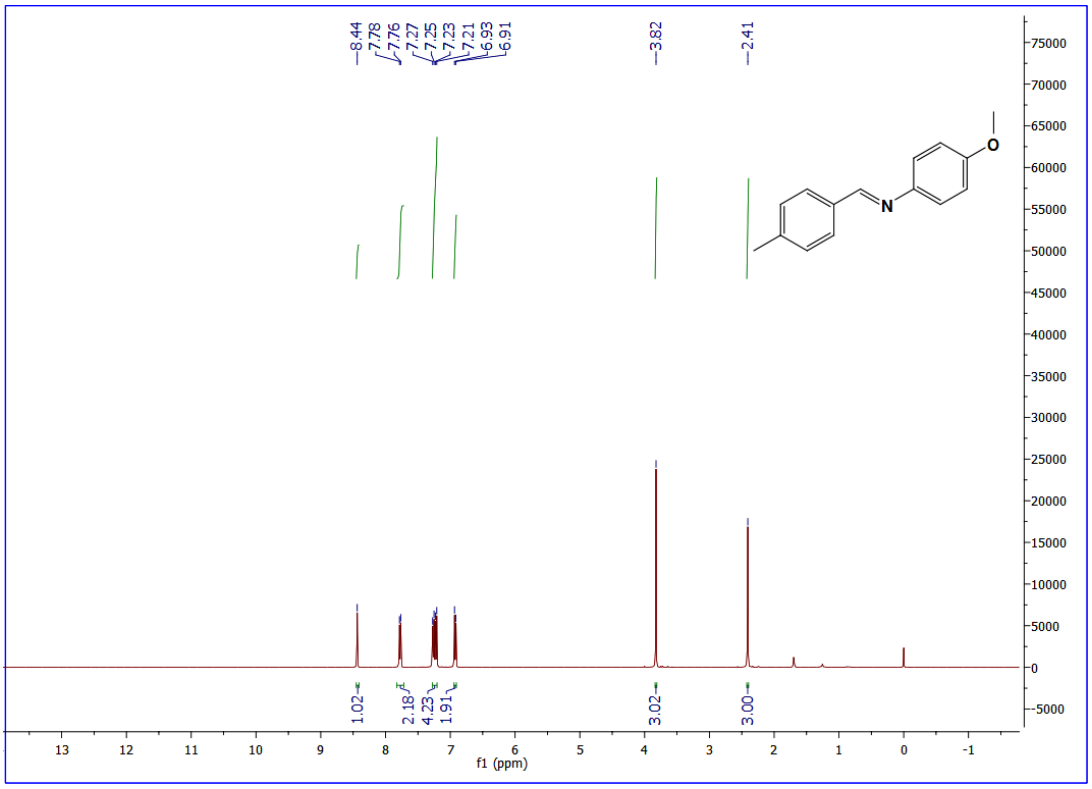

Figure 28. ^{1}H NMR spectrum for (**3g**) in $CDCl_3$ (400MHz, 300K).

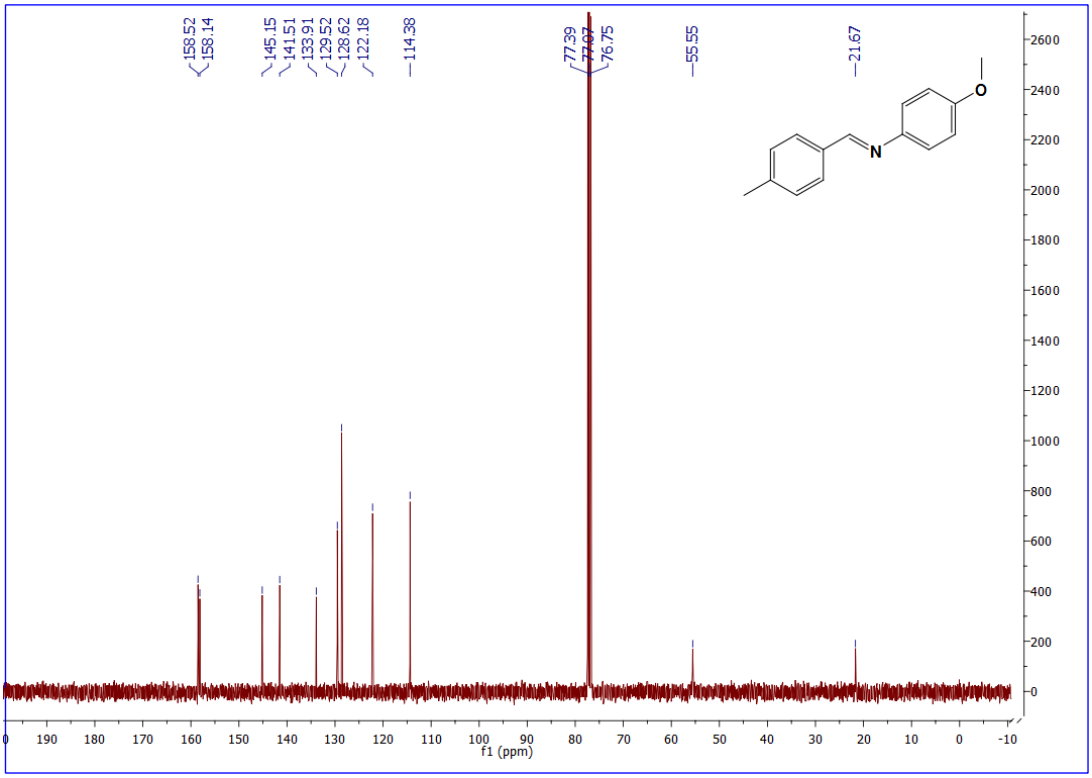

Figure 29. ^{13}C NMR spectrum for (**3g**) in $CDCl_3$ (100MHz, 300K).

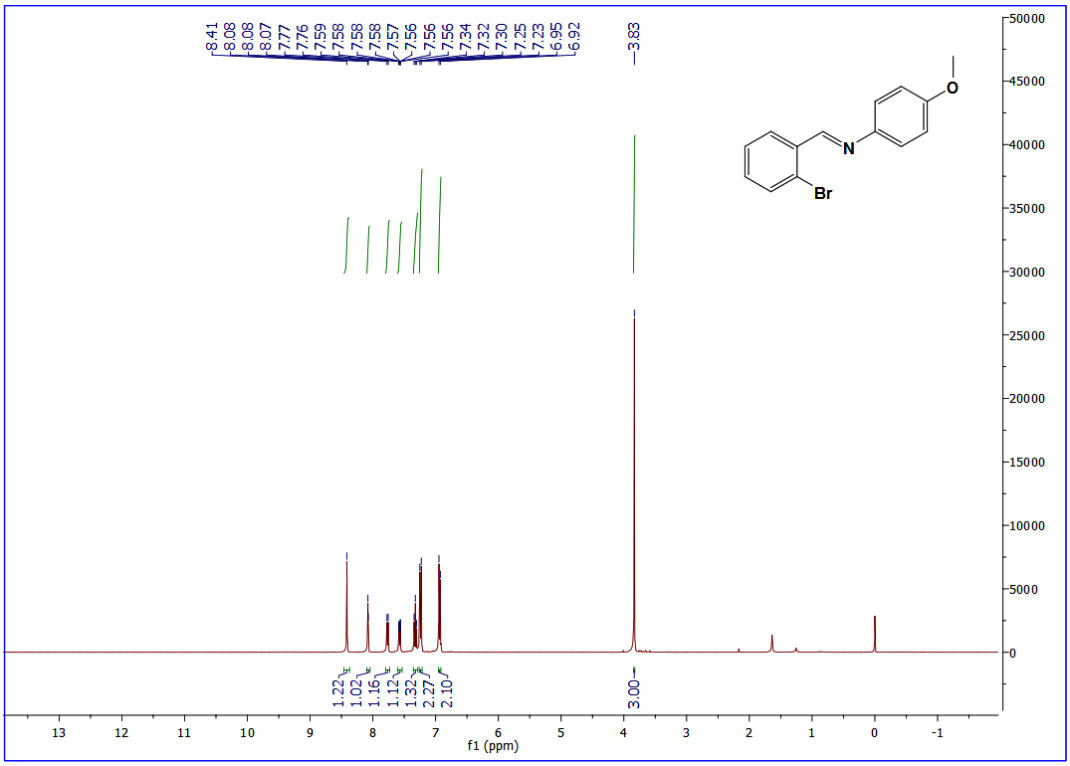

Figure 30. ^{1}H NMR spectrum for (**3h**) in $CDCl_3$ (400MHz, 300K).

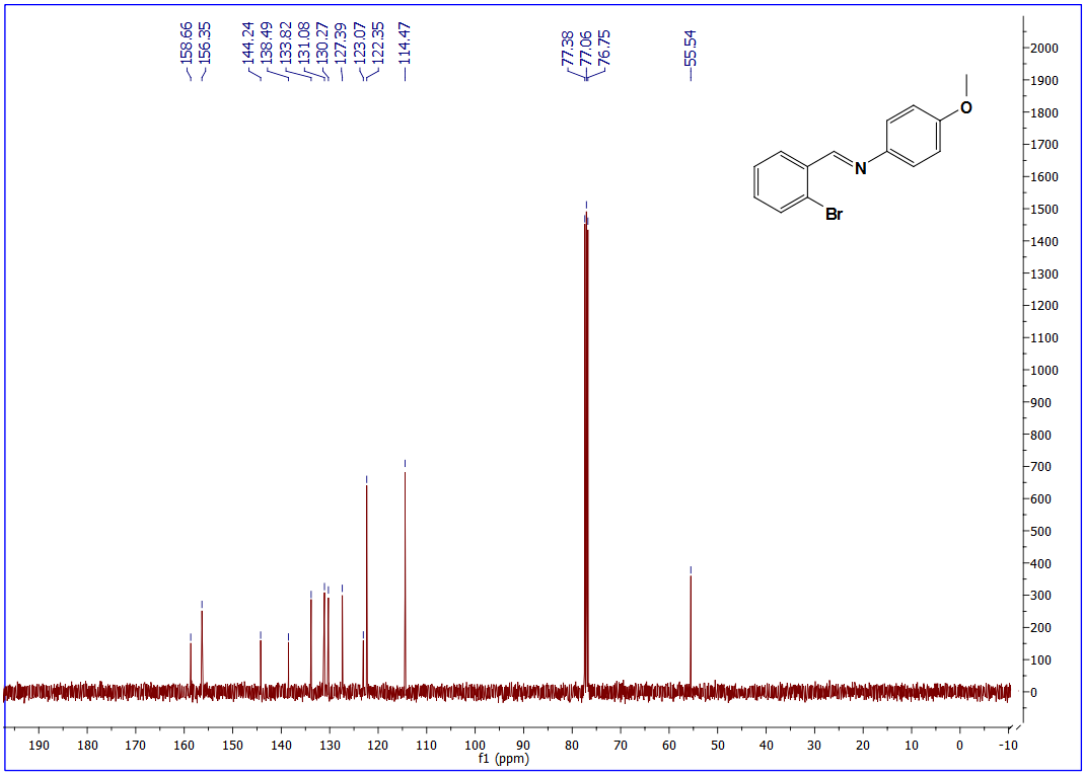

Figure 31. ^{13}C NMR spectrum for (**3h**) in $CDCl_3$ (100MHz, 300K).

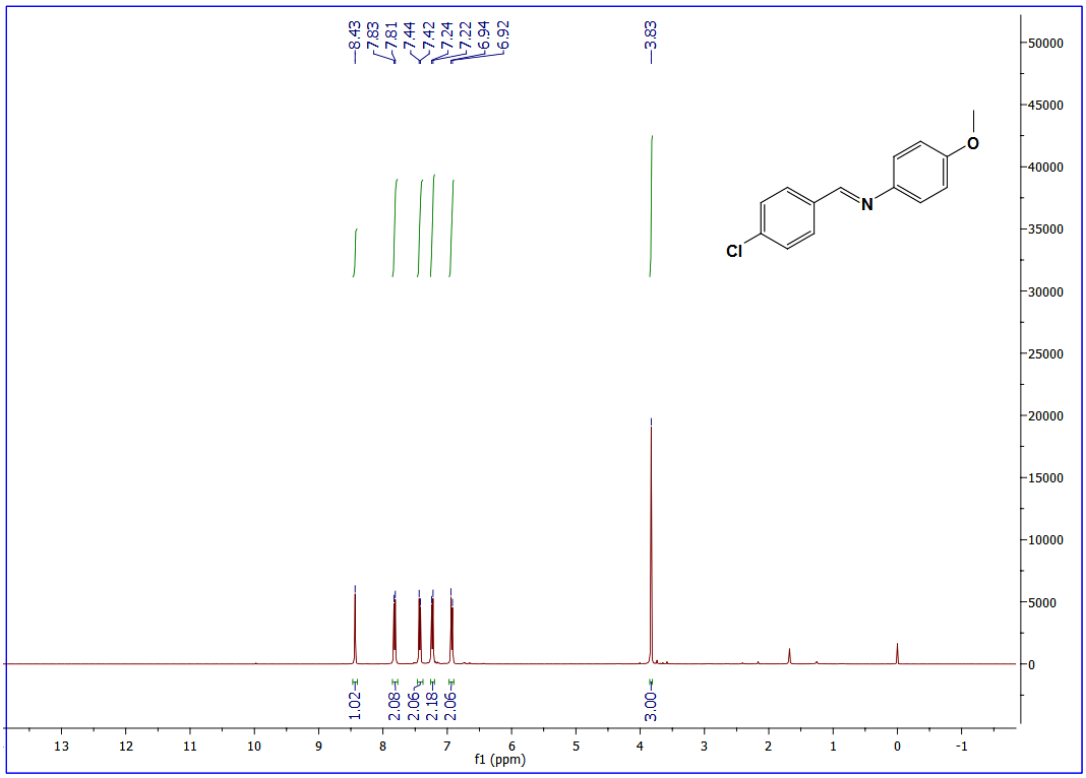

Figure 32. ^{1}H NMR spectrum for (**3i**) in $CDCl_3$ (400MHz, 300K).

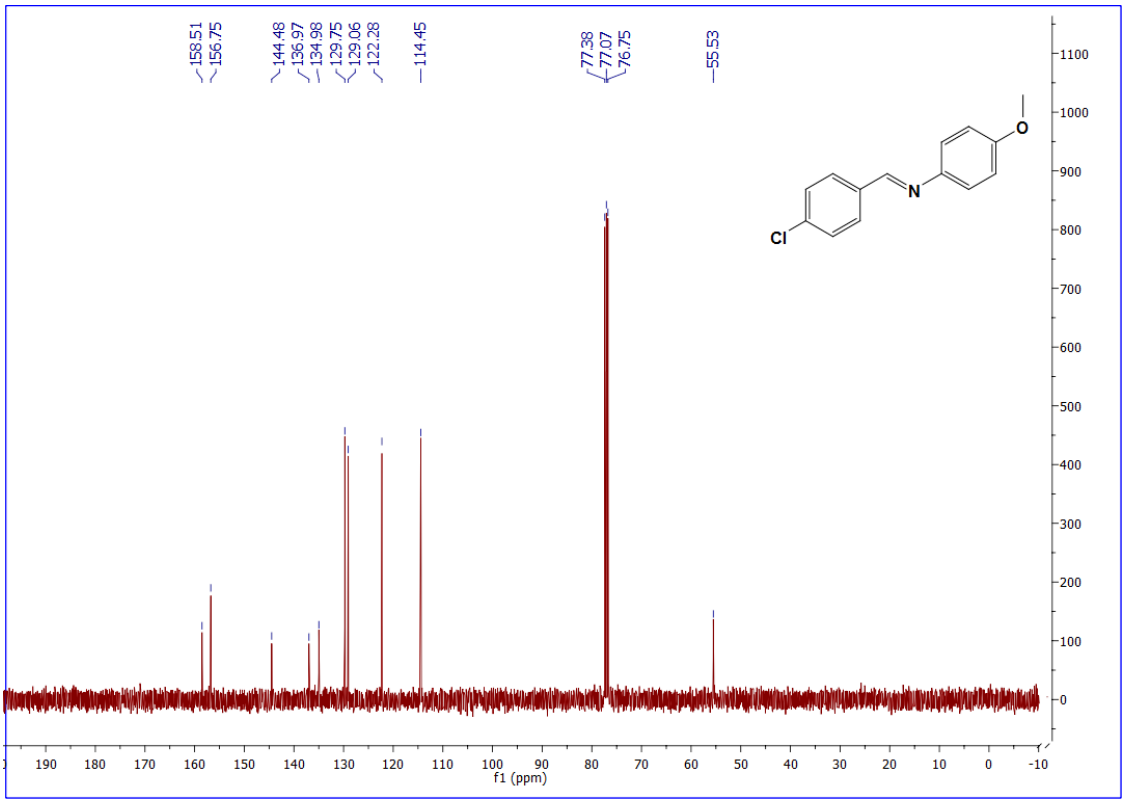

Figure 33. ^{13}C NMR spectrum for (**3i**) in $CDCl_3$ (100MHz, 300K).

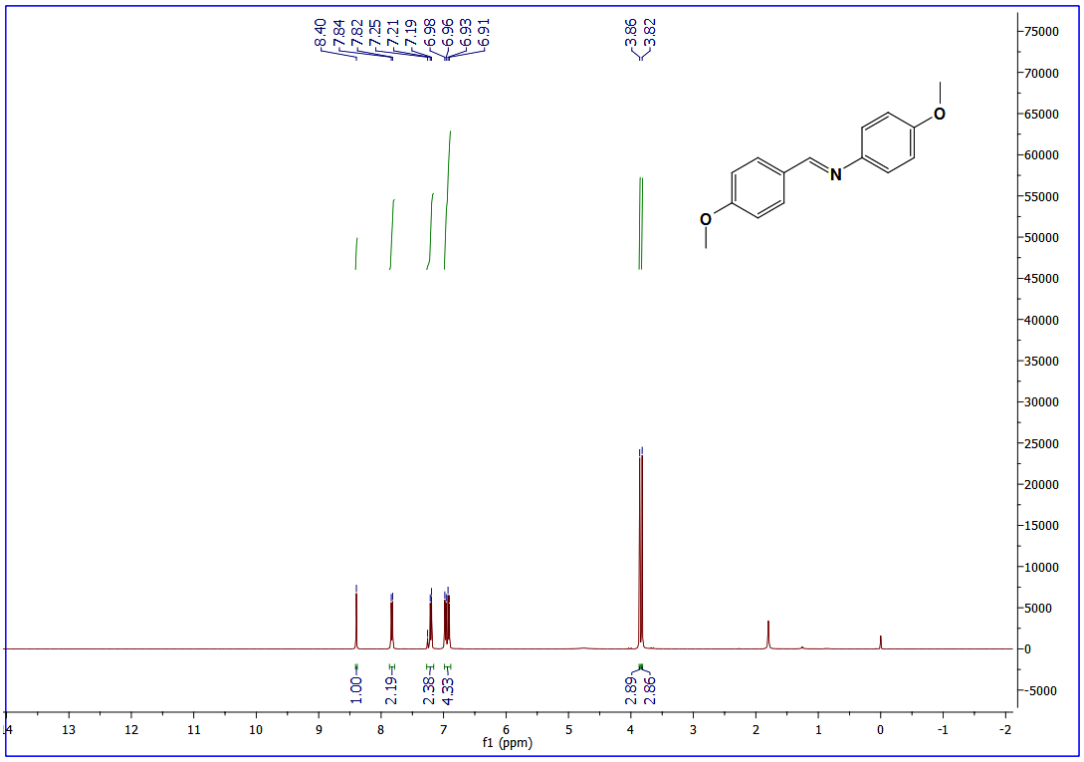

Figure 34. ^{1}H NMR spectrum for (**3j**) in $CDCl_3$ (400MHz, 300K).

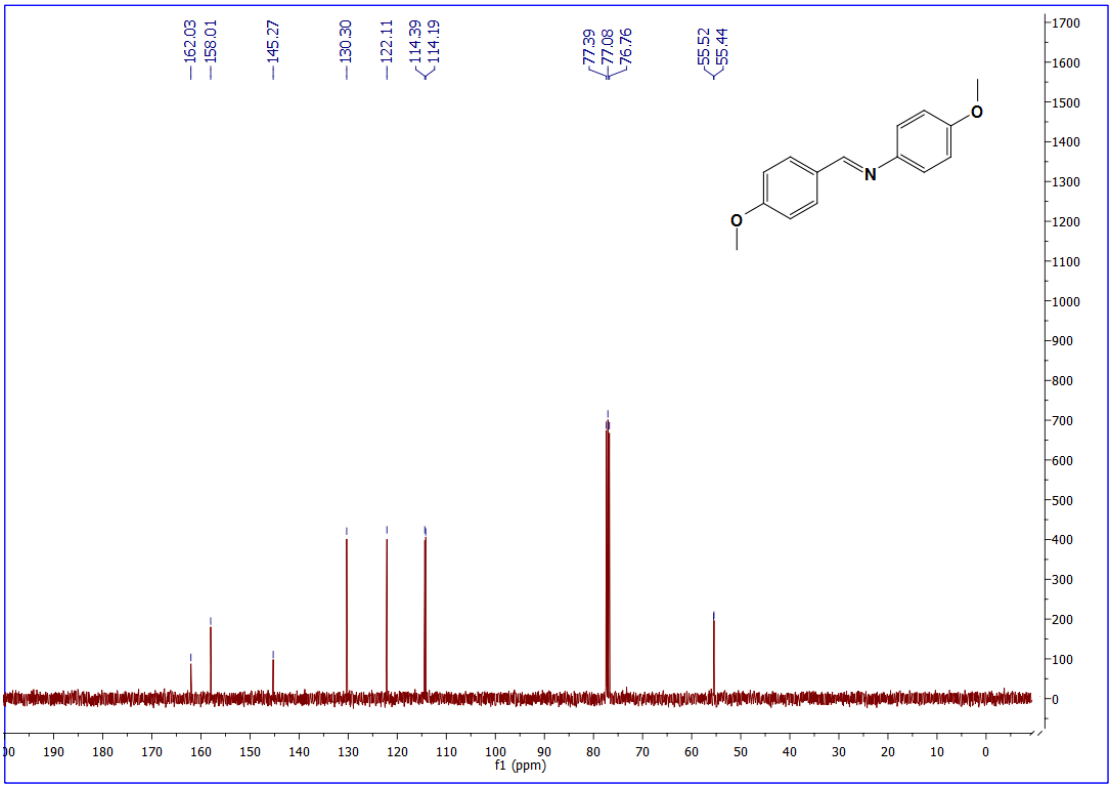

Figure 35. ^{13}C NMR spectrum for (**3j**) in $CDCl_3$ (100MHz, 300K).

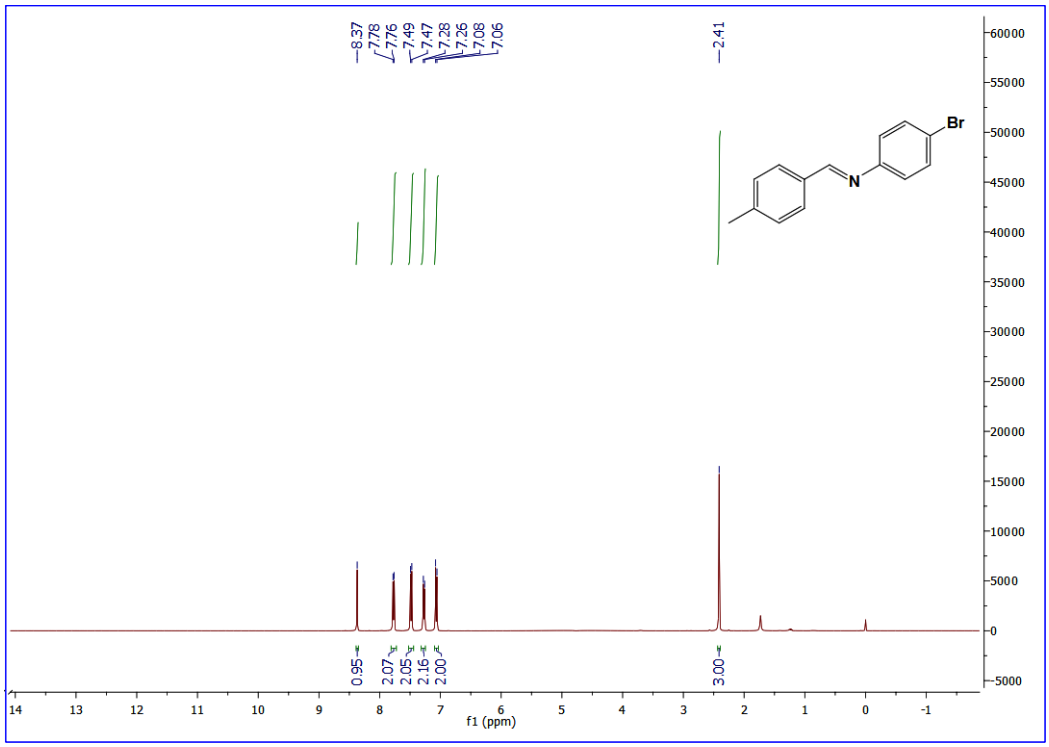

Figure 36. ^{1}H NMR spectrum for (**3k**) in $CDCl_3$ (400MHz, 300K).

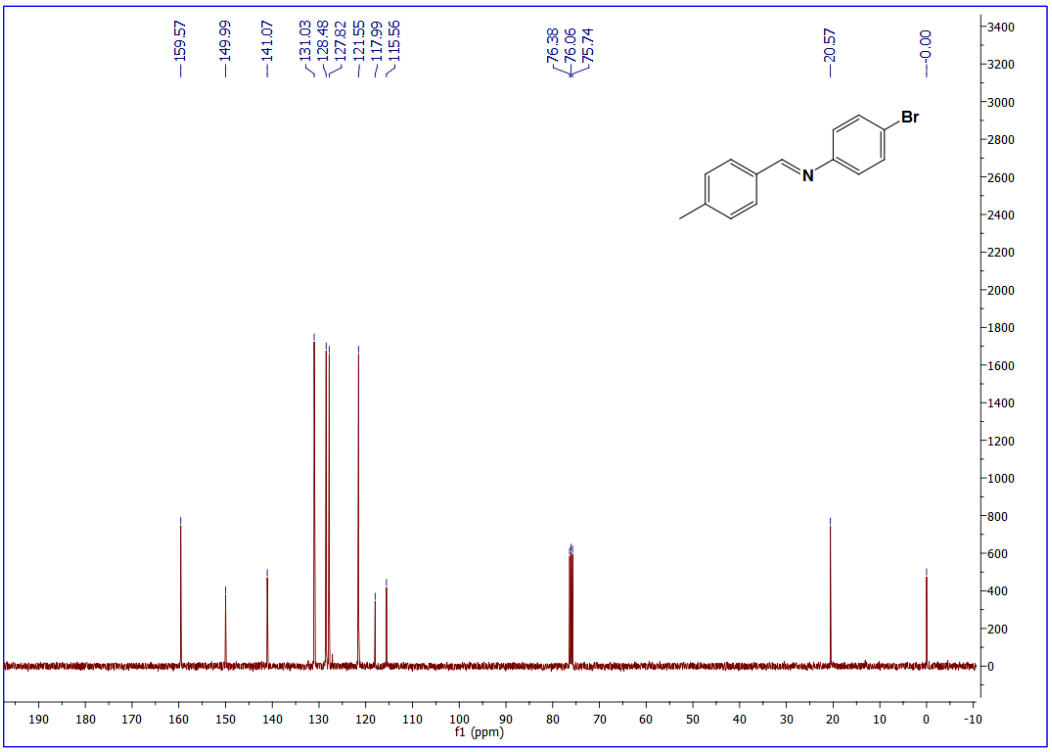

Figure 37. ^{13}C NMR spectrum for (**3k**) in $CDCl_3$ (100MHz, 300K).

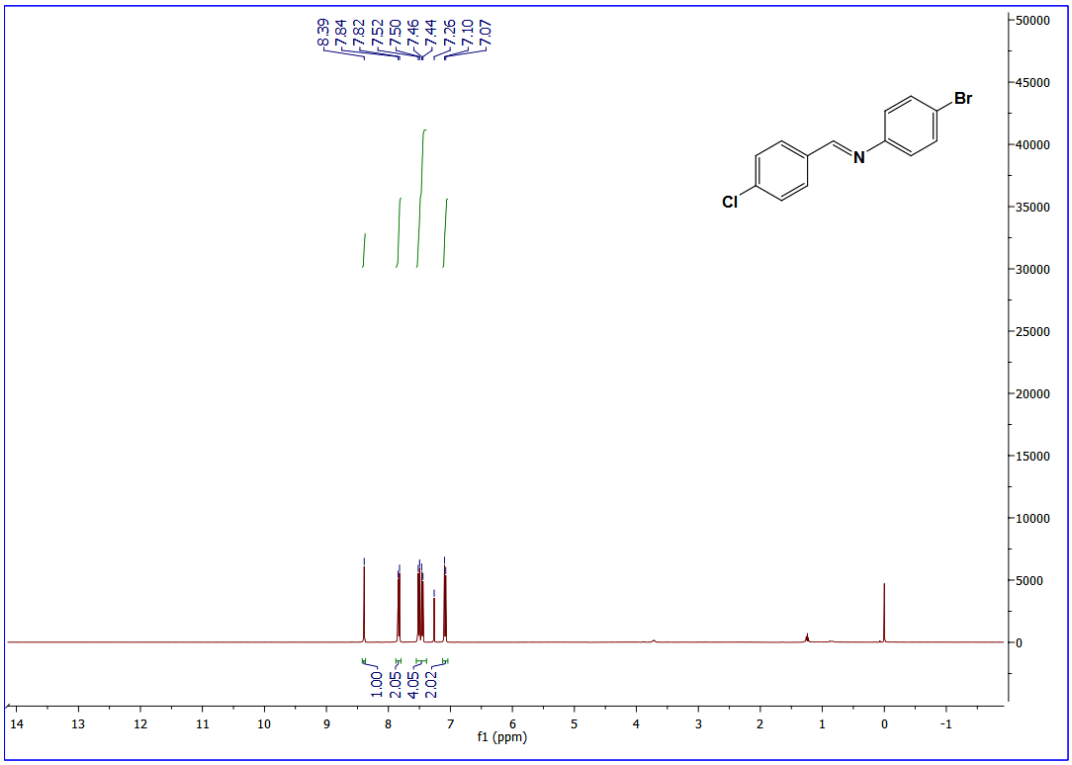

Figure 38. ^{1}H NMR spectrum for (**3l**) in $CDCl_3$ (400MHz, 300K).

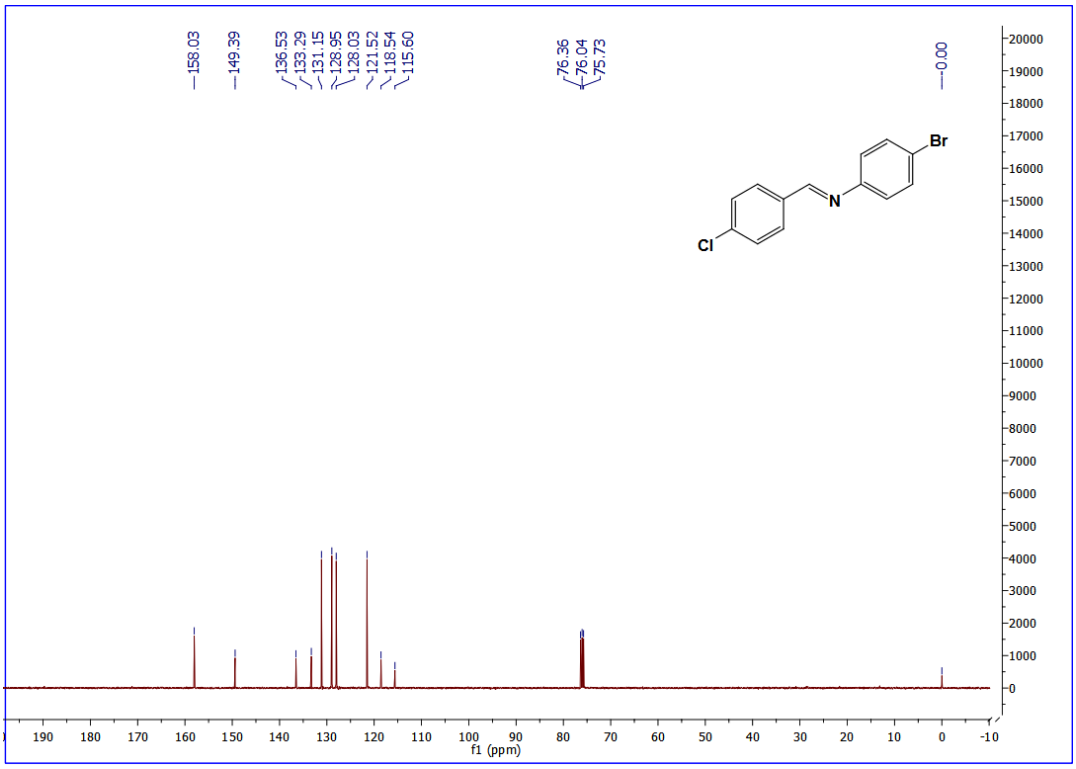

Figure 39. ^{13}C NMR spectrum for (**3l**) in $CDCl_3$ (100MHz, 300K).

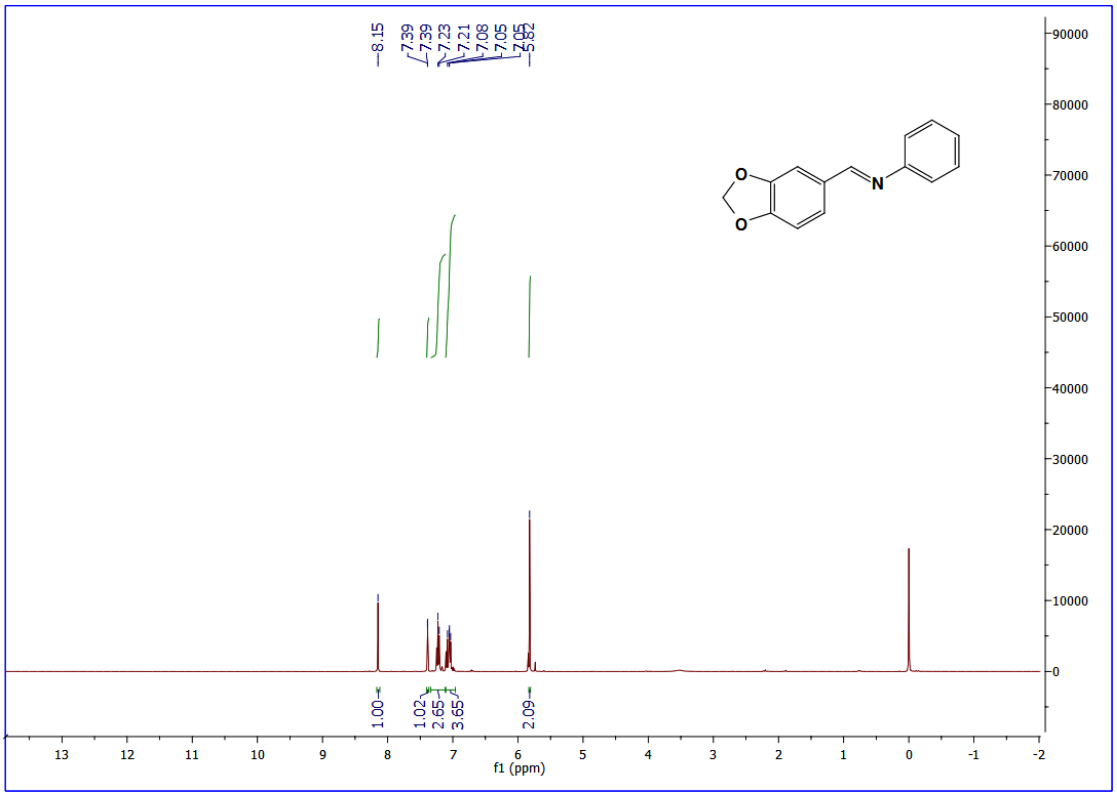

Figure 40. ^{1}H NMR spectrum for (**3m**) in $CDCl_3$ (400MHz, 300K).

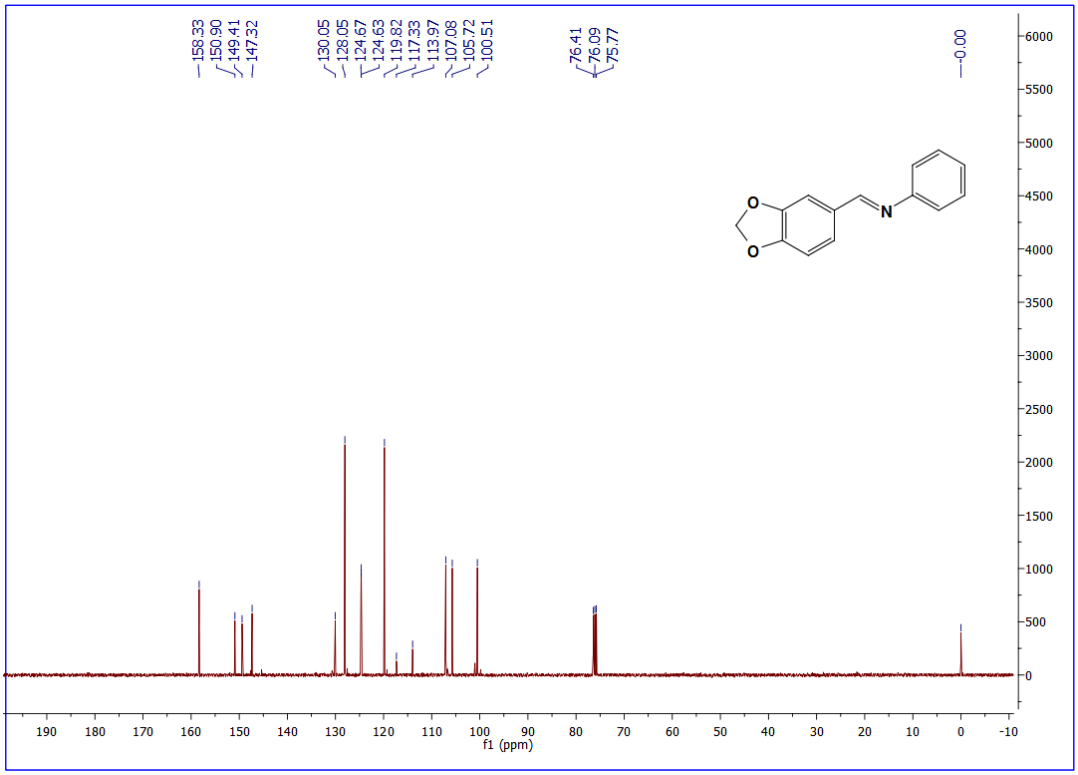

Figure 41. ^{13}C NMR spectrum for (**3m**) in $CDCl_3$ (100MHz, 300K).

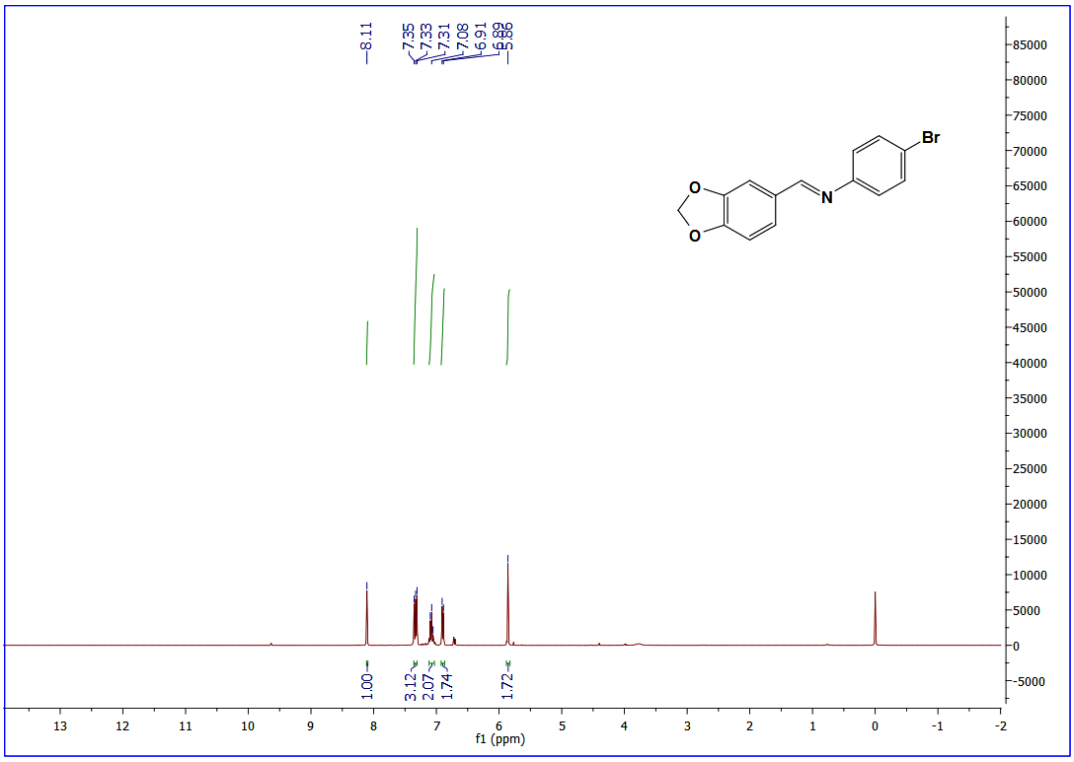

Figure 42. ^{1}H NMR spectrum for (**3n**) in $CDCl_3$ (400MHz, 300K).

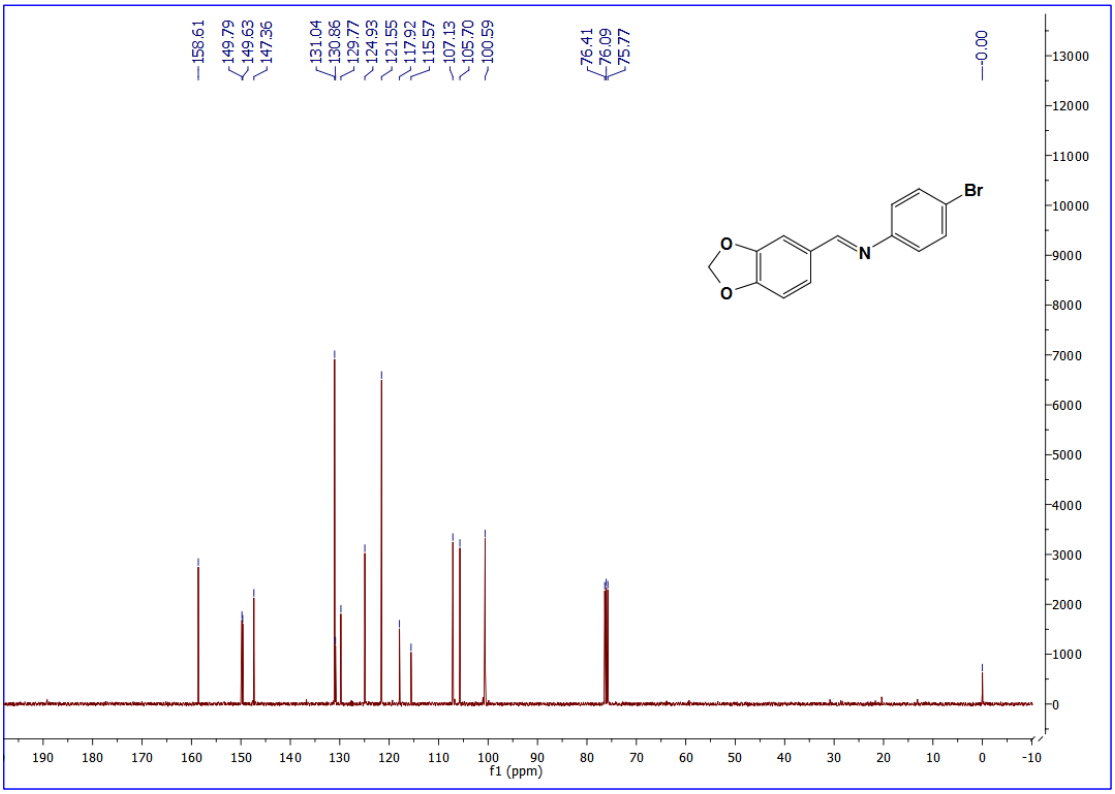

Figure 43. ^{13}C NMR spectrum for (**3n**) in $CDCl_3$ (100MHz, 300K).

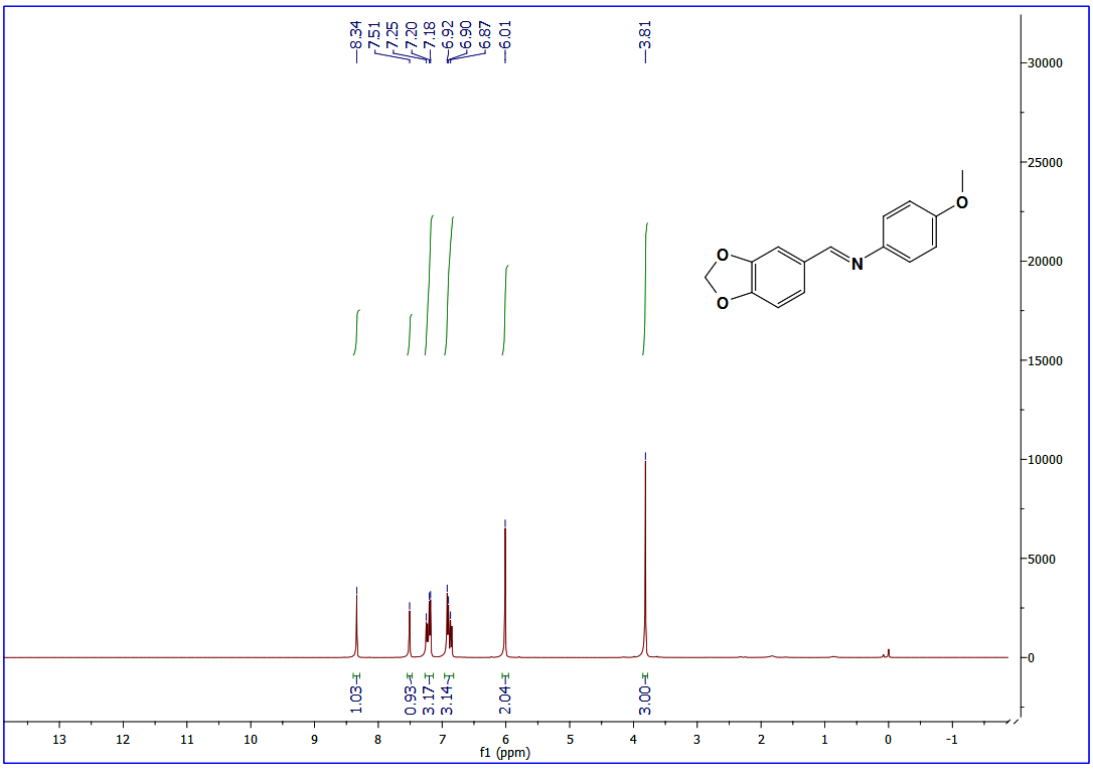

Figure 44. ^{1}H NMR spectrum for (**3o**) in $CDCl_3$ (400MHz, 300K).

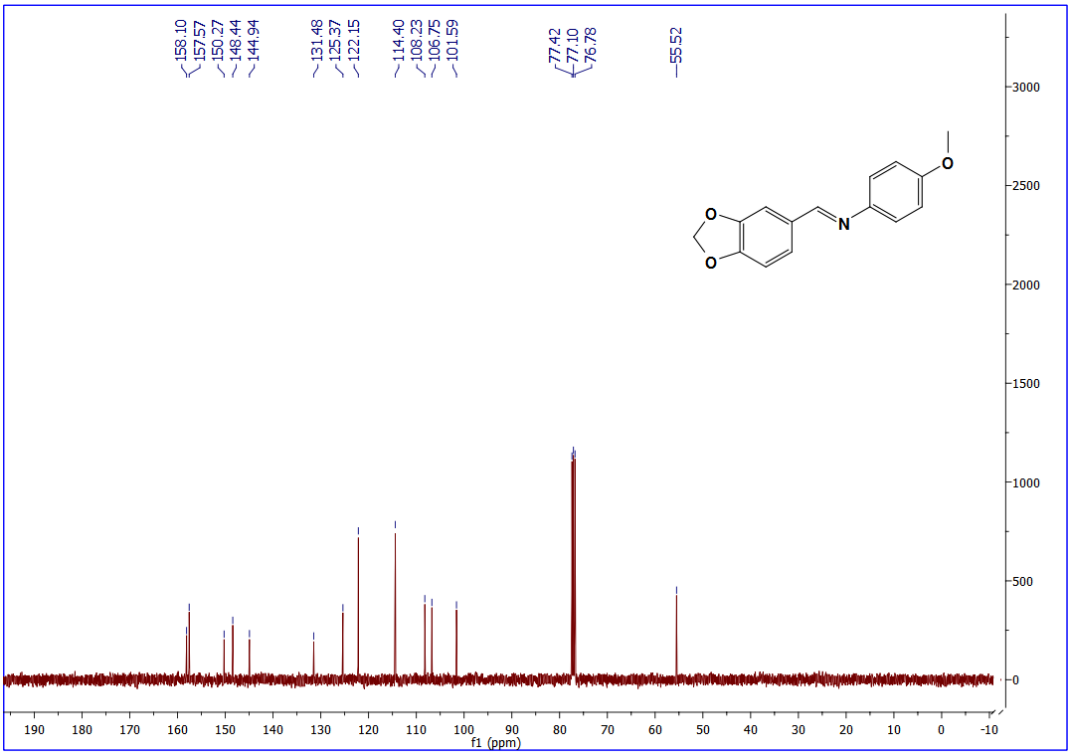

Figure 45. ^{13}C NMR spectrum for (**3o**) in $CDCl_3$ (100MHz, 300K).

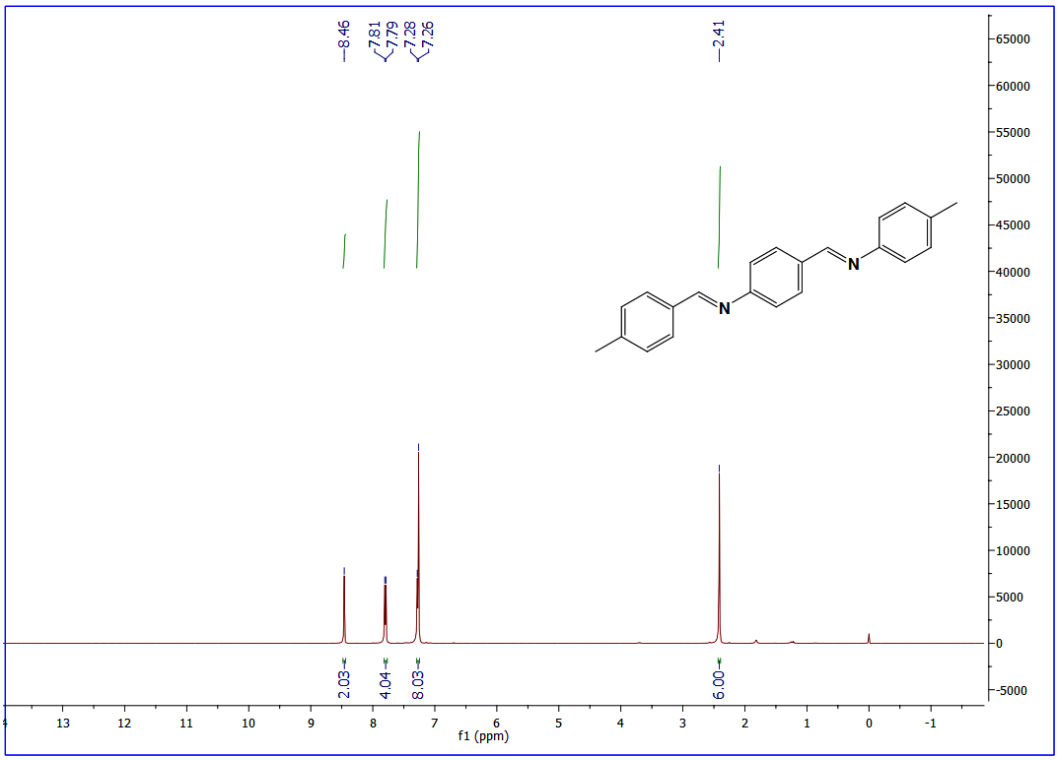

Figure 46. ^{1}H NMR spectrum for (**3p**) in $CDCl_3$ (400MHz, 300K).

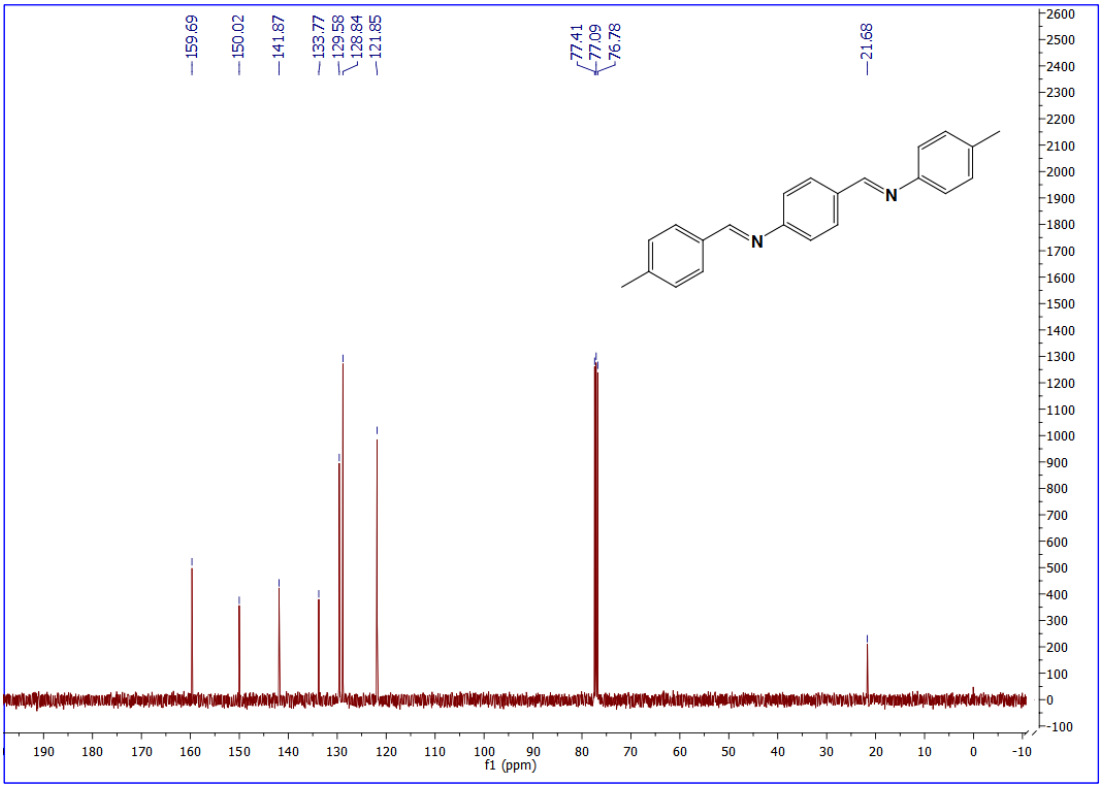

Figure 47. ^{13}C NMR spectrum for (**3p**) in $CDCl_3$ (100MHz, 300K).

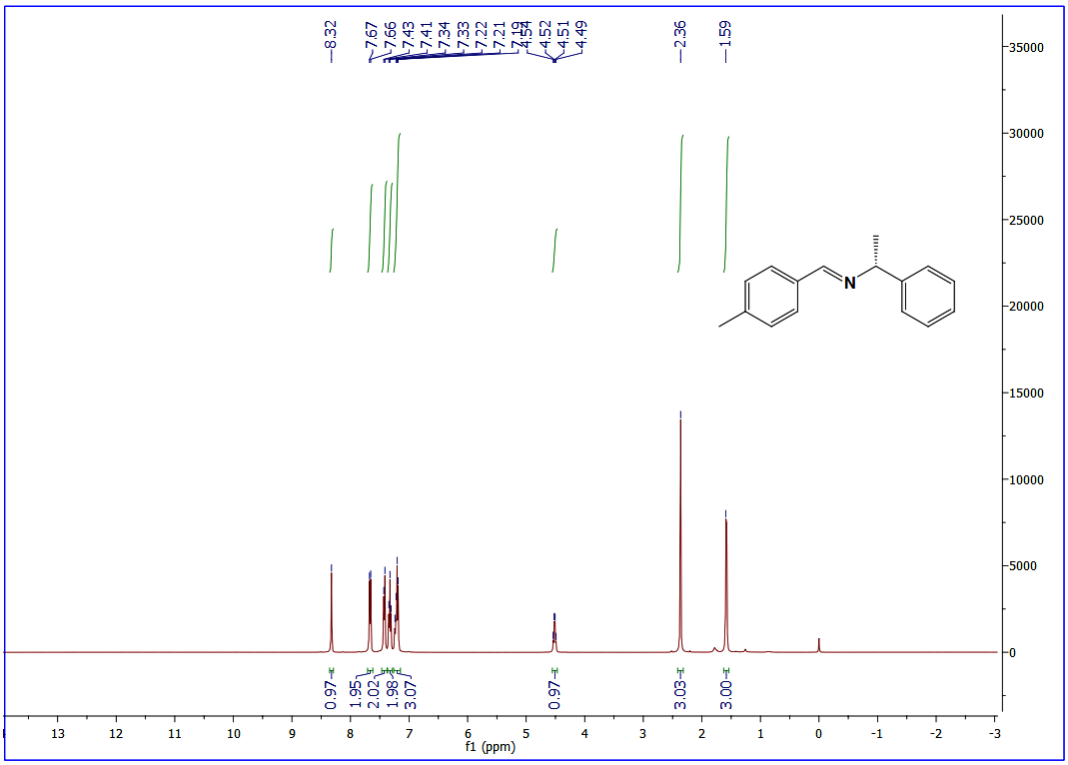

Figure 48. ^{1}H NMR spectrum for (**3q**) in $CDCl_3$ (400MHz, 300K).

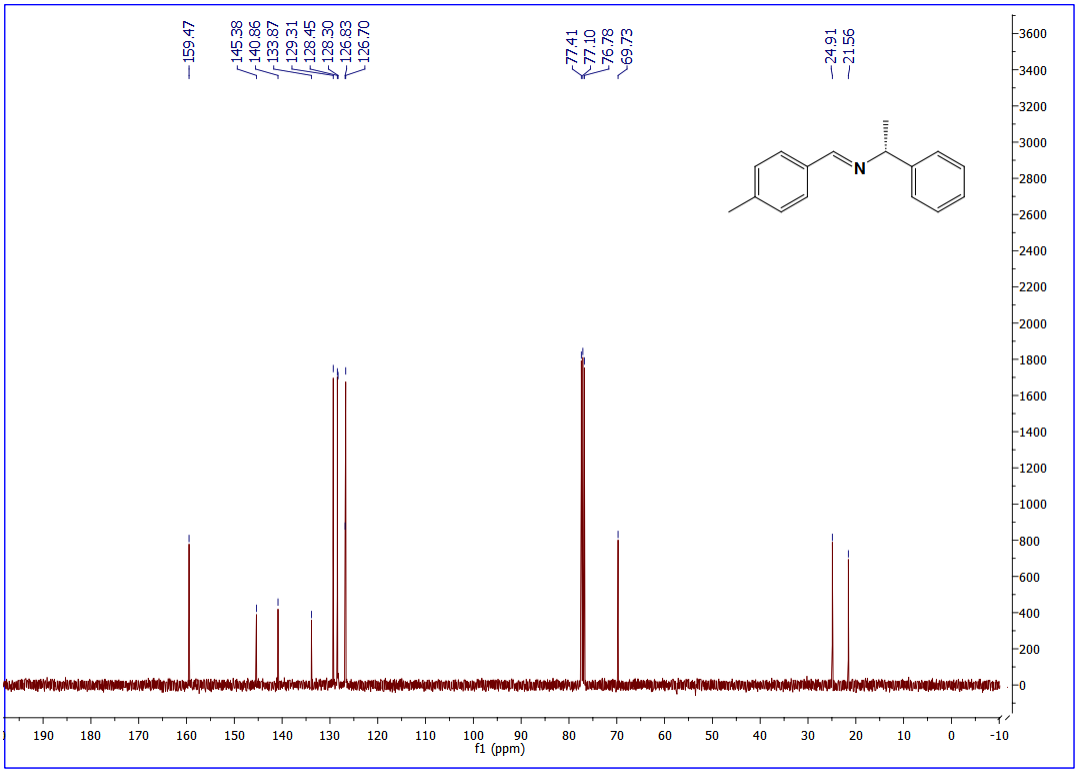

Figure 49. ^{13}C NMR spectrum for (**3q**) in $CDCl_3$ (100MHz, 300K).

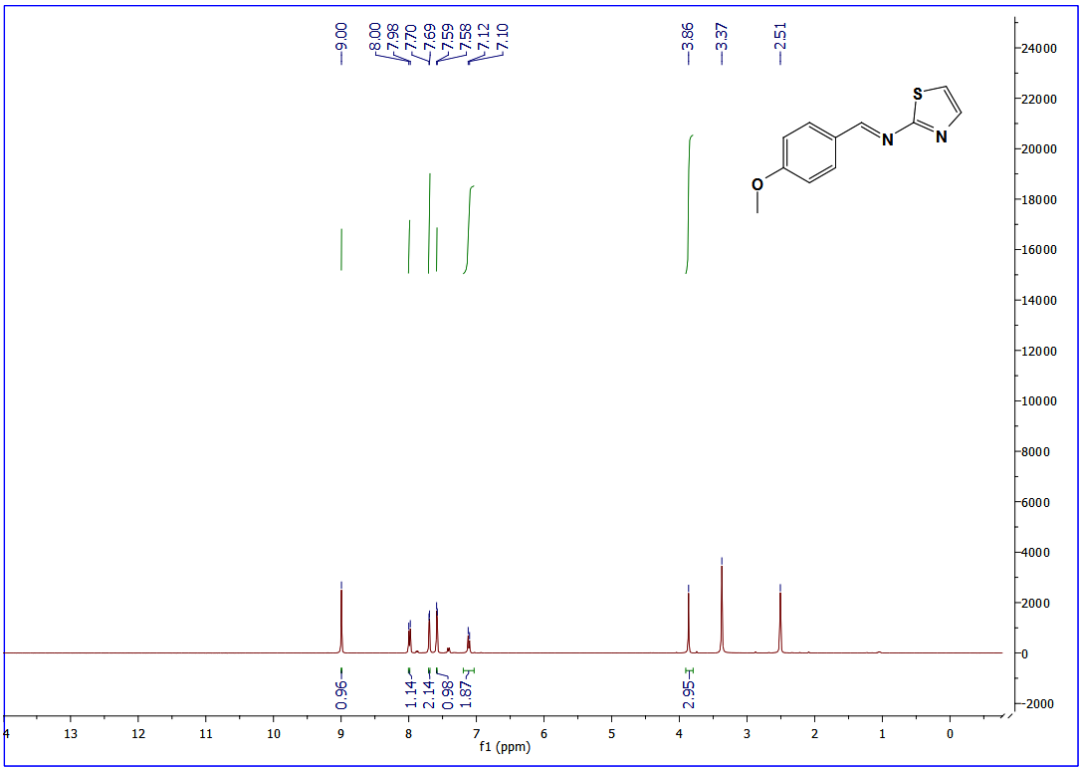

Figure 50. ^{1}H NMR spectrum for (**3r**) in DMSO-d_6 (400MHz, 300K).

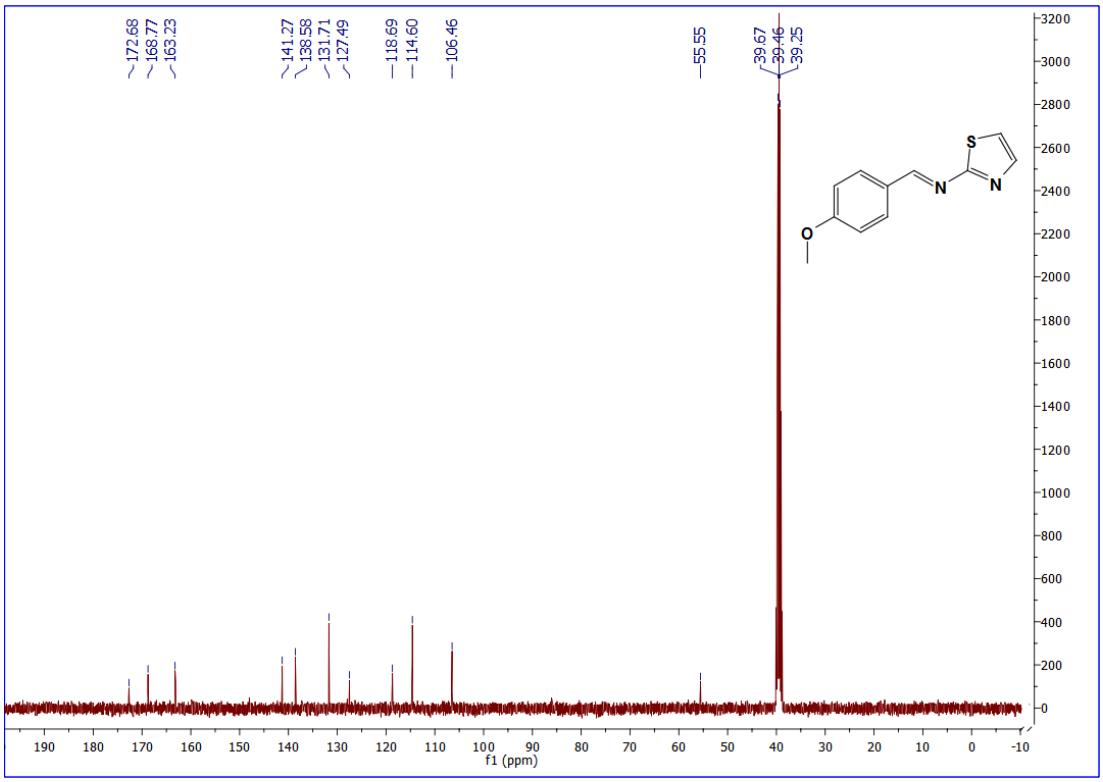

Figure 51. ^{13}C NMR spectrum for (**3r**) in DMSO-d_6 (100MHz, 300K).

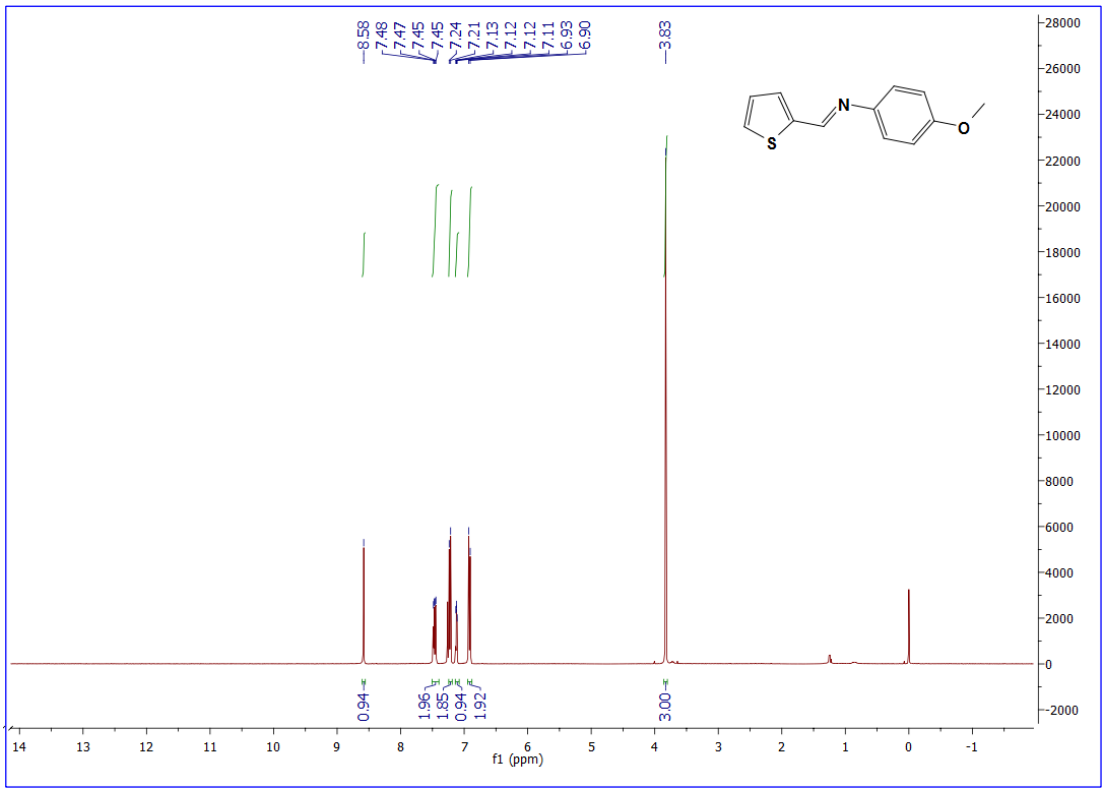

Figure 52. ^{1}H NMR spectrum for (**3s**) in $CDCl_3$ (400MHz, 300K).

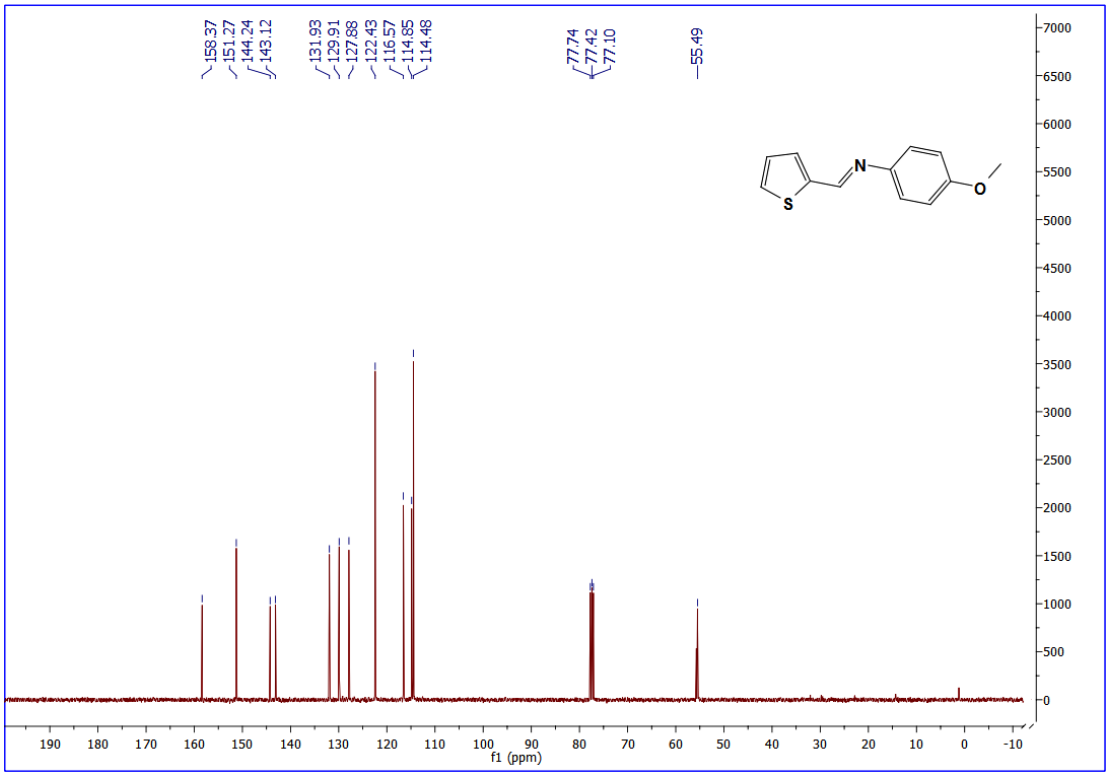

Figure 53. ^{13}C NMR spectrum for (**3s**) in $CDCl_3$ (100MHz, 300K).

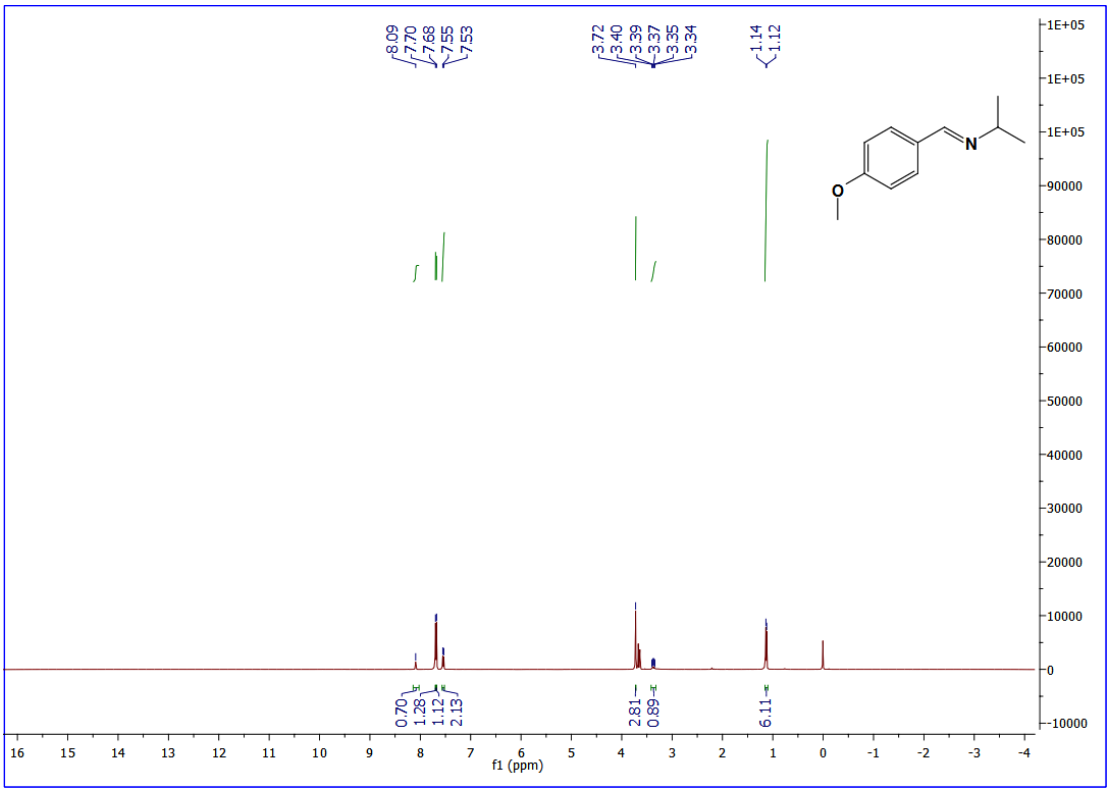

Figure 54. ^{1}H NMR spectrum for (**3t**) in $CDCl_3$ (400MHz, 300K).

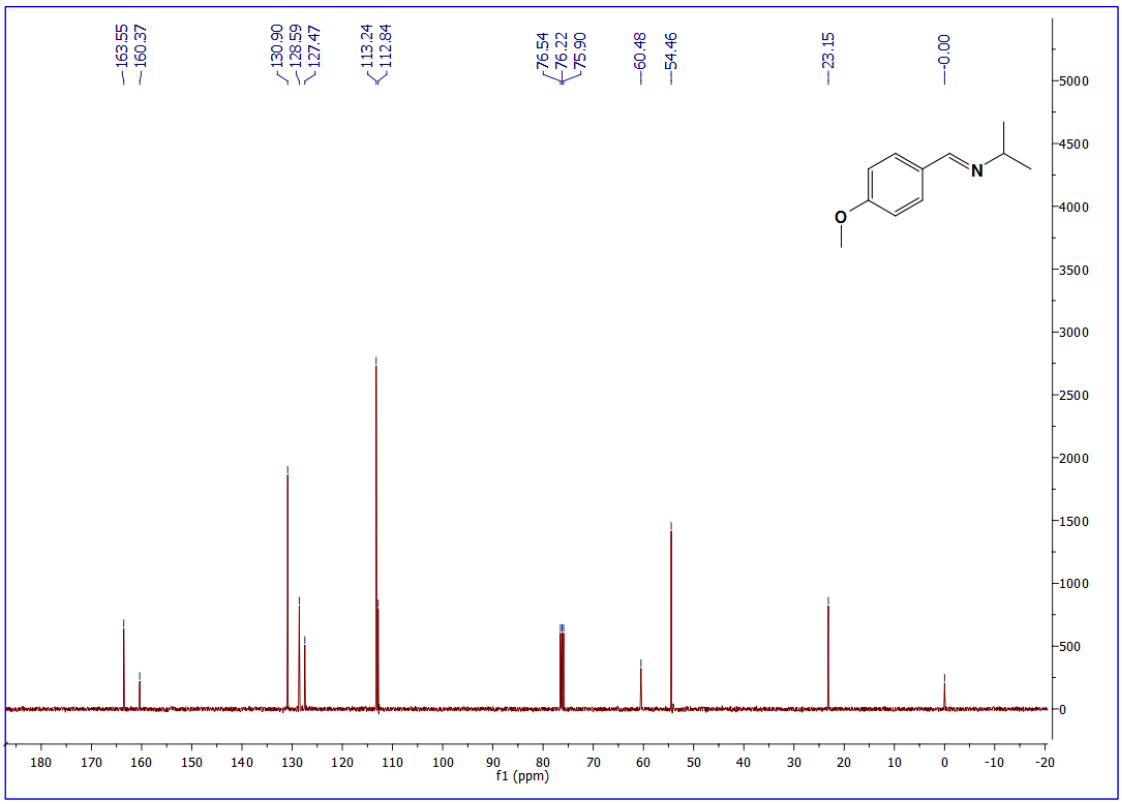

Figure 55. ^{13}C NMR spectrum for (**3t**) in $CDCl_3$ (100MHz, 300K).

NMR spectra for N-(Salicylidene)-2-hydroxyaniline

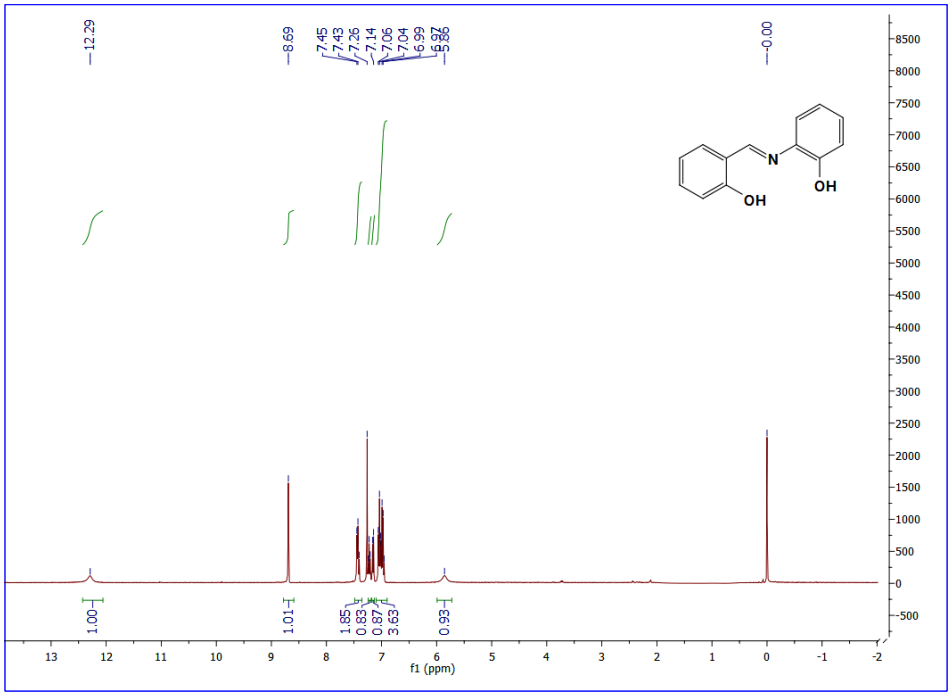

Figure 56. ^{1}H NMR spectrum for N-(Salicylidene)-2-hydroxyaniline in $CDCl_3$ (100MHz, 300K).

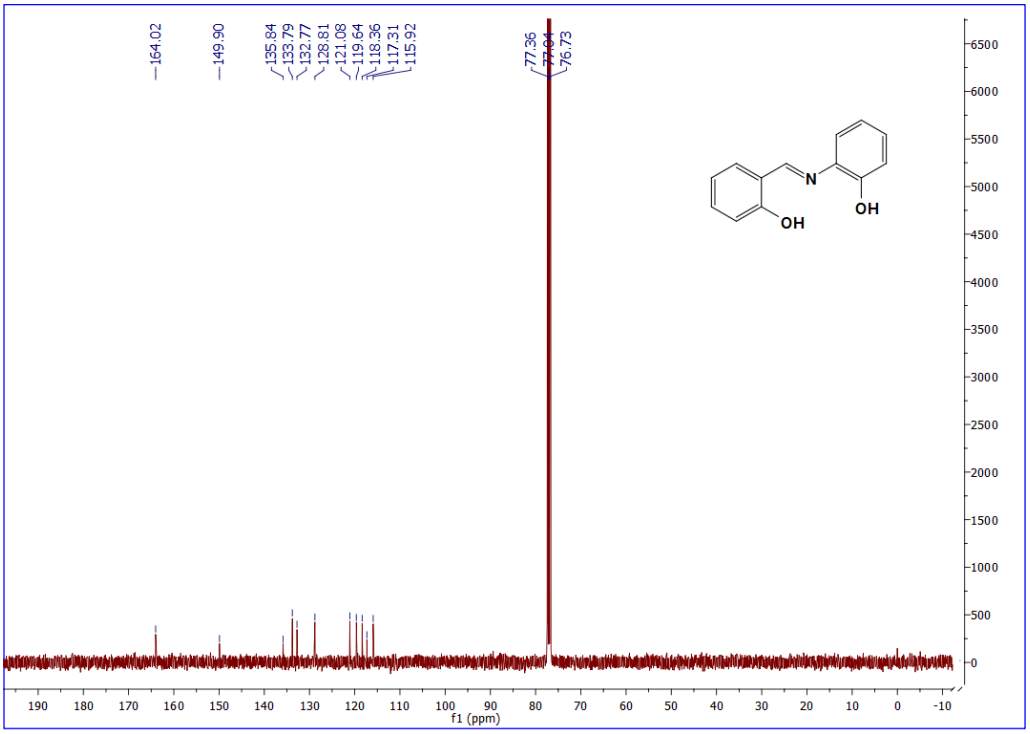

Figure 57. ^{13}C NMR spectrum for N-(Salicylidene)-2-hydroxyaniline in $CDCl_3$ (100MHz, 300K).

2.4. REFERENCES

1. (a) W. R. Layer, *Chem. Rev.* 1963, **63**, 489-510; (b) R. Bloch, *Chem. Rev.* 1998, **98**, 1407-1438; (c) S. Kobayashi and H. Ishitani, *Chem. Rev.* 1999, **99**, 1069-1094; (d) J. P. Adams, *J. Chem. Soc., Perkin Trans,* 2000, **1**, 125-139; (e) A. Erkkila, I. Majander, and P. M. Pihko, *Chem. Rev.* 2007, **107**, 5416-5470.

2. (a) J. Gawronski, N. Wascinska and J. J. Gajewy, *Chem Rev.* 2008, **108**, 5227-5252; (b) J. Adrio and J. C. Carretero, *Chem. Commun.* 2011, **47**, 6784-6794; (c) J. H. Xie, S. F. Zhu and Q. L. Zhou, *Chem. Rev.* 2011, **111**, 1713-1760; (d) S. Kobayashi, Y. Mori, J. S. Fossey and M. M. Salter, *Chem. Rev.* 2011, **111**, 2626-2704.

3. (a) S. Patai, The Chemistry of the Carbon Nitrogen Double Bond (Chemistry of Functional Goups); *Wiley Interscience:* New York, 1970; (b) Z. Guo, R. Xing, S. Liu, Z. Zhong, X. Ji and L. Wang, *Carbohydr Res.* 2007, **342**, 1329-1332; (c) S. F. Martin, *Pure Appl. Chem.* 2009, **81**, 195-204.

4. (a) E. M. Hodnett and P. D. Mooney, *J. Med. Chem.* 1970, **13**, 786-786; (b) C. M. Silva and D. L. Silva, *Journal of Advanced Research.* 2011, **2**, 1-8.

5. (a) R. D. Patil and S. Adimurthy, *Asian J. Org. Chem.* 2013, **2**, 726-744; (b) W. Qin, S. Long, S. M. Panunzio and S. Biondi, *Molecules.* 2013, **18**, 12264-12289.

6. (a) P. T. Lansbury and J. G. Colson, *J. Am. Chem. Soc.* 1962, **84**, 4167-4169; (b) F. Palacios, C. Alonso, D. Aparicio and G. Rubiales, *Tetrahedron.* 2007, **63**, 523-575.

7. (a) M. Ochiai, D. Kajishima and T. Sueda, *Heterocycles.* 1997, **46**, 71-76; (b) K. Orito, T. Hatakeyama, M. Takeo, S. Uchiito, M. Tokuda and H. Suginome, *Tetrahedron.* 1998, **54**, 8403-8410.

8. (a) F. Westheimer and K. J. Taguchi, *Org. Chem.* 1971, **36**, 1570-1572; (b) R. S. Varma, R. Dahiya and S. Kumar, *Tetrahedron Lett.* 1997, **38**, 2039-2042; (c) H. Naeimi, F. Salimi and K. Rabiei, *J. Mol. Catal. A: Chem.* 2006, **260**, 100-104; (d) J. T. Reeves, M. D. Visco, M. A. Marsini, N. Grinberg, C. A. Busacca, A. E. Mattson and C. H. Senanayake, *Org. Lett.* 2015, **17**, 2442-2445.

9. B. Gnanaprakasam, J. Zhang and D. Milstein, *Angew. Chem., Int. Ed.* 2010, **49**, 1468-1471.

10. (a) R. Cano, D. J. Ramon and M. J. Yus, *Org. Chem.* 2011, **76**, 5547-5557; (b) A. Maggi and R. Madsen, *Organometallics.* 2012, **31**, 451-455; (c) G. Vinoth, S. Indira, M. Bharathi, A. Durgadevi, R. Abinaya, L. G. Alves, A. M. Martin and K. S.

Bharathi, *Appl. Organometal. Chem*, 2019, **33**, e5200; (d) X. N. Fan, H. D. Ou, W. Deng and Z. J. Yao, *Inorg. Chem.* 2020, **59**, 4800-4809.

11. (a) M. A. Esteruelas, N. Honczek, M. Oliván, E. Onate and M. Valencia, *Organometallics.*, 2011, **30**, 2468-2471; (b) Y. H. Li, X. L. Liu, Z. T. Yu, Z. S. Li, S. C. Yan, G. H. Chen and Z. G. Zou, *Dalton Trans.* 2016, **45**, 12400-12408.

12. (a) M. S. Kwon, S. Kim, S. Park, W. Bosco, R. K. Chidrala and J. Park, *J. Org. Chem.* 2009, **74**, 2877-2879; (b) L. Jiang, L. Jin, H. Tian, X. Yuan, X. Yu and Q. Xu, *Chem. Commun.* 2011, **47**, 10833-10835.

13. Y. Shiraishi, M. Ikeda, D. Tsukamoto, S. Tanaka and T. Hiraia, *Chem. Commun.* 2011, **47**, 4811-4813.

14. (a) H. Sun, F. Z. Su, J. Ni, Y. Cao, H. Y. He and K. N. Fan, *Angew. Chem., Int. Ed.* 2009, **48**, 4390-4393; (b) S. Kegnæs, J. Mielby, U. V. Mentzel, C. H. Christensen and A. Riisager, *Green Chem.* 2010, **12**, 1437-1441.

15. J. Soule, H. Miyamura and S. Kobayashi, *Chem. Commun.* 2013, **49**, 355-357.

16. R. R. Donthiri, R. D. Patil and S. Adimurthy, *Eur. J. Org. Chem.*, 2012, **24**, 4457-4460.

17. H. Tian, X. Yu, Q. Li, J. Wang and Q. Xua, *Adv. Synth. Catal.* 2012, **354**, 2671-2677.

18. E. Zhang, H. Tian, S. Xu, X. Yu and Q. Xu, *Org. lett.* 2013, **15**, 2704-2707.

19. S. P. Midya, J. Pitchaimani and E. Balaraman, *Catal. Sci. Technol.* 2018, **8**, 3469-3473.

20. (a) A. Furstner, H. Krause and C. W. Lehmann, *Chem. Commun.* 2001, **1**, 2372-2373; (b) J. Buijtenen, J. Meuldijk, J. A. Vekemans, L. A. Hulshof, H. Kooijman and A. L. Spek, *Organometallics.*, 2006, **25**, 873-881; (c) B. Punji, J. T. Mague and M. S. Balakrishna, *Inorg. Chem.* 2007, **46**, 11316-11327; (d) S. Priyarega, D. S. Raja, S. Ganesh Babu, R. Karvembu, T. Hashimoto, A. Endo and K. Natarajan, *Polyhedron.* 2012, **34**, 143-148; (e) K. C. Cheung, L. Wong, M. H. So, Z. Y. Zhou, S. C. Yan and K. Y. Wong, *Chem. Commun.* 2013, **49**, 710-712; (f) N. P. Mankad, *Chem. Eur. J.* 2016, **22**, 5822-5829; (g) D. R. Pye and N. P. Mankad, *Chem. Sci.* 2017, **8**, 1705-1718; (h) T. S. Manikandan, R. Ramesh and D. Semeril, *Organometallics.* 2019, **38**, 319-328.

21. Vogel, A. I.; Test book of practical organic chemistry, Longman, London, 5th edn, 1989, p.395.

22. K. A. Alfallous and M. Aburzeza, *International Journal of Science and Research.* 2015, **4**, 350-352.

23. Farrugia, L. ORTEP-3 for Windows - a version of ORTEP-III with a Graphical User Interface (GUI), *J. Appl. Crystallogr*., 1997, **30**, 565-566.

24. G. M. Sheldrick, *Acta Crystallogr., Sect. A: Found. Crystallogr.* 2008, **64**, 112.

25. Bruker-Nonius (2004), *APEX-II and SAINT-Plus (Version 7.06a),* Bruker AXS Inc., Madison, Wisconsin, USA.

26. K. Yamanari, I. Fukuda S. Yamamoto, Y. Kushi, A. Fuyuhiro, N. Kubota, T. Fukuo and R. J. Arakawa, *Chem. Soc. Dalton Trans.* 2000, 2131-2136.

27. G. Capper, D. L. Davies, J. Fawcett and D. R. Russell, *Acta Crystallogr.* 1995, **51**, 578-580.

28. J. Canivet and B. Therrien, G. S. Fink, *Acta Crystallogr., Sect. E.* 2005, **61**, 1090-1091.

29. (a) M. Arshad, A. R. Bhat, S. Pokharel, J. E. Kim, E. J. Lee, F. Athar and I. Choi, *Eur. J. Med. Chem.* 2014, **71**, 229-236; (b) R. Kholiya, S. I. Khan, A. Bahuguna, M. Tripathi and D. S. Rawat, *Eur. J. Med. Chem.* 2017, **131**, 126-140.

30. S. Musa, S. Fronton, L. Vaccaro and D. Gelman, *Organometallics.* 2013, **32**, 3069-3073.

31. B. Saha, S. M. W. Rahaman, P. Daw, G. Sengupta and J. K. Bera, *Chem. Eur. J.* 2014, **20**, 6542-6551.

32. T. Higuchi, R. Tagawa, A. Iimuro, S. Akiyama, H. Nagae and K. Mashima, *Chem. Eur. J.* 2017, **23**, 12795-12804.

33. S. Huang, X. Hong, H. Z. Cui, B. Zhan, Z. M. Li and X. F. Hou, *Organometallics,* 2020, **39**, 3514–3523.

34. S. Saranya, R. Ramesh and J. G. Małecki, *Eur. J. Org. Chem.* 2017, **45**, 6726-6733.

35. T. S. Manikandan, R. Ramesh, N. Shivalingegowda and L. N. Krishnappagowda, *ChemistrySelect.* 2018, **3**, 1561-1568.

36. J. Xu, R, Zhuang, L. Bao, G. Tang and Y. Zhao, *Green Chem.*, 2012, **14**, 2384-2387.

37. M. D. Jaisingh and S. B. Mhaske, ***New J. Chem.***, 2017, **41**, 470-479

38. A. Subashini, R. Kumaravel, S. Leelaa, H. S. Evans, D. Sastikumar and K. Ramamurthi, *Spectrochimica Acta Part A*, 2011, **78**, 935-941.

39. W. Qin, S. Long, M. Panunzio and S. Biondi, *Molecules*, 2013, **18**, 12264-12289.

Chapter 3

Ru(II)-NNO Pincer Type Complexes Catalyzed E-Olefination of Alkyl Substituted Quinolines/Pyrazines Utilizing Primary Alcohols

Abstract

An efficient and selective E-olefination of alkyl-substituted quinolines and pyrazines through dehydrogenative coupling of alcohols catalyzed by Ru(II) N^N^O pincer type complexes encompassing carbonyl and triphenyl arsines as co-ligands is demonstrated. An array of Ru(II) catalysts has been synthesized and evaluated by analytical and spectral methodologies. The solid-state molecular structure of the synthesized complex (**2**) has been substantiated by X-ray crystallography. The catalytic protocol produces a diverse range of olefinated products up to 90% by employing readily available primary alcohols. The present synthetic strategy is operationally simple, scalable and tolerates various functional groups under mild reaction conditions. Notably, an aldehyde and aryl-2-quinoline-2-yl-ethanol intermediate are involved in the catalytic reaction mechanism. The utility of the present procedure is demonstrated through a facile synthesis of the antifungal drug (E)-2-(2-(pyridin-4-yl)vinyl)quinoline.

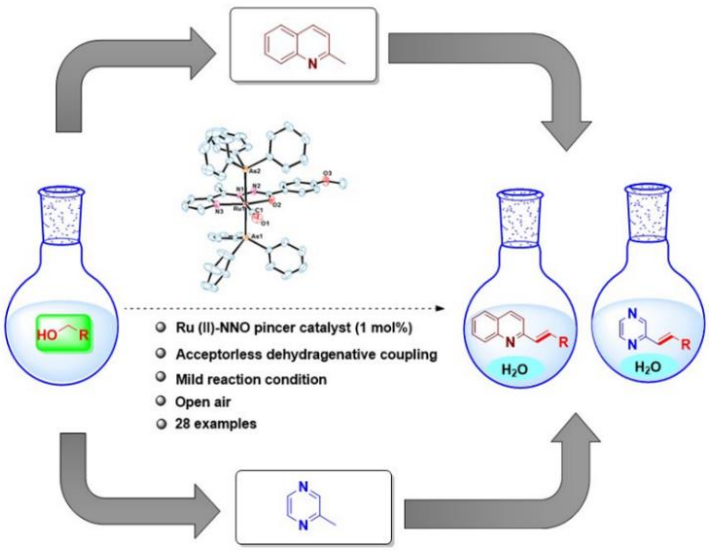

Pub.: *Appl. Organomet. Chem.*, 2022, **36**, e6561

3.1. INTRODUCTION

Olefins especially conjugated E-selective olefins are important key motifs found in various natural products, pharmaceuticals and materials etc.[1] Particularly, N-heteroarenes are widely used as intermediates for the fabrication of valuable materials, conducting polymers and organic light-emitting diodes.[2] Moreover, quinoline based conjugated N-heteroarenes are exhibits biological activities such as antifungal, antiviral, antibacterial and antitumor activities (Figure 1).[3] Owing to the biomedical prominence, the synthesis of such useful quinoline/pyrazine based conjugated N-heteroarene derivatives attracted synthetic chemists and has been broadly explored in catalysis research.

Notably, several conventional approaches were documented for the synthesis of E-olefins by various research groups with an appropriate leaving functional group.[4] In addition, coupling reactions including the Heck, Suzuki and olefin metathesis have been well-known strategies for the fabrication of olefins.[5]

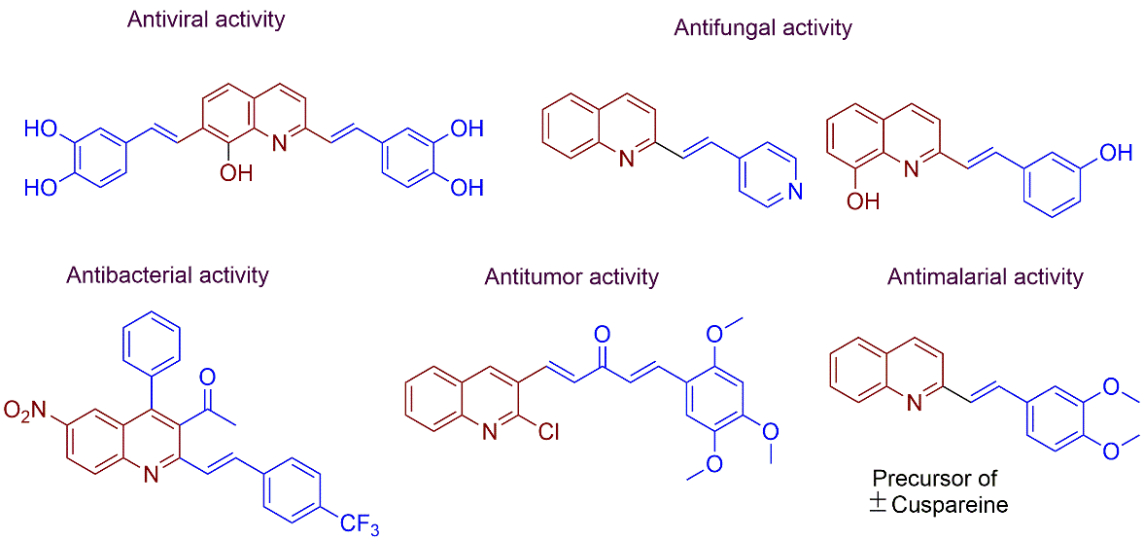

Figure 1. Selective examples for bioactive methyl-N-heteroarene analogues

Construction of E-selective olefins were performed by the condensation of aldehydes with N-heteroarenes in the presence of an oxidant, Lewis acid, organocatalysts, acid or base etc. as well.[6] Nevertheless, the aforementioned reported protocols suffer by

some major shortfalls like (i) harsh synthetic process, (ii) poor selectivity and (iii) stoichiometric waste.[7] Hence, greener and cost-effective methods to the sustainable fabrication of E-selective olefin compounds conjugated with N-heteroarenes is an extremely demanding goal.[8] In this scenario, the transition metal-supported conversion of C(sp^3)-H bonds into olefins would be an alternative approach as it has received significant attention in recent years.[9]

The dehydrogenative coupling strategy symbolizes most atom economical and clearest procedures as a substitute to conventional oxidation with water and hydrogen as only the valuable side products. In this connection, Chepre *et al.* have reported Mn-PNP complexes catalyzed olefination of N-heteroarenes using primary alcohols at longer reaction time.[10] Maji research group demonstrated pincer manganese catalysts mediated alkenation of methyl N-heteroarenes employing primary alcohols under an inert atmosphere.[11] Banerjee and co-workers have explored Ni(II) catalyzed olefination of N-heteroarenes with alcohols at inert condition, concurrently Fe(II) catalyzed olefination reaction was also documented by the same research group.[12] Baidya group reported the synthesis of olefin from 2-methylheteroarene with primary alcohols in presence of *in situ* generated Ni(II) complexes in tertiary butyl alcohol at 140°C for 48 h.[13] Zhang research group have disclosed MnO_2 mediated olefination of N-heteroarenes with alcohols at inert atmosphere.[14] Recently, the Elias group reported N-hetereoarene olefination from alcohols/amines in the presence of TBHP/DMAP in water medium[6a] (Scheme 1).

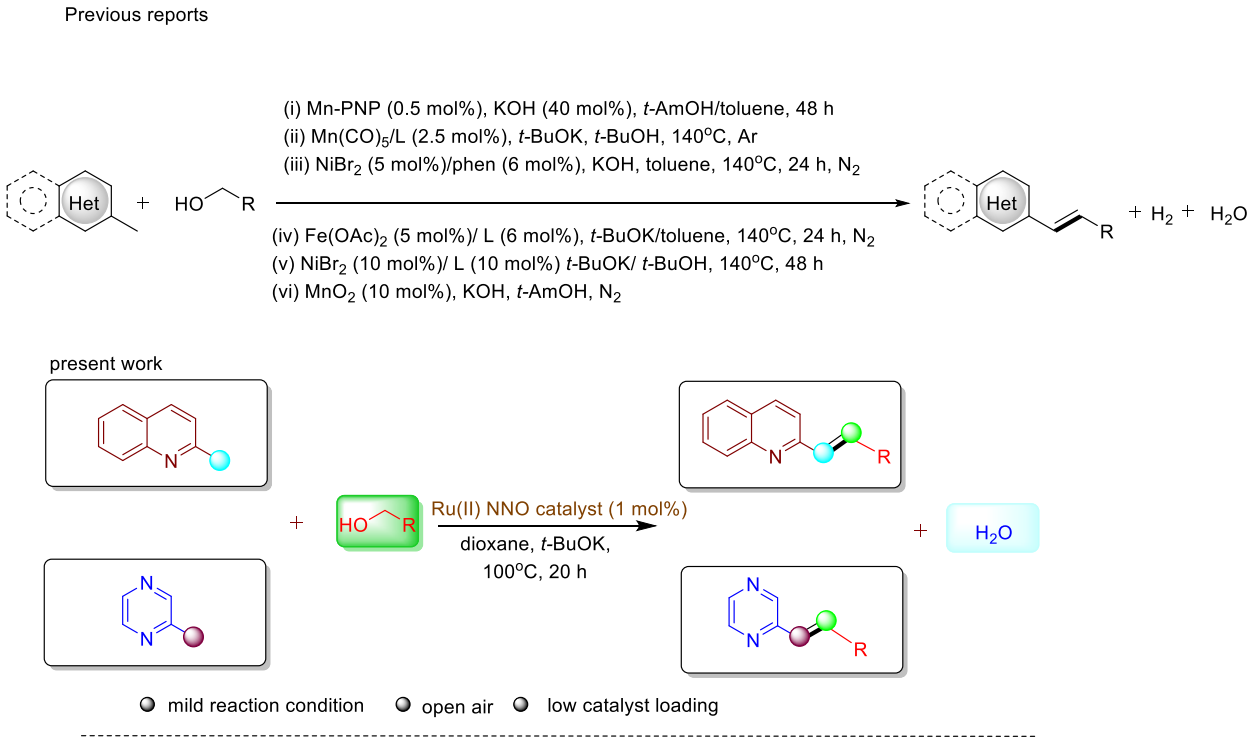

Scheme 1. Methods for E-olefination of methyl N-heteroarenes with Alcohols

Though different metal catalysts with various ligand frameworks were developed for the olefination of N-heteroarenes reaction with alcohols, they are associated with some drawbacks including high catalyst loading, higher temperature, necessity of oxidants, and inert atmospheric conditions. To overcome the above issues by a sustainable protocol, we are interested to execute the olefination of N-heteroarenes with primary alcohols catalyzed by ruthenium complexes with simple NNO pincer type ligands.

In general, ligand partners have been the imperative constituent of the metal catalysts/ pre-catalysts, which can stabilize the metal centre, regulate the stereo-, chemo- and enantioselectivities of chemical transformations, the solution state reactivity, etc. Further, the metal-ligand cooperation depends on their both electronic and steric properties of ligands by the design of suitable donor triads, size of the metallic rings, nature of the ancillary, neutral and anionic ligands. Tridentate ligands possess a perfect balance of control on composition of the coordination geometry by carrying the donor atoms in an orderly

configuration. Upon complexation, these tridentate ligands formed meridional geometry with a metal centre and control the vacant coordination sites which increase the stability of the pincer complexes.[15] Furthermore, the ligands have given a strong *mer*-coordination, planarity around the metal centre that provides a good balance of stability and reactivity, which distinguishes the pincer complexes from other homogeneous catalysts.[16] Moreover, metal complexes comprising pincer type ligands possess enticing catalytic activities and ever-increasing applications in various fields.[17]

Herein, we have reported the synthesis and structural elucidation of new Ru(II) pincer type complexes comprising NNO terdentate ligands with easy leaving $AsPh_3$ as co-ligands and the synthesized complexes were developed as a catalysts for selective E-olefination of methyl N-heteroarenes *via* dehydrogenative coupling of primary alcohols. The present protocol requires only mild reaction conditions and uses low catalyst loading and covers a diverse range of substrates scope with good yields of olefin products.

3.2. Experimental Section

3.2.1. Reagents and materials

All the reagents used were chemically pure and analar grade. Commercially available $RuCl_3.3H_2O$ was supplied from Loba Chemie. Substituted benzhydrazides were purchased from Sigma Aldrich and were used without further purification. The solvents were freshly distilled before use following the standard procedures.[18]

3.2.2. Physical measurements and instrumentation

Melting point was recorded in the Boeties micro heating table and is uncorrected. The elemental analysis of carbon, hydrogen, nitrogen and sulphur were performed at Sophisticated Test and Instrumentation Centre (STIC), Cochin University of Science and Technology, Kochi. Infrared spectra of complexes were recorded in KBr pellets with a Perkin-Elmer 597 spectrophotometer in the range of 4000-400 cm^{-1}. The ^1H and ^{13}C NMR

spectra were recorded in $CDCl_3$ and DMSO-d_6 with Bruker 400 MHz instrument using TMS as internal reference.

3.2.3. Preparation of methyl-2-pyrrolyl hydrazone NNO pincer ligands

Methyl-2-pyrrolyl hydrazone NNO pincer ligands were synthesized from the literature procedure.[19] To a stirred ethanolic solution (10 mL) of methyl-2-pyrrole ketone (1 mmol), 4-substituted benzhydrazide (1 mmol) and few drops of conc. HCl in ethanol (10 mL) was added drop wise (Scheme 2). The reaction mixture was refluxed 12 h. At the end of the reaction the solution was concentrated to 5 mL and poured into cold water 10 mL. The white solid was obtained, filtered and dried in vacuum. Yield: 85-90%.

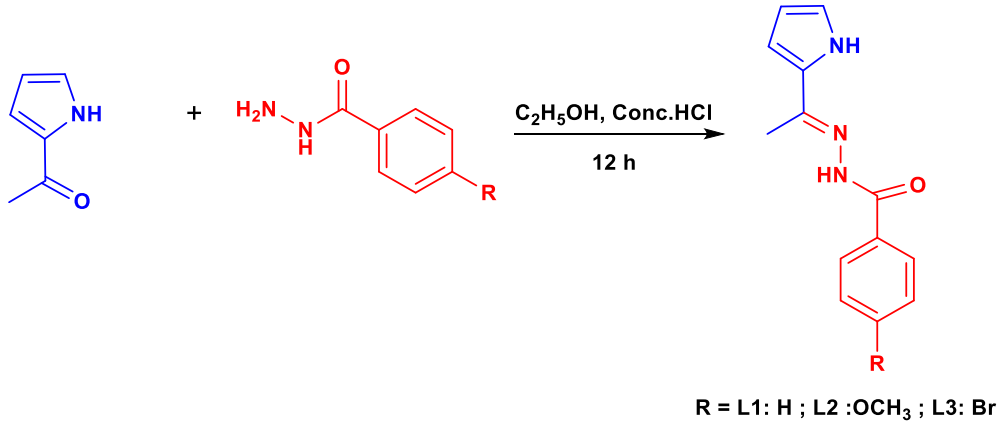

Scheme 2. Preparation of methyl-2-pyrrolyl hydrazone NNO pincer ligands

3.2.4. Synthesis of new Ru(II) hydrazone complexes

An equimolar ratio of 4-substituted pyrrole ketone benzhydrazone (1 mmol), $[RuHCl(CO)(AsPh_3)_3]$ (1 mmol) and triethylamine (1 mmol) were mixed in benzene (15 mL) (Scheme 3). The resulting reaction mixture was refluxed for 6 h. The completion of the reaction was monitored by TLC. The resulting solution was concentrated to 2 mL and the addition of petroleum ether (60-80 °C) in excess gave a brown solid. The synthesized Ru(II) NNO pincer type complexes are stable in air and can be dissolved in most organic solvents.

The structures of the newly formed Ru(II) NNO symmetrical pincer complexes were confirmed by analytical and spectral methods.

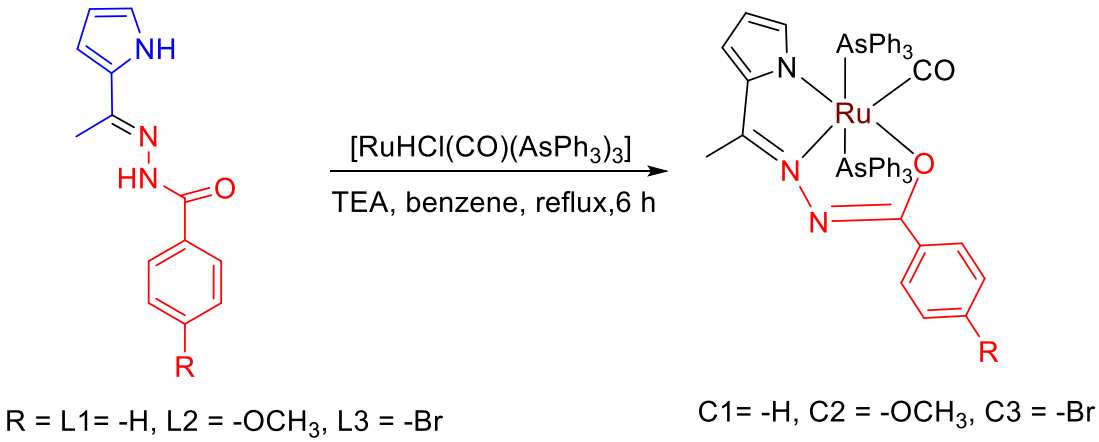

Scheme 3. Synthetic route to Ru(II) NNO pincer type complexes

Spectral characterization of Ru(II)-NNO pincer complexes (1-3)

Complex 1. Brown solid, Yield: 80%, m.p.: 228 °C (with decomposition). Anal. calcd: $C_{50}H_{41}As_2N_3O_2Ru$: C, 62.12; H, 4.27; N, 4.35%. found: C, 62.08; H, 4.24; N, 4.29%. FT-IR (KBr, cm^{-1}): 1514 $\nu_{(C=N)}$, 1228 $\nu_{(C-O)}$, 1510 $\nu_{(C=N-N=C)}$. ^1H NMR (400 MHz, $CDCl_3$): δ (ppm) = 7.49 (d, J = 8 Hz, 3H, ArH (ligand)), 7.24 – 7.06 (m, 32H, ArH (ligand+$(AsPh_3)_2$), 6.11 (s, 1H, pyrrole C-H), 6.04 (d, J = 4 Hz, 1H pyrrole C-H), 5.64 (s, 1H, pyrrole C-H), 1.57 (s, 3H, ligand CH_3). ^{13}C {^1H} NMR (100 MHz, $CDCl_3$): δ (ppm) = 204.05 (Ru-CO), 172.38 (N=C-O), 153.23 (C=N), 137.50, 132.77, 131.36, 128.61, 127.72, 127.52, 127.37, 126.92, 126.18, 112.09, 108.70 (Ar carbons (ligand+$(AsPh_3)_2$), 28.76 (ligand CH_3).

Complex 2. Brown solid, Yield: 85%, m.p.: 235 °C (with decomposition). Anal. calcd: $C_{51}H_{43}As_2N_3O_3Ru$: C, 61.45; H, 4.35; N, 4.22%. found: C, 61.40; H, 4.32; N, 4.18%. FT-IR (KBr, cm^{-1}): 1522 $\nu_{(C=N)}$, 1248 $\nu_{(C-O)}$, 1517 $\nu_{(C=N-N=C)}$. ^1H NMR (400 MHz, $CDCl_3$): δ (ppm) = 7.53 (d, J = 8 Hz, 2H, ArH (ligand)), 7.34 – 7.21 (m, 30H, ArH $(AsPh_3)_2$), 6.67 (d, J = 8 Hz, 2H (ligand)), 6.18 (s, 1H, pyrrole C-H), 6.12 (d, J = 4 Hz, 1H pyrrole C-H), 5.71 (s, 1H, pyrrole C-H), 3.77 (s, 3H, ligand OCH_3), 1.63 (s, 3H, ligand CH_3). ^{13}C {^1H} NMR

(100 MHz, $CDCl_3$): δ (ppm) = 205.07 (Ru-CO), 173.22 (N=C-O), 160.20 (C-OCH_3), 153.65 (C=N), 143.94, 138.28, 133.78, 132.42, 129.55, 129.44, 128.32, 127.68, 112.73, 112.44, 109.50 (Ar carbons (ligand+$(AsPh_3)_2$), 55.19 (ligand OCH_3), 12.77 (ligand CH_3).

Complex 3. Brown solid, Yield: 78%, m.p.: 242°C (with decomposition). Anal. calcd: $C_{50}H_{40}As_2BrN_3O_2Ru$: C, 57.43; H, 3.86; N, 4.02%. found: C, 57.39; H, 3.83; N, 3.99%. FT-IR (KBr, cm^{-1}): 1530 $\nu_{(C=N)}$, 1279 $\nu_{(C-O)}$, 1523 $\nu_{(C=N-N=C)}$. ^1H NMR (400 MHz, $CDCl_3$): δ (ppm) = 7.61 (d, J = 8 Hz, 2H, ArH (ligand)), 7.39 – 7.37 (m, 2H, ArH (ligand), 7.34 – 7.10 (m, 30H, ArH $(AsPh_3)_2$), 6.13 (s, 1H, pyrrole C-H) 6.05 (d, J = 4 Hz, 1H, pyrrole C-H), 5.63 (s, 1H, pyrrole C-H), 1.55 (s, 3H, ligand CH_3). ^{13}C {^1H} NMR (100 MHz, $CDCl_3$): δ (ppm) = 203.87 (Ru-CO), 173.22 (N=C-O), 170.98 (C-Br), 153.48 (C=N), 138.58, 132.65, 132.62, 130.39, 128.58, 128.34, 127.62, 127.43, 127.29, 112.36, 108.91 (Ar carbons (ligand+$(AsPh_3)_2$), 21.59 (ligand CH_3).

3.2.5. X-ray crystallographic data collection

Single crystals of complex **2** were grown by slow evaporation of a chloroform – methanol solution at room temperature. The data collection was carried out using a Bruker AXS Kappa APEX II single crystal X-ray diffractometer using monochromated Mo–Kα radiation (λ = 0.71073 Å). Data was collected at 296 K. The absorption corrections were performed by the multi-scan method using SADABS software.[20] Corrections were made for Lorentz and polarization effects. The structures were solved by direct methods (SHELXS 97) and refined by full-matrix least squares on F^2 using SHELXL 97.[21] All non-hydrogen atoms were refined anisotropically and the hydrogen atoms in these structures were located from the difference Fourier map and constrained to the ideal positions in the refinement procedure. The unit cell parameters were determined by the method of difference vectors using reflections scanned from three different zones of the reciprocal lattice. The intensity data were measured using ω and φ scan with a frame width of 0.5°. Frame integration and

data reduction were performed using the Bruker SAINT-Plus (Version 7.06a) software.[22] Figure 8 was drawn with ORTEP and the structural data have been deposited at the Cambridge Crystallographic Data Centre: CCDC 1844598.

3.2.6. General procedure for the Ru(II)-NNO pincer catalyzed olefination of methyl N-heteroarenes

In a 4 mL of 1,4-dioxane solvent, methyl N- heteroarenes (1 mmol), primary alcohols (1 mmol), *t*-BuOK base (0.5 mmol) and Ru(II)-NNO pincer catalyst (1 mol%) were dissolved in a round-bottom flask. The resulting mixture was stirred at 100 ^{o}C for 20 h under open air atmosphere. Then the solution was quenched by water (5 mL) and followed by extraction with EtOAc (5 × 10 mL). The organic fractions were separated and dried over anhydrous Na_2SO_4. The solvent was removed from the organic fraction under reduced pressure. The resulting crude mixture was purified by using column chromatography with ethyl acetate/hexane (5:95) as an eluent.

3.2.7. Competitive control experiment between EDG and EWG

4-methoxybenzyl alcohol **2d** (1 mmol), 4-chlorobenzyl alcohol **2f** (1 mmol), 2-methylquinoline (1 mmol), *t*-BuOK (0.5 mmol) and Ru(II)-NNO pincer type catalyst (1 mol%) were stirred in 1,4-dioxane medium at 100 ^{o}C for 20 h. The resulting mixture was concentrated and the formed olefin products were isolated by column chromatography. The olefin products **3d** and **3f** were eluted using ethyl acetate/hexane mixture.

3.2.8. Procedure for gram scale synthesis

In a 40 mL of 1,4-dioxane solvent, 2-methyl quinoline (1.43 g, 10 mmol), benzyl alcohol (1.08 g, 10 mmol), *t*-BuOK (0.56 g, 0.5 mmol) and Ru(II)-NNO pincer catalyst (0.1 g, 1 mol%) were dissolved in a round-bottom flask. The resulting mixture was refluxed at 100 ^{o}C for 20 h under open air atmosphere. Then the solution was quenched by adding water (50 mL) and followed by extraction with EtOAc (2 × 100 mL). The organic fractions were

separated and dried over anhydrous Na_2SO_4. The solvent was removed from the organic fraction under reduced pressure. The resulting crude mixture was purified by using column chromatography with ethyl acetate/hexane (5:95) as an eluent.

3.3. Results and Discussion

The simple NNO pincer type ligands (L1-L3) were easily prepared from condensation methyl-2-pyrrole and 4-substituted benzhydrazides in methanol.[19] The synthesis of Ru(II) NNO pincer type complexes were accomplished in good yield from the reaction of $[RuHCl(CO)(AsPh_3)_3]$ with the prepared ligands in 1:1 molar ratio in benzene medium using Et_3N as a base. The synthesized Ru(II) NNO pincer type complexes are stable in air and can be dissolved in most organic solvents. The structures of the newly formed Ru(II) NNO symmetrical pincer complexes were confirmed by analytical and spectral methods.

3.3.1. FT-IR Spectra

In the IR spectra, stretching bands found around 3400-3430 cm^{-1} and 3235-3262 cm^{-1} regions were attributed to pyrrole and hydrazone N-H moieties of L1-L3. Besides, the strong bands around 1640–1684 cm^{-1} and 1684–1710 cm^{-1} have been assigned for C=N and C=O functional groups of ligands, L1-L3. The absence of ν_{N-H} frequencies in the complexes evidenced the bonding of pyrrole nitrogen to ruthenium ion. Further absence of C=O band along with emergence of new intense C-O band (1228–1279 cm^{-1}) indicated the tautomerization and consequent binding of the imidolate oxygen to ruthenium. In all the spectra of complexes, C=N stretching frequencies were lower (1514-1530 cm^{-1}) than free ligands, confirmed that the imine nitrogen possesses the yet another point of attachment to ruthenium ion. Further, the complexes possess strong band around 1920-1928 cm^{-1} due to the terminally binded carbonyl group. The bands in the region 1412–1483 cm^{-1} are attributed to ruthenium-bounded triphenylarsines.[23] From the IR spectral data, the tridentate

coordination of ligand to the ruthenium *via* imidolate oxygen, pyrrole nitrogen and imine nitrogen was corroborated.

3.3.2. NMR spectra

The proton NMR spectra of ligands exhibited two singlets in the region of δ 8.95-10.85 ppm due to the hydrazinic and pyrrole nitrogens. The methyl protons of the ligands were appeared as singlet at δ 1.64 ppm. Another singlet at δ 3.82 ppm was addressed to methoxy protons of ligand 2. The absence of both –NH peaks of the ligand indicates that pyrrole nitrogen and hydrazinic nitrogen are coordinated to Ru(II) centre. Further, aromatic protons of the hydrazone ligand and triphenylarsines resonated as multiplet in the range of δ 5.64-7.62 ppm. Besides, the formation of the synthesized complexes was further evidenced by $^{13}C\{^{1}H\}$ NMR spectra. The bonding of imidolate oxygen and hydrazinic nitrogen to Ru(II) ion was authenticated by the up-shift of C=N (172 ppm) and down-shift C-O (153 ppm) in the spectra of the complexes.

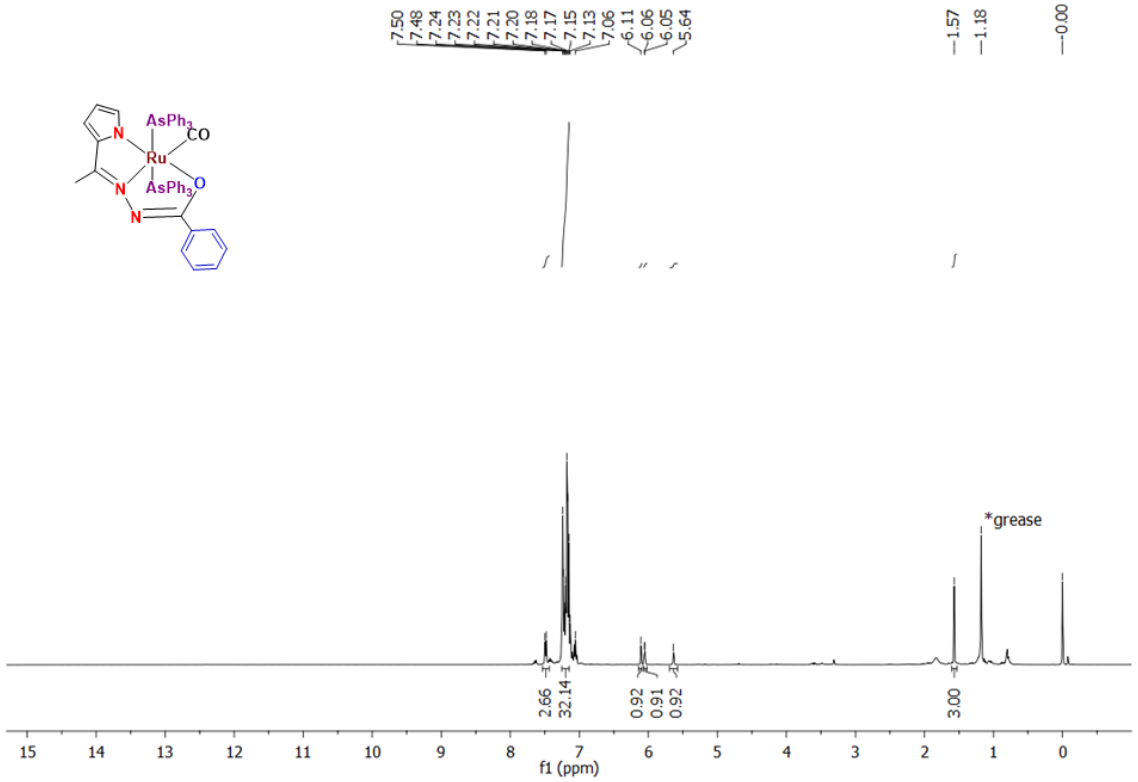

Figure 2: ^{1}H NMR spectrum for complex **1** in $CDCl_3$ (400 MHz, 300K).

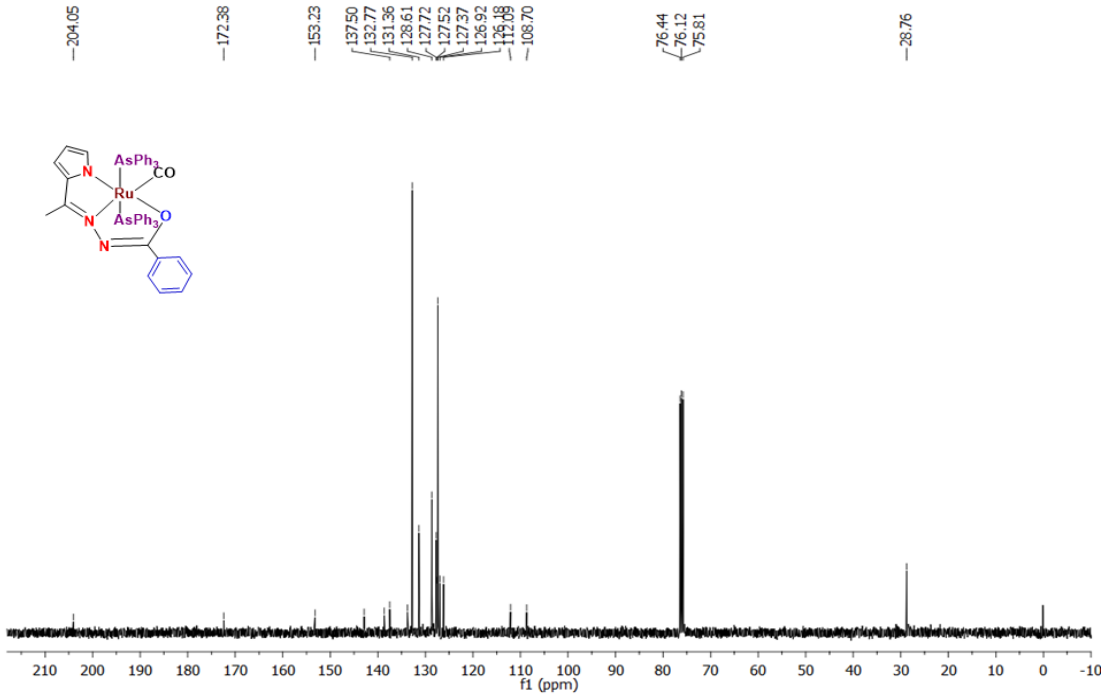

Figure 3: ^{13}C NMR spectrum for complex **1** in $CDCl_3$ (100MHz, 300K).

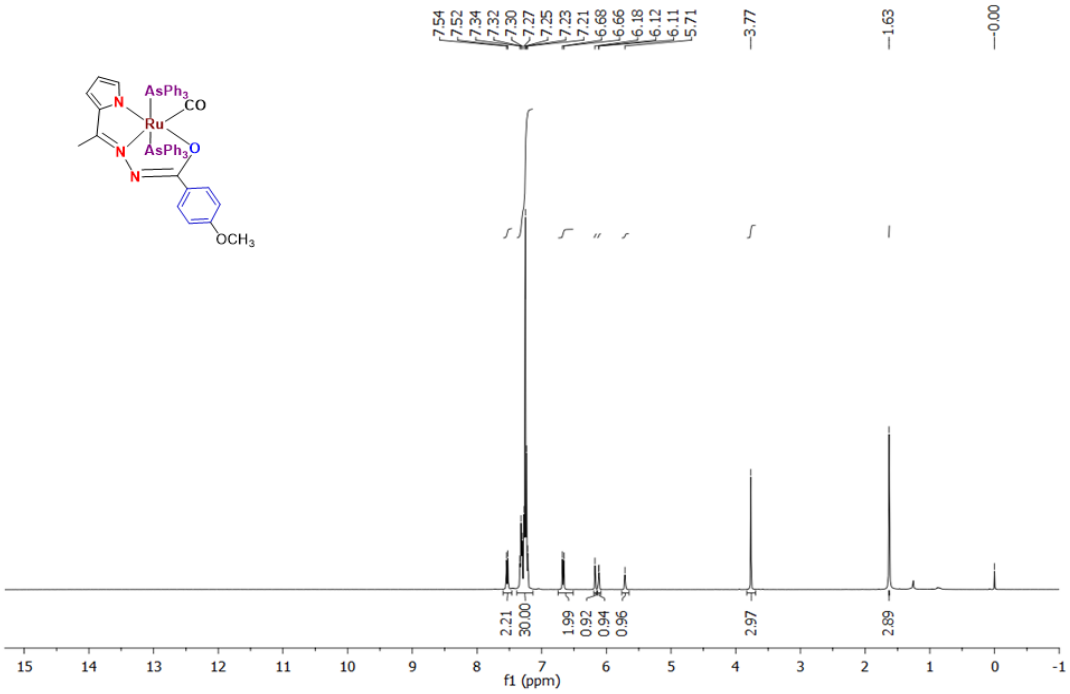

Figure 4: ^{1}H NMR spectrum for complex **2** in $CDCl_3$ (400MHz, 300K).

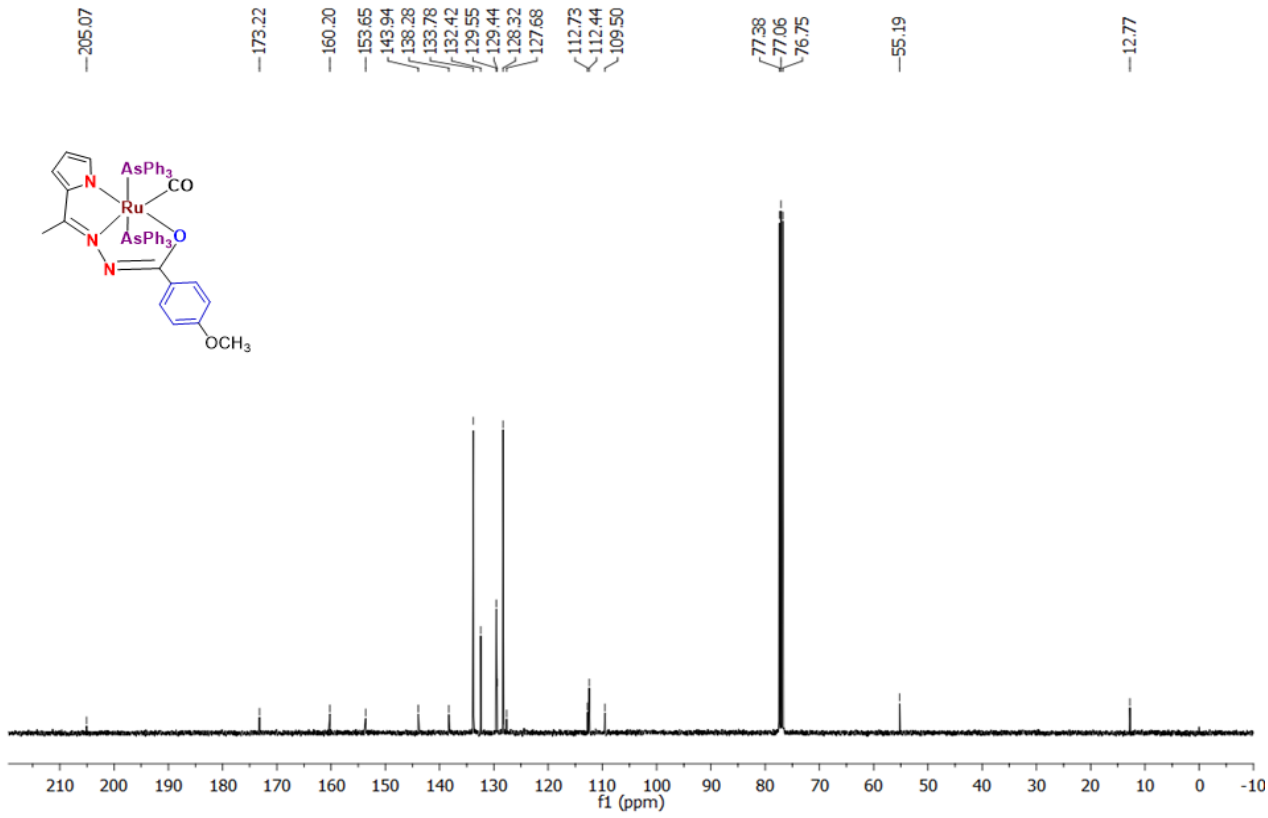

Figure 5: ^{13}C NMR spectrum for complex **2** in $CDCl_3$ (100MHz, 300K).

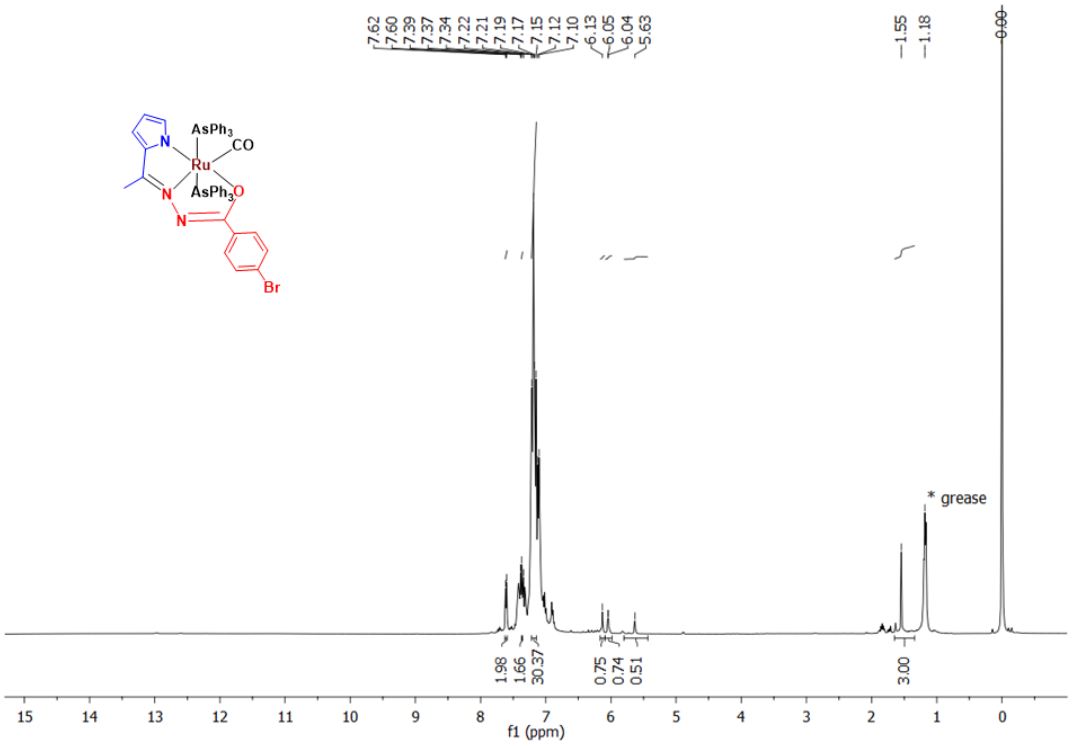

Figure 6: ^{1}H NMR spectrum for complex **3** in $CDCl_3$ (400MHz, 300K).

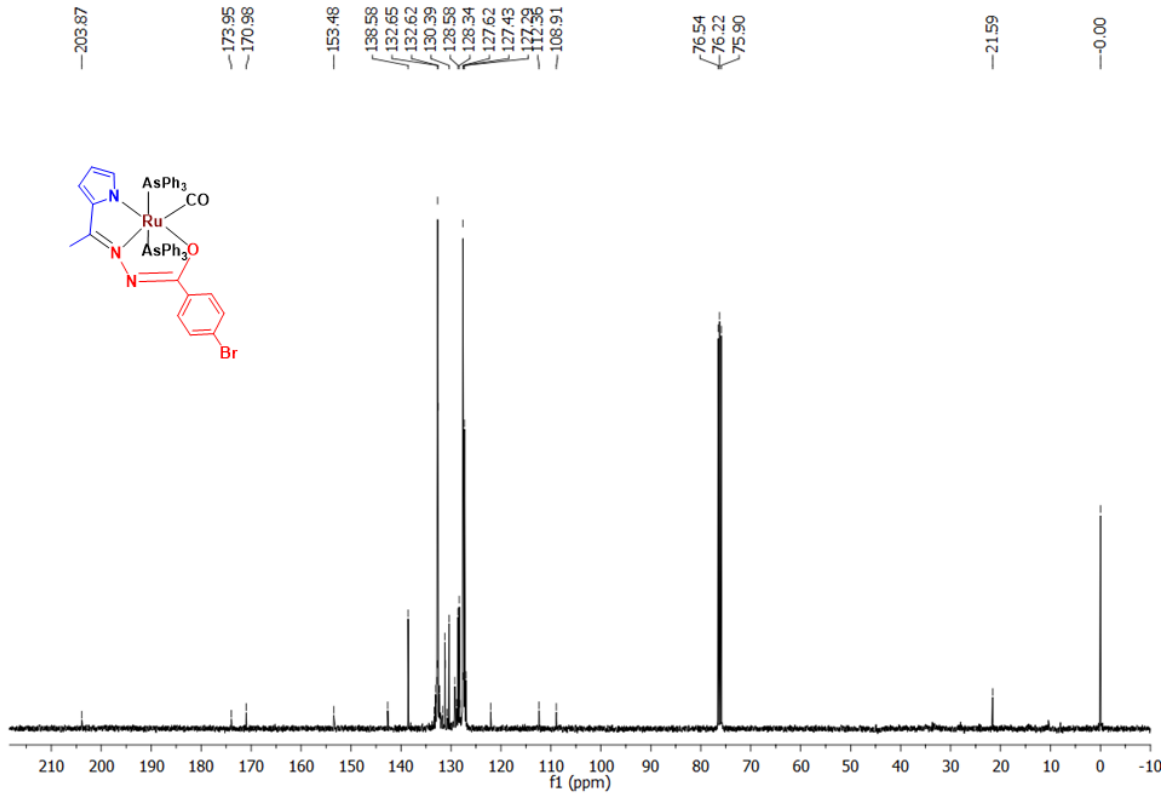

Figure 7: ^{13}C NMR spectrum for complex **3** in $CDCl_3$ (100MHz, 300K).

3.3.3. X-ray molecular structure determination

The suitable quality of crystals were grown by slow evaporation of $CHCl_3$/MeOH solvent (1:1). The X-ray single-crystal diffraction analysis was used to confirm the solid-state structure of complex **2**. The ORTEP diagram of complex **2** is depicted in Figure 8. The complex **2** crystallized in monoclinic space group 'P 2_1/n'. The crystallographic data as well as selected bond lengths and bond angles are described in Tables 1 and 2. The pincer type ligand meridionally binded with ruthenium ion in NNO tridentate manner and resulted in two five-membered chelate rings. The remaining positions were filled by a CO and sterically hindered two triphenylarsine ligands that are trans to each other and thus form a pseudo-octahedral geometry around Ru(II) ion. The Ru(1)-N(1) bond distance of the ligand is significantly shorter (2.025(3) Å) than the Ru(1)-N(3) bond distance (2.078(4) Å), in agreement with the geometrical constraints of the tridentate ligand showing N(1)-Ru(1)-N(3) and N(1)-Ru(1)-O(2) bond angles 77.79(14)^o and 75.98(12)°, respectively. The N(1)-Ru(1)-C(1) angle is slightly distorted from the idealized 180^o to 177.87(16)^o, and the N(1-)Ru(1)-As(1) angle is 88.80(9)^o. Further, the bond distances and bond angles of complex **2** is consistent with other reported Ru(II) complex possess pseudo-octahedral geometry.[24]

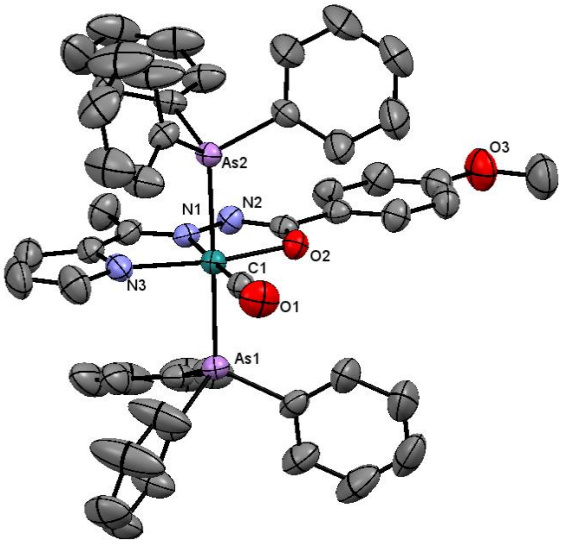

Figure 8. ORTEP view of complex **2**. All hydrogens were omitted for clarity

Table 1. Crystal data and structure refinement for the complex **2**

CCDC	1844598
Empirical formula	$C_{52}H_{44}As_2Cl_3N_3O_3Ru$
Formula weight	1116.16
Temperature/K	295(2)
Crystal system	Monoclinic
Space group	'$P2_1/n$'
a/Å, *b*/Å, *c*/Å	15.5688(4), 18.4229(6), 17.1320(7)
α/°, β/°, γ/°	90, 96.010(3), 90
Volume/Å^3	4886.8(3)
Z	4
ρ_{calc}mg/mm^3	1.517
m/mm^{-1}	1.874
F(000)	2248
Crystal size/mm^3	0.22 × 0.12 × 0.09
Theta range for data collection	3.438 to 29.554°
Index ranges	$-16 \leq h \leq 21$, $-17 \leq k \leq 25$, $-20 \leq l \leq 22$
Reflections collected	25900
Independent reflections	11708[R(int) = 0.0359]
Data/restraints/parameters	11708/0/507
Goodness-of-fit on F^2	1.039
Final *R* indexes [I>2σ (I)]	R_1 = 0.0490, wR_2 = 0.1136
Final *R* indexes [all data]	R_1 = 0.0891, wR_2 = 0.1330
Largest diff. peak/hole / e Å^{-3}	0.693/-0.611

Table 2. Selected bond lengths (Å) and angles (°) for the complex **2**

Bond lengths (Å)		Bond angles (°)	
Ru1-As1	2.4504 (5)	As1-Ru1-As2	176.62 (2)
Ru1-As2	2.4543 (5)	O1-C1-Ru1	178.8 (4)
Ru1-C1	1.858 (4)	O2-Ru1-As1	89.77 (8)
Ru1-N3	2.078 (4)	O2-Ru1-As2	89.82 (8)
Ru1-N1	2.025 (3)	N1-Ru1-As1	88.80 (9)
Ru1-O2	2.097 (3)	N1-Ru1-As2	87.84 (9)
As1-C16	1.930 (2)	N1-Ru1-O2	75.98 (12)
As1-C22	1.926 (4)	N1-Ru1-N3	77.79 (14)
As1-C28	1.925 (3)	N1-C1-S1	112.2 (5)
As2-C34	1.933 (2)	N1-C1-N2	131.0 (6)
As2-C40	1.927 (2)	N2-N1-Ru1	118.5 (2)
As2-C46	1.921 (2)	N2-C8-C9	116.5 (3)
O1-C1	1.140 (5)	N3-Ru1-As1	88.94 (10)
O2-C8	1.299 (5)	N3-Ru1-As2	89.93 (10)
O3-C12	1.350 (4)	N3-Ru1-O2	153.76 (13)
O3-C15	1.402 (7)	C1-Ru1-As1	91.67 (13)
N1-N2	1.379 (5)	C1-Ru1-As2	91.70 (13)
N1-C6	1.301 (5)	C1-Ru1-O2	101.95 (15)
		C1-Ru1-N1	177.87 (16)

3.3.4. Catalytic application to synthesis of styryl quinoline

The remarkable applications of ruthenium catalysts to an extensive variety of coupling reactions motivated us to tune the present Ru(II)-NNO pincer complexes as catalysts in the direct E-olefination of alkyl substituted quinolines/pyrazines *via* dehydrogenative coupling of substituted benzyl alcohols.

3.3.4.1. Optimization of reaction conditions, effect of substituent and catalyst loading[a]

To select the appropriate reaction condition for the fabrication of E-olefins (**3a**), several catalytic variables such as different bases, solvents, time and temperatures have been tested using pincer type Ru(II) complex as catalysts. The model reaction between 2-methyl quinoline **1a** and benzyl alcohol **2a** as test substrates utilizing Ru(II) catalysts in combination with various solvents, bases and temperatures are depicted in Table 3. While employing Ru(II) complex **1** (1 mol%) as a catalyst, in presence of K_2CO_3 and Cs_2CO_3 bases at 110 ^oC in toluene medium, the ADC reaction gives E-Selective olefinated product **3a** with 40%-43% yields (Table 3, entries 1 and 2). Further, the model reaction was performed in toluene/KOH mixture and the yield of **3a** was increased up to 60%. (Table 3, entry 3).

Table 3. Screening of reaction conditions[a]

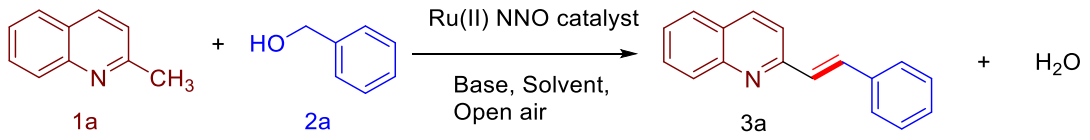

Entry	Complex	Solvent	Base	Temp (° C)	Time (h)	Yield[b]
1	Complex 1	Toluene	K_2CO_3	110	24	40
2	Complex 1	Toluene	Cs_2CO_3	110	24	43
3	Complex 1	Toluene	KOH	110	24	60
4[c]	-	Toluene	KOH	130	24	NR
5[d]	Complex 1	Toluene	-	130	24	NR
6	Complex 1	Toluene	*t*-BuOK	130	24	70
7	Complex 1	*m*-Xylene	*t*-BuOK	130	24	66
8	Complex 1	*t*-BuOH	*t*-BuOK	100	24	50
9	Complex 1	THF	*t*-BuOK	100	24	45
10	Complex 1	Acetonitrile	*t*-BuOK	80	24	20
11	Complex 1	Ethanol	*t*-BuOK	80	24	27
12	Complex 1	1,4-Dioxane	*t*-BuOK	80	20	68
13	**Complex 1**	**1,4-Dioxane**	***t*-BuOK**	**100**	**20**	**77**

[a]**Reaction conditions:** 2-methylquinoline (**1a)** (1 mmol), benzyl alcohol (**2a)** (1 mmol), Complex (1 mol %), *t*-BuOK (0.5 mmol), solvent (4 mL). [b]Isolated yield of **3a** product. [c]Absence of catalyst. [d]Absence of base.

The catalyst and base are essential for the catalytic reaction because the absence of any of them the reaction was unfruitful (Table 3, entries 4 and 5). Conspicuously, when the reaction was accomplished with *t*-BuOK instead of KOH, the yield of **3a** was 79% (Table 3, entry 6). While comparing the yields of the end product, the outperformance of *t*-BuOK over the other bases was distinguished. In the model reaction, switching solvents and temperatures with *t*-BuOK base was performed and among them 1,4-dioxane operated well at 80 ^{o}C (Table 3, entry 7-12**)**. It has been observed that complex **1** gave the maximum yield of 77% of **3a** from the coupling of 2-methyl quinoline with benzyl alcohol under the conditions of 1,4-dioxane/*t*-BuOK at 100 ^{o}C in 20 h (Table 3, entry 13).

Thus, table **3** outlined that the best optimal conditions for the ruthenium complexes catalysed selective E-olefination of methyl N-heteroarenes using primary alcohols. The reaction operated well in 1,4-Dioxane medium with *t*-BuOK as a base at 100 ^{o}C for 20 h under open-air atmosphere.

3.3.4.2. Optimization of effect of substituent

Once the various catalytic parameters were optimized, the effect of substituents of all the complexes on the catalytic reaction has been investigated (Table 4). At most, all the complexes (**1-3**) showed good catalytic activity in the formation of olefin product with appreciable yields. However, based on experimental results, the complex **2** relatively provided a better yield than complexes (**1-3**) due to the presence of electron donating methoxy group[25] (Table 4, entries 1-3). Hence, the complex **2** was kept as a representative catalyst to explore the broad substrate scope using a diverse range of alcohols.

Table 4. Effect of the substituent of catalyst[a]

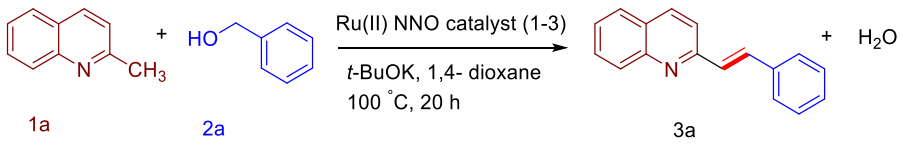

Entry	Ru complexes	Yield(%)[b]
1	Complex 1	72
2	**Complex 2**	**80**
3	Complex 3	65

[a]**Reaction conditions**: 2-methylquinoline (**1a**) (1 mmol), benzyl alcohol (1 mmol), complex (1 mol %), *t*-BuOK (0.5 mmol), 1,4-dioxane (4 mL), 20 h in open air. [b]Isolated yield.

3.3.4.3. Optimization of catalyst loading

Further, the effectiveness of our catalyst was examined with different catalyst loadings for the test reaction (Table 5). Upon reducing the catalyst loading from 1 mol% to 0.1 mol%, there was a substantial decrease in yields (Table 5, entries 1 - 4). Therefore 1 mol% catalyst loading is the best choice for optimization.

Table 5: Effect of catalyst loading[a]

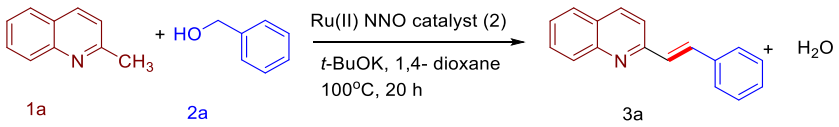

Entry	Catalyst 2 (mol %)	Yield(%)[b]
1	**1.0**	**80**
2	0.5	51
3	0.25	42
4	0.10	20

[a]**Reaction conditions**: 2-methylquinoline (1a) (1 mmol), benzyl alcohol (1 mmol), complex **2** (1 mol %), *t*-BuOK (0.5 mmol), 1,4-dioxane (4 mL), 20 h in open air. [b] Isolated yield.

3.3.4.4. Scope of the reaction

After optimization, the substrate scope of the olefination reaction was examined and the findings are documented in Table 6. The catalytic efficiency exhibited by the complex **2** in the test reaction was conveniently applied to 2-methyl quinoline and 2-methylpyrazines with a variety of electronic and sterically different primary alcohol derivatives and selectivity in E-selective olefin products seen in every case. Benzyl alcohols encompassing electron-rich groups such as 4-methyl, 3-methoxy and 4-methoxy substituents resulted **3b-3d** in high yields up to 90% of the desired olefins. In contrast, electron-deficient groups like 3-chloro, 4-chloro and 3-bromo benzyl alcohols tolerated well with 2-methyl quinoline to deliver olefin products **3e-3g** comparatively low yields (70%-78%). Fabulously, electron-poor 4-nitrobenzyl alcohol was successfully transferred into the respective olefin **3h** in 50% isolated yield. In addition, the complex **2** effectively catalyzed the dehydrogenative coupling of 2-methyl quinoline and benzyl alcohols with two and three electron releasing substituents including 3,4-dimethoxy, 2,6-dimethoxy and 3,4,5-trimethoxy benzyl alcohols and

furnished the corresponding olefins **3i-3k** in 73%-83% yields. Besides, the yield of olefin **3l** has been 60% when the ADC reaction was performed with 2-methyl quinoline and electron deficient 2,6-dichloro benzyl alcohol.

Interestingly, the present catalytic approach can be exploited for sterically fused aromatic alcohols including 1-naphthalene methanol, 9-anthracene methanol, and 1-pyrene methanol are they were smoothly converted into suitable olefins **3m-3o** with 72%-78% isolated yield. Encouraged by the yield of the olefin products, the utility of the present catalytic protocol was further extended to the olefination of 2-methyl pyrazine with various benzyl alcohols derivatives. Under standard conditions, 2-methyl pyrazine smoothly reacted with benzyl alcohol, 4-methyl benzyl alcohol, 4-methoxybenzyl alcohol and 3-methoxybenzyl alcohol to led the respective olefinated pyrazines **5a-5d** up to 83% yields. Strikingly, the reaction operated well for 2-methyl pyrazine with electron-deficient groups including 3-chloro, 4-chloro, and 3-bromobenzyl alcohols in 64%-72% yields of **5e-5g**. Delightfully, the benzyl alcohols comprising electron-rich groups such as 2,6-dimethoxy, 3,4-dimethoxy and 2,3-dimethoxy are tolerated well with 2-methyl pyrazine to provide the equivalent olefins **5h-5j** up to 69% yield. Additionally, the benzyl alcohol with electron-withdrawing substituent, 2,6-dichloro benzyl alcohol was elegantly treated under the optimal condition to deliver the respective **5k** product in 51% yield. Pleasingly, sterically hindered aromatic alcohols produce the appropriate E-olefin products **5l-5m** in moderate yields. Nonetheless, the reactions of 2-methyl pyrazine with heterocyclic and aliphatic alcohols were found to be unproductive **5n-5o**.

Table 6. Ru(II)-NNO catalyzed E-olefination of methyl N Heteroarenes[a],[b]

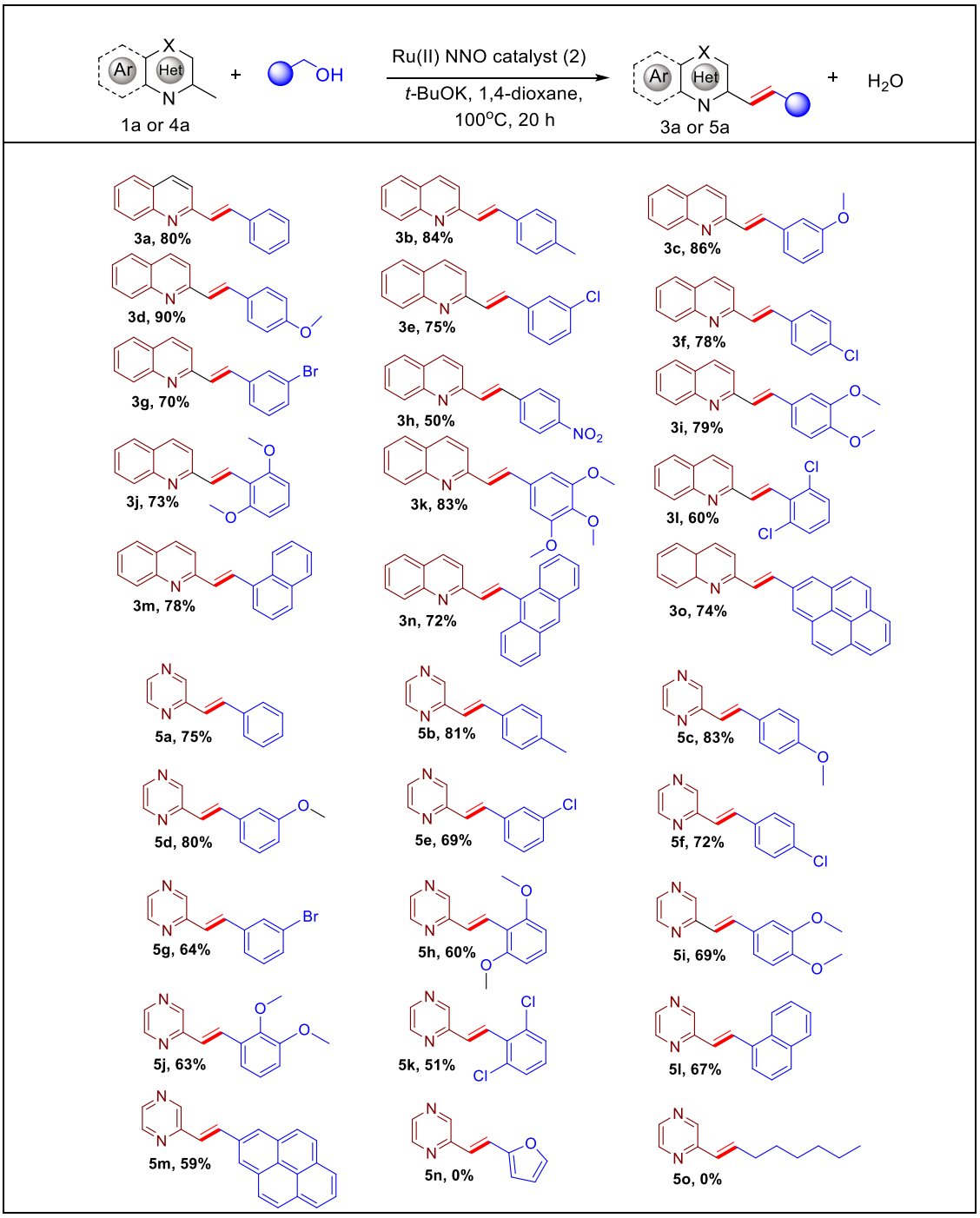

[a]**Reaction conditions:** 2-methylquinoline (**1a**) or 2-methyl pyrazine (**4a**) (1 mmol), alcohol (1 mmol), complex **2** (1 mol %), *t*-BuOK (0.5 mmol), 1,4-dioxane (4 mL), 20 h in open air. [b]Isolated yield.

Overall, the presence of the easily exchangeable $AsPh_3$ groups has promoted the catalytic efficiency of the pincer Ru(II)-NNO complexes towards the synthesis of E-selective olefines in high yields. It should be highlighted that the current catalytic system performed well in the open air without any additive/oxidant at 1 mol% catalyst loading.

3.3.4.5. Control experiments

To get the better understanding of the mechanistic study, a series of control experiments under various reaction conditions has been carried out. Initially, the reaction of benzyl alcohol (**2a**) in the absence of **1a** and catalyst was conducted under standard condition, but it did not proceed (Scheme 4a). However, when benzyl alcohol (**2a**) was treated under optimal conditions in presence of a catalyst, it releases the corresponding aldehyde and hydrogen gas (Scheme 4b). Moreover, no reaction was taken place when **2a** was reacted with **1a** in absence of catalyst. However, the reaction generated **3a** in 80% yield while the coupling has been executed with benzyl alcohol **2a** in the presence of catalyst (Scheme 4c, 4d). In contrast, **1a** reacts with benzaldehyde (**2a'**) under standard conditions to give the olefin product **3a** only with 30% of the yield (Scheme 4e).

In addition, the control experiment was carried out to trap aryl-2-quinoline-2-yl-ethanol intermediate[26] **(1a')** by reacting **1a** and 4-nitro benzyl alcohol (**2h)** in 12 h. Further, **1a'** subsequently underwent dehydration to furnish the desired olefinated products **(**Scheme 4f**)**. Hence, based on control experiments, we strongly believe that the current olefination reaction occurs *via* aldehyde intermediate which is produced through dehydrogenative pathway from benzyl alcohol.

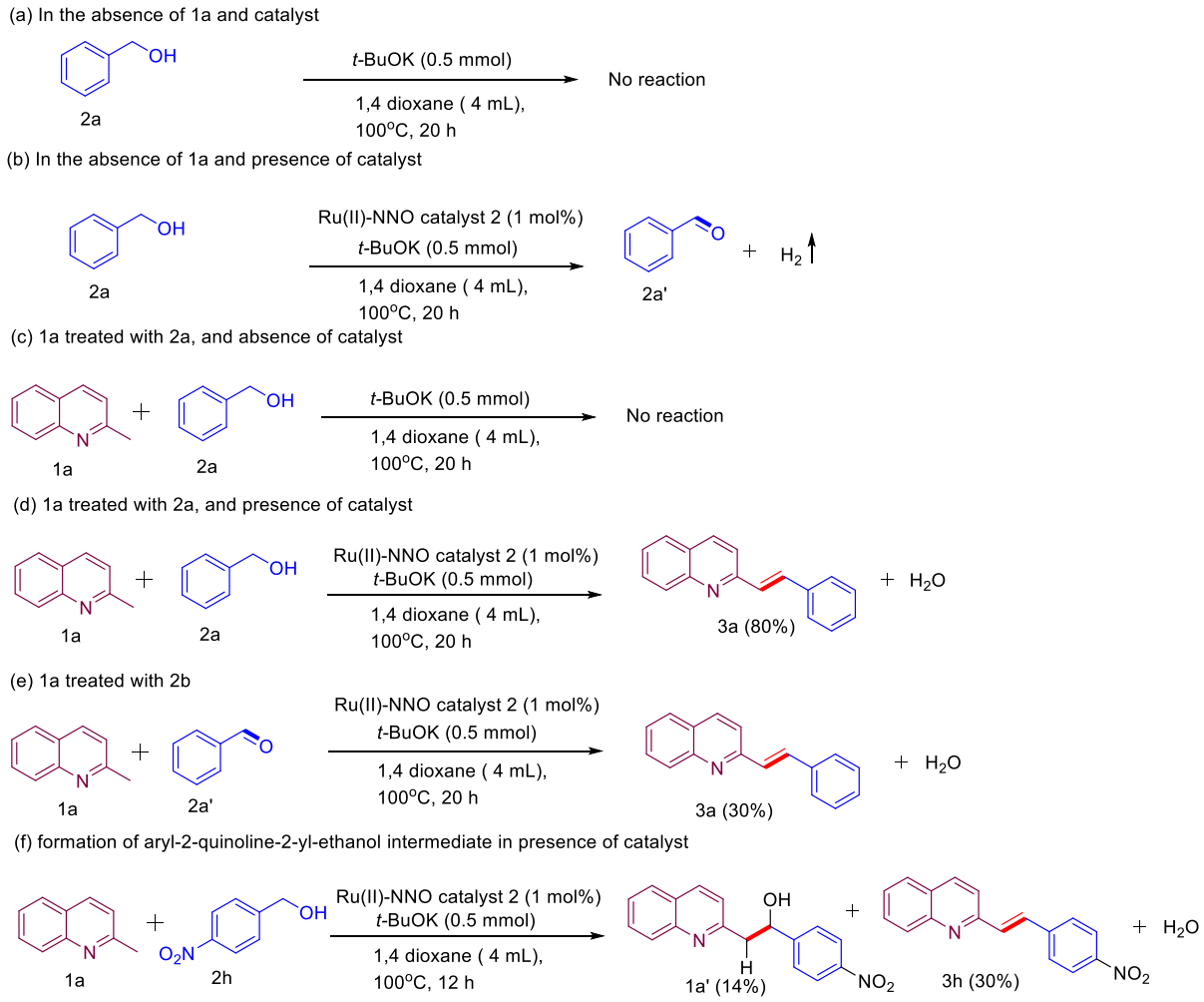

Scheme 4. Control experiments for mechanistic studies

3.3.4.6. Competitive control experiment between EDG and EWG

A competitive experiment was performed under optimized reaction conditions using benzyl alcohol containing electron-donating (4-methoxybenzyl alcohol) and electron-withdrawing groups (4-chlorobenzyl alcohol) with 2-methyl quinoline to gain a better understanding of the electronic effects of substitutes on catalytic activity. The results outlined that the electron-donating group is more reactive than the electron withdrawing group (Scheme 5).

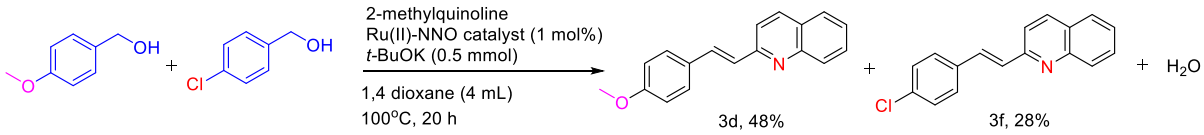

Scheme 5. Competitive control experiment between EDG and EWG

3.3.4.6. Gram-scale synthesis of olefin

Further, gram-scale synthesis was also established to demonstrate the utility of current catalytic protocol (Scheme 6). For that purpose, we performed the reaction of benzyl alcohol (1.08 g, 10 mmol) with 2-methyl quinoline (1.43 g, 10 mmol) in the presence of catalyst (0.1 g, 1 mol%), *t*-BuOK (0.56 g, 0.5 mmol) and 1,4-dioxane (40 mL) furnished desired **3a** in 77% yield.

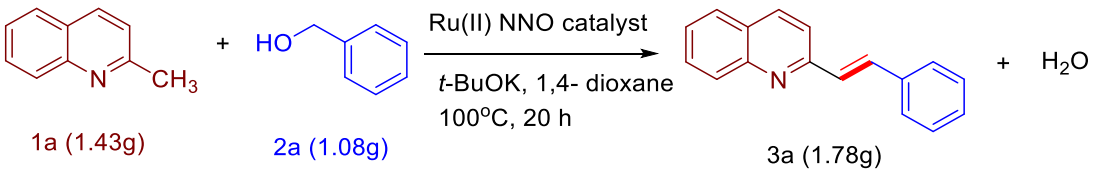

Scheme 6. Gram-scale synthesis of olefin

3.3.4.6. Synthesis of (E)-2-(2-(pyridin-4-yl)vinyl)quinoline antifungal drug

In addition, one of the antifungal drugs, (E)-2-(2-(pyridin-4-yl)vinyl)quinoline (**3p**) has been synthesized utilizing the present methodology from 2-methyl quinoline and 4-pyridinemethanol with a good yield of 80% (Scheme 7).

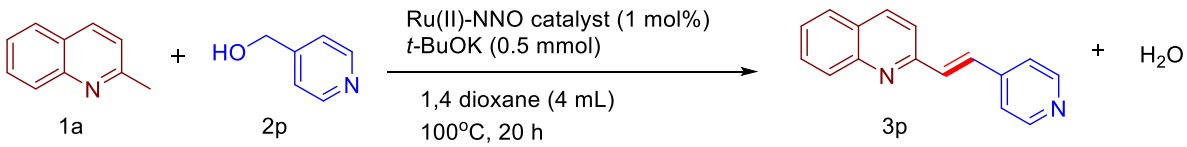

Scheme 7. Synthesis of (E)-2-(2-(pyridin-4-yl)vinyl)quinoline

3.3.4.7. Reaction mechanism for olefination of methyl-N-heteroarenes

From control experiments and previous reports[12,13] a plausible reaction mechanism for olefination of methyl-N-heteroarenes using Ru(II)-NNO pincer catalyst is depicted (Scheme 8).

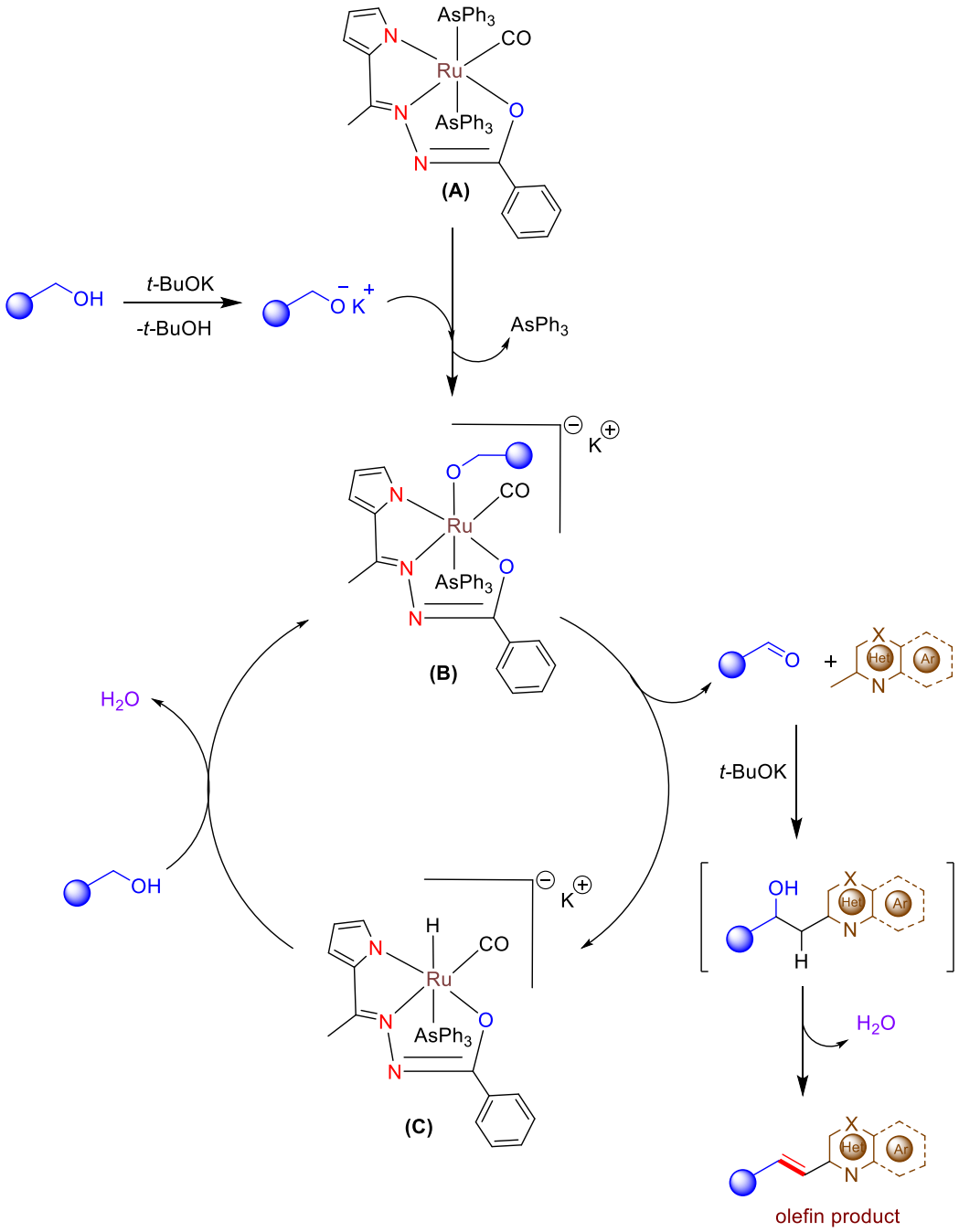

Scheme 8. Plausible reaction mechanism

Initially, the Ru(II) NNO pincer type catalyst (**A**) reacts with alcohols in the presence of a base to form ruthenium alkoxide (**B**). After that, (**B**) underwent *β*-hydride elimination to release aldehyde and Ru-H species (**C**). Further, alcohol reacts with ruthenium hydride species (**C**) to generate ruthenium alkoxide species (**B)** with the liberation of H_2 and thereby catalyst enters into the next catalytic cycle. Afterwards, the liberated aldehyde reacts with 2-methylheteroarenes in the presence of a base to afford aryl-2-quinoline-2-yl-ethanol intermediate followed by dehydration to yield the desired olefinated product.

Characterization data of intermediates, and E-olefin products:

(**2a'**) **Benzaldehyde**. ^{1}H NMR (400 MHz, $CDCl_3$): δ (ppm) 9.96 (s, 1H), 7.83 (d, *J* = 8 Hz, 1H), 7.58-7.41 (m, 4H). ^{13}C {^{1}H} NMR (100 MHz, $CDCl_3$): δ (ppm) 192.64, 136.31, 134.50, 129.73, 128.98.

(1a') 1-(4-nitrophenyl)-2-(quinolin-2-yl)ethan-1-ol[27]. ^{1}H NMR (400 MHz, $CDCl_3$): δ (ppm) 8.21 (d, J = 8.7 Hz, 2H), 8.13 (d, J = 8.4 Hz, 1H), 8.06 (d, J = 8.4 Hz, 1H), 7.82 (d, J = 8.1 Hz, 1H), 7.76 (dd, J = 11.2, 4.2 Hz, 1H), 7.65 (m, 2H), 7.56 (t, J = 7.2 Hz, 1H), 7.26 – 7.21 (m, 1H), 6.77 (s, 1H), 5.45 (dd, J = 8.7, 3.0 Hz, 1H), 3.32 (m, 1H).^{13}C {^{1}H} NMR (100 MHz, $CDCl_3$): δ (ppm) 159.67, 151.44, 146.88, 137.27, 130.17, 128.62, 127.74, 126.97, 126.70, 126.58, 123.68, 121.94, 72.20, 45.28.

(3a) (E)-2-styrylquinoline[28]. ^{1}H NMR (400 MHz, $CDCl_3$): δ (ppm) 8.09 (t, *J* = 8.6 Hz, 2H), 7.76 (d, *J* = 8.0 Hz, 1H), 7.71 (d, *J* = 6.4 Hz, 1H), 7.68 – 7.61 (m, 4H), 7.48 (t, *J* = 7.4 Hz, 1H), 7.42 (d, *J* = 5.0 Hz, 1H), 7.40 – 7.36 (m, 2H), 7.32 (t, *J* = 7.2 Hz, 1H).^{13}C {^{1}H} NMR (100 MHz, $CDCl_3$): δ (ppm) 156.03, 148.31, 136.56, 136.38, 134.47, 129.78, 129.24, 129.06, 128.84, 128.67, 127.54, 127.39, 127.31, 126.21, 119.30.

(3b) (E)-2-(4-methylstyryl)quinoline[28]. ^{1}H NMR (400 MHz, $CDCl_3$): δ (ppm) 8.10 (dd, *J* = 11.2, 8.6 Hz, 2H), 7.81 – 7.75 (m, 1H), 7.69 (m, 4H), 7.54 (d, *J* = 8.0 Hz, 2H), 7.49 (t, *J*

= 7.5 Hz, 1H), 7.39 (t, *J* = 13.9 Hz, 1H), 7.21 (d, *J* = 7.9 Hz, 1H), 2.38 (s, 3H).^{13}C {^{1}H} NMR (100 MHz, $CDCl_3$): δ (ppm) 156.20, 138.84, 136.42, 134.63, 133.76, 129.81, 129.58, 129.07, 128.61, 128.15, 127.91, 127.52, 127.28, 126.14, 119.20, 21.41.

(3c) (E)-2-(3-methoxystyryl)quinoline[29]. ^{1}H NMR (400 MHz, $CDCl_3$): δ (ppm) 8.17 – 8.06 (m, 3H), 7.94 (s, 1H), 7.78-7.70 (m, 2H), 7.67 – 7.65 (m, 2H), 7.54 – 7.47 (m, 1H), 7.33 – 7.26 (m, 1H), 7.23 – 7.19 (m, 1H), 6.88 (d, *J* = 8.0 Hz, 1H), 3.85 (s, 3H). ^{13}C {^{1}H} NMR (100 MHz, $CDCl_3$): δ (ppm) 159.96, 155.95, 148.27, 137.95, 136.39, 134.36, 129.79, 129.34, 129.21, 127.55, 126.24, 120.18, 119.21, 114.79, 111.92, 55.31.

(3d) (E)-2-(4-methoxystyryl)quinoline[28]. ^{1}H NMR (400 MHz, $CDCl_3$): δ (ppm) 8.07 (dd, *J* = 8.4, 4.5 Hz, 2H), 7.75 (d, *J* = 8.0 Hz, 1H), 7.68 (t, *J* = 7.2 Hz, 1H), 7.65 – 7.56 (m, 4H), 7.46 (t, *J* = 7.4 Hz, 1H), 7.28 (d, *J* = 16.3 Hz, 1H), 6.92 (d, *J* = 8.7 Hz, 2H), 3.83 (s, 3H). ^{13}C {^{1}H} NMR (100 MHz, $CDCl_3$): δ (ppm) 160.16, 156.39, 148.29, 136.29, 134.12, 129.72, 129.34, 129.09, 128.69, 127.52, 127.25, 126.87, 125.98, 119.16, 114.30, 55.36.

(3e) (E)-2-(3-chlorostyryl)quinoline[30]. ^{1}H NMR (400 MHz, $CDCl_3$): δ (ppm) 8.19 – 8.07 (m, 3H), 7.94 (s, 1H), 7.83-7.80 (m, 1H), 7.73 (t, *J* = 7.5 Hz, 1H), 7.65 – 7.62 (m, 1H), 7.52 (dd, *J* = 15.6, 7.8 Hz, 1H), 7.41-7.26 (m,1H). ^{13}C {^{1}H} NMR (100 MHz, $CDCl_3$): δ (ppm) 156.29, 148.93, 137.17, 135.74, 135.00, 133.74, 130.55, 130.19, 129.90, 129.71, 129.51, 129.10, 128.23, 127.02, 120.05.

(3f) (E)-2-(4-chlorostyryl)quinoline[28]. ^{1}H NMR (400 MHz, $CDCl_3$): δ (ppm) 8.13 – 8.05 (m, 2H), 7.77 (d, *J* = 8.1 Hz, 1H), 7.72 – 7.59 (m, 4H), 7.55 (d, *J* = 8.0 Hz, 1H), 7.49 (t, *J* = 7.5 Hz, 1H), 7.43 – 7.31 (m, 3H).^{13}C{^{1}H} NMR (100 MHz, $CDCl_3$): δ (ppm) 155.63, 148.32, 136.44, 135.12, 134.34, 133.06, 129.84, 129.58, 129.28, 129.04, 128.42, 127.53, 126.32, 119.39.

(3g) (E)-2-(3-bromostyryl)quinoline[28]. ^{1}H NMR (400 MHz, $CDCl_3$): δ (ppm) 8.19 – 8.05 (m, 3H), 7.93 (s, 1H), 7.82 – 7.76 (m, 4H), 7.73 – 7.69 (m, 2H), 7.63 – 7.57 (m, 1H), 7.53 (d, *J* = 7.4 Hz, 1H).^{13}C{^{1}H} NMR (100 MHz, $CDCl_3$): δ (ppm) 155.38, 148.26, 138.73, 136.53, 134.66, 132.74, 131.39, 130.32, 130.05, 129.90, 129.29, 127.56, 126.43, 125.87, 123.00, 119.47.

(3h) (E)-2-(4-nitrostyryl)quinoline[28]. ^{1}H NMR (400 MHz, $CDCl_3$): δ (ppm) 8.27 (d, *J* = 8.6 Hz, 2H), 8.19 (d, *J* = 8.5 Hz, 1H), 8.11 (d, *J* = 8.4 Hz, 1H), 7.83 – 7.66 (m, 5H), 7.67 (d, *J* = 8.5 Hz, 1H), 7.54 (dd, *J* = 15.5, 6.3 Hz, 2H). ^{13}C{^{1}H} NMR (100 MHz, $CDCl_3$): δ (ppm) 154.69, 143.01, 136.76, 133.18, 131.74, 130.11, 129.43, 127.70, 127.61, 126.84, 124.23, 119.78.

(3i) (E)-2-(3,4-dimethoxystyryl)quinoline[31]. ^{1}H NMR (400 MHz, $CDCl_3$): δ (ppm) 8.11 (m, 3H), 7.97 (d, *J* = 18.4 Hz, 2H), 7.80 – 7.69 (m, 4H), 7.54 – 7.36 (m, 2H), 3.92 (s, 3H), 3.89 (s, 3H). ^{13}C NMR (100 MHz, $CDCl_3$): δ (ppm) 156.49, 155.43, 153.12, 148.35, 147.60, 136.56, 136.25, 134.66, 130.60, 129.86, 128.82, 127.50, 126.64, 124.25, 119.57, 118.94, 112.44, 61.32, 55.90.

(3j) (E)-2-(2,6-dimethoxystyryl)quinoline. ^{1}H NMR (400 MHz, $CDCl_3$): δ (ppm) 8.09 (dd, *J* = 11.8, 8.6 Hz, 2H), 7.98 (d, *J* = 16.6 Hz, 1H), 7.77 (d, *J* = 8.6 Hz, 2H), 7.71 – 7.67 (m, 1H), 7.48 – 7.41 (m, 2H), 7.27 (d, *J* = 9.7 Hz, 1H), 6.86 (d, *J* = 1.4 Hz, 2H), 3.88 (s, 3H), 3.82 (s, 3H). ^{13}C {^{1}H} NMR (100 MHz, $CDCl_3$): δ (ppm) 156.65, 153.77, 151.95, 148.26, 136.21, 129.74, 129.68, 129.19, 129.11, 127.51, 127.32, 126.11, 118.90, 115.78, 112.47, 111.40, 56.26, 55.83.

(3k) (E)-2-(3,4,5-trimethoxystyryl)quinoline. ^{1}H NMR (400 MHz, $CDCl_3$): δ (ppm) 8.14 (d, *J* = 8.6 Hz, 1H), 8.07 (d, *J* = 8.4 Hz, 1H), 7.79 (d, *J* = 8.1 Hz, 1H), 7.72 (m, 2H), 7.59 (d, *J* = 16.3 Hz, 1H), 7.51 (d, *J* = 7.8 Hz, 1H), 7.34 (d, *J* = 16.3 Hz, 1H), 6.89 (s, 6H), 3.93

(s, 5H), 3.90 (s, 3H).$^{13}C\{^{1}H\}$ NMR (100 MHz, $CDCl_3$): δ (ppm) 155.97, 153.46, 148.26, 136.43, 134.35, 132.18, 129.86, 129.12, 128.59, 127.56, 127.35, 126.24, 118.91, 104.30, 61.03, 56.17.

(3l) (E)-2-(2,6-dichlorostyryl)quinoline. ^{1}H NMR (400 MHz, $CDCl_3$): δ (ppm) 8.22 – 8.07 (m, 2H), 7.95 (s, 1H), 7.85 – 7.78 (m, 2H), 7.75 – 7.67 (m, 2H), 7.55 – 7.48 (m, 2H), 7.38 (d, *J* = 8.0 Hz, 1H), 7.15 (t, *J* = 8.1 Hz, 1H). $^{13}C\{^{1}H\}$ NMR (100 MHz, $CDCl_3$): δ (ppm) 155.34, 148.31, 137.16, 136.58, 136.48, 134.86, 134.67, 133.97, 132.94, 129.61, 129.48, 128.65, 127.64, 126.58, 126.54, 119.56, 119.30.

(3m) (E)-2-(2-(naphthalen-1-yl)vinyl)quinoline. ^{1}H NMR (400 MHz, $CDCl_3$): δ (ppm) 8.51 (d, *J* = 16.0 Hz, 1H), 8.33 (d, *J* = 8.3 Hz, 1H), 8.12 (d, *J* = 8.0 Hz, 2H), 7.90 – 7.68 (m, 6H), 7.58 – 7.43 (m, 5H). $^{13}C\ \{^{1}H\}$ NMR (100 MHz, $CDCl_3$): δ (ppm) 156.07, 148.36, 136.48, 134.10, 133.83, 131.77, 131.56, 131.44, 129.84, 129.36, 129.02, 128.75, 127.59, 127.48, 126.40, 126.29, 126.01, 125.77, 124.27, 123.81, 119.62.

(3n) (E)-2-(2-(anthracen-9-yl)vinyl)quinoline. ^{1}H NMR (400 MHz, $CDCl_3$): δ (ppm) 8.64 (d, *J* = 16.5 Hz, 1H), 8.50 – 8.41 (m, 2H), 8.33 (dd, *J* = 5.8, 3.3 Hz, 1H), 8.24 (d, *J* = 8.6 Hz, 1H), 8.17 (d, *J* = 8.3 Hz, 1H), 8.08 – 7.99 (m, 2H), 7.89 – 7.70 (m, 4H), 7.52 (m, 4H), 7.32 (s, 1H).$^{13}C\ \{^{1}H\}$ NMR (100 MHz, $CDCl_3$): δ (ppm) 155.63, 148.38, 137.46, 136.63, 134.14, 133.51, 131.50, 129.88, 129.69, 129.48, 128.77, 127.61, 127.24, 126.39, 125.98, 125.79, 125.30, 119.70.

(3o) (E)-2-(2-(pyren-2-yl)vinyl)-4a,8a-dihydroquinoline. ^{1}H NMR (400 MHz, $CDCl_3$): δ (ppm) 8.59 (d, *J* = 16.0 Hz, 1H), 8.37 (d, *J* = 9.2 Hz, 1H), 8.24 (d, *J* = 8.0 Hz, 1H), 8.12 – 7.95 (m, 5H), 7.93 – 7.78 (m, 4H), 7.62 (d, *J* = 7.7 Hz, 2H), 7.53 – 7.45 (m, 1H), 7.40 – 7.36 (m, 1H). $^{13}C\{^{1}H\}$ NMR (100 MHz, $CDCl_3$): δ (ppm) 156.09, 148.36, 136.31, 134.20,

131.48, 131.41, 131.37, 131.07, 130.82, 130.68, 129.79, 129.30, 128.90, 127.82, 127.58, 127.41, 126.18, 126.02, 125.50, 125.27, 125.15, 125.02, 123.77, 122.86, 119.58.

(5a) (E)-2-styrylpyrazine[28]. ^{1}H NMR (400 MHz, $CDCl_3$): δ (ppm) 8.64 (d, *J* = 1.1 Hz, 1H), 8.58 – 8.51 (m, 1H), 8.40 (d, *J* = 2.4 Hz, 1H), 7.75 (d, *J* = 16.1 Hz, 1H), 7.60 (d, *J* = 7.3 Hz, 2H), 7.40 (t, *J* = 7.4 Hz, 2H), 7.35 (d, *J* = 7.2 Hz, 1H), 7.16 (d, *J* = 16.1 Hz, 1H).^{13}C {^{1}H} NMR (100 MHz, $CDCl_3$): δ (ppm) 151.31, 144.37, 143.79, 142.77, 136.06, 135.23, 129.03, 128.88, 127.36, 124.05.

(5b) (E)-2-(4-methylstyryl)pyrazine[28]. ^{1}H NMR (400 MHz, $CDCl_3$): δ (ppm) 8.60 (s, 1H), 8.50 (s, 1H), 8.36 (s, 1H), 7.70 (d, J = 16 Hz, 1H), 7.59 – 7.40 (m, 2H), 7.26 – 7.07 (m, 3H), 2.36 (s, 3H).^{13}C{^{1}H}NMR (100 MHz, $CDCl_3$): δ (ppm) 151.50, 144.31, 143.66, 142.49, 139.19, 135.17, 133.29, 129.60, 127.84, 127.32, 123.03, 21.42.

(5c) (E)-2-(4-methoxystyryl)pyrazine[28]. ^{1}H NMR (400 MHz, $CDCl_3$) δ (ppm) 8.61 (s, 1H), 8.51 (s, 1H), 8.36 (s, 1H), 7.70 (d, *J* = 16.0 Hz, 1H), 7.54 (d, *J* = 8.0 Hz, 2H), 7.02 (d, *J* = 16.1 Hz, 1H), 6.92 (t, *J* = 8.2 Hz, 2H), 3.85 (s, 3H).^{13}C{^{1}H} NMR (100 MHz, $CDCl_3$): δ (ppm) 160.42, 144.27, 143.56, 142.28, 134.81, 129.25, 128.78, 121.85, 114.34, 55.38.

(5d) (E)-2-(3-methoxystyryl)pyrazine. ^{1}H NMR (400 MHz, $CDCl_3$): δ (ppm) 8.65 (s, 1H), 8.55 (s, 1H), 8.42 (s, 1H), 7.72 (d, *J* = 16.1 Hz, 1H), 7.34-7.27 (m, 2H), 7.21-7.13 (m, 2H), 6.90 (d, *J* = 8.2 Hz, 1H), 3.86 (s, 3H). ^{13}C{^{1}H} NMR (100 MHz, $CDCl_3$): δ (ppm) 159.96, 151.22, 144.38, 143.79, 142.81, 137.46, 135.13, 129.85, 124.36, 120.05, 114.83, 112.39, 55.32.

(5e) (E)-2-(3-chlorostyryl)pyrazine. ^{1}H NMR (400 MHz, $CDCl_3$): δ (ppm) 8.64 (s, 1H), 8.56 (s, 1H), 8.44 (s, 1H), 7.70 (d, *J* = 15.8 Hz, 1H), 7.59 (s, 1H), 7.46 (d, *J* = 6.3 Hz, 1H), 7.32 (m, 2H), 7.16 (d, *J* = 16.1 Hz, 1H). ^{13}C{^{1}H} NMR (100 MHz, $CDCl_3$): δ (ppm) 151.04, 144.51, 143.95, 143.09, 134.82, 134.66, 133.93, 129.19, 128.58, 124.65.

(5f) (E)-2-(4-chlorostyryl)pyrazine[28]. ^{1}H NMR (400 MHz, $CDCl_3$): δ (ppm) 8.63 (d, *J* = 1.2 Hz, 1H), 8.57 – 8.49 (m, 1H), 8.42 (d, *J* = 2.4 Hz, 1H), 7.70 (d, *J* = 16.1 Hz, 1H), 7.52 (d, *J* = 8.5 Hz, 2H), 7.40 – 7.33 (m, 2H), 7.12 (d, *J* = 16.1 Hz, 1H).^{13}C{^{1}H} NMR (100 MHz, $CDCl_3$): δ (ppm) 150.94, 144.43, 143.86, 143.00, 134.73, 134.56, 133.83, 129.10, 128.50, 124.55.

(5g) (E)-2-(3-bromostyryl)pyrazine. ^{1}H NMR (400 MHz, $CDCl_3$): δ (ppm) 8.63 (s, 1H), 8.56 (d, *J* = 1.4 Hz, 1H), 8.43 (d, *J* = 2.3 Hz, 1H), 7.79 – 7.62 (m, 2H), 7.48 (dd, *J* = 15.7, 7.5 Hz, 2H), 7.28 (d, *J* = 7.3 Hz, 1H), 7.15 (d, *J* = 16.0 Hz, 1H).^{13}C{^{1}H} NMR (100 MHz, $CDCl_3$): δ (ppm) 150.73, 144.47, 143.97, 143.19, 138.22, 133.58, 131.77, 130.37, 129.99, 126.07, 125.38, 123.05.

(5h) (E)-2-(2,6-dimethoxystyryl)pyrazine. ^{1}H NMR (400 MHz, $CDCl_3$): δ (ppm) 8.68 (s, 1H), 8.54 (s, 1H), 8.38 (s, 1H), 8.03 (d, *J* = 16.2 Hz, 1H), 7.27 – 7.18 (m, 2H), 6.87 (s, 2H), 3.87 (s, 3H), 3.82 (s, 3H). ^{13}C{^{1}H} NMR (100 MHz, $CDCl_3$) δ (ppm) 153.65, 152.27, 151.85, 144.32, 143.69, 142.48, 130.21, 125.06, 115.55, 112.48, 112.35, 56.14, 55.82.

(5i) (E)-2-(3,4-dimethoxystyryl)pyrazine. ^{1}H NMR (400 MHz, $CDCl_3$): δ (ppm) 8.69 (s, 1H), 8.55 (s, 1H), 8.40 (d, *J* = 2.4 Hz, 1H), 8.04 (d, *J* = 16.3 Hz, 1H), 7.25 (dd, *J* = 26.2, 11.8 Hz, 2H), 7.09 (t, *J* = 8.0 Hz, 1H), 6.91 (d, *J* = 8.0 Hz, 1H), 3.90 (s, 3H), 3.89 (s, 3H).^{13}C{^{1}H} NMR (100 MHz, $CDCl_3$): δ (ppm) 153.18, 151.69, 147.82, 144.36, 143.71, 142.65, 130.26, 129.78, 125.67, 124.22, 118.64, 112.70, 61.26, 55.88.

(5j) (E)-2-(2,3-dimethoxystyryl)pyrazine. ^{1}H NMR (400 MHz, $CDCl_3$): δ (ppm) 8.62 (d, *J* = 1.3 Hz, 1H), 8.49 (dd, *J* = 2.3, 1.6 Hz, 1H), 8.34 (d, *J* = 2.5 Hz, 1H), 7.97 (d, *J* = 16.3 Hz, 1H), 7.23-7.13 (m, 2H), 7.03 (t, *J* = 8.0 Hz, 1H), 6.85 (dd, *J* = 8.1, 1.2 Hz, 1H). ^{13}C{^{1}H} NMR (100 MHz, $CDCl_3$): δ (ppm) 152.44, 150.96, 147.09, 143.62, 142.97, 141.91, 129.53, 129.05, 124.94, 123.48, 117.91, 111.96, 60.52, 55.15.

(5k) (E)-2-(2,6-dichlorostyryl)pyrazine. ^{1}H NMR (400 MHz, $CDCl_3$): δ (ppm) 8.65 (s, 1H), 8.60 (s, 1H), 8.47 (s, 1H), 7.85 (d, *J* = 16.3 Hz, 1H), 7.38 (d, *J* = 8.0 Hz, 2H), 7.31 (s, 1H), 7.17 (t, *J* = 8.0 Hz, 1H).^{13}C{^{1}H} NMR (100 MHz, $CDCl_3$): δ (ppm) 150.54, 144.57, 144.07, 143.55, 134.88, 133.56, 132.38, 129.03, 128.96, 128.77.

(5l) (E)-2-(2-(naphthalen-1-yl)vinyl)pyrazine[28]. ^{1}H NMR (400 MHz, $CDCl_3$): δ (ppm) 8.66 (s, 1H), 8.59 (d, *J* = 15.5 Hz, 2H), 8.42 (d, *J* = 2.0 Hz, 1H), 8.28 (d, *J* = 8.2 Hz, 1H), 7.85 (dd, *J* = 17.6, 8.9 Hz, 3H), 7.52 (m, 3H), 7.20 (d, *J* = 16 Hz, 1H).^{13}C{^{1}H} NMR (100 MHz, $CDCl_3$): δ (ppm) 151.32, 144.47, 143.98, 142.95, 133.78, 133.66, 132.25, 131.52, 129.35, 128.73, 126.73, 126.54, 126.11, 125.64, 124.17, 123.72.

(5m) (E)-2-(2-(pyren-2-yl)vinyl)pyrazine. ^{1}H NMR (400 MHz, $CDCl_3$): δ (ppm) 8.68 (d, *J* = 15.5 Hz, 1H), 8.51 (d, *J* = 28.2 Hz, 2H), 8.39 – 8.32 (m, 2H), 8.15- 8.06 (m, 4H), 8.00 – 7.90 (m, 4H), 7.21 – 7.13 (m, 1H).^{13}C{^{1}H} NMR (100 MHz, $CDCl_3$): δ (ppm) 151.38, 144.40, 143.98, 142.69, 131.71, 131.38, 130.79, 130.07, 129.09, 128.00, 127.90, 127.36, 126.11, 125.62, 125.40, 125.25, 125.06, 124.93, 124.72, 123.55, 122.78.

(E)-2-(2-(pyridin-4-yl)vinyl)quinoline: ^{1}H NMR (400 MHz, $CDCl_3$): δ (ppm) 8.65 (d, *J* = 4.2 Hz, 1H), 8.12 (dd, *J* = 14.7, 8.5 Hz, 2H), 7.81 (dd, *J* = 15.8, 6.9 Hz, 3H), 7.69 (dd, *J* = 15.1, 7.2 Hz, 3H), 7.52 (dd, *J* = 18.0, 10.5 Hz, 2H), 7.20 (dd, *J* = 6.9, 5.2 Hz, 1H). ^{13}C{^{1}H} NMR (100 MHz, $CDCl_3$): δ (ppm) 155.36, 155.09, 149.84, 148.31, 136.68, 136.55, 133.73, 132.65, 129.82, 129.41, 127.57, 126.47, 122.86, 122.79, 120.33.

NMR spectra of catalytic isolated products

(i) Intermediate-benzaldehyde

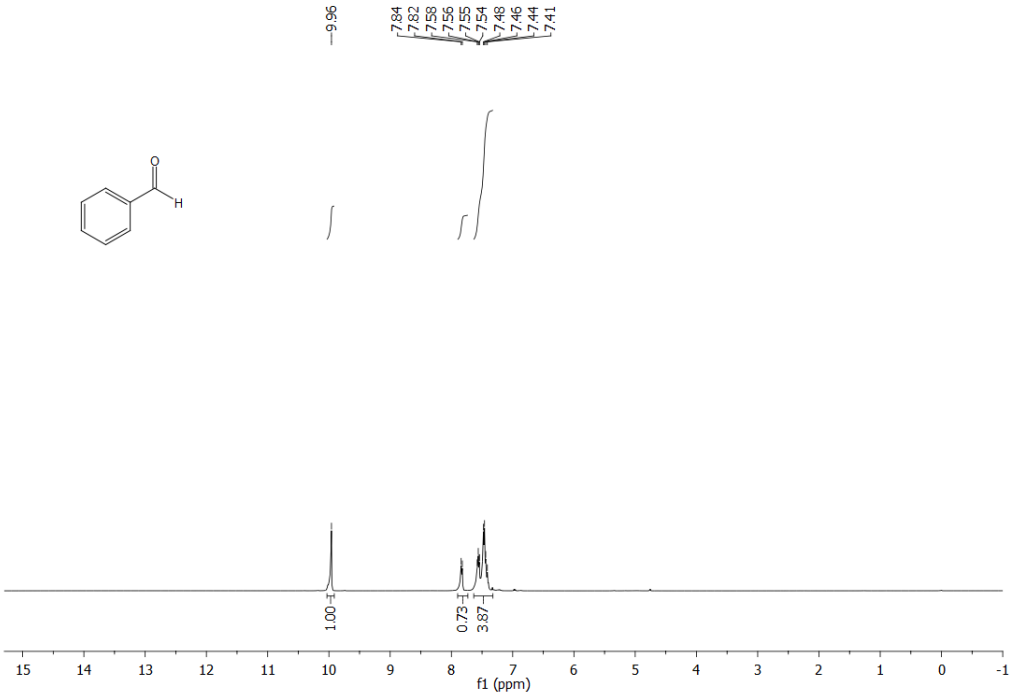

Figure 9: ^{1}H NMR spectrum for (**2a'**) in $CDCl_3$ (400MHz, 300K).

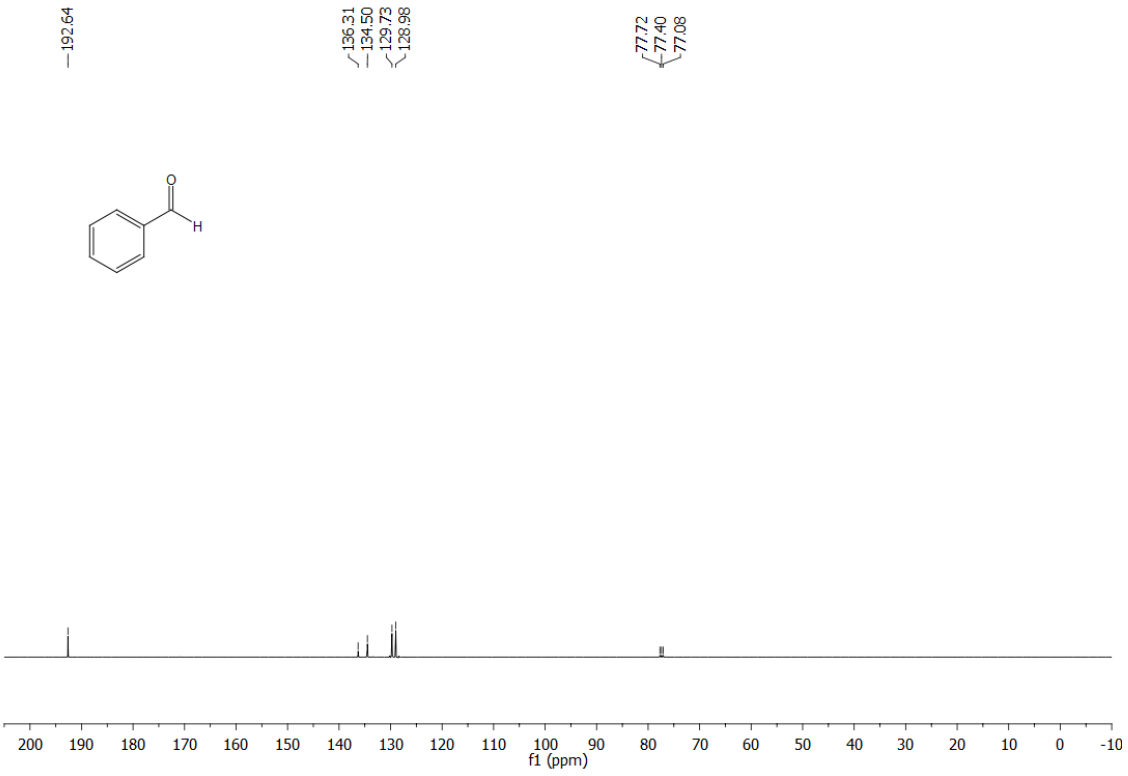

Figure 10: ^{13}C NMR spectrum for (**2a'**) in in $CDCl_3$ (100MHz, 300K).

Intermediate- aryl-2-quinoline-2-yl-ethanol

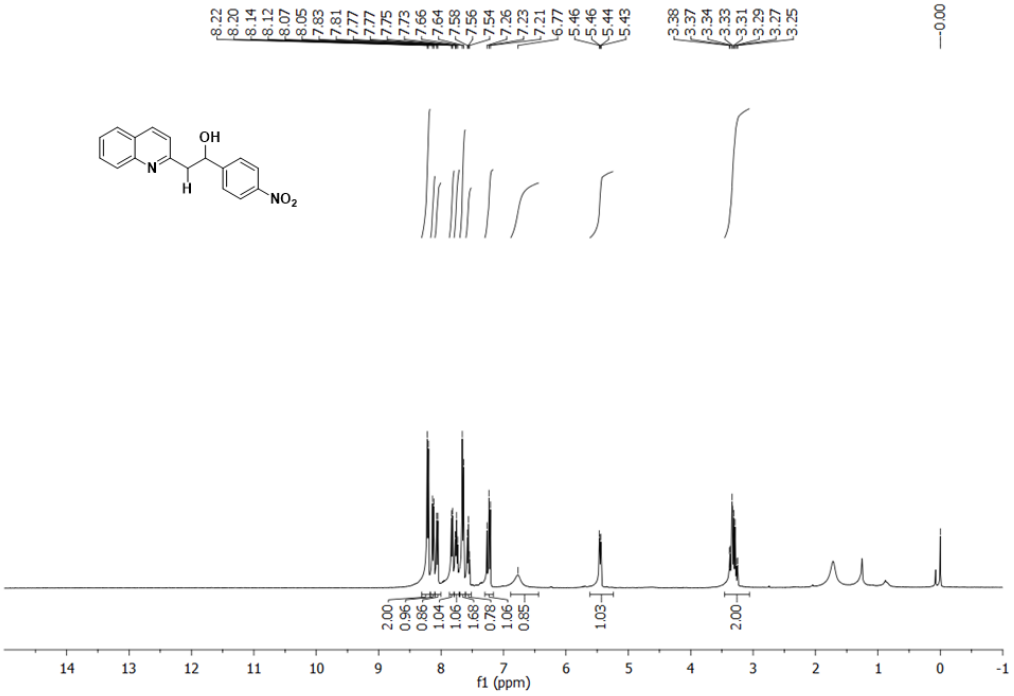

Figure 11: ^{1}H NMR spectrum for (**1a'**) in $CDCl_3$ (400MHz, 300K).

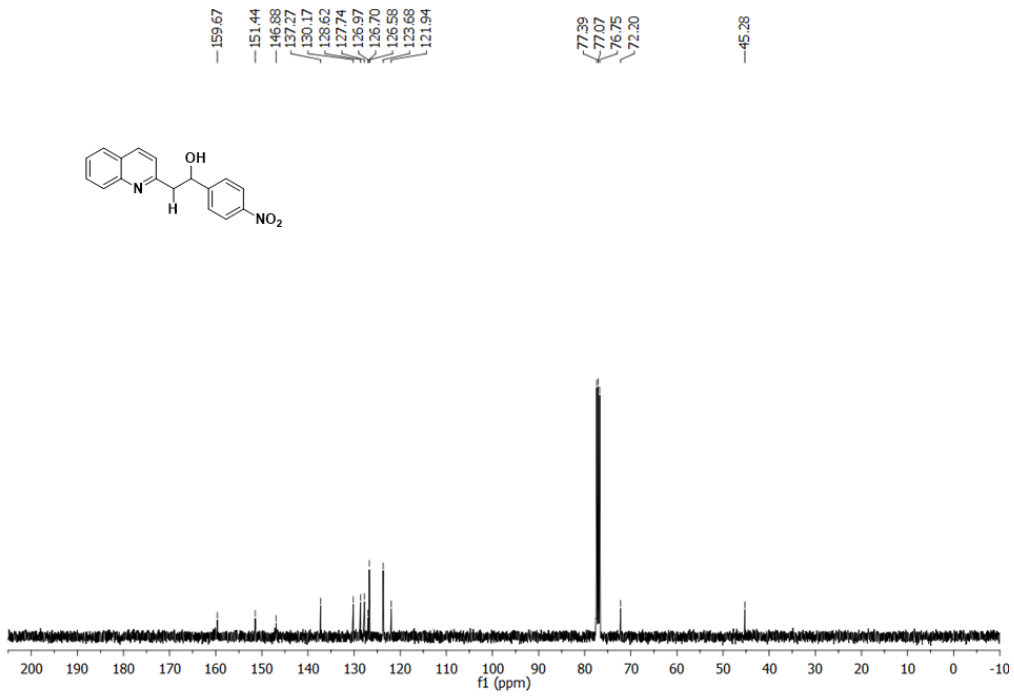

Figure 12: ^{13}C NMR spectrum for (**1a'**) in $CDCl_3$ (100MHz, 300K).

NMR spectrum of E-olefin products (3a-3o and 5a-5m)

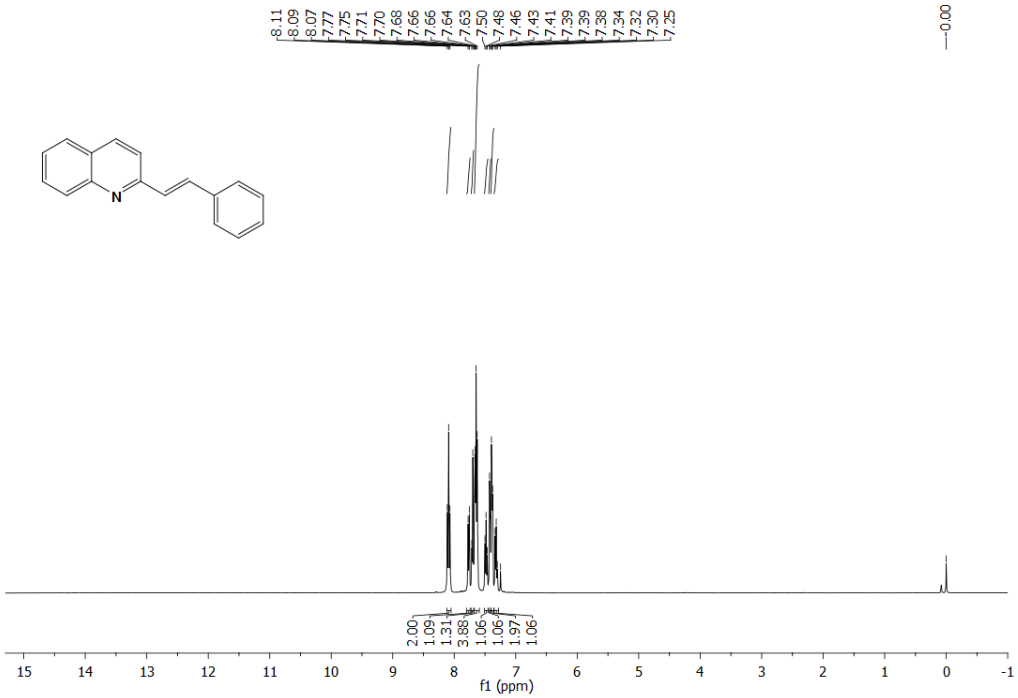

Figure 13: ^{1}H NMR spectrum for (**3a**) in $CDCl_3$ (400MHz, 300K).

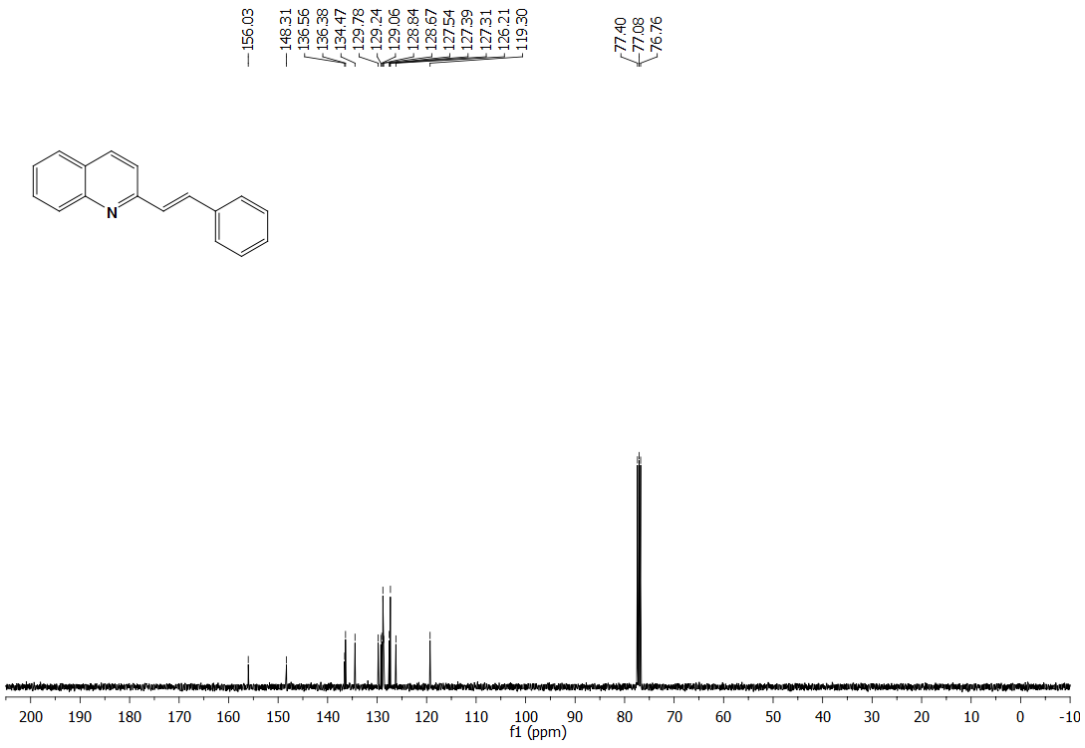

Figure 14: ^{13}C NMR spectrum for (**3a**) in $CDCl_3$ (100MHz, 300K).

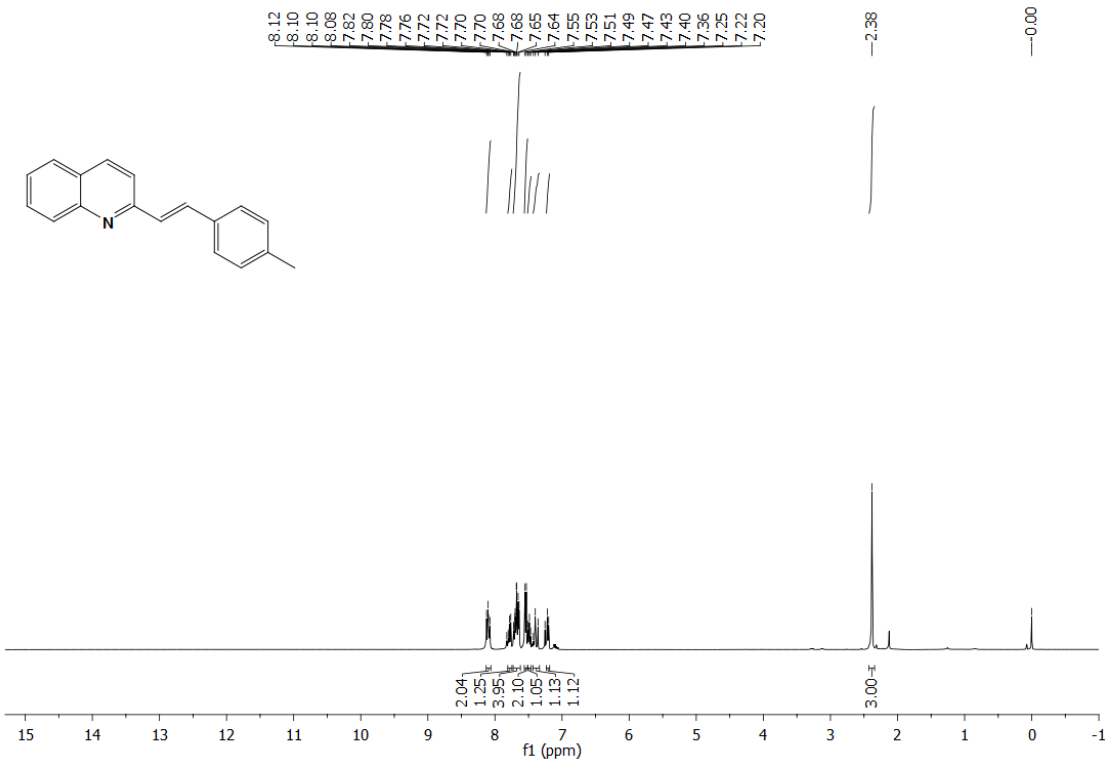

Figure 15: ^{1}H NMR spectrum for (**3b**) in $CDCl_3$ (400MHz, 300K).

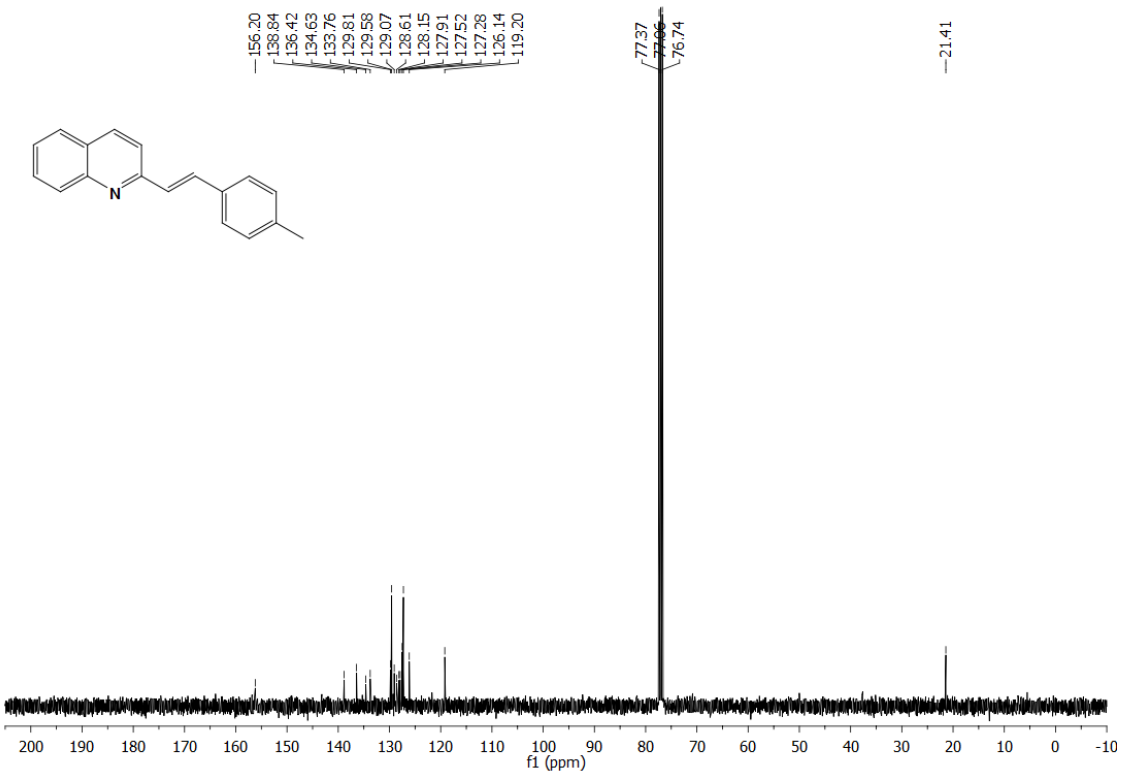

Figure 16: ^{13}C NMR spectrum for (**3b**) in $CDCl_3$ (100MHz, 300K).

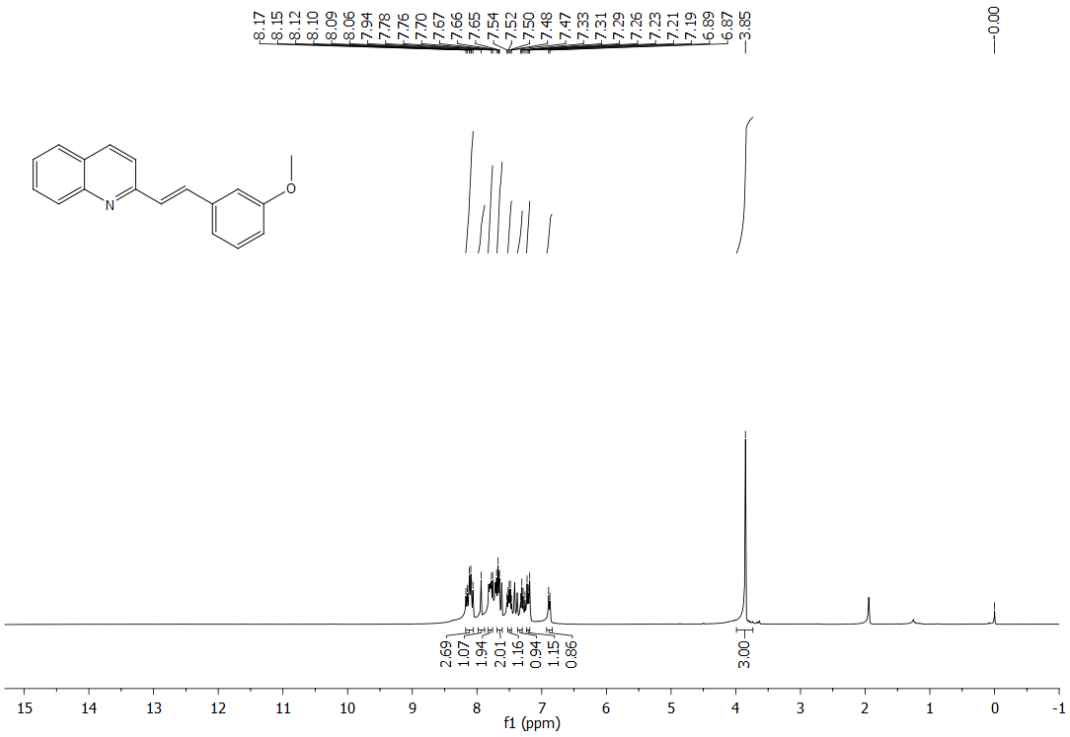

Figure 17: ^{1}H NMR spectrum for (**3c**) in $CDCl_3$ (400MHz, 300K).

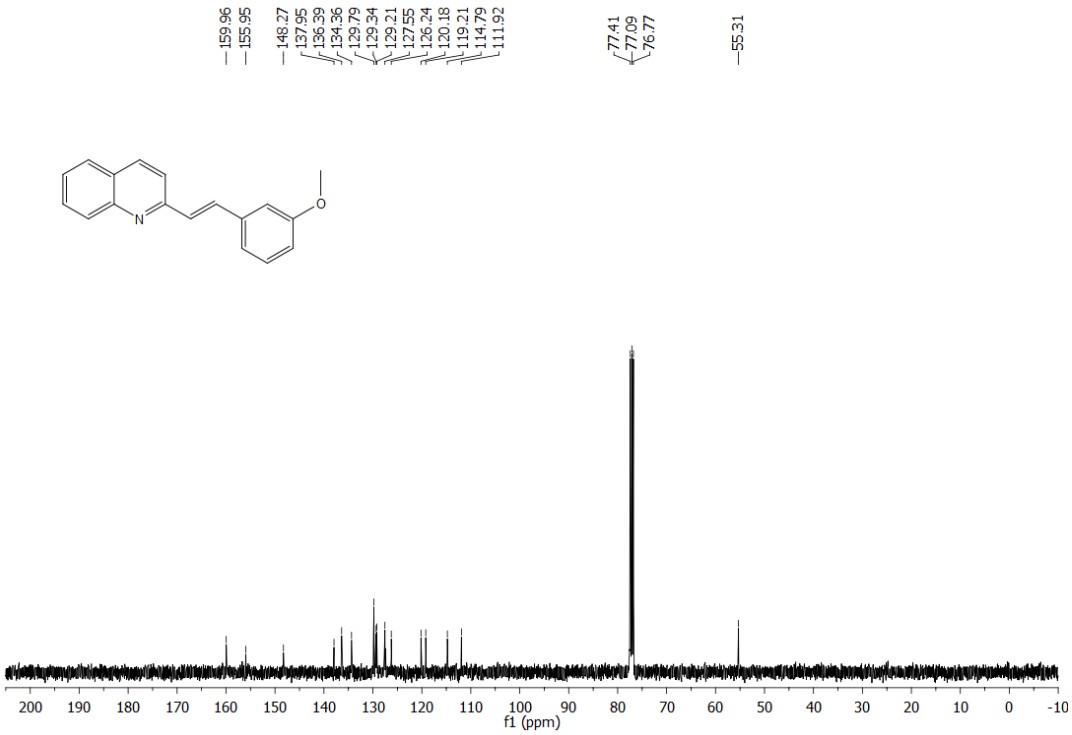

Figure 18: ^{13}C NMR spectrum for (**3c**) in $CDCl_3$ (100MHz, 300K).

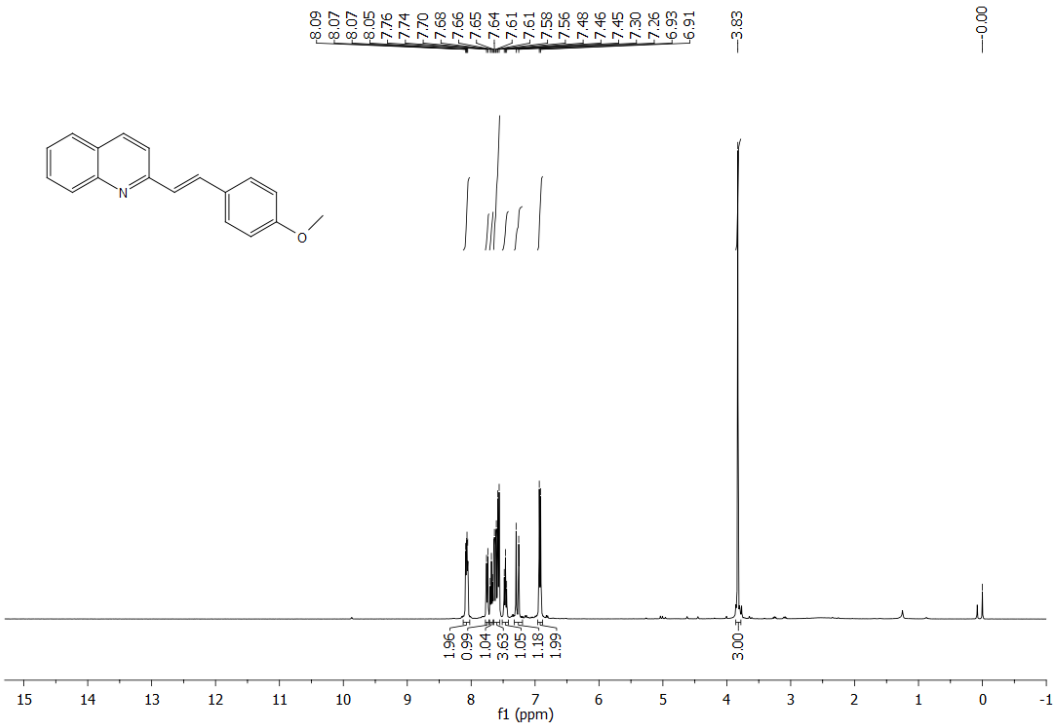

Figure 19: ^{1}H NMR spectrum for (**3d**) in $CDCl_3$ (400MHz, 300K).

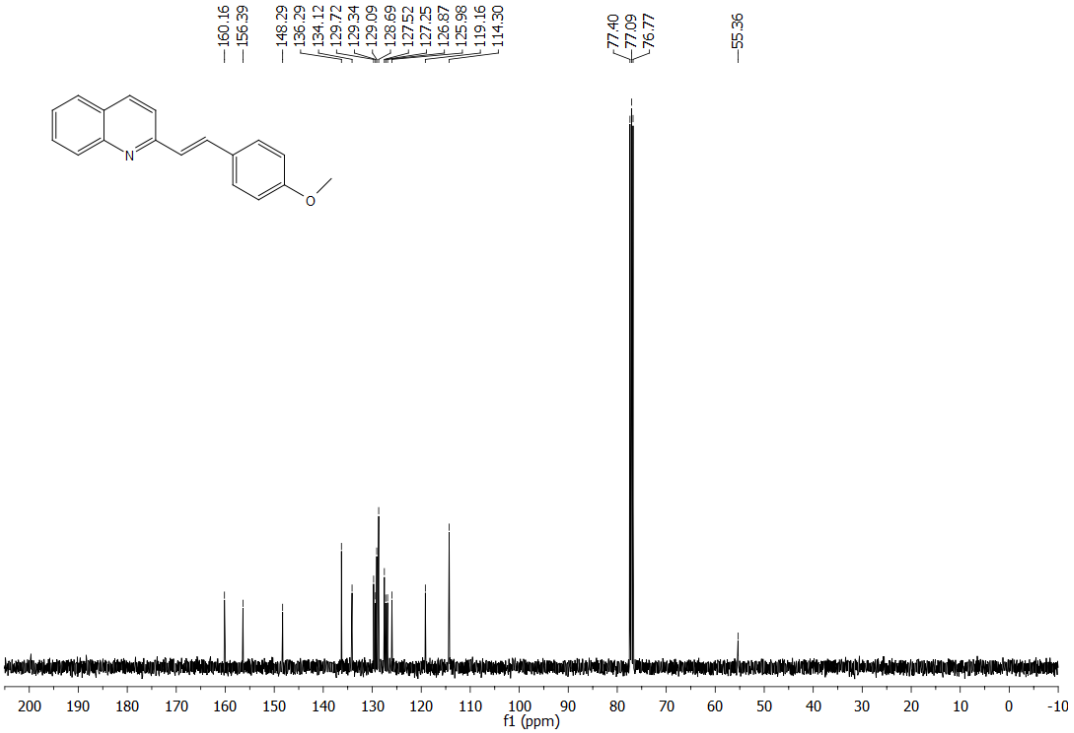

Figure 20: ^{13}C NMR spectrum for (**3d**) in $CDCl_3$ (100MHz, 300K).

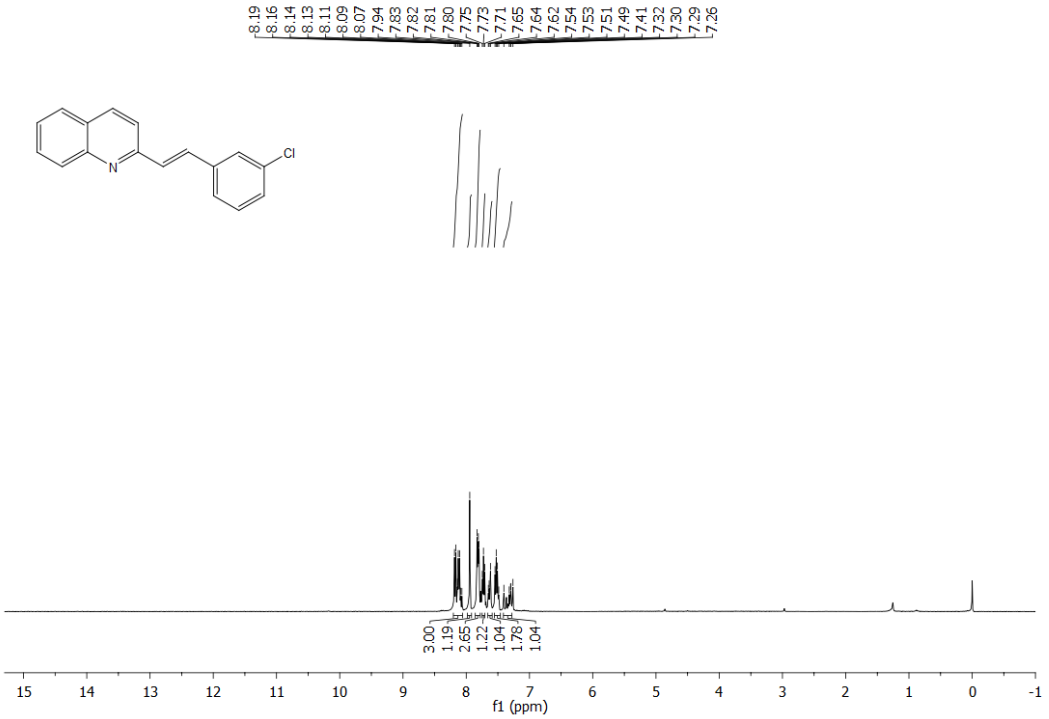

Figure 21: ^{1}H NMR spectrum for (**3e**) in $CDCl_3$ (400MHz, 300K).

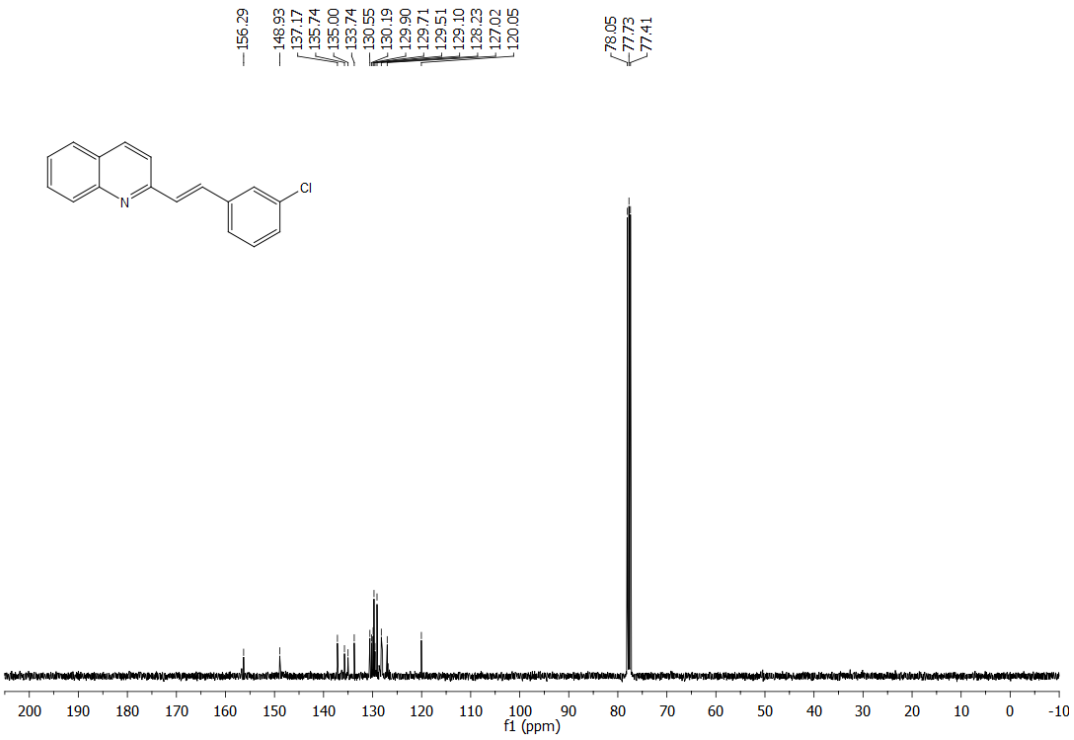

Figure 22: ^{13}C NMR spectrum for (**3e**) in $CDCl_3$ (100MHz, 300K).

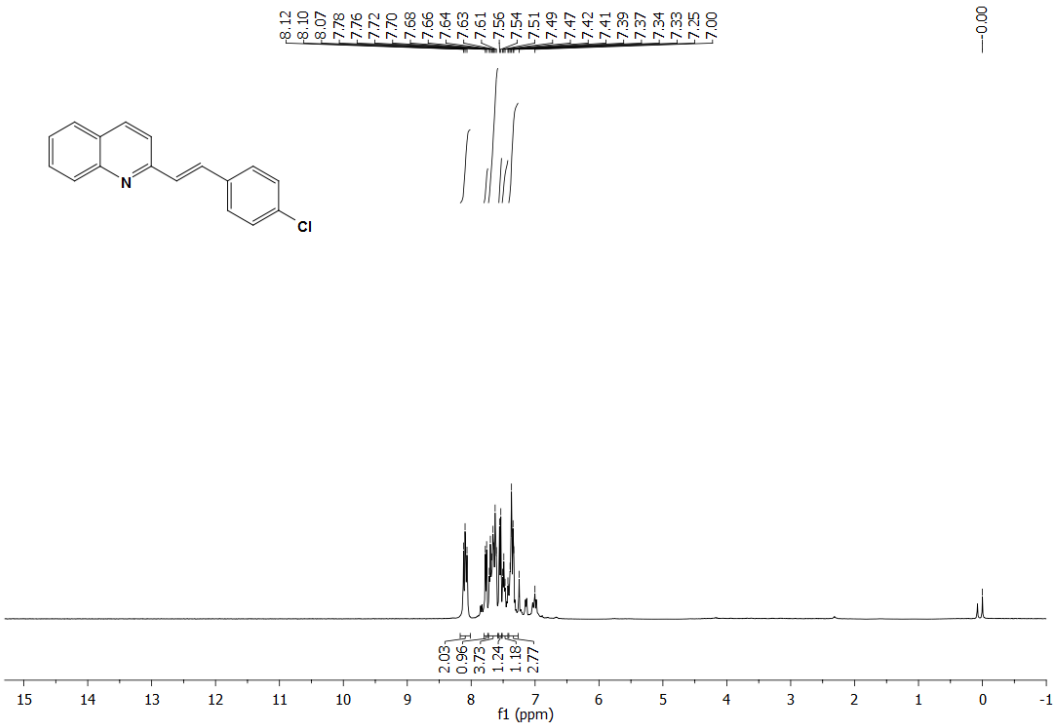

Figure 23: ^{1}H NMR spectrum for (**3f**) in $CDCl_3$ (400MHz, 300K).

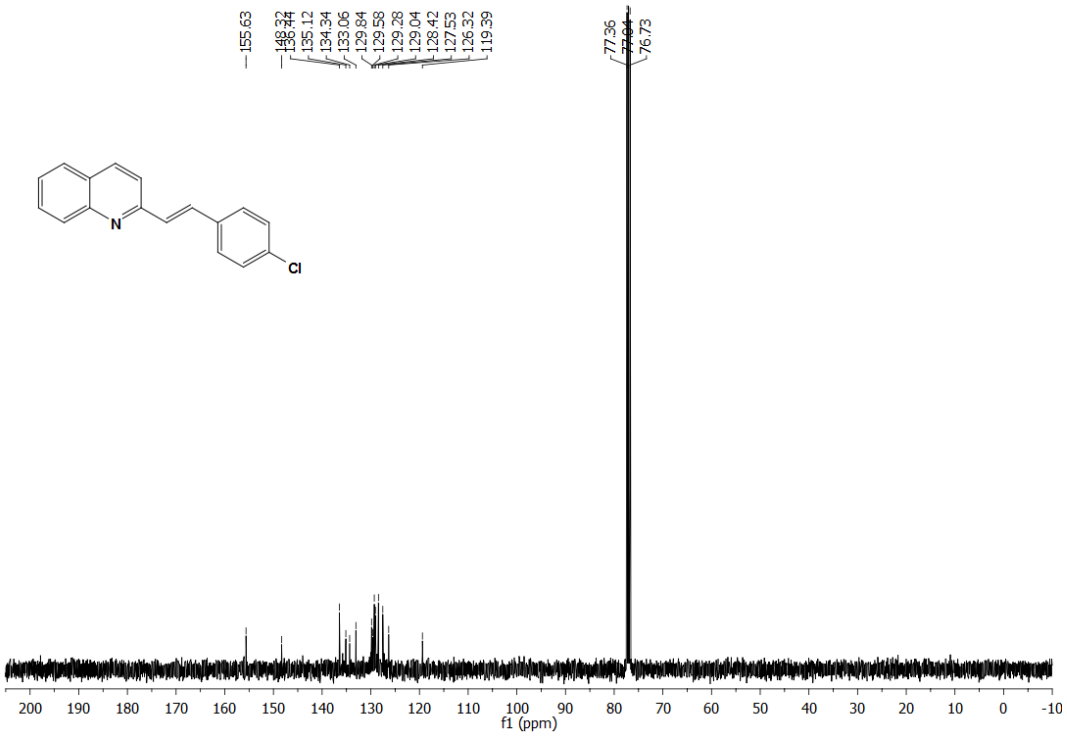

Figure 24: ^{13}C NMR spectrum for (**3f**) in $CDCl_3$ (100MHz, 300K).

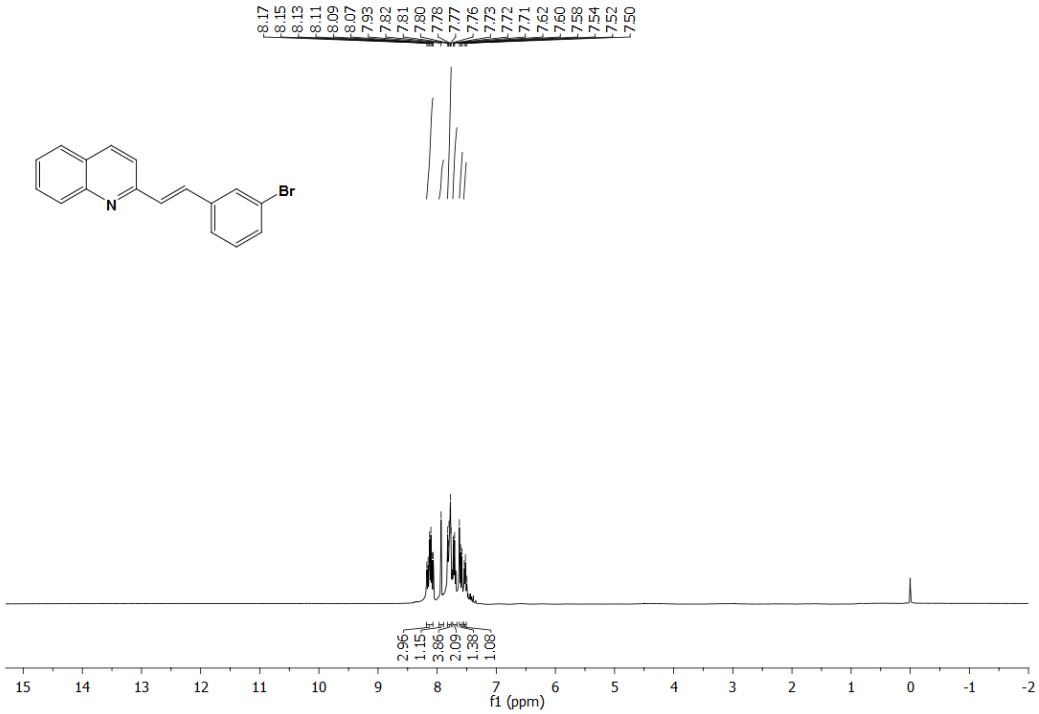

Figure 25: ^{1}H NMR spectrum for (**3g**) in $CDCl_3$ (400MHz, 300K).

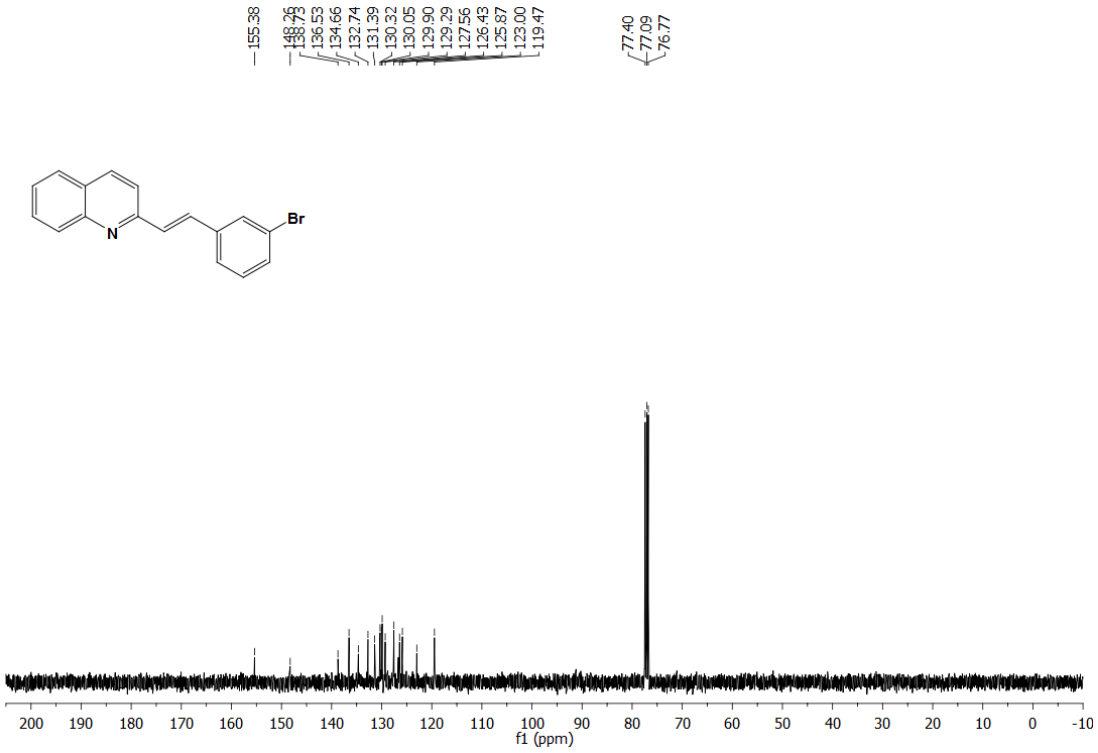

Figure 26: ^{13}C NMR spectrum for (**3g**) in $CDCl_3$ (100MHz, 300K).

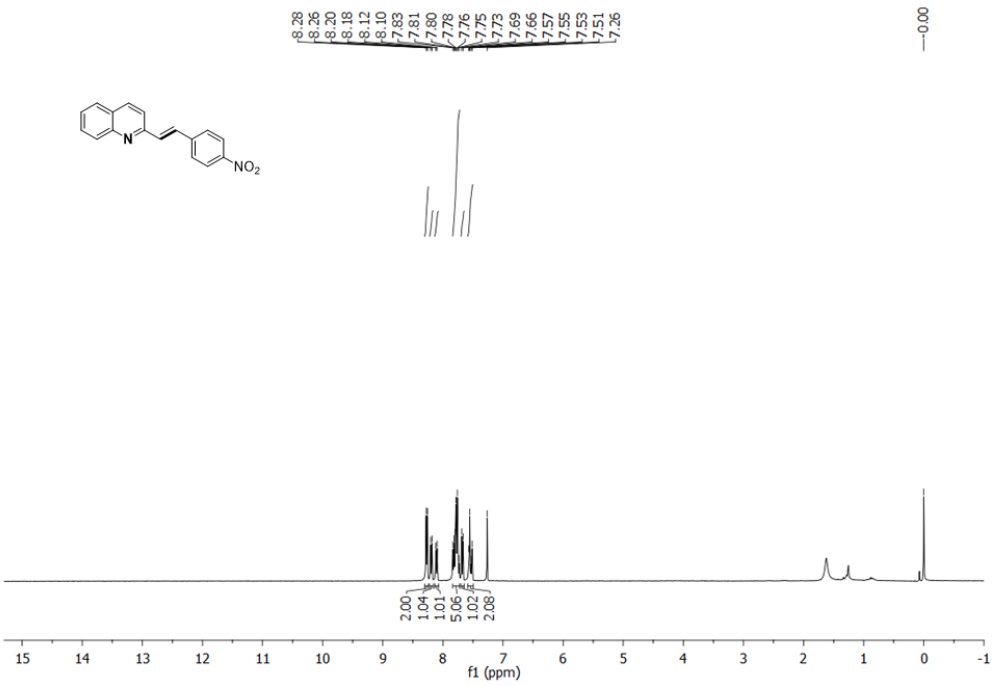

Figure 27: ^{1}H NMR spectrum for (**3h**) in $CDCl_3$ (400MHz, 300K).

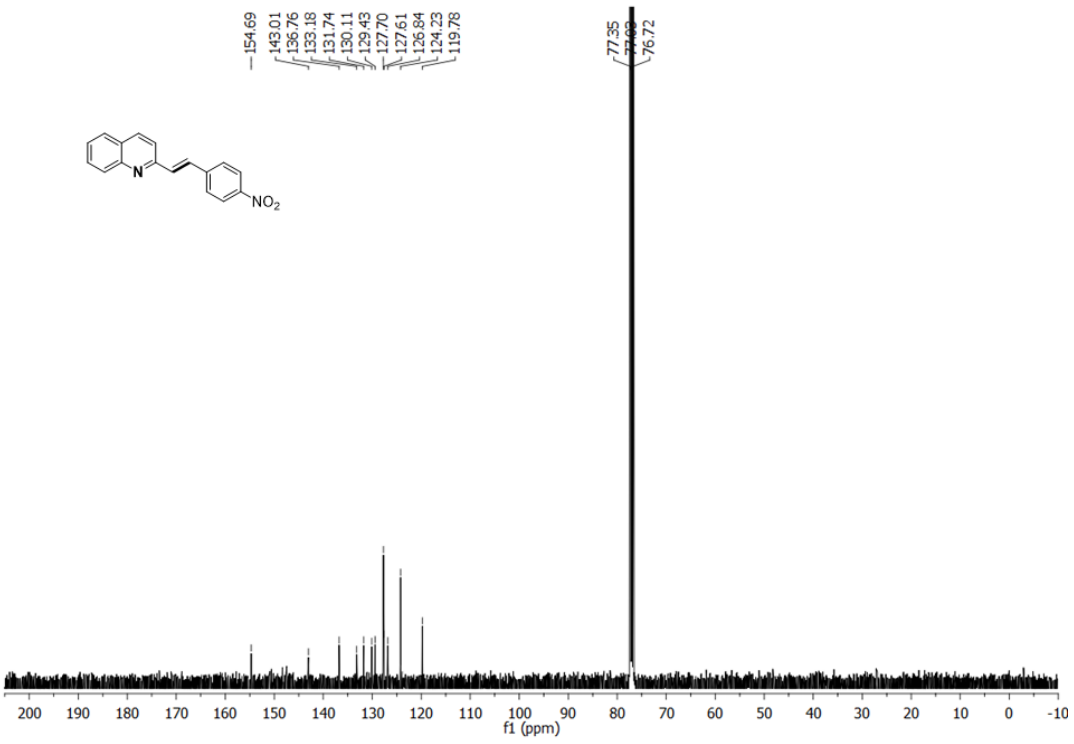

Figure 28: ^{13}C NMR spectrum for (**3h**) in $CDCl_3$ (100MHz, 300K).

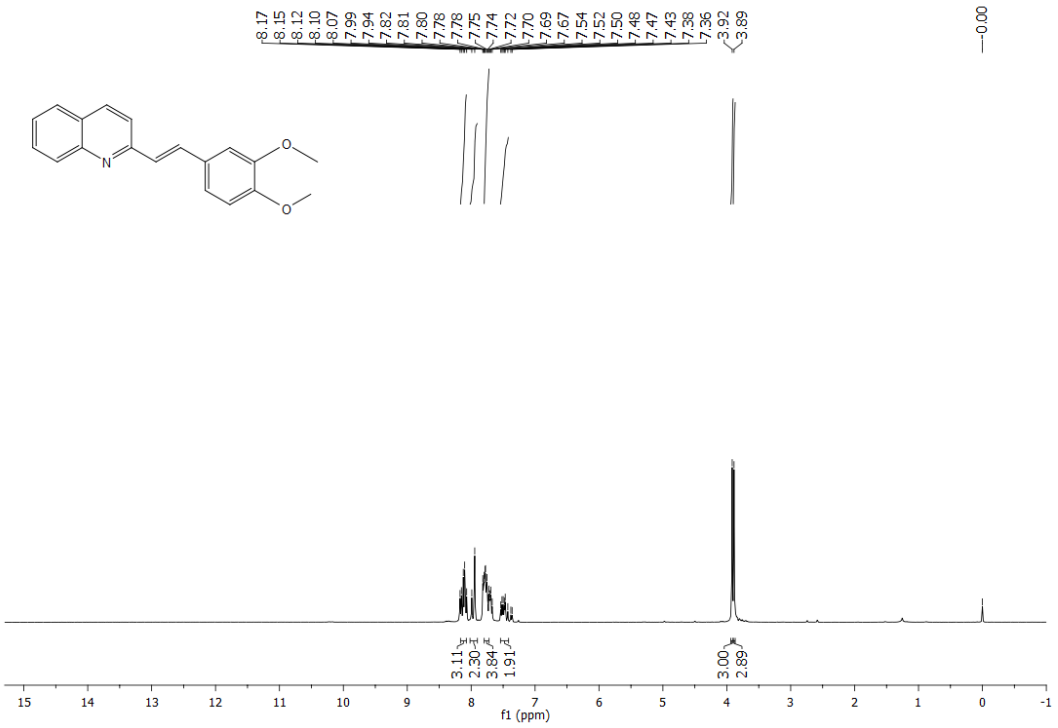

Figure 29: ^{1}H NMR spectrum for (**3i**) in $CDCl_3$ (400MHz, 300K).

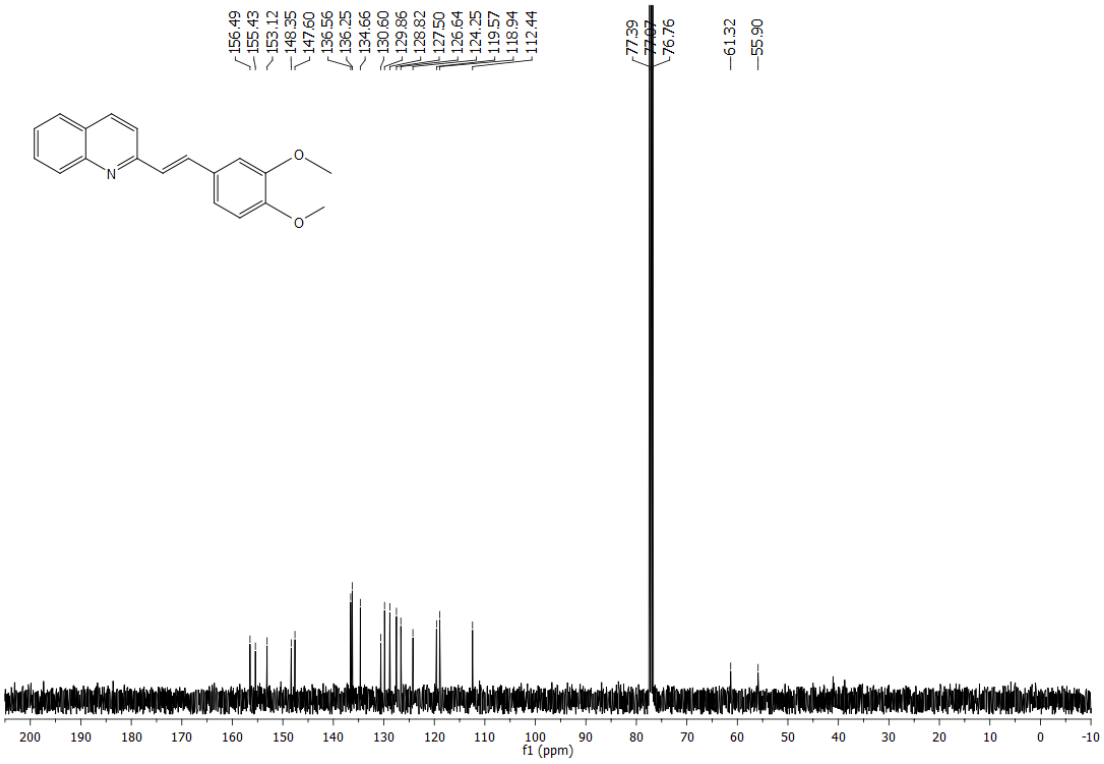

Figure 30: ^{13}C NMR spectrum for (**3i**) in $CDCl_3$ (100MHz, 300K).

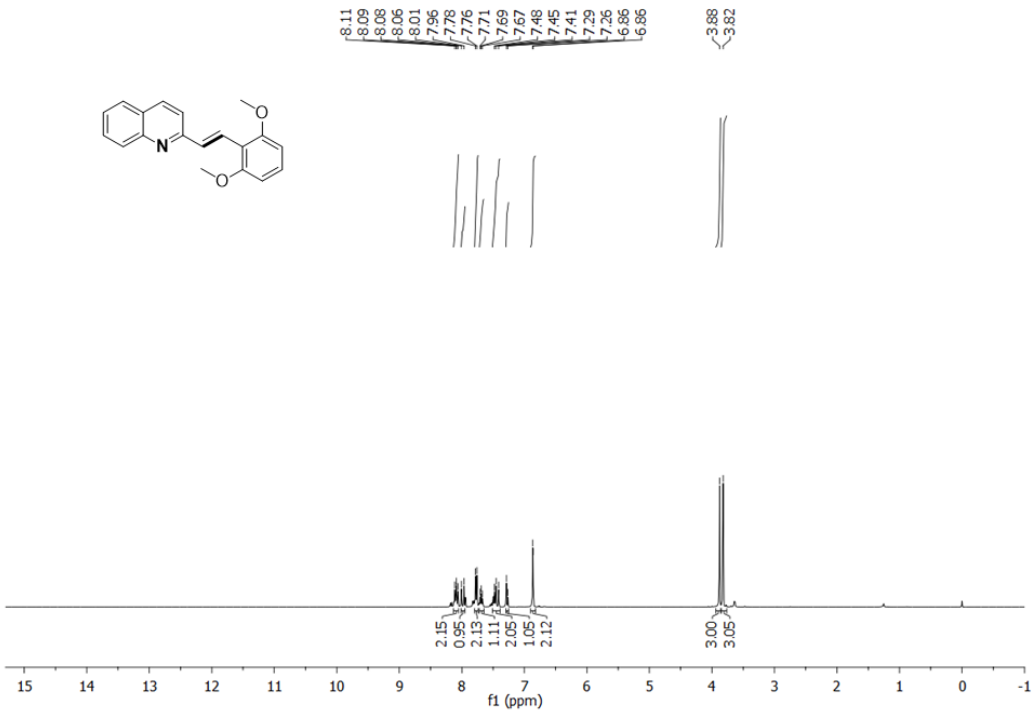

Figure 31: ^{1}H NMR spectrum for (**3j**) in $CDCl_3$ (400MHz, 300K).

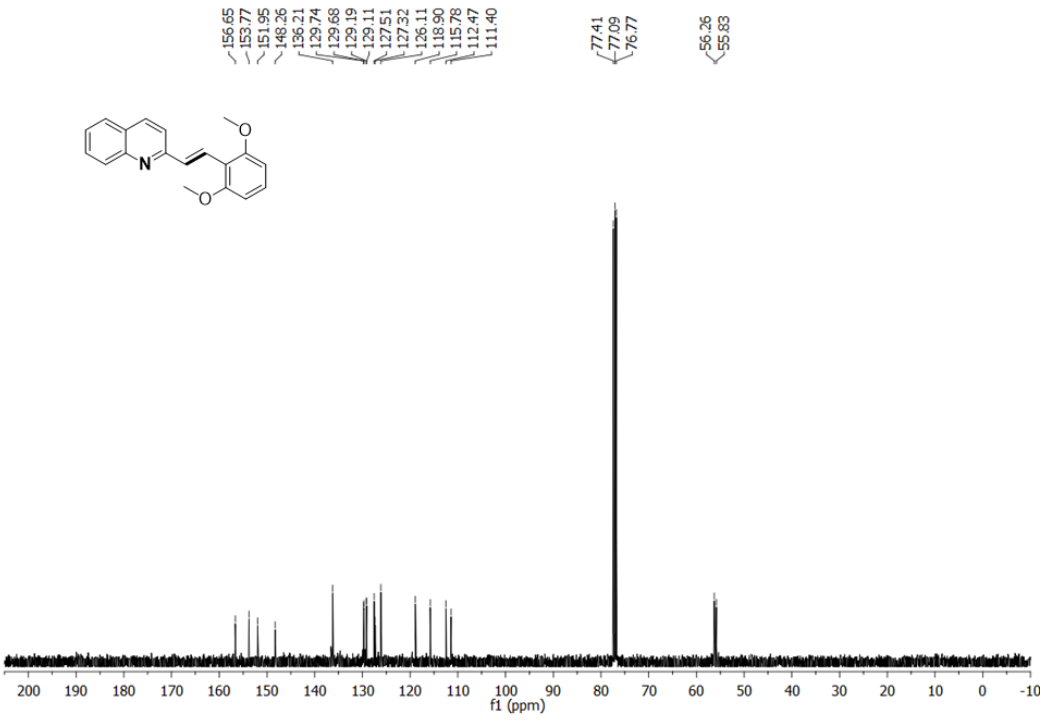

Figure 32: ^{13}C NMR spectrum for (**3j**) in $CDCl_3$ (100MHz, 300K).

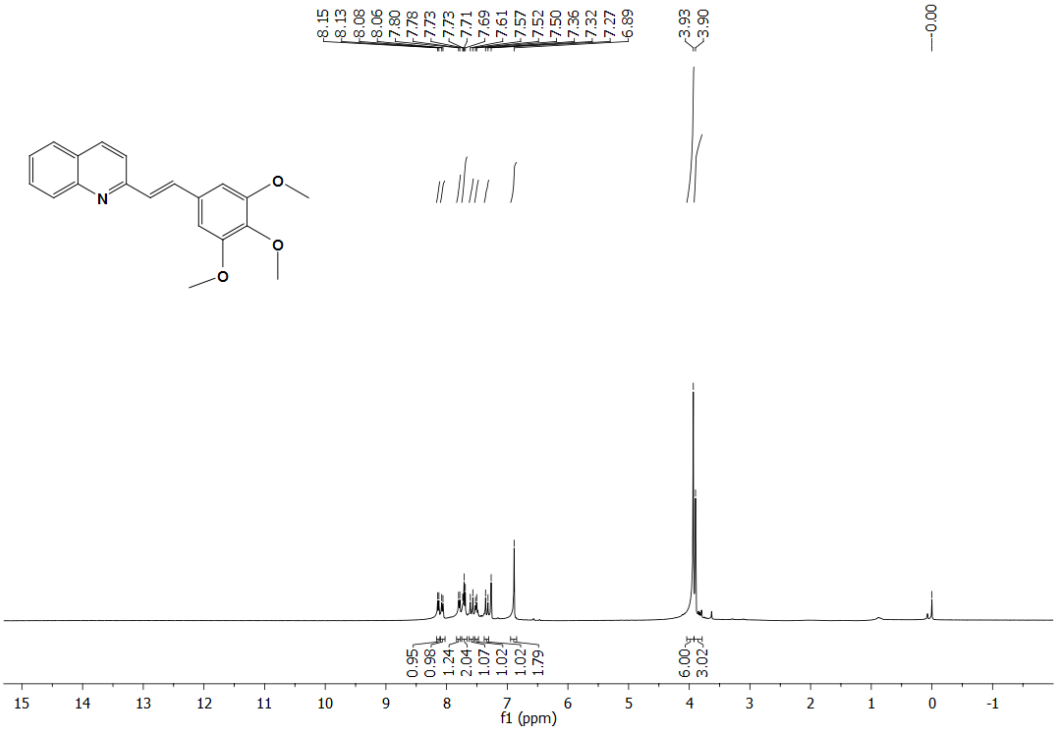

Figure 33: ^{1}H NMR spectrum for (**3k**) in $CDCl_3$ (400MHz, 300K).

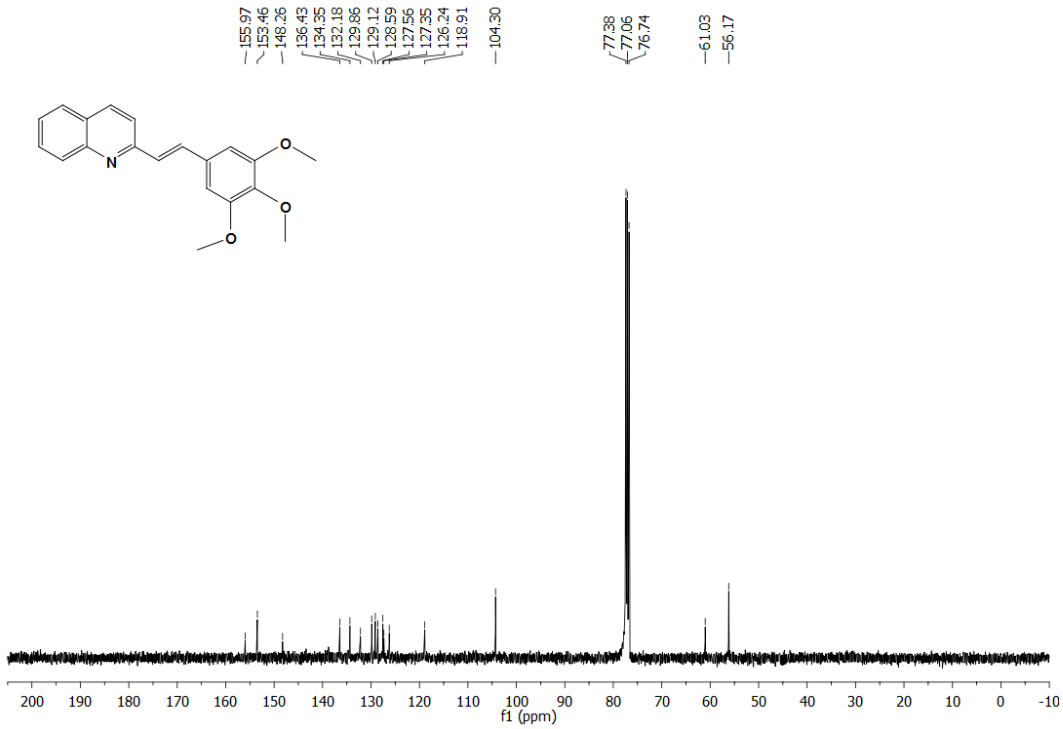

Figure 34: ^{13}C NMR spectrum for (**3k**) in $CDCl_3$ (100MHz, 300K).

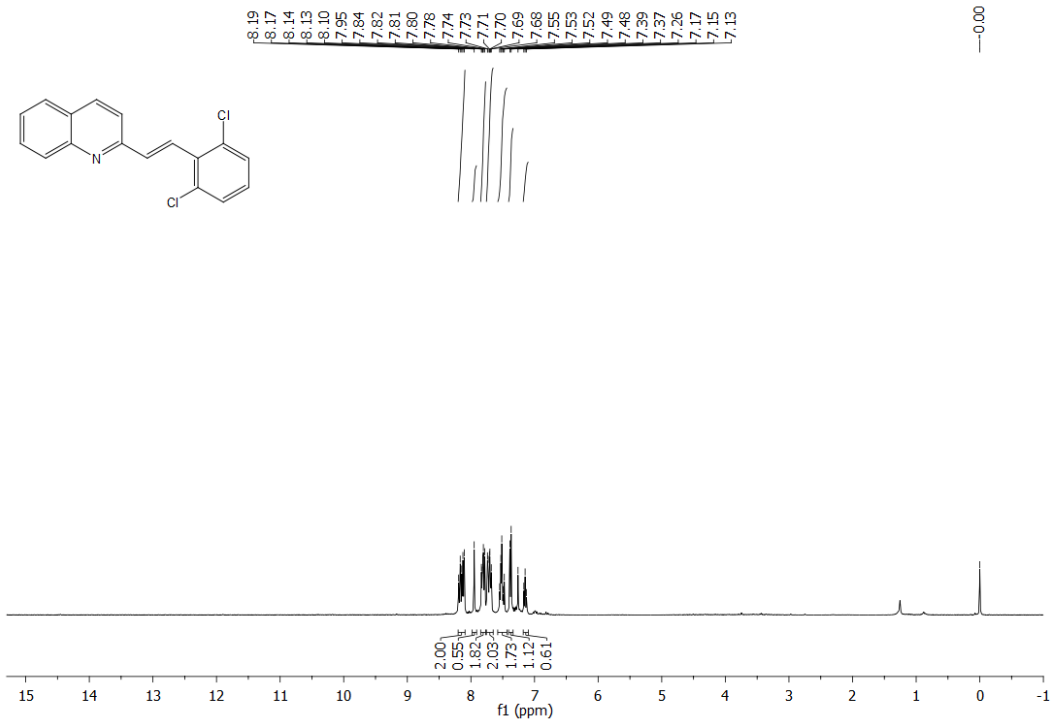

Figure 35: ^{1}H NMR spectrum for (**3l**) in $CDCl_3$ (400MHz, 300K).

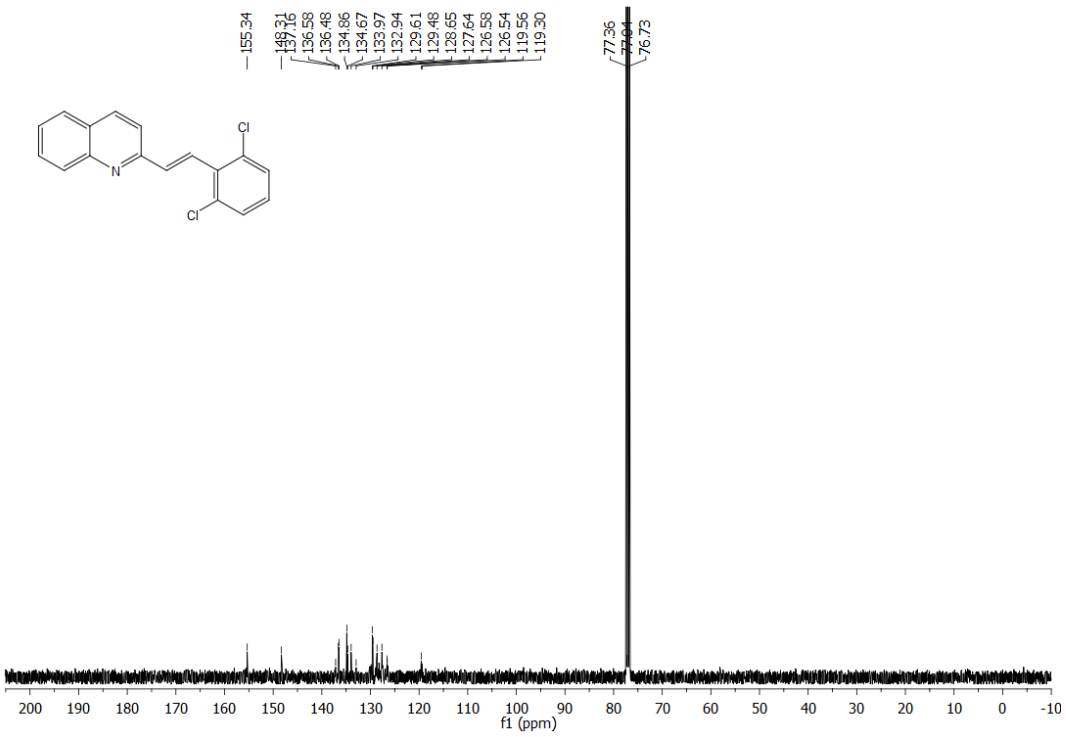

Figure 36: ^{13}C NMR spectrum for (**3l**) in $CDCl_3$ (100MHz, 300K).

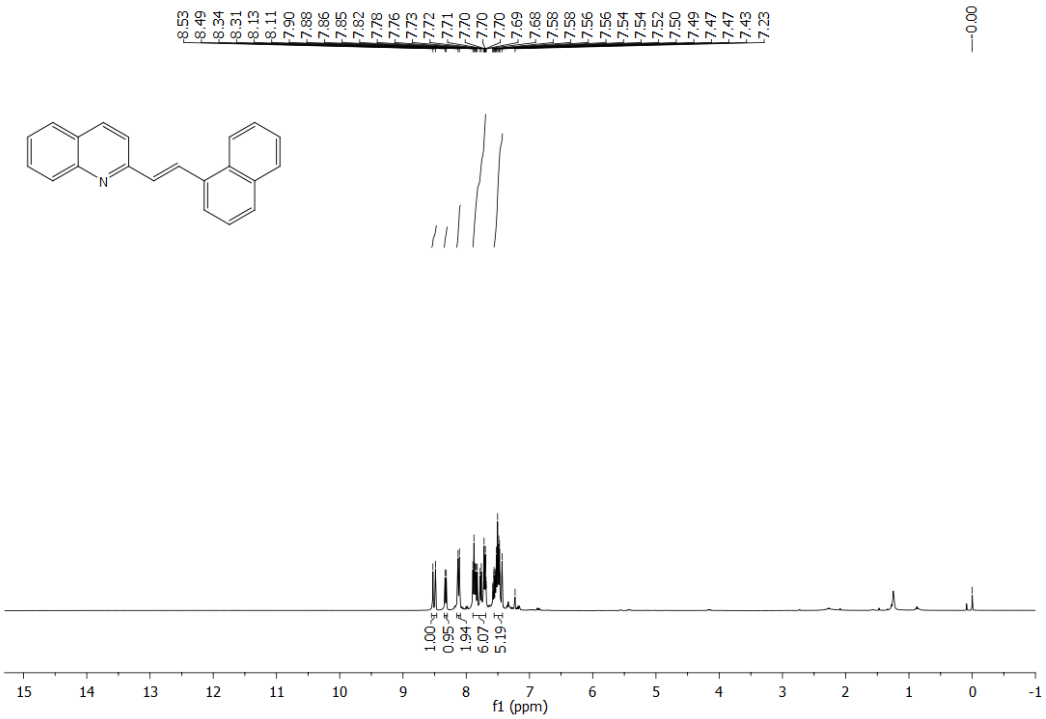

Figure 37: ^{1}H NMR spectrum for (**3m**) in $CDCl_3$ (400MHz, 300K).

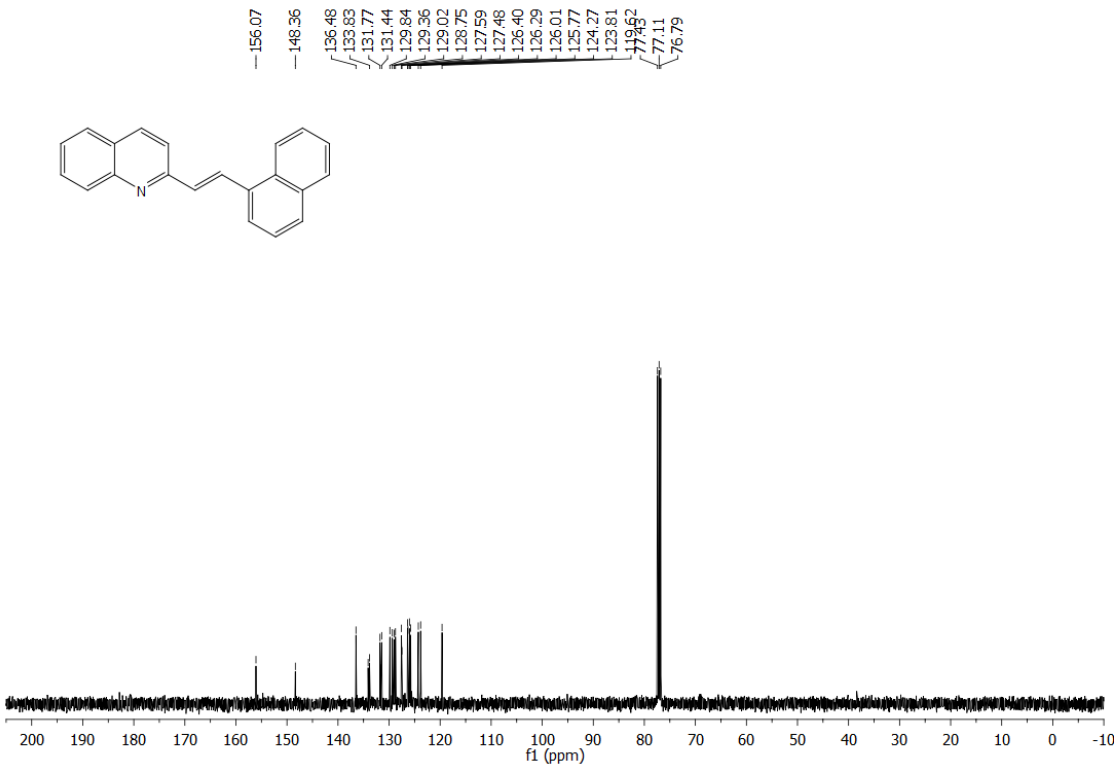

Figure 38: ^{13}C NMR spectrum for (**3m**) in $CDCl_3$ (100MHz, 300K).

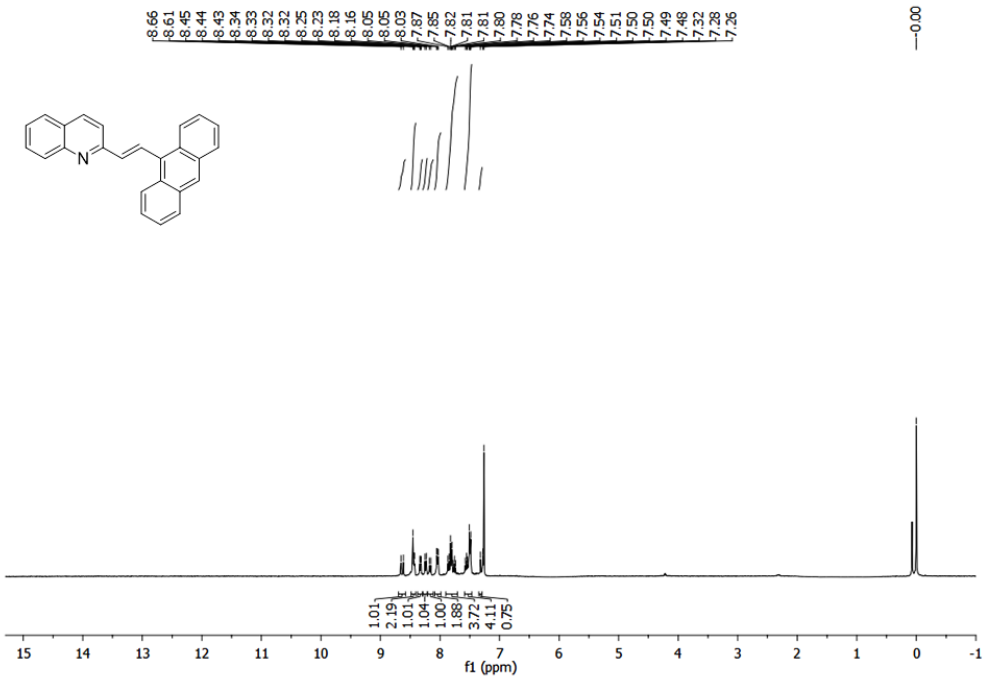

Figure 39: ^{1}H NMR spectrum for (**3n**) in $CDCl_3$ (400MHz, 300K).

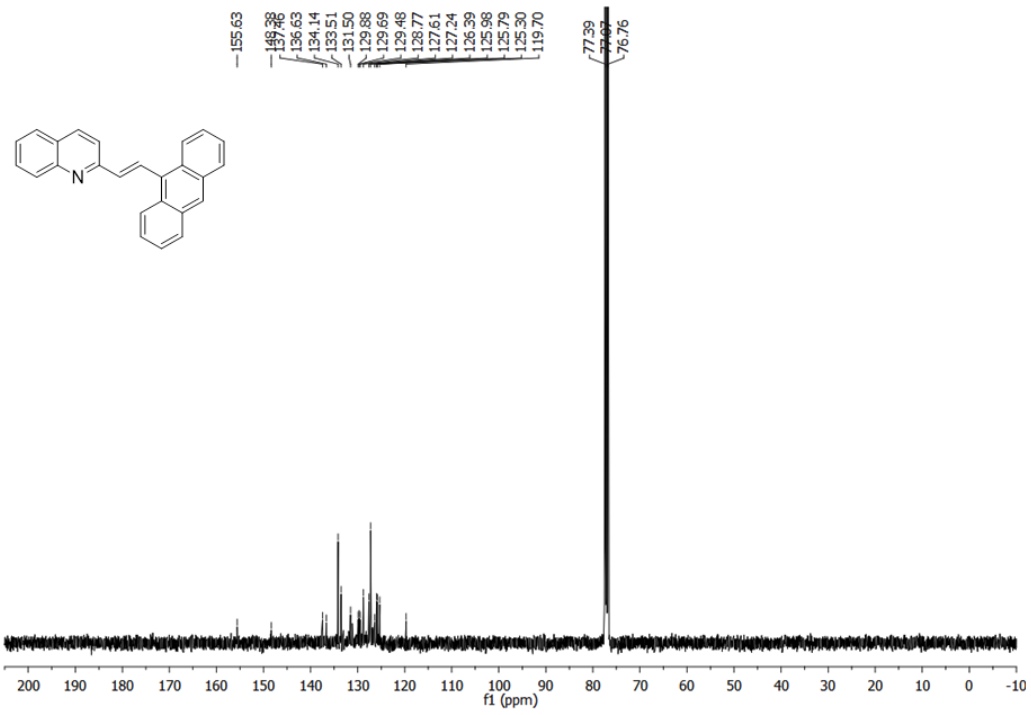

Figure 40: ^{13}C NMR spectrum for (**3n**) in CDCl3 (100MHz, 300K).

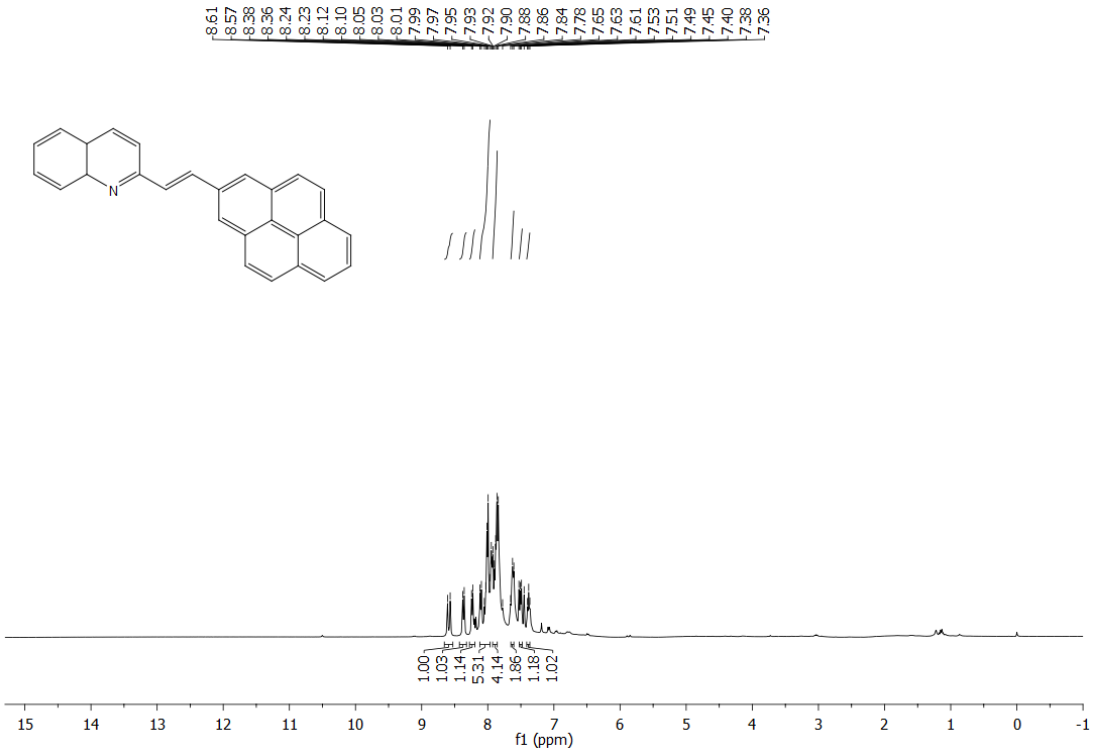

Figure 41: ^{1}H NMR spectrum for (**3o**) in $CDCl_3$ (400MHz, 300K).

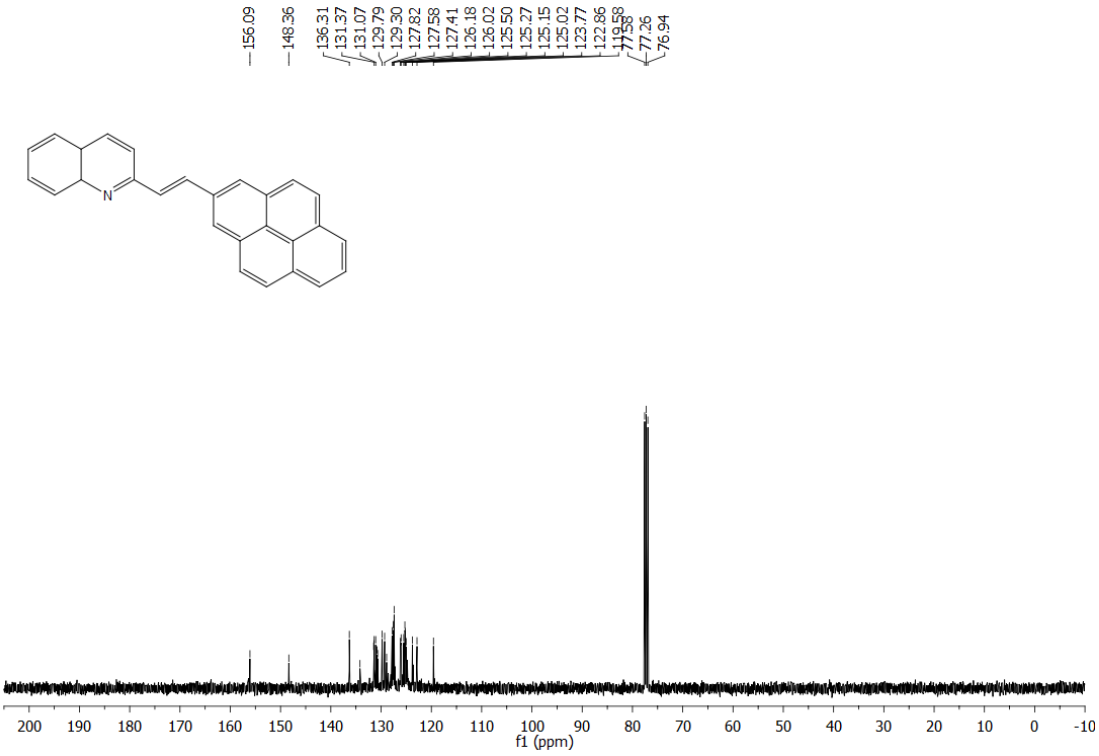

Figure 42: ^{13}C NMR spectrum for (**3o**) in $CDCl_3$ (100MHz, 300K).

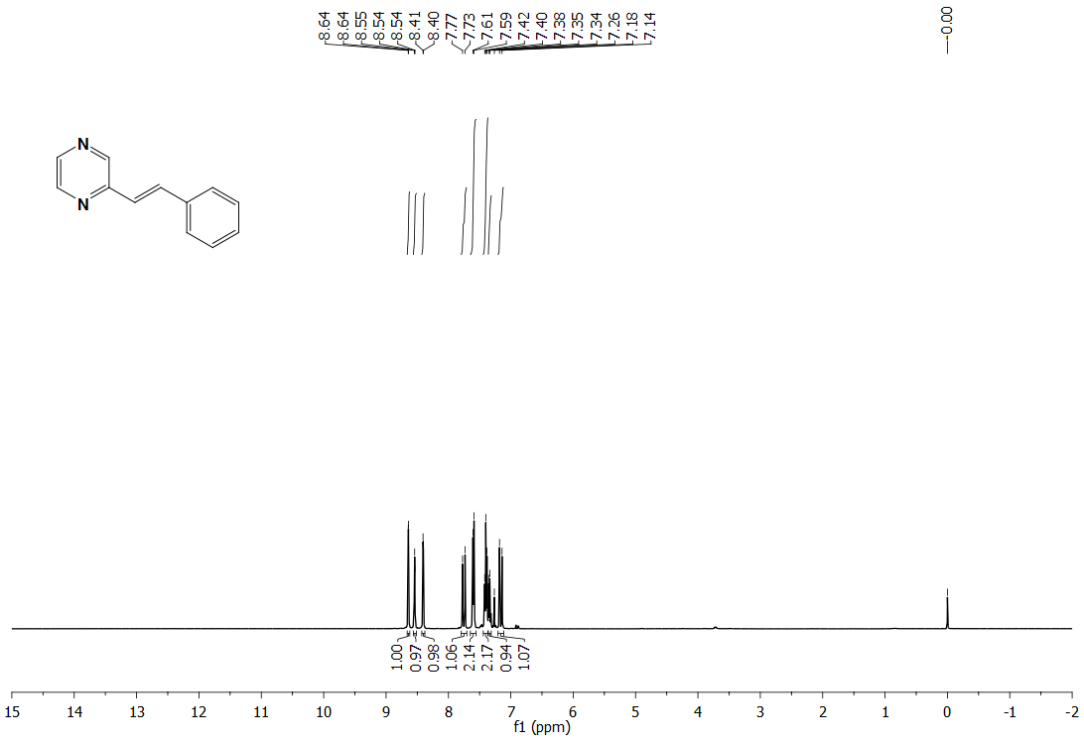

Figure 43: ^{1}H NMR spectrum for (**5a**) in $CDCl_3$ (400MHz, 300K).

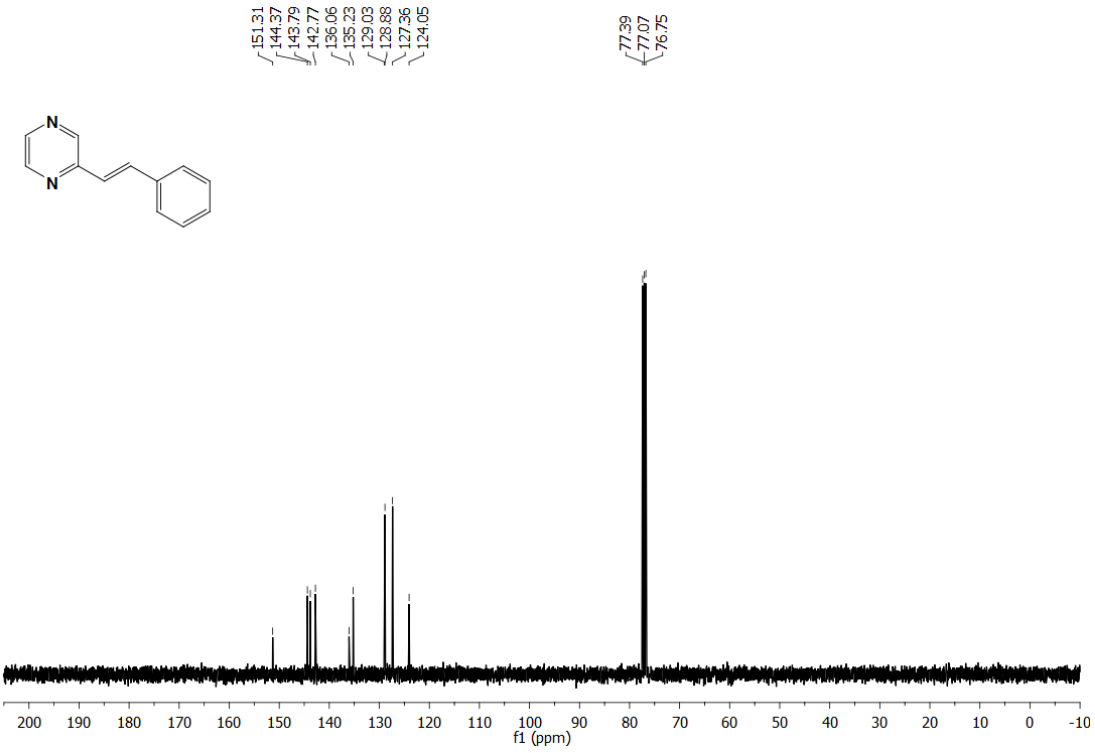

Figure 44: ^{13}C NMR spectrum for (**5a**) in $CDCl_3$ (100MHz, 300K).

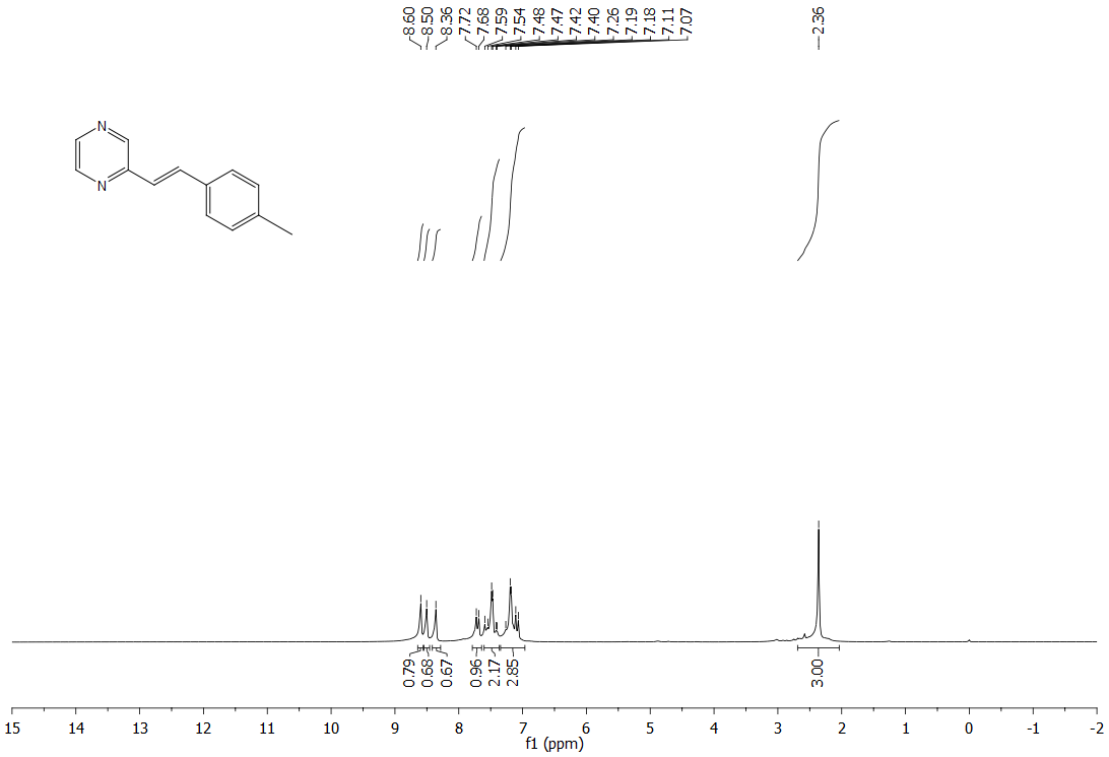

Figure 45: ^{1}H NMR spectrum for (**5b**) in $CDCl_3$ (400MHz, 300K).

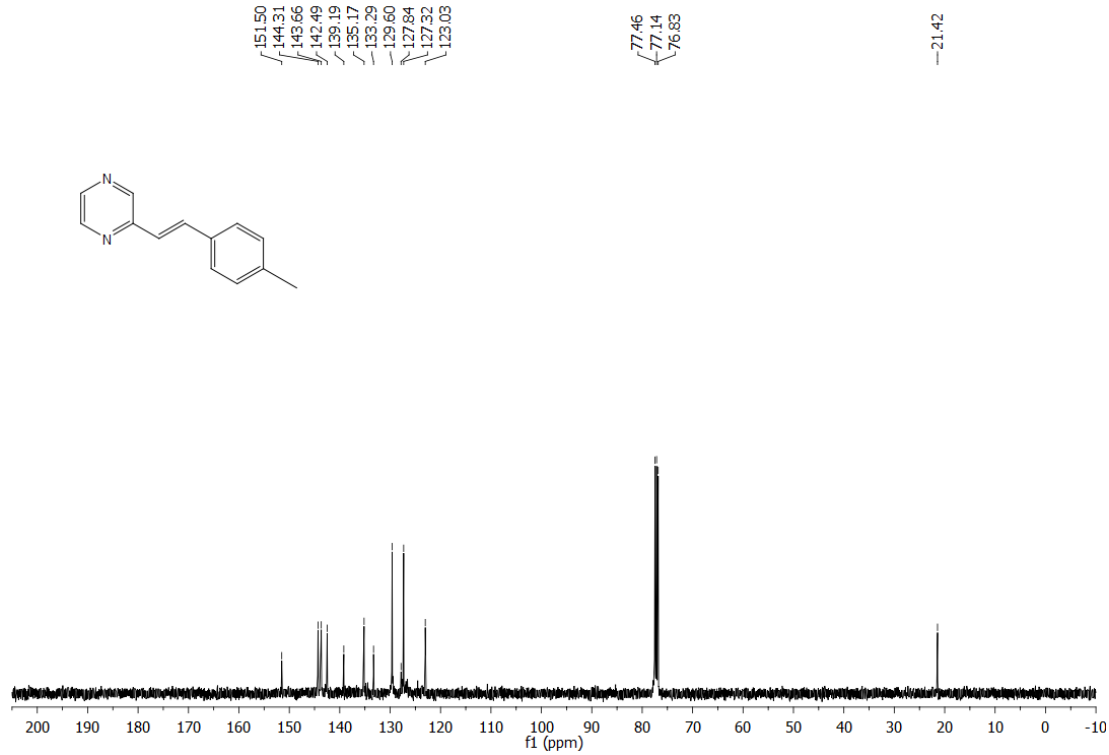

Figure 46: ^{13}C NMR spectrum for (**5b)** in $CDCl_3$ (100MHz, 300K).

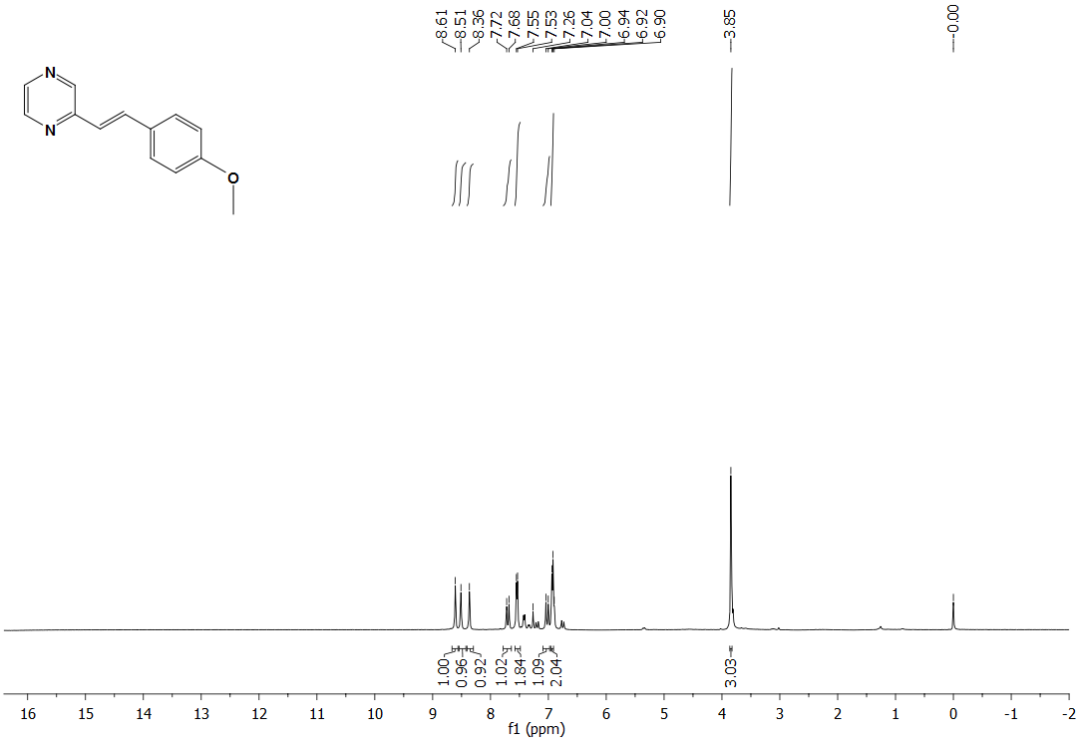

Figure 47: ^{1}H NMR spectrum for (**5c**) in $CDCl_3$ (400MHz, 300K).

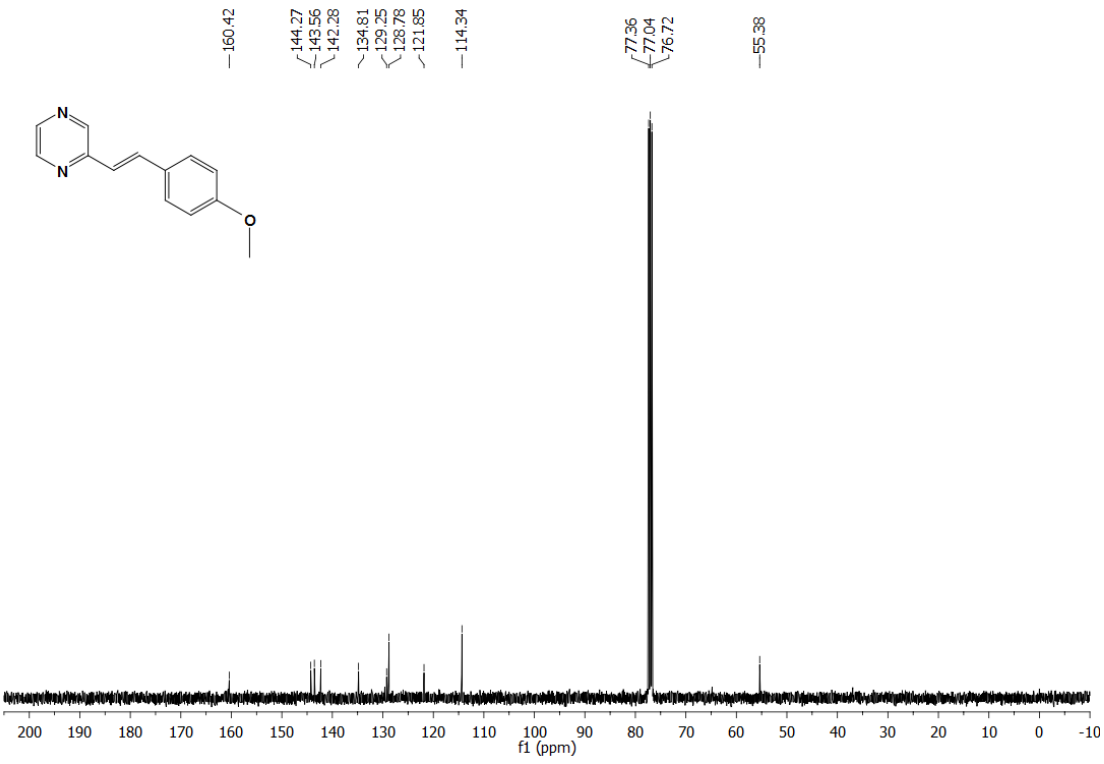

Figure 48: ^{13}C NMR spectrum for (**5c**) in $CDCl_3$ (100MHz, 300K).

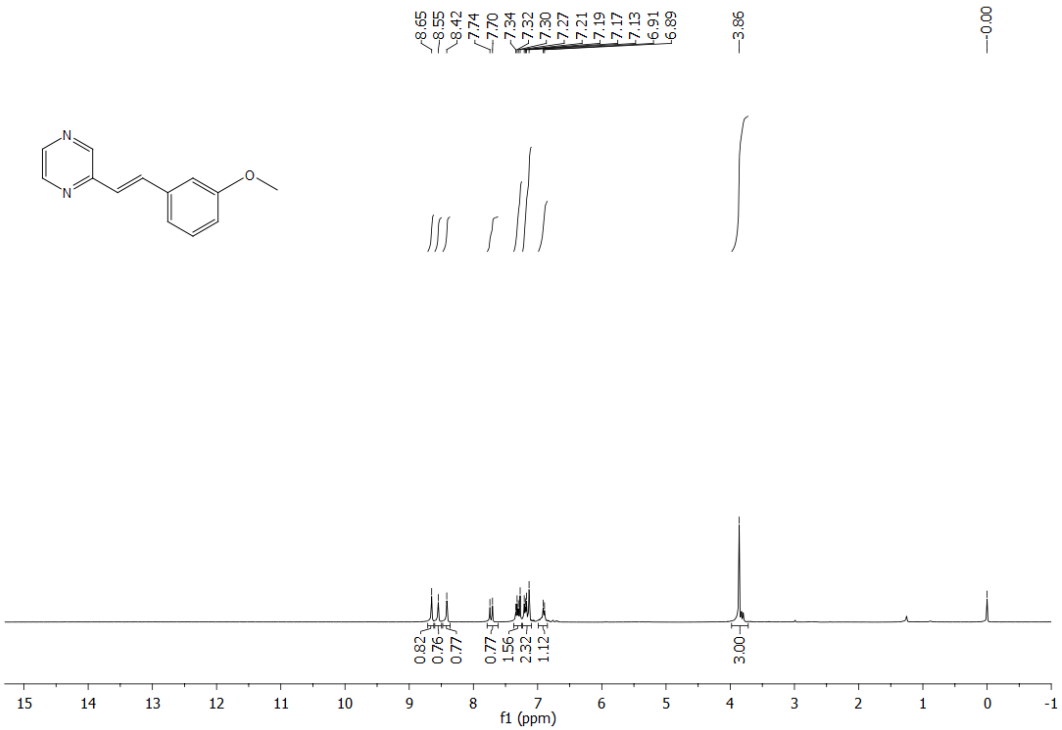

Figure 49: ^{1}H NMR spectrum for (**5d**) in $CDCl_3$ (400MHz, 300K).

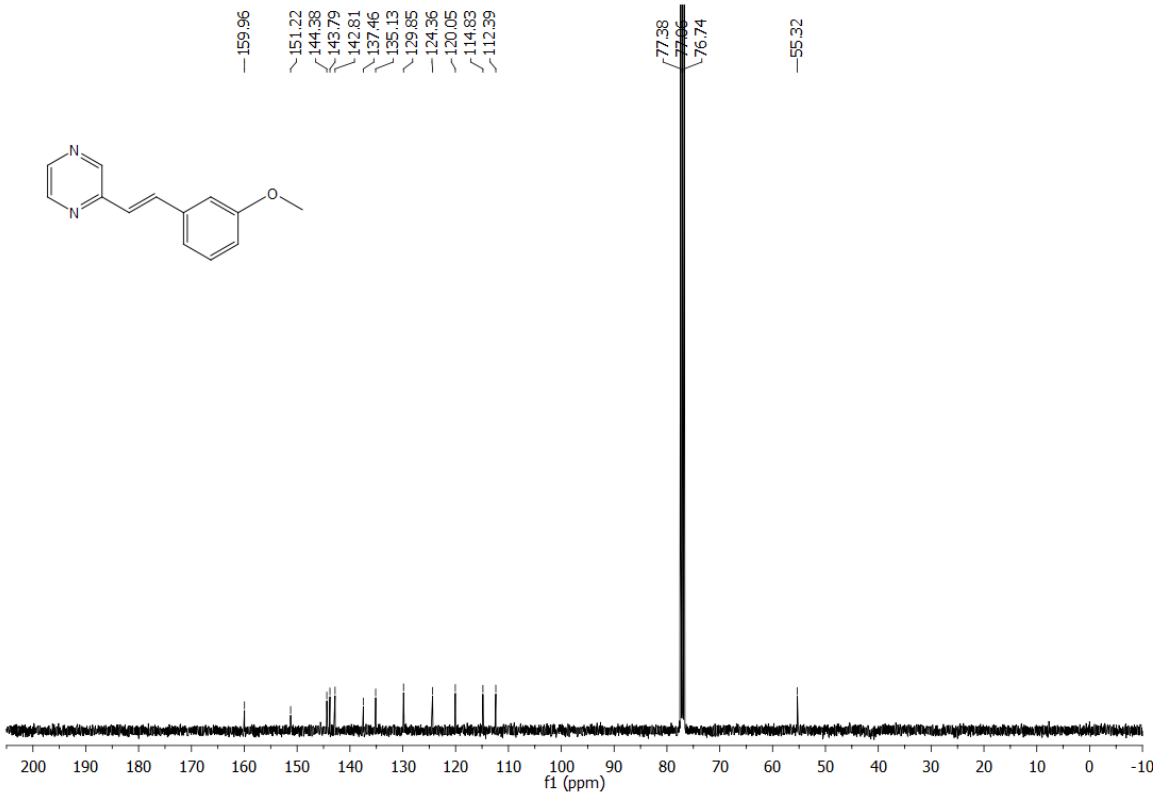

Figure 50: ^{13}C NMR spectrum for (**5d**) in $CDCl_3$ (100MHz, 300K).

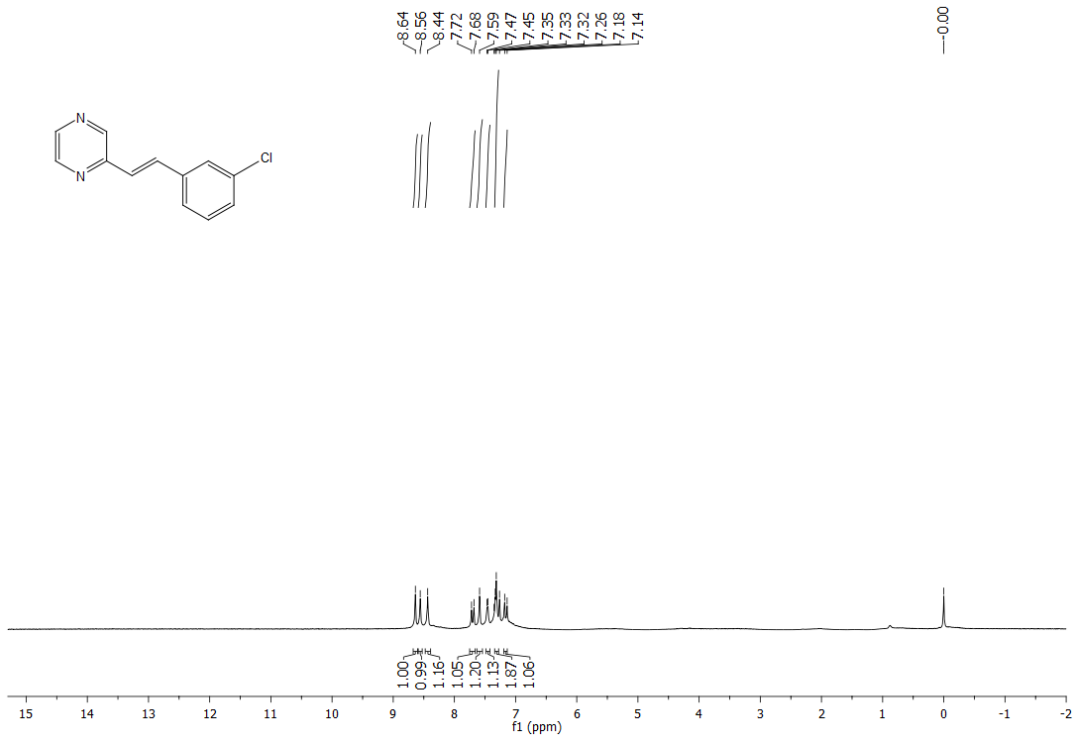

Figure 51: ^{1}H NMR spectrum for (**5e**) in $CDCl_3$ (400MHz, 300K).

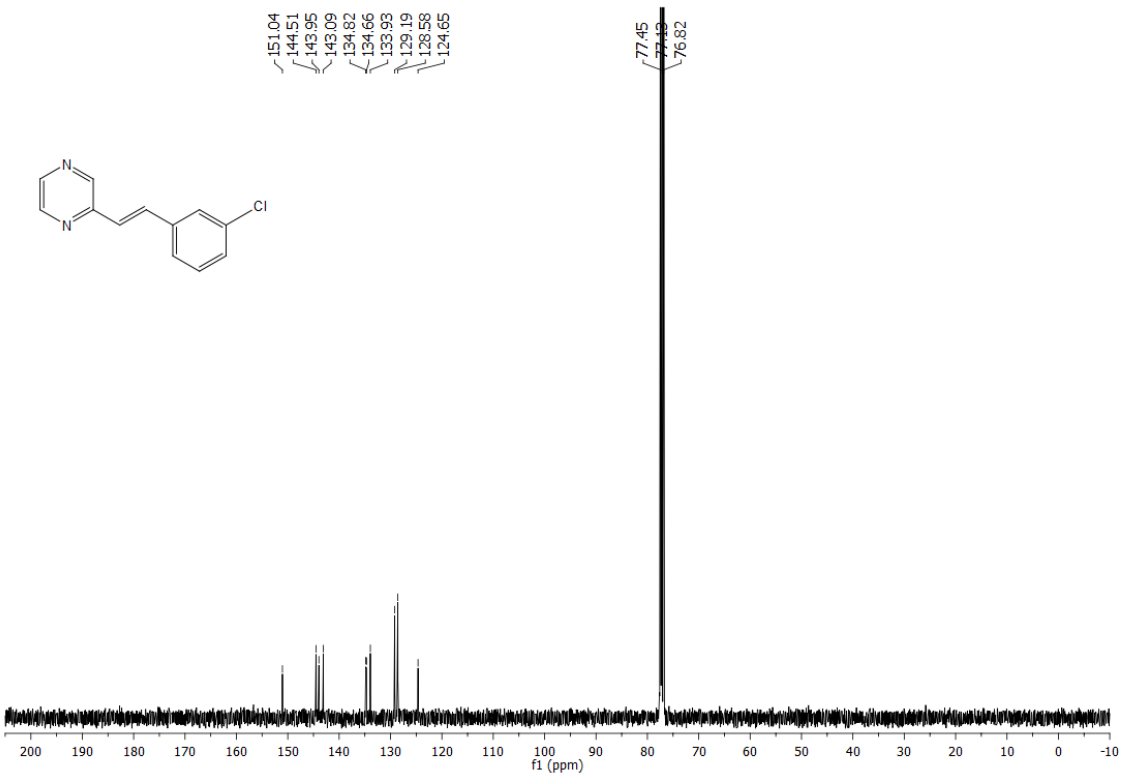

Figure 52: ^{13}C NMR spectrum for (**5e**) in $CDCl_3$ (100MHz, 300K).

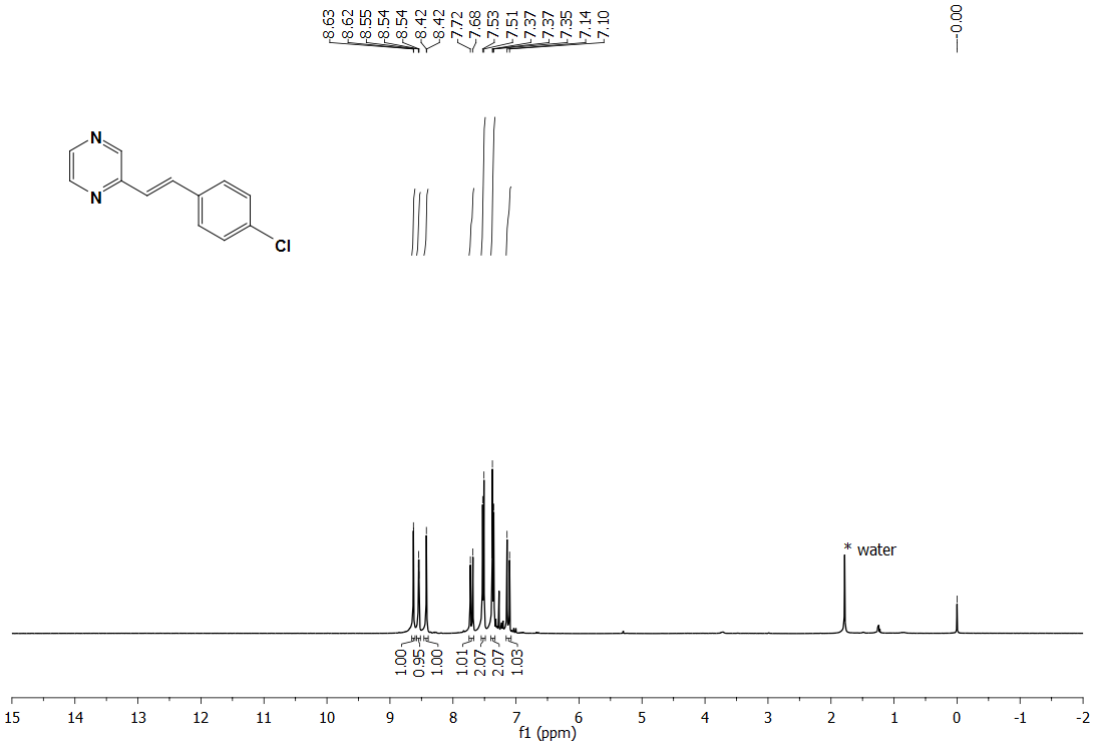

Figure 53: ^{1}H NMR spectrum for (**5f**) in $CDCl_3$ (400MHz, 300K).

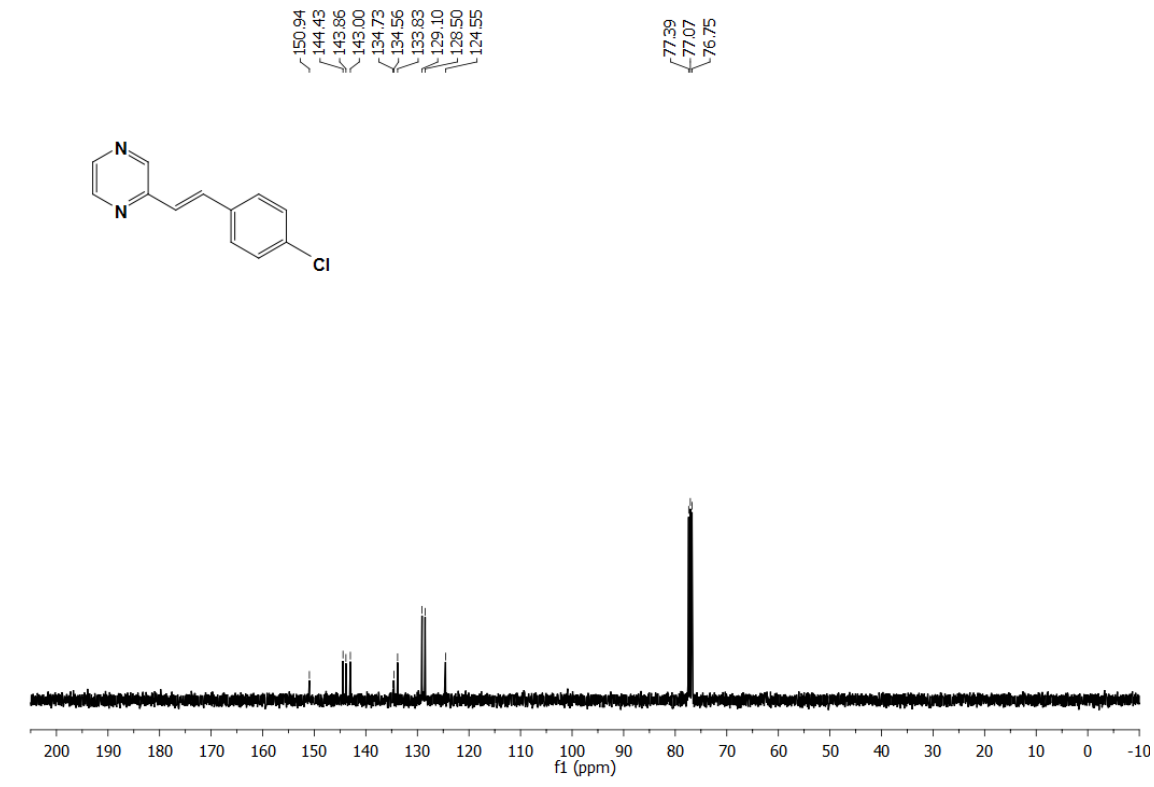

Figure 54: ^{13}C NMR spectrum for (**5f**) in $CDCl_3$ (100MHz, 300K).

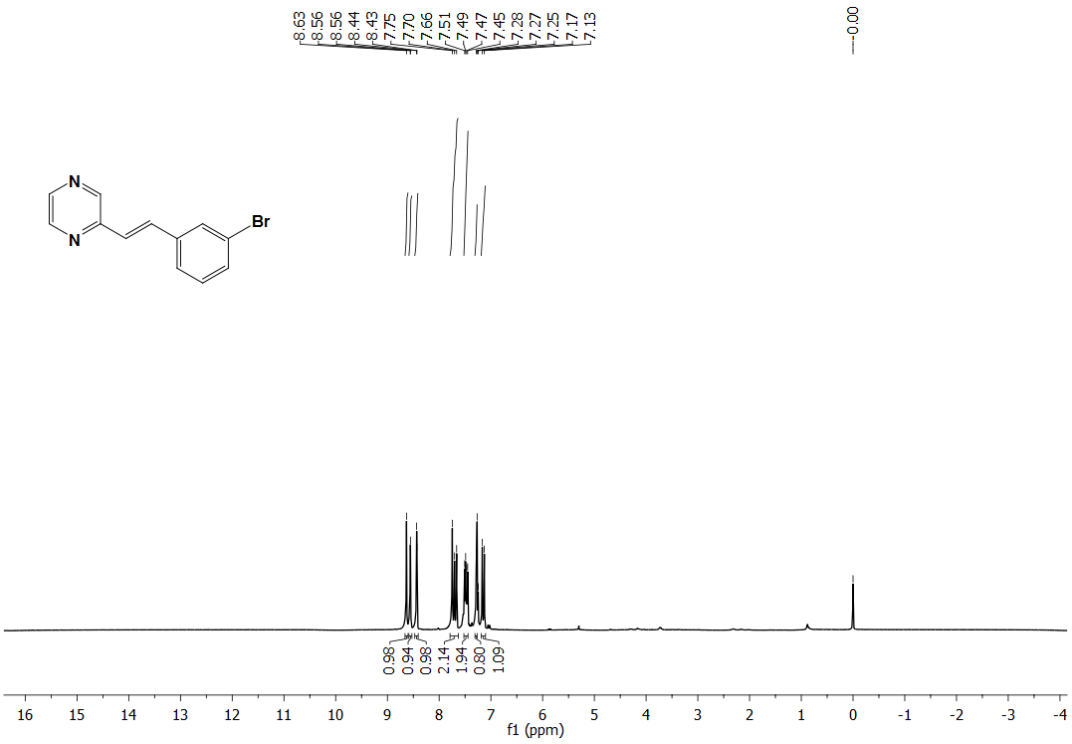

Figure 55: ^{1}H NMR spectrum for (**5g**) in $CDCl_3$ (400MHz, 300K).

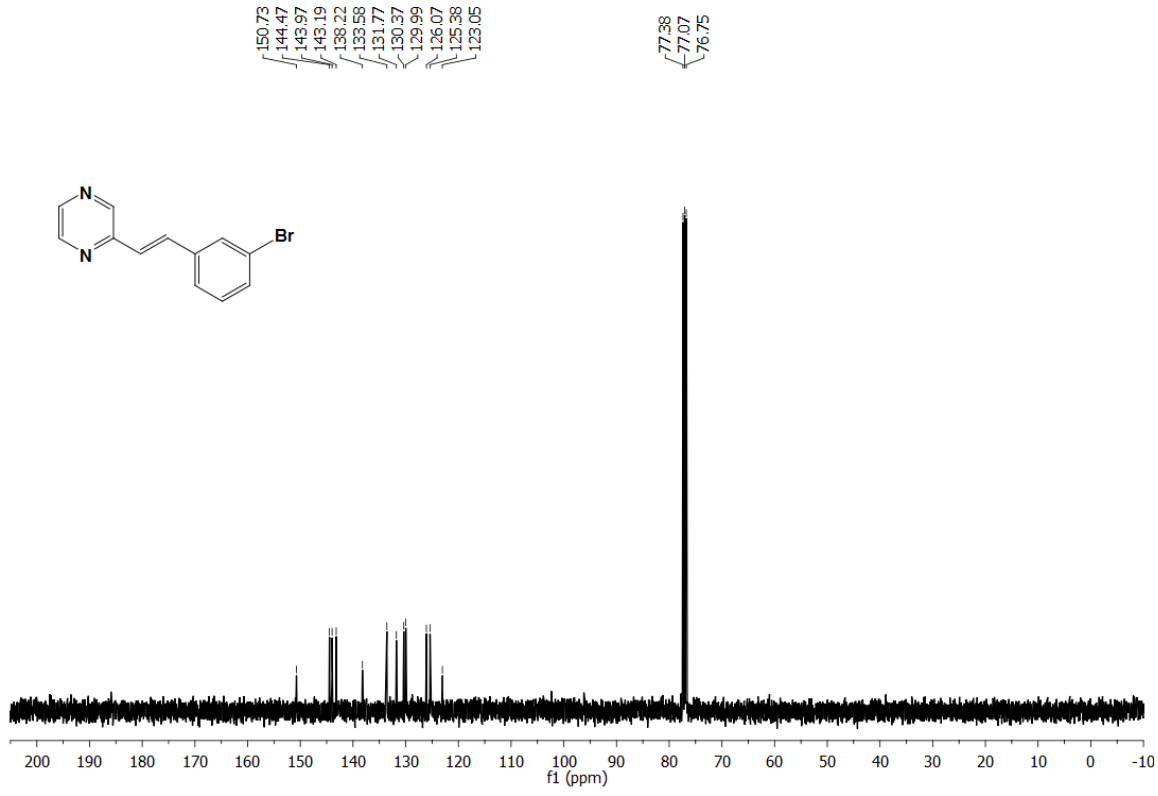

Figure 56: ^{13}C NMR spectrum for (**5g**) in $CDCl_3$ (100MHz, 300K).

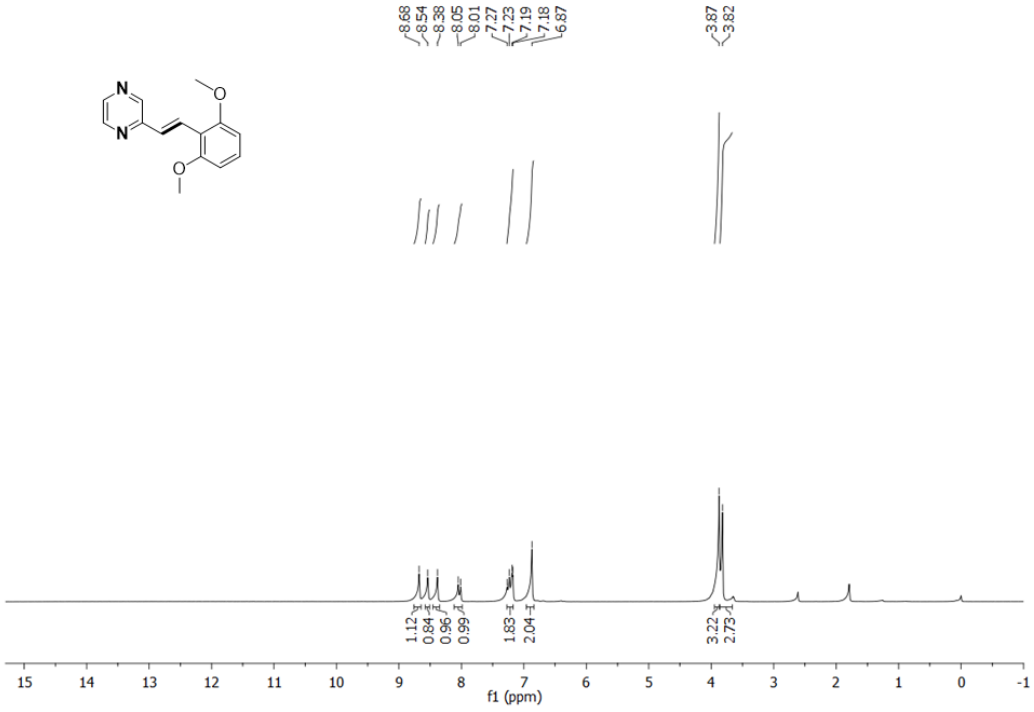

Figure 57: ^{1}H NMR spectrum for (**5h**) in $CDCl_3$ (400MHz, 300K).

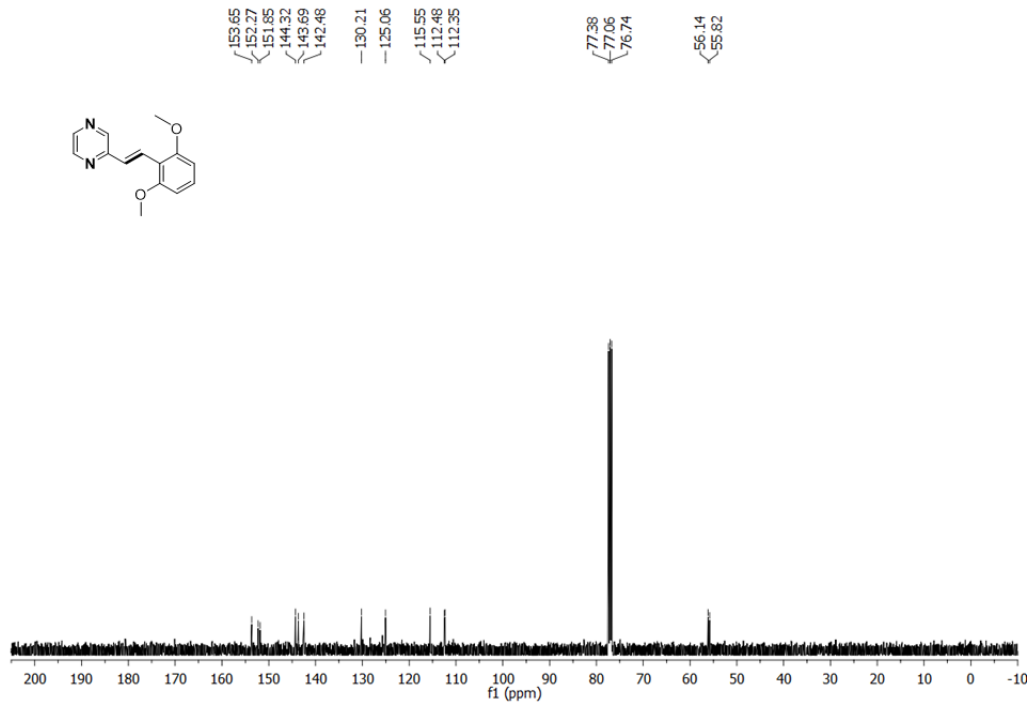

Figure 58: ^{13}C NMR spectrum for (**5h**) in $CDCl_3$ (100MHz, 300K).

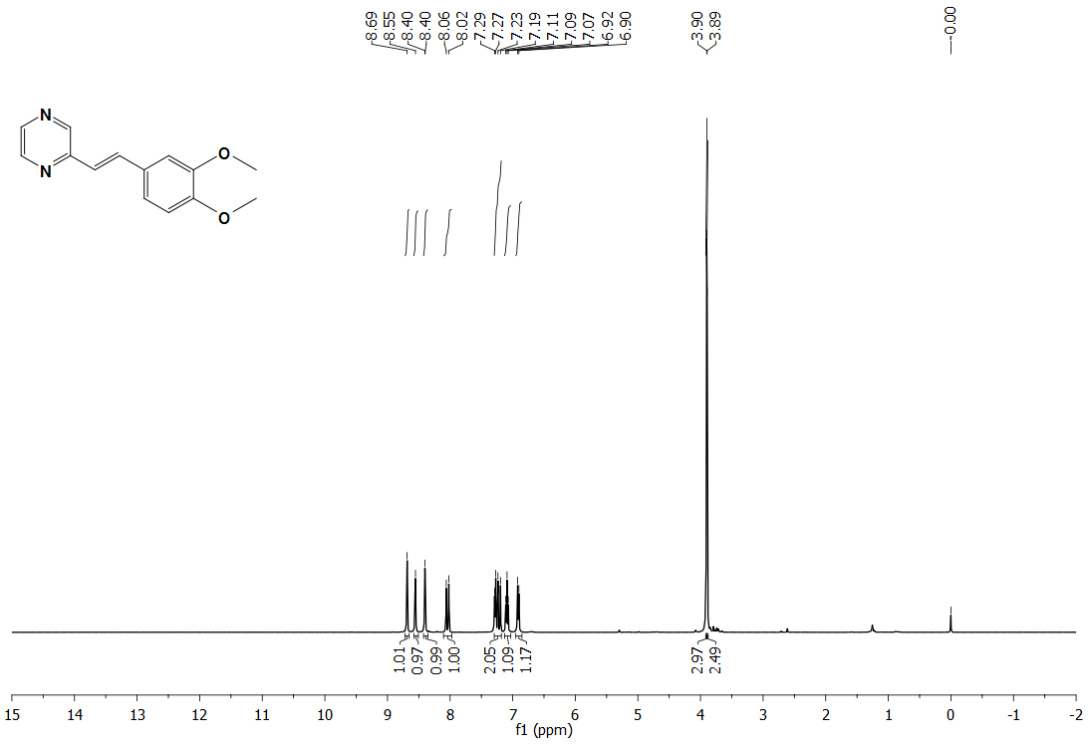

Figure 59: ^{1}H NMR spectrum for (**5i**) in $CDCl_3$ (400MHz, 300K).

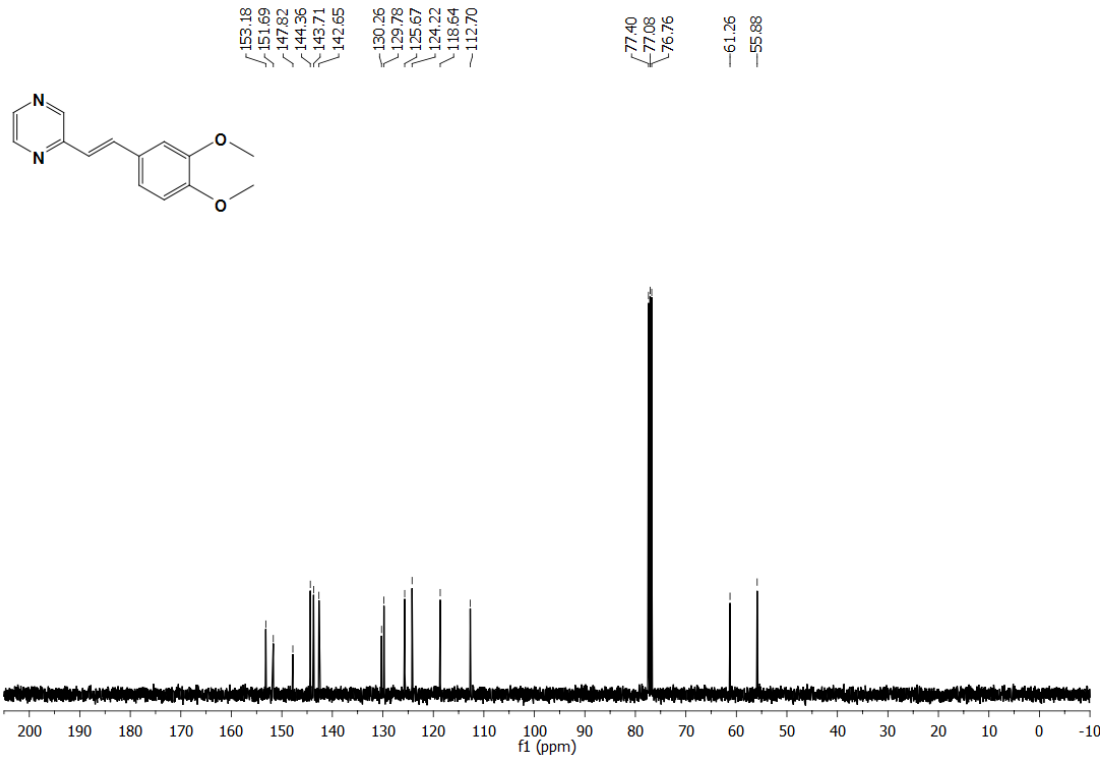

Figure 60: ^{13}C NMR spectrum for (**5i**) in $CDCl_3$ (100MHz, 300K).

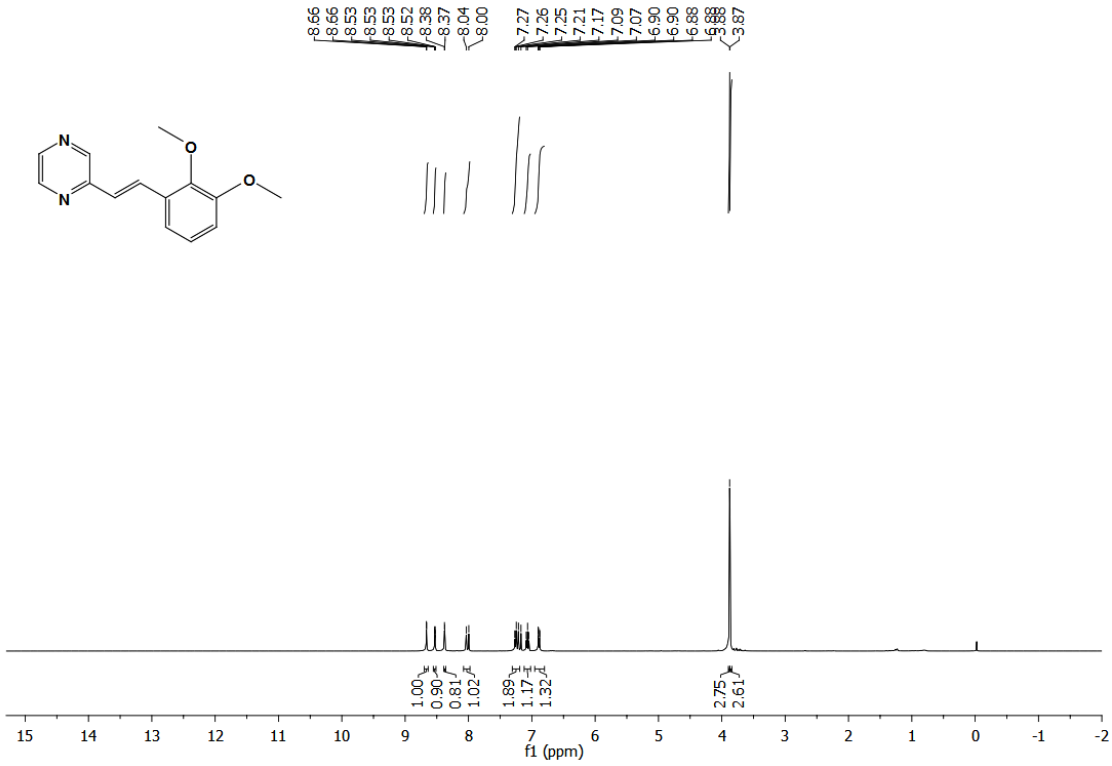

Figure 61: ^{1}H NMR spectrum for (**5j**) in $CDCl_3$ (400MHz, 300K).

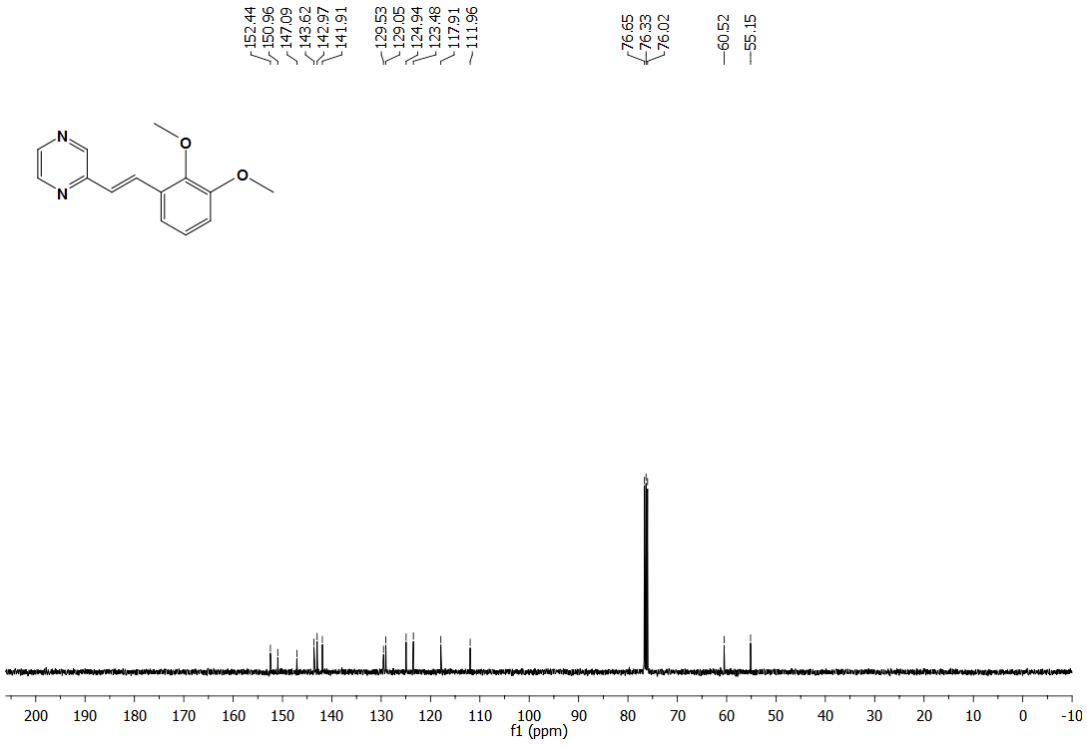

Figure 62: ^{13}C NMR spectrum for (**5j**) in $CDCl_3$ (100MHz, 300K).

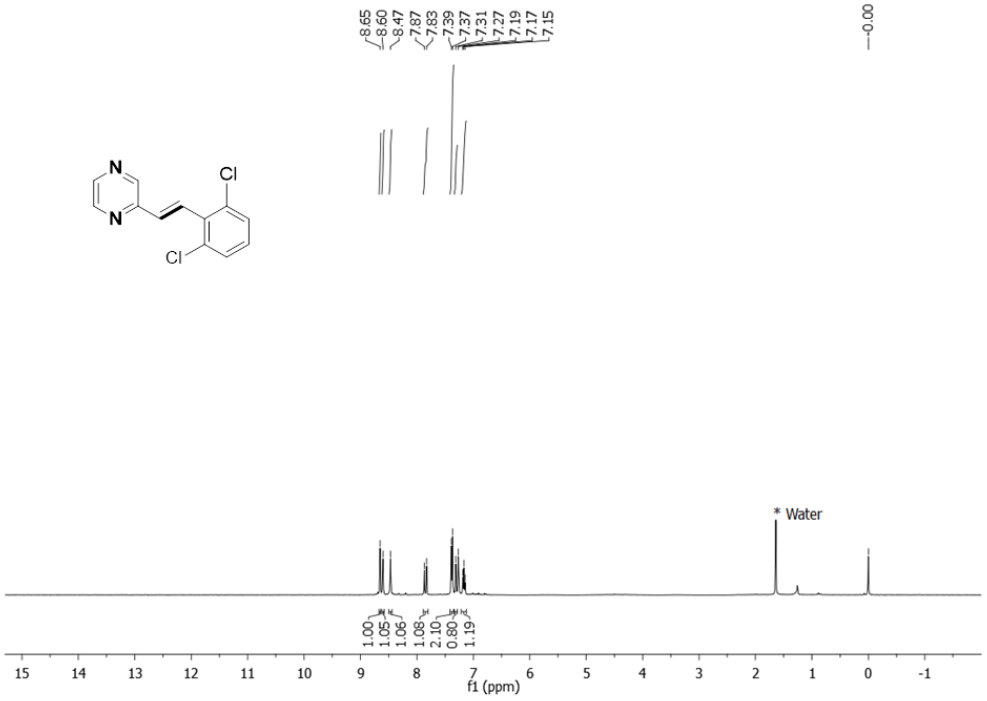

Figure 63: ^{1}H NMR spectrum for (**5k**) in $CDCl_3$ (400MHz, 300K).

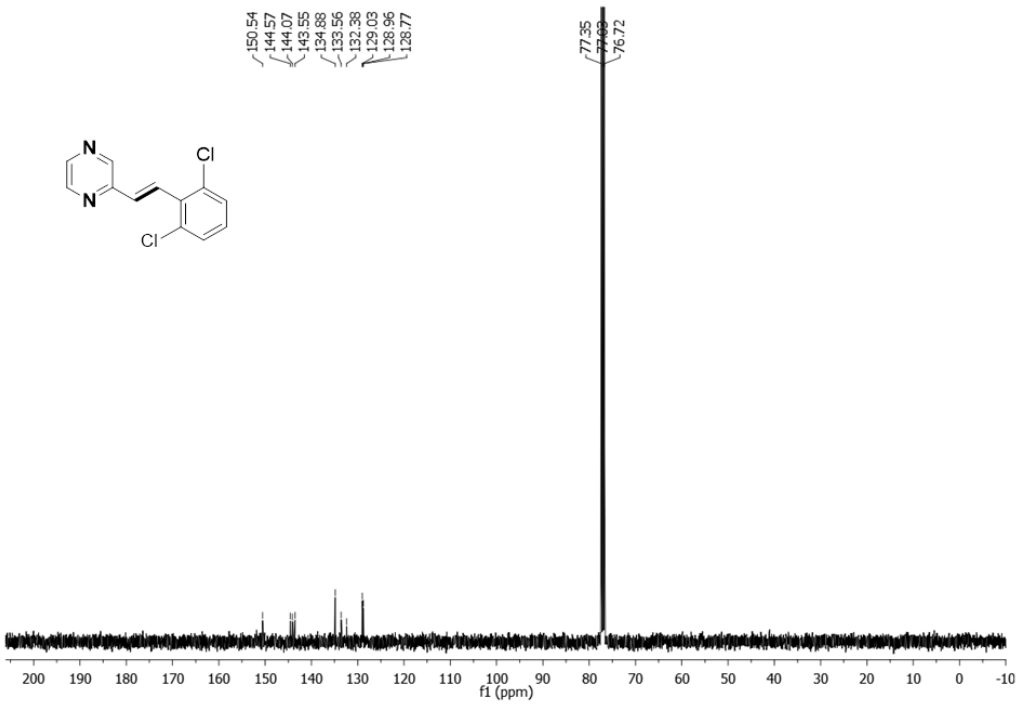

Figure 64: ^{13}C NMR spectrum for (**5k**) in $CDCl_3$ (100MHz, 300K).

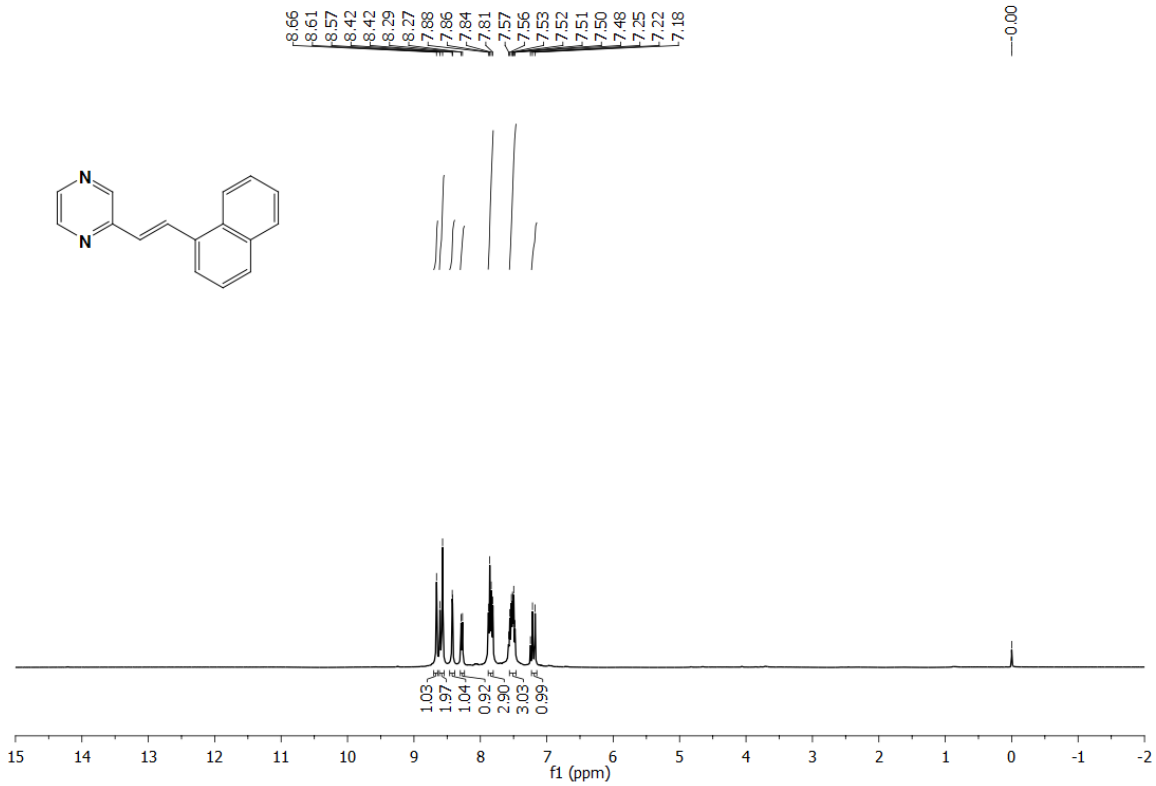

Figure 65: ^{1}H NMR spectrum for (**5l**) in $CDCl_3$ (400MHz, 300K).

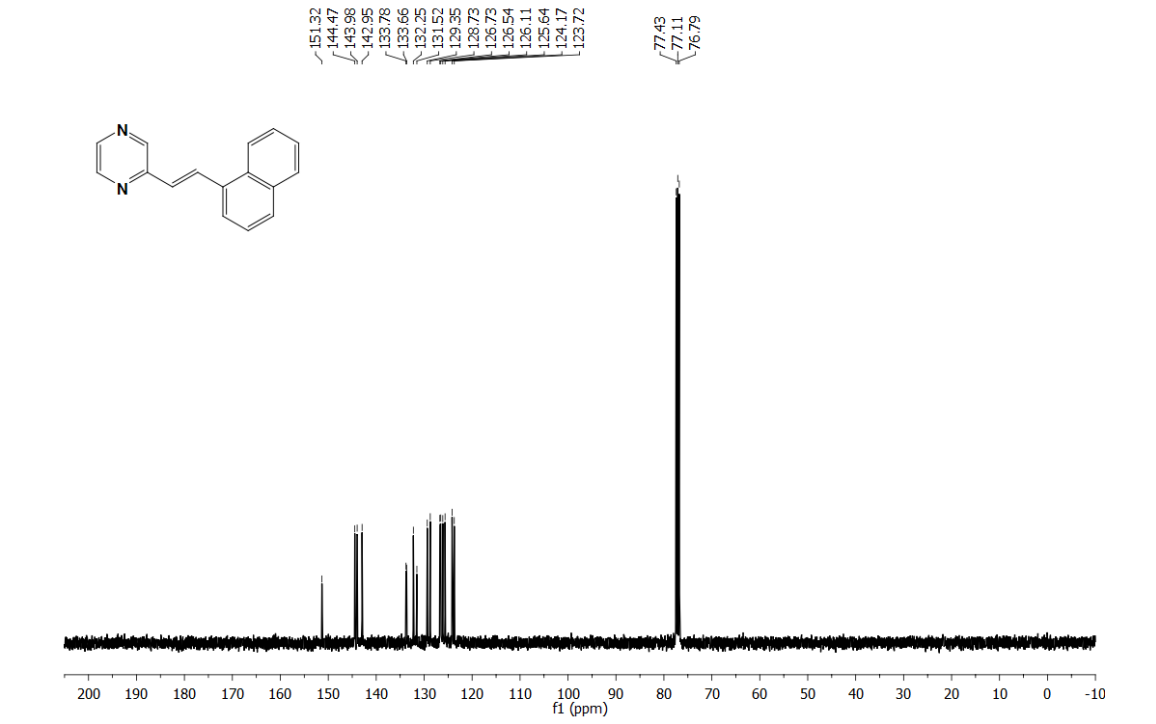

Figure 66: ^{13}C NMR spectrum for (**5l**) in $CDCl_3$ (100MHz, 300K).

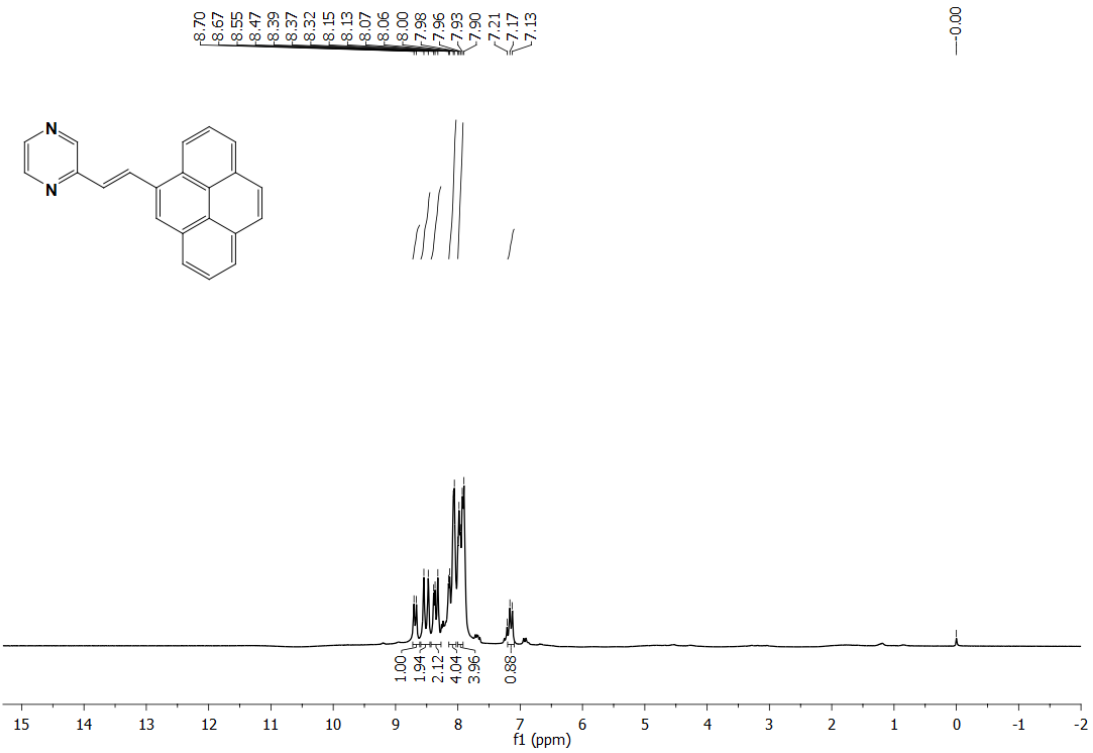

Figure 67: ^{1}H NMR spectrum for (**5m**) in $CDCl_3$ (400MHz, 300K).

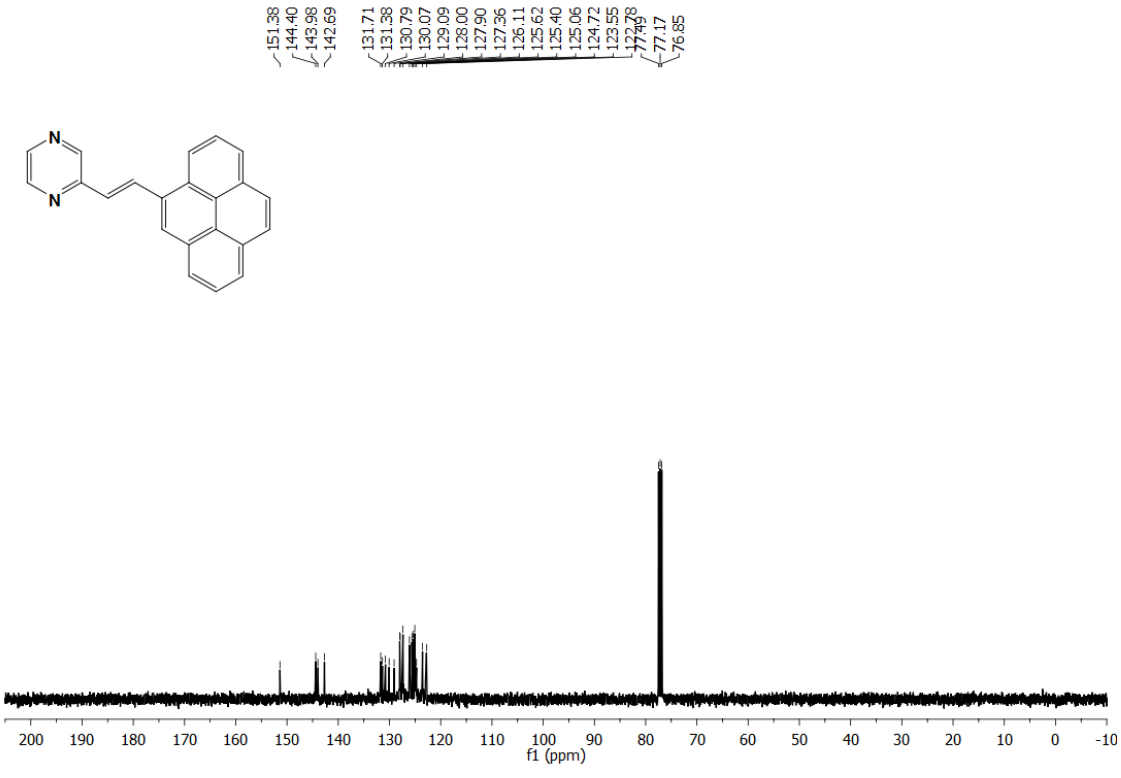

Figure 68: ^{13}C NMR spectrum for (**5m**) in $CDCl_3$ (100MHz, 300K).

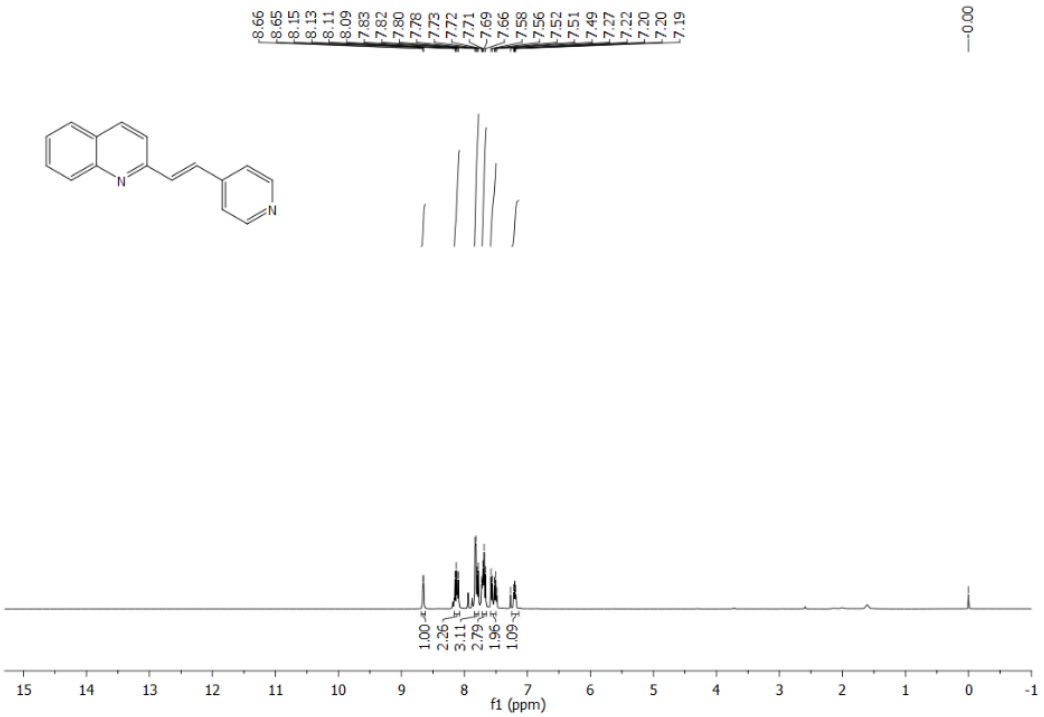

Figure 69: ^{1}H NMR spectrum for (E)-2-(2-(pyridin-4-yl)vinyl)quinoline in $CDCl_3$ (400MHz, 300K).

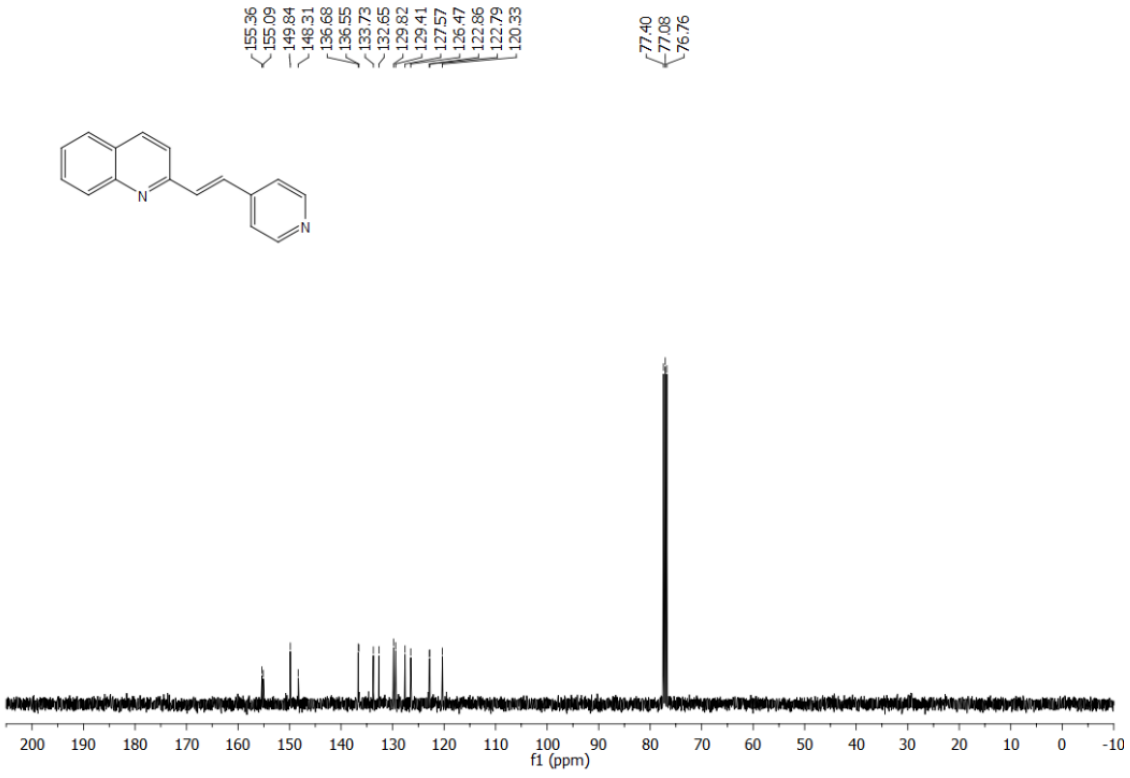

Figure 70: ^{13}C NMR spectrum for (E)-2-(2-(pyridin-4-yl)vinyl)quinoline in $CDCl_3$ (100MHz, 300K).

3.4. REFERENCES

1. (a) S. A. Khalil, A. Alkofahi, D. E. Eisawi and A. A. Shibib, *J. Nat. Prod.* 1998, **61**, 262-263; (b) N. Chatani, T. Asaumi, S. Yorimitsu, T. Ikeda, F. Kakiuchi and S. Murai, *J. Am. Chem. Soc.* 2001, **123**, 10935-10941; (c) X. Franck, A. Fournet, E. Prina, R. Mahieux, R. Hocquemiller and B. Figadère, *Bioorg. Med. Chem. Lett.* 2004, **14**, 3635-3638; (d) R. Dumeunier, I. E. Marko and T. Takeda, Ed. Wiley-VCH: Weinheim, 2004; p 104; (e) C. Torborg and M. Beller, *Adv. Synth. Catal.* 2009, **351**, 3027-3043; (f) F. S. Chang, W. Chen, C. Wang, C. C. Tzeng and Y. L. Chen, *Bioorg. Med. Chem.* 2010, **18**, 124-133; (g) S. Blanchard, A. D. William, A. C. -H. Lee, A. Poulsen, E. L. Teo, W. Deng, N. Tu, E. Tan, K. L. Goh, W. C. Ong, C. P. Ng, K. C. Goh, Z. Bonday and E. T. Sun, *Bioorg. Med. Chem. Lett.* 2010, **20**, 2443-2447.

2. (a) J. H. Burroughes, D. D. C. Bradley, A. R. Brown, R. N. Marks, K. Mackay, R. H. Friend, P. L. Burns and A. B. Holmes, *Nature* 1990, **347**, 539-541; (b) J. Dai, Z. Q. Liu, X. Q. Wang, J. Lin, P. F. Yao, S. L. Huang, T. M. Ou, J. H. Tan, D. Li, L. Q. Gu and Z. S. Huang, *J. Med. Chem.,* 2015, **58**, 3875-3891.

3. (a) K. Mekouar, J.F. Mouscadet, D. Desmaële, F. Subra, H. Leh, D. Savouré, C. Auclair and J. d'Angelo, *J. Med. Chem.,* 1998, **41**, 2846-2857; (b) X. Franck, A. Fournet, E. Prina, R. Mahieux, R. Hocquemiller and B. Figadère, *Bioorg. Med. Chem. Lett*, 2004, **14**, 3635-3638; (c) F. S. Chang, W. Chen, C. Wang, C. C. Tzeng and Y. L. Chen, *Bioorg. Med. Chem.* 2010, **18**, 124-133; (d) W. Cieslik, R. Musiol, J.E. Nycz, J. Jampilek, M. Vejsova, M. Wolff, B. Machura and J. Polanski, *Bioorg. Med. Chem.*, 2012, **20**, 6960-6968; (e) V.V. Kouznetsov, C. Gómez, M. G. Derita, L. Svetaz, E. del Olmo and S. A. Zacchino, *Bioorg. Med. Chem.,* 2012, **20**, 6506-6512; (f) W. Cieslik, R. Musiol, J.E. Nycz, J. Jampilek, M. Vejsova, M. Wolff, B. Machura and J. Polanski, *Bioorg. Med. Chem.*, 2012, **20**, 6960-6968; (f) M. Orhan Puskullu, B. Tekiner and S. Suzen, *Mini reviews in medicinal chemistry*, 2013, **13**, 365-372; (g) K. Gopaul and S. A. N. A. Shintre Koorbanally, *Anti-Cancer Agents Med. Chem.*, 2015, **15**, 631-646; (h) A. Mrozek-Wilczkiewicz, M. Kuczak, K. Malarz, W. E. Cieślik, Spaczyńska and R. Musiol, *Eur. J. Med. Chem.*, 2019, **177**, 338-349; (i) V.V. Kouznetsov, L. Y. V. Méndez, C. E. P. Galvis and M. C. O. Villamizar, *New J. Chem*, 2020, **44**, 12-19.

4. (a) G. Wittig and G. Geissler, *Justus Liebigs Annalen der Chemie.* 1953, **580**, 44-57; (b) D. J. Peterson, *J. Org. Chem.* 1968, **33**, 780-784; (c) M. Julia and J. M. Paris, *Tetrahedron Lett.* 1973, **14**, 4833-4836; (d) B. E. Maryanoff and A. B. Reitz, *Chem. Rev.* 1989, **89**, 863-927; (e) J. Clayden and S. Warren, *Angew. Chem., Int. Ed. Engl.* 1996, **35**, 241-270; (f) L. F. Van Staden and D. Gravestock, D. J. Ager, *Chem. Soc. Rev.* 2002, **31**, 195-200.

5. (a) R. F. Heck and J. P. Nolley, *J. Org. Chem.* 1972, **37**, 2320-2322; (b) R. H. Grubbs, Handbook of Metathesis; Grubbs, R. H., Ed.; Wiley-VCH: Weinheim, 2003; Vols.1-3. (c) K. Ferré-Filmon, L. Delaude, A. Demonceau and A. F. Noels, *Coord. Chem. Rev.* 2004, **248**, 2323-2336.

6. (a) Y. Ogata, A. Kawasaki and H. Hirata, *J. Org. Chem.*, 1970, **35**, 2199-2203; (b) M. Wang, M. Gao, K. D. Miller, G. W. Sledge, G. D. Hutchins and Q. H. Zheng, *Eur. J. Med. Chem.* 2009, **44**, 2300-2306; (c) B. Qian, S. M. Guo, C. G. Xia and H. M. Huang, *Adv. Synth. Catal.* 2010, **352**, 3195-3200; (d) H. omai, T. Yoshino, S. Matsunaga and M. Kanai, *Org. Lett.* 2011, **13**, 1706; (e) B. Qian, D. J. Shi, L. Yang and H. M. Huang, *Adv. Synth. Catal.* 2012, **354**, 2146-2150; (f) V. B. Graves and A. Shaikh, *Tetrahedron Lett*. 2013, **54**, 695-698; (g) L. Xu, Z. Shao, L. Wang, H. Zhao and J. Xiao, *Tetrahedron Lett.*, 2014, **55**, 6856-6860; (h) L. Gong, L. J. Xing, T. Xu, X. P. Zhu, W. Zhou, N. Kang and B. Wang, *Org. Biomol. Chem.*, 2014, **12**, 6557-6560; (i) L. Gong, L. J. Xing, T. Xu, X. P. Zhu, W. Zhou, N. Kang and B. Wang, *Org. Biomol. Chem.*, 2014, **12**, 6557-6560; (j) S. Fu, L. Wang, H. Dong, J. Yu, L. Xu and J. Xiao, *Tetrahedron Lett*. 2016, **57**, 4533-4536; (k) E. Liang, J. Wang, Y. Wu, L. Huang, X. Yao and X. Tang, *Adv. Synth. Catal.* 2019, **361**, 3619-3623; (l) S. Hazra, V. Tiwari, A. Verma, P. Dolui and A. J. Elias, *Org. Lett.* 2020, **22**, 5496-5501.

7. (a) D. J. Peterson, *J. Org. Chem.* 1968, **33**, 780-784; (b) B. E. Maryanoff and A. B. Reitz, *Chem. Rev.* 1989, **89**, 863-927; (c) Y. Yan, K. Xu, Y. Fang and Z. Wang, *J. Org. Chem.* 2011, **76**, 6849-6855; (d) O. M. Ogba, N. C. Warner, D. J. O'Leary and R. H. Grubbs, *Chem. Soc. Rev.* 2018, **47**, 4510-4544.

8. D. S. Latha and S. Yaragorla, *Eur. J. Org. Chem.* 2020, **15**, 2155-2179.

9. (a) V. G. Zaitsev, D. Shabashov and O. Daugulis, *J. Am. Chem. Soc.* 2005, **127**, 13154-13155; (b) T. Watanabe, S. Oishi, N. Fujii and H. Ohno, *Org. Lett.* 2008, **10**, 1759–1762; (c) X. Chen, K. M. Engle, D. H. Wang and J. Q. Yu, *Angew. Chem., Int. Ed.,* 2009, **48**, 5094-5115; (d) D. Shabashov, O. Daugulis, D. Shabashov and O. Daugulis, *J. Am. Chem. Soc*. 2010, **132**, 3965-3972; (e) F. Bellina and R. Rossi, *Chem. Rev.*, 2010, **110**, 1082-1146; (f) R. Jazzar, J. Hitce, A. Renaudat, J. Sofack-Kreutzer and O. Baudoin, *Chem. Eur. J.*, 2010, **16**, 2654-2672; (g) T. W. Lyons and M. S. Sanford, *Chem. Rev*., 2010, **110**, 1147-1169; (h) H. Li, B. J. Li and Z. J. Shi, *Catal. Sci. Technol.*, 2011, **1**, 191-206; (i) S.-Y. Zhang, F.-M. Zhang and Y.-Q. Tu, *Chem. Soc. Rev.*, 2011, **40**, 1937-1949; (j) Z. Jamal, Y. C. Teo and G. S. Lim, *Tetrahedron*, 2016, **72**, 2132-2138.

10. G. Zhang, T. Irrgang, T. Dietel, F. Kallmeier and R. Kempe, *Angew. Chem., Int. Ed*. 2018, **57**, 1-6.

11. M. K. Barman, S. Waiba and B. Maji, *Angew. Chem., Int. Ed.* 2018, **57**, 9126-9130.

12. (a) J. Das, M. Vellakkaran and D. Banerjee, *Chem. Commun.*, 2019, **55**, 7530-7533. (b) J. Das, M. S. M. Vellakkaran and D. Banerjee, *Org. Lett*. 2019, **21**, 7514-7518.

13. B. M. Ramalingam, I. Ramakrishna and M. Baidya, *J. Org. Chem.* 2019, **84**, 9819-9825.

14. C. Zhang, Z. Li, Y. Fang, S. Jiang, M. Wang and G. Zhang, *Tetrahedron*, 2020, **76**, 130968.

15. M. Rauch, S. Kar, A. Kumar, L. Avram, L. J. Shimon and D. Milstein, *J. Am. Chem. Soc.* 2020, **142**, 14513–14521.

16. C. Gunanathan and D. Milstein, *Chem. Rev*, 2014, **114**, 12024–12087

17. H. A. Younus, N. Ahmad, W. Su and F. Verpoort, *Coord. Chem. Rev*. 2014, **276**, 112-152.

18. A. I. Vogel, Test book of practical organic chemistry, Longman, London, 5th edn, 1989, p.395.

19. T.S. Manikandan, R. Ramesh, N. Shivalingegowda and L. N. Krishnappagowda, *ChemistrySelect.*, 2018, **3**, 1561-1568.

20. Farrugia, L. ORTEP - 3 for Windows a version of ORTEP-III with a Graphical User Interface (GUI), Journal of Applied Crystallography,1997, 30, 565-566.

21. G. M. Sheldrick, *Acta Crystallogr., Sect. A: Found. Crystallogr*. 2008, **64**, 112.

22. Bruker-Nonius (2004), APEX-II and SAINT-Plus (Version 7.06a), Bruker AXS Inc., Madison, Wisconsin, USA.

23. M. Cao, L.V. Do, N.W. Hoffman, M.L. Kwan, J. K. Little, J.M. McGilvray, C.B. Morris, B.C. Söderberg, A. Wierzbicki, T.R. Cundari and C.H. Lake, *Organometallics*, 2001, **20**, 2270-2279.

24. R. Manikandan, G. Prakash, R. Kathirvel and P. Viswanathamurthi, *Spectrochim. Acta A Mol. Biomol. Spectrosc.* 2013, **116**, 501- 508.

25. S. Balaji, G. Balamurugan, R. Ramesh and D. Semeril, *Organometallics*, 2021, **40**, 725-734.

26. T. M. Aliyeu, D. V. Berdnikova, O. A. Fedorova, E. N. Gulakova, C. Stremmel and H. Ihmels, *J. Org. Chem*, 2016, **81**, 9075-9085.

27. F. F. Wang, C. P. Luo, Y. Wang, G. Deng, and L. Yang, *Org. Biomol. Chem.* 2012, **10**, 8605-8608.

28. J. Das, M. Vellakkaran, M. Sk, and D. Banerjee, *Org. Lett.* 2019, **21**, 7514–7518.

29. B. M. Ramalingam, I. Ramakrishna, and M. Baidya, *J. Org. Chem.* 2019, **84**, 9819-9825.

30. S. Fu, L. Wang, H. Dong, J. Yu, L. Xu and J. Xiao, *Tetrahedron Lett.* 2016, **57**, 4533- 4536

31. T. M. Aliyeu, D. V. Berdnikova, O. A. Fedorova, E. N. Gulakova, C. Stremmel, and H. Ihmels, *J. Org. Chem,* 2016, **81**, 9075 – 9085.

Chapter 4

Ruthenium(II) Catalyst Mediated Synthesis of 2-amino-4H-chromenes Using Primary Alcohols *via* Acceptorless Dehydrogenative Coupling Pathway

Abstract

A series of biologically important 2-amino-4H-chromenes functionalized with different substituents has been synthesized through one-pot multicomponent reaction catalysed by *p*-cymene Ru(II) organometallic complexes encompassing N^O chelated carbazole based hydrazone ligands. A panel of *p*-cymene Ru(II) complexes were synthesized and characterized by various spectral (FT-IR and NMR) and analytical methods. The molecular structure of one of the complexes was corroborated with the help of single-crystal X-ray diffraction study. 2-amino-4H-chromene derivatives have been readily assessed under mild conditions *via* ruthenium(II) catalyst mediated acceptorless dehydrogenative coupling of substituted benzyl alcohols, resorcinol and malononitrile. The present catalytic protocol furnishes a variety of 2-amino-4H-chromenes in high yields up to 95% from a wide range of readily available primary alcohols without the use of any oxidant/additives utilizing low catalyst loading. A plausible mechanism to the catalytic synthesis of 2-amino-4H-chromene compounds has been described *via* the formation of an aldehyde and benzylidenemalononitrile intermediates with the discharge of water and hydrogen as by-products. Interestingly, medicinally important tacrine analogue was successfully constructed with good yields from the synthesized 2-amino-4H-chromenes.

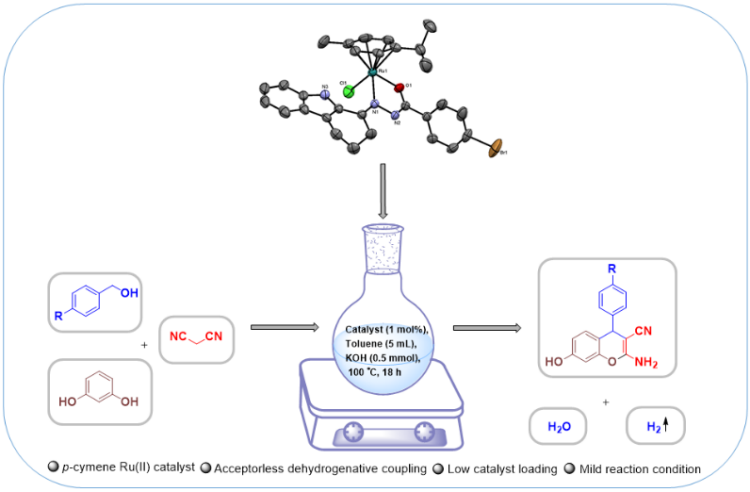

4.1. INTRODUCTION

O-Heterocycles present a broad spectrum of indispensable structural motifs due to their vast biological and pharmacological properties.[1] Among them, chromenes have been one of the imperative classes of O-heterocyclic compounds extensively used as valuable synthetic organic building blocks and are attracted towards a diverse array of research areas exclusively medicinal chemistry and chemical biology.[2] Predominantly, 2-amino-4H-chromenes are interesting biomolecules with notable bioactivities such as antimicrobial, antiviral, and antiproliferative activity (Figure 1).[3]

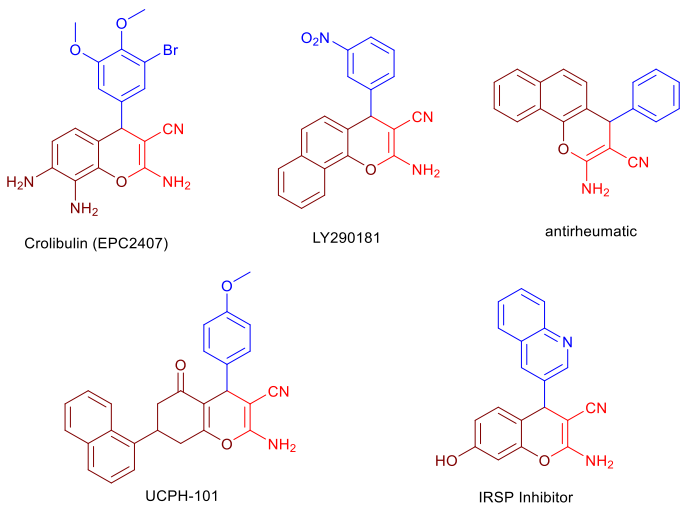

Figure 1. Selective examples for bioactive 2-amino-4H-chromene analogues

Multicomponent reactions (MCR) mediate a facile route to the construction of 2-amino-4H-chromenes in a single step and a huge number of methods have been developed from substituted phenols and compounds comprising active methylene group as starting materials (Scheme 1a).[4] For instance, Zhang *et al.* described the synthesis of 2-amino-4H-chromenes using chiral organocatalysts and aldehyde as substrate in presence of molecular sieves.[5] Dekamin group has reported the Lewis base (5 mol% potassium phthalimide) mediated synthesis of diverse range of chromenes from aldehyde, malononitrile, and resorcinol.[6] Heravi *et al.* have reported the multicomponent fabrication of 2-amino-4H-

chromenes employing the strong methanesulfonic acid (1 mmol) as a catalyst.[7] Imidazole mediated one pot synthesis of 2-amino-4H-chromenes at high catalyst loading (20 mol%) has been demonstrated by Choudhury's group.[8] However, the above approaches have some drawbacks such as the usage of unstable aldehyde reactants, hazardous organic acids, Lewis bases, the requirement of higher reaction temperature, high catalyst loading, longer reaction time and low yields of the chromene products.

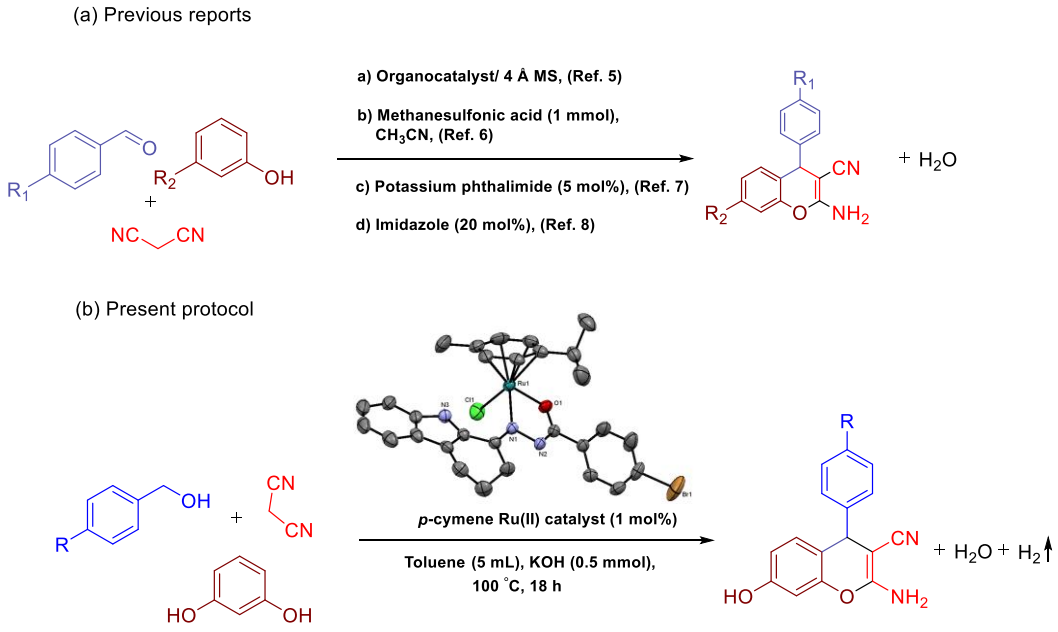

Scheme 1. Synthetic protocol for the synthesis of 2-amino-4H-chromenes

Transition metal catalysed multi-component reactions for the synthesis of heterocyclic compounds have particular interest due to easy workup of intermediates, and a sequence of condensation, addition or cycloaddition reactions can be performed in one pot.[9] Among them, ruthenium-mediated MCR have drawn much attention towards the syntheses of heterocycles due to their atom economy, ready availability and higher catalytic efficiency.[10] Further, MCR for the construction of heterocycles from alcohols through acceptorless dehydrogenative coupling (ADC) strategy has attracted significant interest due to the needless of any oxidants, additives and circumvent of toxic by-products such as permanganate, dichromate, and peroxides.[11] Further, the Kempe *et.al* have explored

multicomponent synthesis of pyrimidines catalyzed by Mn-PNP pincer complexes in 1,4-dioxane at 120 °C for 20 h under argon atmosphere.[12a] Beller and co-workers have described Ru catalyzed synthesis of pyrroles from ADC reaction of alcohols with diol in *t*-amyl alcohol at 130 °C for 18 h.[12b,c] Recently, Srimani group reported Ru-Catalyzed Acceptorless Dehydrogenative MCR towards the synthesis of 1,8-Dioxo-decahydroacridines at 135 °C for 36 h in solvent free condition under nitrogen atmosphere.[12d] Following a thorough review of the literature, it is believed that there are no reports available on ruthenium-mediated MCR for the syntheses of O-heterocycles, especially construction of 2-amino-4H-chromenes through acceptorless dehydrogenative coupling reaction from alcohols.

In recent years, *p*-cymene encapsulated transition metal catalysts have been extensively employed as catalysts in various organic transformation reactions including C-C and C-N bond formations.[13] Hence, we have employed *p*-cymene capped half sandwich organometallic complexes for our present catalytic investigations.

In view of these, herein we have developed and reported the synthesis of carbazole based hydrazone chelated *p*-cymene Ru(II) complexes as catalysts for the direct access of 2-amino-4H-chromenes from benzyl alcohols, malononitrile and resorcinol *via* ADC pathway for the first time. Gratifyingly, the present methodology is considered to be simple and eco-friendly protocol which releases water and hydrogen as the only by-products (Scheme 1b).

4.2. Experimental Section

4.2.1. Reagents and materials

All the reagents used were chemically pure and analytical grade. Benzohydrazide derivatives were purchased from Sigma Aldrich chemicals. The solvents were freshly distilled before use following the standard procedures.[14]

4.2.2. Physical measurements and instrumentation

Commercially available $RuCl_3.3H_2O$ was used as supplied from Loba Chemie Pvt. Ltd. The solvents were freshly distilled before use the standard procedures. The ruthenium(II) precursor complex, $[(\eta^6\text{-}p\text{-cymene})RuCl_2]_2$ was prepared by reported literature method.[15] The microanalysis of carbon, hydrogen and nitrogen were recorded by an analytical function testing Vario EL III CHNS elemental analyzer at the Sophisticated Test and Instrumentation Centre (STIC), Cochin University, Cochin. The Fourier Transform infrared spectra of complexes were recorded in KBr pellets with a Perkin-Elmer 597 spectrophotometers in the range 4000–400 cm^{-1}. The NMR spectra were recorded in $CDCl_3$ with a Bruker 400 MHz instrument using TMS as the internal reference. Chemical shifts are given in ppm referenced to solvents. The electronic spectra of the complexes in acetonitrile solution were recorded with a Jasco V-730 UV-Vis Varian spectrophotometer in the range 800-200 nm. The gas chromatograph analysis for the formation of hydrogen gas was performed on a Shimadzu GC 2014 and TCD detector, injection temperature = 30 °C, column temperature = 50 °C, detector temperature (TCD) = 60 °C, carrier gas = N_2.

4.2.3. Preparation of carbazole based hydrazone ligands

A mixture 2,3,4,9-tetrahydro-1H-carbazol-1-one[16] and substituted benzhydrazide and few drops of conc. HCl in ethanol was stirred at room temperature for 2 h, which resulted a pale-yellow solution. The solution was left to reflux for another 1 h during which time a pale-yellow precipitate was formed. The precipitate was recovered by filtration, washed with ethanol, diethyl ether and air dried (Scheme 2) Yield: 80-90%.

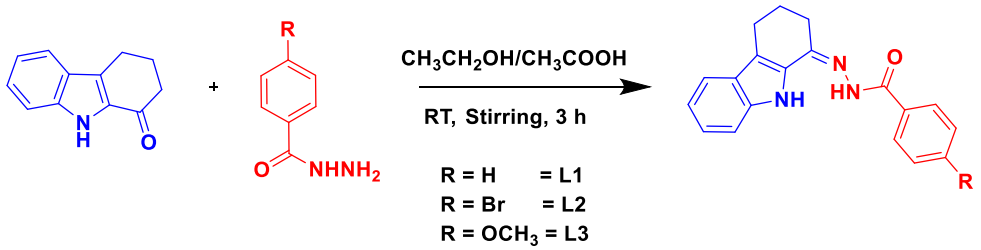

Scheme 2. Preparation of carbazole based hydrazone ligands.

4.2.4. Synthesis of new arene Ru(II) carbazole based hydrazone complexes

Carbazolone based hydrazone derivatives (2 mmol), [(η^6-*p*-cymene)$_2$Ru$_2$Cl$_2$(μ-Cl)$_2$] (1 mmol), and Et$_3$N (1 mmol) were dissolved in toluene solvent. The resultant mixture has been refluxed for 5 h. The formation of the complex was confirmed using thin-layer chromatography. After completion, the reaction mixture was then reduced to 5 mL, and addition of excess diethylether produced brown solid. The solid was collected, washed, and dried (Scheme 3).

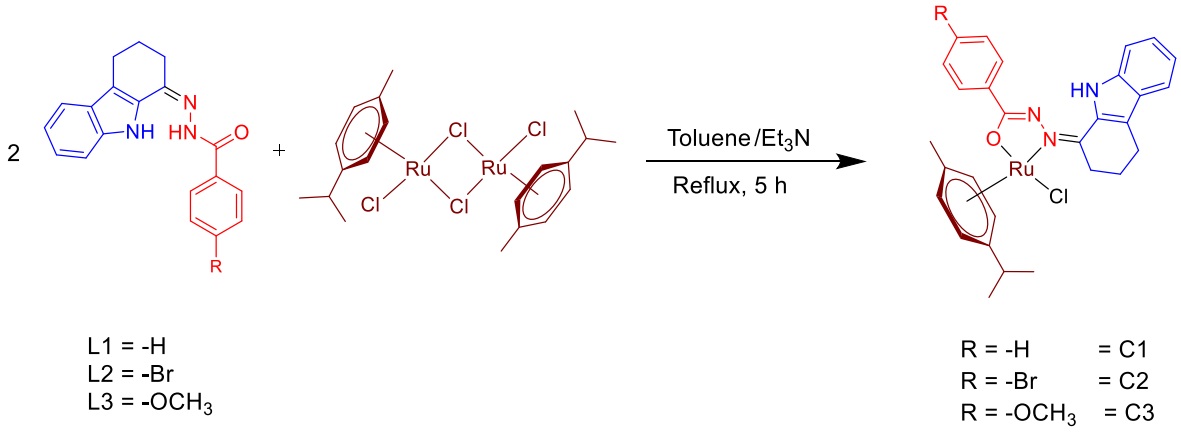

Scheme 3. Synthetic route to *p*-cymene Ru(II) complexes.

Spectral characterization data of complexes (1-3)

Complex 1. Brown solid, Yield: 81%, m.p.: 251°C (with decomposition). Anal. calcd: $C_{29}H_{30}N_3OClRu$: C, 60.78; H, 5.28; N, 7.33%. found: C, 60.74; H, 5.26; N, 7.29%. FT-IR (KBr, cm^{-1}): 3225 $\nu_{(N-H)}$, 1644 $\nu_{(C=N)}$, 1560 $\nu_{(C=O)}$, 1246 $\nu_{(C-O)}$, 1527 $\nu_{(C=N-N=C)}$. ^{1}H NMR (400 MHz, CDCl$_3$): δ (ppm) = 10.80 (*s*, 1H, N-H$_{(carbazole)}$), 8.06 (*d*, J = 8 Hz, 2H, ArH$_{(ligand)}$), 7.59-7.55 (*m*, 1H, ArH$_{(ligand)}$), 7.41-7.36 (*m*, 2H, ArH$_{(ligand)}$), 7.31-7.20 (*m*, 3H, ArH$_{(ligand)}$), 7.11-7.07 (*m*, 1H, ArH$_{(ligand)}$), 5.35-5.26 (*m*, 2H, CH$_{(p\text{-cymene})}$), 4.99 (*d*, J = 8 Hz, 1H, CH$_{(p\text{-cymene})}$), 4.71 (*d*, J = 8 Hz, 1H, CH$_{(p\text{-cymene})}$), 3.02 (*s*, 6H, CH$_{2(cyclohexane)}$), 2.60 (*sept*,1H, CH(CH$_3$)$_{2(p\text{-cymene})}$), 2.23 (*s*, 3H, CH$_{3(p\text{-cymene})}$), 1.30-1.11 (*m*, 6H, CH(CH$_3$)$_{2(p\text{-cymene})}$). ^{13}C {^{1}H} NMR (100MHz, CDCl$_3$): δ (ppm) = 171.85 (C-O), 161.08 (C=N), 136.85, 131.68, 129.10, 128.67,

127.72, 126.78, 125.29, 124.17, 122.76, 118.75, (Ar carbons of ligand), 110.88 and 99.18 (quaternary carbons of *p*-cymene), 83.16, 81.31, 80.92, 80.60 (Ar carbons of *p*-cymene), 45.17 (CH of *p*-cymene), 29.84, 29.75, 23.00, 20.49 ($CH_{2(cyclohexane)}$), 21.23, 21.16 ($2CH_3$, *p*-cymene), 17.70 (CH_3, *p*-cymene).

Complex 2. Brown solid, Yield: 76%, m.p.: 245 °C (with decomposition). Anal. calcd: $C_{29}H_{29}N_3OClBrRu$: C, 53.42; H, 4.48; N, 6.44%. found: C, 53.41; H, 4.47; N, 6.41%. FT-IR (KBr, cm^{-1}): 3247 $\nu_{(N-H)}$, 1662 $\nu_{(C=N)}$, 1578 $\nu_{(C=O)}$, 1268 $\nu_{(C-O)}$, 1516 $\nu_{(C=N-N=C)}$. ^1H NMR (400 MHz, $CDCl_3$): δ (ppm) = 10.77 (*s*, 1H, N-$H_{(carbazole)}$), 7.94 (*d*, J = 8 Hz, 2H, $ArH_{(ligand)}$), 7.56 (*d*, J = 8 Hz, 1H, $ArH_{(ligand)}$), 7.39 (*d*, J = 8 Hz, 2H,$ArH_{(ligand)}$), 7.26-7.21 (*m*, 2H, $ArH_{(ligand)}$), 7.11-7.07 (*m*, 1H, $ArH_{(ligand)}$), 5.35-5.26 (*m*, 2H, $CH_{(p\text{-cymene})}$), 4.99 (*d*, J = 8 Hz, 1H, $CH_{(p\text{-cymene})}$), 4.71 (*d*, J = 8 Hz, 1H, $CH_{(p\text{-cymene})}$), 3.02 (*s*, 6H, $CH_{2(cyclohexane)}$), 2.57 (*sept*, 1H, $CH(CH_3)_{2(p\text{-cymene})}$), 2.23 (*s*, 3H, $CH_{3(p\text{-cymene})}$), 1.30-1.10 (*m*, 6H, $CH(CH_3)_{2(p\text{-cymene})}$). ^{13}C {^1H} NMR (100MHz, $CDCl_3$): δ (ppm) = 170.88 (C-O), 161.49 (C=N), 136.97, 130.70, 129.94, 129.37, 128.60, 125.31, 124.31, 123.58, 123.06, 119.03, 118.81(Ar carbons of ligand), 110.93 and 100.98 (quaternary carbons of *p*-cymene), 83.17, 81.26, 80.96, 80.52(Ar carbons of *p*-cymene), 44.97 (CH of *p*-cymene), 29.87, 29.79, 23.00, 20.51 ($CH_{2(cyclohexane)}$), 21.26, 21.11 ($2CH_3$, *p*-cymene), 17.71 (CH_3, *p*-cymene).

Complex 3. Brown solid, Yield: 85%, m.p.: 260 °C (with decomposition). Anal. calcd: $C_{30}H_{32}N_3O_2ClRu$: C, 59.74; H, 5.35; N, 6.97%. found: C, 59.70; H, 5.33; N, 6.94%. FT-IR (KBr, cm^{-1}): 3273 $\nu_{(N-H)}$, 1679 $\nu_{(C=N)}$, 1605 $\nu_{(C=O)}$, 1295 $\nu_{(C-O)}$, 1520 $\nu_{(C=N-N=C)}$. ^1H NMR (400 MHz, $CDCl_3$): δ (ppm) = 11.76 (*s*, 1H, N-$H_{(carbazole)}$), 8.21 (*d*, J = 8 Hz, 1H, $ArH_{(ligand)}$), 8.06 (*d*, J = 8 Hz, 1H, $ArH_{(ligand)}$), 7.77-7.68 (*m*, 4H, $ArH_{(ligand)}$), 7.52-7.49 (*m*, 2H, $ArH_{(ligand)}$), 5.46-5.29 (*m*, 2H, $CH_{(p\text{-cymene})}$), 4.91 (*d*, J = 4 Hz, 1H, $CH_{(p\text{-cymene})}$), 4.49 (*d*, J = 4 Hz, 1H, $CH_{(p\text{-cymene})}$), 3.83 (*s*, 3H, $OCH_{3(ligand)}$), 3.09 (*s*, 6H, $CH_{2(cyclohexane)}$), 2.62 (*sept*, 1H, $CH(CH_3)_{2(p\text{-cymene})}$), 2.27 (*s*, 3H, $CH_{3(p\text{-cymene})}$), 1.38 (*m*, 6H, $CH(CH_3)_{2(p\text{-cymene})}$). ^{13}C {^1H}

NMR (100MHz, $CDCl_3$): δ (ppm) = 174.48 (C-O), 161.51 (C=N), 158.16 (C-OCH_3),142.72, 139.90, 134.44, 131.03, 130.51, 129.07, 128.14, 127.11, 126.85, 124.65, 113.16, (Ar carbons of ligand), 101.65 and 101.20 (quaternary carbons of *p*-cymene), 85.15, 81.59, 81.47, 80.99 (Ar carbons of *p*-cymene), 55.28 (OCH_3), 45.93 (CH of *p*-cymene), 38.76, 30.96, 29.70, 28.94 ($CH_{2(cyclohexane)}$), 22.42, 22.13 ($2CH_3$, *p*-cymene), 18.94 (CH_3, *p*-cymene).

4.2.5. X-ray crystallographic data collection

Single crystals of complex **2** were grown by slow evaporation of a dichloromethane - methanol solution at room temperature. The data collection was carried out using a Bruker AXS Kappa APEX II single crystal X-ray diffractometer using monochromated Mo–Kα radiation (λ = 0.71073 Å). Data was collected at 296 K. The absorption corrections were performed by the multi-scan method using SADABS software.[17] Corrections were made for Lorentz and polarization effects. The structures were solved by direct methods (SHELXS 97) and refined by full-matrix least squares on F^2 using SHELXL 97.[18] All non-hydrogen atoms were refined anisotropically and the hydrogen atoms in these structures were located from the difference Fourier map and constrained to the ideal positions in the refinement procedure. The unit cell parameters were determined by the method of difference vectors using reflections scanned from three different zones of the reciprocal lattice. The intensity data were measured using ω and φ scan with a frame width of 0.5°. Frame integration and data reduction were performed using the Bruker SAINT-Plus (Version 7.06a) software.[19] Figure 8 was drawn with ORTEP and the structural data have been deposited at the Cambridge Crystallographic Data Centre: CCDC 2025903.

4.2.6. General procedure for the *p*-cymene Ru(II) catalyzed synthesis of 2-amino-4H-chromenes

Aromatic alcohols (1 mmol), malononitrile (1 mmol), resorcinol (1 mmol), KOH (0.5 mmol), and catalyst (1 mol %) have been dissolved with 5 mL of toluene solvent. Then

the mixture was refluxed for 18 h at 100 ^{o}C in nitrogen atmosphere. The reaction mixture has been quenched with water and extracted using EtOAc. The organic fractions were separated and dried over anhydrous Na_2SO_4, and the solvent was removed under vacuum. The products have been isolated by column chromatography with petroleum ether/EtOAc (80:20).

4.2.7. Competitive control experiment between EDG and EWG

p-methylbenzyl alcohol **1b** (1 mmol), *p*-chlorobenzyl alcohol **1e** (1 mmol), resorcinol (1 mmol), malononitrile (1 mmol), KOH (0.5 mmol) and catalyst (1 mol%) were refluxed in toluene for 18 hours at 100 ^{o}C under nitrogen atmosphere. The reaction mixture has been reduced and the 2-amino-4H-chromene derivatives have been isolated by column chromatography. petroleum ether/EtOAc (80:20) combination was used to elute the chromenes **4b** and **4e**.

4.2.8. Procedure for gram scale synthesis

Benzyl alcohol (1.08 g, 10 mmol), malononitrile (0.66 g, 10 mmol), resorcinol (1.10 g, 10 mmol), KOH (0.23 g, 0.5 mmol), and catalyst (0.56 g, 1 mol%) were taken in 50 mL of toluene solvent. The resultant mixture has been refluxed for 18 h at 100 ^{o}C under nitrogen atmosphere. After that, the final mixture has been quenched with water and extracted with ethyl acetate. The EtOAc fractions have been collected separately dried using Na_2SO_4 and filtered. The evaporation of solvent under vacuum provided the crude mixture which has been purified using column chromatography with petroleum ether/ethyl acetate (80:20).

4.2.9. Experiment for confirmation of hydrogen gas using Gas chromatography

Benzyl alcohol **1a** (1 mmol), malononitrile **2** (1 mmol), resorcinol **3** (1 mmol), Ru (II) catalyst **3** (1 mol%), KOH (0.5 mmol), 2 mL of toluene were transferred in a dried 10 mL Schlenk flask under N_2 atmosphere, and the reaction mixture was heated at 100 °C for

5 h. The reaction mixture was then analysed using GC (TCD detector), confirming the liberation of hydrogen gas.

4.3. Results and Discussion

The carbazole ligands were easily prepared from the reaction of 2,3,4,9-tetrahydro-1H-carbazol-1-one with substituted benzhydrazide in ethanol. Complexation was accomplished by reacting these ligands with the Ru(II) precursor [Ru(II)(η^6-arene)Cl_2] in a 1:2 molar ratio in the presence of toluene solvent. The resulted complexes yellow in color. All the complexes are stable in air and readily dissolved in most organic solvents. The newly formed arene ruthenium(II) complexes were authenticated with the help of analytical and different spectral techniques.

4.3.1. FT-IR Spectra

In FT-IR spectra, stretching frequencies were observed around 3225-3273 and 3317–3460 cm^{-1} and assignable to carbazole and hydrazone N–H fragments of the ligands (L1– L3). Moreover, the intense bands around 1644-1679 and 1560 - 1605 cm^{-1} were attributed to C═N and C═O moieties of L1– L3. In the spectra of the complexes, one of the $\nu_{(N–H)}$ frequencies and $\nu_{(C=O)}$ were absent which suggested the tautomerization and the formation of a new sharp band characteristic to $\nu_{(C-O)}$ (1246-1295 cm^{-1}) demonstrated the subsequent coordination of the imidolate oxygen to ruthenium. Further, $\nu_{(C=N)}$ in the complexes were decreased (1516-1527 cm^{-1}) relative to free ligands and witnessed that another active binding cite of ligand to ruthenium ion is ylidene nitrogen and authenticated the bidentate N^O coordination of L1-L3 to Ru metal centre.

4.3.2. NMR spectra

The proton NMR spectra of L1-L3 displayed two distinctive downfield singlets around δ 9.13–11.36 ppm due to the carbazole and hydrazone NH protons. The aliphatic protons of the carbazole ring exhibited three multiplets from δ 2.26-4.02 ppm. Another

singlet at δ 3.82 ppm was endorsed to methoxy protons of ligand L3. The coordination *via* imidolate oxygen to ruthenium ion was entailed by the absence of hydrazone –NH peak in the spectra of the complexes after enolization and subsequent deprotonation. All aromatic protons of the ligands and complexes were appeared as multiplets in the range of δ 7.09-8.07 ppm. In the complexes, arene protons were found at δ 4.69-5.35 ppm. The $-CH_3$ protons of the isopropyl group in *p*-cymene moiety were resonated as a singlet in the region δ 1.11-1.13 ppm and methine proton was emerged as septet around δ 2.50 ppm. Furthermore, methyl protons of *p*-cymene moiety were noticed as a singlet at δ 2.23-2.66 ppm. The formation of the synthesized complexes was further evidenced by $^{13}C\{^1H\}$ NMR spectra. The downfield shifts of C=N (161.08-161.49 ppm) and C-O (170.34-171.45 ppm) in the spectra of the complexes supported the bonding of imidolate oxygen and ylidene nitrogen to Ru(II) ion.

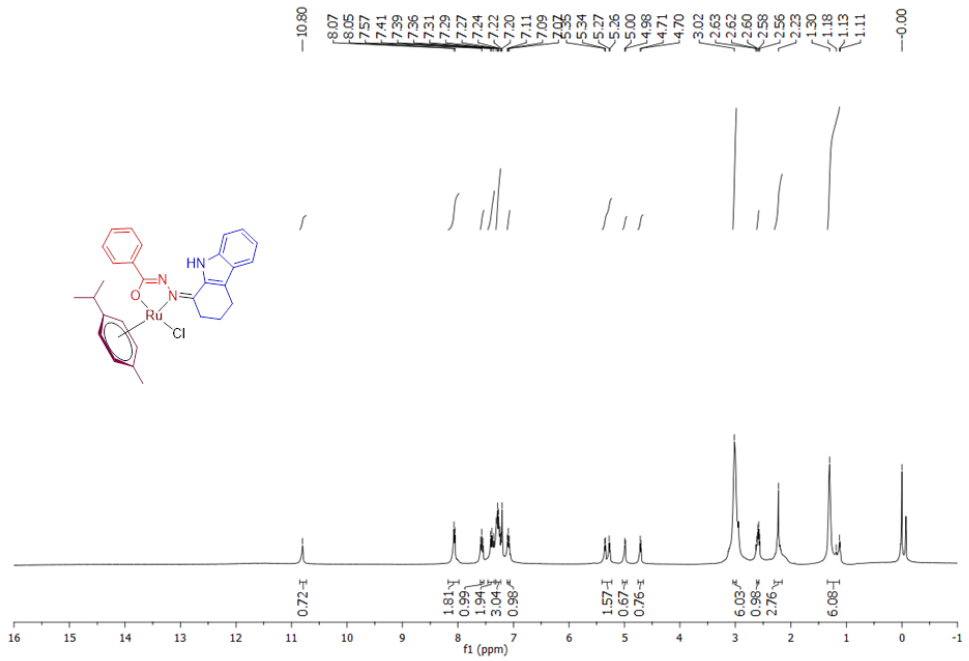

Figure 2. ^{1}H NMR spectrum of complex **1** in $CDCl_3$ (400 MHz, 293 K).

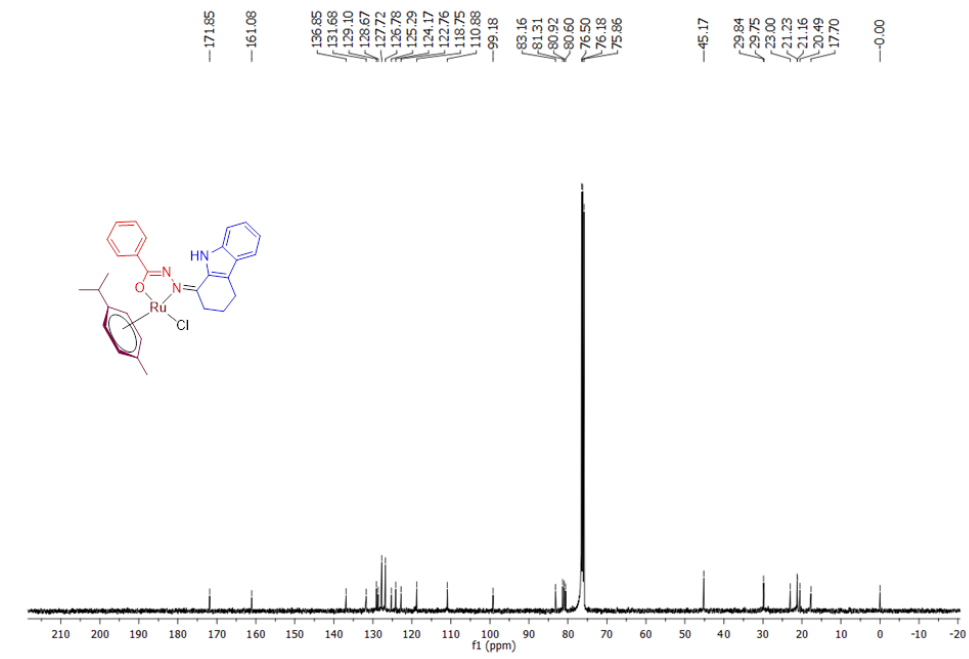

Figure 3. ^{13}C NMR spectrum of complex **1** in $CDCl_3$ (100 MHz, 293 K).

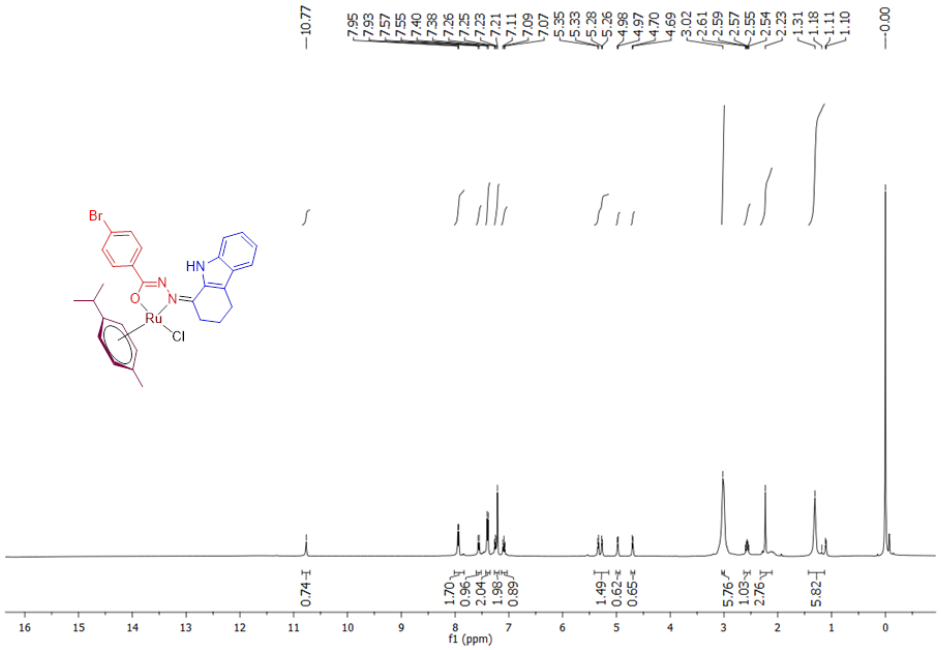

Figure 4. ^{1}H NMR spectrum of complex **2** in $CDCl_3$ (400 MHz, 293 K).

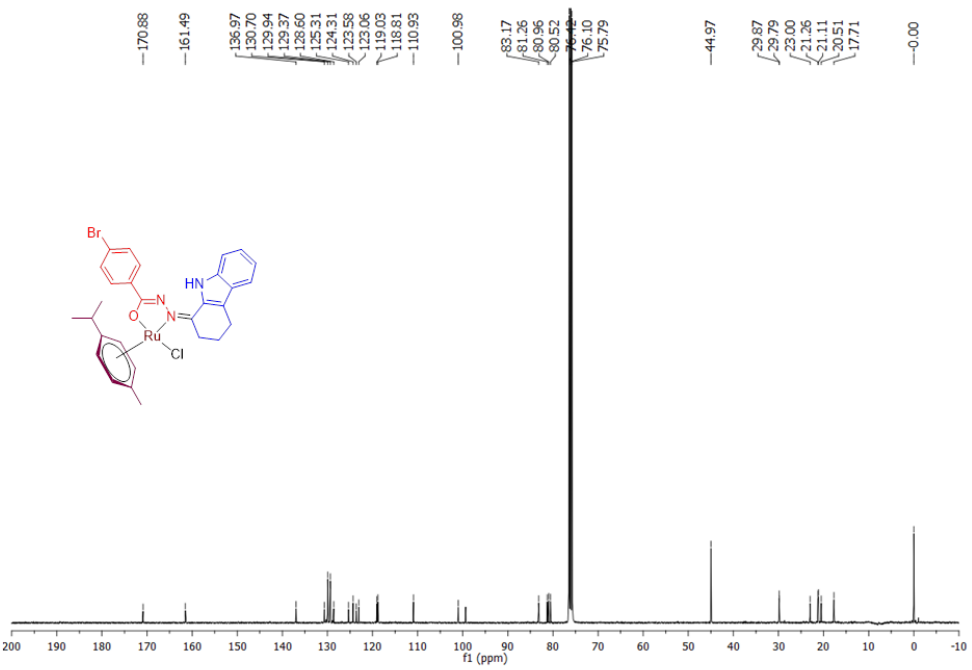

Figure 5. ^{13}C NMR spectrum of complex **2** in $CDCl_3$(100 MHz, 293 K).

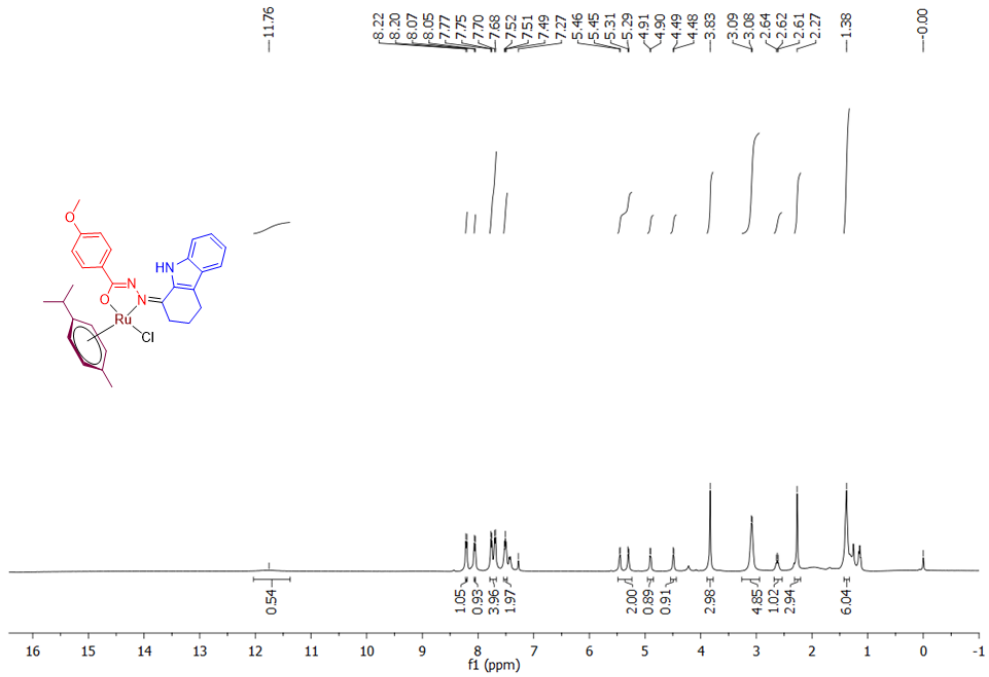

Figure 6. ^{1}H NMR spectrum of complex **3** in $CDCl_3$ (400 MHz, 293 K).

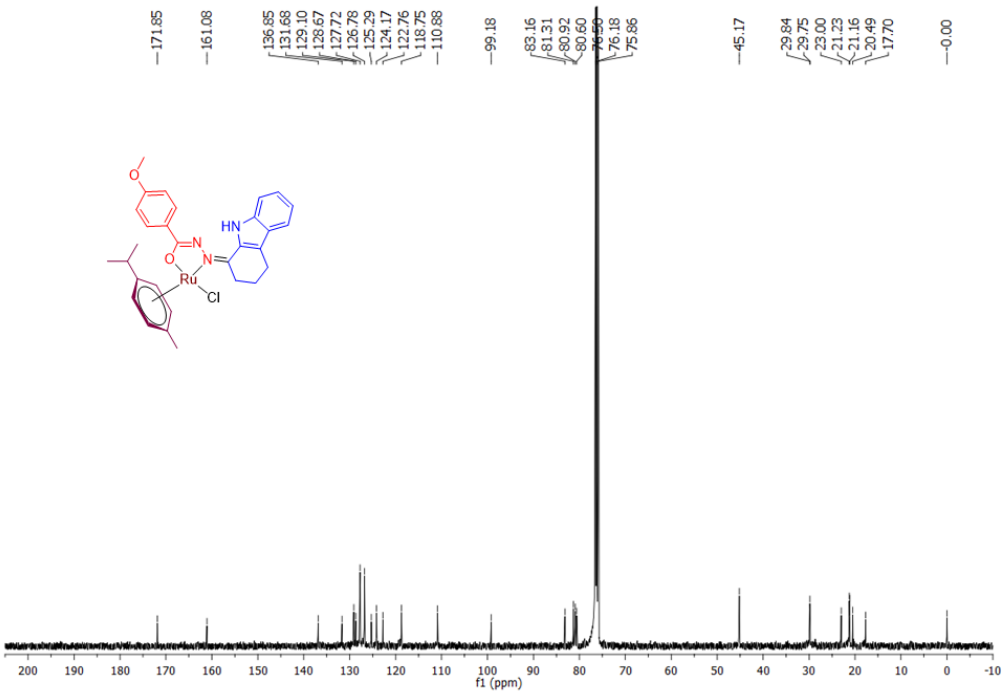

Figure 7. ^{13}C NMR spectrum of complex **3** in $CDCl_3$ (100 MHz, 293 K).

4.3.3. X-ray molecular structure determination

The molecular structure for the representative complex **2** is confirmed by X-ray diffraction studies and the ORTEP diagram is portrayed in Figure 8. The crystal structure refinement parameters have been provided in Table 1, and important bond distances and angles have been presented in Table 2. The orthorhombic system of complex **2** belongs to the "P 21 21 21" space group with Z = 4. The bite angle O(1)-Ru(1)-N(1) of the complex is 76.37 (15)^{o}. Ru(1)-N(1) and Ru(1)-O(1) have bond lengths of 2.107(4) and 2.051(4) A˚, respectively. The Ru-Cl has a bond length of 2.4093(16) A˚, and Ru-centroid distance of 1.677 Å which is comparable with other reported *p*-cymene ruthenium(II) complexes.[20] Therefore, the XRD studies corroborated the binding of hydrazone ligand with the Ru(II) ion through the ylidene nitrogen and imidolate oxygen to form a five-member metallacycle. The residual cites of the octahedron have been occupied by *p*-cymene and chloride ligands resulting in the formation of piano-stool geometry.

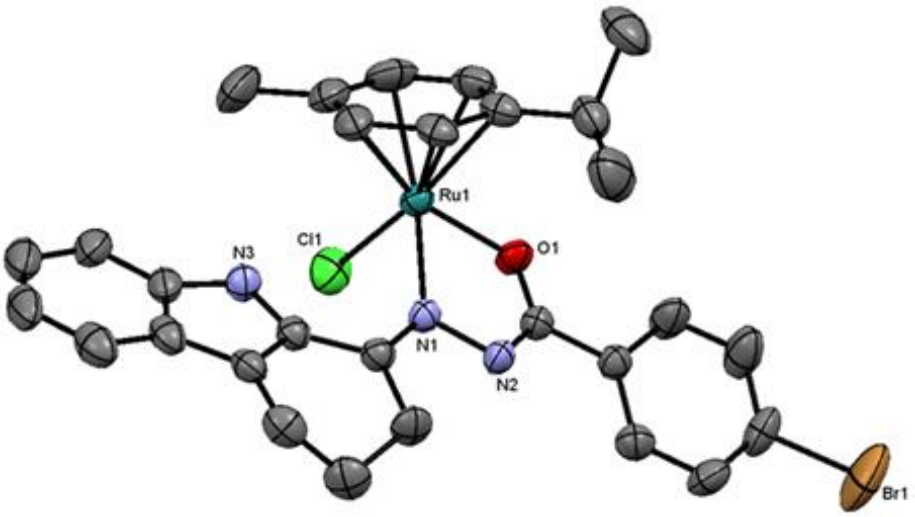

Figure 8. ORTEP diagram of the complex **2** with 30% probability. All the hydrogen atoms were omitted for clarity.

Table 1. Crystal data and structure refinement for complex **2**

CCDC	2025903
Empirical formula	$C_{29}H_{29}BrClN_3ORu$
Formula weight	651.98
Temperature/K	295(2)
Crystal system	Orthorhombic
Space group	P 21 21 21
a/Å, *b*/Å, *c*/Å	8.0310(4), 16.1519(7), 20.7720(8)
α/°, β/°, γ/°	90, 90, 90
Volume/Å3	2694.47(19)
Z	4
ρcalcmg/mm^3	1.607
m/mm^{-1}	2.191
F(000)	1312
Crystal size/mm^3	0.42 × 0.13 × 0.07
Theta range for data collection	3.446 to 29.330°
Index ranges	$-8 \leq h \leq 10$, $-15 \leq k \leq 22$, $-25 \leq l \leq 28$
Reflections collected	16543
Independent reflections	6452[R(int) = 0.0353]
Data/restraints/parameters	6452/0/332
Goodness-of-fit on F^2	1.025
Final *R* indexes [I>2σ (I)]	*R1* = 0.0412, *wR2* = 0.0859
Final *R* indexes [all data]	*R1* = 0.0624, *wR2* = 0.0928
Largest diff. peak/hole / e $Å^{-3}$	0.353/-0.726

Table 2. Selected bond lengths (Å) and angles (°) for the complex **2**

Bond lengths (Å)	
Ru1-Cl1	2.409 (16)
Ru1-O1	2.051 (4)
Ru1-N1	2.107 (4)
Ru1-C20	2.193 (5)
Ru1-C21	2.166 (5)
Ru1-C22	2.195 (6)
Ru1-C23	2.227 (6)
Ru1-C24	2.191 (6)
Ru1-C25	2.158 (6)
Br1-C17	1.893 (6)
O1-C13	1.292 (6)
N1-N2	1.409 (6)
N1-C1	1.304 (6)
N2-C13	1.296 (7)
N3-C11	1.377 (7)
C1-C2	1.514 (7)
C1-C12	1.446 (7)
C5-C12	1.379 (7)

Bond angles (°)	
O(1)-Ru(1)-Cl(1)	86.51 (12)
O(1)-Ru(1)-N(1)	76.37 (15)
Cl(1)-Ru(1)-C(21)	152.89 (15)
N(2)- C(13)-O(1)	126.3 (5)
N(1)-Ru(1)-Cl(1)	85.12 (12)
N(1)-N(2)-C(13)	110.5 (4)
C(11)-N(3)-C(12)	108.6 (5)
C(16)-C(17)-Br(1)	119.0 (5)
C(12)-C(1)-N(1)	123.9 (5)
C(11)-N(3)-C(12)	108.6 (5)
C(20)-Ru(1)-Cl(1)	161.71 (15)
C(21)-Ru(1)-Cl(1)	152.89 (15)
C(22)-Ru(1)-Cl(1)	116.13 (17)
C(23)-Ru(1)-Cl(1)	93.12 (18)
C(24)-Ru(1)-Cl(1)	96.30 (19)
C(25)-Ru(1)-Cl(1)	123.62 (19)
C(26)-C(20)-Ru(1)	126.0 (4)
C(29)-C(23)-Ru(1)	129.7 (5)
C(13)-O(1)-Ru(1)	111.7 (3)

4.3.4. Catalytic application to synthesis of 2-amino-4H-chromenes

Based on the development of ruthenium catalysts towards noteworthy applications in coupling reactions, the *p*-cymene Ru(II) complexes have been tuned as a catalysts in the direct synthesis of 2-amino-4H-chromene derivatives under mild conditions. The catalytic synthesis was carried out *via* ADC of substituted benzyl alcohols with malononitrile, and resorcinol.

4.3.4.1. Optimization of bases, solvents and temperature

The optimization for the multicomponent synthesis of 2-amino-4H-chromene has been started with benzyl alcohol (**1a**), resorcinol (**2**), and malononitrile (**3**) as a benchmark substrate employing 1 mol % of *p*-cymene ruthenium complex **1** and demonstrated in **Table 3**. The trail reaction influenced us to check the catalytic variables including different solvents, bases, times, catalyst loadings and temperatures. Initially, complex **1** was utilized as a catalyst with 1 mol% catalyst loading in presence of K_2CO_3 base in *m*-xylene solvent at 140 ℃ for 24 h to provide 2-amino-4H-chromene **4a** with 74% of isolated yield (Table 3, entry 1). Upon screening the solvents, the multicomponent synthesis performed in toluene medium furnished better yield of **4a** (81%) when compared to *m*-xylene, 1,4-dioxane, *t*-BuOH, THF, CH_3CN, and ethanol medium that afforded only upto 74 % (Table 3, entries 2-7). The key role of the base towards catalyst activation was evidenced by the outcomes of previous optimization reactions and for the current multicomponent chromene synthesis, the same KOH base proved as suitable choice among the all-other bases screened (Table 3, entries 8-13). Further, the yield of **4a** was decreased marginally when lowering the temperature from 110 °C (85%) to 100 °C (83%) (Table 3, entry 14). Hence, complex **1** has been carry out the chromene synthesis at a little shortened time (18 h) time (Table 3, entry 15) and almost same amount of **4a** was attained (79 %). The inevitability of catalyst and base to the catalytic reaction was further evidenced by the no formation or non-quantitative yields (<10 %) of the products when the synthesis was performed without the catalyst and KOH (Table 3, entries 16 and 17). From the results of optimization reactions, the suitable condition has been streamlined as $PhCH_3$/KOH medium at 100 °C for 18 h for extending the substrate scope of desired 2-amino-4H-chromene.

Table 3. Screening of reaction conditions[a]

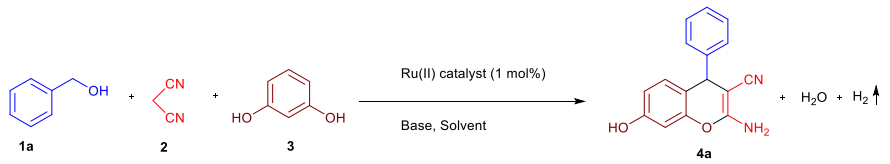

#	Complex	Solvent	Base	T (°C)	T (h)	Yield[b]
1	1	*m*-Xylene	K_2CO_3	140	24	74
2	1	$PhCH_3$	K_2CO_3	110	24	81
3	1	Dioxane	K_2CO_3	100	24	52
4	1	*t*-BuOH	K_2CO_3	82	24	48
5	1	THF	K_2CO_3	66	24	26
6	1	CH_3CN	K_2CO_3	80	24	35
7	1	Ethanol	K_2CO_3	78	24	42
8	1	$PhCH_3$	Na_2CO_3	110	24	64
9	1	$PhCH_3$	$NaHCO_3$	110	24	53
10	1	$PhCH_3$	Cs_2CO_3	110	24	67
11	1	$PhCH_3$	KOH	110	24	85
12	1	$PhCH_3$	NaOH	110	24	72
13	1	$PhCH_3$	*t*-BuOK	110	24	69
14	1	$PhCH_3$	KOH	100	24	83
15	**1**	**$PhCH_3$**	**KOH**	**100**	**18**	79
16[c]	-	$PhCH_3$	KOH	100	24	<10
17[d]	1	$PhCH_3$	-	100	24	NR

[a]**Reaction Conditions:** Benzyl alcohol (**1a**) (1 mmol), malononitrile (**2**) (1 mmol), resorcinol (**3**) (1 mmol), complex (1 mol %), base (0.5 mmol), solvent (5 mL). N_2 atm. [b] Isolated yield of **4a**. [c] No catalyst. [d] No base.

4.3.4.2. Optimization of effect of substituent

Once the various catalytic parameters were optimized, the effect of substituents of all the complexes on the catalytic reaction has been investigated (Table 4). At most, all the complexes (**1-3**) showed good catalytic activity in the formation of 2-amino-4H-chromene product with appreciable yields. However, based on experimental results, the complex **3** relatively provided a better yield than complexes (**1-3**) due to the presence of electron donating methoxy group (Table 4, entries 1-3). Hence, the complex **3** was kept as a representative catalyst to explore the broad substrate scope using a diverse range of alcohols.

Table 4. Effect of the substituent of catalyst[a]

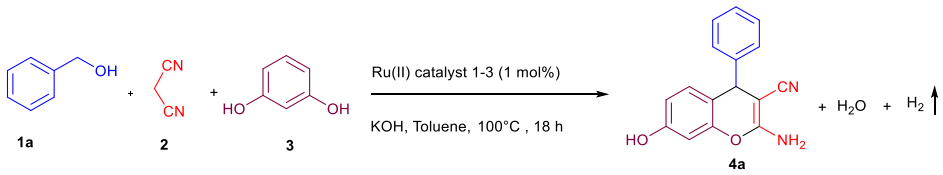

Entry	Ru complexes	Yield(%)[b]
1	Complex 1	83
2	Complex 2	81
3	**Complex 3**	**89**

[a]**Reaction conditions:** Benzyl alcohol (**1a**) (1 mmol), malononitrile (**2**) (1 mmol), resorcinol (**3**) (1 mmol), complex (1 mol %), KOH (0.5 mmol), $PhCH_3$ (5 mL). N_2 atm, 100 °C, 18 h. [b] Isolated yield.

4.3.4.3. Optimization of catalyst loading

Further, the effectiveness of our catalyst was examined with different catalyst loadings for the test reaction (Table 5). Upon reducing the catalyst loading from 1 mol% to 0.1 mol%, there was a substantial decrease in yields (Table 5, entries 1-4). Therefore 1 mol% catalyst loading is the best choice for optimization.

Table 5: Effect of catalyst loading[a]

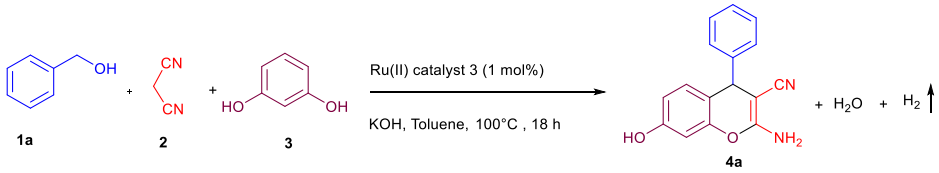

Entry	Catalyst 3 (mol %)	Yield(%)[b]
1	**1.0**	**87**
2	0.5	45
3	0.25	23
4	0.10	<10

[a]**Reaction conditions:** Benzyl alcohol (**1a**) (1 mmol), malononitrile (**2**) (1 mmol), resorcinol (**3**) (1 mmol), complex **3** (1 mol %), KOH (0.5 mmol), $PhCH_3$ (5 mL). N_2 atm, 100 °C, 18 h. [b] Isolated yield.

4.3.4.4. Scope of the reactions

The broad substrate scope to the ruthenium-catalysed synthesis of 2-amino-4H-chromenes from the coupling of resorcinol and malononitrile with primary alcohols with different structural diversities were given in Table 6. The optimized reaction conditions were applied for benzyl alcohols containing different electron-donating (*p*-CH_3, *m*-OCH_3, *p*-OCH_3, and *m*-OH) and deficient (*p*-Cl, *o*-Cl, *m*-Br and *o*-Br) substituents to the construction of corresponding chromene derivatives **4b-4i** in 69-95% isolated yields. It is worth to note that, benzyl alcohols bearing electron-donating substituents were found to be effective to provide the final products than the electron-withdrawing benzyl alcohol analogues. In addition, the catalytic reaction with benzyl alcohols comprising more electron-donating groups including dimethoxy, and trimethoxy benzyl alcohols afforded **4j-4m** in 65%-80% yields. The reaction of benzyl alcohol encompassing isopropyl group provided **4n** in 73% yield. 4-nitro benzyl alcohol reacted with resorcinol and malononitrile smoothly to give the chromene **4o** with moderate yield (61%). Further, 2,6-dichloro benzyl alcohol resulted the preferred **4p** with 58% yield. Noticeably, 1,4-benzenedimethanol underwent ADC reaction with malononitrile and resorcinol to form **4q** in 70% yield. Aliphatic and heterocyclic alcohols were also tested for the synthesis of 2-amino-4H-chromenes **4r** and **4s** and it was observed as unsuccessful.

Table 6. *p*-cymene-Ru(II) catalyzed 2-amino-4H-chromene synthesis from acceptorless dehydrogenative coupling of various benzyl alcohols[a,b]

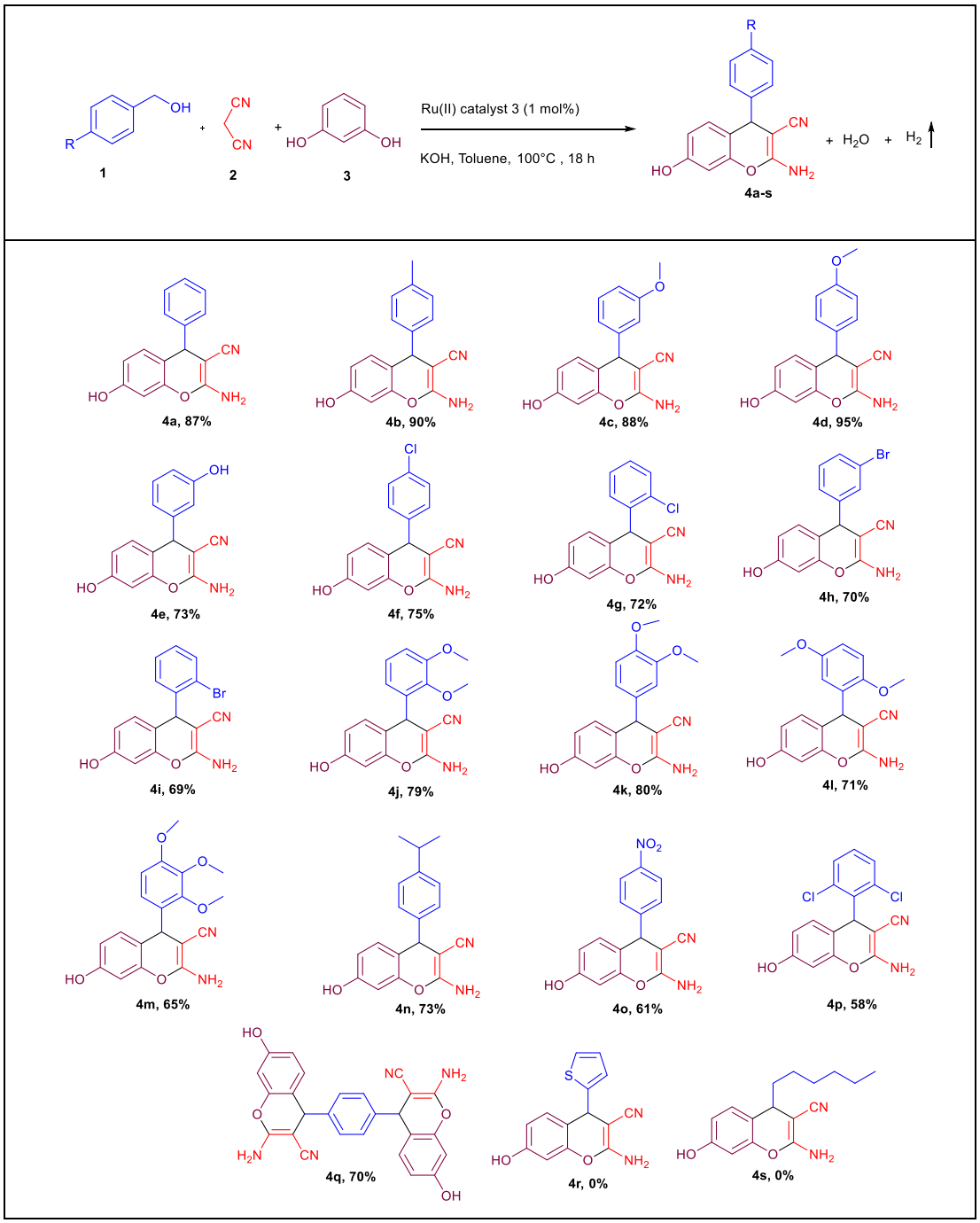

[a]**Reaction conditions:** Benzyl alcohol (**1a**) (1 mmol), malononitrile (**2**) (1 mmol), resorcinol (**3**) (1 mmol), complex **3** (1 mol %), KOH (0.5 mmol), $PhCH_3$ (5 mL). N_2 atm, 100 °C, 18 h. [b] Isolated yield.

4.3.4.5. Control experiments

A sequence of control experiments has been carried out to propose the possible mechanistic pathway behind the catalytic synthesis of 2-amino-4H-chromene. Initially, dehydrogenation of benzyl alcohol (**1a**) formed benzaldehyde (**1a'**) with the discharge of hydrogen gas under the influence of the Ru(II) catalyst in 4-5 h under the optimized reaction condition.[21]

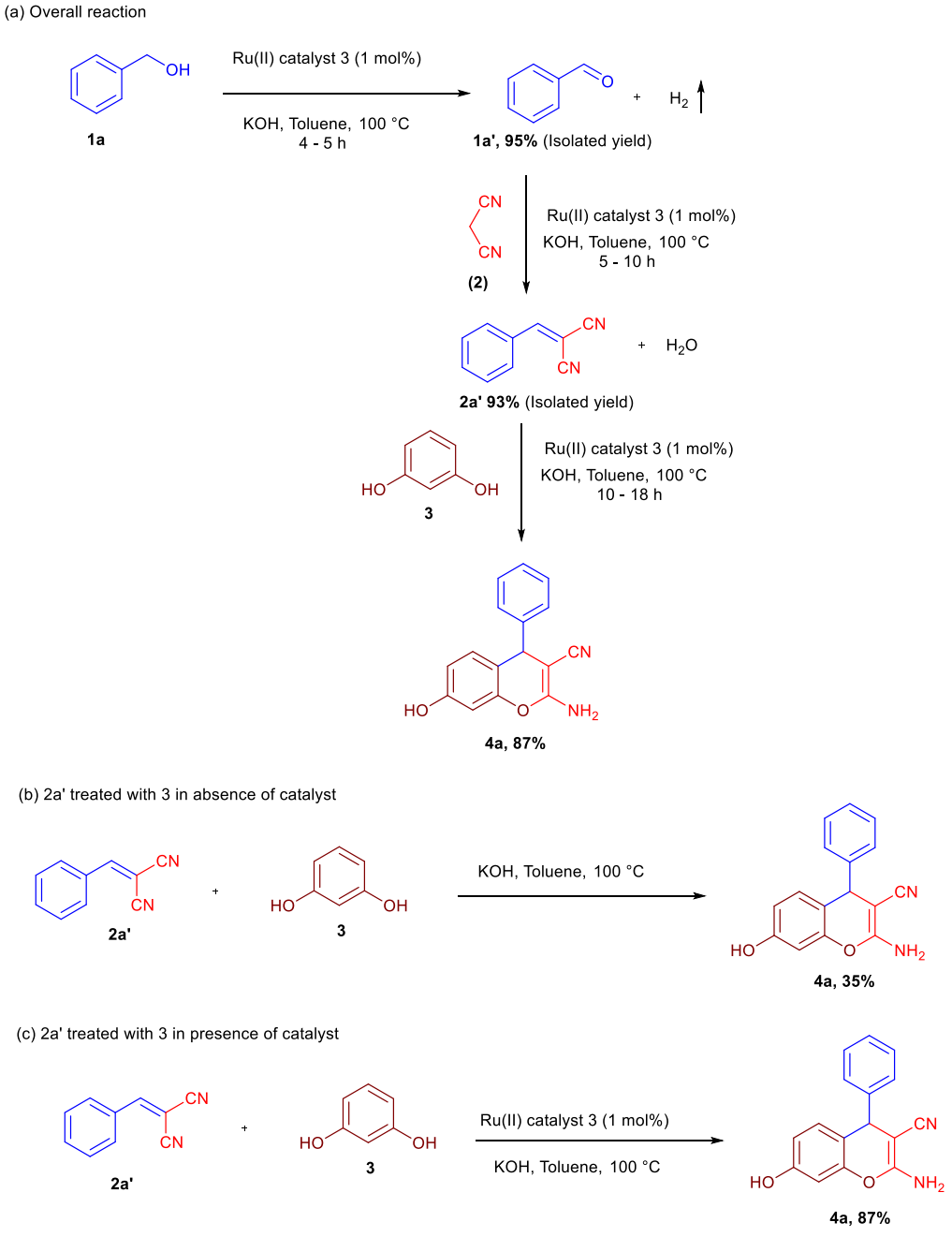

Scheme 4. Control experiments for the synthesis of 2-amino-4H-chromene

Further, the benzaldehyde **1a'** formed was reacted with malononitrile (**2**) in presence of catalyst to give **2a'** in 93% of isolated yield in 10 h. After, Ru(II) catalyst mediated reaction of **2a'** with resorcinol (**3**) provided 2-amino-4H-chromene **4a** with 87% yield in 18 h (Scheme 4a).

To attest the vital role of the synthesized Ru(II) catalyst towards the construction of the desired chromene, a test reaction with **2a'** and resorcinol (**3**) has been performed without the complex **3**. As expected, the reaction ended with the chromene **4a** only in 35% yield (Scheme 4b). However, in contrary to the above reaction, 87% of **4a** was attained while **2a'** coupled with resorcinol (**3**) in the presence of complex **3** under optimal conditions (Scheme 4c) which corroborated the active involvement of ruthenium catalyst in catalytic cycle.[12d]

4.3.4.6. Competitive control experiment between EDG and EWG

An intermolecular competitive experiment was carried out between *p*-methylbenzyl alcohol and *p*-chlorobenzyl alcohol with malononitrile and resorcinol under optimized reaction conditions. From this reaction, we have gained a better understanding of the impact of the electron-donating and electron-deficient substituents of substrates on catalytic efficiency. The results expressed that the electron releasing benzyl alcohol is more reactive than the electron-deficient benzyl alcohol (Scheme 5).

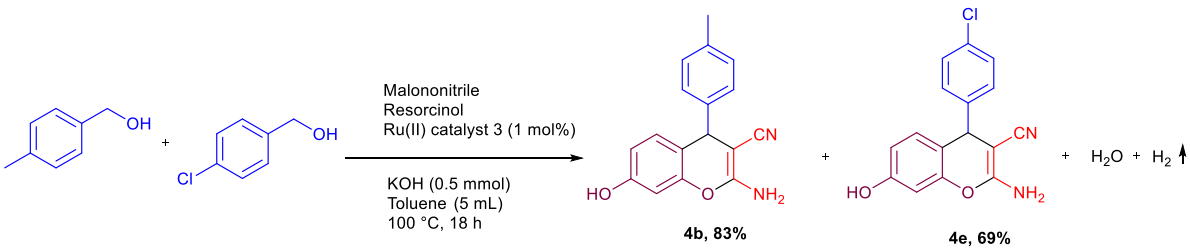

Scheme 5. Competition reaction among electron releasing and electron deficient alcohols

4.3.4.7. Large-scale synthesis of 2-amino-4H-chromene

Large-scale synthesis has been carried out to illustrate the usefulness of the titled catalysts for the enlightenment to large-scale synthesis of 2-amino-4H-chromene. Advantageously, the gram-scale reaction of benzyl alcohol (**1a**), malononitrile (**2**), and resorcinol (**3**) at the optimized reaction condition furnished **4a** in 65 % isolated yield (1.62 g) (Scheme 6).

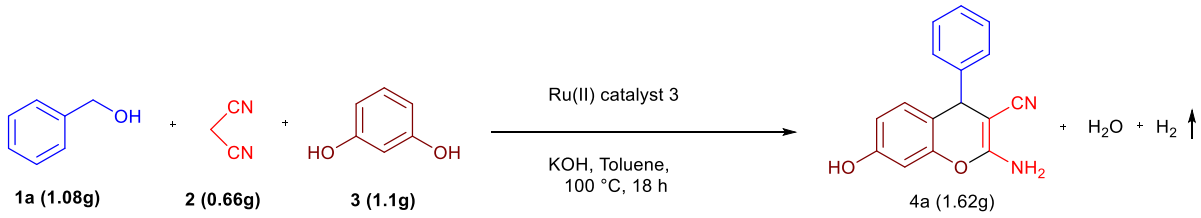

Scheme 6. Large scale synthesis of 2-amino-4H-chromenes

4.3.4.8. Synthesis of Tacrine analogue

2-amino-3-cyano-4H-chromenes exist as core structural fragment in multitude of natural and man-made compounds demonstrating fascinating therapeutic and pharmacological applications. They are used as key intermediates for the fabrication of tacrine analogues. Tacrine is one of the important drugs used for the treatment of Alzheimer's disease.[22] Further, research of tacrine and its analogues is still of interest to researchers investigating in the field of Alzheimer medicine. Hence, here we have fabricated tacrine analogue **5** with good yields from the synthesized 2-amino-7-hydroxy-4-phenyl-4H-chromene-3-carbonitrile (**4a**) with cyclohexanone in presence of $AlCl_3$ in 1,4-dioxane (Scheme 7).[23]

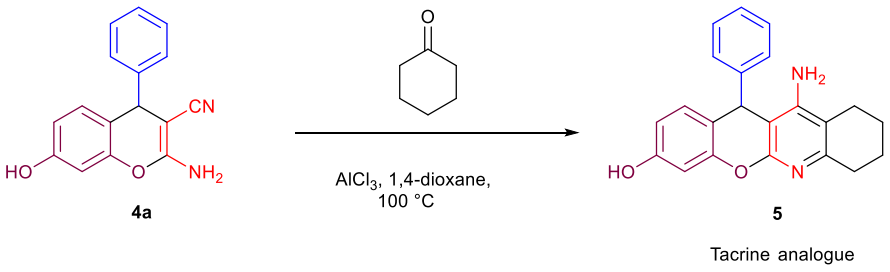

Scheme 7. Synthesis of Tacrine analogue

4.3.4.9. Reaction mechanism for 2-amino-4H-chromenes

Based on the control experiments and previous literature reports[24] a plausible mechanism for Ru(II) catalysed synthesis of 2-amino-4H-chromene has proposed (Scheme 8).

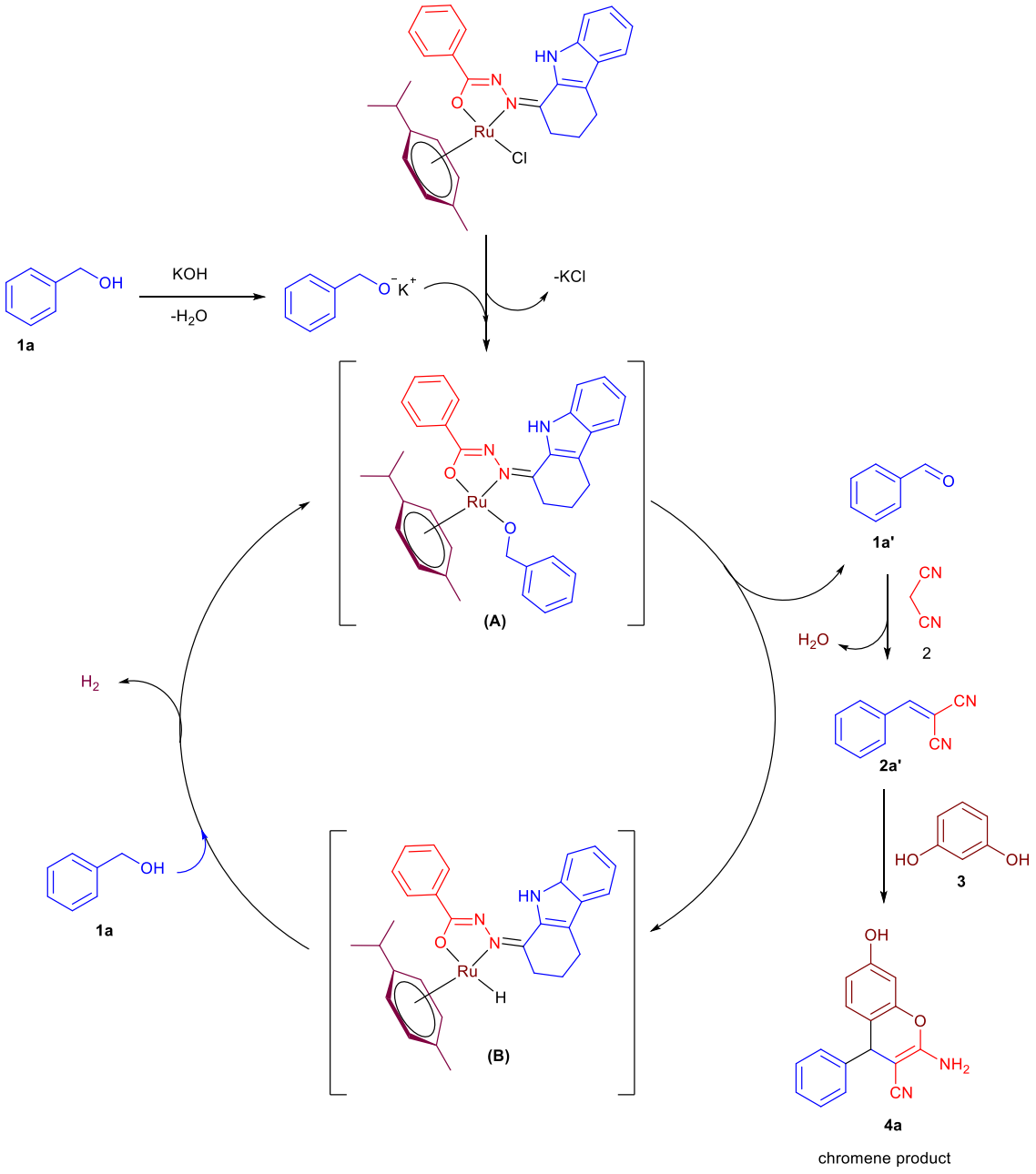

Scheme 8. A plausible mechanism for 2-amino-4H-chromene synthesis

At first, the catalyst reacts with alcohol with the aid of KOH to give Ru-alkoxide species (**A**). Further, **A** undergoes *β*-hydride elimination to discharge benzaldehyde (**1a'**) along with the generation of Ru-H species (**B**). Further, the *in-situ* generated benzaldehyde (**1a'**) underwent Knoevenagel condensation with malononitrile (**2**) to form benzylidenemalononitrile intermediate (**2a'**). Later, Michael addition[25] of **2a'** and resorcinol (**3**) followed by intramolecular cyclization to result the 2-amino-4H-chromene (**4a**). Finally, Ru-hydride species (**B**) reacts with another molecule of benzyl alcohol (**1a**) to regenerate the catalyst with the evolution of hydrogen gas.[26] The liberated H_2 gas was confirmed by Gas chromatography.

Spectral data of the catalytic products

Benzaldehyde (**1a'**)[27]. ^{1}H NMR (400 MHz, $CDCl_3$): δ (ppm) δ 9.96 (s, 1H), 7.83 (d, *J* = 7.6 Hz, 1H), 7.58-7.41 (m, 4H), 2.91-2.83 (s, 1H), 1.19 (s, 6H). ^{13}C {^{1}H} NMR (100 MHz, $CDCl_3$): δ (ppm) 192.63, 136.36, 134.55, 129.79, 129.03.

2-benzylidenemalononitrile (**2a'**)[28]. ^{1}H NMR (400 MHz, $CDCl_3$): δ (ppm) 7.91 (d, *J* = 7.6 Hz, 2H), 7.79 (s, 1H), 7.64 (t, *J* = 7.4 Hz, 1H), 7.55 (t, *J* = 7.6 Hz, 2H). ^{13}C {^{1}H} NMR (100 MHz, $CDCl_3$): δ (ppm) 160.05, 134.70, 130.96, 130.79, 129.68, 113.77, 112.61, 82.86.

2-amino-7-hydroxy-4-phenyl-4H-chromene-3-carbonitrile (4a)[29]. ^{1}H NMR (400 MHz, DMSO-d_6): δ (ppm) 9.72 (s, 1H), 7.30 (t, *J* = 7.4 Hz, 2H), 7.23 – 7.14 (m, 3H), 6.88 (s, 2H), 6.81 (d, *J* = 8.5 Hz, 1H), 6.49 (dd, *J* = 8.4, 1.3 Hz, 1H), 6.42 (d, *J* = 2.2 Hz, 1H), 4.62 (s, 1H). ^{13}C {^{1}H} NMR (100 MHz, DMSO-d_6): δ (ppm) 160.22, 157.04, 148.82, 146.34, 129.88, 128.55, 127.34, 126.60, 120.65, 113.71, 112.34, 102.14, 56.22

2-amino-7-hydroxy-4-(p-tolyl)-4H-chromene-3-carbonitrile (4b)[29]. ^{1}H NMR (400 MHz, DMSO-d_6): δ (ppm) 9.74 (s, 1H), 7.11 (d, *J* = 7.9 Hz, 2H), 7.05 (d, *J* = 7.9 Hz, 2H), 6.84 (s, 2H), 6.78 (d, *J* = 8.4 Hz, 1H), 6.48 (dd, *J* = 8.4, 2.1 Hz, 1H), 6.42 (d, *J* = 2.1 Hz, 1H), 4.57

(s, 1H), 2.25 (s, 3H). ^{13}C {^{1}H} NMR (100 MHz, DMSO-d_6): δ (ppm) 160.12, 156.96, 148.75, 143.39, 135.68, 129.87, 129.09, 127.26, 120.67, 113.85, 112.30, 102.10, 56.36, 20.54.

2-amino-7-hydroxy-4-(3-methoxyphenyl)-4H-chromene-3-carbonitrile (4c)[30]. ^{1}H NMR (400 MHz, DMSO-d_6): δ (ppm) 9.76 (s, 1H), 7.22 (t, *J* = 8.0 Hz, 1H), 6.89 (s, 2H), 6.85 (d, *J* = 8.5 Hz, 1H), 6.76 (m, 3H), 6.51 (dd, *J* = 8.3, 1.7 Hz, 1H), 6.45 (s, 1H), 4.61 (s, 1H), 3.71 (s, 3H).^{13}C{^{1}H} NMR (100 MHz, DMSO-d_6): δ (ppm) 160.30, 159.31, 157.06, 148.79, 147.93, 129.85, 129.71, 120.67, 119.56, 113.60, 113.46, 112.35, 111.43, 102.17, 56.11, 54.90.

2-amino-7-hydroxy-4-(4-methoxyphenyl)-4H-chromene-3-carbonitrile (4d)[31]. ^{1}H NMR (400 MHz, DMSO-d_6): δ (ppm) 9.71 (s, 1H), 6.94-6.82 (m, 5H), 6.75 (d, *J* = 6.8 Hz, 1H), 6.56 (s, 1H), 6.49 (d, *J* = 8.3 Hz, 1H), 6.44 (s, 1H), 4.95 (s, 1H), 3.71 (s, 3H).^{13}C{^{1}H} NMR (100 MHz, DMSO-d_6): δ (ppm) 160.94, 156.91, 153.26, 150.57, 149.09, 135.27, 129.21, 120.76, 115.06, 113.76, 112.75, 112.18, 111.47, 102.10, 56.19, 55.13.

2-amino-7-hydroxy-4-(3-hydroxyphenyl)-4H-chromene-3-carbonitrile (4e)[32]. ^{1}H NMR (400 MHz, DMSO-d_6): δ (ppm) 9.53 (s, 1H), 7.09 (t, *J* = 7.8 Hz, 1H), 6.85 – 6.81 (m, 3H), 6.64-6.58 (m, 2H), 6.54 (s, 1H), 6.50 (dd, *J* = 8.4, 2.0 Hz, 1H), 6.42 (d, *J* = 1.9 Hz, 1H), 4.51 (s, 1H).^{13}C {^{1}H} NMR (100 MHz, DMSO-d_6): δ (ppm) 160.20, 157.48, 156.99, 148.79, 147.82, 129.83, 129.44, 120.70, 118.05, 114.06, 113.78, 113.69, 112.31, 102.12, 56.31.

2-amino-4-(4-chlorophenyl)-7-hydroxy-4H-chromene-3-carbonitrile (4f)[31]. ^{1}H NMR (400 MHz, DMSO-d_6): δ (ppm) 9.75 (s, 1H), 7.37 (d, *J* = 8.4 Hz, 2H), 7.19 (d, *J* = 8.4 Hz, 2H), 6.93 (s, 2H), 6.79 (d, *J* = 8.5 Hz, 1H), 6.49 (dd, *J* = 8.4, 2.1 Hz, 1H), 6.42 (s, 1H), 4.67 (s, 1H).^{13}C{^{1}H} NMR (100 MHz, DMSO-d_6): δ (ppm) 160.21, 157.18, 148.78, 145.30, 131.20, 129.87, 129.25, 128.54, 120.49, 113.16, 112.45, 102.19, 55.79.

2-amino-4-(2-chlorophenyl)-7-hydroxy-4H-chromene-3-carbonitrile (4g)[30]. ^{1}H NMR (400 MHz, DMSO-d_6): δ (ppm) 9.82 (s, 1H), 7.41 (d, *J* = 7.6 Hz, 1H), 7.29 – 7.18 (m, 3H), 6.95 (s, 2H), 6.75 (d, *J* = 8.5 Hz, 1H), 6.50 (dd, *J* = 8.4, 2.2 Hz, 1H), 6.45 (d, *J* = 2.1 Hz, 1H), 5.15 (s, 1H).^{13}C{^{1}H} NMR (100 MHz, DMSO-d_6): δ (ppm) 160.49, 157.28, 148.97, 142.77, 131.80, 130.74, 129.70, 129.22, 128.53, 127.77, 120.32, 112.49, 112.44, 102.24, 54.84.

2-amino-4-(3-bromophenyl)-7-hydroxy-4H-chromene-3-carbonitrile (4h)[29]. ^{1}H NMR (400 MHz, $CDCl_3$): δ (ppm) 9.77 (s, 1H), 7.41 (d, *J* = 7.7 Hz, 1H), 7.35 (s, 1H), 7.28 (t, *J* = 7.8 Hz, 1H), 7.18 (d, *J* = 7.6 Hz, 1H), 6.96 (s, 2H), 6.82 (d, *J* = 8.4 Hz, 1H), 6.51 (d, *J* = 8.4 Hz, 1H), 6.42 (d, *J* = 1.4 Hz, 1H), 4.68 (s, 1H). ^{13}C{^{1}H} NMR (100 MHz, $CDCl_3$): δ (ppm) 160.32, 157.25, 149.08, 148.77, 130.89, 129.93, 129.57, 126.55, 121.81, 120.45, 112.94, 102.23, 56.00.

2-amino-4-(2-bromophenyl)-7-hydroxy-4H-chromene-3-carbonitrile (4i)[29]. ^{1}H NMR (400 MHz, DMSO-d_6): δ (ppm) 9.78 (s, 1H), 7.58 (d, *J* = 6.8 Hz, 1H), 7.32 (s, 1H), 7.15 (d, *J* = 6.5 Hz, 2H), 6.95 (s, 2H), 6.75 (d, *J* = 7.4 Hz, 1H), 6.49 (d, *J* = 7.6 Hz, 1H), 6.44 (s, 1H), 5.16 (s, 1H). ^{13}C{^{1}H} NMR (100 MHz, DMSO-d_6): δ (ppm) 160.38, 157.33, 148.85, 144.56, 132.82, 130.96, 129.13, 128.79, 128.43, 122.28, 120.22, 112.54, 102.27, 55.10.

2-amino-4-(2,3-dimethoxyphenyl)-7-hydroxy-4H-chromene-3-carbonitrile (4j)[33]. ^{1}H NMR (400 MHz, DMSO-d_6): δ (ppm) 9.72 (s, 1H), 6.98 (t, *J* = 7.9 Hz, 1H), 6.89 (d, *J* = 7.5 Hz, 1H), 6.81 (s, 2H), 6.74 (d, *J* = 8.4 Hz, 1H), 6.64 (d, *J* = 7.5 Hz, 1H), 6.46 (dd, *J* = 8.4, 2.2 Hz, 1H), 6.41 (d, *J* = 2.1 Hz, 1H), 4.86 (s, 1H), 3.78 (s, 3H), 3.62 (s, 3H).^{13}C{^{1}H} NMR (100 MHz, DMSO-d_6): δ (ppm) 160.37, 156.87, 152.38, 148.95, 145.96, 139.22, 129.48, 124.04, 120.84, 120.74, 113.68, 112.12, 111.17, 102.10, 60.18, 55.63, 55.48.

2-amino-4-(3,4-dimethoxyphenyl)-7-hydroxy-4H-chromene-3-carbonitrile (4k)[30]. ^{1}H NMR (400 MHz, DMSO-d_6): δ (ppm) 9.68 (s, 1H), 6.83-6.89 (m, 5H), 6.67 (d, *J* = 7.9 Hz, 1H), 6.49 (d, *J* = 8.3 Hz, 1H), 6.40 (s, 1H), 4.57 (s, 1H), 3.71 (s, 6H). ^{13}C {^{1}H} NMR (100 MHz, DMSO-d_6): δ (ppm) 160.13, 156.92, 148.65, 147.52, 138.84, 129.86, 120.72, 119.35, 113.91, 112.25, 111.92, 111.20, 102.06, 56.34, 55.45, 55.41.

2-amino-4-(2,5-dimethoxyphenyl)-7-hydroxy-4H-chromene-3-carbonitrile (4l)[31]. ^{1}H NMR (400 MHz, $CDCl_3$): δ (ppm) 9.66 (s, 1H), 7.53 (d, *J* = 2.5 Hz, 3H), 7.30-7.27 (m, 2H), 7.16 (d, *J* = 9.2 Hz, 2H), 6.50 (dd, *J* = 29.8, 5.5 Hz, 1H), 6.39 (s, 1H), 4.91 (s, 1H), 3.85 (s, 3H), 3.75 (s, 3H). ^{13}C {^{1}H} NMR (100 MHz, $CDCl_3$): δ (ppm) 155.27, 153.20, 152.65, 122.77, 119.92, 114.35, 113.63, 112.31, 81.36, 56.35, 55.54.

2-amino-7-hydroxy-4-(2,3,4-trimethoxyphenyl)-4H-chromene-3-carbonitrile (4m)[33]. ^{1}H NMR (400 MHz, DMSO-d_6): δ (ppm) 9.67 (s, 1H), 6.77-6.73 (m, 5H), 6.46 (dd, *J* = 8.4, 2.2 Hz, 1H), 6.40 (d, *J* = 2.1 Hz, 1H), 4.75 (s, 1H), 3.75 (s, 3H), 3.74 (s, 3H), 3.64 (s, 3H).^{13}C{^{1}H} NMR (100 MHz, DMSO-d_6): δ (ppm) 160.26, 156.78, 152.26, 150.90, 148.97, 141.64, 131.54, 129.44, 123.34, 120.89, 113.93, 112.05, 107.82, 102.03, 60.68, 60.18, 55.84, 55.68.

2-amino-7-hydroxy-4-(4-isopropylphenyl)-4H-chromene-3-carbonitrile (4n)[34]. ^{1}H NMR (400 MHz, DMSO-d_6): δ (ppm) 9.69 (s, 1H), 7.17 (d, *J* = 8.1 Hz, 2H), 7.07 (d, *J* = 8.1 Hz, 2H), 6.85 (s, 2H), 6.81 (d, *J* = 8.5 Hz, 1H), 6.48 (dd, *J* = 8.4, 2.3 Hz, 1H), 6.40 (d, *J* = 2.2 Hz, 1H), 4.57 (s, 1H), 2.88 – 2.78 (sept, 1H), 1.18 (s, 3H), 1.16 (s, 3H). ^{13}C {^{1}H} NMR (100 MHz, DMSO-d_6): δ (ppm) 160.21, 156.97, 148.81, 146.56, 143.82, 129.86, 127.16, 126.45, 120.74, 113.92, 112.31, 102.10, 56.31, 32.98, 23.84.

2-amino-7-hydroxy-4-(4-nitrophenyl)-4H-chromene-3-carbonitrile (4o)[30]. ^{1}H NMR (400 MHz, DMSO-d_6): δ (ppm) 9.86 (s, 1H), 8.21 (d, *J* = 8.6 Hz, 2H), 7.47 (d, *J* = 8.6 Hz,

2H), 7.07 (s, 2H), 6.83 (d, *J* = 8.4 Hz, 1H), 6.53 (dd, *J* = 8.4, 2.2 Hz, 1H), 6.48 (d, *J* = 2.1 Hz, 1H), 4.88 (s, 1H). ^{13}C {^{1}H} NMR (100 MHz, DMSO-d_6): δ (ppm) 160.39, 157.47, 153.71, 148.85, 146.26, 129.92, 128.66, 123.96, 120.31, 112.61, 112.29, 102.38, 55.09.

2-amino-4-(2,6-dichlorophenyl)-7-hydroxy-4H-chromene-3-carbonitrile (4p)[32]. ^{1}H NMR (400 MHz, DMSO-d_6): δ (ppm) 9.81 (s, 1H), 7.53 (d, *J* = 7.7 Hz, 1H), 7.30-7.37 (m, 2H), 6.95 (s, 2H), 6.59 (d, *J* = 8.4 Hz, 1H), 6.47 (dd, *J* = 8.4, 1.9 Hz, 1H), 6.40 (s, 1H), 5.70 (s, 1H).^{13}C{^{1}H} NMR (100 MHz, DMSO-d_6): δ (ppm) 160.73, 157.45, 149.57, 137.86, 135.28, 134.68, 130.68, 129.55, 128.37, 120.01, 112.24, 110.05, 102.01, 52.12.

4,4'-(1,4-phenylene)bis(2-amino-7-hydroxy-4H-chromene-3-carbonitrile (4q)[35]. ^{1}H NMR (400 MHz, DMSO-d_6): δ (ppm) 9.97 (s, 1H), 7.10 (s, 4H), 6.84 (d, *J* = 11.7 Hz, 6H), 6.50 (d, *J* = 8.1 Hz, 2H), 6.43 (s, 2H), 4.58 (s, 2H). ^{13}C {^{1}H} NMR (100 MHz, DMSO-d_6): δ (ppm) 160.28, 157.09, 148.86, 144.65, 129.85, 127.43, 120.71, 113.62, 112.42, 102.18, 56.23, 56.02.

11-amino-12-phenyl-7,9,10,12-tetrahydro-8H-chromeno[2,3-b]quinolin-3-ol (5)[36]. ^{1}H NMR (400 MHz, DMSO-d_6): δ (ppm) 7.21 (d, *J* = 9.5 Hz, 4H), 7.10 (s, 1H), 6.98 (d, *J* = 7.6 Hz, 1H), 6.47 – 6.43 (m, 2H), 5.50 (s, 2H), 5.20 (s, 1H), 2.30 – 2.17 (m, 2H), 1.84 (s, 2H), 1.69 (s, 4H). ^{13}C {^{1}H} NMR (100 MHz, DMSO-d_6): δ (ppm) 156.85, 155.33, 152.22, 151.31, 145.95, 129.44, 128.43, 127.03, 126.24, 115.88, 111.96, 111.11, 102.60, 98.58, 31.92, 22.87, 22.28, 22.08.

NMR spectra for the catalytic isolated products

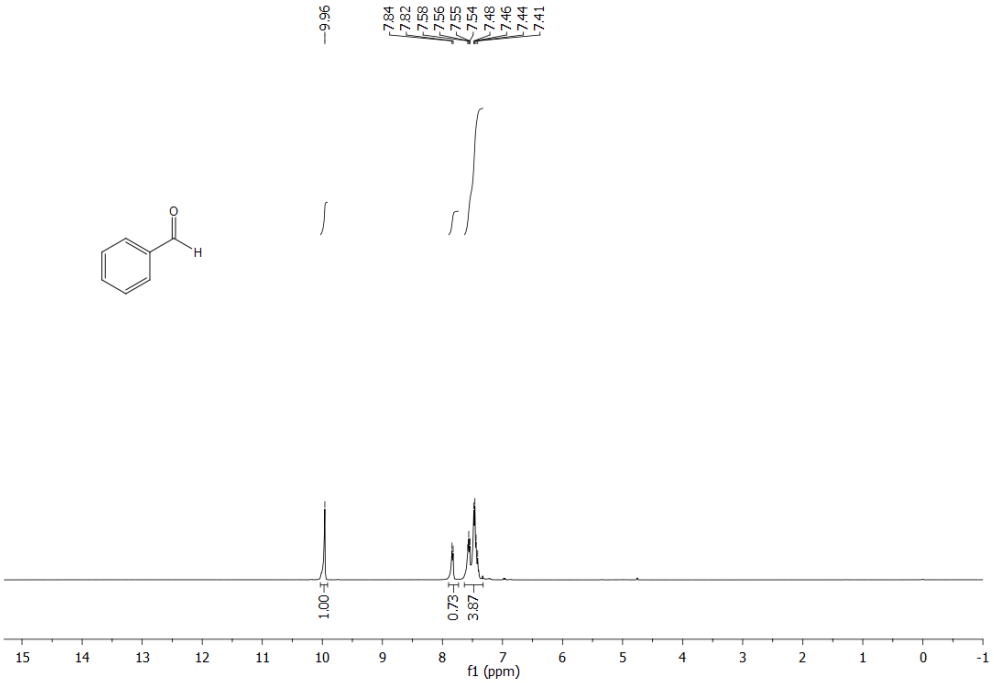

Figure 9: ^{1}H NMR spectrum for (**1a'**) in $CDCl_3$ (400MHz, 300K).

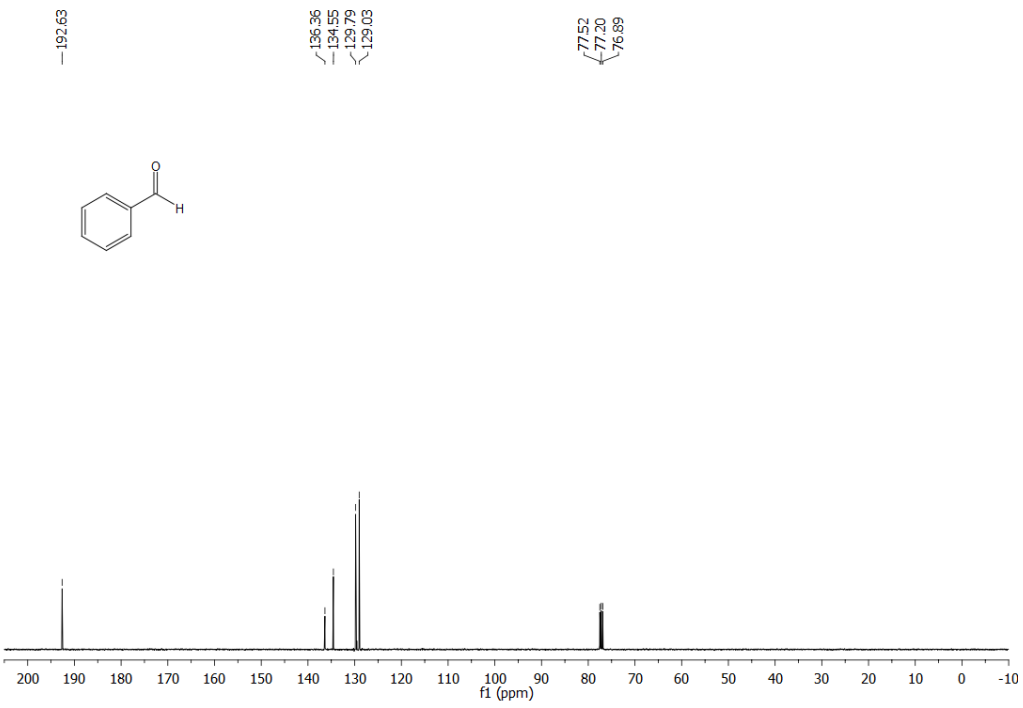

Figure 10: ^{13}C NMR spectrum for (**1a'**) in $CDCl_3$ (100MHz, 300K).

NMR spectra for benzylidinemalonitrile intermediate

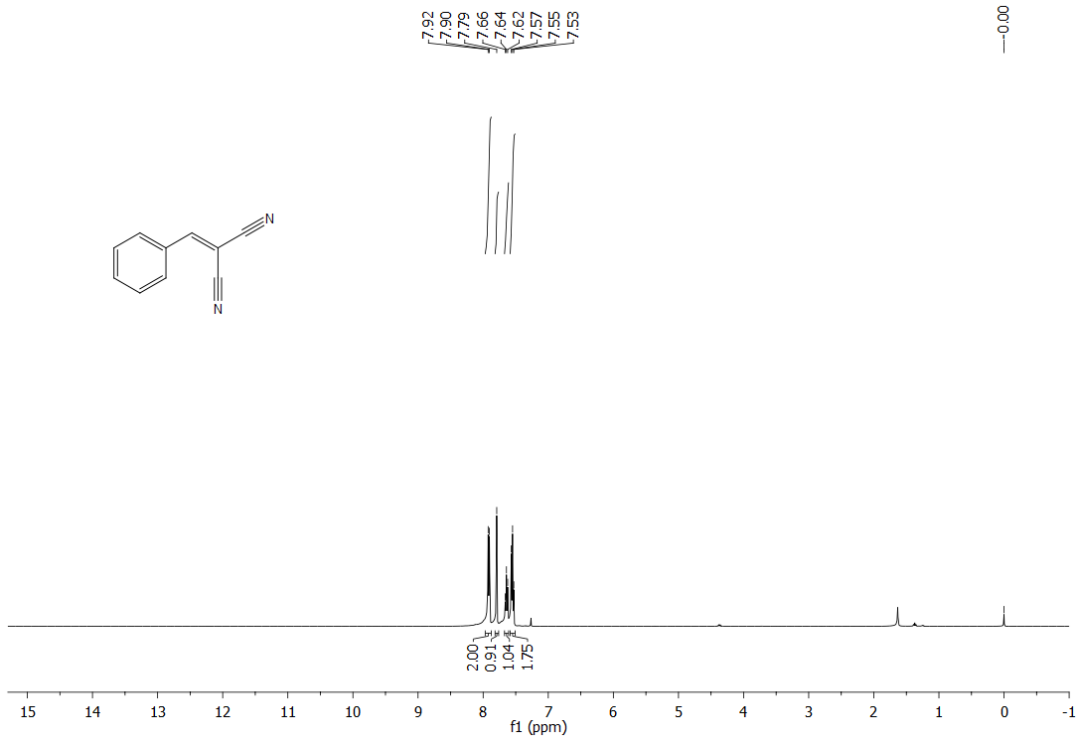

Figure 11: ^{1}H NMR spectrum for (**2a'**) in $CDCl_3$ (400MHz, 300K).

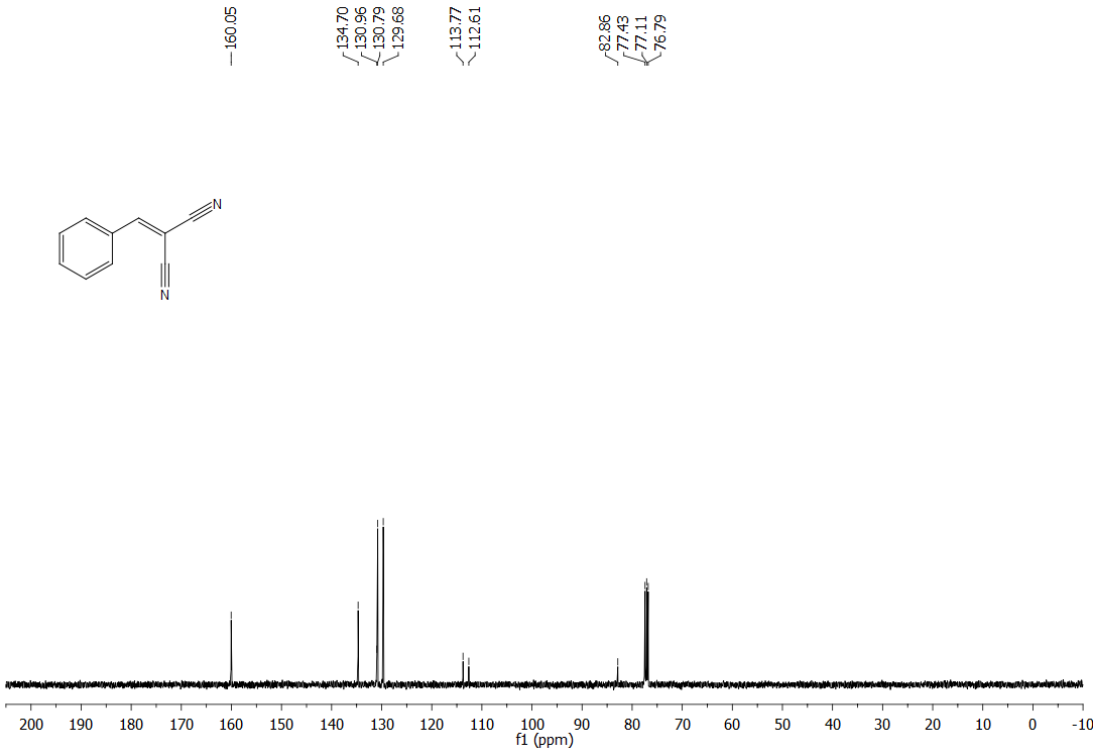

Figure 12: ^{13}C NMR spectrum for (**2a'**) in $CDCl_3$ (100MHz, 300K).

NMR spectra for chromene products

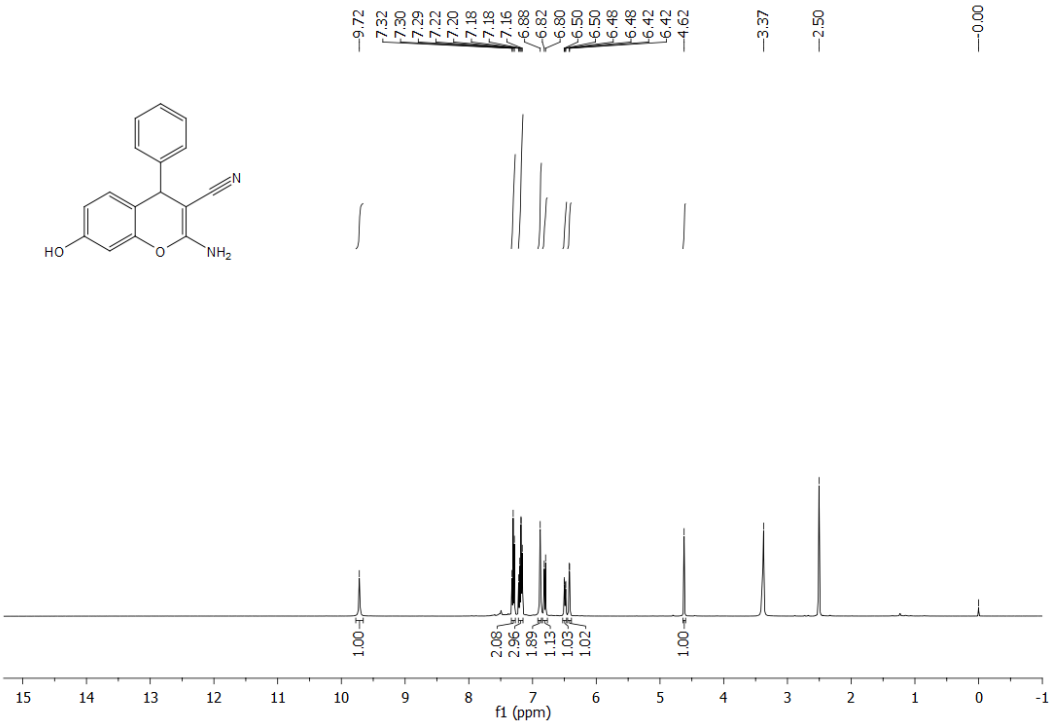

Figure 13: ^{1}H NMR spectrum for (**4a**) in DMSO-d_6 (400MHz, 300K).

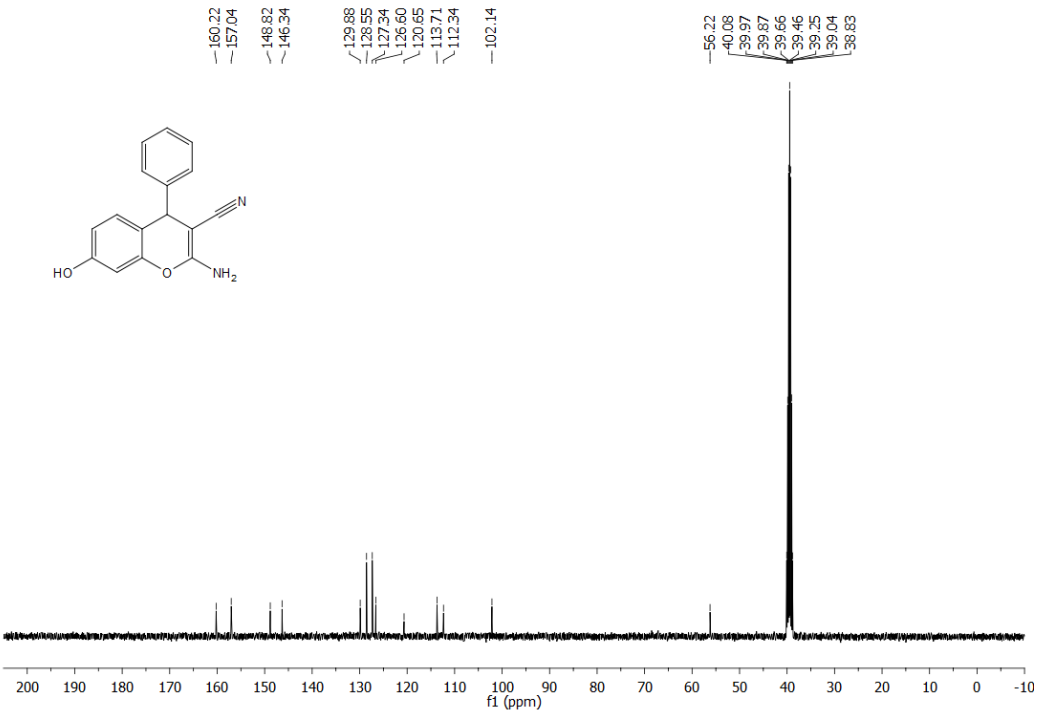

Figure 14: ^{13}C NMR spectrum for (**4a**) in DMSO-d_6 (100MHz, 300K).

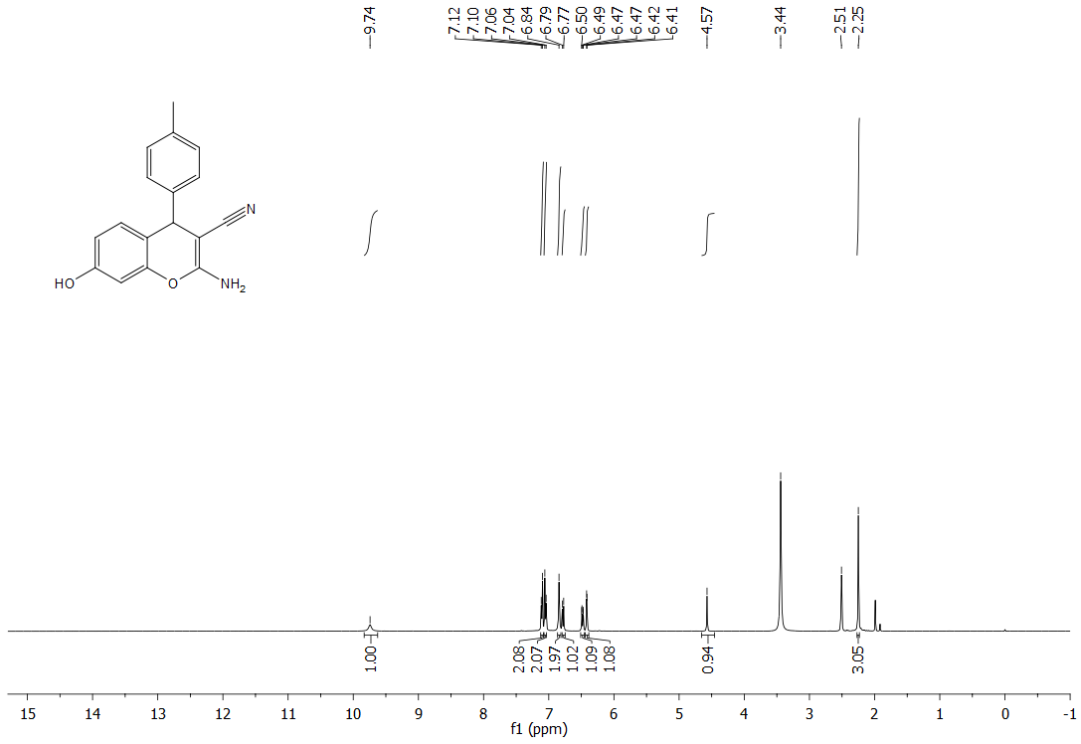

Figure 15: ^{1}H NMR spectrum for (**4b**) in DMSO-d_6 (400MHz, 300K).

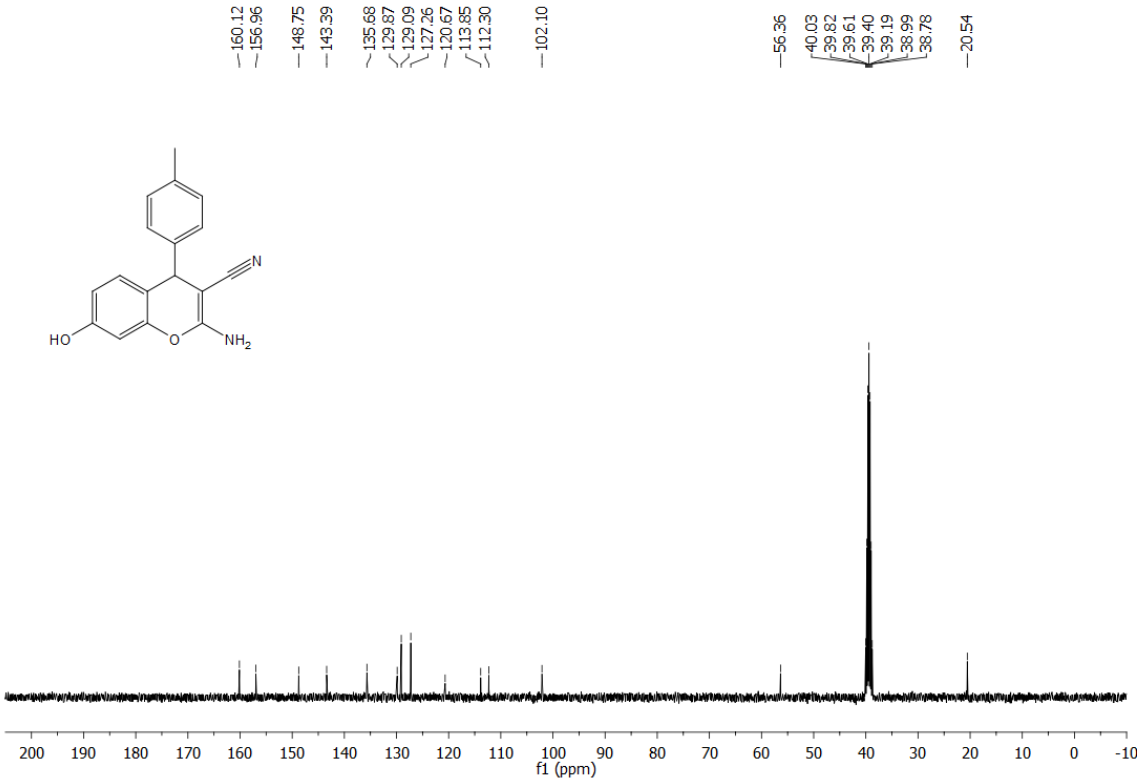

Figure 16: ^{13}C NMR spectrum for (**4b**) in DMSO-d_6 (100MHz, 300K).

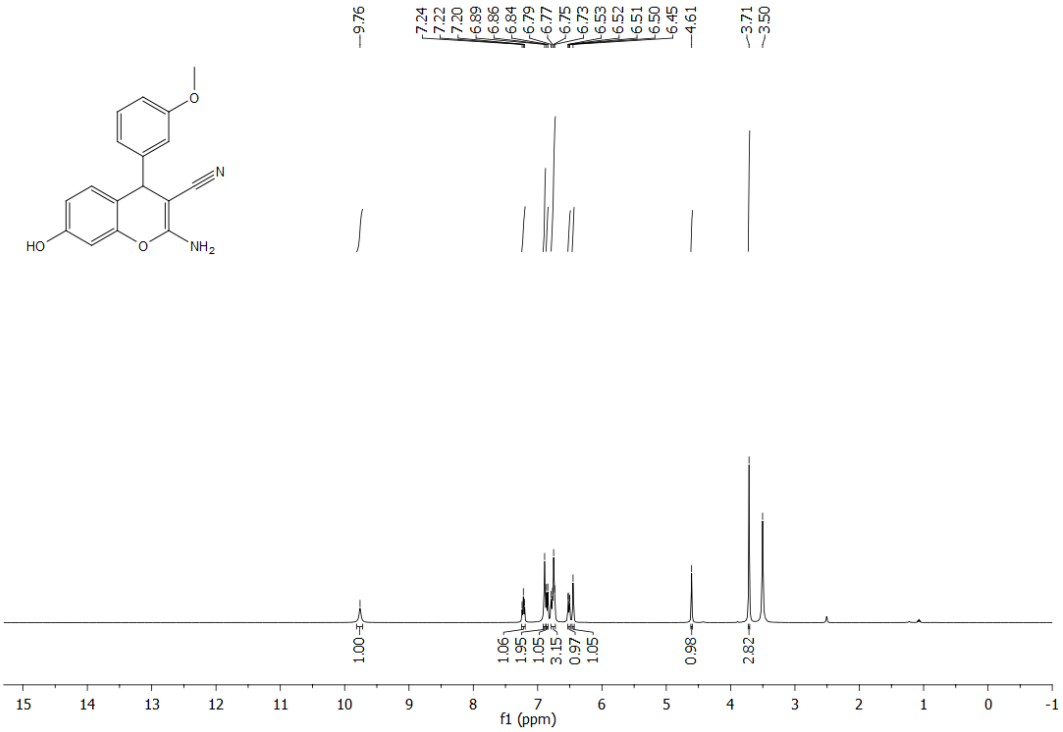

Figure 17: ^{1}H NMR spectrum for (**4c**) in DMSO-d_6 (400MHz, 300K).

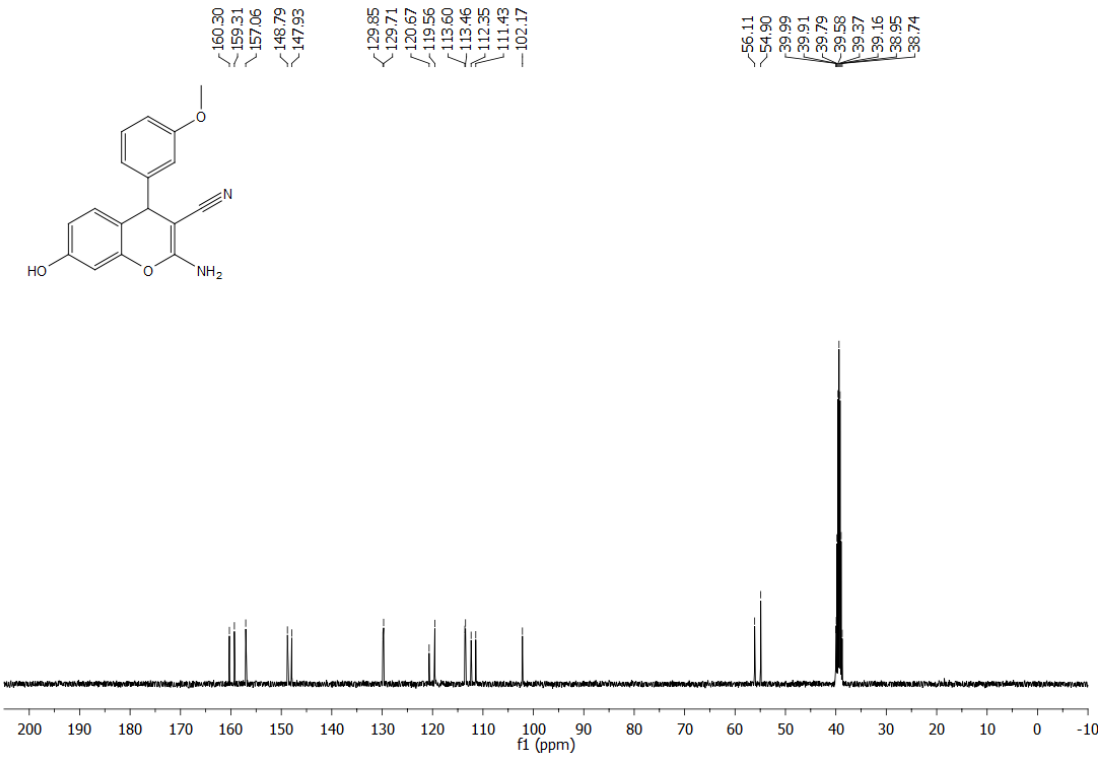

Figure 18: ^{13}C NMR spectrum for (**4c**) in DMSO-d_6 (100MHz, 300K).

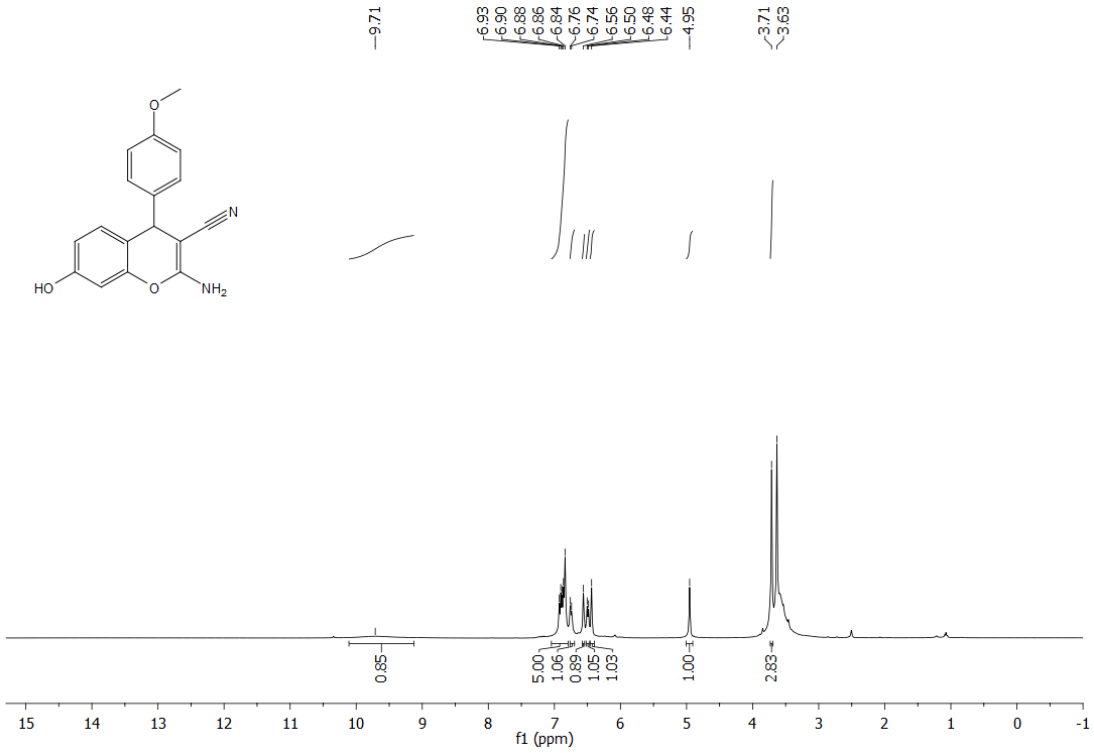

Figure 19: ^{1}H NMR spectrum for (**4d**) in DMSO-d_6 (400MHz, 300K).

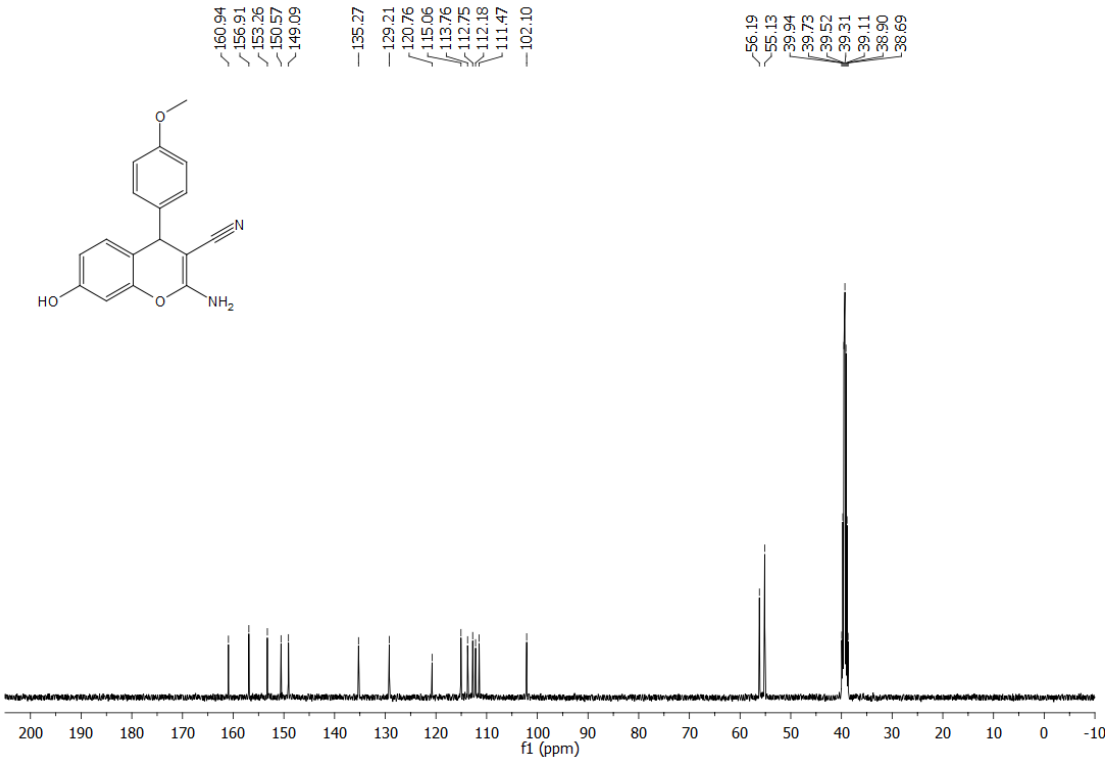

Figure 20: ^{13}C NMR spectrum for (**4d**) in DMSO-d_6 (100MHz, 300K).

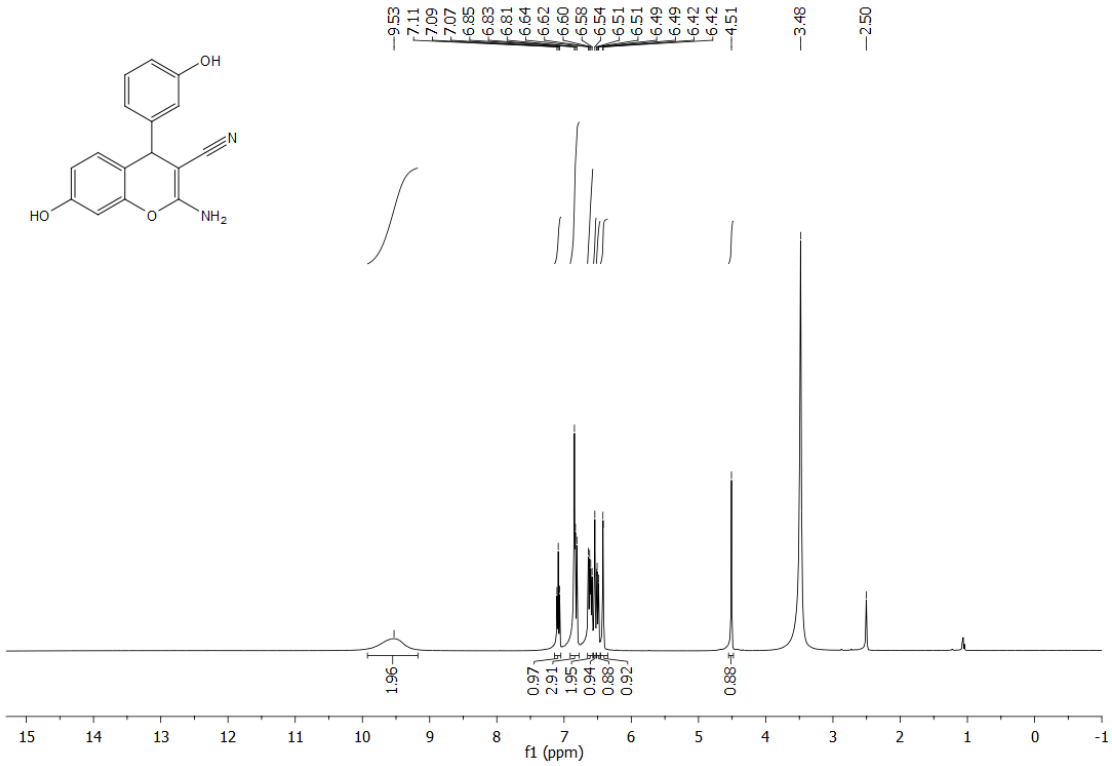

Figure 21: ^{1}H NMR spectrum for (**4e**) in DMSO-d_6 (400MHz, 300K).

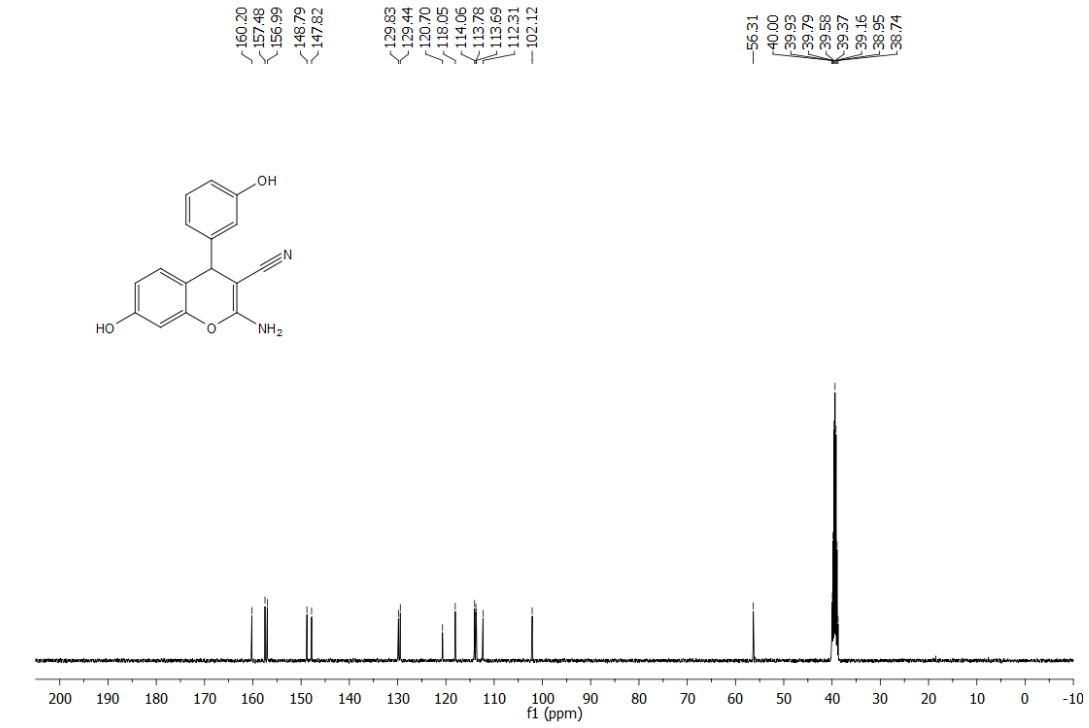

Figure 22: ^{13}C NMR spectrum for (**4e**) in DMSO-d_6 (100MHz, 300K).

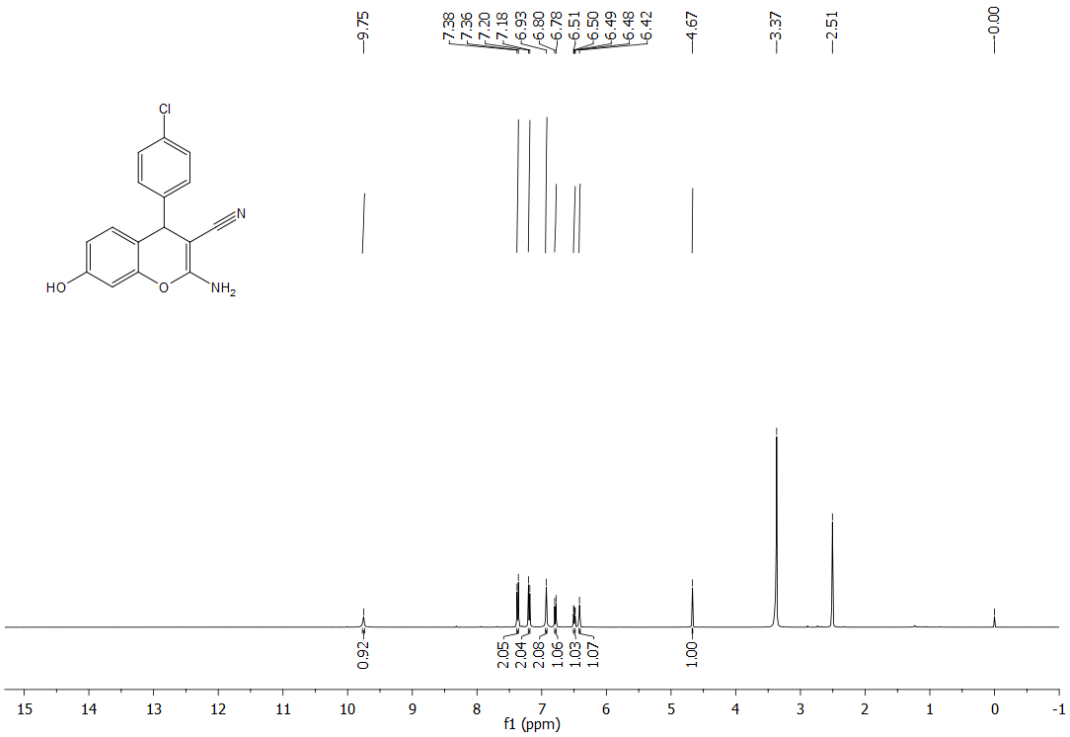

Figure 23: ^{1}H NMR spectrum for (**4f**) in DMSO-d_6 (400MHz, 300K).

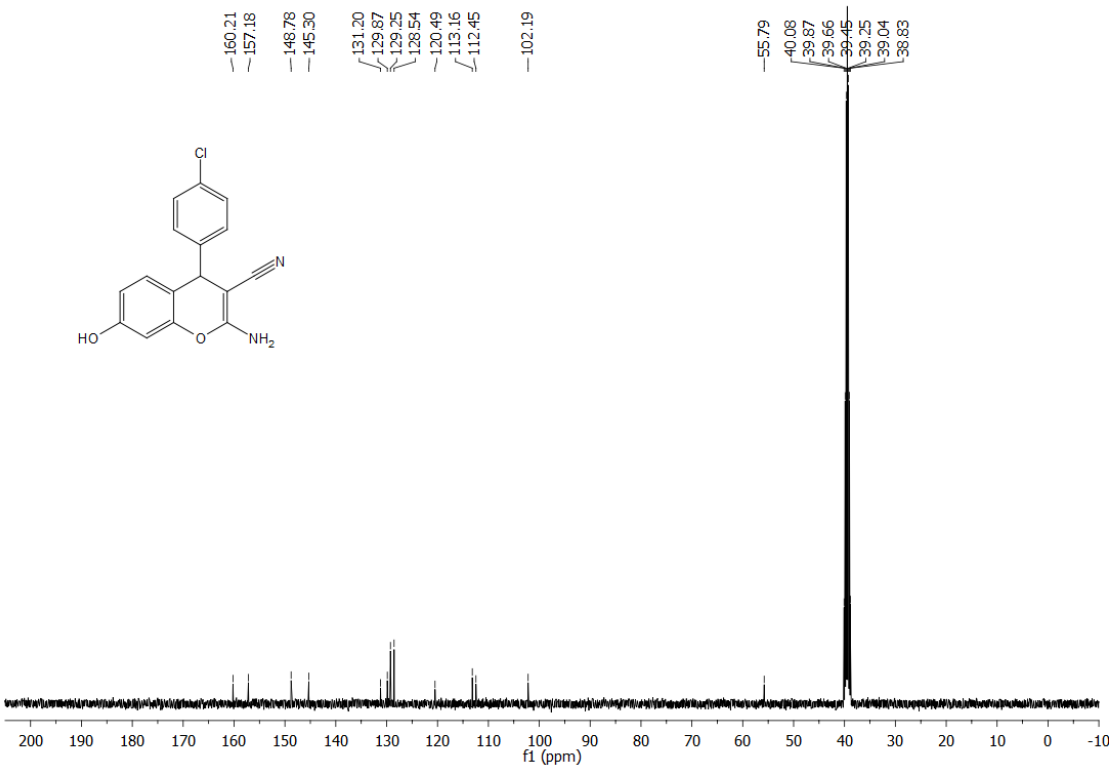

Figure 24: ^{13}C NMR spectrum for (**4f**) in DMSO-d_6 (100MHz, 300K).

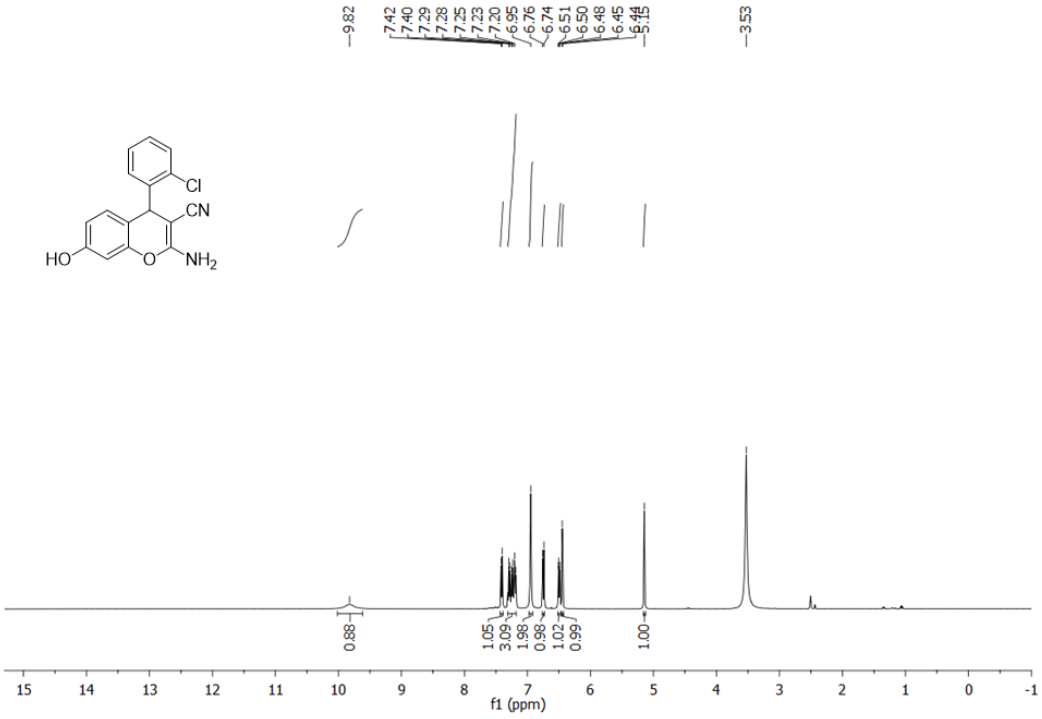

Figure 25: ^{1}H NMR spectrum for (**4g**) in DMSO-d_6 (400MHz, 300K).

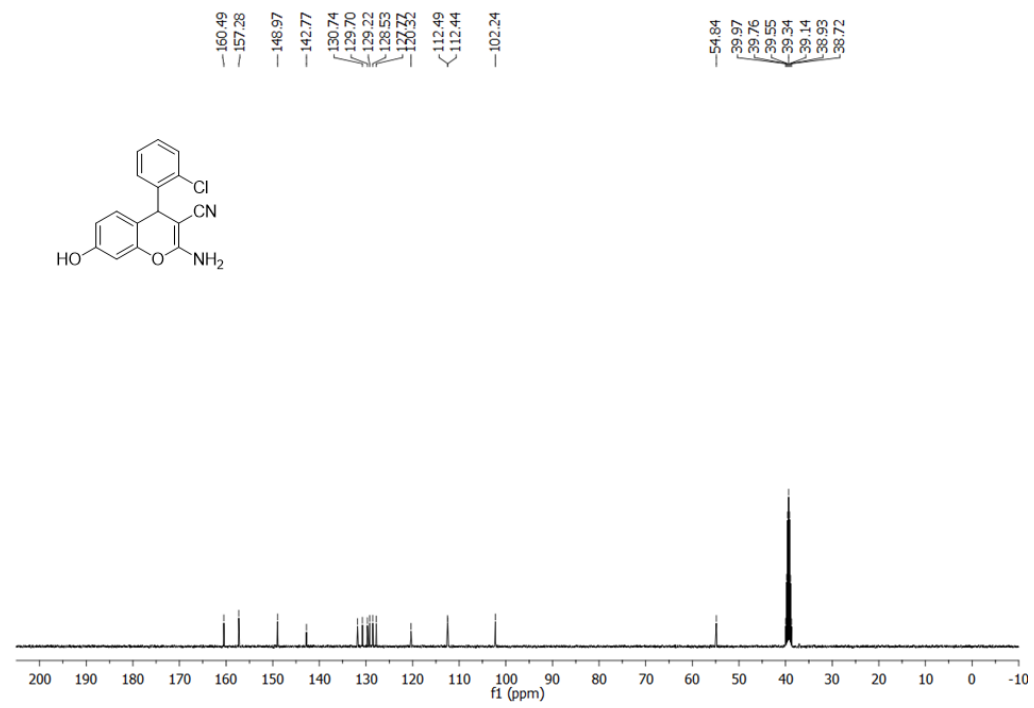

Figure 26: ^{13}C NMR spectrum for (**4g**) in DMSO-d_6 (100MHz, 300K).

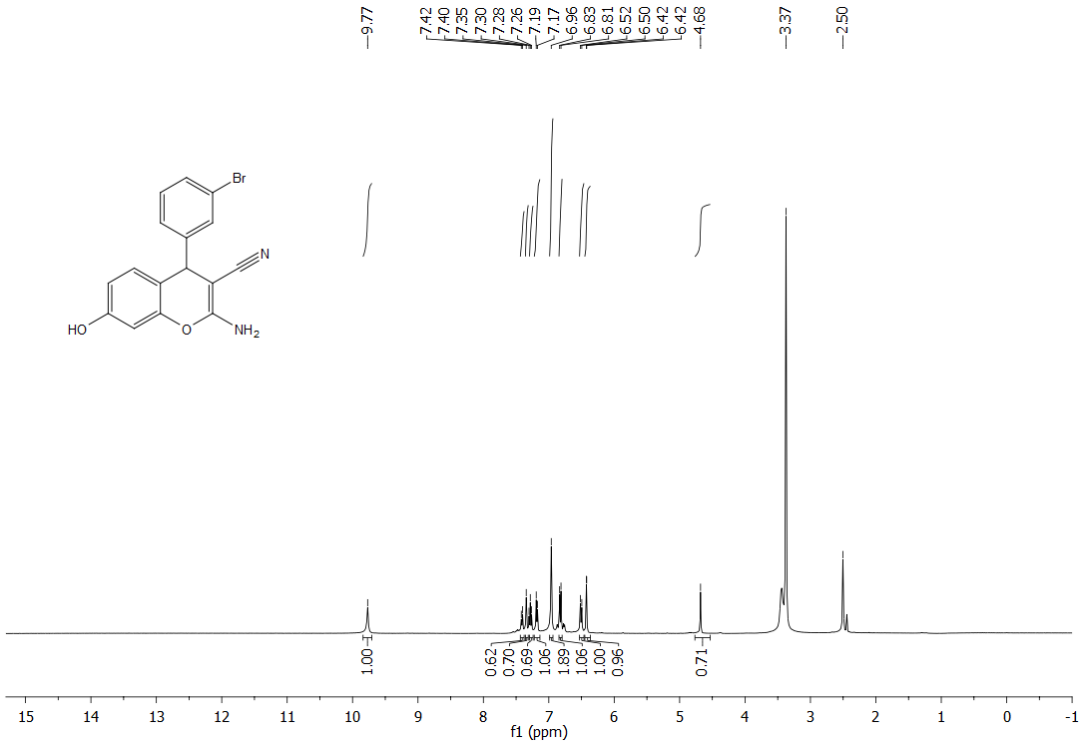

Figure 27: ^{1}H NMR spectrum for (**4h**) in DMSO-d_6 (400MHz, 300K).

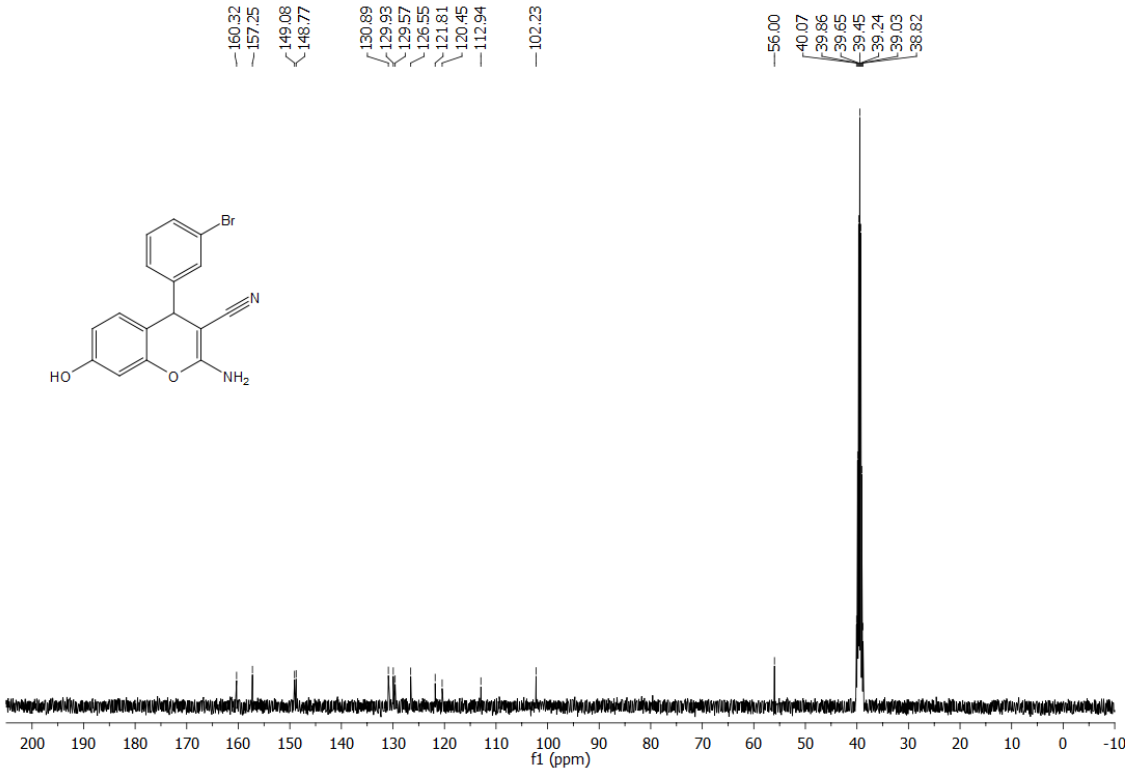

Figure 28: ^{13}C NMR spectrum for (**4h**) in DMSO-d_6 (100MHz, 300K).

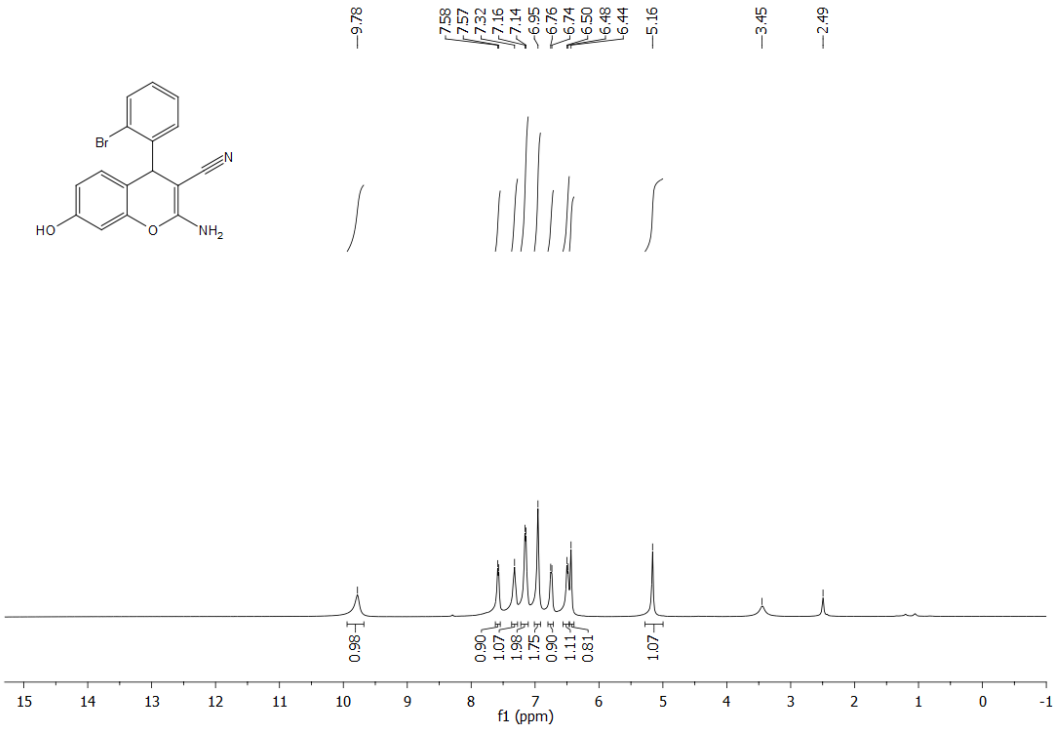

Figure 29: ^{1}H NMR spectrum for (**4i**) in DMSO-d_6 (400MHz, 300K).

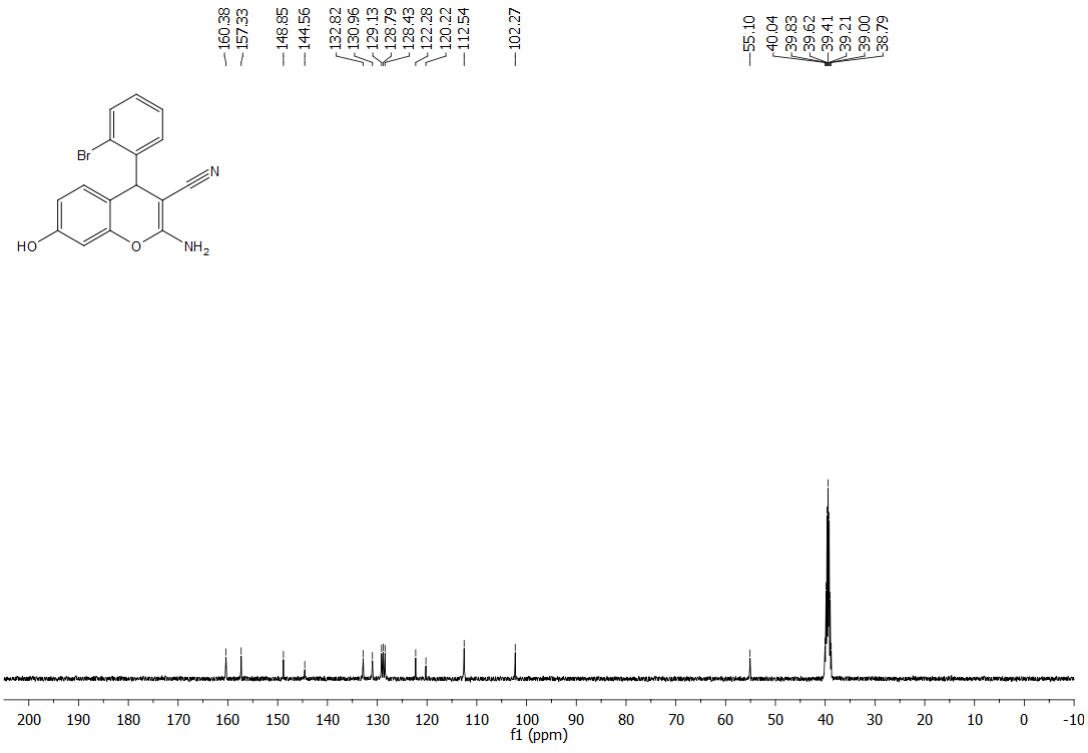

Figure 30: ^{13}C NMR spectrum for (**4i**) in DMSO-d_6 (100MHz, 300K).

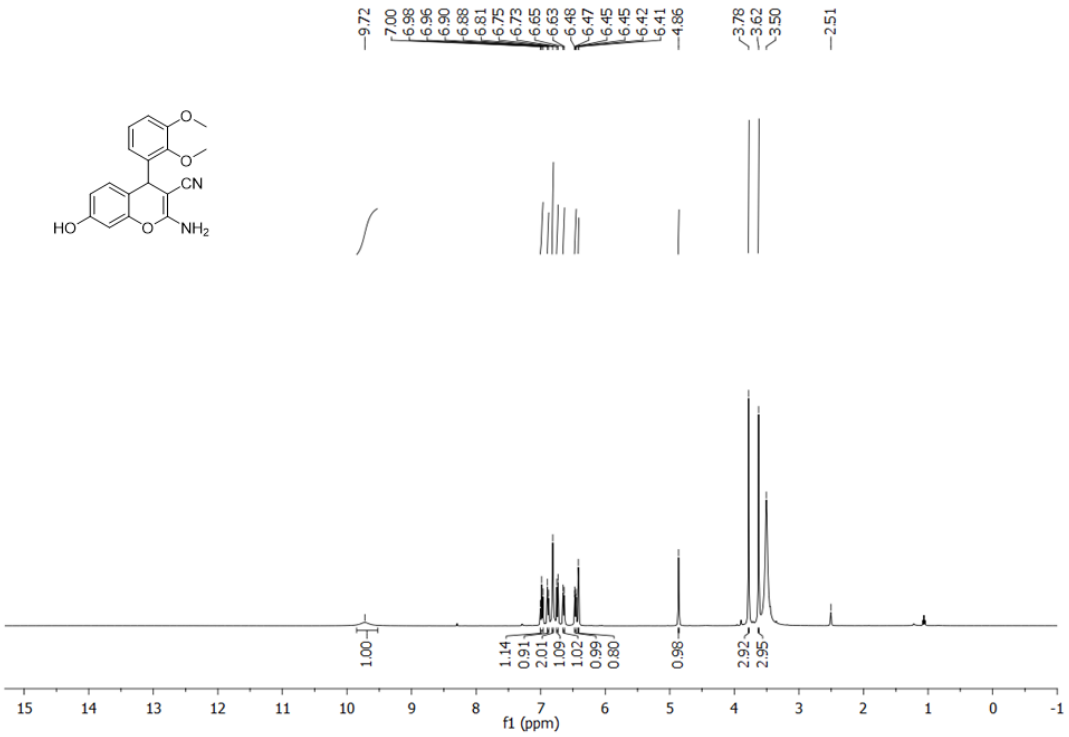

Figure 31: ^{1}H NMR spectrum for (**4j**) in DMSO-d_6 (400MHz, 300K).

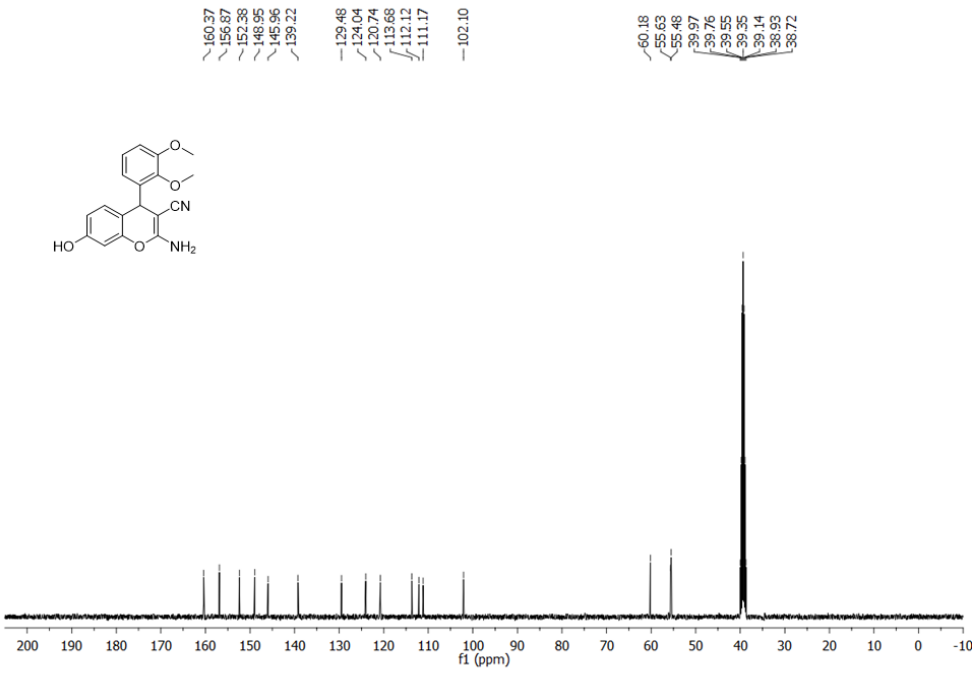

Figure 32: ^{13}C NMR spectrum for (**4j**) in DMSO-d_6 (100MHz, 300K).

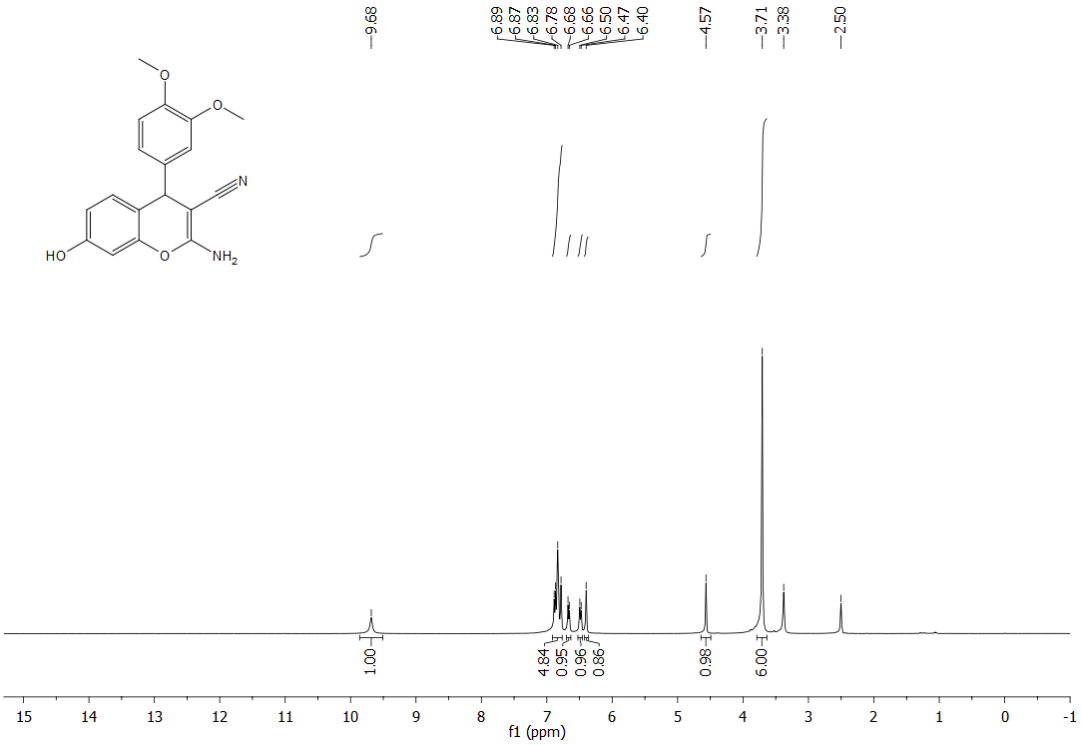

Figure 33: ^{1}H NMR spectrum for (**4k**) in DMSO-d_6 (400MHz, 300K).

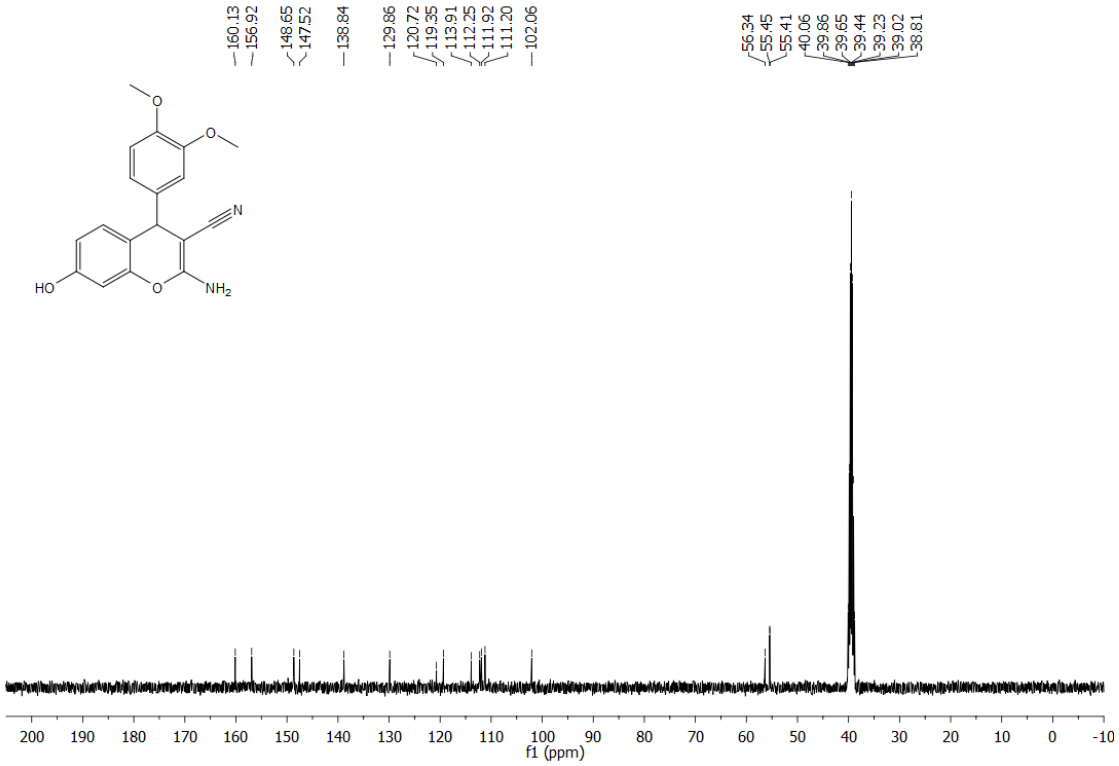

Figure 34: ^{13}C NMR spectrum for (**4k**) in DMSO-d_6 (100MHz, 300K).

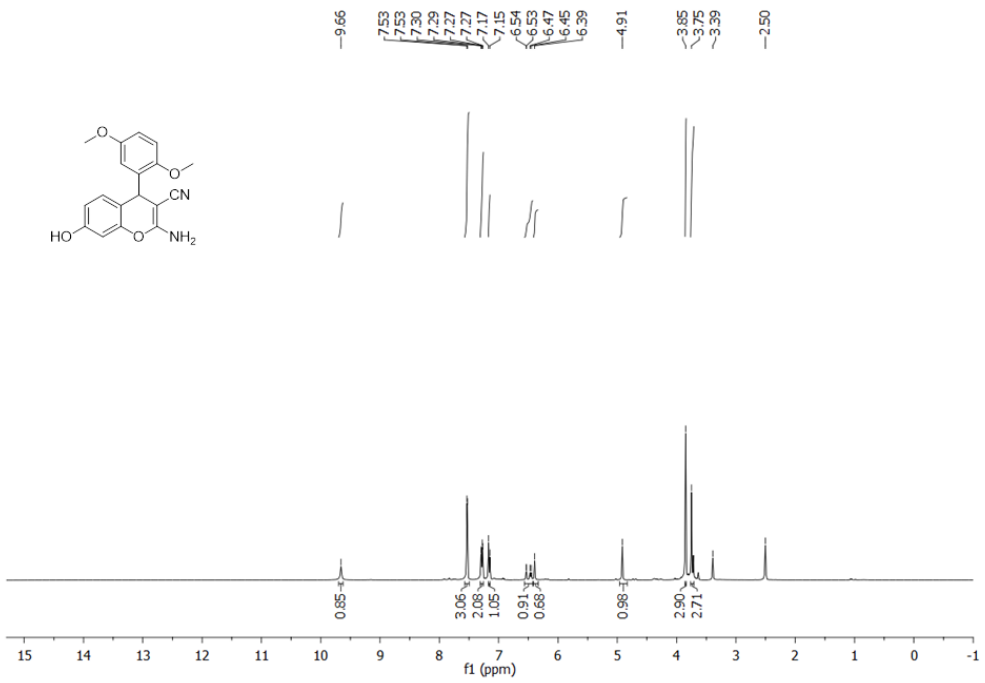

Figure 35: ^{1}H NMR spectrum for (**4l**) in DMSO-d_6 (400MHz, 300K).

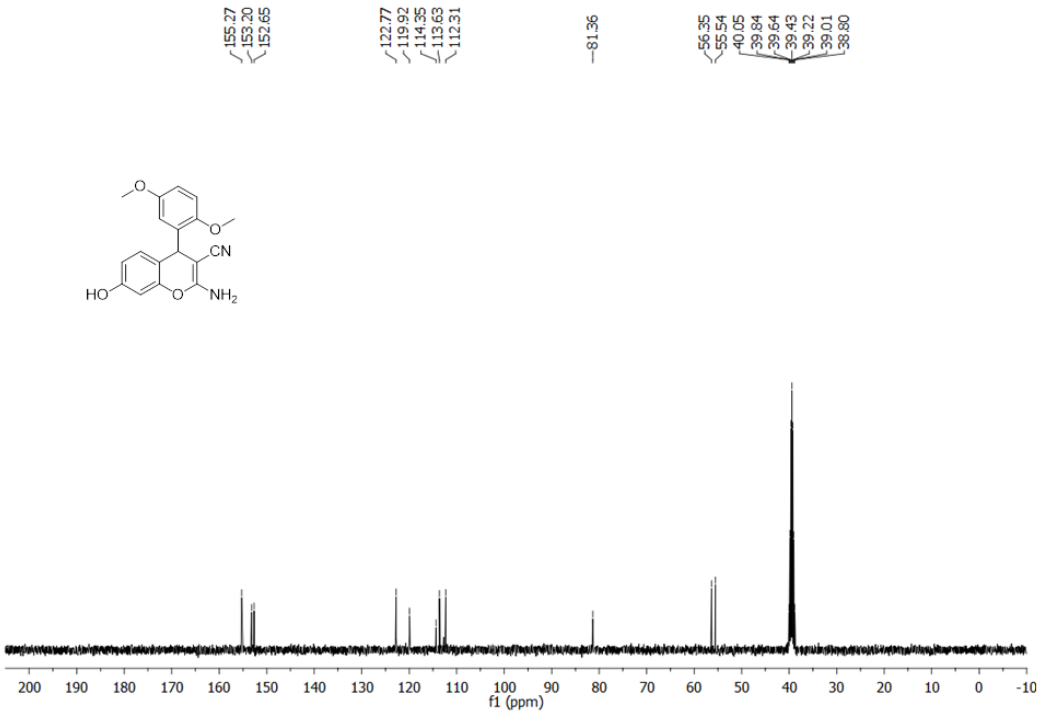

Figure 36: ^{13}C NMR spectrum for (**4l**) in DMSO-d_6 (100MHz, 300K).

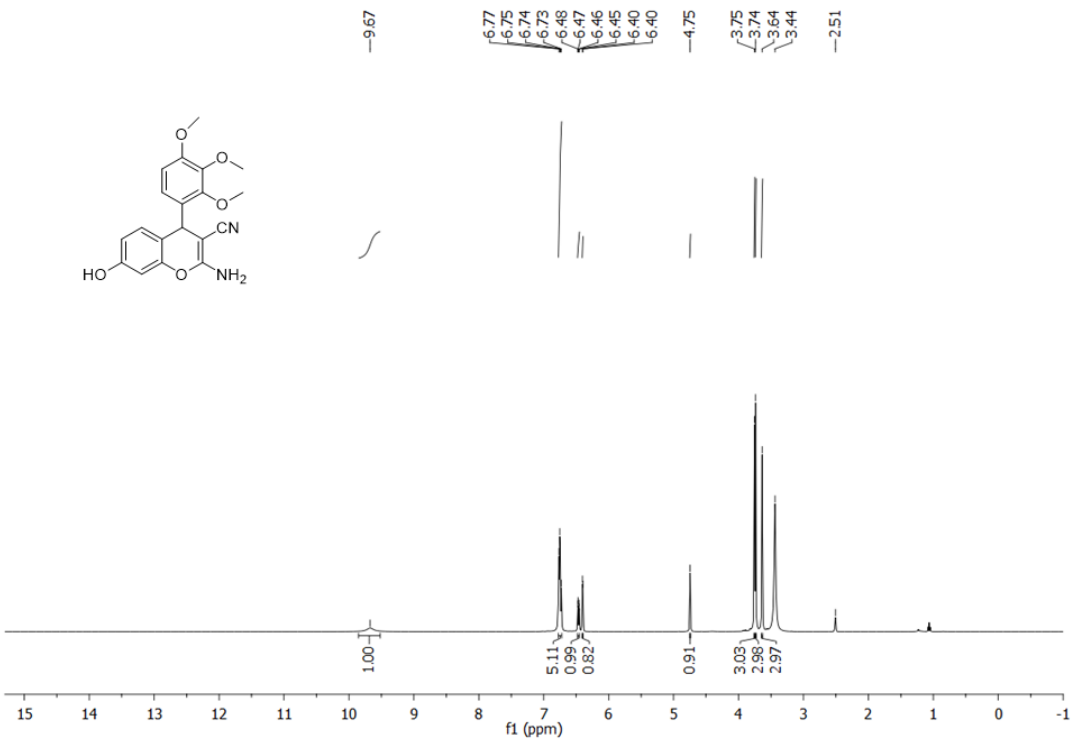

Figure 37: ^{1}H NMR spectrum for (**4m**) in DMSO-d_6 (400MHz, 300K).

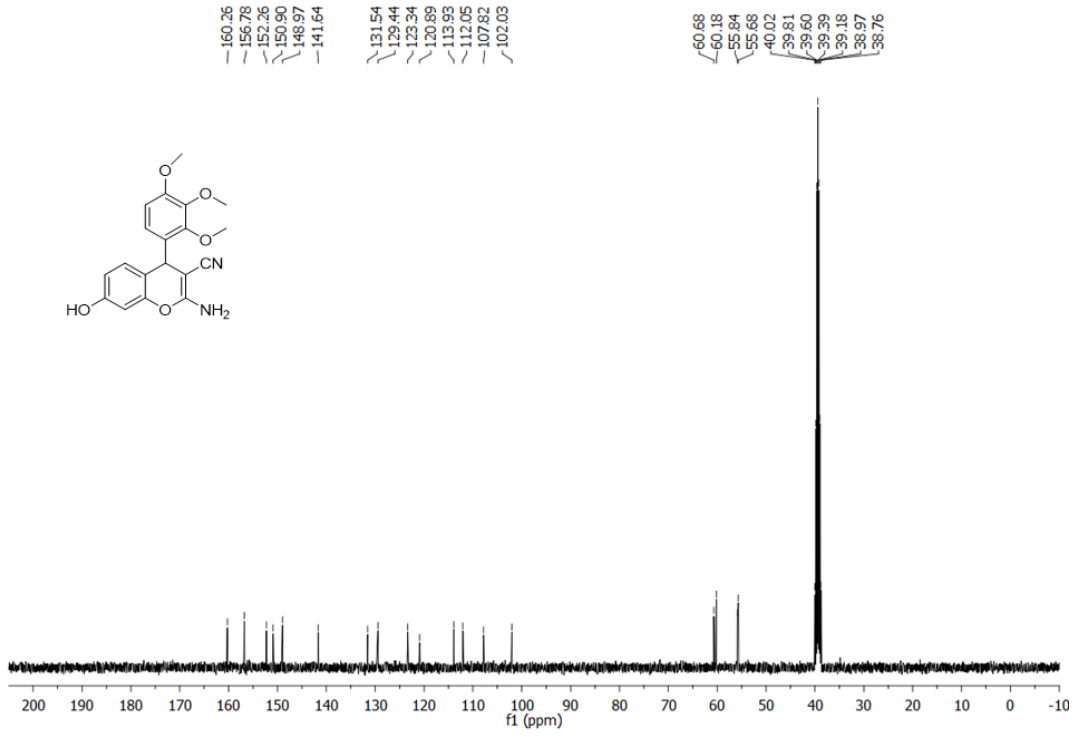

Figure 38: ^{13}C NMR spectrum for (**4m**) in DMSO-d_6 (100MHz, 300K).

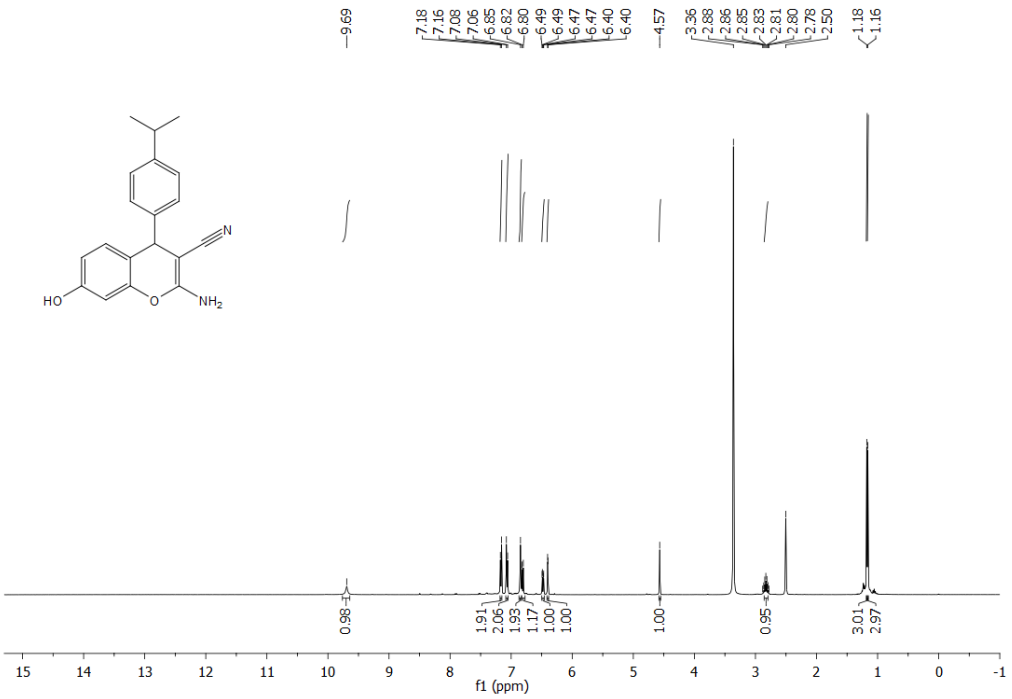

Figure 39: ^{1}H NMR spectrum for (**4n**) in DMSO-d_6 (400MHz, 300K).

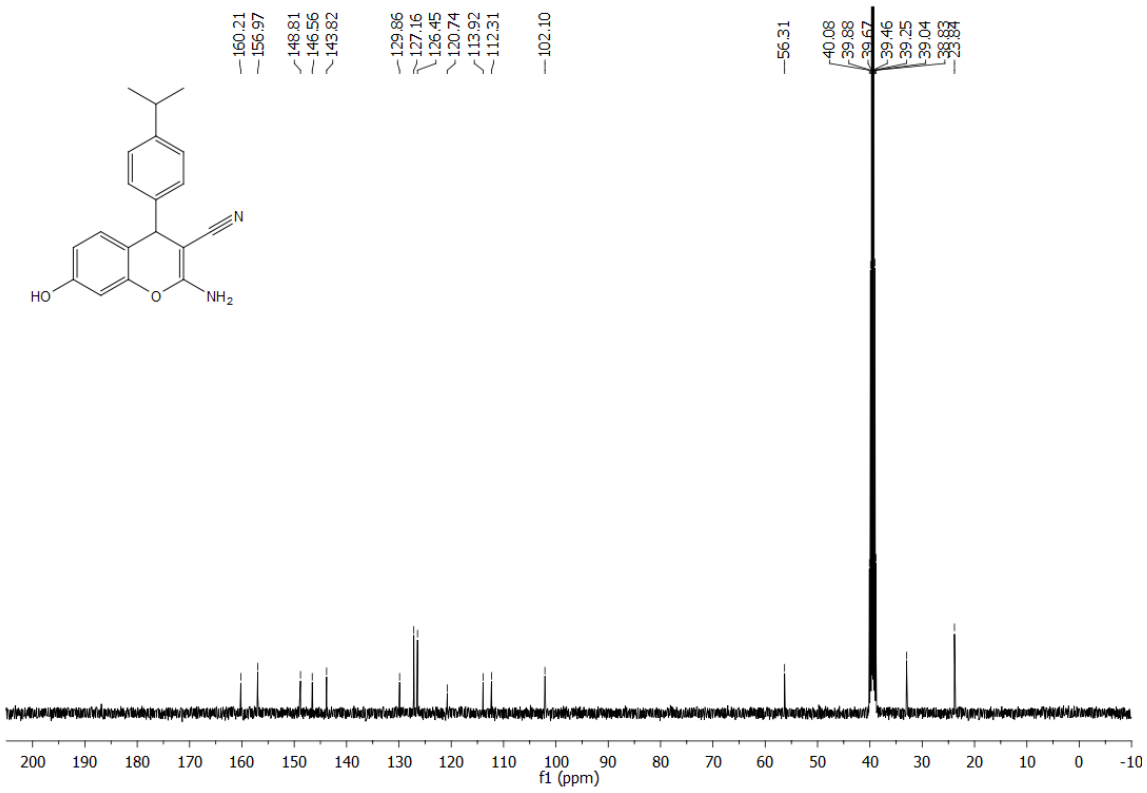

Figure 40: ^{13}C NMR spectrum for (**4n**) in DMSO-d_6 (100MHz, 300K).

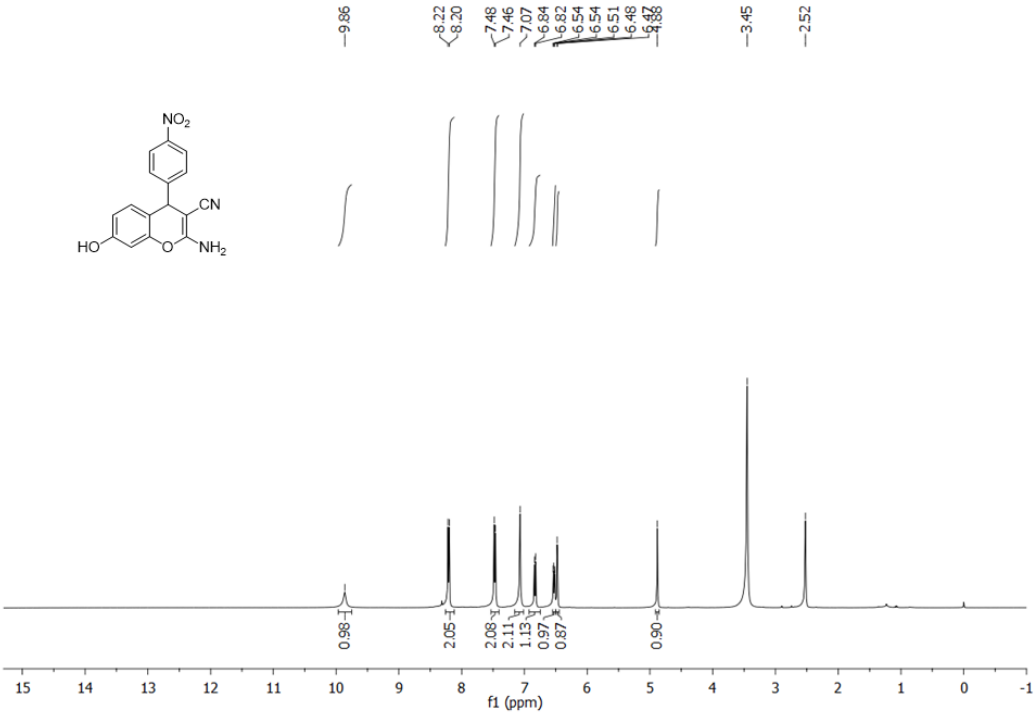

Figure 41: ^{1}H NMR spectrum for (**4o**) in DMSO-d_6 (400MHz, 300K).

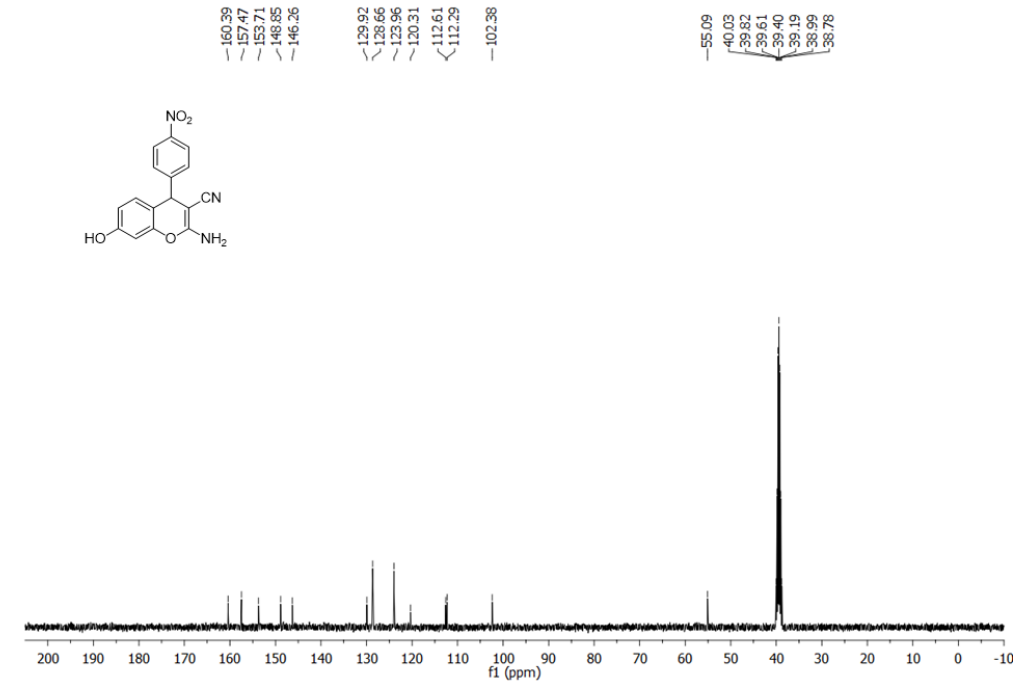

Figure 42: ^{13}C NMR spectrum for (**4o**) in DMSO-d_6 (100MHz, 300K).

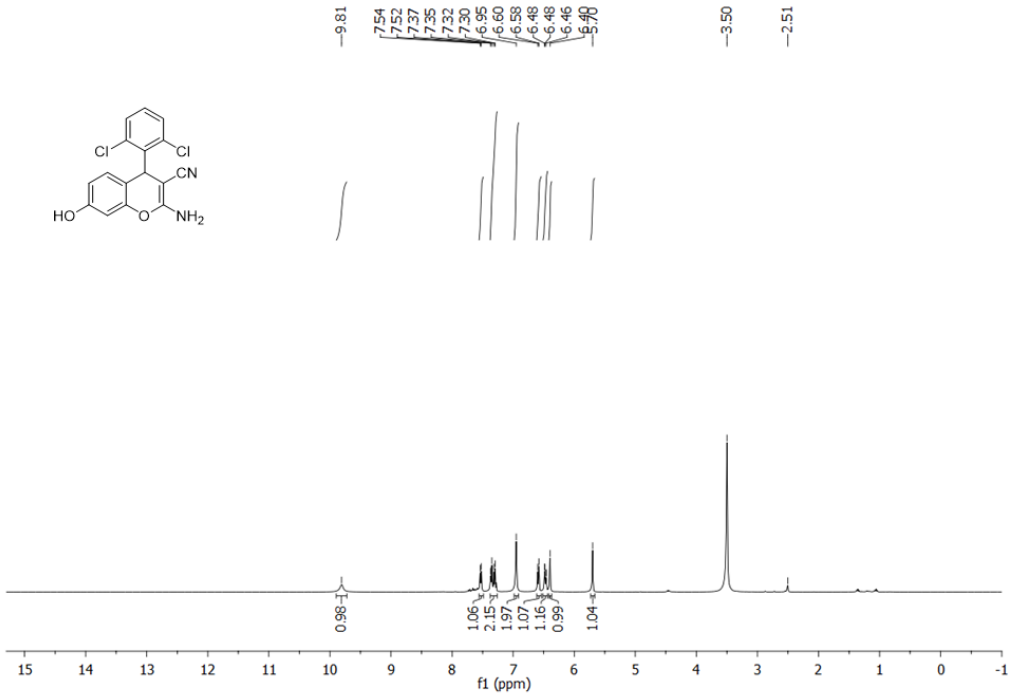

Figure 43: ^{1}H NMR spectrum for (**4p**) in DMSO-d_6 (400MHz, 300K).

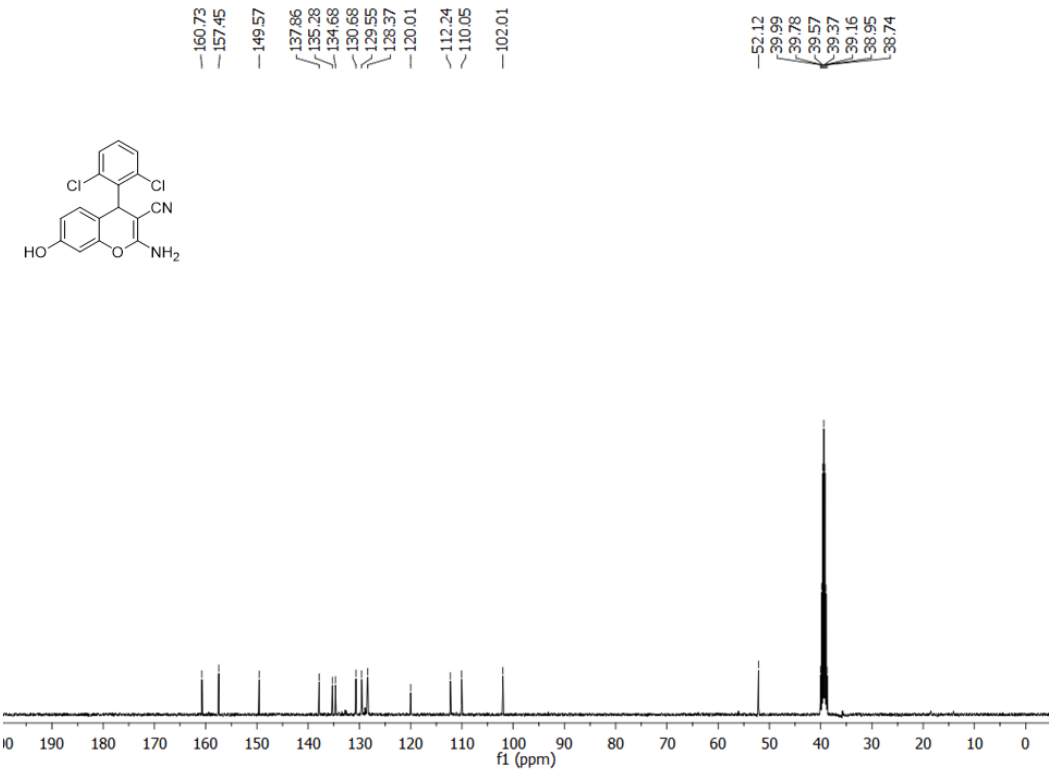

Figure 44: ^{13}C NMR spectrum for (**4p**) in DMSO-d_6 (100MHz, 300K).

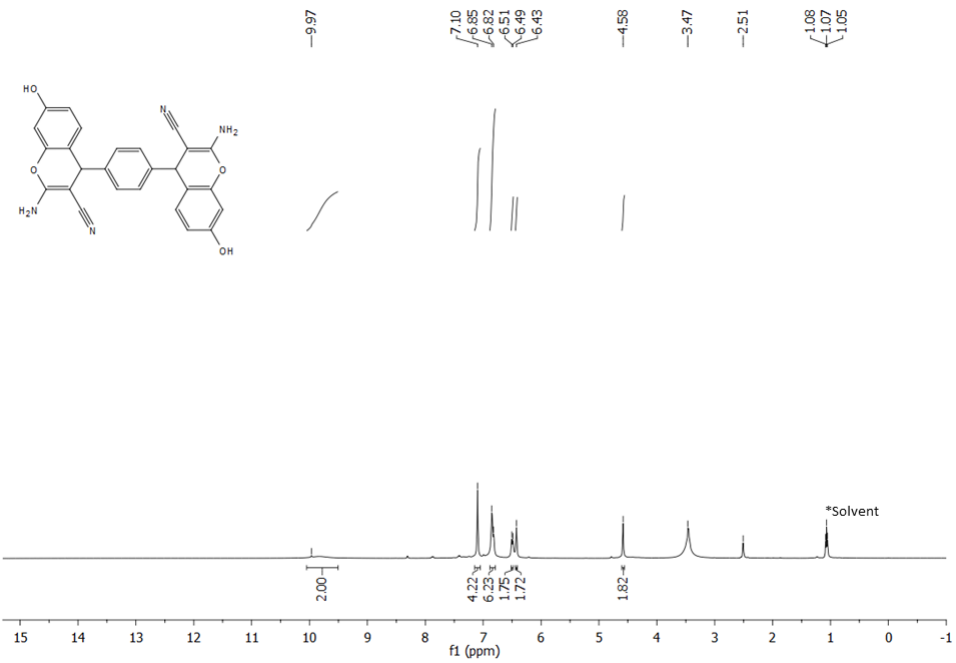

Figure 45: ^{1}H NMR spectrum for (**4q**) in DMSO-d_6 (400MHz, 300K).

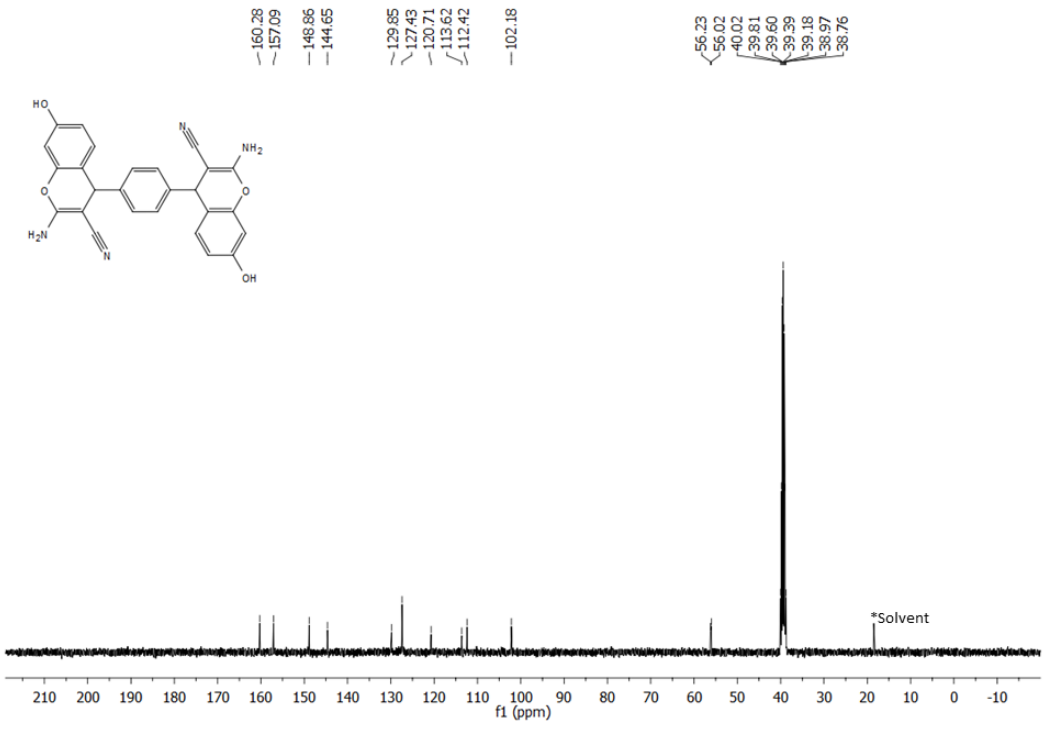

Figure 46: ^{13}C NMR spectrum for (**4q**) in DMSO-d_6 (100MHz, 300K).

NMR spectra for tacrine analogue (5)

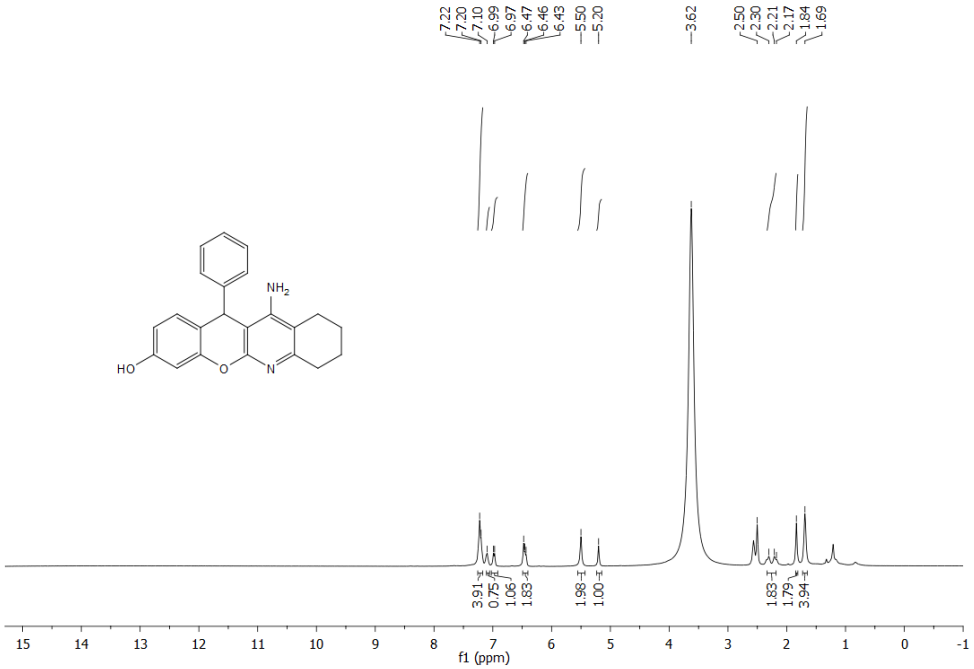

Figure 47: ^{1}H NMR spectrum for (**5**) in DMSO-d_6 (400MHz, 300K).

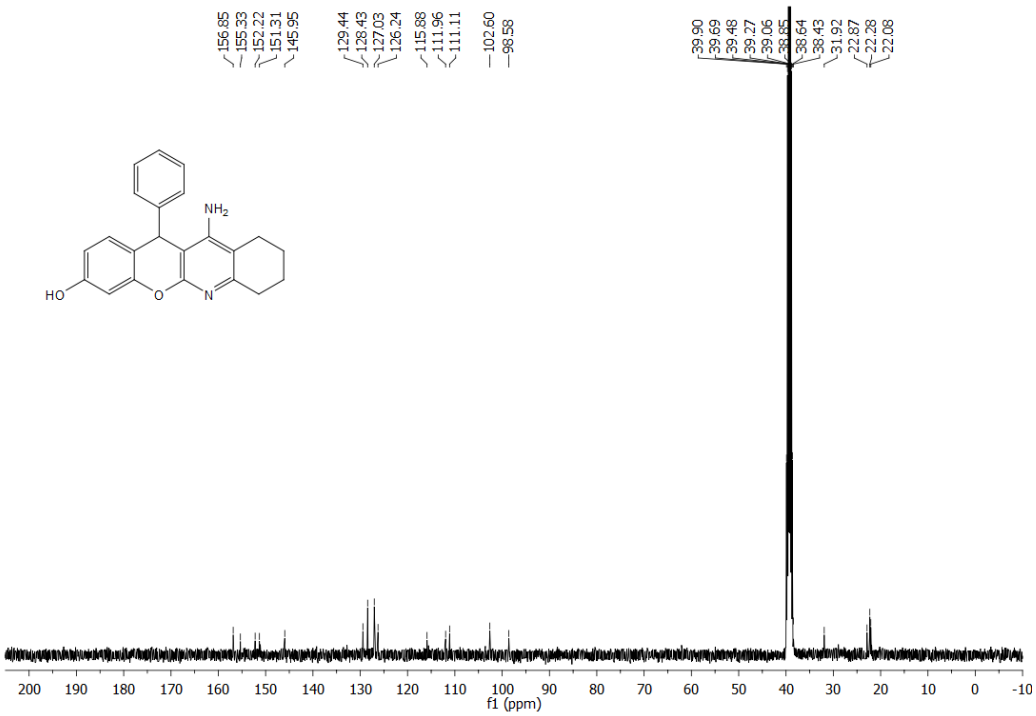

Figure 48: ^{13}C NMR spectrum for (**5**) in DMSO-d_6 (100MHz, 300K).

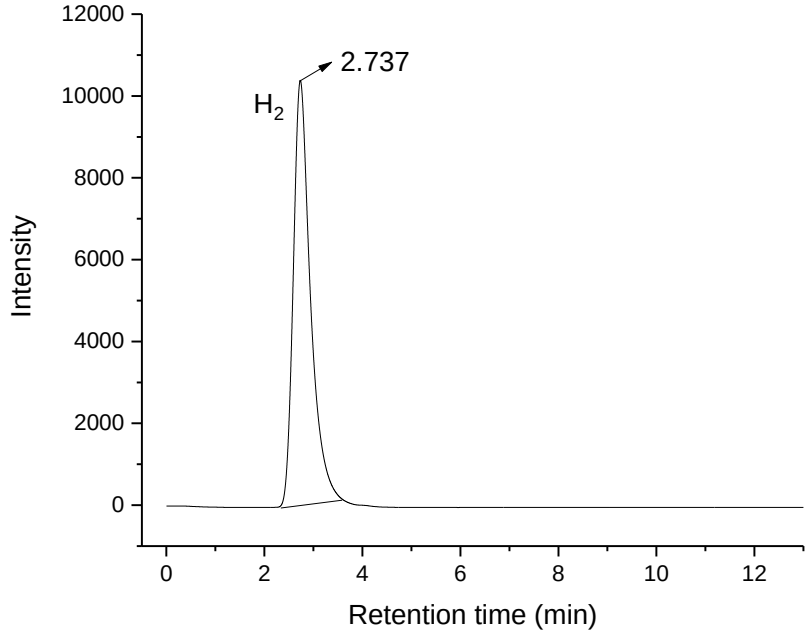

Figure 49: Chromatogram of H_2

4.4. REFERENCES

1. (a) J. D. Hepworth, In Comprehensive Heterocyclic Chemistry; Katritzky, A. R., Rees, C. W., Boulton, A. J., McKillop, A., Eds.; Pergamon Press: Oxford, U.K., 1984, **3**, 737-883; (b) G. Zeni, and R. Larock, C. *Chem. Rev.* 2004, **104**, 2285-2309; (c) M. A. Brimble, J. S. Gibson, Sperry, J. Pyrans and their Benzo Derivatives: Synthesis. In Comprehensive Heterocyclic Chemistry III; Katritzky, A. R., Ramsden, C. A., Scriven, E. F. V., Taylor, R. J. K., Eds.; Elsevier Ltd.: Oxford, 2008; Vol. **7**, pp 419-699; (d) Handbook of Heterocyclic Chemistry, 3rd ed.; Katritzky, A. R., Ramsden, C. A., Joule, J. A. and Zhdankin, V. V., Eds.; Elsevier: Oxford, 2010; pp 815.

2. (a) N. Majumdar, N.D. Paul, S. Mandal, B. de Bruin and W. D. Wulff, *ACS Catal*. 2015, **5**, 2329-2366; (b) G. P. Ellis and Lockhart, I. M. In The Chemistry of Heterocyclic Compounds: Chromenes, Chromanones, and Chromones; Ellis, G. P., Ed.; Wiley-VCH: Weinheim, Germany, 2007, **31**, 11196.

3. (a) S. J. Mohr, M. A. Chirigos, F. S. Fuhrman and J. W. Pryor, *Cancer Res.*, 1975, **35**, 3750-3754; (b) A. G. Martinez and L. J. Marco, *Bioorg. Med. Chem. Lett.*, 1997, **7**, 3165-3170; (c) K. Hiramoto, A. Nasuhara, K. Michiloshi, T. Kato and K. Kikugawa, *Mutat. Res.*, 1997, **395**, 47-56; (d) W. P. Smith, L. S. Sollis, D. P. Howes, C. P. Cherry, D. I. Starkey and N. K. Cobley, *J. Med. Chem.*, 1998, **41**, 787-797; (e) M. M. Khafagy, A. H. F. A. El-Wahas, F. A Eid and A. M. El-Agrody, *Farmaco*, 2002, **57**, 715-722; (f) M. Kidwai, S. Saxena, M. K. R. Khan and S. S. Thukral, *Bioorg. Med. Chem. Lett.*, 2005, **15**, 4295-4298.

4. (a) S. Yadav, M. Srivastava, P. Rai, J. Singh, K.P. Tiwari and J. Singh, *New. J. Chem.*, 2015, **39**, 4556-4561; (b) A. Khalafi-Nezhad, M. Nourisefat and F. Panahi, *Org. Biomol. Chem.*, 2015, **13**, 7772-7779; (c) M. Esmaeilpour, J. Javidi, F. Dehghani and F.N. Dodeji, *RSC Adv.*, 2015, **5**, 26625-26633; (d) P. Sagar Vijay Kumar, L. Suresh, T. Vinodkumar, B.M. Reddy and G. V. P. Chandramouli, *ACS Sustainable Chem. Eng.* 2016, **4**, 2376-2386; (e) J. Safari, M. Heydarian and Z. Zarnegar, *Arab. J. Chem.*, 2017, **10**, S2994-S3000; (f) M. A. Wanzheng, A. G. Ebadi, R. Javahershenas and G. Jimenez, *RSC Adv.*, 2019, **9**, 12801-12812; (g) P. Singh, P. Yadav, A. Mishra and S. K. Awasthi, *ACS Omega.*, 2020, **5**, 4223-4232; (h) H. Naeimi and S. Mohammadi, *ChemistrySelect.*, 2020, **5**, 2627-2633; (i) F. Matloubi Moghaddam, M. Eslami and G. Hoda, *Sci. Rep.*, 2020, **10**, 1-14; (j) S. Saneinezhad, L. Mohammadi, V. Zadsirjan, F. F. Bamoharram and M. M. Heravi, *Sci. Rep.*, 2020, **10**, 1-26; (k) F. Auria-Luna, V. Fernández-Moreira, E. Marqués-López, M. C. Gimeno and R. P. Herrera, *Sci. Rep.*, 2020, **10**, 1-17.

5. G. Zhang, Y. Zhang, J. Yan, R. Chen, S. Wang, Y. Ma and R. Wang, *J. Org. Chem.*, 2012, **77,** 878-888.

6. M.G. Dekamin and M. Eslami, *Green Chem.*, 2014, **16**, 4914-4921.

7. M.M. Heravi, B. Baghernejad and H.A. Oskooie, A *J. Chin. Chem. Soc.*, 2008, **55**, 659-662.

8. M.N. Khan, S. Pal, S. Karamthulla and L.H. Choudhury, *RSC Adv.*, 2014, **4**, 3732-3741.

9. (a) M. Alvarez-Corral, M. Munoz-Dorado and I. Rodriguez-Garcia, *Chem. Rev.* 2008, **108**, 3174-3198. (b) J.M. Weibel, A. Blanc and P. Pale, *Chem. Rev.* 2008, **108**, 3149-3173.

10. T. Naota, H. Takaya and S.I. Murahashi, *Chem. Rev.*, 1998, **98**, 2599-2660.

11. (a) T. Punniyamurthy, S. Velusamy and J. Iqbal, *Chem. Rev.*, 2005, **105**, 2329-2364. (b) C. Gunanathan and D. Milstein, *Science*, 2013, **341**, 1229712.

12. (a) M. Zhang, H. Neumann and M. Beller, *Angew. Chem., Int. Ed.* 2013, **52**, 597-601; (b) M. Zhang, X. Fang, H. Neumann and M. Beller, *J. Am. Chem. Soc.* 2013, **135**, 11384-11388; (c) N. Deibl, and R. Kempe, *Angew. Chem., Int. Ed.* 2017, **56**, 1663-1666; (d) N. Biswas and D. Srimani, *J. Org. Chem.* 2021, **86**, 9733-9743.

13. V. V. Matveevskaya, D. I. Pavlov, T. S. Sukhikh, A.L. Gushchin, A. Y. Ivanov, T. B. Tennikova, V. V. Sharoyko, S. V. Baykov, E. Benassi and A. S. Potapov, *ACS omega.*, 2020, **5**, 11167-11179.

14. Vogel, A. I.; Test book of practical organic chemistry, Longman, London, 5th edn, 1989, p.395.

15. M. A. Bennett and A. K. Smith, *J. Chem. Soc., Dalton Trans.*, 1974, 233

16. T. S. Kamatchi, M. K. M. Subarkhan, R. Ramesh, H. Wang and J.G. Małecki, *Dalton Trans*, 2020, **49**, 11385-11395.

17. Farrugia, L. ORTEP-3 for Windows - a version of ORTEP - III with a Graphical User Interface (GUI), *J. Appl. Crystallogr.*,1997, **30**, 565-566.

18. G. M. Sheldrick, *Acta Crystallogr., Sect. A: Found. Crystallogr*. 2008, **64**, 112.

19. Bruker-Nonius (2004), APEX-II and SAINT-Plus (Version 7.06a), Bruker AXS Inc., Madison, Wisconsin, USA.

20. T.S. Manikandan, R. Ramesh, N. Shivalingegowda and L. N. Krishnappagowda, *ChemistrySelect*, 2018, **3**, 1561-1568.

21. L.U. Nordstrøm, H. Vogt and R. Madsen, *J. Am. Chem. Soc.* 2008, **130**,17672-17673.

22. (a) S. Hamulakova, L. Janovec, M. Hrabinova, K. Spilovska, J. Korabecny, P. Kristian, K. Kuca and J. Imrich, *J. Med. Chem.* 2014, **57**, 7073-7084; (b) M. Digiacomo, Z. Chen, S. Wang, A. Lapucci, M. Macchia, X. Yang, J. Chu, Y. Han, R. Pi and S. Rapposelli, *Bioorg. Med. Chem. Lett.* 2015, **25**, 807-810; (c) G. Wu, Y. Gao, D. Kang, B. Huang, Z. Huo, H. Liu, V. Poongavanam, P. Zhan and X. Liu, Design, *MedChemComm*, 2018, **9**, 149-159.

23. E. Maalej, F. Chabchoub, M.J. Oset-Gasque, M. Esquivias-Pérez, M.P. González, L. Monjas, C. Pérez, C. de los Ríos, M.I.I. Rodríguez-Franco, I. riepa and I. Moraleda, *Eur. J. Med. Chem.*, 2012, **54**,750-763.

24. (a) W. Chen, Y. Cai, X. Fu, X. Liu L. Lin, and X. Feng, *Org. Lett.*, 2011, **13**, 4910-4913; (b) A. H. F. Abd El-Wahab, H. M. Mohamed, A.M. El-Agrody and A. H. Bedair, *Chem. Eur. J.* 2013, **4**, 467-483; (b) N. Thomas, S. M. Zachariah and P. Ramani, *J. Heterocycl. Chem.* 2016, **53**, 1778-178; (c) A. Aminkhani, M. Talati, R. Sharifi, F. Chalabian and F. Katouzian, *J. Heterocycl. Chem.*, 2019, **5**, 1812-1819.

25. S.I. Murahashi, T. Naota, H. Taki, M. Mizuno, H. Takaya, S. Komiya, Y. Mizuho, N. Oyasato and M. Hiraoka, *J. Am. Chem. Soc*, 1995, **117**, 12436-12451.

26. A. Maggi and R. Madsen, *Organometallics*, 2012, **31**, 451-455.

27. G. Balamurugan, and R. Ramesh, *ChemCatChem*, 2022, **14**, e202101455.

28. S. Kumará Panja, *RSC. Adv.*, 2015, **5**, 65526-65531.

29. S.K. Kundu, J. Mondal and A. Bhaumik, *Dalton. Trans.*, 2013, **42**,10515-10524.

30. M. Kamalzare, M. Bayat and A. Maleki, *R. Soc. Open. Sci.*, 2020, **7,** 200385.

31. S.R. Kale, S.S. Kahandal, A.S. Burange, M.B. Gawande and R.V. Jayaram, *Catal. Sci. Tech.*, 2013, **3**, 2050-2056.

32. J. Safari, Z. Zarnegar and M. Heydarian, *Bull. Chem. Soc. Japan,* 2012, **85**, 1332-1338.

33. A.M. El-Maghraby, *Org. Chem. Int.*, 2014, 715091.

34. I.N. Bardasov, A.U. Alekseeva, O.V. Ershov and D.A. Grishanov, *Heterocycl. Comm.* 2015, **21**, 175-177.

35. J. Safari, M. Heydarian and Z. Zarnegar, *Arab. J. Chem.* 2017, **10**, S2994-S3000.

36. S. Damavandi, *Arab. J. Chem.* 2016, **9**, S941-S945.

Chapter 5

Binuclear Arene Ru(II) Mediated C-N Bond Formation for One-Pot Synthesis of Pyrazoles from Benzohydrazides and Alcohols *via* Acceptorless Dehydrogenative Pathway

Abstract

We present a new route to synthesis of pyrazoles through one-pot reaction facilitated by binuclear *p*-cymene Ru(II) complexes encapsulated N^O hydrazine ligands. A set of new binuclear *p*-cymene Ru(II) complexes were synthesized and characterized by analytical and spectroscopic techniques. The molecular structure of one of the complexes was confirmed by a single crystal X-ray diffraction study. The synthesized complexes were employed as effective catalysts for the synthesis of pyrazole derivatives using alcohols, malononitrile and benzohydrazides through acceptorless dehydrogenative pathway. The current catalytic approach provides a variety of pyrazole derivatives in high yields up to 95% without any oxidant/additives using low catalyst loading under mild reaction conditions.

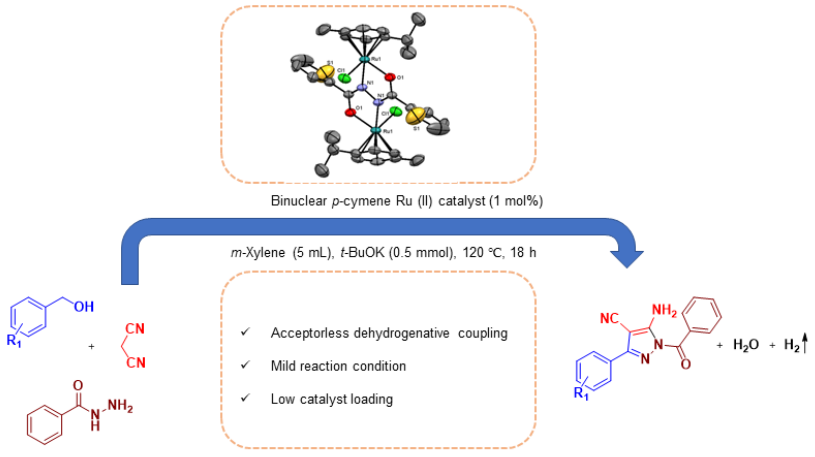

5.1. INTRODUCTION

N-heterocycles are ubiquitous nature and important key motifs in various synthetic and natural organic compounds.[1] Among them, pyrazole and its derivatives forms an imperative framework in pharmacological (Figure 1) and agrochemical sciences.[2] For example, a several pyrazole-containing compounds have been successfully achieved into commercial available drugs[3] and employed as ligands for transition-metal-catalyzed cross-coupling reactions,[4] precursors to N-heterocyclic carbenes (NHCs)[5] and directing groups for C-H activations.[6] Due to the functional flexibility of the pyrazole skeleton, their synthesis has been extensively explored.[7]

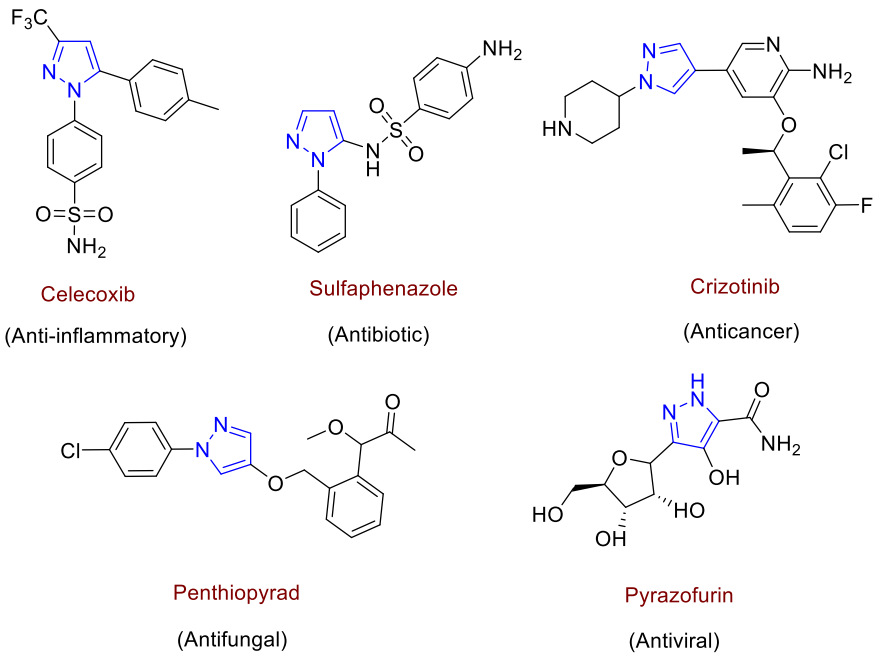

Figure 1. Selective examples for bioactive pyrazole analogues

The traditional procedures for the construction of pyrazoles derivatives include the condensation of monosubstituted hydrazine with carbonyl compounds and cyclocondensation between dicarbonyl or *α,β*-unsaturated carbonyl compounds and hydrazines.[8] Besides the above two strategies, another straightforward approach to synthesize the pyrazole analogues is oxidative cyclization reaction of hydrazones catalyzed

by iodine or DDQ could provide derivatives of pyrazoles.[9] However, these methods have some drawbacks such as higher reaction temperature, use of microwave, additives/oxidants and limited substrate scope. Therefore, the synthetic community remains interested in current synthetic procedures for substituted pyrazoles with good selectivity using benign and economic conditions.

Transition metal mediated synthesis of N-heterocycles have received considerable interest due to easy workup process of intermediates, and a series of condensation, addition or cycloaddition reactions can be performed in one pot.[10] Among them, ruthenium-mediated syntheses of heterocycles has been particular attention due to their atom economy, ready availability and higher catalytic efficiency.[11]

The previous reports are available on transition-metal-catalyzed synthesis of pyrazole from hydrazones.[12] However, these methods have certain limitations such as limited substrate scope and inferior yields due to the low stability of the intermediates. Thus, the development of more convenient and efficient method for fabrication of pyrazoles still highly desirable.

Further, the construction of heterocycles from alcohols using acceptorless dehydrogenative coupling (ADC) strategy has received extensive attention due to the needless of any oxidants, additives and avoid the production of toxic by-products like permanganate, dichromate, and peroxides.[13] Furthermore, the synthesis of N-heterocycles using acceptorless dehydrogenative coupling promoted by transition metal catalysts has also received attention recently. Particularly, ruthenium mediated N-heterocycles synthesis *via* ADC strategy is enticing approach due to the efficiency of ruthenium metal. Hence, Ru(II) catalyzed ADC reaction for the production of N-heterocycles has been well-explored.[14]

Recently, *p*-cymene moiety supported ruthenium(II) catalysts have been widely employed as catalysts in various organic transformation reactions including C-C and C-N bond formations.[15] However, the bimetallic catalytic system has cooperative effect between the two metal centres which increases the strong metal-metal interaction that interacts with the substrates, increasing the rate of the reaction over the monometallic system.

The earlier reports[16] for synthesis of pyrazole derivatives from aldehydes/alcohols react with malononitrile and phenylhydrazine. Herein, we have attempted to synthesis of pyrazole derivatives from alcohols with malononitrile and benzohydrazides catalyzed by newly synthesized binuclear *p*-cymene Ru(II) complexes *via* ADC pathway (Scheme 1).The catalytic protocol is considered an atom economical and eco-friendly which releases water and hydrogen are the only by-products.

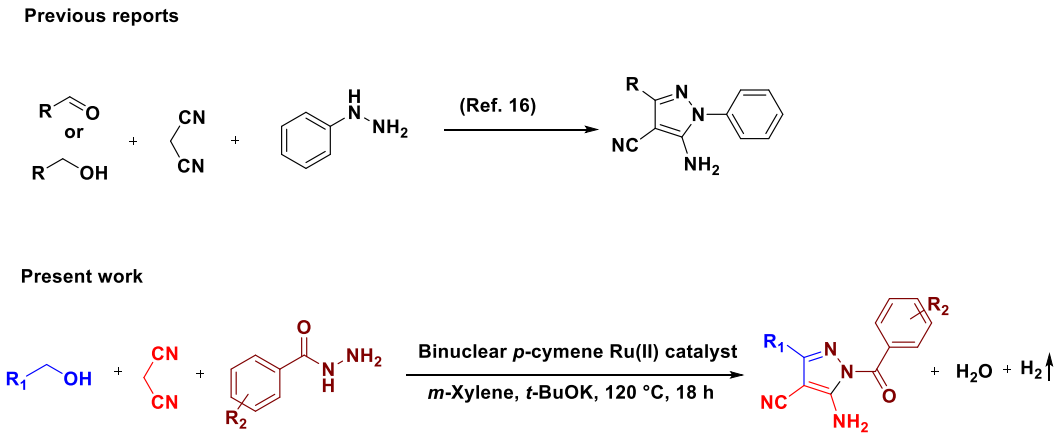

Scheme 1. Synthetic strategies for pyrazole derivatives.

5.2. Experimental Section

5.2.1. Reagents and materials

All the reagents used were chemically pure and analytical grade. Thiophene-2-carbonyl chloride and different benzhydrazides were purchased from Sigma Aldrich chemicals. The solvents were freshly distilled before use following the standard procedures.[17]

5.2.2. Physical measurements and instrumentation

Commercially available $RuCl_3.3H_2O$ was used as supplied from Loba Chemie Pvt. Ltd. The ruthenium(II) precursor complex, $[(\eta^6\text{-}p\text{-cymene})RuCl_2]_2$ was prepared by reported literature method.[18] The microanalysis of carbon, hydrogen and nitrogen were recorded by an analytical function testing Vario EL III CHNS elemental analyzer at the Sophisticated Test and Instrumentation Centre (STIC), Cochin University, Cochin. The Fourier Transform infrared spectra of complexes were recorded in KBr pellets with a Perkin-Elmer 597 spectrophotometers in the range 4000-400 cm^{-1}. The NMR spectra were recorded in $CDCl_3$ and DMSO-d_6 with a Bruker 400 MHz instrument using TMS as the internal reference. Chemical shifts are given in ppm referenced to solvents.

5.2.3. Preparation of thiophene based hydrazine ligands

N-benzoylthiophene-2-carbohydrazide ligands (HL) ligands were synthesized from the literature procedure.[19] To a stirred solution of the thiophene-2-carbonyl chloride (1 mmol) in dry tetrahydrofuran (5 mL) at 0 °C was added a hydrazide (1 mmol) and anhydrous sodium carbonate (1 mmol) in dry tetrahydrofuran (10 mL) and water (10 mL). The mixture was stirred at 0 °C for 1 h, and room temperature for 4 h. Diethyl ether was then added and a precipitation was observed. The residue was collected by filtration, washed with cold diethyl ether and dried in vacuum (Scheme 2) (Yield: 80-85%).

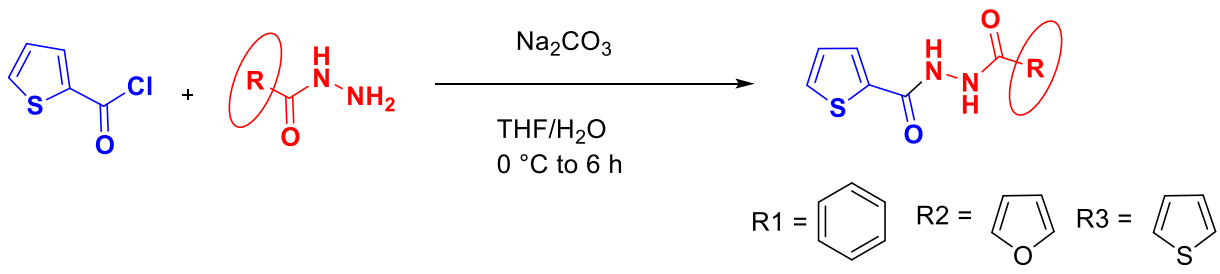

Scheme 2. Preparation of thiophene based hydrazine ligands

5.2.4. Synthesis of new binuclear arene Ru(II) complexes

To a benzene solution of N-benzoylthiophene-2-carbohydrazide ligands (1 mmol) and [(η^6-*p*-cymene)$_2$Ru$_2$Cl$_2$(μ-Cl)$_2$] (1 mmol) in the presence of triethylamine base this reaction mixture was stirred for 5 h. The formation of complexes were monitored by TLC. At the end of the reaction, the solution was concentrated to 3 mL and addition of petroleum ether (60-80 ^{o}C) resulted in the formation of yellow solid (Scheme 3).

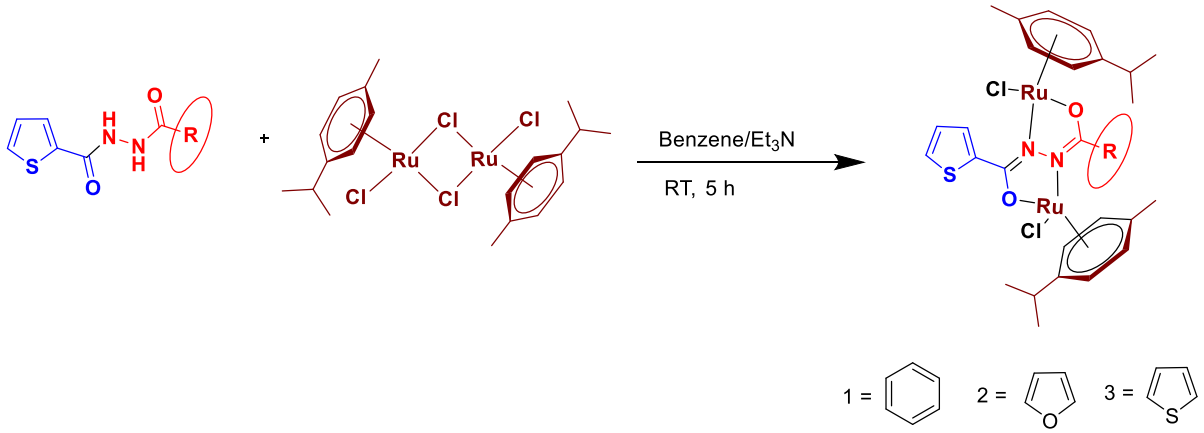

Scheme 3. Synthetic route to *p*-cymene binuclear Ru(II) complexes.

Spectral characterization data of complexes (1-3)

Complex 1. Yellow solid, Yield: 85%, m.p.: 228 °C (with decomposition). Anal. calcd: $C_{32}H_{36}Cl_2N_2O_2Ru_2S$: C, 48.92; H, 4.62; N, 3.57%. found: C, 48.72, H, 4.58, N, 3.45%. FT-IR (KBr, cm^{-1}): 3275 $\nu_{(N-H)}$, 1668 $\nu_{(C=N)}$, 1578 $\nu_{(C=O)}$, 1250 $\nu_{(C-O)}$, 1520 ν(C=N-N=C). ^{1}H NMR (400 MHz, $CDCl_3$): δ (ppm) = 8.02 (*dd*, J = 3.6 Hz, 1.2Hz, 2H, $ArH_{(ligand)}$), 7.48-7.44 (*m*, 4H, $ArH_{(ligand)}$), 7.27 (*s*, 1H, $ArH_{(ligand)}$), 7.07 (*dd*, J = 4.8 Hz, 3.6 Hz, 1H, $ArH_{(ligand)}$), 5.14 (*t*, J = 6 Hz, 2H, $CH_{(p\text{-cymene})}$), 5.06 (*d*, J = 8 Hz, 1H, $CH_{(p\text{-cymene})}$), 5.03 (*d*, J = 4 Hz, 1H, $CH_{(p\text{-cymene})}$), 4.74 (*d*, J = 4 Hz, 1H, $CH_{(p\text{-cymene})}$), 4.49 (*d*, J = 4 Hz, 1H, $CH_{(p\text{-cymene})}$), 4.14 (*d*, J = 4 Hz, 1H, $CH_{(p\text{-cymene})}$), 3.71 (*d*, J = 4 Hz, 1H, $CH_{(p\text{-cymene})}$), 2.68-2.62 (*sept*,1H, $CH(CH_3)_{2(p\text{-cymene})}$), 2.55-2.48 (*sept*,1H, $CH(CH_3)_{2(p\text{-cymene})}$), 2.19 (*s*, 3H, $CH_{3(p\text{-cymene})}$), 2.13

(*s*, 3H, $CH_{3(p\text{-cymene})}$),1.14-1.05 (*m*, 12H, $CH(CH_3)_{2(p\text{-cymene})}$). ^{13}C {^1H} NMR (100MHz, $CDCl_3$): δ (ppm) = 173.05 (C-O), 167.51 (C=N), 136.79, 136.43, 131.66, 129.48, 127.81, 126.36 (Ar carbons of ligand), 100.71, 100.19, 99.85, 99.78 (quaternary carbons of *p*-cymene), 83.57, 82.88, 81.53, 81.49, 80.40, 80.33, 79.90, 79.64 (Ar carbons of *p*-cymene), 46.01 (CH of *p*-cymene), 30.40 (CH of *p*-cymene), 22.62, 22.25 ($2CH_3$, *p*-cymene), 18.80, 8.69 ($(CH_3)_2$ of *p*-cymene).

Complex 2. Yellow solid, Yield: 82%, m.p.: 221 °C (with decomposition). Anal. calcd: $C_{30}H_{34}Cl_2N_2O_3Ru_2S$: C, 46.45; H, 4.42; N, 3.61%. found: C, 46.25, H, 4.40, N, 3.56%. FT-IR (KBr, cm^{-1}): 3175 $\nu_{(N\text{-}H)}$, 1627 $\nu_{(C=N)}$, 1560 $\nu_{(C=O)}$, 1230 $\nu_{(C\text{-}O)}$, 1542 ν(C=N-N=C). ^1H NMR (400 MHz, $CDCl_3$): δ (ppm) = 8.04 (*s*, 1H, $ArH_{(ligand)}$), 7.58-7.38 (*m*, 3H, $ArH_{(ligand)}$), 7.06 (*s*, 1H, $ArH_{(ligand)}$), 6.49 (*s*, 1H, $ArH_{(ligand)}$), 5.20-5.08 (*m*, 4H, $CH_{(p\text{-cymene})}$), 4.79 (*s*, 1H, $CH_{(p\text{-cymene})}$), 4.65 (*s*, 1H, $CH_{(p\text{-cymene})}$), 4.43 (*s*, 1H, $CH_{(p\text{-cymene})}$), 4.19 (*s*, 1H, $CH_{(p\text{-cymene})}$), 2.68-2.60 (*sept*, 2H, $CH(CH_3)_{2(p\text{-cymene})}$), 2.20 (*s*, 6H, $CH_{3(p\text{-cymene})}$), 1.11 (*s*, 12H, $CH(CH_3)_{2(p\text{-cymene})}$). ^{13}C {^1H} NMR (100MHz, $CDCl_3$): δ (ppm) = 168.15 (C-O), 164.33 (C=N), 147.15, 143.38, 136.60, 131.94, 127.99, 126.38 (Ar carbons of ligand), 114.70, 110.79, 101.12, 100.12 (quaternary carbons of *p*-cymene), 82.87, 82.70, 81.54, 81.25, 80.32, 80.25, 80.07, 79.82 (Ar carbons of *p*-cymene), 45.98 (CH of *p*-cymene), 30.47 (CH of *p*-cymene), 22.71, 22.23 ($2CH_3$, *p*-cymene), 18.79, 8.70 ($(CH_3)_2$ of *p*-cymene).

Complex 3. Yellow solid, Yield: 86%, m. p.: 210 °C (with decomposition). Anal. calcd: $C_{30}H_{34}Cl_2N_2O_2Ru_2S_2$: C, 45.51; H, 4.33; N, 3.54%. found: C, 45.37, H, 4.28, N, 3.44%. FT-IR (KBr, cm^{-1}): 3257 $\nu_{(N\text{-}H)}$, 1675 $\nu_{(C=N)}$, 1568 $\nu_{(C=O)}$, 1283 $\nu_{(C\text{-}O)}$, 1510 ν(C=N-N=C). ^1H NMR (400 MHz, $CDCl_3$): δ (ppm) = 8.04 (*d*, J = 4 Hz, 2H, $ArH_{(ligand)}$), 7.48-7.46 (*m*, 2H, $ArH_{(ligand)}$), 7.07 (*dd*, J = 4.8 Hz, 3.6 Hz, 2H, $ArH_{(ligand)}$), 5.14 (*d*, J = 4 Hz, 2H, $CH_{(p\text{-cymene})}$), 5.07 (*d*, J = 4 Hz, 2H, $CH_{(p\text{-cymene})}$), 4.67 (*d*, J = 4 Hz, 2H, $CH_{(p\text{-cymene})}$), 4.14 (*d*, J = 4 Hz, 2H, $CH_{(p\text{-cymene})}$), 2.64-2.57 (*sept*, 2H, $CH(CH_3)_{2(p\text{-cymene})}$), 2.19 (*s*, 6H, $2CH_{3(p\text{-cymene})}$), 1.12-

1.08 (*m*, 12H, $CH(CH_3)_{2(p\text{-cymene})}$). ^{13}C {^1H} NMR (100MHz, $CDCl_3$): δ (ppm) = 173.23 (C-O), 167.85 (C=N), 136.77, 131.83, 127.86, 126.35 (Ar carbons of ligand), 100.80, 100.07 (quaternary carbons of *p*-cymene), 83.04, 81.62, 80.22, 80.14 (Ar carbons of *p*-cymene), 45.84 (CH of *p*-cymene), 30.44 (CH of *p*-cymene), 22.56, 22.28 ($2CH_3$, *p*-cymene), 18.82, 8.65 ($(CH_3)_2$ of *p*-cymene).

5.2.5. X-ray crystallographic data collection

Single crystals of complex **3** were grown by slow evaporation of a dichloromethane-methanol solution at room temperature. The data collection was carried out using a Bruker AXS Kappa APEX II single crystal X-ray diffractometer using monochromated Mo–Kα radiation (λ = 0.71073 Å). Data was collected at 296 K. The absorption corrections were performed by the multi-scan method using SADABS software.[20] Corrections were made for Lorentz and polarization effects. The structures were solved by direct methods (SHELXS 97) and refined by full-matrix least squares on F^2 using SHELXL 97.[21] All non-hydrogen atoms were refined anisotropically and the hydrogen atoms in these structures were located from the difference Fourier map and constrained to the ideal positions in the refinement procedure. The unit cell parameters were determined by the method of difference vectors using reflections scanned from three different zones of the reciprocal lattice. The intensity data were measured using ω and φ scan with a frame width of 0.5°. Frame integration and data reduction were performed using the Bruker SAINT-Plus (Version 7.06a) software.[22] Figure 8 was drawn with ORTEP and the structural data have been deposited at the Cambridge Crystallographic Data Centre: CCDC 2179018.

5.2.6. General procedure for the binuclear *p*-cymene Ru(II) catalyzed synthesis of pyrazoles

Aromatic alcohols (1 mmol), malononitrile (1 mmol), benzohydrazide derivatives (1 mmol), *t*-BuOK (0.5 mmol), and catalyst (1 mol %) have been dissolved with 5 mL of xylene solvent. Then the mixture was refluxed for 18 h at 120 ^oC in nitrogen atmosphere.

The reaction mixture has been quenched with water and extracted using EtOAc. The organic fractions were separated and dried over anhydrous Na_2SO_4, and the solvent was removed under vacuum. The products have been isolated by column chromatography with petroleum ether/EtOAc (95:5).

5.2.7. Competitive control experiment between EDG and EWG.

The round bottom flask with 4-methyl and 4-chloro benzyl alcohol (1 mmol), malononitrile (1 mmol), benzohydrazide (1 mmol), *t*-BuOK (0.5 mmol) and catalyst (1 mol%) and another reaction performed with 4-methoxy and 4-chloro benzohydrazide (1 mmol), benzyl alcohol (1 mmol), malononitrile (1 mmol), *t*-BuOK (0.5 mmol) and catalyst (1 mol%) both reactions were refluxed in *m*-Xylene solvent for 18 h at 120 ^oC under nitrogen atmosphere. The reaction mixture has been reduced and the pyrazole derivatives have been isolated by column chromatography. petroleum ether/EtOAc (95:5) combination was used to elute the desired pyrazole products.

5.2.8. Procedure for gram scale synthesis.

Benzyl alcohol (1.08 g, 10 mmol), malononitrile (0.66 g, 10 mmol), benzohydrazide (1.36 g, 10 mmol), *t*-BuOK (0.56 g, 0.5 mmol), and catalyst (0.77 g, 1 mol%) were taken in 50 mL of *m*-xylene solvent. The resultant mixture has been refluxed for 18 h at 120 ^oC under nitrogen atmosphere. After that, the final mixture has been quenched with water and extracted with ethyl acetate. The EtOAc fractions have been collected separately dried using Na_2SO_4 and filtered. The evaporation of solvent under vacuum provided the crude mixture which has been purified using column chromatography with petroleum ether/ethyl acetate (95:5).

5.3. Results and Discussion

Thiophene derived different set of hydrazine ligands have been prepared in accordance with previously described literature. The synthesis of new *p*-cymene binuclear

Ru(II)complexes have been accomplished in good yields from the reaction of [(η^6-*p*-cymene)$_2$Ru$_2$Cl$_2$(μ-Cl)$_2$] with hydrazine ligand in benzene medium and presence of Et_3N base.

5.3.1. FT-IR Spectra

The synthesized *p*-cymene binuclear Ru(II) complexes are stable to air and dissolvable in most organic solvents. In FT-IR spectra, stretching frequencies were observed around 3205-3089 cm^{-1} assignable to hydrazine N–H fragments of the ligands (L1-L3). Moreover, the intense bands around 1654-1689 cm^{-1} were attributed C=O moiety of ligands. On complexation, both of the ν_{N-H} frequencies and $\nu_{(C=O)}$ were absent which suggested the tautomerization and the formation of a new sharp band characteristic to ν(C-O) (1219-1300 cm^{-1}). The shift in these bands revealed that coordination of ligand to the metal *via* hydrazine nitrogen and imidolate oxygen to ruthenium (II) centre.

5.3.2. NMR spectra

The proton NMR spectra of L1-L3 displayed two distinctive downfield singlets around δ 10.12–11.86 ppm due to the hydrazine NH protons. The coordination *via* imidolate oxygen to ruthenium ion was entailed by the absence of hydrazone –NH peak in the spectra of the complexes after enolization and subsequent deprotonation. All aromatic protons of the ligands and complexes were appeared as multiplets in the range of 7.05-8.04 ppm. In the complexes, arene protons were found at δ 5.20-3.70 ppm. The $-CH_3$ protons of the isopropyl group in *p*-cymene moiety were resonated as a singlet in the region δ1.08-1.40 ppm and methine proton was emerged as septet around δ 2.60 ppm. Furthermore, methyl protons of *p*-cymene moiety were noticed as a singlet at 2.13-2.20 ppm. The formation of the synthesized complexes was further evidenced by $^{13}C\{^1H\}$ NMR spectra. The downfield shift of C-O (167.85-173.07 ppm) in the spectra of the complexes supported the bonding of imidolate oxygen and hydrazine nitrogen to Ru(II) ion.

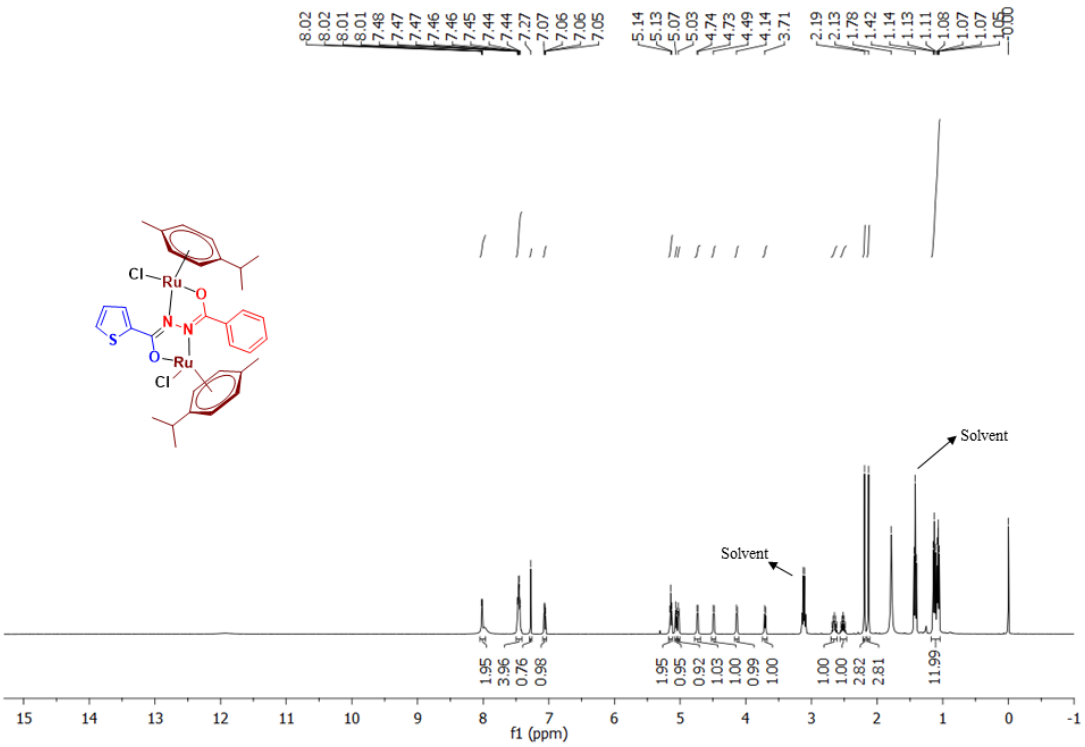

Figure 2. ^{1}H NMR spectrum of complex **1** in $CDCl_3$ (400 MHz, 293 K).

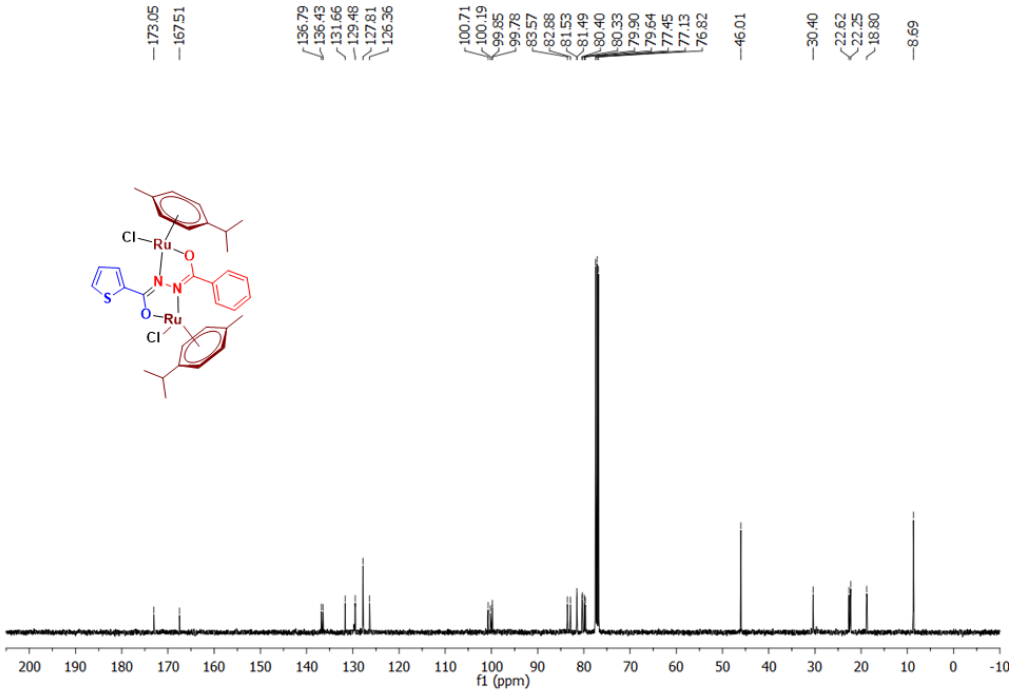

Figure 3. ^{13}C NMR spectrum of complex **1** in $CDCl_3$ (100 MHz, 293 K).

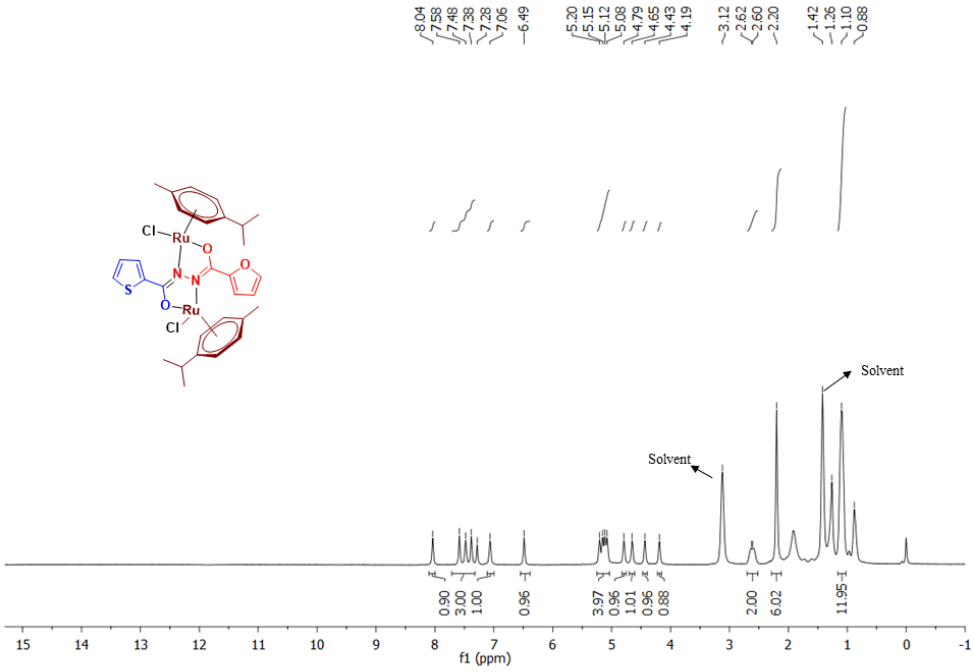

Figure 4. ^{1}H NMR spectrum of complex **2** in $CDCl_3$ (400 MHz, 293 K).

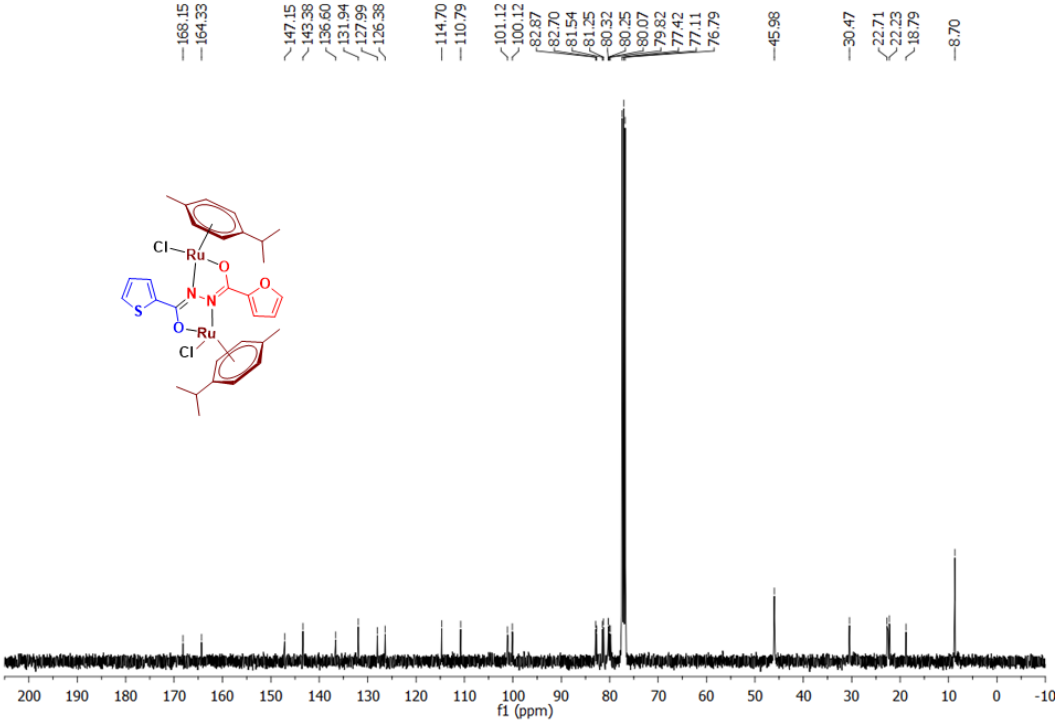

Figure 5. ^{13}C NMR spectrum of complex **2** in $CDCl_3$(100 MHz, 293 K).

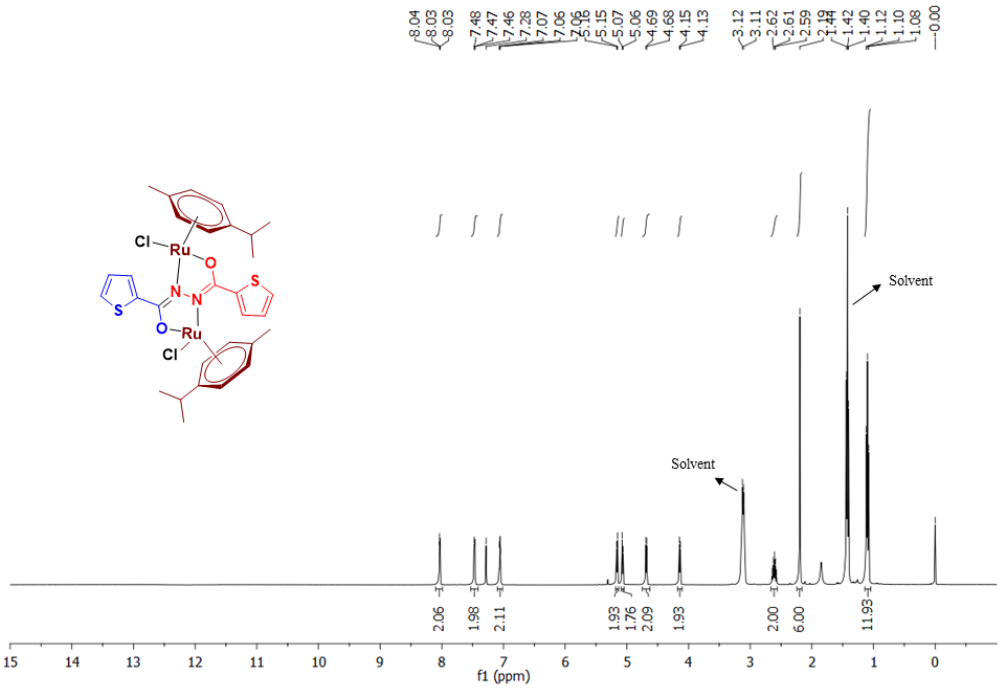

Figure 6. ^{1}H NMR spectrum of complex **3** in $CDCl_3$ (400 MHz, 293 K).

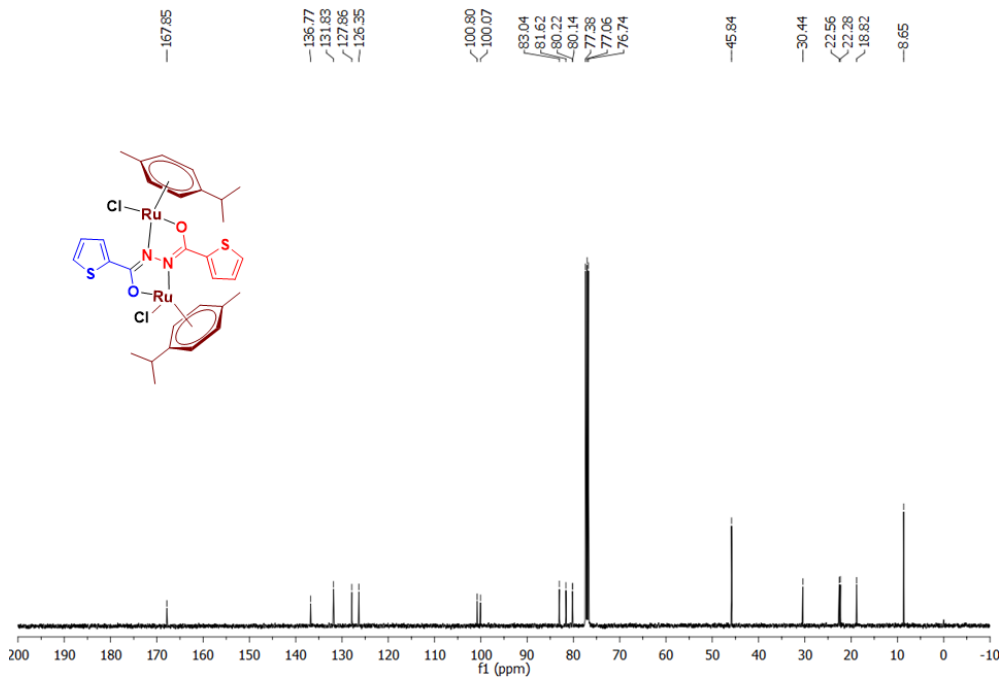

Figure 7. ^{13}C NMR spectrum of complex **3** in $CDCl_3$ (100 MHz, 293 K).

5.3.3. Single crystal X-ray studies

The solid-state molecular structure for the representative complex **3** is corroborated by X-ray diffraction studies and the ORTEP diagram is depicted in Figure 8. The crystal structure refinement parameters have been provided in Table 1, and important bond distances and angles have been presented in Table 2. The triclinic system of complex **3** belongs to the "P-1" space group with Z = 2. The bite angle O(1)-Ru(1)-N(1) of the complex is 76.34 (8)º. Ru(1)-N(1) and Ru(1)-O(1) have bond lengths of 2.093(2) and 2.070(2) A˚, respectively. The Ru-Cl has a bond length of 2.413(8) A˚, and Ru-centroid distance 1.656 Å which is comparable with other reported *p*-cymene ruthenium(II) complexes.[23] Therefore, X-ray studies confirm the formation of the arene binuclear Ru(II) complexes by the coordination of the ligand in a monoionised bidentate manner to each ruthenium(II) ion *via* the hydrazine nitrogen and carbonyl oxygen including one chlorine atom and *p*-cymene ring. It adopts a piano-stool pseudo octahedral geometry around each Ru(II) ion.

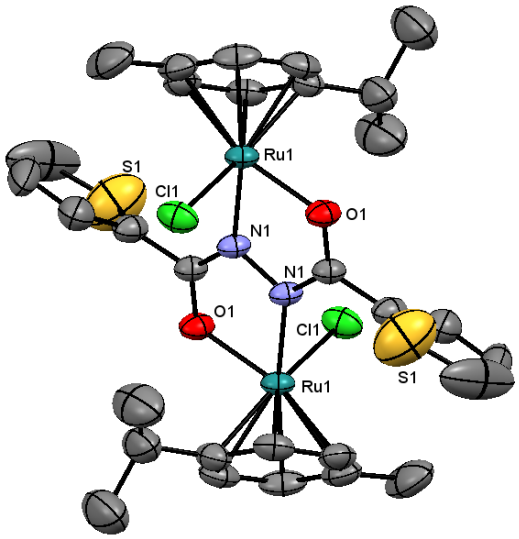

Figure 8. ORTEP view of complex **3**. All hydrogens were omitted for clarity.

Table 1. Crystal data and structure refinement for complex **3**

CCDC	2179018
Empirical formula	$C_{30}H_{34}Cl_2N_2O_2Ru_2S_2$
Formula weight	395.88
Temperature/K	298(2)
Crystal system	triclinic
Space group	P-1
a/Å	9.3518(10)
b/Å	9.6547(10)
c/Å	9.9074(11)
α/°	72.253(3)
β/°	85.331(3)
γ/°	69.299(3)
Volume/Å^3	796.61(15)
Z	2
ρcalcg/cm^3	1.650
μ/mm^{-1}	1.277
F(000)	398.0
Crystal size/mm^3	0.28 × 0.25 × 0.16
Radiation	MoKα (λ = 0.71073 Å)
Theta range for data collection	4.658 to 60.146
Index ranges	-13 ≤ h ≤ 13, -13 ≤ k ≤ 13, -13 ≤ l ≤ 13
Reflections collected	20735
Independent reflections	4578 [*R* int = 0.0227, *R* sigma = 0.0172]

Table 2. Selected bond lengths (Å) and angles (°) for the complex **3**

Bond lengths (Å)	
Ru1-O1	2.070(2)
Ru1-N1	2.093(2)
Ru1-Cl1	2.413(8)
Ru1-C4	2.153(3)
Ru1-C2	2.175(3)
Ru1-C6	2.186(3)
Ru1-C5	2.191(3)
Ru1-C3	2.193(3)
S1-C12	1.652(4)
S1-C15	1.672(12)
O1-C1	1.286(3)
N1-N2	1.409(6)
N1-C1	1.312(3)
N2-N1	1.422(4)
C1-C12	1.476(4)
N3-C12	1.378(7
C1-C2	1.514(7)
C1-C12	1.446(7)

Bond angles (°)	
O1-Ru1-N1	76.34 (8)
O1-Ru1-C4	123.16 (12)
N1-Ru1-C4	94.42 (10)
O1-Ru1-C2	89.31 (12)
N1-Ru1-C2	146.04 (13)
C4-Ru1-C2	67.76 (13)
O1-Ru1-C6	148.67 (13)
C4-Ru1-C6	68.49(14)
C2-Ru1-C6	67.45(15)
O1-Ru1-C5	160.84(13)
N1-Ru1-C5	104.46(11)
Ru1-C20	38.2(2)
C4-Ru1-C5	37.96(16)
Ru1-C22	79.1(2)
Ru1-C23	67.6(2)
Ru1-C24	37.4(3)

5.3.4. Catalytic application to synthesis of pyrazoles

The *p*-cymene Ru(II) complexes have been tailored as catalysts for the direct access of pyrazole derivatives under benign conditions based on the development of ruthenium catalysts towards significant applications in coupling reactions. The catalytic synthesis was carried out *via* ADC of substituted benzyl alcohols with malononitrile and benzohydrazide.

5.3.4.1. Optimization of bases, solvents and temperature

We started the optimization for the one-pot synthesis of pyrazole with benzyl alcohol (**1a**), malononitrile (**2**) and benzohydrazide (**3a**) as a benchmark substrates utilising 1 mol% of *p*-cymene binuclear Ru(II) complex **1** as catalyst and results are illustrated in Table 3.The trail reaction encouraged us to investigate the catalytic factors such as various solvents, bases, time and temperatures. At first, complex **1** was used as a catalyst with 1 mol % catalyst loading in *m*-xylene solvent at 140 °C for 24 h to produce 5-amino-1-benzoyl-3-phenyl-1H-pyrazole-4-carbonitrile **4a** with 72% isolated yield (Table 3, entry 1). Encouragingly, the one-pot synthesis reaction was performed in various solvents like toluene, 1,4-dioxane, *t*-BuOH, THF, acetonitrile and ethanol. Amongst them, *m*-xylene was the best medium for the reaction and furnished good yield of **4a** (81%) when compared other solvents (Table 3, entries 2-7). After complete screening, revealing that *t*-BuOK as suitable base for current pyrazole **4a** synthesis when compared to the all-other bases (Table 3, entries 8-13). Reducing the temperature to 120 °C the yield of **4a** was decreased (88%) marginally (Table 3, entry 14). Additionally, the reaction has been carried out at a little shortened time (18 h) time (Table 3, entry 15) and almost same amount of **4a** was attained (86 %). In absence of catalyst and *t*-BuOK in catalytic reaction only trace (<10 %) amount of product **4a** was detected (Table 3, entries 16 and 17). Further, the effectiveness of catalyst complexes **2** and **3** was evaluated under optimum conditions (*m*-Xylene/*t*-BuOK at 120 °C for 18h) and pyrazole **4a** was produced with 94% and 89% respectively. (Table 3, entries 18 and 19). From optimization reaction outcomes, the suitable condition has been streamlined as *m*-xylene / *t*-BuOK medium at 120 °C for 18 h for extending the substrate scope of desired pyrazole product.

Table 3. Screening of reaction conditions[a]

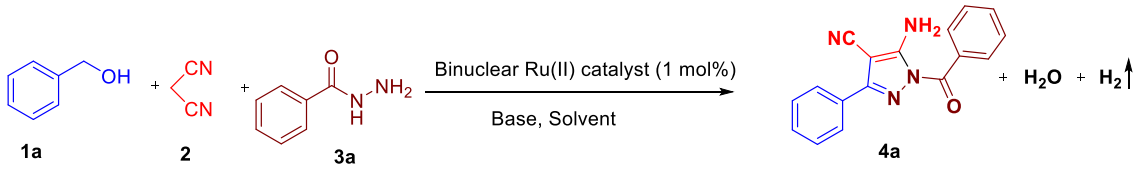

Entry	Complex	Solvent	Base	Temp (° C)	Time (h)	Yield[b]
1	Complex **1**	*m*-Xylene	Na_2CO_3	140	24	72
2	Complex **1**	$PhCH_3$	Na_2CO_3	110	24	61
3	Complex **1**	1,4-dioxane	Na_2CO_3	100	24	54
4	Complex **1**	*t*-BuOH	Na_2CO_3	82	24	42
5	Complex **1**	THF	Na_2CO_3	66	24	34
6	Complex **1**	Acetonitrile	Na_2CO_3	80	24	39
7	Complex **1**	Ethanol	Na_2CO_3	78	24	46
8	Complex **1**	*m*-Xylene	K_2CO_3	140	24	68
9	Complex **1**	*m*-Xylene	Cs_2CO_3	140	24	62
10	Complex **1**	*m*-Xylene	$NaHCO_3$	140	24	50
11	Complex **1**	*m*-Xylene	NaOH	140	24	76
12	Complex **1**	*m*-Xylene	KOH	140	24	79
13	Complex **1**	*m*-Xylene	*t*-BuOK	140	24	92
14	Complex **1**	*m*-Xylene	*t*-BuOK	120	24	88
15	Complex **1**	*m*-Xylene	*t*-BuOK	120	18	86
16[c]	-	*m*-Xylene	*t*-BuOK	120	18	<10
17[d]	Complex **1**	*m*-Xylene	-	120	18	NR
18	**Complex 2**	***m*-Xylene**	***t*-BuOK**	**120**	**18**	**94**
19	Complex **3**	*m*-Xylene	*t*-BuOK	120	18	89

[a]**Reaction conditions:** Benzyl alcohol (**1a)** (1 mmol), malononitrile (**2**) (1 mmol), benzohydrazide (**3a**) (1 mmol), complex (1 mol %), base (0.5 mmol), solvent (5 mL). N_2 atm. [b]Isolated yield of **4a**. [c] No catalyst. [d] No base.

5.3.4.2. Optimization of effect of substituent

Once the various catalytic parameters were optimized, the effect of substituents of all the complexes on the catalytic reaction has been investigated (Table 4). At most, all the complexes (**1-3**) showed good catalytic activity in the formation of pyrazole product with appreciable yields. However, based on experimental results, the complex **2** relatively provided a better yield than complexes (1-3) and explore the broad substrate scope using a diverse range of alcohols.

Table 4. Effect of the substituent of catalyst[a]

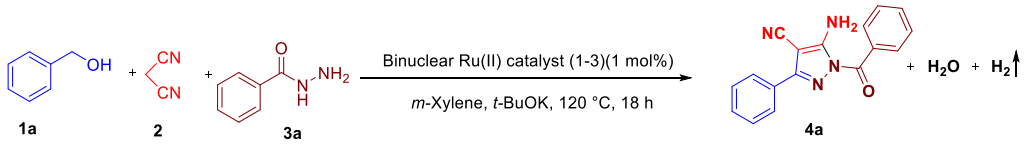

Entry	Ru complexes	Yield(%)[b]
1	Complex 1	86
2	**Complex 2**	**94**
3	Complex 3	89

[a]**Reaction conditions:** Benzyl alcohol (**1a**) (1 mmol), malononitrile (**2**) (1 mmol), benzohydrazide (**3a**) (1 mmol), complex (1 mol %), *t*-BuOK (0.5 mmol), *m*-Xylene (5 mL). N_2 atm, 120 °C, 18 h. [b] Isolated yield.

5.3.4.3. Optimization of catalyst loading

Further, the effectiveness of our catalyst was examined with different catalyst loadings for the test reaction (Table 5). Upon reducing the catalyst loading from 1 mol% to 0.1 mol%, there was a substantial decrease in yields (Table 5, entries 1 - 4). Therefore 1 mol% catalyst loading is the best choice for optimization.

Table 5: Effect of catalyst loading[a]

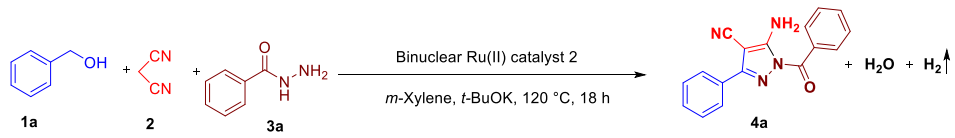

Entry	Catalyst 2 (mol %)	Yield(%)[b]
1	**1.0**	**94**
2	0.5	41
3	0.25	20
4	0.10	<10

[a]**Reaction conditions:** Benzyl alcohol (**1a**) (1 mmol), malononitrile (**2**) (1 mmol), benzohydrazide (**3a**) (1 mmol), *t*-BuOK (0.5 mmol), *m*-Xylene (5 mL). N_2 atm, 120 °C, 18 h. [b] Isolated yield.

5.3.4.4. Scope of the reactions

The optimization results inspired us to further demonstrate broad substrate scope of the ruthenium-catalysed synthesis of pyrazoles from the coupling of benzohydrazide and malononitrile with primary alcohols was surveyed and the outcomes are depicted in Table 6. The benzyl alcohols have substituted by electron-donating groups (4-CH_3, 3-OCH_3, 4-^{i}Pr, and 3-OH) gave the products in good to excellent yields up to 95% (**4b-4e**), while the reactions of the benzyl alcohols with electron-withdrawing groups (4-Cl, 3-Cl, 2-Cl, 3-Br, 4-NO_2, 2-NO_2 and 4-$CONH_2$) proceeded well and furnished good to moderate yields of desired products (**4f-4l**). These results showed that electron-donating groups had more favourable effects than electron-withdrawing groups. Further, the catalytic reaction

employing more electron-donating groups (2,5-dimethoxy and 3, 4-dimethoxy) on benzyl alcohols to deliver **4m** and **4n** in 78% and 80% yields. However, 2,6-dichloro benzyl alcohol was tolerated well and conferred target product **4o** in 68% of isolated yield. Notably, 2-naphthalenemethanol was operated well in ADC reaction with malononitrile and benzohydrazide to afford **4p** in 85% yield. In addition, substituted benzohydrazides (4-Cl, 4-OCH_3) undergone smoothly react with benzyl alcohol, 4-methyl and 4-chloro benzyl alcohols to give equivalent pyrazole products **4q-4s** in good yields up to 94%. Heterocyclic and aliphatic alcohols were also tested for this reaction and it was observed as ineffective.

Table 6. Binuclear Ru(II) catalyzed pyrazoles from acceptorless dehydrogenative coupling of various benzyl alcohols and benzohydrazides[a]

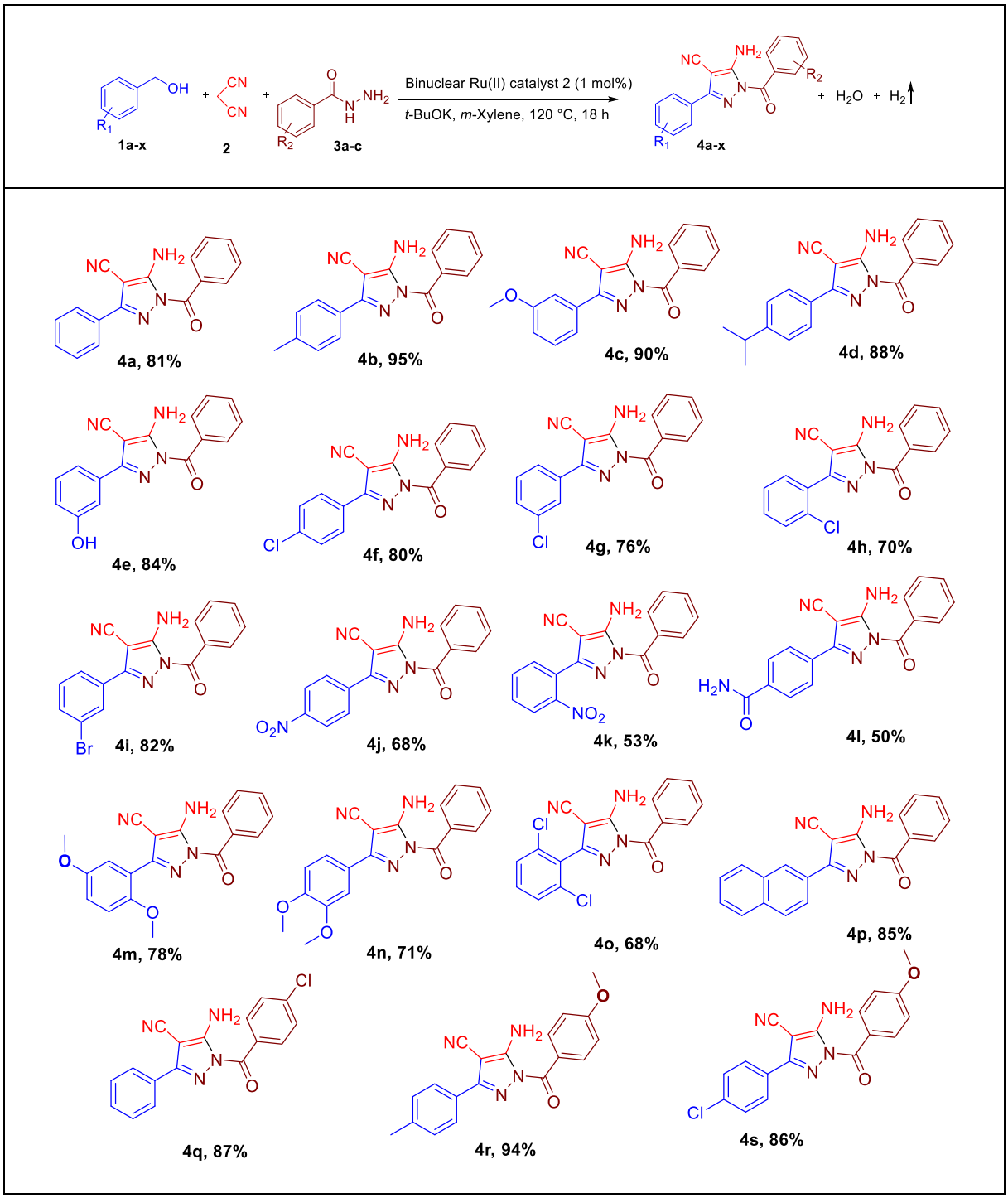

[a]**Reaction conditions**: Benzyl alcohol (**1a**) (1 mmol), malononitrile (**2**) (1 mmol), benzohydrazide derivatives (**3a-c**) (1 mmol), catalyst **2** (1 mol %), *t*-BuOK (0.5 mmol), *m*-Xylene (5 mL). N_2 atm, 120 °C, 18 h.

5.3.4.5. Control experiments

Control experiments were carried out to elucidate the reaction path of the acceptorless dehydrogenative coupling reaction facilitated by a binuclear Ru(II) catalyst. Initially, benzyl alcohol underwent dehydrogenation (**1a**) to formed benzaldehyde (**1a'**) with the liberation of H_2 under the involvement of the binuclear Ru(II) catalyst in 5 h.

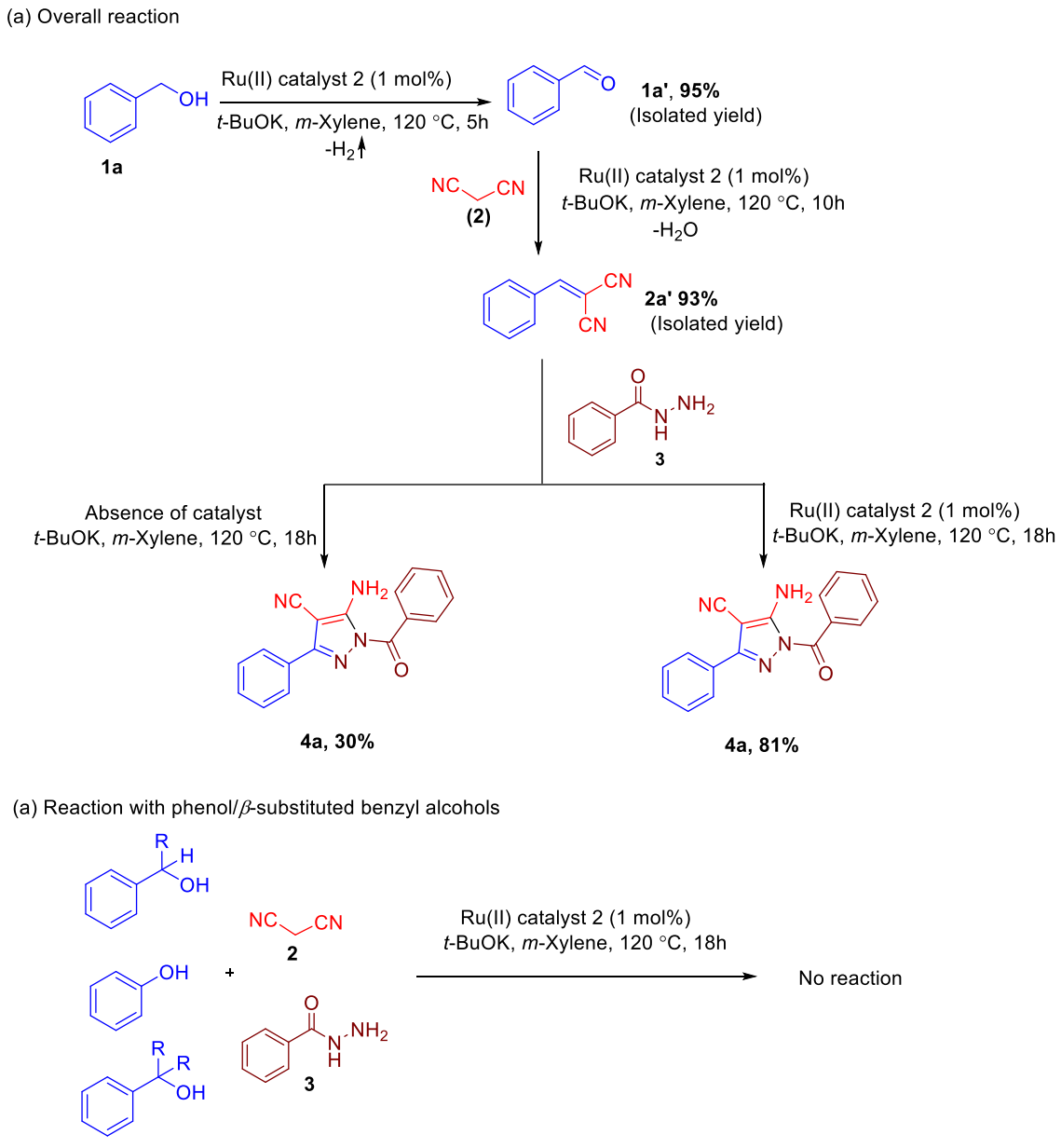

Scheme 4. Control experiments for the synthesis of pyrazole

Further, the formed benzaldehyde **1a'** was reacted with malononitrile in presence of catalyst to give **2a'** in 93% of yield in 10 h. After, presence of catalyst mediated reaction of **2a'** with benzohydrazide (**3**) provided pyrazole product **4a** with 81% yield in 18 h. However, in contrary to the above reaction was performed in absence of catalyst the reaction ended with only 30% of pyrazole **4a** which indicates the active involvement of binuclear ruthenium catalyst in catalytic cycle. Hence, the acceptorless dehydrogenation reaction leads to the formation of expected pyrazole under the influence of binuclear ruthenium catalysts through acceptorless dehydrogenative coupling[24] of alcohols.

5.3.4.6. Competitive control experiment between EDG and EWG

An intermolecular competitive experiment was carried out between 4-methyl, 4-chlorobenzyl alcohols and 4-methoxy, 4-chlorobenzohydrazides under optimized reaction conditions. From this reaction, we have gained a better understanding of the impact of the electron-donating and electron-deficient substituents of substrates on catalytic efficiency. The results expressed that the electron releasing group has more reactive than the electron-deficient group on both benzyl alcohols and benzohydrazides (Scheme 5).

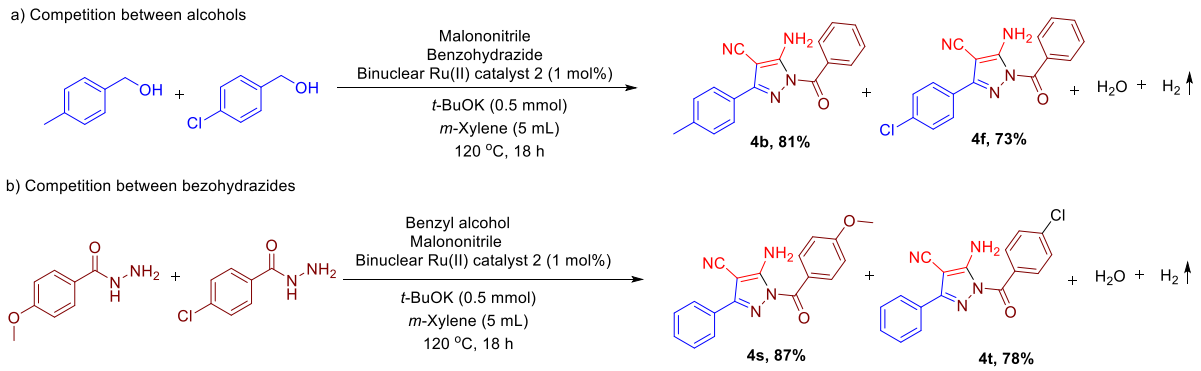

Scheme 5. Competition reaction among electron releasing and electron deficient benzyl alcohols and benzohydrazides

5.3.4.7. Large-scale synthesis of pyrazole

We then succeeded in performing the reaction on a large scale to illustrate the practical usefulness of the developed methodology in a one-pot reaction. Advantageously, the large-scale reaction of benzyl alcohol (**1a**), malononitrile (**2**) and benzohydrazide (**3**) at the optimized reaction condition furnished **4a** in 76 % isolated yield (2.18g) (Scheme 6).

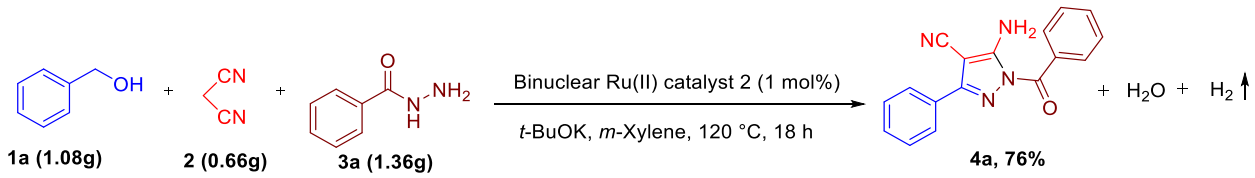

Scheme 6. Large scale synthesis of pyrazole

5.3.4.8. Reaction mechanism for pyrazole

Based on the control experiment studies and literature reports[16] a plausible mechanism for binuclear Ru(II) catalysed synthesis of pyrazole has been proposed (Scheme 7). At first, the binuclear Ru(II) catalyst reacts with benzyl alcohol with the aid of *t*-BuOK to give Ru-alkoxide species (**A**). Further, **A** undergoes *β*-hydride elimination to discharge benzaldehyde (**1a'**) along with the generation of Ru-H species (**B**). Further, the *in-situ* generated benzaldehyde (**1a'**) underwent condensation with malononitrile (**2**) to form benzylidenemalononitrile intermediate (**2a'**). After that, **2a'** reacted with benzohydrazide (**3**) to form intermediate (**4a'**) followed by coordination of more basic nitrogen on **4a'** to the ruthenium ion to generate ruthenium amino species **C**. Thereafter, the formed **C** reacts with another molecule of benzyl alcohol (**1a**) to regenerate the catalyst with the formation of the product **4a** along with the release of H_2.

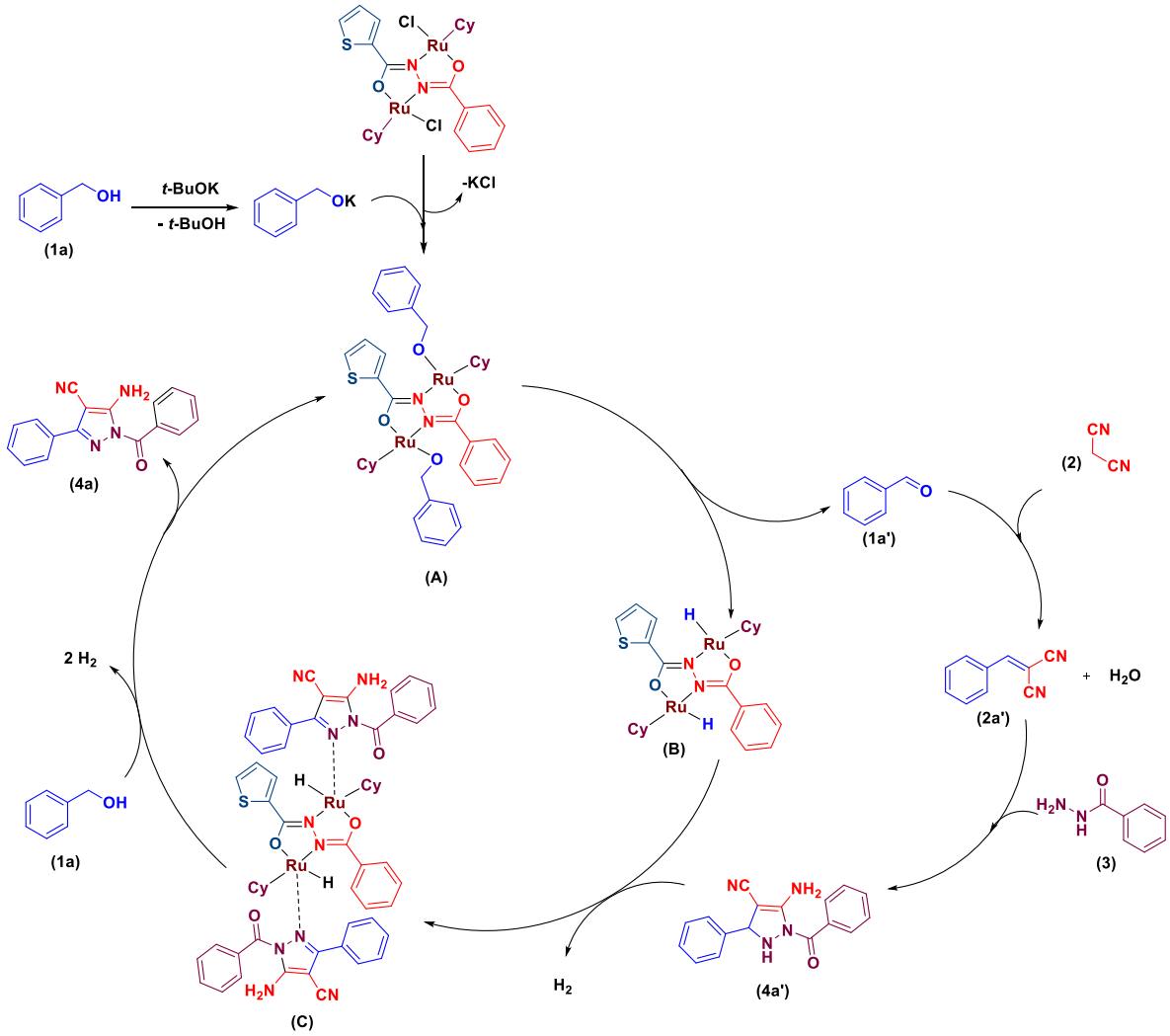

Scheme 7. A plausible mechanism for pyrazole synthesis

Spectral data of the catalytic products

(4a) 5-amino-1-benzoyl-3-phenyl-1H-pyrazole-4-carbonitrile. ^{1}H NMR (400 MHz, DMSO-d_6): δ (ppm) 11.91 (s, 1H), 8.50 (s, 1H), 7.95 (d, *J* = 7.2 Hz, 2H), 7.75 (d, *J* = 6.2 Hz, 2H), 7.59 – 7.45 (m, 6H). ^{13}C {^{1}H} NMR (100 MHz, DMSO-d_6): δ (ppm) 163.17 (C=O), 147.80, 134.32, 133.41, 131.73, 130.05, 128.80, 128.45, 127.61, 127.07.

(4b) 5-amino-1-benzoyl-3-(p-tolyl)-1H-pyrazole-4-carbonitrile. ^{1}H NMR (400 MHz, DMSO-d_6): δ (ppm) δ ^{1}H NMR (400 MHz, DMSO) δ 11.84 (s, 1H), 8.45 (s, 1H), 7.94 (d, J = 8 Hz, 2H), 7.65 – 7.50 (m, 5H), 7.25 (d, J = 8 Hz, 2H).^{13}C {^{1}H} NMR (100 MHz, DMSO-

d_6): δ (ppm) 163.15 (C=O), 147.90, 139.88, 133.45, 131.67, 131.59, 129.40, 128.42, 127.57, 127.06, 20.98.

(4c) 5-amino-1-benzoyl-3-(3-methoxyphenyl)-1H-pyrazole-4-carbonitrile. ^{1}H NMR (400 MHz, DMSO-d_6): δ (ppm) 11.91 (s, 1H), 8.45 (s, 1H), 7.93 (d, *J* = 8 Hz, 2H), 7.60-7.51 (m, 4H), 7.39-7.31 (m, 3H), 3.81 (s, 4H). ^{13}C {^{1}H} NMR (100 MHz, DMSO-d_6): δ (ppm) 163.21 (C=O), 159.52, 147.72, 135.73, 133.36, 131.74, 129.91, 128.45, 127.60, 120.07, 116.22, 111.15, 55.12.

(4d) 5-amino-1-benzoyl-3-(4-isopropylphenyl)-1H-pyrazole-4-carbonitrile. ^{1}H NMR (400 MHz, DMSO-d_6): δ (ppm) 11.81 (s, 1H), 8.45 (s, 1H), 7.93 (d, *J* = 4 Hz, 2H), 7.66 (d, *J* = 8 Hz, 2H), 7.67-7.51 (m, 3H), 7.33 (d, *J* = 8 Hz, 2H), 2.95-2.89 (sept, 1H), 1.22-1.21 (d, *J* = 4 Hz, 6H). ^{13}C {^{1}H} NMR (100 MHz, DMSO-d_6): δ (ppm) 163.06 (C=O), 150.67, 147.84, 133.46, 132.00, 131.66, 128.43, 127.56, 127.17, 126.77, 33.35, 23.62.

(4e) 5-amino-1-benzoyl-3-(3-hydroxyphenyl)-1H-pyrazole-4-carbonitrile. ^{1}H NMR (400 MHz, DMSO-d_6): δ (ppm) 11.82 (s, 1H), 9.66 (s, 1H), 8.40 (s, 1H), 7.93 (d, *J* = 8 Hz, 2H), 7.58-7.52 (m, 3H), 7.24 (s, 2H), 7.12 (s, 1H), 6.86 (d, *J* = 4 Hz, 1H). ^{13}C {^{1}H} NMR (100 MHz, DMSO-d_6): δ (ppm) 163.13 (C=O), 157.67, 147.92, 135.57, 133.41, 131.70, 129.85, 128.43, 127.58, 118.81, 117.44, 112.63.

(4f) 5-amino-1-benzoyl-3-(4-chlorophenyl)-1H-pyrazole-4-carbonitrile. ^{1}H NMR (400 MHz, DMSO-d_6): δ (ppm) 11.94 (s, 1H), 8.46 (s, 1H), 7.93 (d, *J* = 8 Hz, 2H), 7.76 (d, *J* = 8 Hz, 2H), 7.60-7.51 (m, 5H). ^{13}C {^{1}H} NMR (100 MHz, DMSO-d_6): δ (ppm) 163.18 (C=O), 146.42, 134.49, 133.25, 131.78, 128.89, 128.67, 128.45, 127.61.

(4g) 5-amino-1-benzoyl-3-(3-chlorophenyl)-1H-pyrazole-4-carbonitrile. ^{1}H NMR (400 MHz, DMSO-d_6): δ (ppm) 12.01 (s, 1H), 8.46 (s, 1H), 7.94 (d, *J* = 8 Hz, 2H), 7.79 (s, 1H), 7.69 (s, 1H), 7.60 – 7.49 (m, 5H). ^{13}C {^{1}H} NMR (100 MHz, DMSO-d_6): δ (ppm) 163.27

(C=O), 146.05, 136.56, 133.64, 133.21, 131.84, 130.68, 129.65, 128.45, 127.65, 126.23, 125.78.

(4h) 5-amino-1-benzoyl-3-(2-chlorophenyl)-1H-pyrazole-4-carbonitrile. ^{1}H NMR (400 MHz, DMSO-d_6): δ (ppm) δ 12.13 (s, 1H), 8.89 (s, 1H), 8.05 (s, 1H), 7.97 (d, *J* = 8 Hz, 2H), 7.50-7.42 (m, 6H).^{13}C {^{1}H} NMR (100 MHz, DMSO-d_6): δ (ppm) 163.20 (C=O), 143.69, 133.20, 133.10, 131.89, 131.57, 131.42, 129.86, 128.46, 127.65, 127.54, 126.85.

(4i) 5-amino-1-benzoyl-3-(3-bromophenyl)-1H-pyrazole-4-carbonitrile. ^{1}H NMR (400 MHz, DMSO-d_6): δ (ppm) 12.02 (s, 1H), 8.44 (s, 1H), 7.94 (s, 3H), 7.72 (d, *J* = 8 Hz, 1H), 7.60 – 7.53 (m, 5H), 7.43 – 7.40 (m, 1H). ^{13}C {^{1}H} NMR (100 MHz, DMSO-d_6): δ (ppm) 163.29 (C=O), 145.94, 136.78, 133.20, 132.53, 131.84, 130.94, 129.07, 128.45, 127.66, 126.22, 122.16, 40.10, 39.89, 39.68, 39.47, 39.26, 39.06, 38.85.

(4j) 5-amino-1-benzoyl-3-(4-nitrophenyl)-1H-pyrazole-4-carbonitrile. ^{1}H NMR (400 MHz, DMSO-d_6): δ (ppm) 12.14 (s, 1H), 8.54 (s, 1H), 8.27 (s, 2H), 7.95 (s, 4H), 7.56 (d, *J* = 24 Hz, 3H). ^{13}C {^{1}H} NMR (100 MHz, DMSO-d_6): δ (ppm) 163.41 (C=O), 147.76, 145.20, 140.60, 133.02, 131.97, 128.47, 127.92, 127.70, 123.97.

(4k) 5-amino-1-benzoyl-3-(2-nitrophenyl)-1H-pyrazole-4-carbonitrile. ^{1}H NMR (400 MHz, DMSO-d_6): δ (ppm) 12.22 (s, 1H), 8.89 (s, 1H), 8.10 (d, *J* = 28 Hz, 2H), 7.95 (s, 2H), 7.81 (s, 1H), 7.67 – 7.54 (m, 4H).^{13}C {^{1}H} NMR (100 MHz, DMSO-d_6): δ (ppm) 163.32, (C=O) 148.18, 142.90, 133.65, 132.94, 131.98, 130.60, 128.69, 128.46, 127.90, 127.70, 124.61.

(4l) 4-(5-amino-1-benzoyl-4-cyano-1H-pyrazol-3-yl)-3-nitrobenzamide. ^{1}H NMR (400 MHz, DMSO-d_6): δ (ppm) 11.80 (s, 1H), 10.16 (s, 2H), 8.42 (s, 1H), 7.93 (d, *J* = 4. Hz, 2H), 7.68 (s, 4H), 7.54 (d, *J* = 20 Hz, 3H). ^{13}C {^{1}H} NMR (100 MHz, DMSO-d_6): δ (ppm) 168.57, 163.09, 147.66, 140.99, 133.46, 131.63, 128.88, 128.41, 127.78, 127.55, 118.92.

(4m) 5-amino-1-benzoyl-3-(2,5-dimethoxyphenyl)-1H-pyrazole-4-carbonitrile. ^{1}H NMR (400 MHz, DMSO-d_6): δ (ppm) 11.90 (s, 1H), 8.81 (s, 1H), 7.94 (d, *J* = 7.4 Hz, 2H), 7.59-7.50 (m, 3H), 7.40 (d, *J* = 2.3 Hz, 1H), 7.07-6.99 (m, 2H), 3.82 (s, 3H), 3.76 (s, 3H). ^{13}C {^{1}H} NMR (100 MHz, DMSO-d_6): δ (ppm) 162.94 (C=O), 153.22, 152.27, 143.12, 133.30, 131.70, 128.41, 127.58, 122.89, 117.60, 113.36, 109.13, 56.17, 55.40.

(4n) 5-amino-1-benzoyl-3-(3,4-dimethoxyphenyl)-1H-pyrazole-4-carbonitrile. ^{1}H NMR (400 MHz, DMSO-d_6): δ (ppm) 11.75 (s, 1H), 8.39 (s, 1H), 7.91 (d, *J* = 8 Hz, 2H), 7.61-7.51 (m, 3H), 7.36 (s, 1H), 7.21 (d, *J* = 8.0 Hz, 1H), 7.03 (d, *J* = 8 Hz, 1H), 3.83 (s, 3H), 3.81 (s, 3H).^{13}C {^{1}H} NMR (100 MHz, DMSO-d_6): δ (ppm) 163.00 (C=O), 150.74, 149.05, 148.03, 133.55, 131.61, 128.42, 127.52, 127.01, 121.88, 111.46, 108.22, 55.53, 55.43.

(4o) 5-amino-1-benzoyl-3-(2,6-dichlorophenyl)-1H-pyrazole-4-carbonitrile. ^{1}H NMR (400 MHz, DMSO-d_6): δ (ppm) 12.16 (s, 1H), 8.69 (s, 1H), 7.95 (d, *J* = 4 Hz, 2H), 7.61 – 7.41 (m, 6H).^{13}C {^{1}H} NMR (100 MHz, DMSO-d_6): δ (ppm) 163.23 (C=O), 143.16, 133.92, 132.99, 131.95, 131.10, 130.57, 129.04, 128.48, 127.68.

(4p) 5-amino-1-benzoyl-3-(naphthalen-2-yl)-1H-pyrazole-4-carbonitrile. ^{1}H NMR (400 MHz, DMSO-d_6): δ (ppm) 11.99 (s, 1H), 9.16 (s, 1H), 8.90 (s, 1H), 8.01 (s, 4H), 7.59 (s, 7H). ^{13}C {^{1}H} NMR (100 MHz, DMSO-d_6): δ (ppm) 163.12, 147.68, 133.53, 133.40, 131.79, 130.53, 130.23, 129.57, 128.76, 128.50, 127.71, 127.61, 127.30, 126.24, 125.53, 124.19.

(4q) 5-amino-1-(4-chlorobenzoyl)-3-phenyl-1H-pyrazole-4-carbonitrile. ^{1}H NMR (400 MHz, DMSO-d_6): δ (ppm) δ ^{1}H NMR (400 MHz, DMSO) δ 11.93 (s, 1H), 8.47 (s, 1H), 7.96 (d, *J* = 8 Hz, 2H), 7.74 (s, 2H), 7.60 (d, *J* = 8 Hz, 2H), 7.45 (s, 3H). ^{13}C {^{1}H} NMR (100

MHz, DMSO-d_6): δ (ppm) 167.34, 153.40, 141.85, 139.46, 137.32, 135.40, 134.79, 134.07, 133.81, 132.38.

(4r) 5-amino-1-(4-methoxybenzoyl)-3-(p-tolyl)-1H-pyrazole-4-carbonitrile. ^{1}H NMR (400 MHz, DMSO-d_6): δ (ppm) δ ^{1}H NMR (400 MHz, DMSO) δ 11.69 (s, 1H), 8.42 (s, 1H), 7.92 (d, *J* = 8 Hz, 2H), 7.62 (d, *J* = 8 Hz, 2H), 7.26 (d, *J* = 4 Hz, 2H), 7.06 (d, *J* = 12 Hz, 2H), 3.83 (s, 3H), 2.33 (s, 3H). ^{13}C {^{1}H} NMR (100 MHz, DMSO-d_6): δ (ppm) 162.52, 161.96, 147.25, 139.71, 131.70, 129.48, 129.39, 126.96, 125.45, 113.67, 55.36, 20.97.

(4s) 5-amino-3-(4-chlorophenyl)-1-(4-methoxybenzoyl)-1H-pyrazole-4-carbonitrile. ^{1}H NMR (400 MHz, DMSO-d_6): δ (ppm) δ ^{1}H NMR (400 MHz, DMSO) δ 11.81 (s, 1H), 8.44 (s, 1H), 7.92 (s, 2H), 7.73 (s, 2H), 7.55 (s, 2H), 7.05 (d, *J* = 8 Hz, 2H), 3.82 (s, 3H). ^{13}C {^{1}H} NMR (100 MHz, DMSO-d_6): δ (ppm) 162.61, 162.03, 145.80, 134.33, 133.36, 130.19, 129.55, 128.84, 128.55, 125.28, 113.67, 55.35.

NMR spectra for pyrazole products

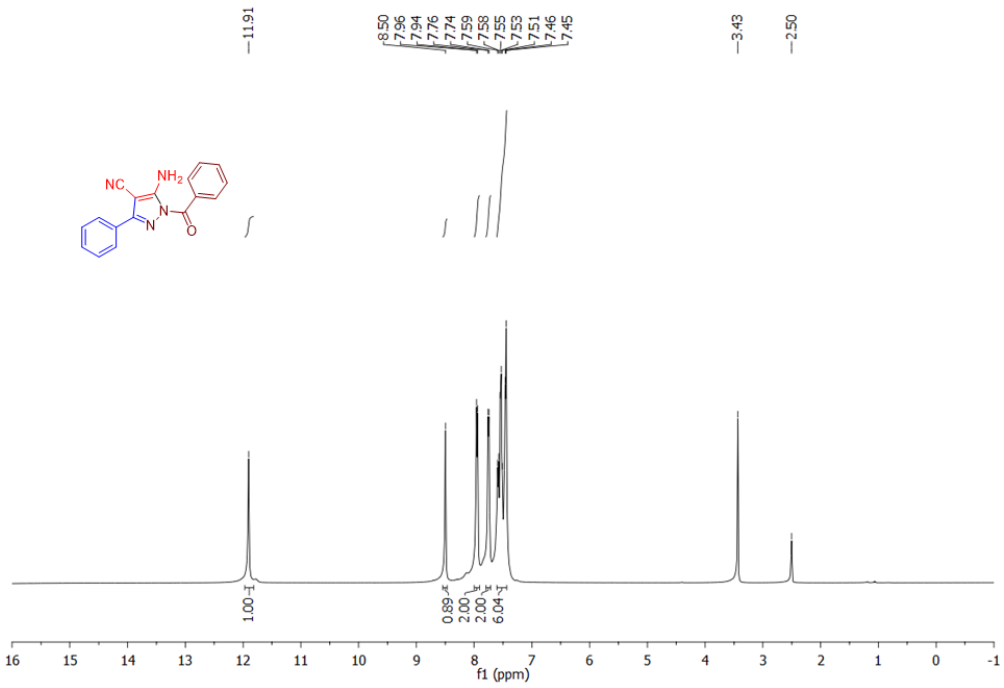

Figure 9: ^{1}H NMR spectrum for (**4a**) in DMSO-d_6 (400MHz, 300K).

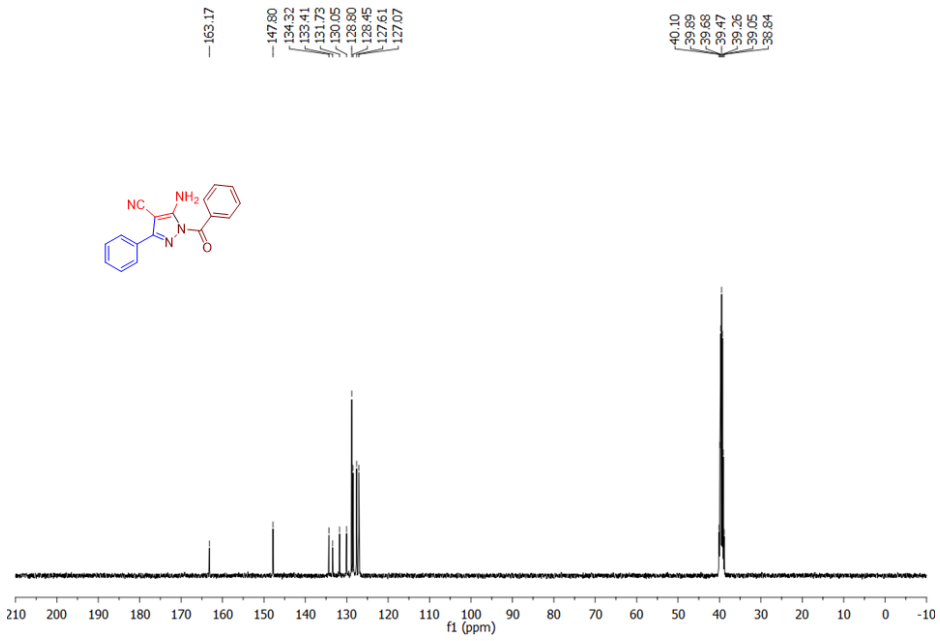

Figure 10: ^{13}C NMR spectrum (**4a**) in DMSO-d_6 (100MHz, 300K).

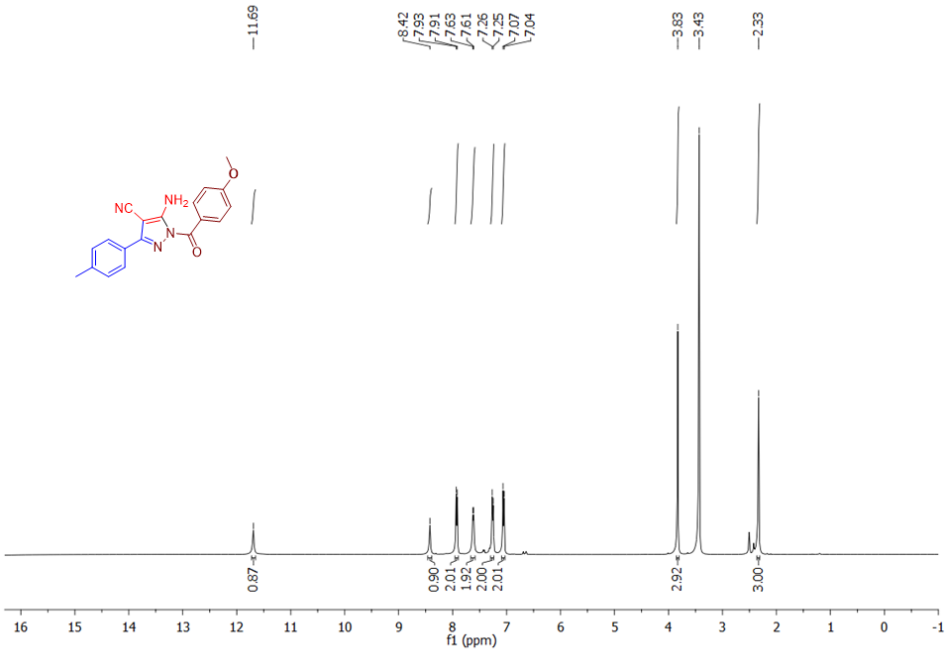

Figure 11: ^{1}H NMR spectrum for (**4b**) in DMSO-d_6 (400MHz, 300K).

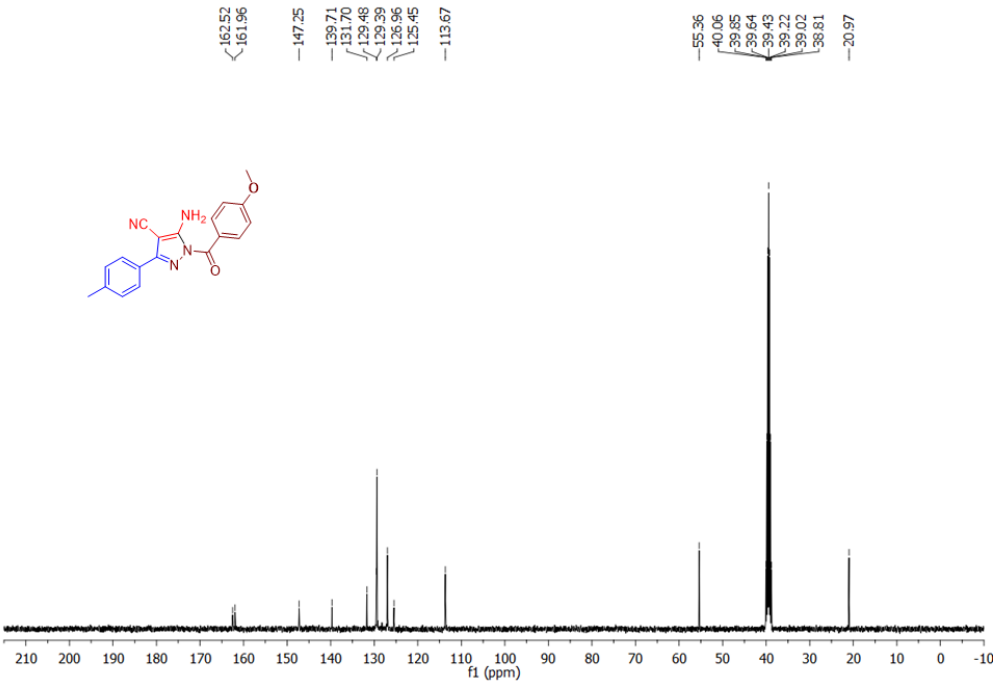

Figure 12: ^{13}C NMR spectrum (**4b**) in DMSO-d_6 (100MHz, 300K).

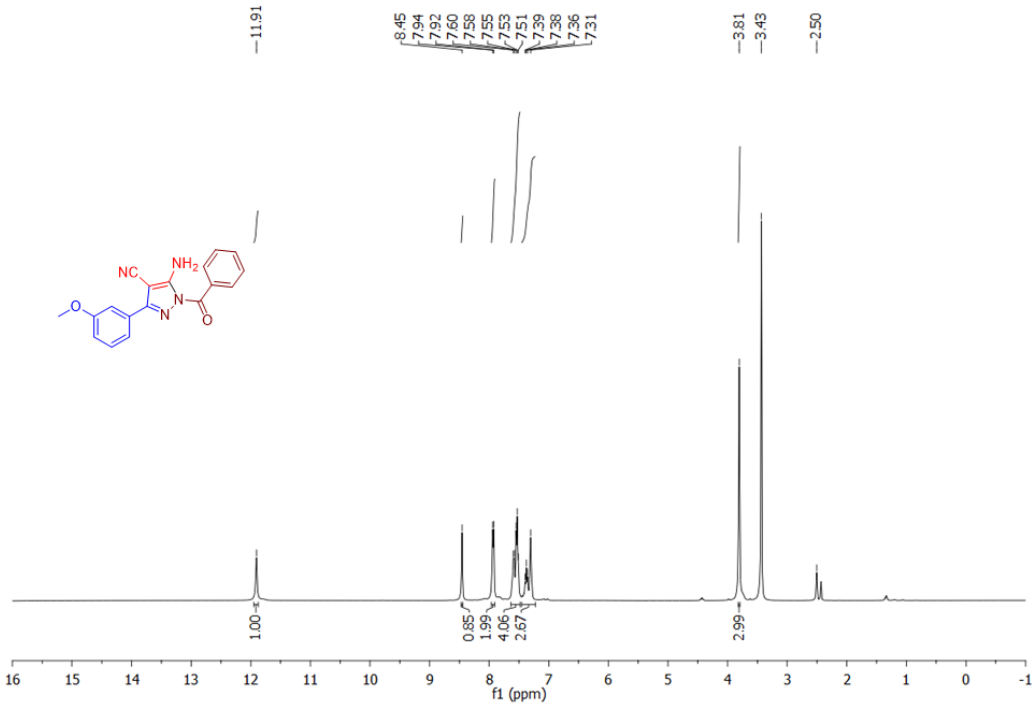

Figure 13: ^{1}H NMR spectrum for (**4c**) in DMSO-d_6 (400MHz, 300K).

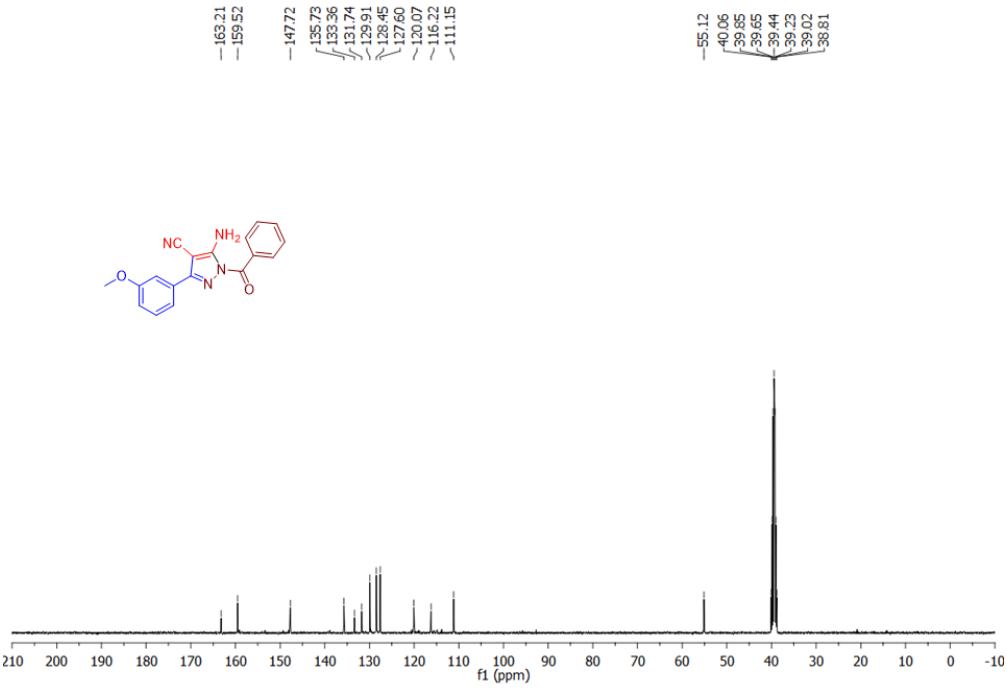

Figure 14: ^{13}C NMR spectrum (**4c**) in DMSO-d_6 (100MHz, 300K).

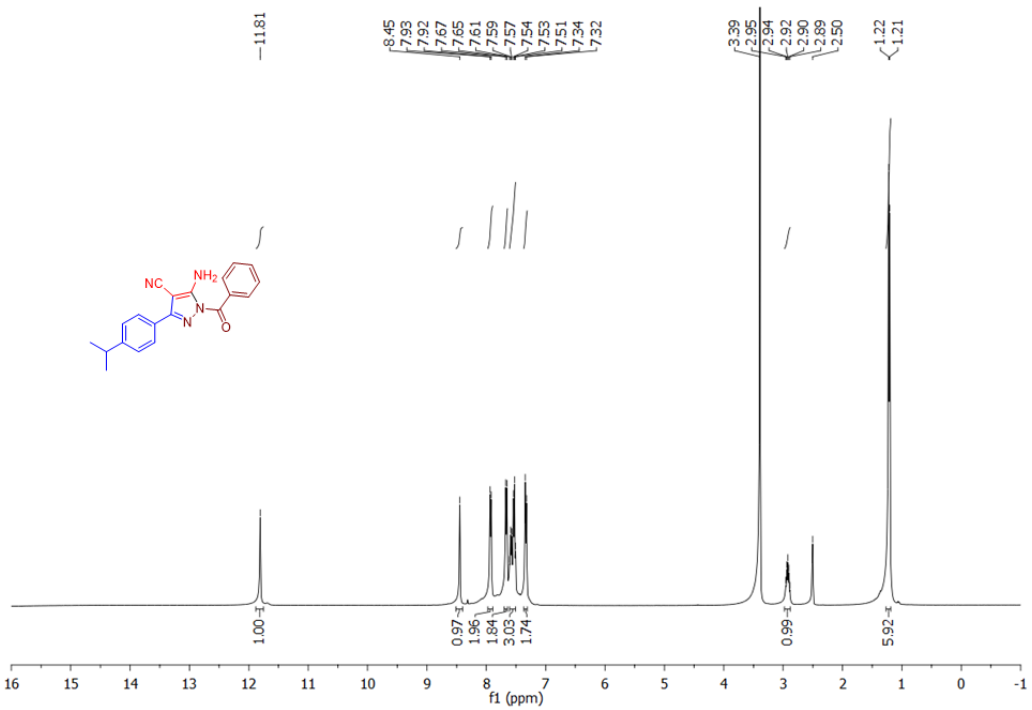

Figure 15: ^{1}H NMR spectrum for (**4d**) in DMSO-d_6 (400MHz, 300K).

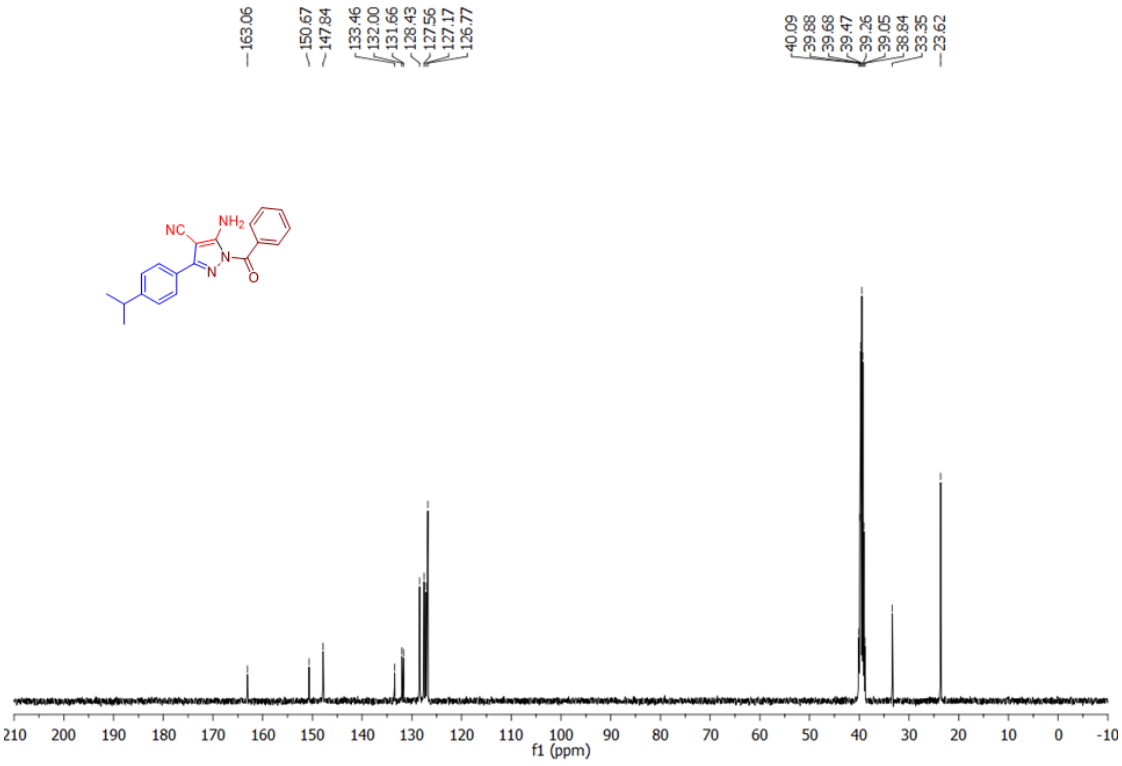

Figure 16: ^{13}C NMR spectrum (**4d**) in DMSO-d_6 (100MHz, 300K).

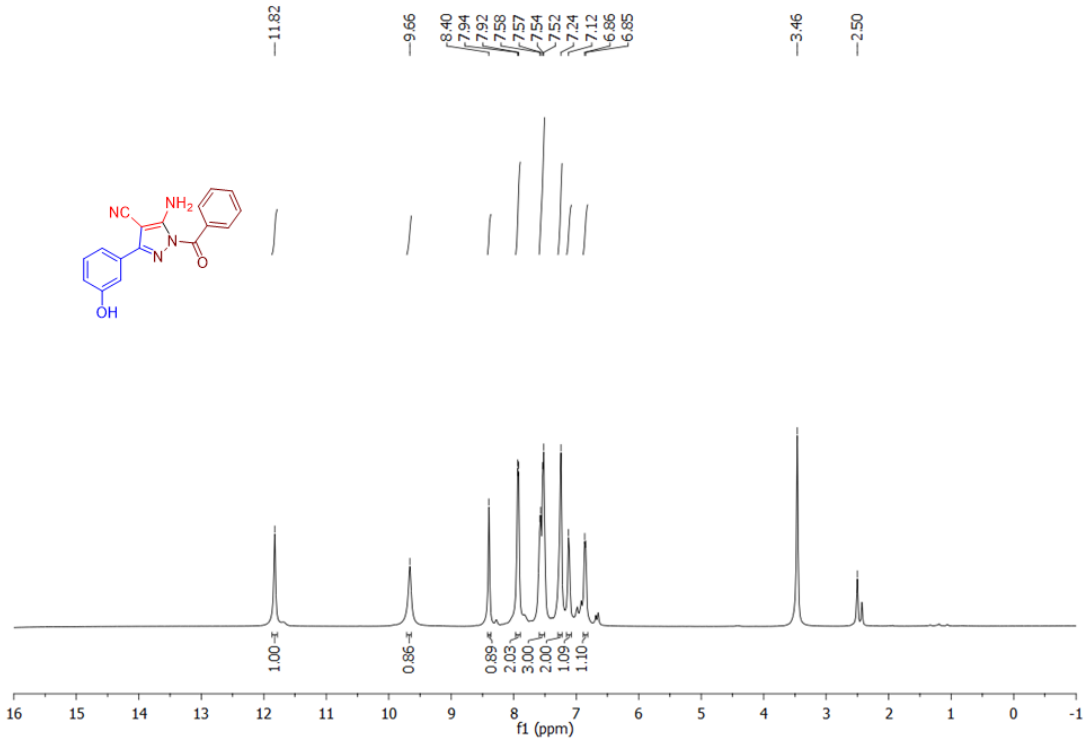

Figure 17: ^{1}H NMR spectrum for (**4e**) in DMSO-d_6 (400MHz, 300K).

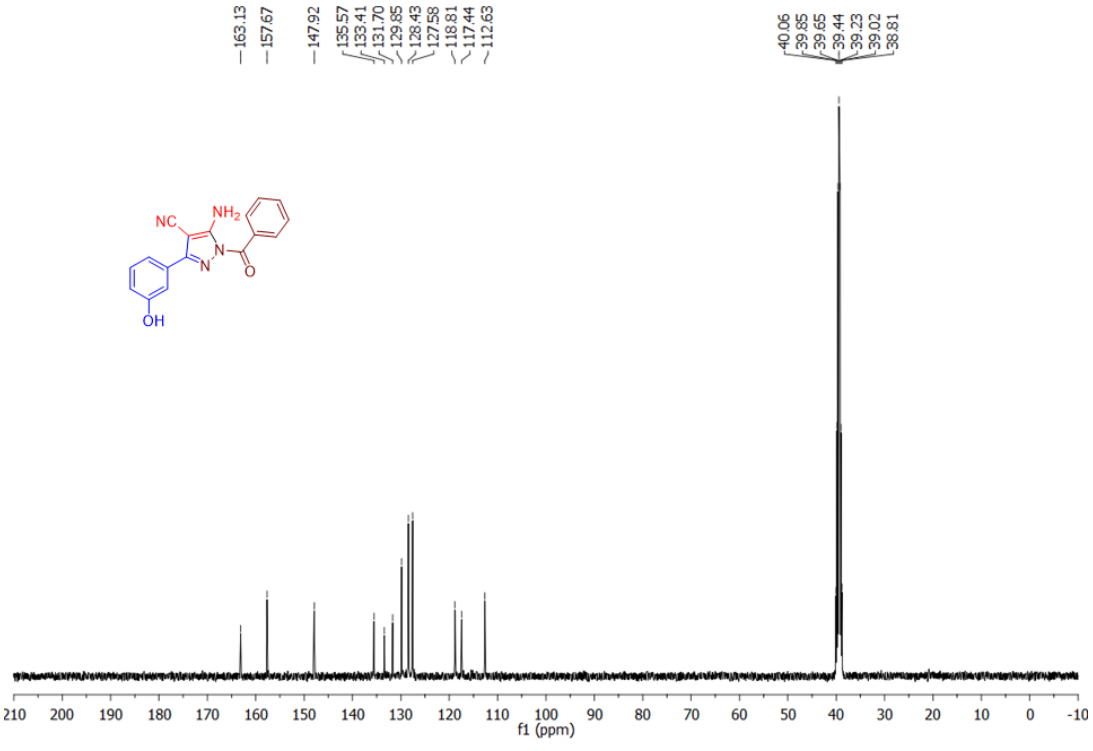

Figure 18: ^{13}C NMR spectrum (**4e**) in DMSO-d_6 (100MHz, 300K).

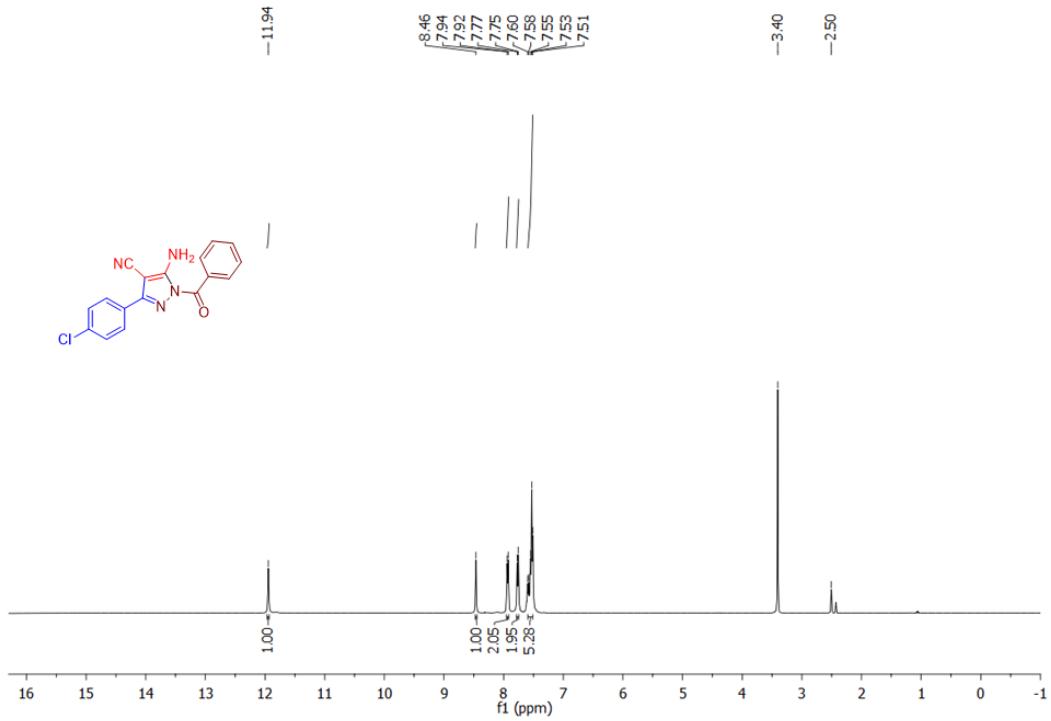

Figure 19: ^{1}H NMR spectrum for (**4f**) in DMSO-d_6 (400MHz, 300K).

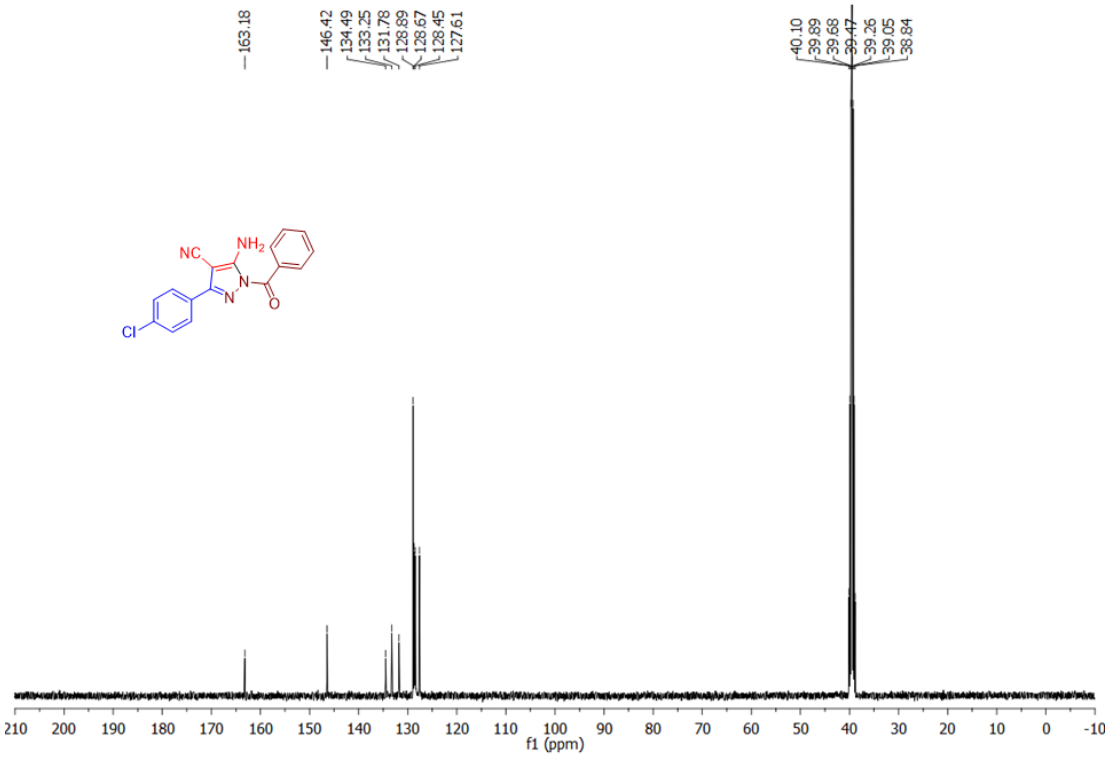

Figure 20: ^{13}C NMR spectrum (**4f**) in DMSO-d_6 (100MHz, 300K).

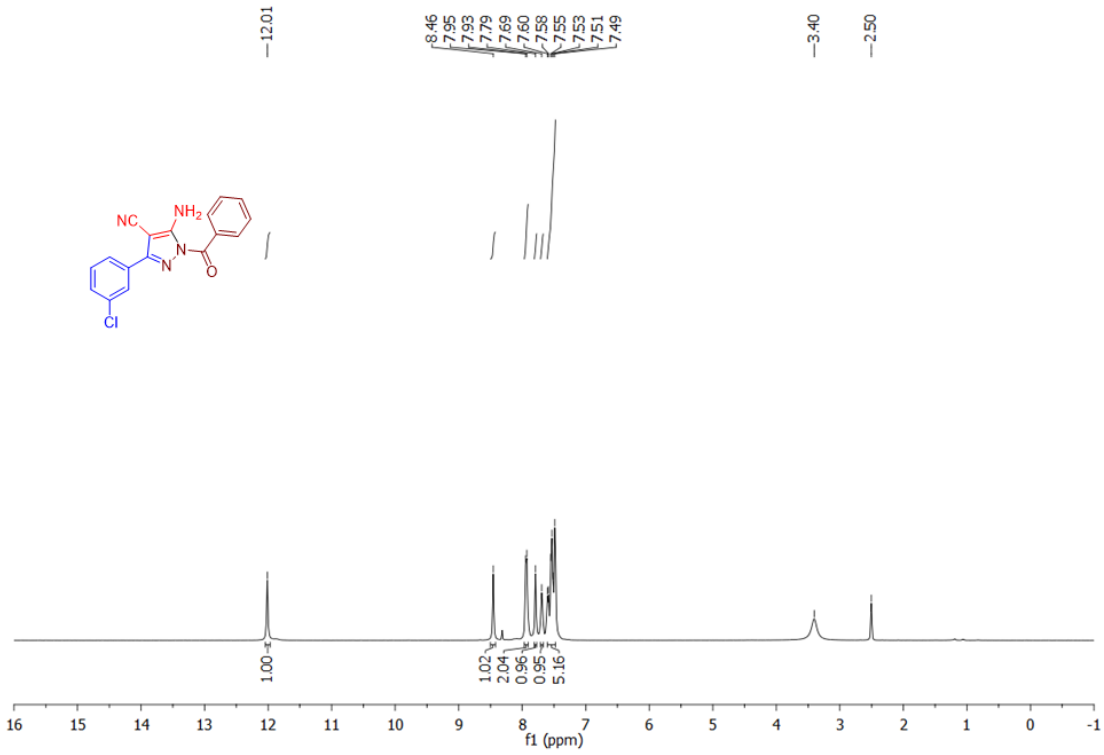

Figure 21: ^{1}H NMR spectrum for (**4g**) in DMSO-d_6 (400MHz, 300K).

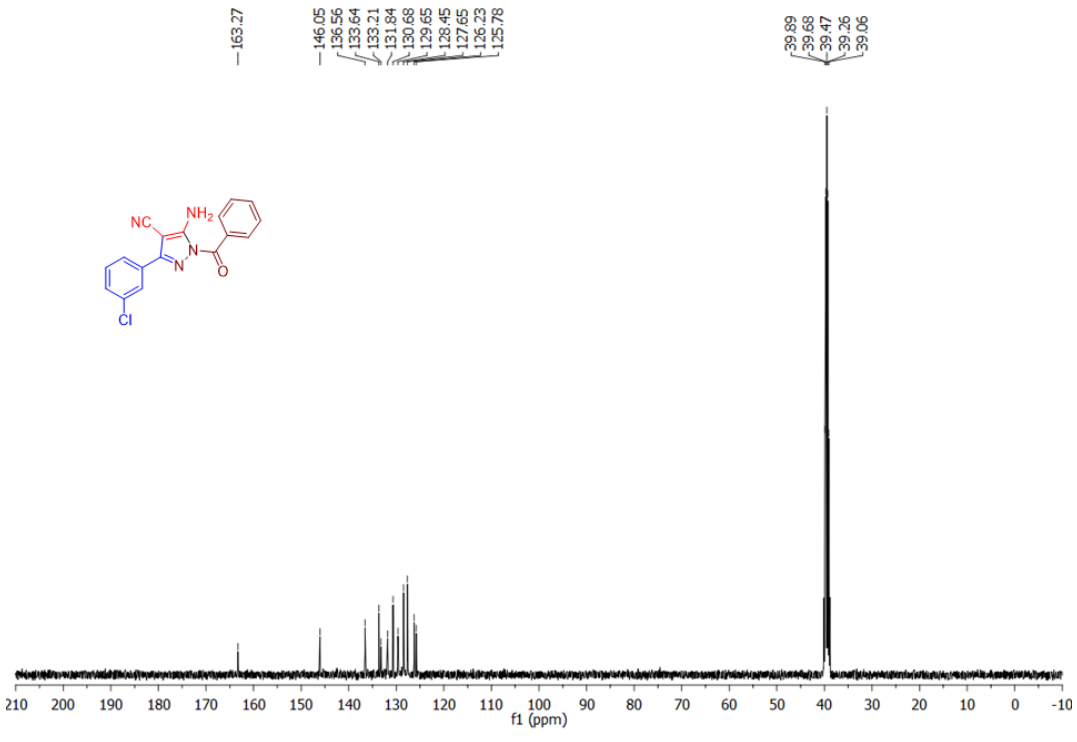

Figure 22: ^{13}C NMR spectrum (**4g**) in DMSO-d_6 (100MHz, 300K).

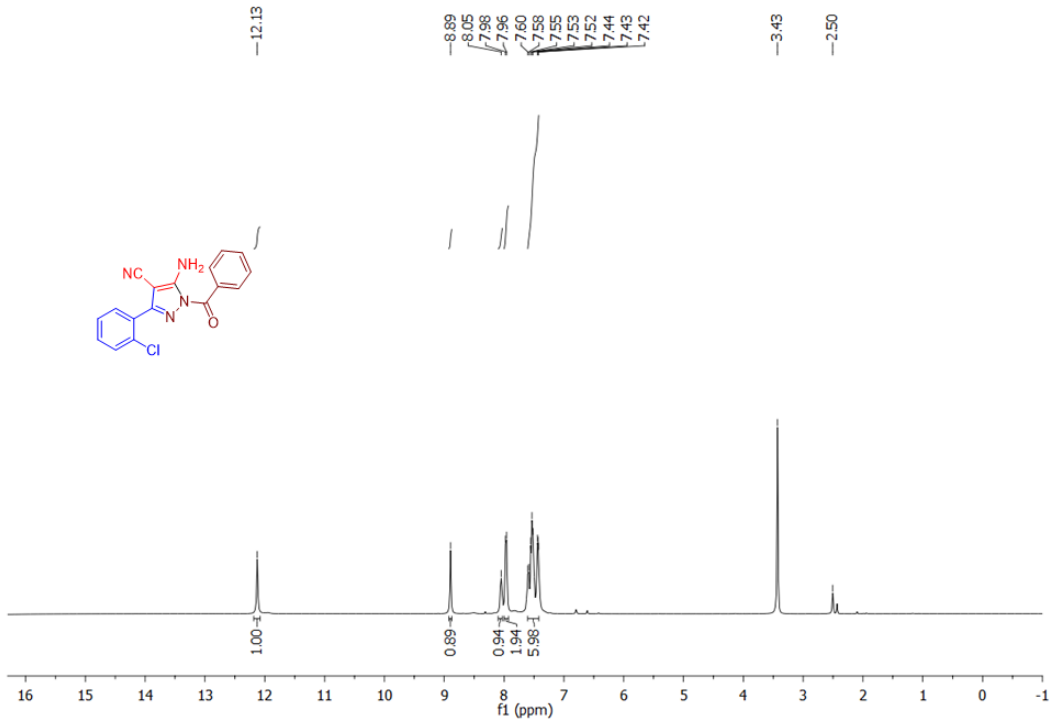

Figure 23: ^{1}H NMR spectrum for (**4h**) in DMSO-d_6 (400MHz, 300K).

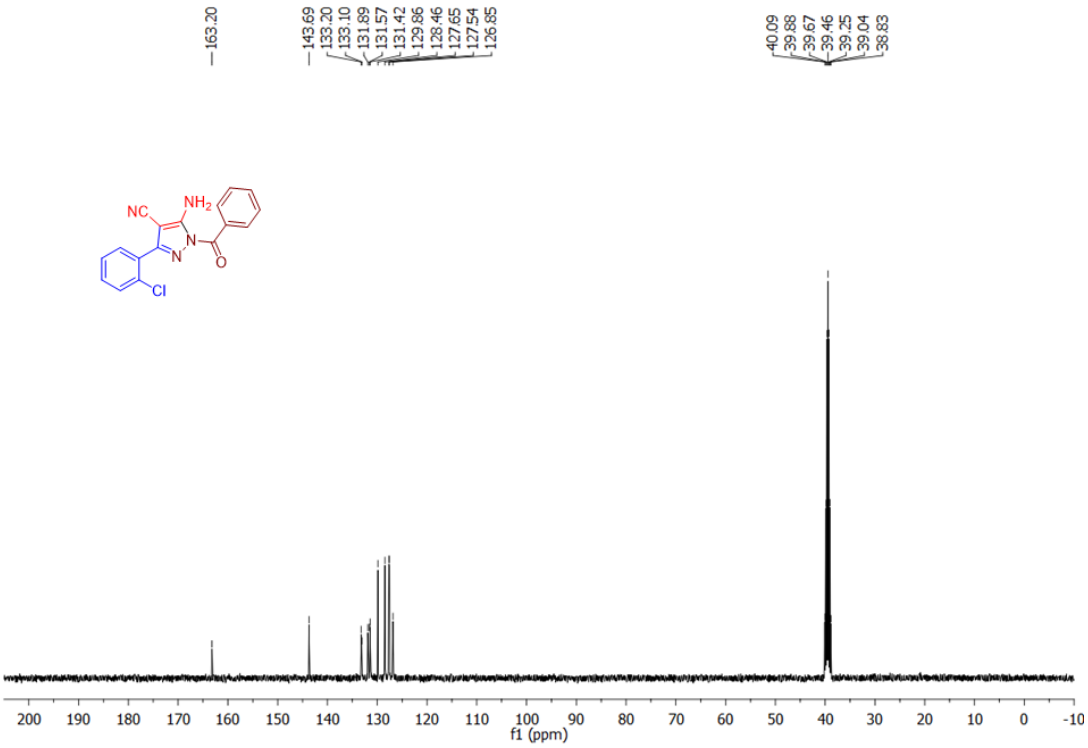

Figure 24: ^{13}C NMR spectrum (**4h**) in DMSO-d_6 (100MHz, 300K).

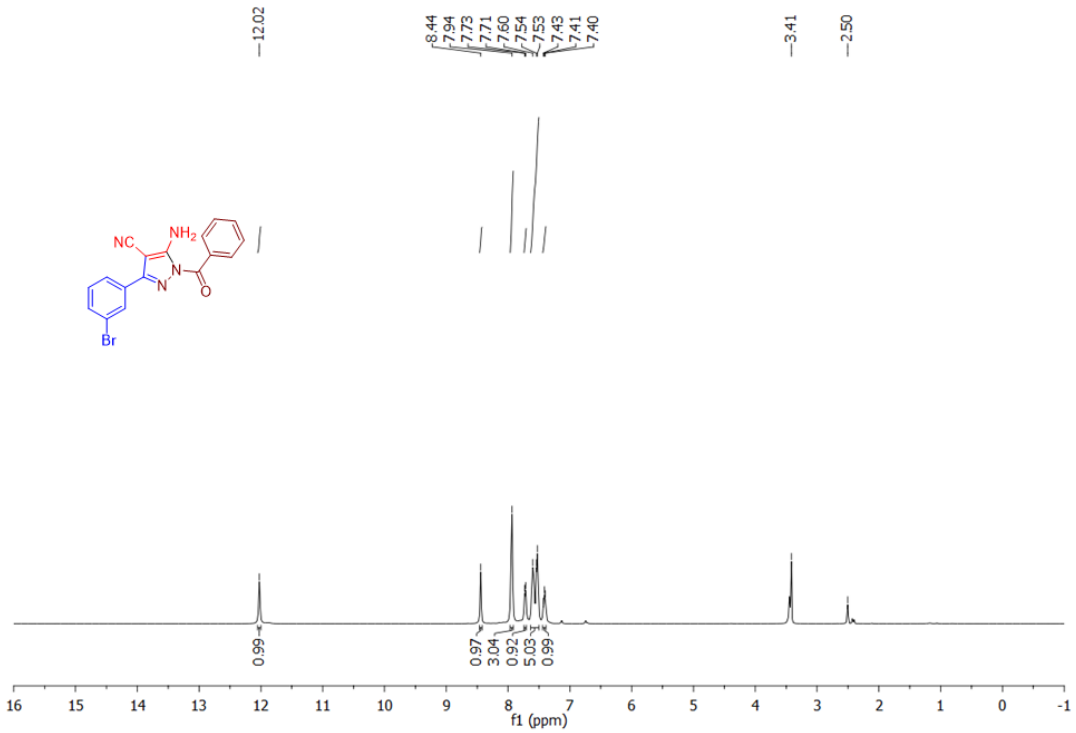

Figure 25: ^{1}H NMR spectrum for (**4i**) in DMSO-d_6 (400MHz, 300K).

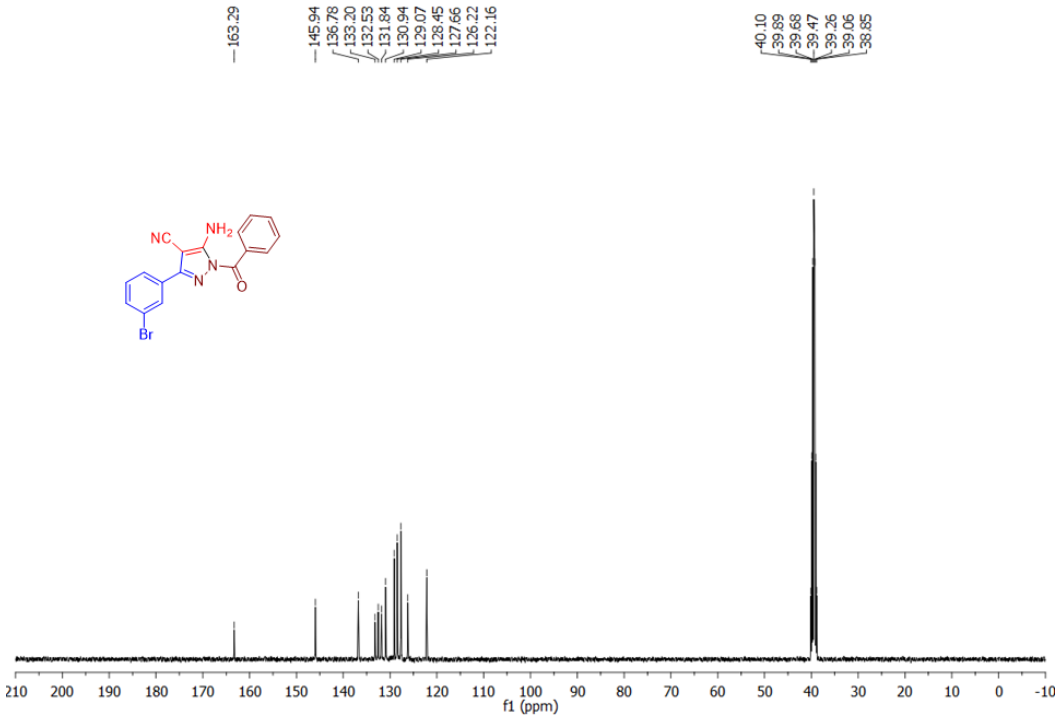

Figure 26: ^{13}C NMR spectrum (**4i**) in DMSO-d_6 (100MHz, 300K).

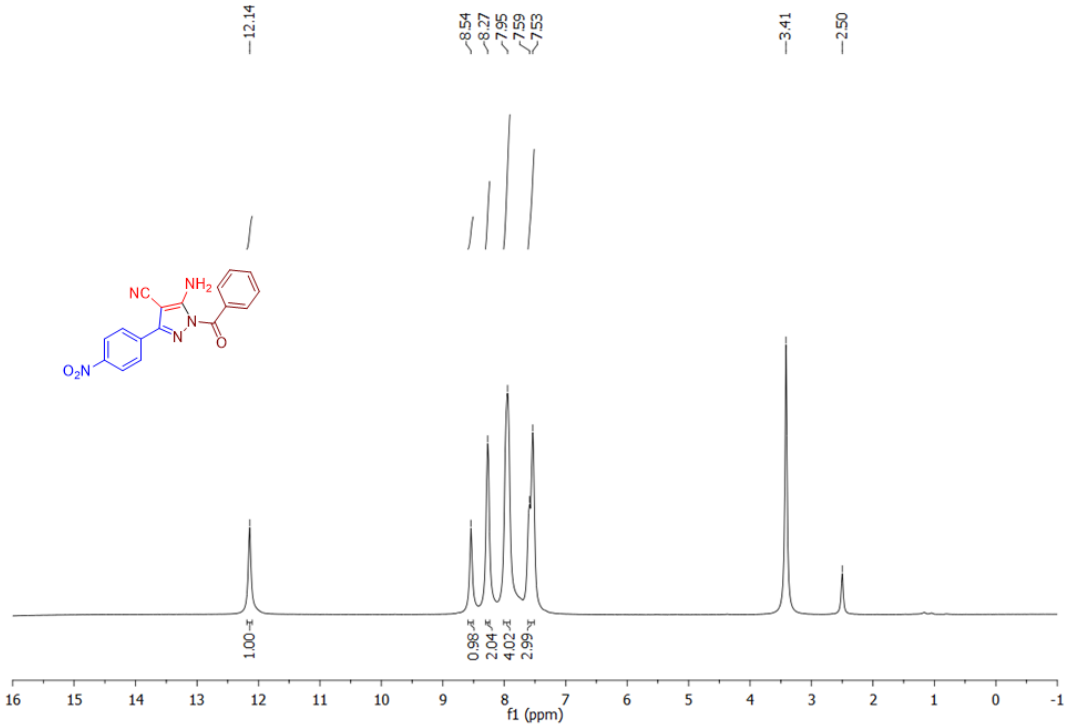

Figure 27: ^{1}H NMR spectrum for (**4j**) in DMSO-d_6 (400MHz, 300K).

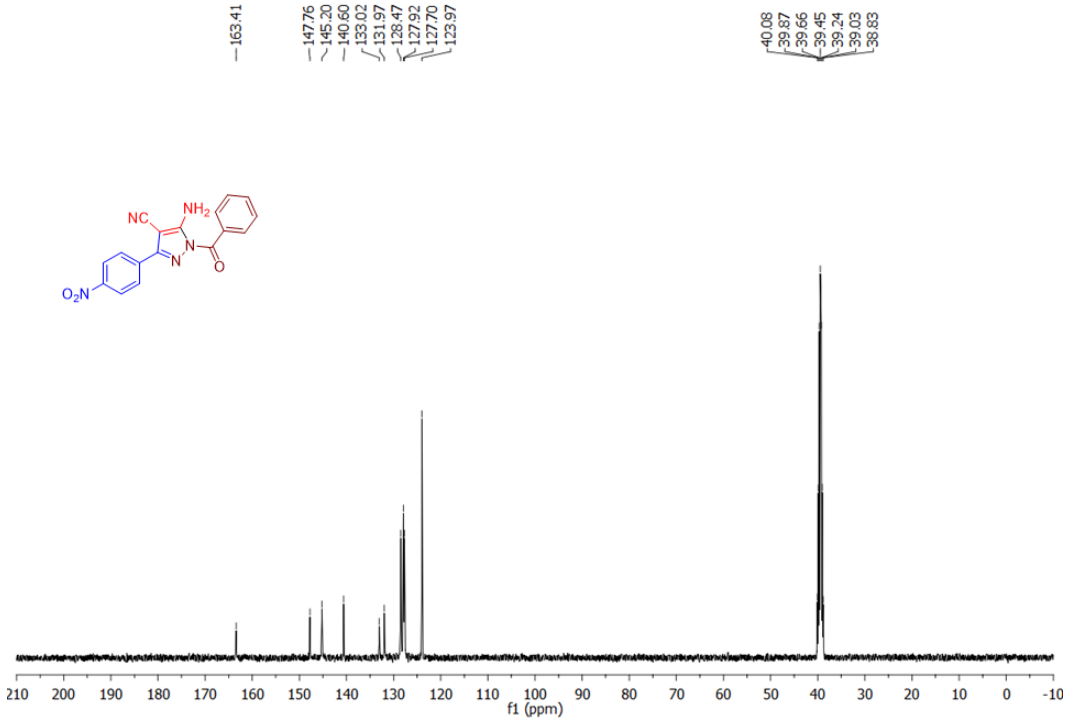

Figure 28: ^{13}C NMR spectrum (**4j**) in DMSO-d_6 (100MHz, 300K).

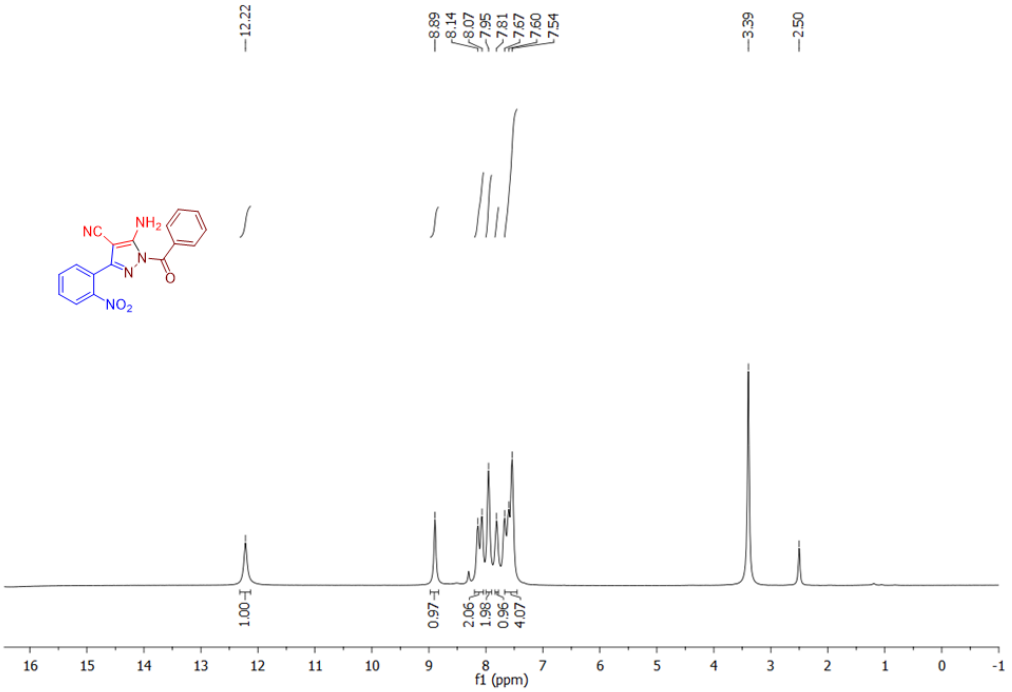

Figure 29: ^{1}H NMR spectrum for (**4k**) in DMSO-d_6 (400MHz, 300K).

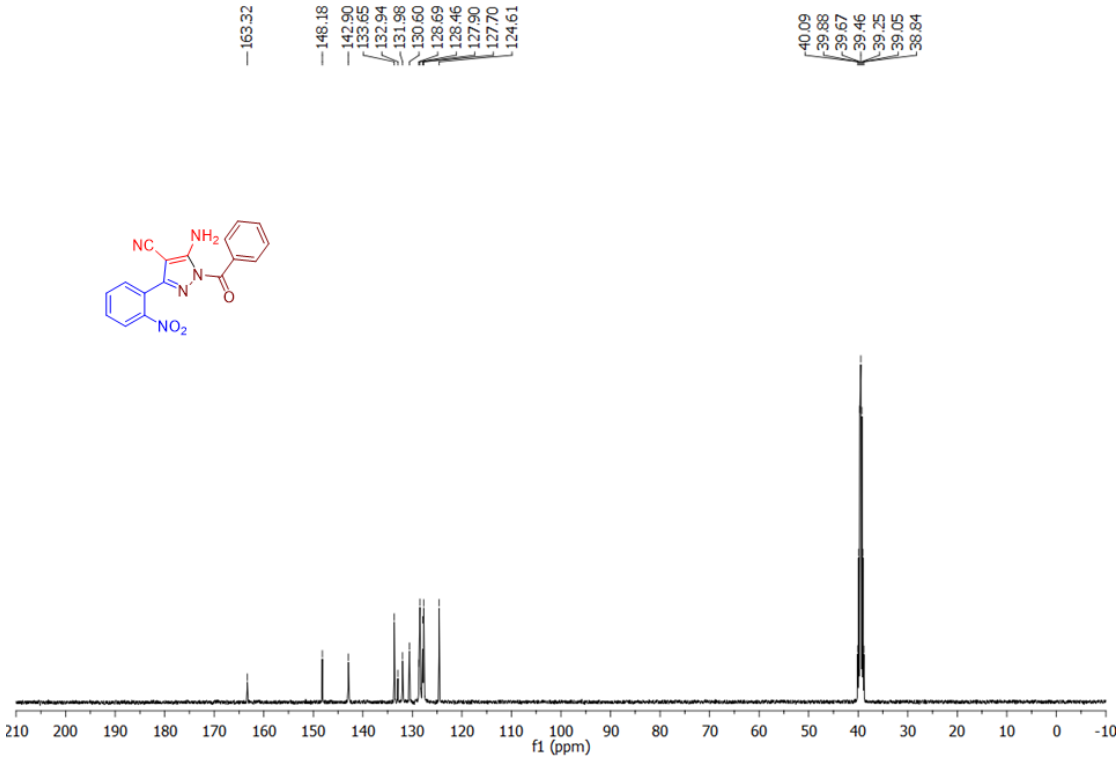

Figure 30: ^{13}C NMR spectrum (**4k**) in DMSO-d_6 (100MHz, 300K).

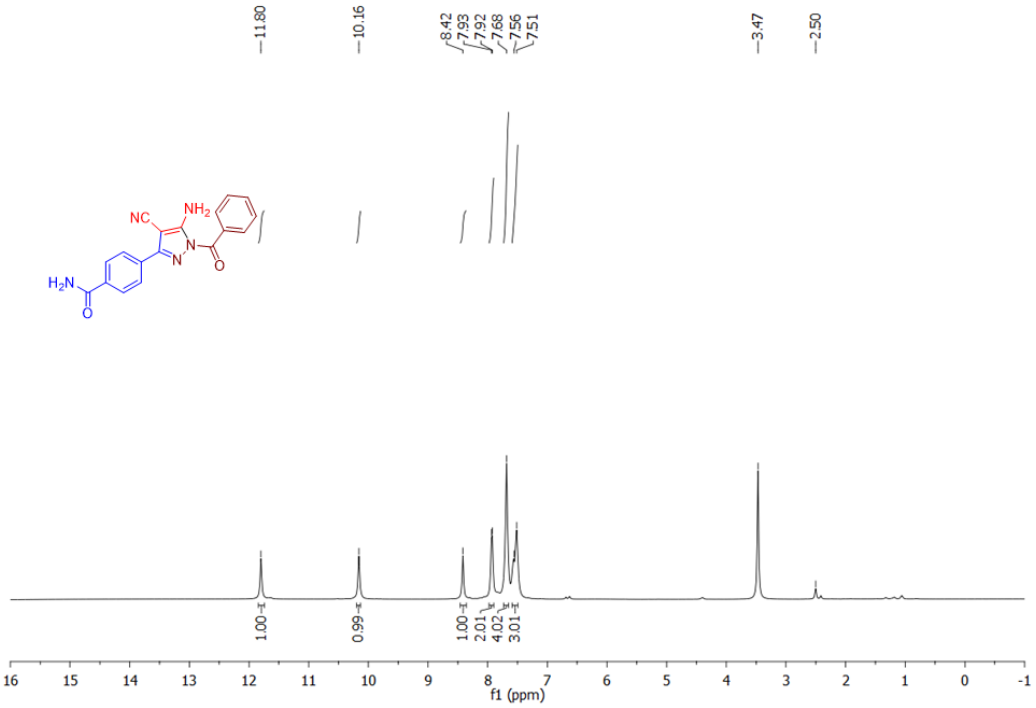

Figure 31: ^{1}H NMR spectrum for (**4l**) in DMSO-d_6 (400MHz, 300K).

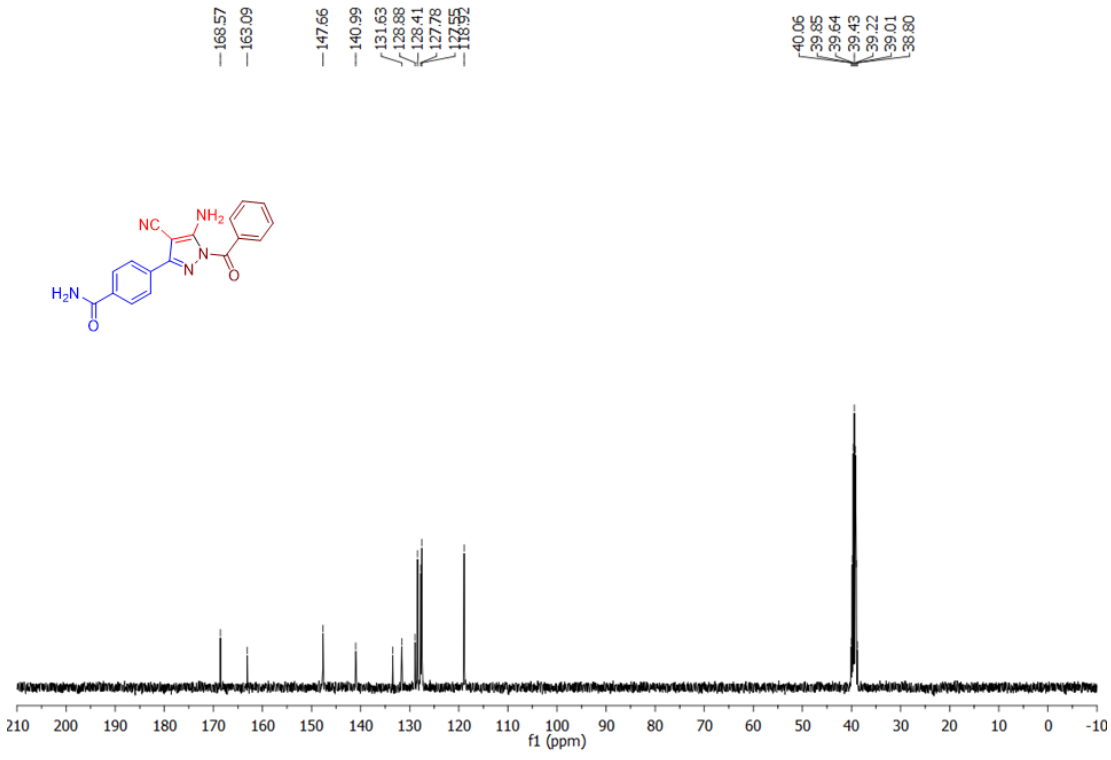

Figure 32: ^{13}C NMR spectrum (**4l**) in DMSO-d_6 (100MHz, 300K).

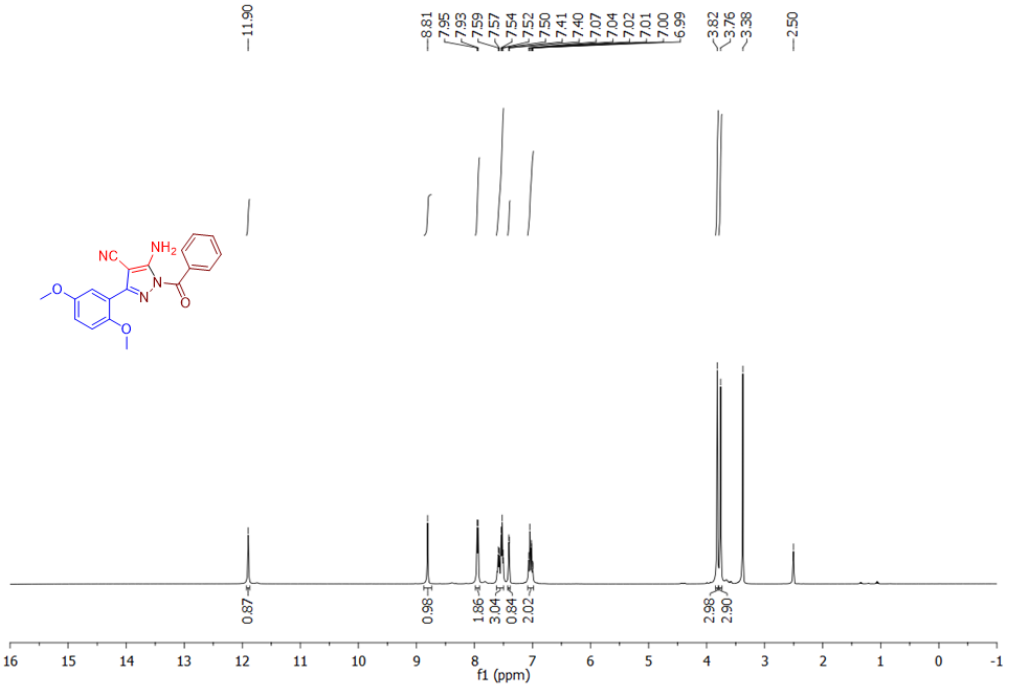

Figure 33: ^{1}H NMR spectrum for (**4m**) in DMSO-d_6 (400MHz, 300K).

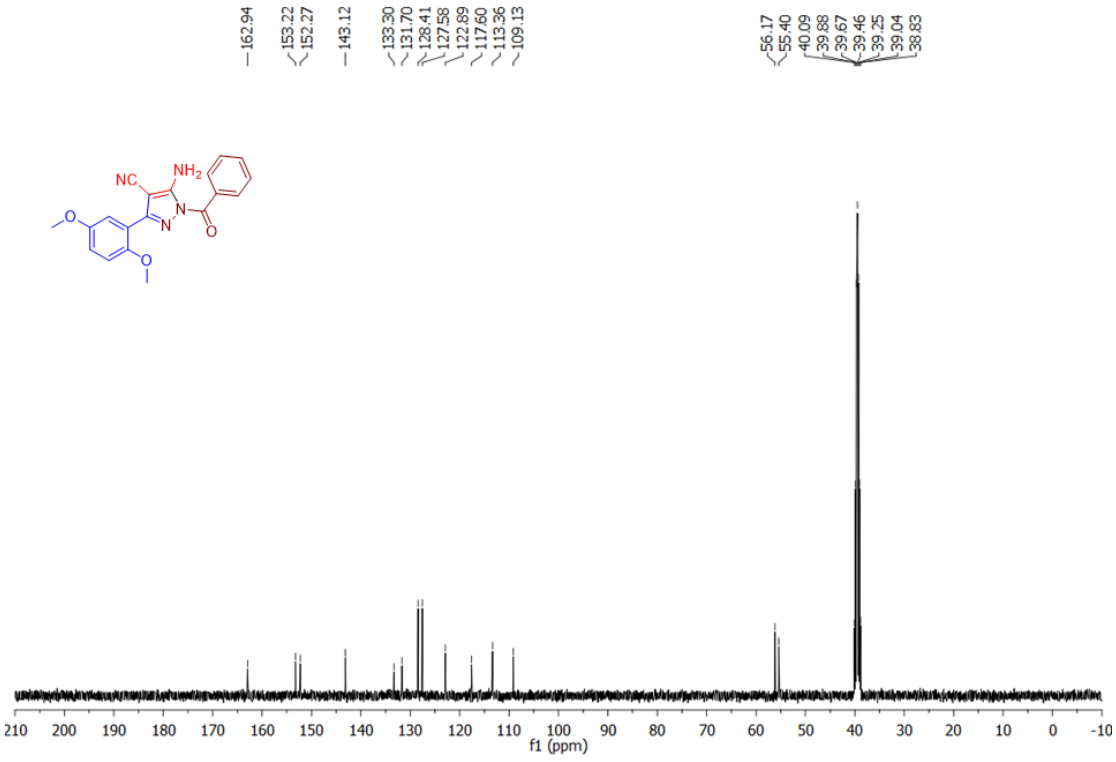

Figure 34: ^{13}C NMR spectrum (**4m**) in DMSO-d_6 (100MHz, 300K).

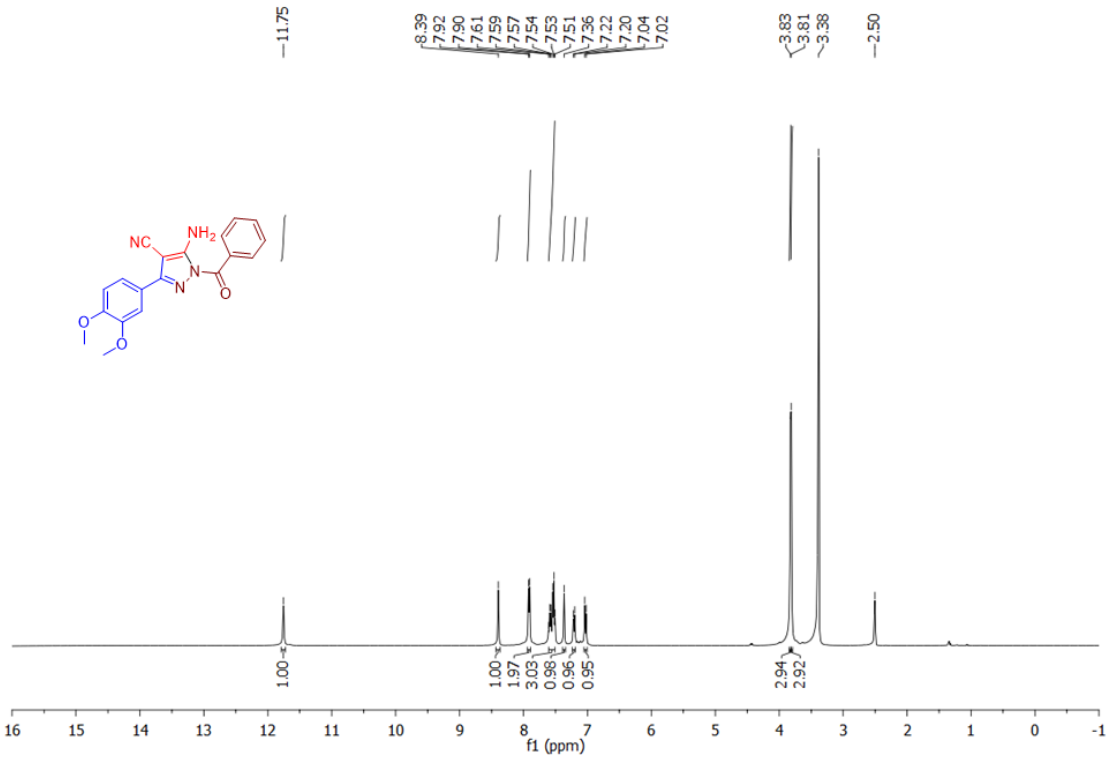

Figure 35: ^{1}H NMR spectrum for (**4n**) in DMSO-d_6 (400MHz, 300K).

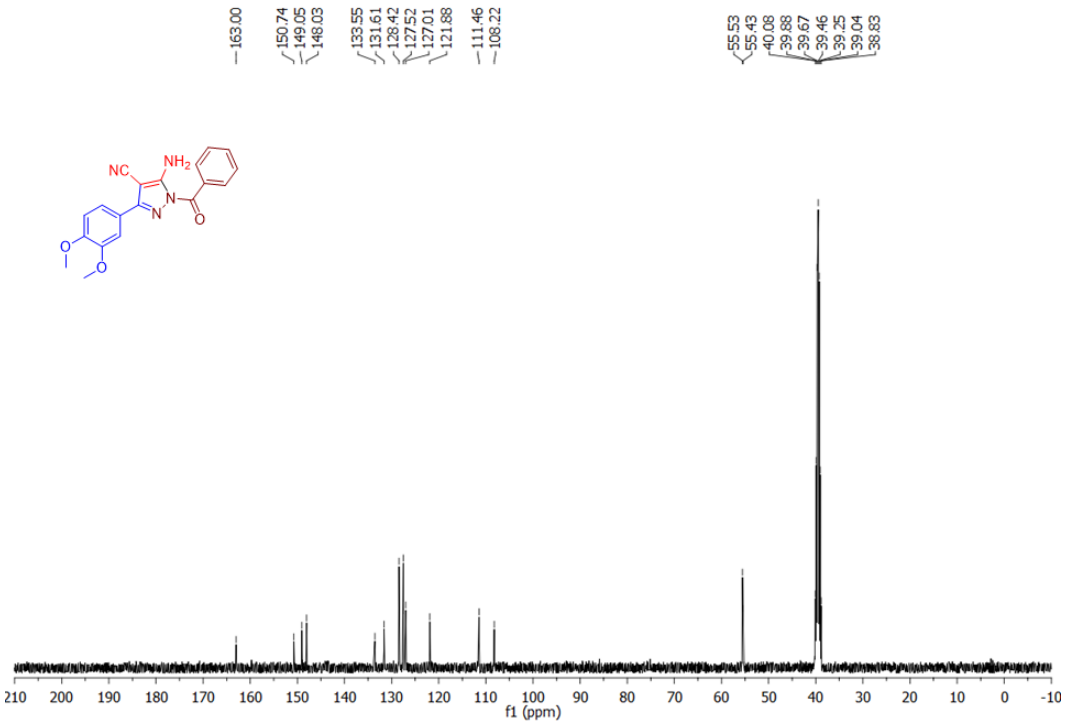

Figure 36: ^{13}C NMR spectrum (**4n**) in DMSO-d_6 (100MHz, 300K).

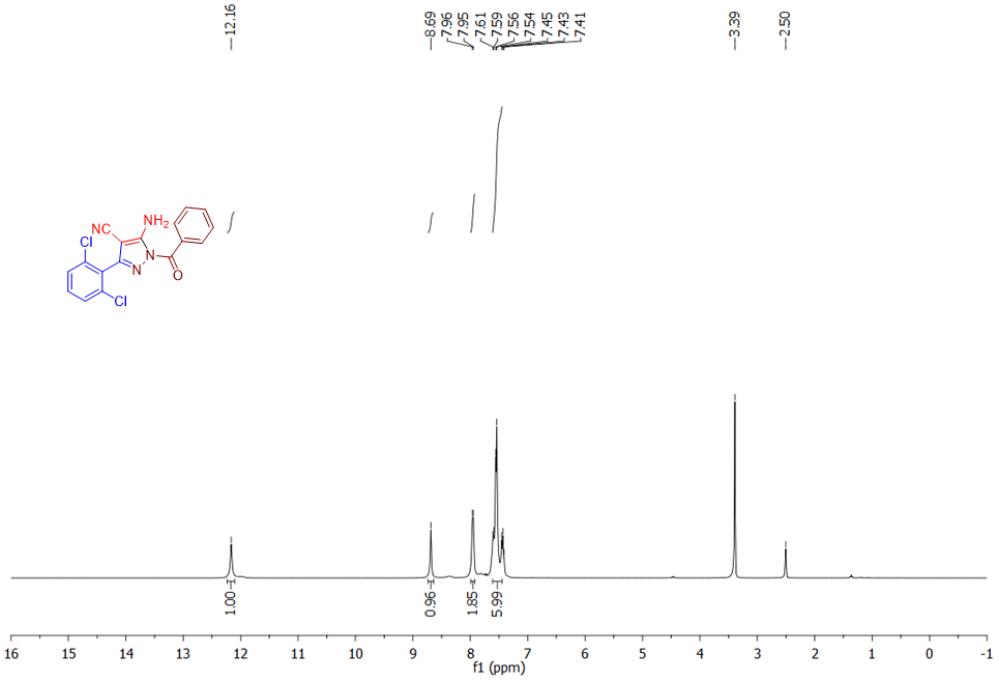

Figure 37: ^{1}H NMR spectrum for (**4o**) in DMSO-d_6 (400MHz, 300K).

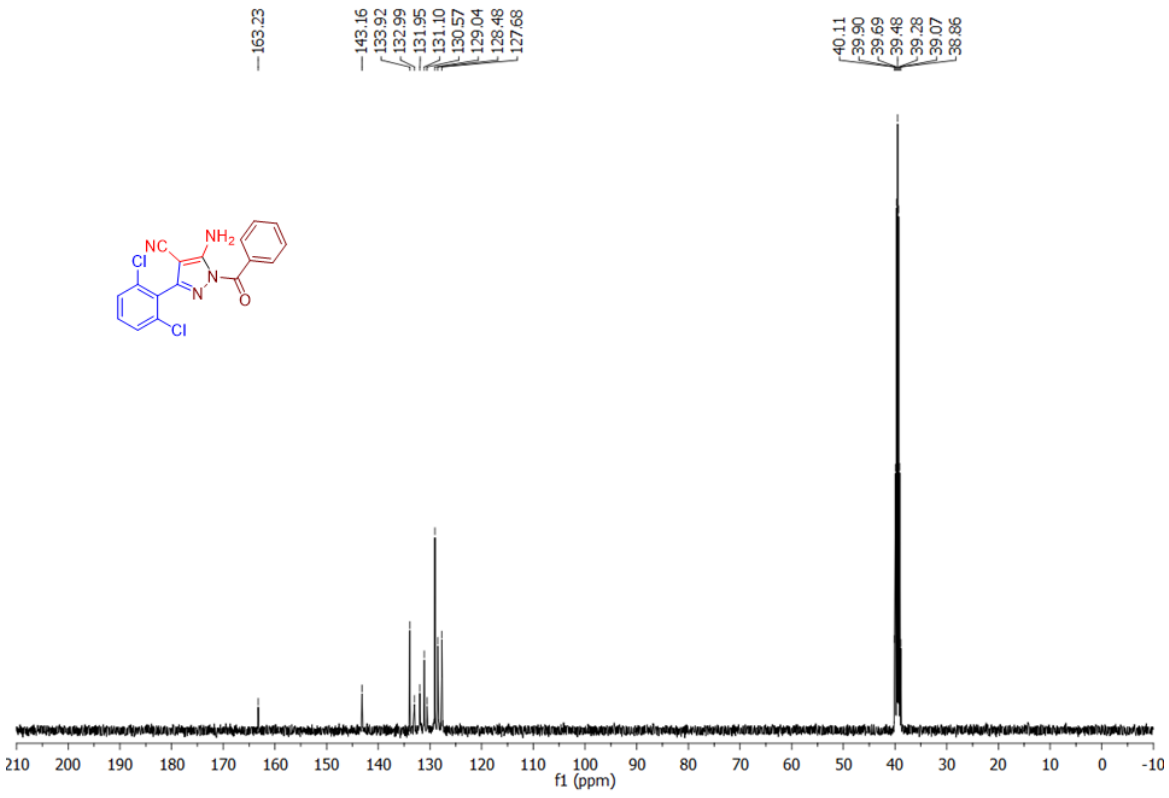

Figure 38: ^{13}C NMR spectrum (**4o**) in DMSO-d_6 (100MHz, 300K).

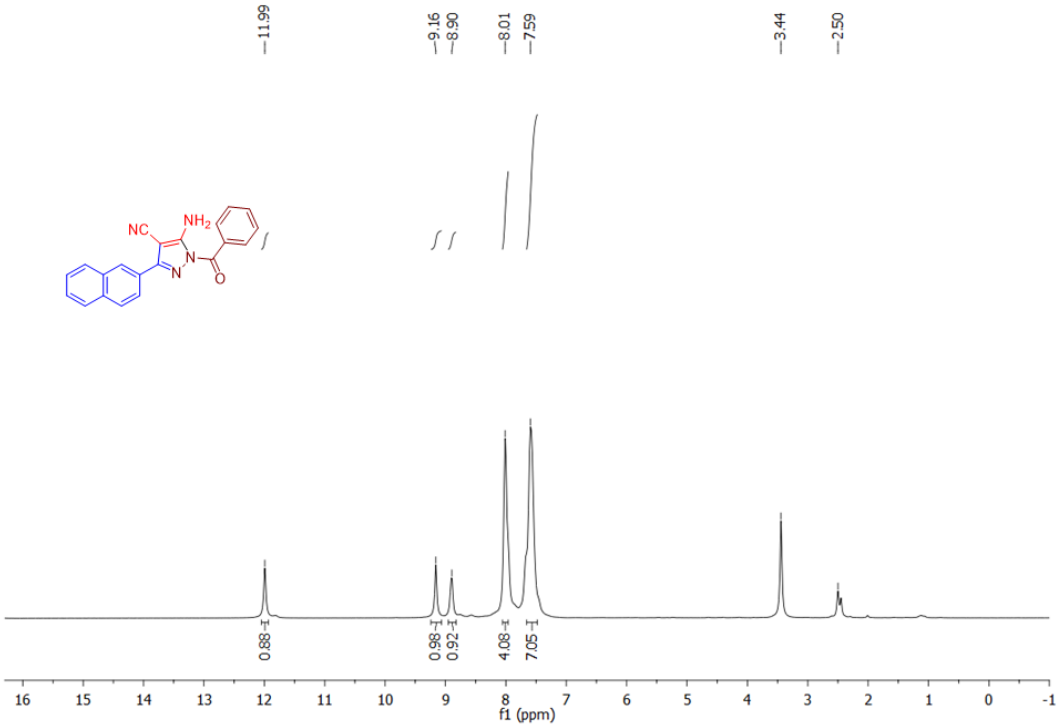

Figure 39: ^{1}H NMR spectrum for (**4p**) in DMSO-d_6 (400MHz, 300K).

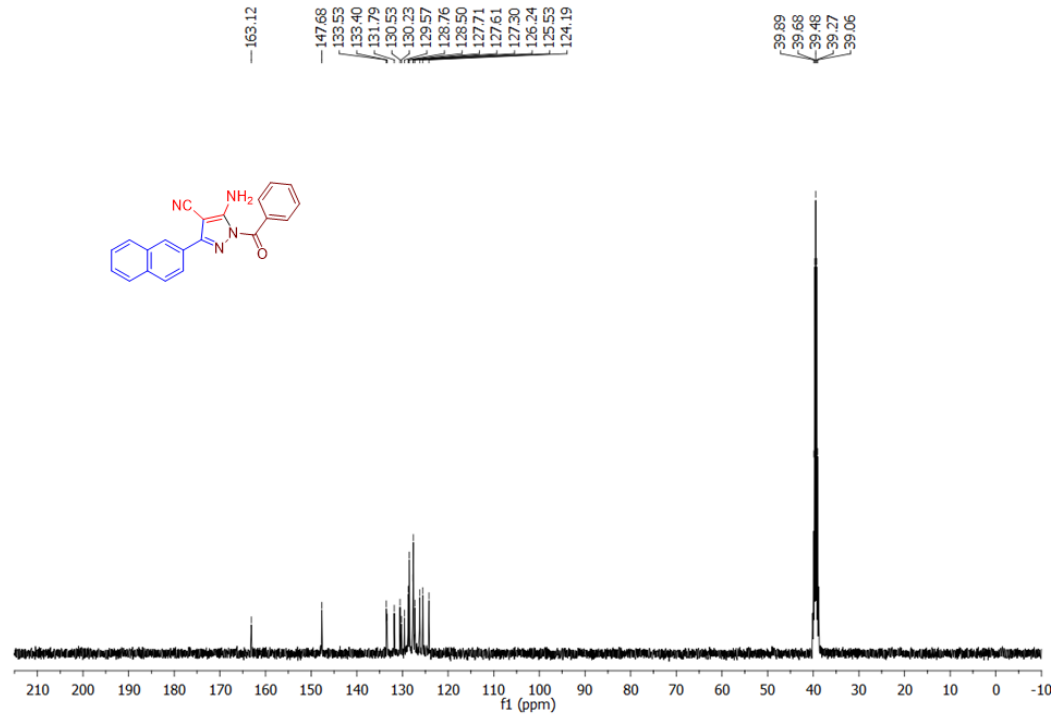

Figure 40: ^{13}C NMR spectrum (**4p**) in DMSO-d_6 (100MHz, 300K).

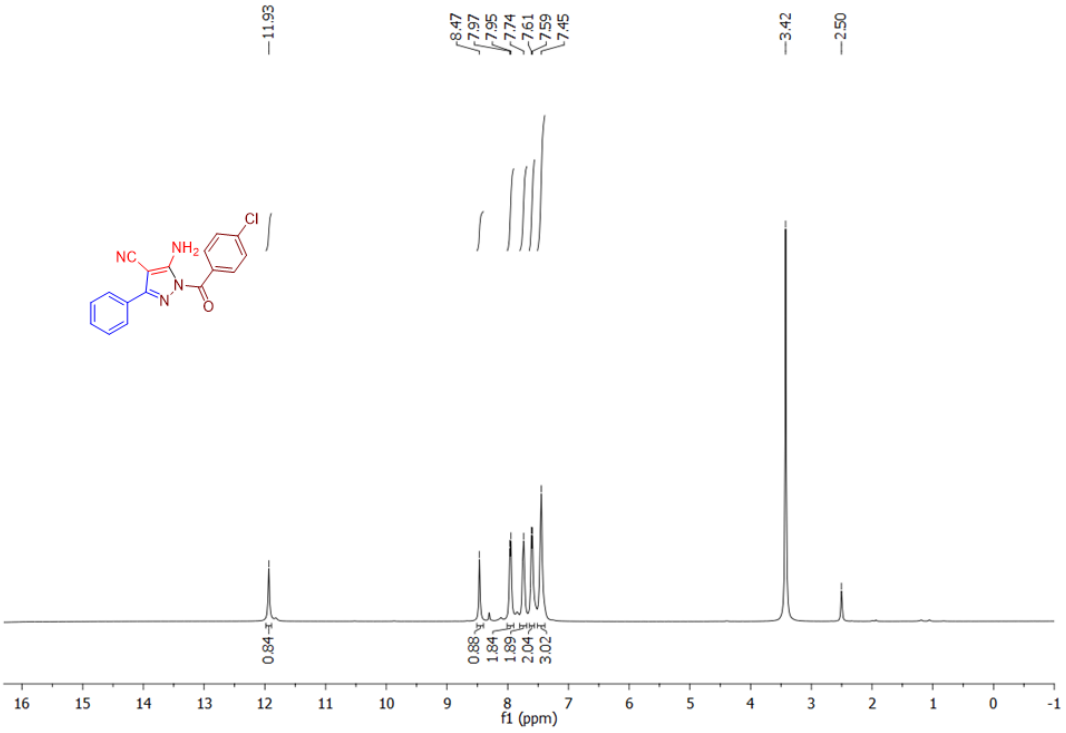

Figure 41: ^{1}H NMR spectrum for (**4q**) in DMSO-d_6 (400MHz, 300K).

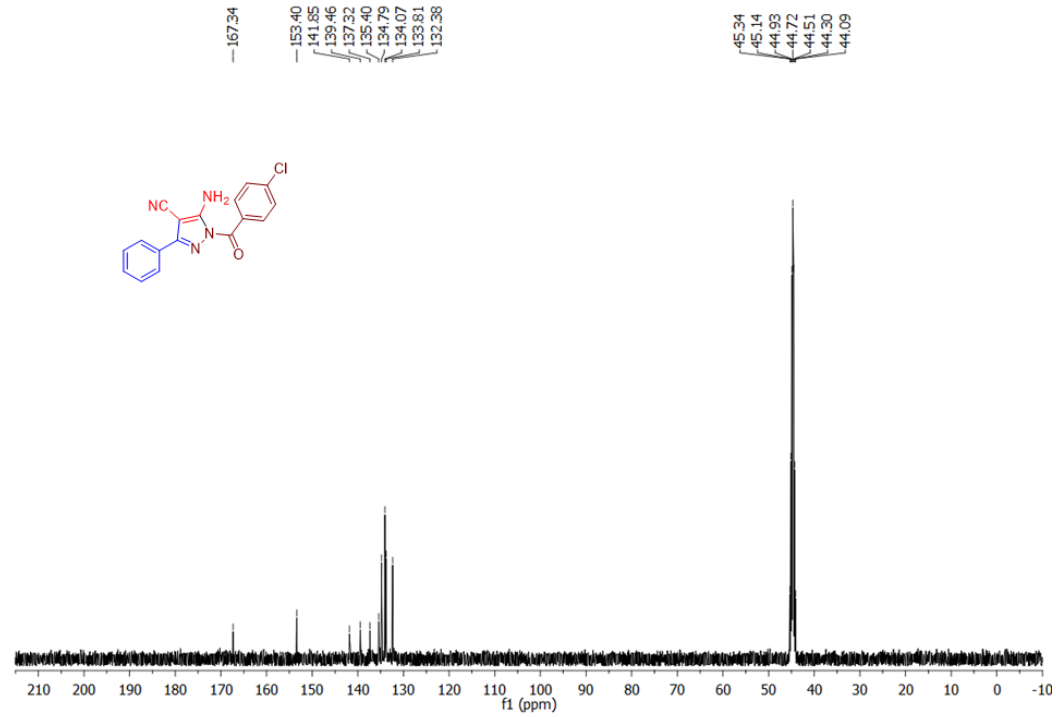

Figure 42: ^{13}C NMR spectrum (**4q**) in DMSO-d_6 (100MHz, 300K).

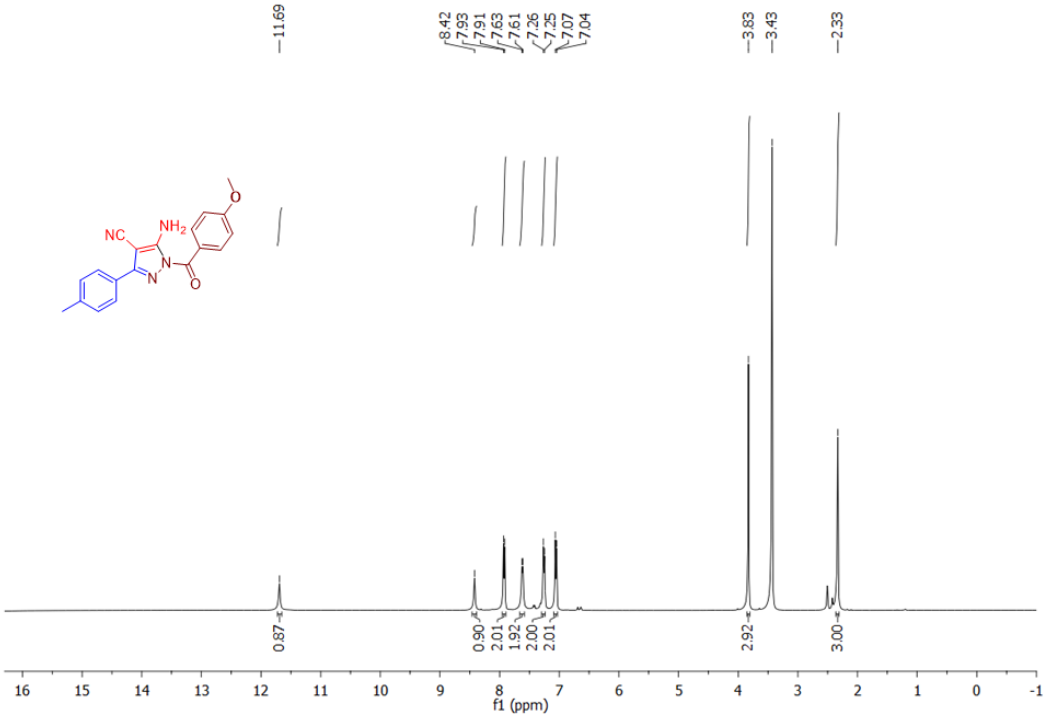

Figure 43: ^{1}H NMR spectrum for (**4r**) in DMSO-d_6 (400MHz, 300K).

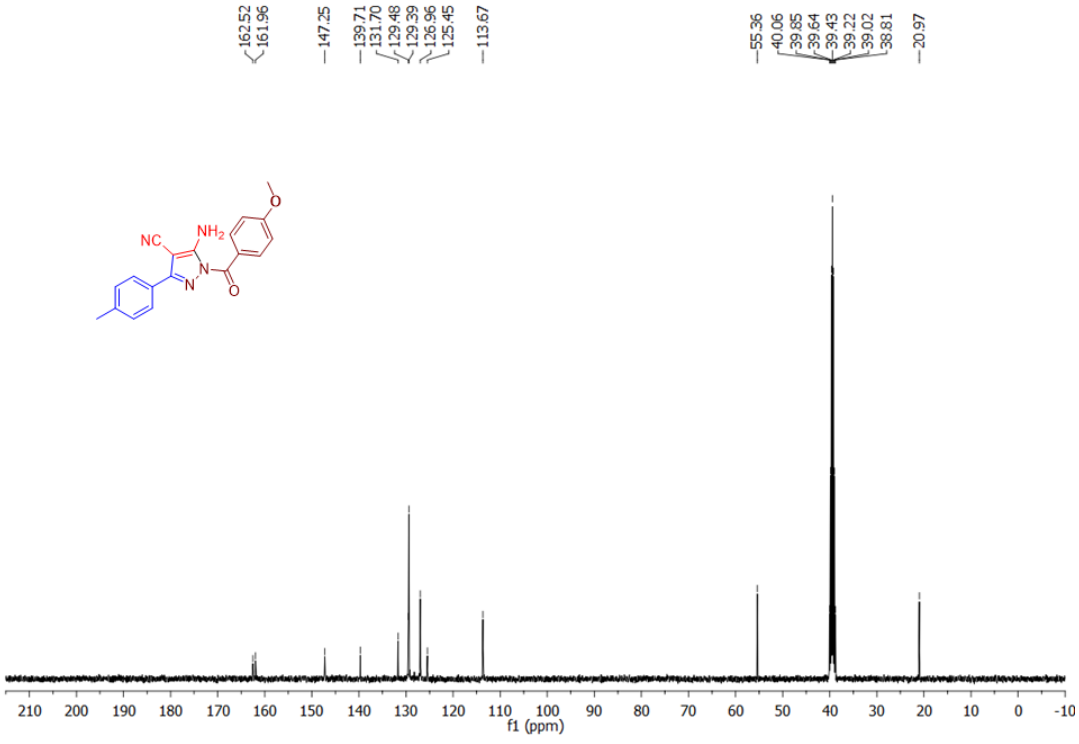

Figure 44: ^{13}C NMR spectrum for (**4r**) in DMSO-d_6 (100MHz, 300K).

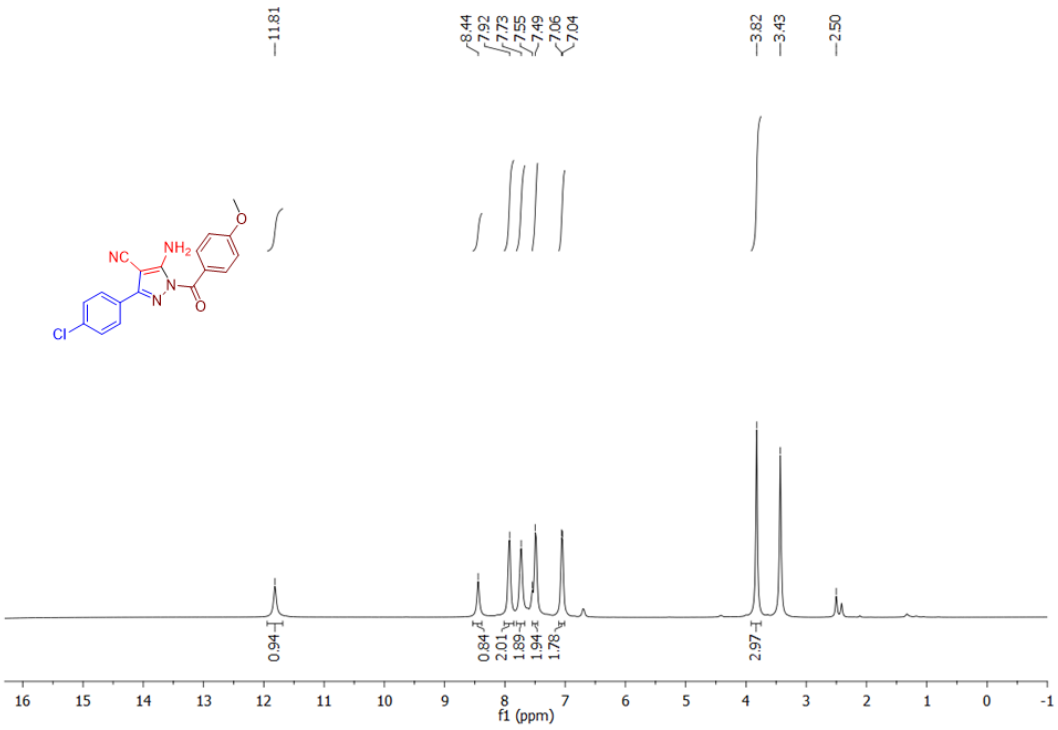

Figure 45: ^{1}H NMR spectrum for (**4s**) in DMSO-d_6 (400MHz, 300K).

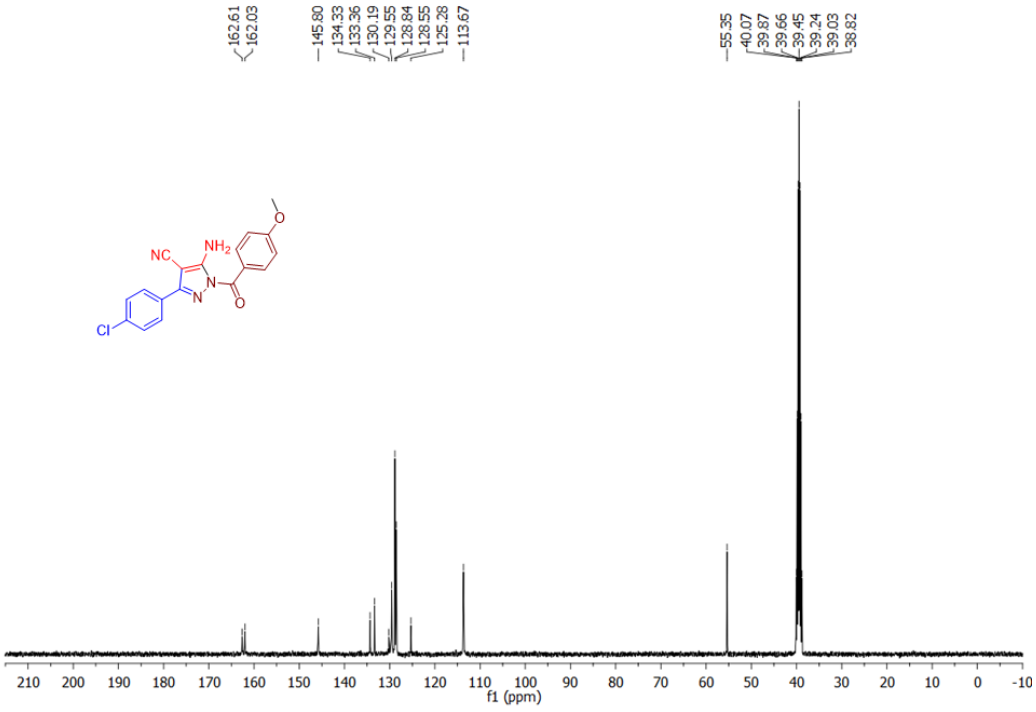

Figure 46: ^{13}C NMR spectrum for (**4s**) in DMSO-d_6 (100MHz, 300K).

5.4. REFERENCES

1. (a) A. R. Katritzky and C. W. Rees, Comprehensive Heterocyclic Chemistry II Eds.; Elsevier: Oxford, 1996; (b) T. Nomura, Z. Z. Ma, Y. Hano and Y. J. Chen, *Heterocycles.,* 1997, **46**, 541-546; (c) I. J. S. Fairlamb, *Chem. Soc. Rev.,* 2007, **36**, 1036-1045.

2. (a) N. K. Terrett, A. S. Bell, D. Brown and P. Ellis, Bioorg. *Med. Chem. Lett.,* 1996, **6**, 1819-1824; (b) J. Elguero, P. Goya, N. Jagerovic and A. M. S. Silva, *Targets Heterocycl. Syst.* 2002, **6**, 52-98; (c) W. R. Tracey, M. C. Allen, D. E. Frazier, A. A. Fossa, C. G. Johnson, R. B. Marala, D. R. Knight and A. Guzman-Perez, *Cardiovasc. Drug Rev.,* 2003, **21**, 17-32; (d) P. G. Wyatt, A. J. Woodhead, V. Berdini, J. A. Boulstridge, M. G. Carr, D. M. Cross, D. J. Davis, L. A. Devine, T. R. Early, R. E. Feltell, E. J. Lewis, R. L. McMenamin, E. F. Navarro, M. A. O'Brien, M. O'Reilly, M. Reule, G. Saxty, L. A. Seavers, D. M. Smith, M. Squires, G. Trewartha, M. T. Walker and A. J. A. Woolford, *J. Med. Chem.,* 2008, **51**, 4986-4999; (e) F. K. Keter and J. Darkwa, *BioMetals*., 2012, **25**, 9-21; (f) D. Havrylyuk, B. Zimenkovsky, O. Vasylenko, A. Gzella and R. Lesyk, *J. Med. Chem.,* 2012, **55**, 8630-8641.

3. (a) S. R. Donohue, C. Halldin and V. W. Pike, *Bioorg. Med. Chem.,* 2006, **14**, 3712-3720; (b) S. H. Hwang, K. M. Wagner, C. Morisseau, J. Y. Liu, H. Dong, A. T. Wecksler and B. D. Hammock, *J. Med. Chem.,* 2011, **54**, 3037-3050; (c) H. X. Dai, A. F. Stepan, M. S. Plummer, Y. H. Zhang and J. Q. Yu, *J. Am. Chem. Soc*., 2011, **133**, 7222-7228.

4. (a) R. A. Singer, S. Caron, R. E. McDermott, P. Arpin and N. M. Do, *Synthesis.,* 2003, **2003**, 1727-1731; (b) R. Kowalczyk, and J. Skarzewski, *Tetrahedron.,* 2005, **61**, 623-628; (c) R. A. Singer, M. Dore, J. E. Sieser and M. A. Berliner, *Tetrahedron Lett.,* 2006, **47**, 3727-3731.

5. A. Schmidt and A. Dreger, *Curr. Org. Chem.,* 2011, **15**, 2897-2970.

6. (a) V. S. Thirunavukkarasu, K. Raghuvanshi and L. Ackermann, *Org. Lett.*, 2013, **15**, 3286-3289; (b) P. M. Liu and C. G. Frost, *Org. Lett.,* 2013, **15**, 5862-5865.

7. For reviews: (a) K. Makino, S. H. Kim and Y. Kurasawa, *J. Heterocycl. Chem.,* 1998, **35**, 489-497; (b) J. Svete, *ARKIVOC* 2006, **7**, 35-56; (c) S. Fustero, A. Simon-Fuentes and J. F. Sanz-Cervera, *Org. Prep. Proced. Int.* 2009, **41**, 253-290; (d) J. J. Neumann, M. Suri and F. Glorius, *Angew. Chem., Int. Ed.,* 2010, **49**, 7790-7794; (e) S. Fustero, M. Sanchez-Rosello, P. Barrio and A. Simon-Fuentes, *Chem. Rev.,* 2011, **111**, 6984-7034; (f) G. Shan, P. Liu and Rao, *Org. Lett.*, 2011, **13**, 1746-1749; (g) Y. Wang, X. Bi, W. Q. Li, D. Li, Q. Zhang, Q. Liu and B. S. Ondon, *Org. Lett.*,

2011, **13**, 1722-1725; (h) J. Qian, Y. Liu, J. Zhu, B. Jiang and Z. Xu, *Org. Lett.*, 2011, **13**, 4220-4223; (i) Y. L. Janin, *Chem. Rev.*, 2012, **112**, 3924-3958; (j) R. S. Foster, H. Jakobi and J. P. A. Harrity, *Org. Lett.*, 2012, **14**, 4858-4861; (k) J. R. Chen, W. R. Dong, M. Candy, F. F. Pan, M. Jorres and C. Bolm, *J. Am. Chem. Soc.*, 2012, **134**, 6924-6927; (l) G. Zhang, H. Ni, W. Chen, J. Shao, H. Liu, B. Chen and Y. Yu, *Org. Lett.*, 2013, **15**, 5967-5969; (m) X. Zhu, Y. F. Wang, W. Ren, F. L. Zhang and S. Chiba, *Org. Lett.*, 2013, **15**, 3214-3217; (n) X. Li, L. He, H. Chen, W. Wu and H. Jiang, *J. Org. Chem.*, 2013, **78**, 3636-3646; (o) T. Zhang and W. Bao, *J. Org. Chem.*, 2013, **78**, 1317-1332; (p) J. Zhang, Y. Shao, H. Wang, Q. Luo, J. Chen, D. Xu and X. Wan, *Org. Lett.*, 2014, **16**, 3312-3315; (q) Y. Kong, M. Tang and Y. Wang, *Org. Lett.*, 2014, **16**, 576-579; (r) Y. Schneider, J. Prevost, M. Gobin and C. Y. Legault, *Org. Lett.*, 2014, **16**, 596-599; (s) F. G. Zhang, Y. Wei, Y. P. Yi, J. Nie and J. A. Ma, *Org. Lett.*, 2014, **16**, 3122-3125.

8. (a) K. Y. Lee, J. M. Kim and J. N. Kim, *Tetrahedron Lett.*, 2003, **44**, 6737-6740; (b) B. S. Gerstenberger, M. R. Rauckhorst and J. T. Starr, *Org. Lett.*, 2009, **11**, 2097-2100; (c) T. Okitsu, K. Sato and A. Wada, *Org. Lett.*, 2010, **12**, 3506-3509; (d) M. Zora, A. Kivrak and C. Yazici, *J. Org. Chem.*, 2011, **76**, 6726-6742.

9. (a) R. Aggarwal and R. Kumar, *Synth. Commun.*, 2009, **39**, 2169-2177; (b) V. G. Desai, P. C. Satardekar, S. Polo and K. Dhumaskar, *Synth. Commun.*, 2012, **42**, 836-842.

10. (a) M. Alvarez-Corral, M. Munoz-Dorado and I. Rodriguez-Garcia, *Chem. Rev.*, 2008, **108**, 3174-3198; (b) J. M. Weibel, A. Blanc and P. Pale, *Chem. Rev.*, 2008, **108**, 3149-3173.

11. T. Naota, H. Takaya and S. I. Murahashi, *Chem. Rev.*, 1998, **98**, 2599-2660.

12. (a) J. Hu, S. Chen, Y. Sun, J. Yang and Y. Rao, *Org. Lett.*, 2012, **14**, 5030-5033; (b) X. Li, L. He, H. Chen, W. Wu and H. Jiang, *J. Org. Chem.*, 2013, **78**, 3636-3646; (c) T. Zhang and W. Bao, *J. Org. Chem.*, 2013, **78**, 1317-1322.

13. T. Punniyamurthy, S. Velusamy and J. Iqbal, *Chem. Rev.*, 2005, **105**, 2329-2364; (b) C. Gunanathan and D. Milstein, Science, 2013, 341, 1229712.

14. A. J. Watson, A. C. Maxwell and J. M. Williams, *Org. Biomol. Chem.*, 2012, **10**, 240-243.

15. V.V. Matveevskaya, D.I. Pavlov, T.S. Sukhikh, A.L. Gushchin, A.Y. Ivanov, T.B. Tennikova, V.V. Sharoyko, S.V. Baykov, E. Benassi and A.S. Potapov, *ACS omega.*, 2020, **5**, 11167-11179.

16. (a) D. Mishra, R. Singh and C. Rout, *Journal of Chemical and Pharmaceutical Research.*, 2017, **9**, 16-19; (b) H. Kiyani and M. Bamdad, *Research on Chemical*

Intermediates, 2018, **44**, 2761-2778; (c) H. T. Nguyen, T. Van Le, and P. H. Tran, *Journal of Environmental Chemical Engineering.*, 2021, **9**, 105228; (d) H. T. Nguyen, M. N. H.Truong, T. V. Le, N. T. Vo, H. D. Nguyen and P. H. Tran, *ACS Omega.,* 2022, **20**, 17432-17443.

17. Vogel, A. I.; Test book of practical organic chemistry, Longman, London, 5th edn, 1989, p.395.

18. M. A. Bennett and A. K. Smith, J. Chem. Soc., *Dalton Trans.,* 1974, 233.

19. S. Saranya, R. Ramesh and J. G. Małecki, *Eur. J. Org. Chem.,* 2017, **2017**, 6726-6733.

20. Farrugia, L. ORTEP-3 for Windows - a version of ORTEP-III with a Graphical User Interface (GUI), *Journal of Applied Crystallography*,1997, **30**, 565-566.

21. G. M. Sheldrick, *Acta Crystallogr., Sect. A: Found. Crystallogr.* 2008, **64**, 112.

22. Bruker-Nonius (2004), APEX-II and SAINT-Plus (Version 7.06a), Bruker AXS Inc., Madison, Wisconsin, USA.

23. S. Sundar and R. Rengan, *Org. Biomol. Chem.,* 2019, **17**, 1402-1409.

24. (a) W. Yin, C. Wang and Y. Huang, *Org. Lett.,* 2013, **15**, 1850-1853; (b) S. Muthumari, S. Saranya and R. Ramesh, *Appl. Organomet. Chem.,* 2018, **32**, 4582; (c) A. Alanthadka, S. Bera, M. Vellakkaran and D. Banerjee, *J. Org. Chem.,* 2019, **84**, 21, 13557-13564.

Chapter 6

CONCLUSIONS

The construction of heterocycles is an emerging area of chemical research and plays a vital role due to their high importance in pharmaceuticals, material chemistry, and natural product synthesis etc. The development of sustainable methodologies by employing easily available starting materials has been a long thirst for synthetic chemists. Thus, the development of much greener and more effective methodologies by using abundant starting materials under milder reaction conditions is highly desirable. Alcohol is an economical and abundantly available greener substrate produced from diverse sustainable resources. The transition metal-catalyzed dehydrogenative coupling of alcohols offers the environmentally benign synthesis of numerous N-heterocycles *via* C-C, C-N and C-O bond formation, since only water and hydrogen are produced as the eco-friendly by-products compared to conventional protocols. In particular, ruthenium metal catalyzed dehydrogenative coupling reaction of alcohols with suitable coupling partners is one of the alternatives and sustainable routes for the synthesis of potent heterocyclic compounds.

In this context, the current investigation involves the synthesis of new mono and binuclear ruthenium(II) complexes featuring chelating ligands such as thiourea, aroylhydrazone and aroylhydrazine ligands. The structural characterization of synthesized complexes was established by elemental analysis, spectroscopic (FT-IR, UV-Vis and NMR) and single crystal X-ray diffraction methods. Further, the synthesized complexes were promoted as effective catalysts for the synthesis of bioactive compounds *via* acceptorless/oxidative dehydrogenative coupling of alcohols.

The thesis is divided to six chapters. Chapter -1 provides a quick overview of thiourea, aroylhydrazone, aroylhydrazine and metal-arene frameworks. Further, the transition metal catalyzed acceptorless/oxidative dehydrogenative coupling of alcohols with suitable partner towards the synthesis of imines, E-olefins, 2-amino-4H-chromenes and pyrazoles have been described. Furthermore, literature reports on the catalytic applications of ruthenium(II) complexes containing various multidentate ligands in organic synthesis were given.

Chapter - 2 outlined the arene diruthenium(II) complexes mediated synthesis of imines from alcohols and amines under aerobic condition. The new complexes were synthesized in good yields using $[RuCl_2(arene)]_2$ and thiourea ligands. The structural compositions of synthesized complexes were evidenced with aid of analytical and spectral techniques. The molecular structure of one of the complexes was substantiated with the help of single-crystal X-ray diffraction method and confirmed the unprecedented formation of the thiolato-bridged dinuclear ruthenium complexes. The synthesized complexes were developed as catalysts for the synthesis of a wide range of imines through dehydrogenative coupling of alcohols and amines. The desirable imines were obtained in good to excellent yields up to 98% with water as the only by-product. This catalytic reaction is a concise atom economical protocol operated with 1 mol% of the catalyst loading without the use of any oxidant or additives.

In chapter – 3, Ru(II)–N^N^O pincer-type complexes catalyzed E-olefination of alkyl-substituted quinolines/pyrazines has been described. An array of N^N^O pincer type Ru(II) methyl-2-pyrrole benzhydrazone complexes containing carbonyl and triphenyl arsines as co-ligands has been synthesized. The structural composition of the complexes was elucidated by analytical and spectral techniques. The solid-state molecular structure of the representative complex has been substantiated by single crystal X-ray crystallography.

Further, the synthesized complexes were employed as catalysts for selective E-olefination of alkyl-substituted quinolines and pyrazines. The catalytic protocol produces a diverse range of olefinated products up to 90% *via* dehydrogenative coupling of readily available primary alcohols. This synthetic strategy is operationally simple, scalable and tolerates various functional groups under mild reaction conditions and discovers a chance for the production of biologically important olefins using Ru(II)–N^N^O pincer-type catalysts.

Chapter - 4 deals with the one-pot three-component synthesis of 2-amino-4H-chromenes catalyzed by new Ru(II) complexes. The complexes were synthesized from carbazole-based hydrazone ligands and $[RuCl_2(p\text{-cymene})]_2$. Analytical and spectral techniques demonstrated the formation of new Ru(II) complexes comprising N^O chelating carbazolone benzhydrazone ligands. The molecular structure of one of the complexes was corroborated with the help of single-crystal X-ray diffraction study. A broad variety of 2-amino-4H-chromenes derivatives were synthesized from acceptorless dehydrogenative coupling of substituted benzyl alcohols with malononitrile and resorcinol. This synthetic approach is amenable and constructed a broad variety of 2-amino-4H-chromenes derivatives with the maximum yield up to 95% at low catalyst loading (1 mol %). Interestingly, the medicinally important tacrine analogue has been successfully derived from the synthesized 2-amino-4H-chromenes. The environmentally friendly protocol operates under mild conditions and discharges water and hydrogen as only by-products.

In chapter – 5, binuclear arene Ru(II) complexes promoted one-pot synthesis of pyrazoles from benzohydrazides and alcohols has been portrayed. A series of binuclear *p*-cymene Ru(II) thiazole-based hydrazine complexes were synthesized and characterized by analytical and spectroscopic techniques. The solid-state molecular structure of one of the complexes was confirmed by a single crystal X-ray diffraction study. The synthesized complexes were promoted as effective catalysts for the synthesis of pyrazole derivatives

from alcohols, malononitrile and benzohydrazides through acceptorless dehydrogenative pathway. This catalytic protocol provides a variety of pyrazole derivatives in high yields up to 50% - 95% using low catalyst loading. This approach is efficient, highly facile and environmentally friendly as hydrogen and water are gentle by-products and do not use any oxidant/additives.

Chapter - 6 concisely gives the summary of all the five chapters.

Overall, the thesis focuses on the synthesis and characterization of mono and binuclear ruthenium(II) complexes featuring thiourea, aroylhydrazone and aroylhydrazine ligands. Further, the complexes were developed as catalysts for the direct synthesis of imines, E-olefins, 2-amino-4H-chromenes and pyrazoles involving C-C, C-N and C-O bond formation reaction proceeds through acceptorless / oxidative dehydrogenative coupling of alcohols with suitable coupling partners.

List of Publications

1.	Arene diruthenium(II)-mediated synthesis of imines from alcohols and amines under aerobic condition V. Tamilthendral, R. Ramesh* and J. G. Malecki, ***Appl. Organomet. Chem.,*** 2021, 35, e6122.	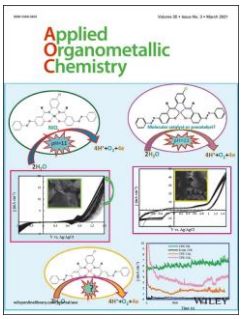
2.	Ru(II)-NNO pincer-type complexes catalysed E-olefination of alkyl-substituted quinolines/pyrazines utilizing primary alcohols V. Tamilthendral, G. Balamurugan, R. Ramesh* and J. G. Malecki, ***Appl. Organomet. Chem.,*** 2022, 36, e6561.	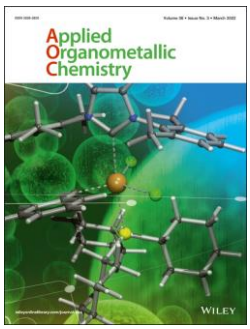
3.	Ruthenium(II) Catalyst Mediated Synthesis of 2-amino-4H-chromenes Using Primary Alcohols *via* Acceptorless Dehydrogenative Coupling Pathway V. Tamilthendral, R. Ramesh* and J. G. Malecki, ***New J. Chem.,*** (Under revision)	
4.	Binuclear Arene Ru(II) Mediated C-N Bond Formation for One-Pot Synthesis of Pyrazoles from Benzohydrazides and alcohols *via* Acceptorless Dehydrogenative Pathway V. Tamilthendral, T. S. Kamatchi and R. Ramesh*, ***Organometallics.,*** (Communicated)	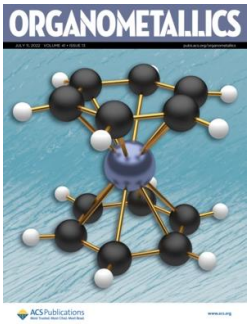

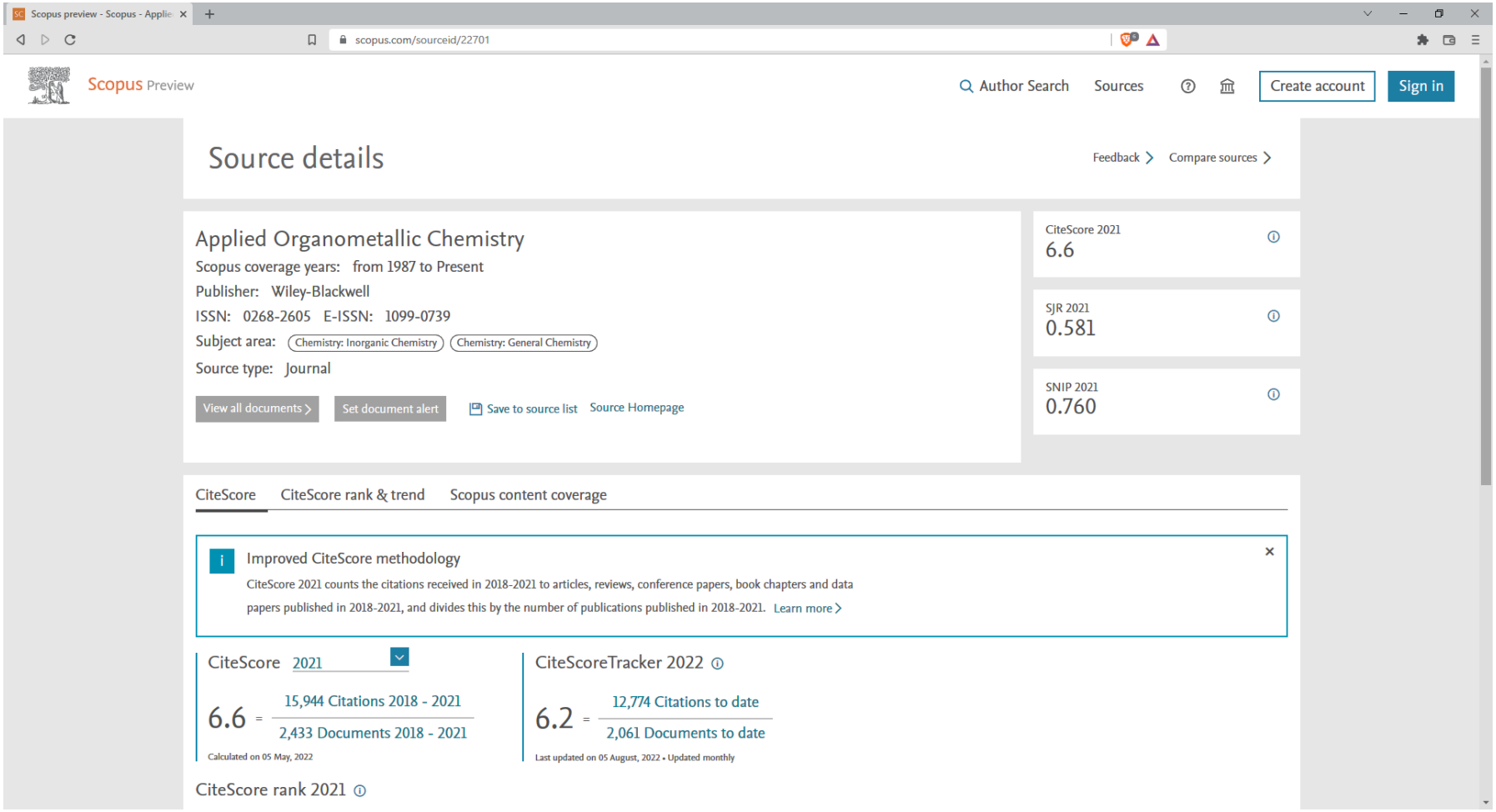
Scopus preview - Scopus - Applie
scopus.com/sourceid/22701
Scopus Preview
Author Search
Sources
Create account
Sign in
Source details
Feedback
Compare sources
Applied Organometallic Chemistry
Scopus coverage years: from 1987 to Present
Publisher: Wiley-Blackwell
ISSN: 0268-2605 E-ISSN: 1099-0739
Subject area: Chemistry: Inorganic Chemistry Chemistry: General Chemistry
Source type: Journal
View all documents
Set document alert
Save to source list
Source Homepage
CiteScore 2021
6.6
SJR 2021
0.581
SNIP 2021
0.760
CiteScore
CiteScore rank & trend
Scopus content coverage
Improved CiteScore methodology
CiteScore 2021 counts the citations received in 2018-2021 to articles, reviews, conference papers, book chapters and data papers published in 2018-2021, and divides this by the number of publications published in 2018-2021. Learn more
CiteScore 2021
6.6 = 15,944 Citations 2018 - 2021 / 2,433 Documents 2018 - 2021
Calculated on 05 May, 2022
CiteScoreTracker 2022
6.2 = 12,774 Citations to date / 2,061 Documents to date
Last updated on 05 August, 2022 • Updated monthly
CiteScore rank 2021

Received: 28 October 2020 | Revised: 27 November 2020 | Accepted: 28 November 2020

DOI: 10.1002/aoc.6122

FULL PAPER

Applied Organometallic Chemistry WILEY

Arene diruthenium(II)-mediated synthesis of imines from alcohols and amines under aerobic condition

Veerappan Tamilthendral[1] | **Rengan Ramesh**[1] | **Jan Grzegorz Malecki**[2]

[1]Centre for Organometallic Chemistry, School of Chemistry, Bharathidasan University, Tiruchirappalli, India

[2]Department of Crystallography, Institute of Chemistry, University of Silesia, Katowice, Poland

Correspondence
Rengan Ramesh, Centre for Organometallic Chemistry, School of Chemistry, Bharathidasan University, Tiruchirappalli, 620 024 Tamilnadu, India.
Email: rramesh@bdu.ac.in

Funding information
Science and Engineering Research Board, Grant/Award Number: EMR/2016/004952

The utility and selectivity of the newly synthesized dinuclear arene Ru(II) complex were demonstrated towards the synthesis of imines from coupling of alcohols and amines in the aerobic condition. Analytical and various spectral methods have been used to establish the unprecedented formation of the new thiolato-bridged dinuclear ruthenium complex. The molecular structure of the titled complex was evidenced with aid of X-ray crystallographic technique. A wide range of imines were obtained in good-to-excellent yields up to 98% and water as the by-product through an acceptorless dehydrogenative coupling of alcohols with amines. The catalytic reaction operated a concise atom economical without any oxidant with 1 mol% of the catalyst load. Further, the role of base, solvent and catalyst loading of the coupling reaction has been investigated. A plausible mechanism has been described and was found to proceed via the formation of an aldehyde intermediate. Short synthesis of antibacterial drug *N*-(salicylidene)-2-hydroxyaniline illustrated the utility of the present protocol.

KEYWORDS

aerobic oxidation, imine synthesis, thiolato Ru(II) catalyst, thiourea

1 | INTRODUCTION

Imines are profound important class of nitrogen compounds owing to their high reactivity.[1] They are ubiquitous intermediates in many organic reactions such as cyclization, cycloaddition, multicomponent reactions and condensation.[2] They are adaptable nitrogen sources that find applications in pharmaceuticals, industrial and agriculture.[3] Further, many nitrogen-containing bioactive compounds such as amines, amides and pyrrolines can be constructed from imine functional group (Figure 1).[4] Hence, synthesis and applications of imines are essentially ever-appealing topics in synthetic organic chemistry.

The conventional approach for imine synthesis involves the direct coupling of amines with aldehydes or ketones with Lewis acid or dehydrating agents and higher reaction time are required in many situations.[5] Imines have been also synthesized in different circumstances includes Schmidt reaction, Aza-Wittig reaction[6] and oxidation of secondary amines using oxidizing agents (Scheme 1).[7]

Although a number of methods are known for imine synthesis in the literature, they largely suffer from drawbacks like use of toxic reagents, poor atom economy, harsh synthetic process and low level of selectivity.[8]

To overcome the aforementioned limitations, the metal-catalyzed direct synthesis of imines from alcohols with amines through acceptorless dehydrogenation coupling mechanism is an alternative approach. The strategy consists of two steps: (i) aerobic oxidation of alcohol in the presence of a transition metal catalyst and (ii) generation of imine. More advantageously, the acceptorless dehydrogenative methodology is a greener protocol

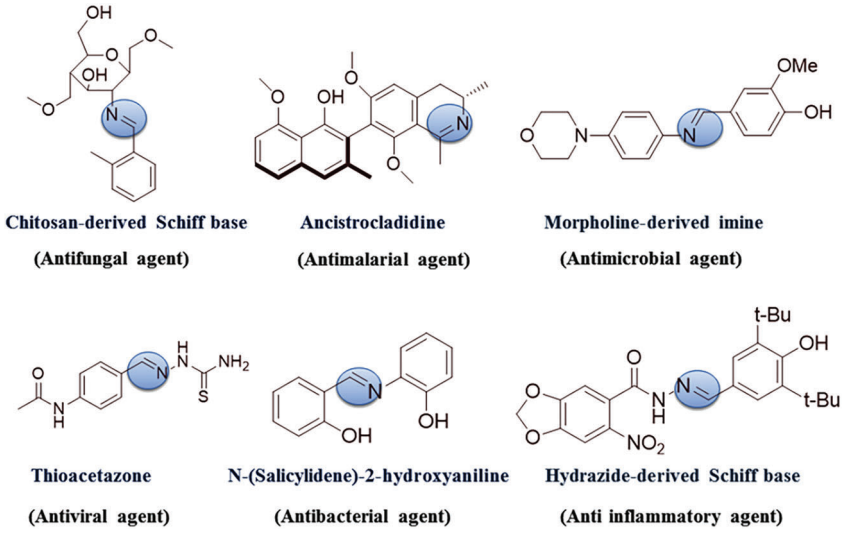

FIGURE 1 Examples for bioactive imine analogues

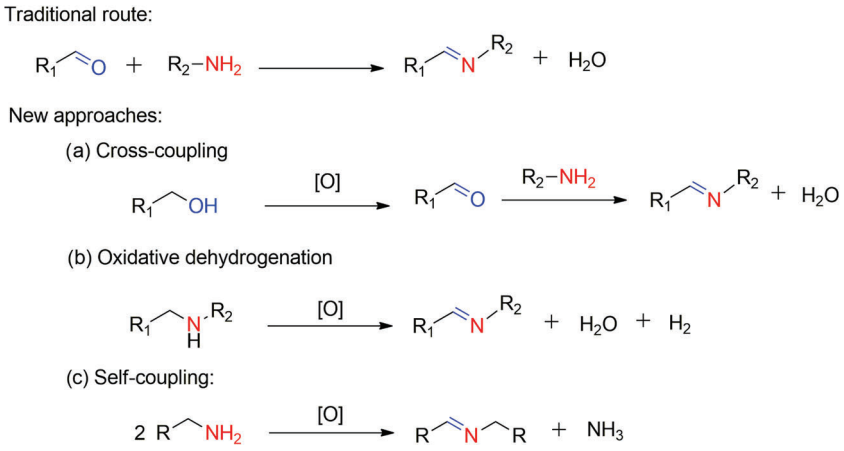

SCHEME 1 Imine formation via traditional method and new approaches by aerobic oxidation of alcohols and amines (a, b and c)

for the coupling of alcohol and amine to desired imine with the water as the by-product.

Milstein and co-workers reported Ru–PNP-type pincer complex that promoted synthesis of imines from alcohols and amines under nitrogen atmosphere.[9] This significant breakthrough methodology has garnered much attention from the researchers towards imine synthesis. Several wide transition metal complexes such as Ru, Os, Pd, Pt and Au have been reported as catalysts for imine synthesis under high temperature, inert atmosphere, special condition and long reaction time.[10–14] Shiraishi and co-workers employed a Pt/TiO_2 heterogeneous catalyst for the imine synthesis with UV radiation and used nitrogen atmosphere protection.[13] Soule and co-workers have reported synthesis of imines by gold/palladium alloy nanoparticles (1.5 mol%) in the presence of oxidant.[15] Donthiri et al. have described synthesis of imines by using NaOH (10 mol%) as a catalyst at high temperature.[16] The Tian research group explored imine formation by employing CuI/bipyridine/TEMPO under neat conditions.[17] Later, the Zhang group reported mild one-pot synthesis of imines using as $Fe(NO_3)_3$/TEMPO system used as a catalyst in the presence of additives.[18] Maggi et al. demonstrated the catalytic performance of Ru–NHC complex (5 mol%) in imine synthesis using DABCO ligand in the presence of molecular sieves for 24 h.[10b] The catalytic activity of Co(II)–NNN pincer complex has been explored for imine synthesis, and the reaction was carried out with *n*-octane as a solvent at high temperature[19] (Scheme 2).

Overall, a large number of metal complexes with different ligand systems have been explored as catalysts for this reaction. In particular, metal-based catalysts for the synthesis of imines with phosphine labile ligands have been well explored. However, the catalytic condition showed some drawbacks such as higher temperature, higher catalyst load and inert atmosphere. To overcome the above issues, we are interested to execute the imine synthesize protocol using metal complexes with phosphine-free ligands. Generally, metal complex containing phosphorus-free ligands has salient features like ease of synthesis and air stability, to avoid tedious separation and catalyst recovery. In the present art of research, we have described the synthesis and characterization of

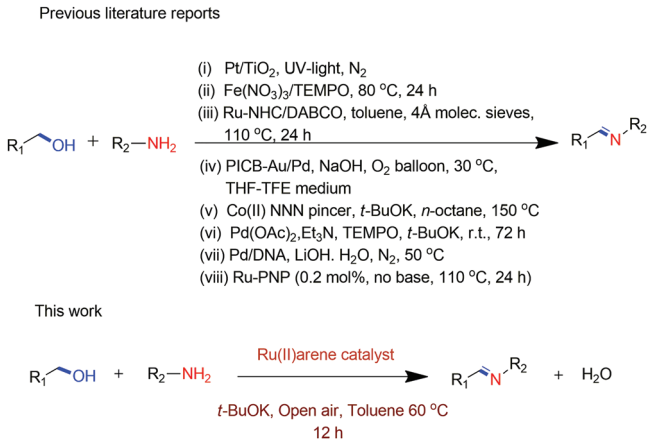

SCHEME 2 Synthetic strategies of imine reaction

new binuclear Ru(II) complex of thiourea ligand and used as a catalyst for imine synthesis under the aerobic catalytic condition. A catalyst featuring two closely associated metal active sites is one of the emerging areas in homogeneous catalysis. This bimetallic catalytic system complements the traditional focus on parameters in order to optimize catalytic behaviour in a better way. Change of the steric and electronic properties of the ligands can fine-tune the performance of the bimetallic system. Such catalysts introduce new optimization parameters such as catalyst nuclearity and synergistic cooperation between the two metal active sites and the bridging ligands.[20] Hence, controlling selectivity and activity of the catalytic transformations will be offered by the suitable design of bimetallic catalysts. Exquisite levels of activities of these catalysts could be achieved by careful design of two metal active sites (Figure 2).

2 | RESULTS AND DISCUSSION

1-(5-Methylthiazole-2-yl)-3-phenylthiourea ligand (HL) was prepared from phenyl isothiocyanate with 5-methylthiazole-2-amine in the equimolar ratio in the presence of dimethylformamide (DMF) medium.[21] The synthesis cationic arene Ru(II) thiourea complex can be accomplished in good yield from complexation of ruthenium starting precursor $[(\eta^6\text{-}p\text{-cymene})RuCl_2]_2$ (1.0 mmol) with thiourea ligand in 1:2 molar respectively in benzene under the open-air condition. The complex was yellow in colour and air stable. It was easily soluble in solvents like CH_2Cl_2, $CHCl_3$, CH_3CN, dimethyl sulfoxide (DMSO), and tetrahydrofuran (THF). The resulting complex was crystallized from the mixture of solvents dichloromethane and methanol (1:1) (Scheme 3).

In the IR spectrum, thiazole N–H and phenyl group N–H in the ligand showed bands in the regions 3,366 and 3,162 cm^{-1}, respectively. Also, free ligand displayed the thiocarbonyl ($\nu_{C=S}$) stretching frequencies at 1,254 cm^{-1}. On complexation, thiazole-attached N–H stretching vibration was not observed in the complex, indicating that the ligand underwent enolization and decrease in $\nu_{C=S}$ (1,150 cm^{-1}). The shift in these bands revealed the coordination of ligand to the metal via thiazole nitrogen and thiocarbonyl sulfur.

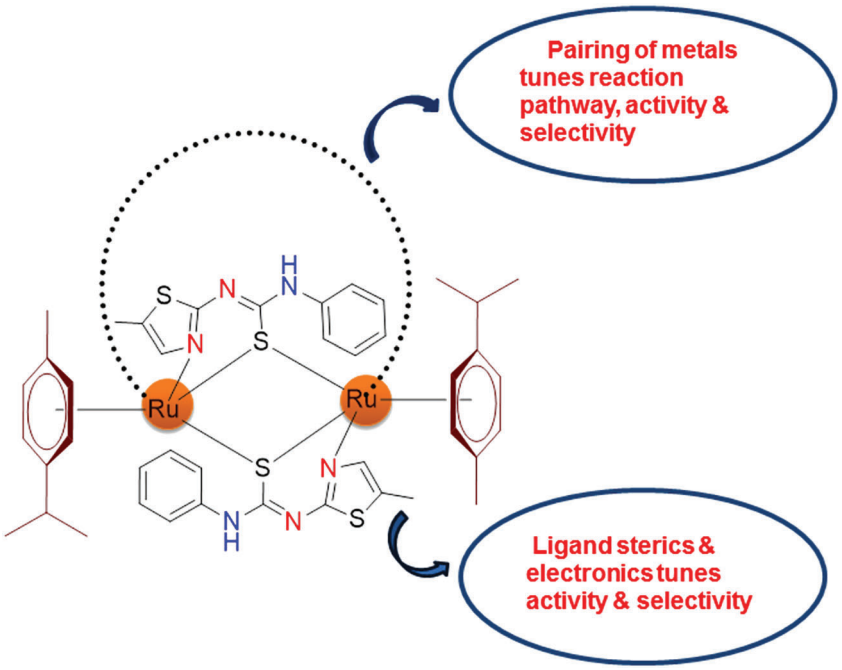

FIGURE 2 Structure–function relationship available in bimetallic catalysis

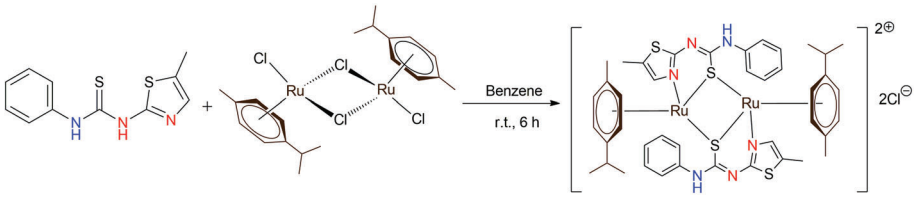

SCHEME 3 Synthetic route to [Ru(η^6-*p*-cymene)(HL)]$_2$Cl$_2$ complex

In the ^{1}H NMR spectrum, the free ligand showed signals at 12.30 and 10.23 ppm due to N–H protons. Upon complexation, the thiazole-connected –NH proton disappeared from the complex, further supporting enolization and coordination through thiocarbonyl sulfur to the Ru(II) ion. All aromatic protons of the complex appeared as multiplet in the region of 7.30–7.60 ppm. The arene protons of the complex were observed at 5.30–5.56 ppm. The methyl protons of isopropyl group in *p*-cymene moiety exhibited as singlet in the region 1.21–1.26 ppm. A septet appeared in the range of 2.80 ppm due to a methine proton of the isopropyl group. Further, signals due to the methyl protons of the *p*-cymene were observed at 2.43 ppm as singlet (Figures S1, S2).

The solid state structure of the complex [Ru(η^6-*p*-cymene)(HL)]$_2$Cl$_2$ has been studied by X-ray crystallographic technique. Crystals of suitable size were obtained from mixed solvents of dichloromethane and methanol (1:1). The Oak Ridge thermal ellipsoid plot (ORTEP) view of the complex is shown in Figure 3, and the crystallographic data and selected bond distances and bond angles are shown in the supporting information (Table S1, S2). The crystal belongs to the monoclinic space group '*C* 2/*c*' with $Z = 4$. The thiourea chelates to Ru(II) ion through the two thiolato sulfur ions and thiazole nitrogen, and the remaining position is occupied by arene moiety forming a pseudo octahedral geometry. A four-membered Ru–S–Ru–S ring system is formed owing to the bridging position of sulfur atoms between the two Ru ions. The unprecedented formation of bridging system is due to pushing of electron density by the thiazole group through the amino nitrogen atom. This enabled the sulfur atom to make the new Ru–S bond, resulting in dimer formation. The observed dimeric structure is similar to the related compound containing a [Rh–N–C–S]$_2$ sulfur-bridged dinuclear unit.[22] The Ru_2S_2 core is essentially planar, which indicated that the cymene ligands adopted *cis* arrangement in the complex, similar to the arrangement observed in [(η^6-$C_6H_3Me_3$)Ru{$SCMe_2CH$–(CO_2H)NH_2}$_2$]$_2$.[23] All of the Ru–S distances of complex are basically of equal length [range 2.3765(15)–2.4204(16) Å], indicating symmetrical sulfur atoms. It has been observed that the Ru–S–Ru bond angle [99.25 (6)°] is slightly larger than the corresponding chloride bridging Ru–Cl–Ru [98.22°] bond angle.[24] Hence, the single-crystal X-ray diffraction studies confirmed the structure proposed with the aid of other spectroscopic techniques.

With the novel dinuclear arene Ru(II) thiourea complex in hand, we wish to study the catalytic utility in the synthesis of imines from coupling of alcohols and amines at open atmospheric conditions. For that, we initiated with test reaction between the equimolar amounts of 4-methylbenzyl alcohol and aniline with complex (1 mol%) as a catalyst with various solvents and KOH as a base to optimize the reaction condition (Table 1). When toluene was used as solvent, the corresponding imine product **3a** was obtained 83% yield in 12 h (Table 1, entry 1). Switching the solvent to xylene and benzene is also effective, furnishing imines up to 80% and 72% yield, respectively (Table 1, entries 2 and 3). Moderate yields of imines were obtained when the reaction was performed in various polar solvents like dioxane, THF, acetonitrile, DMF

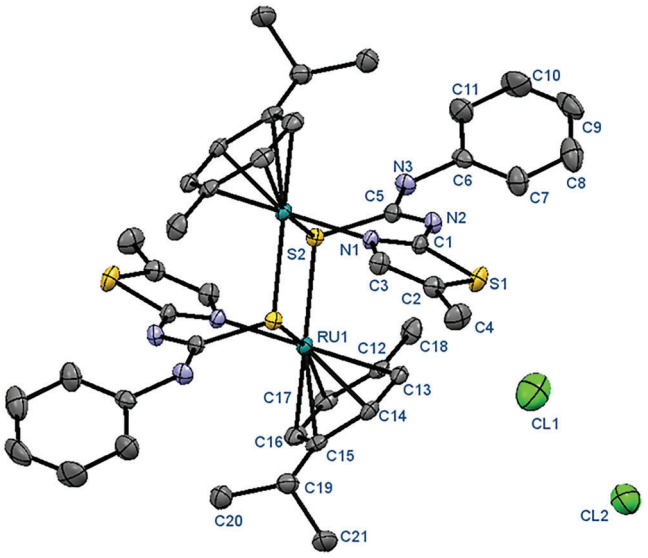

FIGURE 3 Oak Ridge thermal ellipsoid plot (ORTEP) representation of complex [Ru(η^6-*p*-cymene)(HL)]$_2$Cl$_2$ with 50% probability level. All hydrogen atoms were omitted for clarity. Selected bond lengths [Å] and angles [°]: Ru(1)–S [2] = 2.3765 [15], Ru(2)–S [2] = 2.4204 [16], Ru(1)–N [1] = 2.120 [5], Ru(1)–C [12] = 2.261 [6], Ru(1)–C [13] = 2.189 [6]; Ru(1)–S(2)–Ru [2] = 99.25 [6], S(2)–Ru(1)–S [1] = 80.75 [6], N(1)–Ru(1)–S [2] = 86.99 [14], N(1)–Ru(1)–C [12] = 122.3 [2], N(1)–C(1)–S [1] = 112.2 [5], C(5)–S(2)–Ru [1] = 103.4 [2], C(12)–Ru(1)–S [2] = 97.35 [17]

TABLE 1 Screening of solvents, bases and temperatures[a]

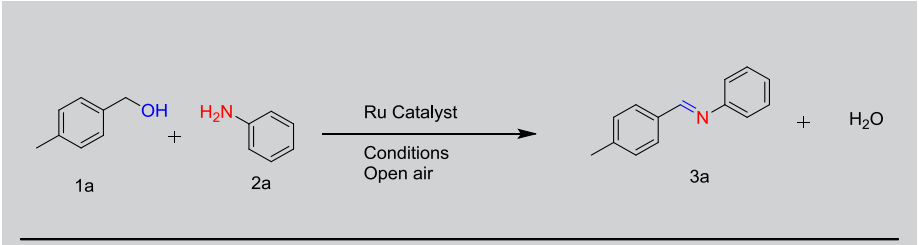

Entry	Solvent	Base	Temp. (°C)	Yield(%)[b]
1	Toluene	KOH	110	83
2	Xylene	KOH	140	80
3	Benzene	KOH	80	72
4	1,4-Dioxane	KOH	100	65
5	THF	KOH	66	78
6	Acetonitrile	KOH	82	60
7	DMF	KOH	150	52
8	Methanol	KOH	65	70
9[c]	Toluene	—	r.t	NR
10[c]	Toluene	—	80	NR
11[d]	Toluene	*t*-BuOK	110	10
12	Toluene	NaOH	110	82
13	Toluene	NaOMe	110	85
14	Toluene	K_2CO_3	110	79
15	Toluene	CS_2CO_3	110	80
16	Toluene	*t*-BuOK	110	88
17	Toluene	*t*-BuOK	80	90
18	**Toluene**	***t*-BuOK**	**60**	**98**
19[e]	Toluene	*t*-BuOK	r.t	70

Abbreviations: DMF, dimethylformamide; THF, tetrahydrofuran.
The bold data in the table 1 indicates the best optimized reaction condition.
[a]Conditions: 4-methyl benzyl alcohol (1 mmol), aniline (1 mmol), catalyst, (1.0 mol%) and base (0.5 mmol) in the presence of solvent (5 ml) at 60°C for 12 h.
[b]Isolated yield.
[c]Absence of base.
[d]Absence of catalyst.
[e]Time for 24 h.

and methanol (Table 1, entries 4–8). These results indicated that nonpolar solvents outperformed polar solvents in the test reaction. No further reaction proceeded in the absence of a base or a catalyst (Table 1, entries 9–11). Furthermore, good product yields are observed in the presence of NaOH and NaOMe (Table 1, entries 12 and 13). In addition, up to 80% of imines were noted when K_2CO_3 and Cs_2CO_3 are present (Table 1, entries 14 and 15). Further, it has been observed that *t*-BuOK outperformed other bases, which afforded **3a** in 90% yield of imine (Table 1, entries 16 and 17). Notably, the cationic dinuclear ruthenium complex catalyzed effectively the coupling of alcohol and amine and yielded 98% of selective imine under the optimized condition of toluene/*t*-BuOK at 60°C (Table 1, entry 18).

Further, the effectiveness of our catalyst was examined with different catalyst loadings for the test reaction (Table 2). Upon reducing the catalyst loading from 1 mol % to 0.25 mol%, there was a substantial decrease in yields (Table 2, entries 1–4). Therefore, 1 mol% catalyst loading is the best choice for optimization.

The substrate scope of the reaction with respect to various types of alcohols and amines under the optimized catalytic conditions is displayed in Table 3. Fabulously, electron-rich functionalities of benzyl alcohols (–CH_3, –OCH_3) are efficiently reacted with aniline to yield the respective imines **3a**–**3c** in 83–95% of isolated yields

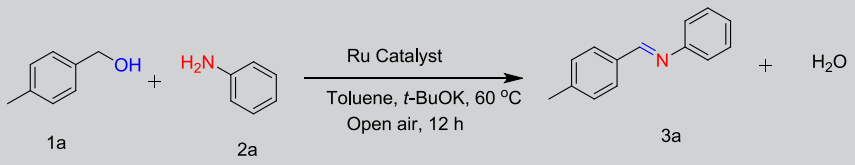

TABLE 2 The screening of the catalyst loadings[a]

Entry	Catalyst (mol %)	Yield (%)
1	**1.0**	**97**
2	0.5	80
3	0.3	61
4	0.1	39

The bold data in the table 2 indicates the best optimized condition.
[a]Conditions: 4-methylbenzyl alcohol (1 mmol), aniline (1 mmol) and base (0.5 mmol) in the presence of solvent (5 ml) at 60°C for 12 h.

(Figures S3–S8). Further, electron-withdrawing substituents (–Cl, –F) on benzyl alcohols were tolerated well with aniline that acquired desired imines **3d** and **3e** in the yields of 88–78% (Figures S9–S12). In addition, the coupling reactions between different benzyl alcohols and 4-ethoxy and 4-methoxy anilines afforded the corresponding imines **3f** and **3g** in 80–83% of isolated yields (Figures S13–S16). More interestingly, the complex catalysed well in the coupling of sterically hindered 2-bromobenzyl alcohol with 4-methoxy aniline to afford the respective imine **3h** in 75% of yield (Figures S17, S18). However, the electron-withdrawing substituent of 4-chlorobenzyl alcohol with 4-methoxy aniline showed a better result in the formation of respective imine **3i** in 79% of yield (Figures S19, S20). The high yield of 82% for **3j** was obtained by the reaction of 4-methoxybenzyl alcohol and 4-methoxy aniline (Figures S21, S22). Coupling of benzyl alcohol-bearing electron-donating and withdrawing substituents (4-methyl and 4-chloro) with 4-bromoaniline gave respective imines **3k** and **3l** in 98% and 90% of yields (Figures S23–S26). Importantly, piperonyl-based imine moieties were found to be effective in pharmaceutically active ingredients. But the synthesis of piperonyl-derived imines is less covered in previous literature.[25] Hence, we are interested in coupling the piperonyl alcohol with various amines. More significantly, we attained the piperonyl-derived imines **3m**–**3o** up to 94% of yields (Figures S27–S32). Gratifyingly, the catalytic efficiency of the present complex proved the synthesis of bis-imine product **3p** with the appreciable yield of 75% under the optimized condition (Figures S33, S34). Deliberately, a chiral imine **3q** was achieved from the coupling of 4-methylbenzyl alcohol with (*R*)-(+)-α-methylbenzylamine gave an 84% yield (Figures S35, S36). Notably, the complex efficiently promoted the synthesis of imines from heterocyclic alcohols, and amines resulted in good yields of imine products **3r** and **3s** (Figures S37–S40). The attempt taken for coupling of alcohol and aliphatic amine to provide the expected product **3t** was successful (Figures S41, S42). Further, the catalytic condition was found to be ineffective for the coupling of aliphatic alcohols with amines.

It is crucial at this point to compare the catalytic efficiency and scope of our catalytic system with other reported ruthenium(II) catalysts. Maggi et al. demonstrated the catalytic performance of Ru–NHC complex (5 mol%) in imine synthesis using DABCO ligand in the presence of molecular sieves for 24 h.[10b] Musa et al. have reported the catalytic activity of bifunctional Ru(II) PCP pincer complexes towards synthesis of imine from alcohols and amines in *p*-xylene medium with 2 mol% catalyst loading for 24 h under argon atmosphere.[26] The binuclear Ru catalyst was documented to catalyze an imine formation reaction with 5 mol% DABCO ligand, and molecular sieves for 24 h were reported.[27] In addition, Higuchi and co-workers reported the ruthenium complex catalyzed imination reaction with Zn $(OCOCF_3)_2$ (1 mol%) and KO^{t}Bu (20 mol%) as a base in dioxane medium.[28] The arene Ru(II) complex has considerable benefits over other reported catalysts. In contrast, the salient features of titled catalysts are insensitive towards air and simple, convenient catalytic method for the synthesis of imines. Further, the bimetallic catalytic system, with a cooperative effect between the two metal centres, enhances the strong metal–metal interaction, which interact with the substrates, increasing the rate of the reaction than the monometallic system. We speculated that the

TABLE 3 Synthesis of imines from alcohols and amine[a]

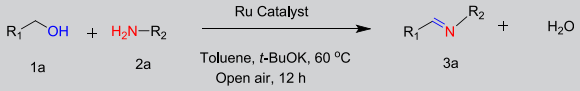

Entry	1	2	3		Yield[b] %
1	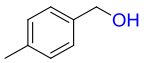	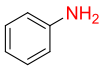	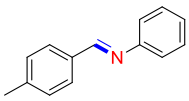	(**3a**)	95
2	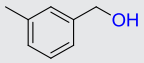	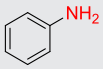	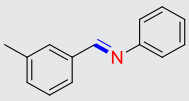	(**3b**)	80
3	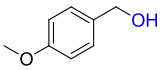	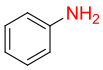	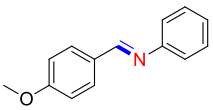	(**3c**)	83
4	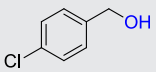	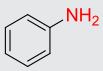	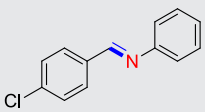	(**3d**)	88
5	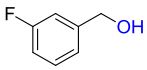	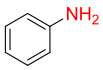	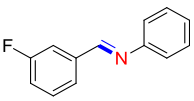	(**3e**)	78
6	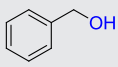	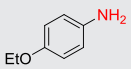	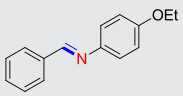	(**3f**)	80
7	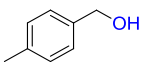	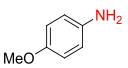	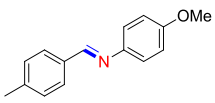	(**3g**)	83
8	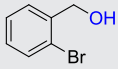	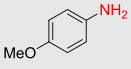		(**3h**)	75

(Continues)

TABLE 3 (Continued)

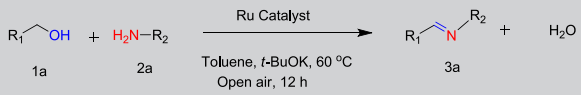

Entry	1	2	3		Yield[b] %
			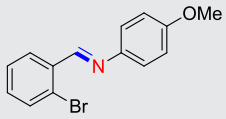		
9	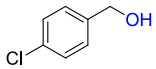	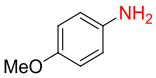	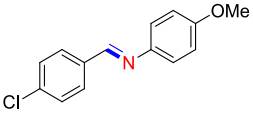	(**3i**)	79
10	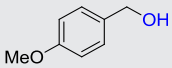	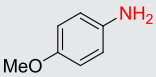	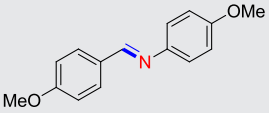	(**3j**)	82
11	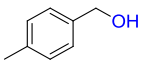	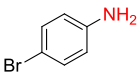	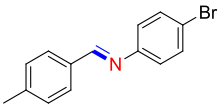	(**3 k**)	98
12	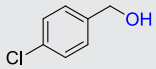	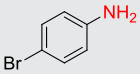	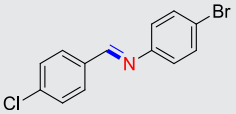	(**3 l**)	90
13	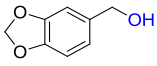	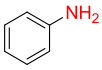	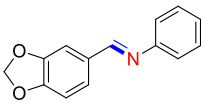	(**3m**)	70
14	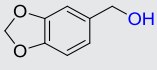	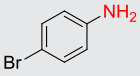	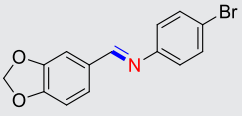	(**3n**)	94
15				(**3o**)	82

TABLE 3 (Continued)

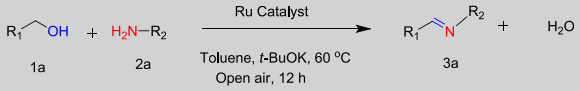

Entry	1	2	3		Yield[b] %
	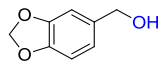	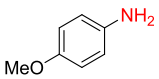	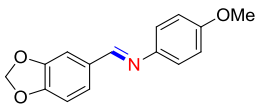		
16[c]	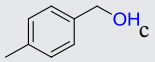	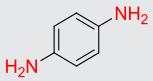	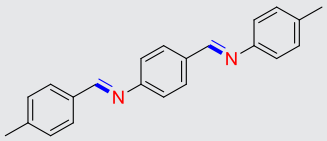	(**3p**)	75
17	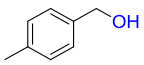	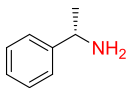	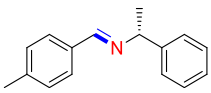	(**3q**)	84
18	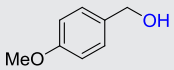	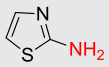	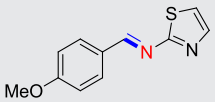	(**3r**)	70
19	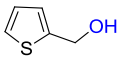	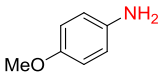	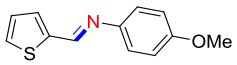	(**3s**)	87
20	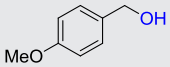		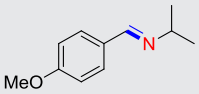	(**3t**)	60

[a]Reaction conditions: **1a** (1 mmol), **2a** (1 mmol), catalyst (1 mol%), *t*-BuOK (0.5 mmol) and toluene (5 ml) stirred for 12 h in open air.
[b]Isolated yields.
[c]Reaction for 24 h.

SCHEME 4 Preparation of *N*-(salicylidene)-2-hydroxyaniline using our protocol

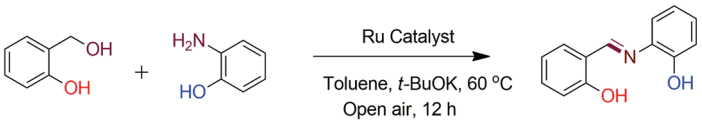

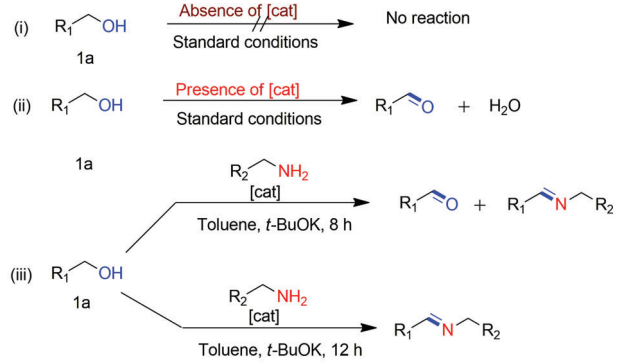

[a] Reaction conditions: alcohol 1a (1 mmol), amine (1 mmol) catalyst (1 mol %), *t*-BuOK (0.5 mmol), Toluene (5 mL) stirred for 12 h in open air.

SCHEME 5 Control experiments

catalytic performance may be from two active metal centres of the complex working independently, or only an active metal centre under the electronic influence of the second one. Hence, the catalyst loading is 1 mol% sufficient to catalyse the reaction with good-to-excellent yields.[29]

It is worth to note that one of the antibacterial drugs, namely, *N*-(salicylidene)-2-hydroxyaniline, was synthesized from 2-hydroxybenzyl alcohol and 2-amino phenol using our present protocol (Scheme 4), and an excellent yield of 95% was obtained (Figures S43, S44).

3 | CONTROL EXPERIMENTS FOR THE MECHANISTIC INVESTIGATIONS[A]

Control experiments were performed under standard conditions in order to examine the mechanism of the imination (Scheme 5). Initially, oxidation of alcohol leads to the formation of aldehyde. Further, a mixture of products aldehyde and imine was obtained when the reaction was conducted in the presence of amine for 8 h. Complete imine product was obtained only after 12 h of the reaction. Hence, the formation of aldehyde clearly indicates that the reaction proceeds via oxidation of alcohol as an initial step (Figures S45–S50).

A plausible mechanism has been proposed based on the results from the control experiments and on the previously reported literature (Scheme 6). The reaction involves the formation of ruthenium alkoxide species from the catalyst through deprotonation of the alcohol followed by β-hydride elimination to form aldehyde. This aldehyde intermediate further reacts with amines to produce imines, and water is eliminated as a by-product. Further, the ruthenium hydride[10b,30] complex reacts with alcohol to form the next catalytic cycle with the release of two molecules of water. The detailed studies on the mechanism for imine synthesis are under investigation.

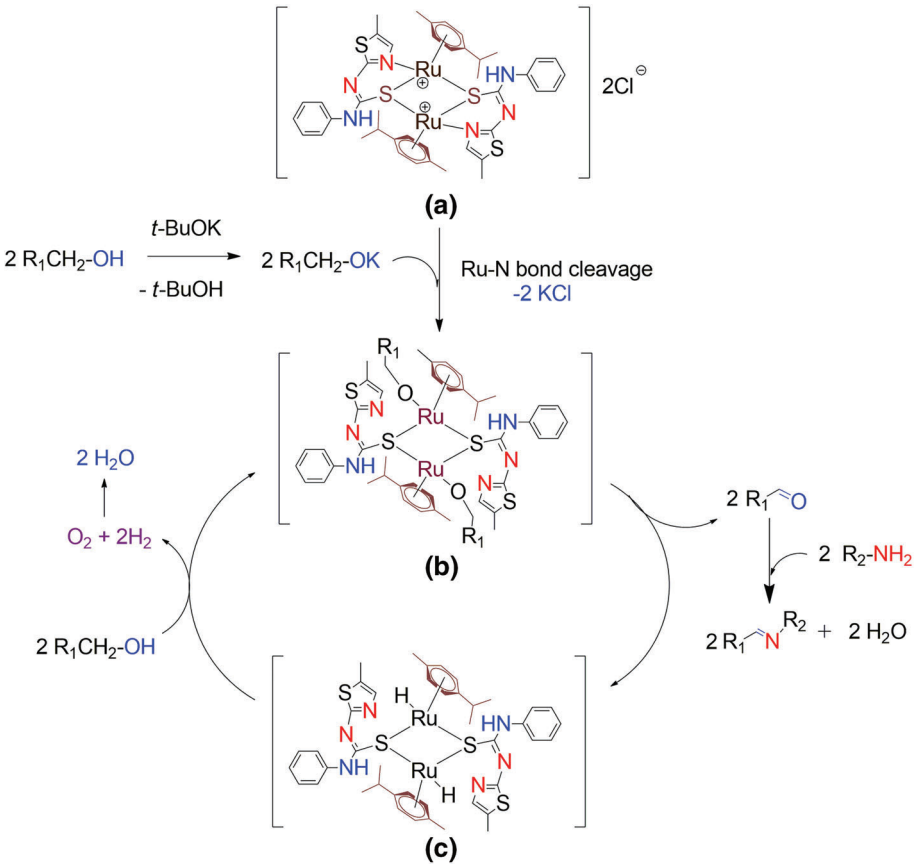

SCHEME 6 Plausible mechanism for imine formation

4 | CONCLUSIONS

Summing up, we have presented the first example of thiolato-bridged dinuclear arene Ru(II) arene complex that promoted green synthesis of highly desirable imines obtained from readily available alcohols and amines in open air as an eco-friendly oxidant. To our knowledge, this is a convenient and straightforward method for one-pot synthesis of imines from alcohols and amines. The catalyst system provides selective imination reactions of substituted alcohols with various amines with good tolerance to reducible functional groups. The complex was demonstrated as an efficient catalyst with 1 mol% loading under optimized conditions to afford up to 98% yield.

5 | EXPERIMENTAL SECTION

5.1 | General method for the synthesis of binuclear *p*-cymene ruthenium(II) complex

$[RuCl_2(\eta^6\text{-}p\text{-cymene})]_2$ (1 equiv) and 1-(5-methylthiazole-2-yl)-3-phenylthiourea(HL) (2 equiv) were dissolved in 25 ml of benzene and stirred for 6 h. The solution was reduced to 2 ml, and addition of petroleum ether (60–80°C) in excess gave a clear yellow solid.

5.1.1 | $[Ru(\eta^6\text{-}p\text{-cymene})(HL)]_2Cl_2$

Yellow solid. Yield: 92%: Anal. Calcd. For $C_{42}H_{48}Cl_2N_6Ru_2S_4$: C, 48.59; H, 4.66; N, 8.09. Found: C, 48.62; H, 4.60; N, 8.01. ^{1}H NMR (400 MHz, $CDCl_3$): δ (ppm) = 11.55 (*s*, 2H, $N\text{–}H_{(phenyl)}$), 7.58–7.60 (*m*, 4H, $ArH_{(ligand)}$), 7.43–7.47 (*m*, 4H, $ArH_{(ligand)}$), 7.36–7.38 (*m*, 4H, $ArH_{(ligand)}$), 5.43–5.57 (*m*, 2H, $CH_{(p\text{-cymene})}$), 5.30–5.38 (*m*, 6H, $CH_{(p\text{-cymene})}$), 2.80 (*sept*, 2H, CH $(CH_3)_{2\ (p\text{-cymene})}$), 2.43 (*s*, 6H, $CH_{3(p\text{-cymene})}$), 2.08 (*s*, 6H, $CH_{3\ (ligand)}$), 1.21–1.26 (*m*, 12H, CH $(CH_3)_{2(p\text{-cymene})}$). $^{13}C\{^1H\}$ NMR (100 MHz, $CDCl_3$): δ (ppm) = 175.35 (C–S), 158.22 (C═N), 140.52, 136.32, 129.19, 128.95, 127.89, 125.28 (Ar carbons of ligand), 106.66 and 100.06 (quaternary carbons of *p*-cymene), 86.29, 84.89, 84.73, 84.24 (Ar carbons of *p*-cymene), 30.78 (CH of *p*-cymene), 22.52, 22.17 ($2CH_3$, *p*-cymene), 18.54 (CH_3, *p*-cymene), 12.53 (CH_3 of ligand). Fourier transform infrared (FT-IR) (cm^{-1}): 2,925 (N–H), 1,642 (C═N), 1,594 (C═C), 1,261 (N–C═S), 1,149 and 910 (C═S). UV–vis ($CHCl_3$): λ_{max} (nm) 280, 340, 463.

5.2 | Typical procedure for imine formation reaction

The alcohol (1 mmol), an amine (1 mmol), *t*-BuOK (0.5 mmol), and a catalyst (1 mol%) were stirred at 60°C for 12 h under open-air atmosphere in 5 ml of toluene, and the reaction was monitored by thin-layer chromatography (TLC) until completion. Then, the reaction mixture was cooled and diluted with ethyl acetate (10 ml). For calculation of isolated yield, the layers were formed upon addition of water (5 ml), and organic layer was separated. The organic phase was dried over Na_2SO_4 and concentrated in vacuo. The resulting residue was purified by column chromatography using EtOAc:hexane to afford imine products.

ACKNOWLEDGMENTS

The authors are thankful to the Science and Engineering Research Board (SERB) (Scheme No. EMR/2016/004952) for providing financial support and for Junior Research Fellow to V. T. We are also thankful to the DST-India (FIST Programme) for the use of instrumental facilities at the School of Chemistry, Bharathidasan University, India.

AUTHOR CONTRIBUTIONS

Veerappan Tamilthendral: Investigation; methodology; writing-original draft. **Rengan Ramesh:** Conceptualization; supervision; validation; writing-review and editing. **Jan Grzegorz Malecki:** Software.

CONFLICT OF INTEREST

The authors declare no competing financial interest.

DATA AVAILABILITY STATEMENT

The data that support the findings of this study are available in the supplementary material of this article.

ORCID

Rengan Ramesh https://orcid.org/0000-0001-8358-9583

REFERENCES

[1] a)W. R. Layer, *Chem. Rev.* **1963**, *63*, 489. b)R. Bloch, *Chem. Rev.* **1998**, *98*, 1407. c)S. Kobayashi, H. Ishitani, *Chem. Rev.* **1999**, *99*, 1069. d)J. P. Adams, *J. Chem. Soc. Perkin Trans.* **2000**, *1*, 125. e)A. Erkkila, I. Majander, P. M. Pihko, *Chem. Rev.* **2007**, *107*, 5416.

[2] a)J. Gawronski, N. Wascinska, J. J. Gajewy, *Chem. Rev.* **2008**, *108*, 5227. b)J. Adrio, J. C. Carretero, *Chem. Commun.* **2011**, *47*, 6784. c)S. Kobayashi, Y. Mori, J. S. Fossey, M. M. Salter, *Chem. Rev.* **2011**, *111*, 2626. d)J. H. Xie, S. F. Zhu, Q. L. Zhou, *Chem. Rev.* **2011**, *111*, 1713.

[3] a)S. Patai, *The Chemistry of the Carbon Nitrogen Double Bond (Chemistry of Functional Goups)*, New York, Wiley Interscience **1970**. b)S. F. Martin, *Pure Appl. Chem.* **2009**, *81*, 195. c) Z. Guo, R. Xing, S. Liu, Z. Zhong, X. Ji, L. Wang, *Carbohydr. Res.* **2007**, *342*, 1329.

[4] a)E. M. Hodnett, P. D. Mooney, *J. Med. Chem.* **1970**, *13*, 786. b) C. M. Silva, D. L. Silva, *J. Adv. Res.* **2011**, *2*, 1.

[5] a)R. D. Patil, S. Adimurthy, *Asian J. Org. Chem.* **2013**, *2*, 726. b)W. Qin, S. Long, S. M. Panunzio, S. Biondi, *Molecules* **2013**, *18*, 12264.
[6] a)P. T. Lansbury, J. G. Colson, *J. Am. Chem. Soc.* **1962**, *84*, 4167. b)F. Palacios, C. Alonso, D. Aparicio, G. Rubiales, *Tetrahedron* **2007**, *63*, 523.
[7] a)M. Ochiai, D. Kajishima, T. Sueda, *Heterocycles* **1997**, *46*, 71. b)K. Orito, T. Hatakeyama, M. Takeo, S. Uchiito, M. Tokuda, H. Suginome, *Tetrahedron* **1998**, *54*, 8403.
[8] a)F. Westheimer, K. J. Taguchi, *Org. Chem.* **1971**, *36*, 1570. b) R. S. Varma, R. Dahiya, S. Kumar, *Tetrahedron Lett.* **1997**, *38*, 2039. c)H. Naeimi, F. Salimi, K. Rabiei, *J. Mol. Catal. A: Chem.* **2006**, *260*, 100. d)J. T. Reeves, M. D. Visco, M. A. Marsini, N. Grinberg, C. A. Busacca, A. E. Mattson, C. H. Senanayake, *Org. Lett.* **2015**, *17*, 2442.
[9] B. Gnanaprakasam, J. Zhang, D. Milstein, *Angew. Chem., Int. Ed.* **2010**, *49*, 1468.
[10] a)R. Cano, D. J. Ramon, M. J. Yus, *Org. Chem.* **2011**, *76*, 5547. b)A. Maggi, R. Madsen, *Organometallics* **2012**, *31*, 451. c)X. N. Fan, H. D. Ou, W. Deng, Z. J. Yao, *Inorg. Chem.* **2020**, *59*, 4800. d)G. Vinoth, S. Indira, M. Bharathi, A. Durgadevi, R. Abinaya, L. G. Alves, A. M. Martin, K. S. Bharathi, *Appl. Organomet. Chem.* **2019**, *33*, e5200.
[11] a)M. A. Esteruelas, N. Honczek, M. Oliván, E. Onate, M. Valencia, *Organometallics* **2011**, *30*, 2468. b)Y. H. Li, X. L. Liu, Z. T. Yu, Z. S. Li, S. C. Yan, G. H. Chen, Z. G. Zou, *Dalton Trans.* **2016**, *45*, 12400.
[12] a)M. S. Kwon, S. Kim, S. Park, W. Bosco, R. K. Chidrala, J. Park, *J. Org. Chem.* **2009**, *74*, 2877. b)L. Jiang, L. Jin, H. Tian, X. Yuan, X. Yu, Q. Xu, *Chem. Commun.* **2011**, *47*, 10833.
[13] Y. Shiraishi, M. Ikeda, D. Tsukamoto, S. Tanaka, T. Hiraia, *Chem. Commun.* **2011**, *47*, 4811.
[14] a)S. Kegnæs, J. Mielby, U. V. Mentzel, C. H. Christensen, A. Riisager, *Green Chem.* **2010**, *12*, 1437. b)H. Sun, F. Z. Su, J. Ni, Y. Cao, H. Y. He, K. N. Fan, *Angew. Chem., Int. Ed.* **2009**, *48*, 4390.
[15] J. Soule, H. Miyamura, S. Kobayashi, *Chem. Commun.* **2013**, *49*, 355.
[16] R. R. Donthiri, R. D. Patil, S. Adimurthy, *Eur. J. Org. Chem.* **2012**, *24*, 4457.
[17] H. Tian, X. Yu, Q. Li, J. Wang, Q. Xua, *Adv. Synth. Catal.* **2012**, *354*, 2671.
[18] E. Zhang, H. Tian, S. Xu, X. Yu, Q. Xu, *Org. Lett.* **2013**, *15*, 2704.
[19] S. P. Midya, J. Pitchaimani, E. Balaraman, *Catal. Sci. Technol.* **2018**, *8*, 3469.
[20] a)A. Furstner, H. Krause, C. W. Lehmann, *Chem. Commun.* **2001**, *1*, 2372. b)J. Buijtenen, J. Meuldijk, J. A. Vekemans, L. A. Hulshof, H. Kooijman, A. L. Spek, *Organometallics* **2006**, *25*, 873. c)B. Punji, J. T. Mague, M. S. Balakrishna, *Inorg. Chem.* **2007**, *46*, 11316. d)S. Priyarega, D. S. Raja, S. Ganesh Babu, R. Karvembu, T. Hashimoto, A. Endo, K. Natarajan, *Polyhedron* **2012**, *34*, 143. e)K. C. Cheung, L. Wong, M. H. So, Z. Y. Zhou, S. C. Yan, K. Y. Wong, *Chem. Commun.* **2013**, *49*, 710. f)N. P. Mankad, *Chem. – Eur. J.* **2016**, *22*, 5822. g)D. R. Pye, N. P. Mankad, *Chem. Sci.* **2017**, *8*, 1705. h)T. S. Manikandan, R. Ramesh, D. Semeril, *Organometallics* **2019**, *38*, 319.
[21] K. A. Alfallous, M. Aburzeza, *Int. J. Sci. Res.* **2015**, *4*, 350.
[22] K. Yamanari, I. Fukuda, S. Yamamoto, Y. Kushi, A. Fuyuhiro, N. Kubota, T. Fukuo, R. J. Arakawa, *J. Chem. Soc. Dalton Trans.* **2000**, (13), 2131.
[23] G. Capper, D. L. Davies, J. Fawcett, D. R. Russell, *Acta Crystallogr.* **1995**, *51*, 578.
[24] J. Canivet, B. Therrien, G. S. Fink, *Acta Crystallogr. Sect. E* **2005**, *61*, 1090.
[25] a)R. Kholiya, S. I. Khan, A. Bahuguna, M. Tripathi, D. S. Rawat, *Eur. J. Med. Chem.* **2017**, *131*, 126. b)M. Arshad, A. R. Bhat, S. Pokharel, J. E. Kim, E. J. Lee, F. Athar, I. Choi, *Eur. J. Med. Chem.* **2014**, *71*, 229.
[26] S. Musa, S. Fronton, L. Vaccaro, D. Gelman, *Organometallics* **2013**, *32*, 3069.
[27] B. Saha, S. M. W. Rahaman, P. Daw, G. Sengupta, J. K. Bera, *Chem. – Eur. J.* **2014**, *20*, 6542.
[28] T. Higuchi, R. Tagawa, A. Iimuro, S. Akiyama, H. Nagae, K. Mashima, *Chem. – Eur. J.* **2017**, *23*, 12795.
[29] S. Huang, X. Hong, H. Z. Cui, B. Zhan, Z. M. Li, X. F. Hou, *Organometallics* **2020**, *39*, 3514.
[30] S. Saranya, R. Ramesh, J. G. Małecki, *Eur. J. Org. Chem.* **2017**, *45*, 6726.

SUPPORTING INFORMATION

Additional supporting information may be found online in the Supporting Information section at the end of this article.

How to cite this article: Tamilthendral V, Ramesh R, Malecki JG. Arene diruthenium(II)-mediated synthesis of imines from alcohols and amines under aerobic condition. *Appl Organomet Chem*. 2020;e6122. https://doi.org/10.1002/aoc.6122

Received: 20 October 2021 | Revised: 10 November 2021 | Accepted: 26 November 2021

DOI: 10.1002/aoc.6561

FULL PAPER

Applied Organometallic Chemistry WILEY

Ru(II)–NNO pincer-type complexes catalysed E-olefination of alkyl-substituted quinolines/pyrazines utilizing primary alcohols

Veerappan Tamilthendral[1] | **Gunasekaran Balamurugan**[1] | **Rengan Ramesh**[1] | **Jan Grzegorz Malecki**[2]

[1]Centre for Organometallic Chemistry, School of Chemistry, Bharathidasan University, Tiruchirappalli, Tamil Nadu, India

[2]Department of Crystallography, Institute of Chemistry, University of Silesia, Katowice, Poland

Correspondence
Rengan Ramesh, Centre for Organometallic Chemistry, School of Chemistry, Bharathidasan University, Tiruchirappalli, Tamil Nadu 620 024, India.
Email: rramesh@bdu.ac.in

Funding information
Science and Engineering Research Board, Grant/Award Number: EMR/2016/004952

Abstract

An efficient and selective E-olefination of alkyl-substituted quinolines and pyrazines through acceptorless dehydrogenative coupling of alcohols catalysed by Ru(II)–N^N^O pincer-type complexes encompassing carbonyl and triphenylarsines as co-ligands is demonstrated. An array of Ru(II) catalysts has been synthesized and evaluated by analytical and spectral methodologies. The solid-state molecular structure of the synthesized complex (**2**) has been substantiated by x-ray crystallography. The catalytic protocol produces a diverse range of olefinated products up to 90% by employing readily available primary alcohols. The present synthetic strategy is operationally simple and scalable and tolerates various functional groups under mild reaction conditions. Notably, an aldehyde and aryl-2-quinoline-2-yl-ethanol intermediate are involved in the catalytic reaction mechanism. The utility of the present procedure is demonstrated through a facile synthesis of the antifungal drug (E)-2-(2-(pyridin-4-yl)vinyl)quinoline.

KEYWORDS

acceptorless dehydrogenative coupling, alcohols, E-olefination, quinolines/pyrazines, Ru(II)–NNO pincer-type complexes

1 | INTRODUCTION

Olefins, especially conjugated E-selective olefins, are important key motifs found in various natural products, pharmaceuticals and materials.[1] Particularly, *N*-heteroarenes are widely used as intermediates for the fabrication of valuable materials, conducting polymers and organic light-emitting diodes.[2] Moreover, quinoline-based conjugated *N*-heteroarenes exhibit biological activities such as antifungal, antiviral, antibacterial and antitumour activities (Figure 1).[3] Owing to the biomedical prominence, the synthesis of such useful quinoline/pyrazine-based conjugated *N*-heteroarene derivatives attracted synthetic chemists and has been broadly explored in catalysis research.

Notably, several conventional approaches were documented for the synthesis of E-olefins by various research groups with an appropriate leaving functional group.[4] In addition, coupling reactions including Heck, Suzuki and olefin metathesis have been well-known strategies for the fabrication of olefins.[5]

Construction of E-selective olefins was performed by the condensation of aldehydes with *N*-heteroarenes in the presence of an oxidant, Lewis acid, organocatalysts, acid or base as well.[6] Nevertheless, the aforementioned reported protocols suffer by some major shortfalls like

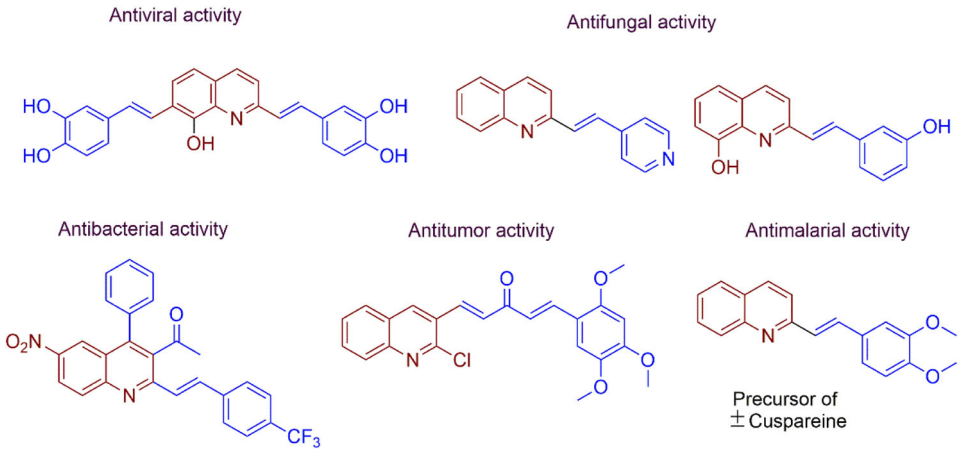

FIGURE 1 Selective examples for bioactive methyl *N*-heteroarene analogues

(a) harsh synthetic process, (b) poor selectivity and (c) stoichiometric waste.[7] Hence, greener and cost-effective methods to the sustainable fabrication of E-selective olefin compounds conjugated with *N*-heteroarenes are an extremely demanding goal.[8] In this scenario, the transition metal-supported conversion of C(sp^3)—H bonds into olefins would be an alternative approach as it has received significant attention in recent years.[9]

The acceptorless dehydrogenative coupling (ADC) strategy symbolizes most atom economical and clearest procedures as a substitute to conventional oxidation with water and hydrogen as only the valuable side products. In this connection, Zhang et al. have reported that Mn–PNP complexes catalysed olefination of *N*-heteroarenes using primary alcohols at longer reaction time.[10] Maji research group demonstrated pincer manganese catalysts mediated alkenation of methyl *N*-heteroarenes employing primary alcohols under an inert atmosphere.[11] Banerjee and co-workers have explored Ni(II) catalysed olefination of *N*-heteroarenes with alcohols at inert condition; concurrently, Fe(II) catalysed olefination reaction was also documented by the same research group.[12] Baidya group reported the synthesis of olefin from 2-methylheteroarene with primary alcohols in the presence of in situ generated Ni(II) complexes in tertiary butyl alcohol at 140°C for 48 h.[13] Zhang research group has disclosed MnO_2-mediated olefination of *N*-heteroarenes with alcohols at inert atmosphere.[14] Recently, the Elias group reported *N*-heteroarene olefination from alcohols/amines in the presence of tert-Butyl hydroperoxide (TBHP)/4-Dimethylaminopyridine (DMAP) in water medium[6a] (Scheme 1).

Though different metal catalysts with various ligand frameworks were developed for the olefination of *N*-heteroarenes' reaction with alcohols, they are associated with some drawbacks including high catalyst loading, higher temperature, necessity of oxidants and inert atmospheric conditions. To overcome the above issues by a sustainable protocol, we are interested to execute the olefination of *N*-heteroarenes with primary alcohols catalysed by ruthenium complexes with simple NNO pincer-type ligands.

In general, ligand partners have been the imperative constituent of the metal catalysts/pre-catalysts, which can stabilize the metal centre and regulate the stereoselectivity, chemoselectivity and enantioselectivity of chemical transformations, the solution state reactivity and so forth. Further, the metal–ligand cooperation depends on their both electronic and steric properties of ligands by the design of suitable donor triads, size of the metallic rings, nature of the ancillary and neutral and anionic ligands. Tridentate ligands possess a perfect balance of control on composition of the coordination geometry by carrying the donor atoms in an orderly configuration. Upon complexation, these tridentate ligands formed meridional geometry with a metal centre and control the vacant coordination sites, which increase the stability of the pincer complexes.[15] Furthermore, the ligands have given a strong *mer*-coordination, planarity around the metal centre that provides a good balance of stability and reactivity, which distinguishes the pincer complexes from other homogeneous catalysts.[16] Moreover, metal complexes comprising pincer-type ligands possess enticing catalytic activities and ever-increasing applications in various fields.[17]

Herein, we have reported the synthesis and structural elucidation of new Ru(II) pincer-type complexes comprising NNO terdentate ligands with easy leaving $AsPh_3$ as co-ligands, and the synthesized complexes were developed as catalysts for selective E-olefination of methyl *N*-heteroarenes via ADC of primary alcohols. The present protocol requires only mild reaction conditions and uses low catalyst loading and covers a diverse range of substrate scope with good yields of olefin products.

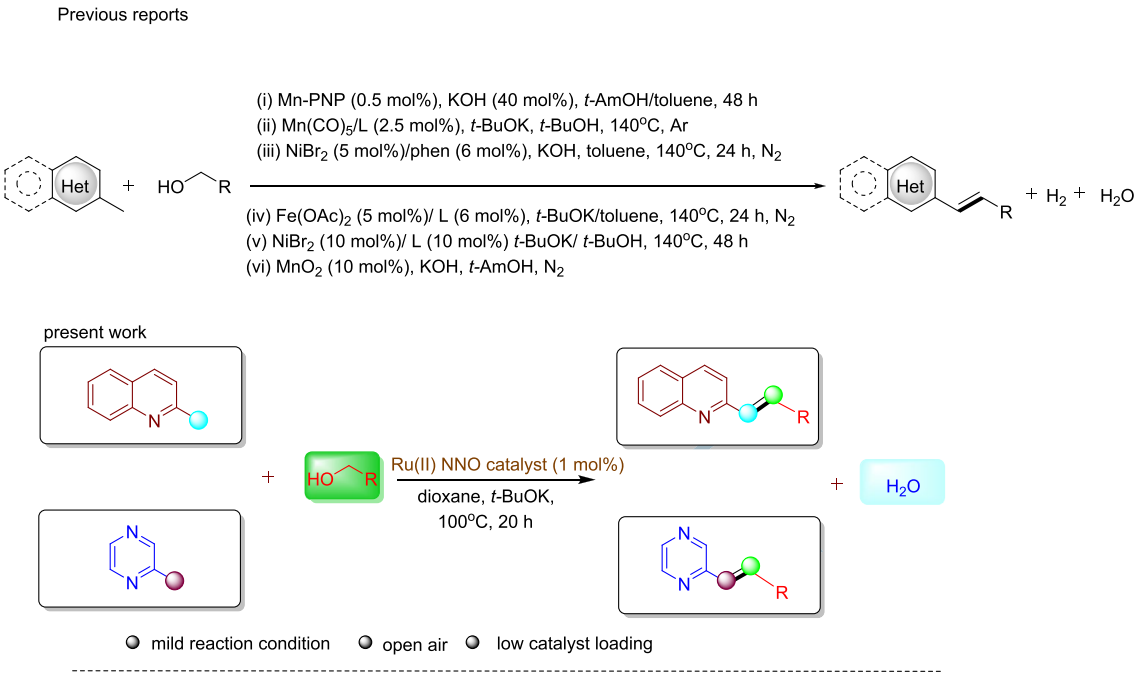

SCHEME 1 Methods for E-olefination of methyl *N*-heteroarenes with alcohols

2 | RESULTS AND DISCUSSION

The simple NNO pincer-type ligands (L1–L3) were easily prepared from condensation methyl-2-pyrrole and 4-substituted benzohydrazides in methanol.[18] The synthesis of Ru(II)–NNO pincer-type complexes was accomplished in good yield from the reaction of [RuHClCO $(AsPh_3)_3$] with the prepared ligands in 1:1 molar ratio in benzene medium using Et_3N as a base (Scheme 2). The synthesized Ru(II)–NNO pincer-type complexes are stable in air and can be dissolved in most organic solvents. The structures of the newly formed Ru(II)–NNO symmetrical pincer complexes were confirmed by analytical and spectral methods.

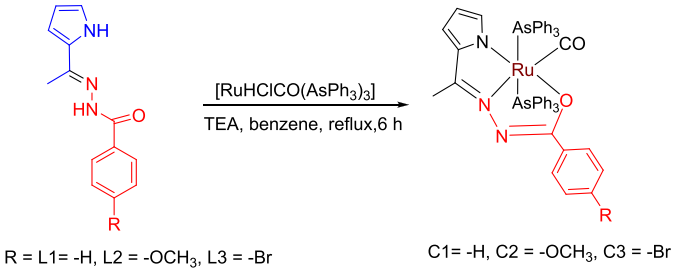

SCHEME 2 Synthetic route to Ru(II)–NNO pincer-type complexes

In the infrared (IR) spectra, stretching bands found around 3400–3430 and 3235–3262 cm^{-1} regions were attributed to pyrrole and hydrazone N–H moieties of L1–L3. Besides, the strong bands around 1640–1684 and 1684–1710 cm^{-1} have been assigned for C═N and C═O functional groups of ligands, L1–L3. The absence of ν_{N-H} frequencies in the complexes evidenced the bonding of pyrrole nitrogen to ruthenium ion. Further absence of C═O band along with emergence of new intense C—O band (1228–1279 cm^{-1}) indicated the tautomerization and consequent binding of the imidolate oxygen to ruthenium. In all the spectra of complexes, C═N stretching frequencies were lower (1514–1530 cm^{-1}) than free ligands and confirmed that the imine nitrogen possesses the yet another point of attachment to ruthenium ion. Further, the complexes possess strong band around 1920–1928 cm^{-1} due to the terminally binded carbonyl group. The bands in the region 1412–1483 cm^{-1} are attributed to ruthenium-bounded triphenylarsines.[19] From the IR spectral data, the tridentate coordination of ligand to the ruthenium via imidolate oxygen, pyrrole nitrogen and imine nitrogen was corroborated.

The ultraviolet–visible (UV–vis) spectra of all the Ru(II)–NNO pincer-type complexes revealed strong bands in the 250–460 nm range. The π–π* and n–π* ligand-centred transitions have been observed with high intensity at 246–355 nm. Moreover, the complexes showed a band in the 451–460 nm range, which was attributed to metal to ligand-centred transitions and comparable with other similar Ru(II) complexes.[20]

The proton nuclear magnetic resonance (NMR) spectra of ligands exhibited two singlets in the region of δ 8.95–10.85 ppm due to the hydrazinic and pyrrole

nitrogens. The methyl protons of the ligands were appeared as singlet at δ 1.64 ppm. Another singlet at δ 3.82 ppm was addressed to methoxy protons of ligand **2**. The absence of both –NH peaks of the ligand indicates that pyrrole nitrogen and hydrazinic nitrogen are coordinated to Ru(II) centre. Further, aromatic protons of the hydrazone ligand and triphenylarsines resonated as multiplet in the range of δ 5.64–7.62 ppm. Besides, the formation of the synthesized complexes were further evidenced by $^{13}C\{^{1}H\}$ NMR spectra. The bonding of imidolate oxygen and hydrazinic nitrogen to Ru(II) ion was authenticated by the upshift of C═N (172 ppm) and downshift C—O (153 ppm) in the spectra of the complexes.

The suitable quality of crystals was grown by slow evaporation of $CHCl_3$/MeOH solvent (1:1). The x-ray single-crystal diffraction analysis was used to confirm the solid-state structure of complex **2**. The Oak Ridge thermal ellipsoid plot (ORTEP) diagram of complex **2** is depicted in Figure 2. The complex **2** crystallized in monoclinic space group '$P2_1/n$'. The crystallographic data as well as selected bond lengths and bond angles are described in Tables S1 and S2. The pincer-type ligand meridionally binded with ruthenium ion in NNO tridentate manner and resulted in two five-membered chelate rings. The remaining positions were filled by a CO and sterically hindered two triphenylarsine ligands that are trans to each other and thus form a pseudo-octahedral geometry around Ru(II) ion. The Ru(1)–N(1) bond distance of the ligand is significantly shorter (2.025(3) Å) than the Ru(1)–N(3) bond distance (2.078(4) Å), in agreement with the geometrical constraints of the tridentate ligand showing N(1)–Ru(1)–N(3) and N(1)–Ru(1)–O(2) bond angles 77.79(14)° and 75.98(12)°, respectively. The N(1)–Ru(1)–C(1) angle is slightly distorted from the idealized 180° to 177.87(16)°, and the N(1)–Ru(1)–As(1) angle is 88.80(9)°. Further, the bond distances and bond angles of complex **2** are consistent with other reported Ru(II) complex possess pseudo-octahedral geometry.[21]

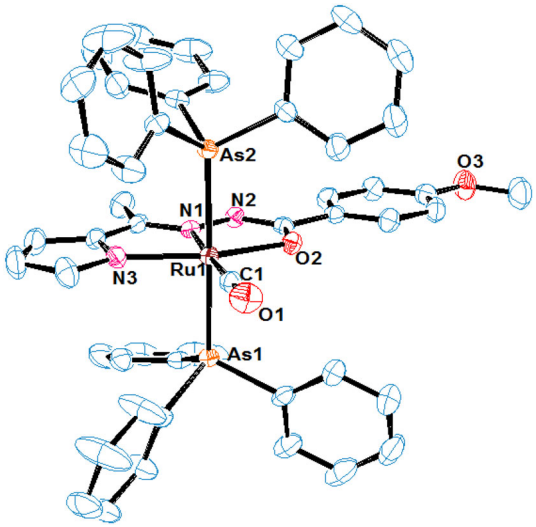

FIGURE 2 ORTEP view of complex **2**. All hydrogens were omitted for clarity. Selected bond lengths (Å) and angles (°): Ru(1)–N(1) = 2.025(3), Ru(1)–N(3) = 2.078(4), Ru(1)–C(1) = 1.858(4), Ru(1)–As(1) = 2.4504(5), Ru(1)–As(2) = 2.4543(5), N(1)–Ru(1)–C(1) = 177.87(16), N(3)–Ru(1)–O(2) = 153.76(13), As(1)–Ru(1)–As(2) = 176.62(2), N(1)–Ru(1)–As(1) = 88.80(9), N(1)–Ru(1)–As(2) = 87.84(9), N(1)–Ru(1)–O(2) = 75.98(12), N(1)–Ru(1)–N(3) = 77.79(14)

To select the appropriate reaction condition for the fabrication of E-olefins (**3a**), several catalytic variables such as different bases, solvents, time and temperatures have been tested using pincer-type Ru(II) complex as catalysts. The model reaction between 2-methylquinoline **1a** and benzyl alcohol **2a** as test substrates utilizing Ru(II) catalysts in combination with various solvents, bases and temperatures is depicted in Table 1. While employing Ru(II) complex **1** (1 mol%) as a catalyst, in the presence of K_2CO_3 and Cs_2CO_3 bases at 110°C in toluene medium, the ADC reaction gives E-selective olefinated product **3a** with 40%–43% yields (Table 1, entries 1 and 2). Further, the model reaction was performed in toluene/KOH mixture, and the yield of **3a** was increased up to 60% (Table 1, entry 3). Furthermore, the catalytic efficiency of the complexes **2** and **3** as catalysts was evaluated by allowing the test substrates to perform in toluene medium, and the product **3a** was isolated in 71% and 53% yields, respectively (Table 1, entries 4 and 5). Among the three complexes, we found that complex **2** was the most effective catalyst for this reaction because the electron-donating group (–OCH_3) enhances the catalytic activity.[22]

The catalyst and base are essential for the catalytic reaction because in the absence of any of them, the reaction was unfruitful (Table 1, entries 6 and 7). Conspicuously, when the reaction was accomplished with *t*-BuOK instead of KOH, the yield of **3a** was 79% (Table 1, entry 8). While comparing the yields of the end product, the outperformance of *t*-BuOK over the other bases was distinguished. In the model reaction, switching solvents and temperatures with *t*-BuOK base was performed, and among them, 1,4-dioxane operated well at 80°C (Table 1, entries 9–14). It has been observed that complex **2** gave the maximum yield of 80% of **3a** from the coupling of 2-methylquinoline with benzyl alcohol under the conditions of 1,4-dioxane/*t*-BuOK at 100°C in 20 h (Table 1, entry 15).

In addition, the impact of catalyst loading was investigated. While reducing the catalyst loading from 1 to 0.5 and 0.25 mol%, a decrease of yield of the product **3a** was observed in 51% and 42%, respectively (Table 1, entries 16 and 17).

TABLE 1 Screening of reaction conditions

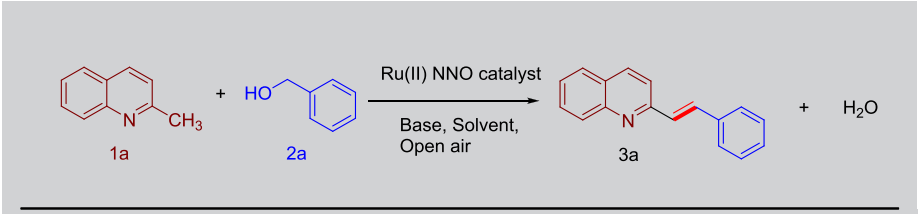

Entry	Complex	Solvent	Base	Temp (°C)	Time (h)	Yield[a]
1	**1**	Toluene	K_2CO_3	110	24	40
2	**1**	Toluene	Cs_2CO_3	110	24	43
3	**1**	Toluene	KOH	110	24	60
4	**2**	Toluene	KOH	110	24	71
5	**3**	Toluene	KOH	110	24	53
6[b]	—	Toluene	KOH	130	24	NR
7[c]	**3**	Toluene	—	130	24	NR
8	**2**	Toluene	*t*-BuOK	130	24	79
9	**2**	*m*-Xylene	*t*-BuOK	130	24	66
10	**2**	*t*-BuOH	*t*-BuOK	100	24	50
11	**2**	THF	*t*-BuOK	100	24	45
12	**2**	Acetonitrile	*t*-BuOK	80	24	20
13	**2**	Ethanol	*t*-BuOK	80	24	27
14	**2**	1,4-Dioxane	*t*-BuOK	80	20	68
15	**2**	**1,4-Dioxane**	***t*-BuOK**	**100**	**20**	**80**
16	**2** (0.50 mol%)	1,4-Dioxane	*t*-BuOK	100	20	51
17	**2** (0.25 mol%)	1,4-Dioxane	*t*-BuOK	100	20	42

Note: Reaction conditions: 2-Methylquinoline (**1a**; 1 mmol), benzyl alcohol (**2a**; 1 mmol), complex (1 mol%), *t*-BuOK (0.5 mmol) and solvent (4 ml). The bold data in the table indicate the best optimized reaction condition.

[a]Isolated yield of **3a** product.

[b]Absence of catalyst.

[c]Absence of base.

Thus, Table 1 outlined that the best optimal conditions for the ruthenium complexes catalysed selective E-olefination of methyl *N*-heteroarenes using primary alcohols. The reaction operated well at 1 mol% of complex **2** as a catalyst with *t*-BuOK as a base in 1,4-dioxane medium at 100°C for 20 h under open-air atmosphere.

After optimization, the substrate scope of the olefination reaction was examined, and the findings are documented in Table 2. The catalytic efficiency exhibited by the complex **2** in the test reaction was conveniently applied to 2-methylquinoline and 2-methylpyrazines with a variety of electronic and sterically different primary alcohol derivatives and selectivity in E-selective olefin products seen in every case. Benzyl alcohols encompassing electron-rich groups such as 4-methyl, 3-methoxy and 4-methoxy substituents resulted **3b–3d** in high yields up to 90% of the desired olefins (Figures S7–S14). In contrast, electron-deficient groups like 3-chloro, 4-chloro and 3-bromo benzyl alcohols tolerated well with 2-methylquinoline to deliver olefin products **3e–3g** (Figures S15–S20) comparatively low yields (70%–78%). Fabulously, electron-poor 4-nitrobenzyl alcohol was successfully transferred into the respective olefin **3h** in 50% isolated yield (Figures S21 and S22). In addition, the complex **2** effectively catalysed the dehydrogenative coupling of 2-methylquinoline and benzyl alcohols with two and three electron-releasing substituents including 3,4-dimethoxy, 2,6-dimethoxy and 3,4,5-trimethoxy benzyl alcohols and furnished the corresponding olefins **3i–3k** (Figures S23–S28) in 73%–83% yields. Besides, the yield of olefin **3l** has been 60% when the ADC reaction was performed with 2-methylquinoline and electron-deficient 2,6-dichloro benzyl alcohol (Figures S29 and S30).

Interestingly, the present catalytic approach can be exploited for sterically fused aromatic alcohols including 1-naphthalene methanol, 9-anthracene methanol and 1-pyrene methanol, and they were smoothly converted into suitable olefins **3m–3o** with 72%–78% isolated yield

TABLE 2 Ru(II)–NNO catalysed E-olefination of methyl *N*-heteroarenes

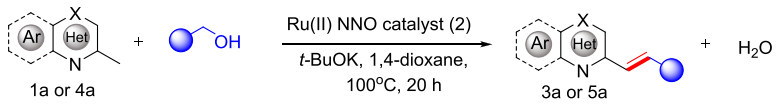

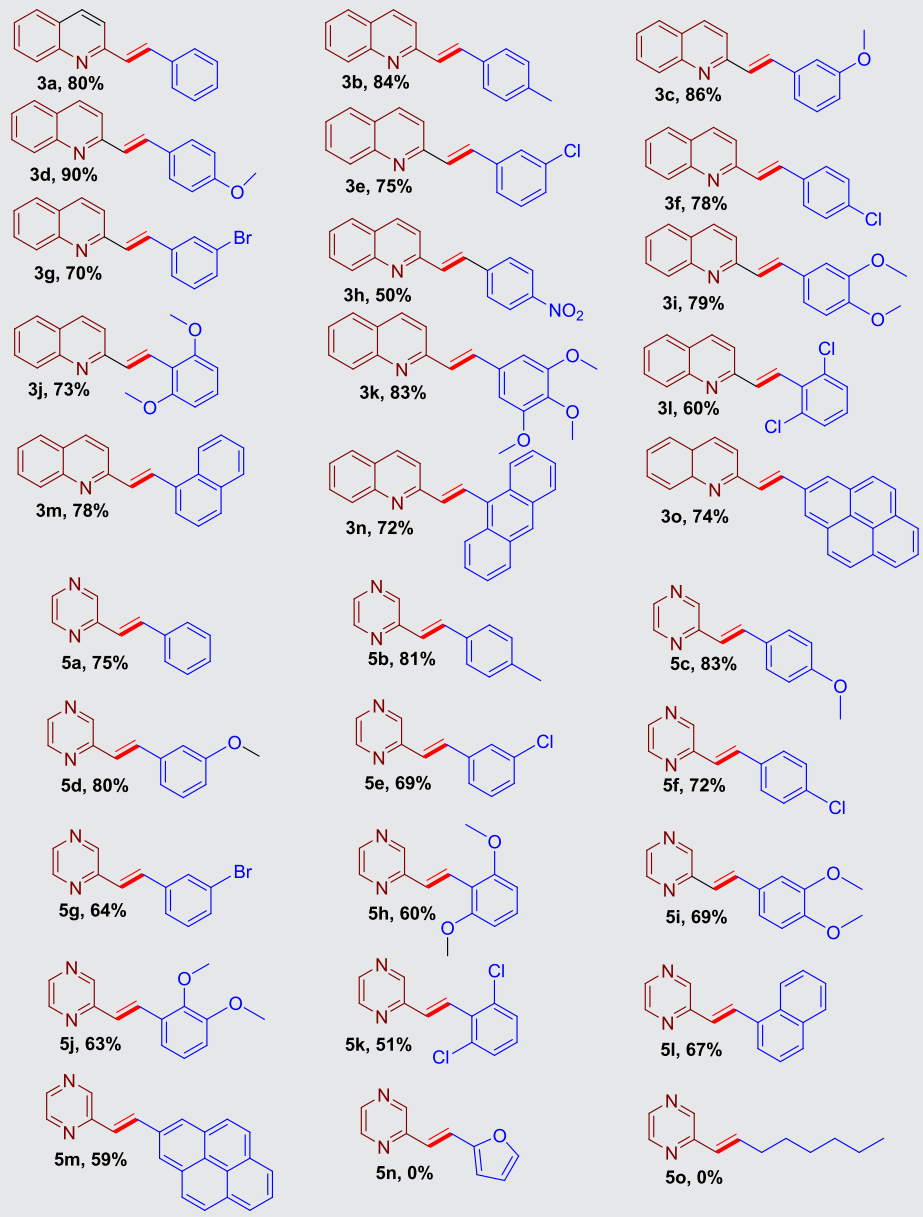

Note: Reaction conditions: 2-Methylquinoline (**1a**) or 2-methylpyrazine (**4a**; 1 mmol), alcohol (1 mmol), Complex **2** (1 mol%), *t*-BuOK (0.5 mmol), 1,4-dioxane (4 ml), 20 h in open air.

(Figures S31–S36). Encouraged by the yield of the olefin products, the utility of the present catalytic protocol was further extended to the olefination of 2-methylpyrazine with various benzyl alcohols derivatives. Under standard conditions, 2-methylpyrazine smoothly reacted with benzyl alcohol, 4-methylbenzyl alcohol, 4-methoxybenzyl alcohol and 3-methoxybenzyl alcohol to led the respective olefinated pyrazines **5a**–**5d** (Figures S37–S44) up to 83% yields. Strikingly, the reaction operated well for 2-methylpyrazine with electron-deficient groups

including 3-chloro, 4-chloro and 3-bromobenzyl alcohols in 64%–72% yields of **5e**–**5g** (Figures S45–S50). Delightfully, the benzyl alcohols comprising electron-rich groups such as 2,6-dimethoxy, 3,4-dimethoxy and 2,3-dimethoxy are tolerated well with 2-methylpyrazine to provide the equivalent olefins **5h**–**5j** (Figures S51–S56) up to 69%

SCHEME 3 Synthesis of (E)-2-(2-(pyridin-4-yl)vinyl)quinoline

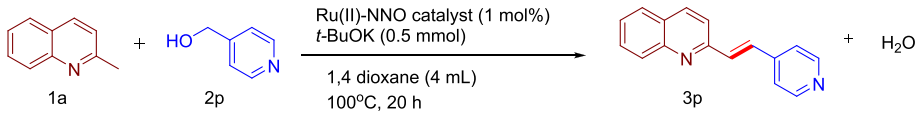

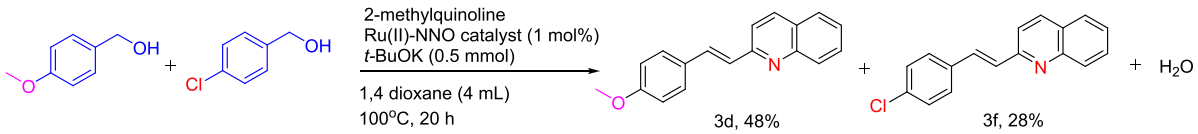

SCHEME 4 Competitive experiment between electron-donating and electron-withdrawing groups

SCHEME 5 Gram-scale synthesis of olefin

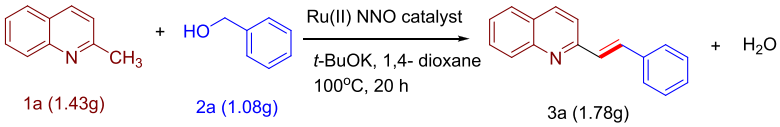

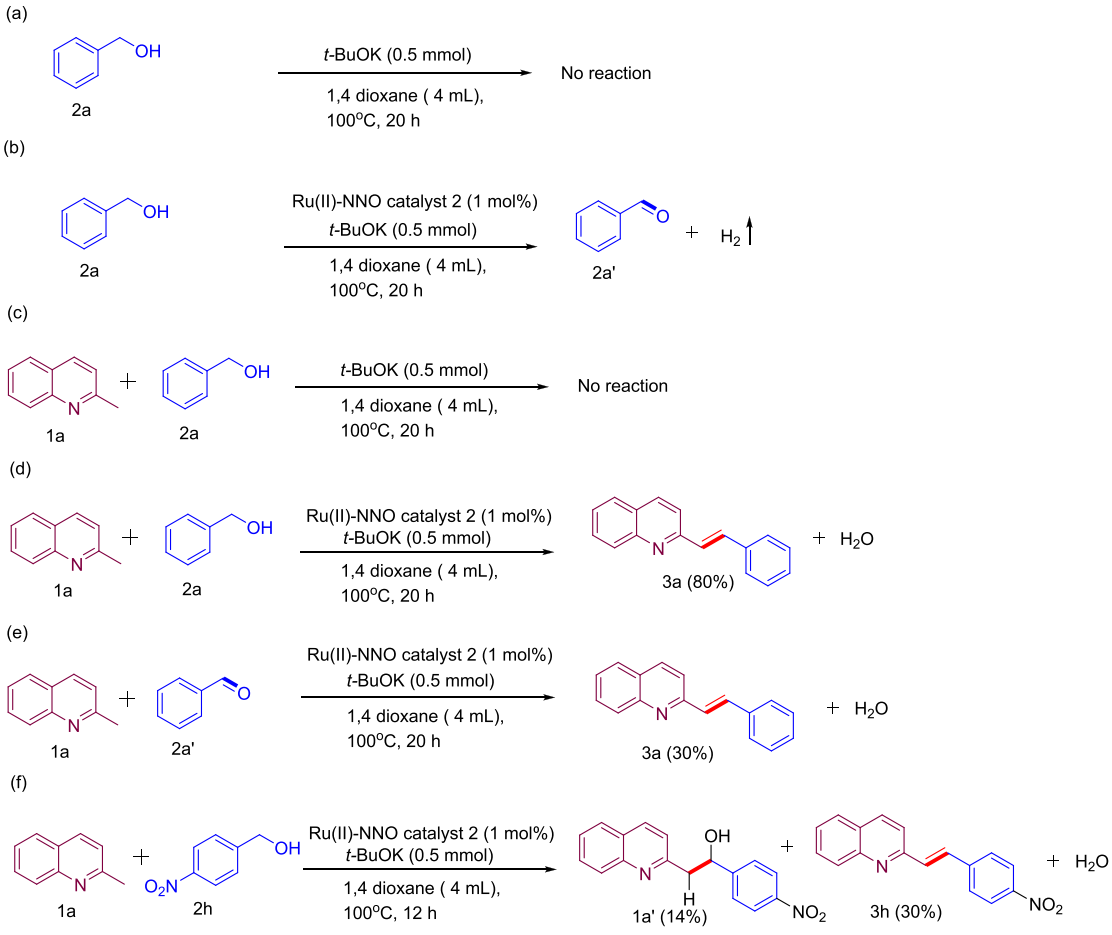

SCHEME 6 Control experiments: (a) in the absence of **1a** and catalyst; (b) in the absence of **1a** and the presence of catalyst; (c) **1a** treated with **2a**, and absence of catalyst; (d) **1a** treated with **2a** and the presence of catalyst; (e) **1a** treated with **2b**; and (f) formation of aryl-2-quinoline-2-yl-ethanol intermediate in presence of catalyst

yield. Additionally, the benzyl alcohol with electron-withdrawing substituent, 2,6-dichlorobenzyl alcohol was elegantly treated under the optimal condition to deliver the respective **5k** (Figures S57 and S58) product in 51% yield. Pleasingly, sterically hindered aromatic alcohols produce the appropriate E-olefin products **5l**–**5m** (Figures S59–S62) in moderate yields. Nonetheless, the reactions of 2-methylpyrazine with heterocyclic and aliphatic alcohols were found to be unproductive (Table 2, **5n**–**5o**).

Overall, the presence of the easily exchangeable $AsPh_3$ groups has promoted the catalytic efficiency of the pincer Ru(II)–NNO complexes towards the synthesis of E-selective olefines in high yields. It should be highlighted that the current catalytic system performed well in the open air without any additive/oxidant at 1 mol% catalyst loading.

In addition, one of the antifungal drugs, (E)-2-(2-(pyridin-4-yl)vinyl)quinoline (**3p**), has been synthesized utilizing the present methodology from 2-methylquinoline and 4-pyridinemethanol with a good yield (Figures S63 and S64) of 80% (Scheme 3).

A competitive experiment was performed under optimized reaction conditions using benzyl alcohol containing electron-donating (4-methoxybenzyl alcohol) and electron-withdrawing groups (4-chlorobenzyl alcohol) with 2-methylquinoline to gain a better understanding of the electronic effects of substitutes on catalytic activity. The results outlined that the electron-donating group is more reactive than the electron-withdrawing group (Scheme 4).

Further, gram-scale synthesis was also established to demonstrate the utility of current catalytic protocol. For that purpose, we performed the reaction of benzyl alcohol (1.08 g, 10 mmol) with 2-methylquinoline (1.43 g, 10 mmol) in the presence of catalyst (0.1 g, 1 mol%), *t*-BuOK (0.56 g, 0.5 mmol) and 1,4-dioxane (40 ml) furnished desired **3a** in 77% yield (Scheme 5).

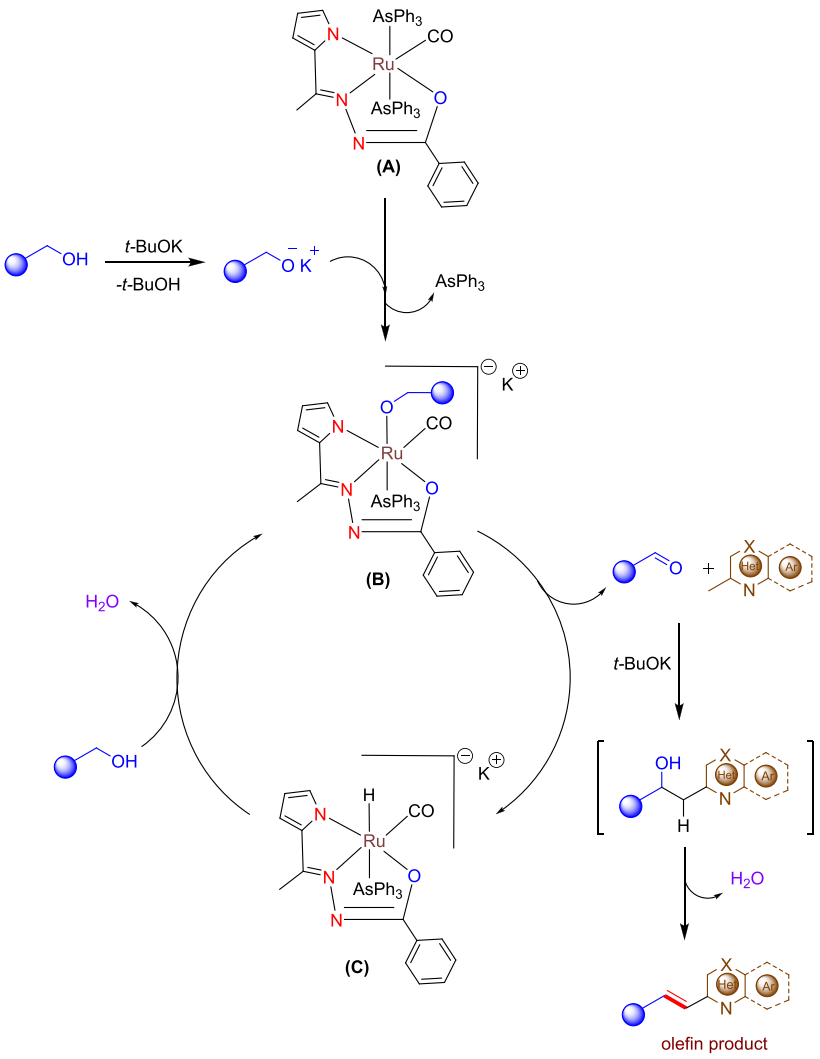

SCHEME 7 Plausible reaction mechanism

3 | CONTROL EXPERIMENTS FOR THE MECHANISTIC INVESTIGATIONS

To get better understanding of the mechanistic study, a series of control experiments under various reaction conditions has been carried out. Initially, the reaction of benzyl alcohol (**2a**) in the absence of **1a** and catalyst was conducted under standard condition, but it did not proceed (Scheme 6a). However, when benzyl alcohol (**2a**) was treated under optimal conditions in the presence of a catalyst, it releases the corresponding aldehyde and hydrogen gas (Scheme 6b). Moreover, no reaction was taken place when **2a** was reacted with **1a** in the absence of catalyst. However, the reaction generated **3a** in 80% yield, whereas the coupling has been executed with benzyl alcohol **2a** in the presence of catalyst (Scheme 6c,d). In contrast, **1a** reacts with benzaldehyde (**2a′**; Figures S65 and S66) under standard conditions to give the olefin product **3a** only with 30% of the yield (Scheme 6e).

In addition, the control experiment was carried out to trap aryl-2-quinoline-2-yl-ethanol intermediate[23] (**1a′**; Figures S67 and S68) by reacting **1a** and 4-nitrobenzyl alcohol (**2h**) in 12 h. Further, **1a′** subsequently underwent dehydration to furnish the desired olefinated products (Scheme 6f). Hence, on the basis of control experiments, we strongly believe that the current olefination reaction occurs via aldehyde intermediate, which is produced through an acceptorless dehydrogenative pathway from benzyl alcohol.

From control experiments and previous reports,[12,13] a plausible reaction mechanism for olefination of methyl *N*-heteroarenes using Ru(II)–NNO pincer catalyst is depicted (Scheme 7). Initially, the Ru(II)–NNO pincer-type catalyst (**A**) reacts with alcohols in the presence of a base to form ruthenium alkoxide (**B**). After that, (**B**) underwent *β*-hydride elimination to release aldehyde and Ru–H species (**C**). Further, alcohol reacts with ruthenium hydride species (**C**) to generate ruthenium alkoxide species (**B**) with the liberation of H_2, and thereby, catalyst enters into the next catalytic cycle. Afterwards, the liberated aldehyde reacts with 2-methylheteroarenes in the presence of a base to afford aryl-2-quinoline-2-yl-ethanol intermediate followed by dehydration to yield the desired olefinated product.

4 | CONCLUSIONS

In summary, the first report on the synthesis of Ru(II)–NNO pincer-type complexes mediated selective E-olefination of methyl *N*-heteroarenes using primary alcohols under mild reaction conditions was described. This present approach unveiled the synthesis of a variety of E-selective olefinated products in the maximum yield of 90% using 1 mol% of Ru(II) catalyst loading. The present approach is efficient, highly facile and environmentally friendly as hydrogen and water are gentle by-products. Control experiments and the mechanistic insights evidenced that the olefination reaction of *methyl N* heteroarenes proceeds via ADC pathway. Undoubtedly, this catalytic strategy discovers a chance for the production of biologically important olefins using Ru(II)–NNO pincer-type catalysts.

5 | EXPERIMENTAL SECTION

5.1 | The general method for the synthesis of Ru(II)–NNO pincer complexes

An equimolar ratio of 4-substituted pyrrole ketone benzhydrazone (1 mmol), $[RuHClCO(AsPh_3)_3]$ (1 mmol) and triethylamine (1 mmol) was mixed in benzene (15 ml; Scheme 2). The resulting reaction mixture was refluxed for 6 h. The completion of the reaction was monitored by thin-layer chromatography. The resulting solution was concentrated to 2 ml, and the addition of petroleum ether (60–80°C) in excess gave a brown solid.

5.2 | Characterization data of complexes

Complex **1**. Brown solid, Yield: 80%, m.p.: 228°C (with decomposition). Anal. Calcd: $C_{50}H_{41}As_2N_3O_2Ru$: C, 62.12; H, 4.27; N, 4.35%. Found: C, 62.08, H, 4.24, N, 4.29%. Fourier transform infrared (FT-IR; KBr, cm^{-1}): 1514 $\nu_{(C=N)}$, 1,228 $\nu_{(C-O)}$, 1510 ν(C═N—N═C). UV–vis (CH_3CN): λ_{max} (nm) 248, 353, 458. ^1H NMR (400 MHz, $CDCl_3$): δ (ppm) = 7.49 (d, J = 8 Hz, 3H, ArH (ligand)), 7.24–7.06 (m, 32H, ArH (ligand + $(AsPh_3)_2$)), 6.11 (s, 1H, pyrrole C—H), 6.04 (d, J = 4 Hz, 1H pyrrole C—H), 5.64 (s, 1H, pyrrole C—H), 1.57 (s, 3H, ligand CH_3). ^{13}C $\{^1H\}$ NMR (100 MHz, $CDCl_3$): δ (ppm) = 204.05 (Ru—CO), 172.38 (N═C—O), 153.23 (C═N), 137.50, 132.77, 131.36, 128.61, 127.72, 127.52, 127.37, 126.92, 126.18, 112.09, 108.70 (Ar carbons (ligand + $(AsPh_3)_2$)), 28.76 (ligand CH_3).

Complex **2**. Brown solid, Yield: 85%, m.p.: 235°C (with decomposition). Anal. Calcd: $C_{51}H_{43}As_2N_3O_3Ru$: C, 61.45; H, 4.35; N, 4.22%. Found: C, 61.40, H, 4.32, N, 4.18%. FT-IR (KBr, cm^{-1}): 1522 $\nu_{(C=N)}$, 1248 $\nu_{(C-O)}$, 1517 ν(C═N—N═C). UV–vis (CH_3CN): λ_{max} (nm) 246, 347, 451. ^1H NMR (400 MHz, $CDCl_3$): δ (ppm) = 7.53 (d, J = 8 Hz, 2H, ArH (ligand)), 7.34–7.21 (m, 30H, ArH $(AsPh_3)_2$), 6.67 (d, J = 8 Hz, 2H (ligand)), 6.18 (s, 1H, pyrrole C—H), 6.12 (d, J = 4 Hz, 1H pyrrole

C—H), 5.71 (s, 1H, pyrrole C—H), 3.77 (s, 3H, ligand OCH_3), 1.63 (s, 3H, ligand CH_3). ^{13}C {^1H} NMR (100 MHz, $CDCl_3$): δ (ppm) = 205.07 (Ru—CO), 173.22 (N=C—O), 160.20 (C—OCH_3), 153.65 (C=N), 143.94, 138.28, 133.78, 132.42, 129.55, 129.44, 128.32, 127.68, 112.73, 112.44, 109.50 (Ar carbons (ligand + $(AsPh_3)_2$)), 55.19 (ligand OCH_3), 12.77 (ligand CH_3).

Complex **3**. Brown solid, Yield: 78%, m.p.: 242°C (with decomposition). Anal. Calcd: $C_{50}H_{40}As_2BrN_3O_2Ru$: C, 57.43; H, 3.86; N, 4.02%. Found: C, 57.39, H, 3.83, N, 3.99%. FT-IR (KBr, cm^{-1}): 1530 $\nu_{(C=N)}$, 1279 $\nu_{(C-O)}$, 1523 ν(C=N—N=C). UV–vis (CH_3CN): λ_{max} (nm) 250, 355, 460. ^1H NMR (400 MHz, $CDCl_3$): δ (ppm) = 7.61 (d, J = 8 Hz, 2H, ArH (ligand)), 7.39–7.37 (m, 2H, ArH (ligand)), 7.34–7.10 (m, 30H, ArH $(AsPh_3)_2$), 6.13 (s, 1H, pyrrole C—H) 6.05 (d, J = 4 Hz, 1H, pyrrole C—H), 5.63 (s, 1H, pyrrole C—H), 1.55 (s, 3H, ligand CH_3). ^{13}C {^1H} NMR (100 MHz, $CDCl_3$): δ (ppm) = 203.87 (Ru—CO), 173.22 (N=C—O), 170.98 (C—Br), 153.48 (C—N), 138.58, 132.65, 132.62, 130.39, 128.58, 128.34, 127.62, 127.43, 127.29, 112.36, 108.91 (Ar carbons (ligand + $(AsPh_3)_2$)), 21.59 (ligand CH_3).

5.3 | General procedure for the Ru(II)–NNO pincer catalysed olefination of methyl *N*-heteroarenes

In a 4 ml of 1,4-dioxane solvent, methyl *N*-heteroarenes (1 mmol), primary alcohols (1 mmol), *t*-BuOK base (0.5 mmol) and Ru(II)–NNO pincer catalyst (1 mol%) were dissolved in a round-bottom flask. The resulting mixture was stirred at 100°C for 20 h under open-air atmosphere. Then, the solution was quenched by water (5 ml) and followed by extraction with EtOAc (5 × 10 ml). The organic fractions were separated and dried over anhydrous Na_2SO_4. The solvent was removed from the organic fraction under reduced pressure. The resulting crude mixture was purified by using column chromatography with ethyl acetate/hexane (5:95) as an eluent.

5.4 | Competitive experiment between electron-donating and electron-withdrawing groups

4-Methoxybenzyl alcohol **2d** (1 mmol), 4-chlorobenzyl alcohol **2f** (1 mmol), 2-methylquinoline (1 mmol), *t*-BuOK (0.5 mmol) and Ru(II)–NNO pincer-type catalyst (1 mol%) were stirred in 1,4-dioxane medium at 100°C for 20 h. The resulting mixture was concentrated, and the formed olefin products were isolated by column chromatography. The olefin products **3d** and **3f** were eluted using ethyl acetate/hexane mixture.

5.5 | Procedure for gram-scale synthesis

In a 40 ml of 1,4-dioxane solvent, 2-methylquinoline (1.43 g, 10 mmol), benzyl alcohol (1.08 g, 10 mmol), *t*-BuOK (0.56 g, 0.5 mmol) and Ru(II)–NNO pincer catalyst (0.1 g, 1 mol%) were dissolved in a round-bottom flask. The resulting mixture was refluxed at 100°C for 20 h under open-air atmosphere. Then, the solution was quenched by adding water (50 ml) and followed by extraction with EtOAc (2 × 100 ml). The organic fractions were separated and dried over anhydrous Na_2SO_4. The solvent was removed from the organic fraction under reduced pressure. The resulting crude mixture was purified by using column chromatography with ethyl acetate/hexane (5:95) as an eluent.

ACKNOWLEDGEMENTS

The authors are thankful to the Science and Engineering Research Board (SERB; scheme no. EMR/2016/004952) for providing financial support and for junior research fellow to V. T. We are also thankful to the DST-India (FIST Programme) for the use of instrumental facilities at the School of Chemistry, Bharathidasan University, Tiruchirappalli 620 024, India. The authors declare no competing financial interest.

AUTHOR CONTRIBUTIONS

Veerappan Tamilthendral: contributed in the investigation, methodology and writing of the original draft. **Gunasekaran Balamurugan**: contributed in the investigation and methodology. **Rengan Ramesh**: contributed in the conceptualization, supervision, validation and writing—review and editing—of the manuscript. **Jan Grzegorz Malecki**: contributed in software support.

DATA AVAILABILITY STATEMENT

The data that support the findings of this study are available in the supporting information of this article.

REFERENCES

[1] a) N. Chatani, T. Asaumi, S. Yorimitsu, T. Ikeda, F. Kakiuchi, S. Murai, *J. Am. Chem. Soc.* **2001**, *123*, 10935; b) F. S. Chang, W. Chen, C. Wang, C. C. Tzeng, Y. L. Chen, *Bioorg. Med. Chem.* **2010**, *18*, 124; c) X. Franck, A. Fournet, E. Prina, R. Mahieux, R. Hocquemiller, B. Figadère, *Bioorg. Med. Chem. Lett.* **2004**, *14*, 3635; d) C. Torborg, M. Beller, *Adv. Synth. Catal.* **2009**, *351*, 3027; e) R. Dumeunier, I. E. Marko, Takeda, T. Ed. Wiley-VCH: Weinheim, **2004**; p 104; f) S. Blanchard, A. D. William, A. C.-H. Lee, A. Poulsen, E. L. Teo, W. Deng, N. Tu, E. Tan, K. L. Goh, W. C. Ong, C. P. Ng, K. C. Goh, Z. Bonday,

E. T. Sun, *Bioorg. Med. Chem. Lett.* **2010**, *20*, 2443; g) S. A. Khalil, A. Alkofahi, D. E. Eisawi, A. A. Shibib, *J. Nat. Prod.* **1998**, *61*, 262.

[2] a) J. H. Burroughes, D. D. C. Bradley, A. R. Brown, R. N. Marks, K. Mackay, R. H. Friend, P. L. Burns, A. B. Holmes, *Nature* **1990**, *347*, 539; b) J. Dai, Z. Q. Liu, X. Q. Wang, J. Lin, P. F. Yao, S. L. Huang, T. M. Ou, J. H. Tan, D. Li, L. Q. G. Z. S. Huang, *J. Med. Chem.* **2015**, *58*, 3875.

[3] a) W. Cieslik, R. Musiol, J. E. Nycz, J. Jampilek, M. Vejsova, M. Wolff, B. Machura, J. Polanski, *Bioorg. Med. Chem.* **2012**, *20*, 6960; b) K. Mekouar, J. F. Mouscadet, D. Desmaële, F. Subra, H. Leh, D. Savouré, C. Auclair, J. d'Angelo, *J. Med. Chem.* **1998**, *41*, 2846; c M. O. Puskullu, B. Tekiner, S. Suzen, *Mini Rev. Med. Chem.* **2013**, *13*, 365; d V. V. Kouznetsov, C. Gómez, M. G. Derita, L. Svetaz, E. del Olmo, S. A. Zacchino, *Bioorg. Med. Chem.* **2012**, *20*, 6506; e V. V. Kouznetsov, L. Y. V. Méndez, C. E. P. Galvis, M. C. O. Villamizar, *New J. Chem.* **2020**, *44*, 12; f K. Gopaul, S. A. N. A. S. Koorbanally, *Anti Cancer Agents Med. Chem.* **2015**, *15*, 631; g A. Mrozek-Wilczkiewicz, M. Kuczak, K. Malarz, W. E. Cieślik, R. M. Spaczyńska, *Eur. J. Med. Chem.* **2019**, *177*, 338.

[4] a) G. Wittig, G. Geissler, J. Liebigs, *Ann. Chem.* **1953**, *580*, 44; b) D. J. Peterson, *J. Org. Chem.* **1968**, *33*, 780; c) M. Julia, J. M. Paris, *Tetrahedron Lett.* **1973**, *14*, 4833; d) B. E. Maryanoff, A. B. Reitz, *Chem. Rev.* **1989**, *89*, 863; e) J. Clayden, S. Warren, *Angew. Chem. Int. Ed. Engl.* **1996**, *35*, 241; f) L. F. Van Staden, D. Gravestock, D. J. Ager, *Chem. Soc. Rev.* **2002**, *31*, 195.

[5] a) R. F. Heck, J. P. Nolley, *J. Org. Chem.* **1972**, *37*, 2320; b) K. Ferré-Filmon, L. Delaude, A. Demonceau, A. F. Noels, *Coord. Chem. Rev.* **2004**, *248*, 2323; c) R. H. Grubbs, in *Handbook of Metathesis*, (Ed: R. H. Grubbs) Vol. 1–3, Wiley-VCH, Weinheim **2003**.

[6] a) S. Hazra, V. Tiwari, A. Verma, P. Dolui, A. J. Elias, *Org. Lett.* **2020**, *22*, 5496; b) L. Gong, L. J. Xing, T. Xu, X. P. Zhu, W. Zhou, N. Kang, B. Wang, *Org. Biomol. Chem.* **2014**, *12*, 6557; c) E. Liang, J. Wang, Y. Wu, L. Huang, X. Yao, X. Tang, *Adv. Synth. Catal.* **2019**, *361*, 3619; d) Y. Ogata, A. Kawasaki, H. Hirata, *J. Org. Chem.* **1970**, *35*, 2199; e) B. Qian, D. J. Shi, L. Yang, H. M. Huang, *Adv. Synth. Catal.* **2012**, *354*, 2146; f) B. Qian, S. M. Guo, C. G. Xia, H. M. Huang, *Adv. Synth. Catal.* **2010**, *352*, 3195; g) H. Omai, T. Yoshino, S. Matsunaga, M. Kanai, *Org. Lett.* **2011**, *13*, 1706; h) L. Xu, Z. Shao, L. Wang, H. Zhao, J. Xiao, *Tetrahedron Lett.* **2014**, *55*, 6856; i) V. B. Graves, A. Shaikh, *Tetrahedron Lett.* **2013**, *54*, 695; j) S. Fu, L. Wang, H. Dong, J. Yu, L. Xu, J. Xiao, *Tetrahedron Lett.* **2016**, *57*, 4533; k M. Wang, M. Gao, K. D. Miller, G. W. Sledge, G. D. Hutchins, Q. H. Zheng, *Eur. J. Med. Chem.* **2009**, *44*, 2300.

[7] a) O. M. Ogba, N. C. Warner, D. J. O'Leary, R. H. Grubbs, *Chem. Soc. Rev.* **2018**, *47*, 4510; b) Y. Yan, K. Xu, Y. Fang, Z. Wang, *J. Org. Chem.* **2011**, *76*, 6849.

[8] D. S. Latha, S. Yaragorla, *Eur. J. Org. Chem.* **2020**, *15*, 2155.

[9] For selected examples on sp^3 C–H bonds transformations:a) V. G. Zaitsev, D. Shabashov, O. Daugulis, *J. Am. Chem. Soc.* **2005**, *127*, 13154; b) T. Watanabe, S. Oishi, N. Fujii, H. Ohno, *Org. Lett.* **2008**, *10*, 1759; c) D. Shabashov, O. Daugulis, D. Shabashov, O. Daugulis, *J. Am. Chem. Soc.* **2010**, *132*, 3965; d) H. Li, B. J. Li, Z. J. Shi, *Catal. Sci. Technol.* **2011**, *1*, 191; e) S.-Y. Zhang, F.-M. Zhang, Y.-Q. Tu, *Chem. Soc. Rev.* **2011**, *40*, 1937; f) R. Jazzar, J. Hitce, A. Renaudat, J. S.-K. O. Baudoin, *Chem. Eur. J.* **2010**, *16*, 2654; g) F. Bellina, R. Rossi, *Chem. Rev.* **2010**, *110*, 1082; h) T. W. Lyons, M. S. Sanford, *Chem. Rev.* **2010**, *110*, 1147; i) X. Chen, K. M. Engle, D. H. W. J. Q. Yu, *Angew. Chem. Int. Ed.* **2009**, *48*, 5094; j) Z. Jamal, Y. C. Teo, G. S. Lim, *Tetrahedron* **2016**, *72*, 2132.

[10] G. Zhang, T. Irrgang, T. Dietel, F. Kallmeier, R. Kempe, *Angew. Chem. Int. Ed.* **2018**, *57*, 1.

[11] M. K. Barman, S. Waiba, B. Maji, *Angew. Chem. Int. Ed.* **2018**, *57*, 9126.

[12] a) J. Das, M. Vellakkaran, D. Banerjee, *Chem. Commun.* **2019**, *55*, 7530; b) J. Das, M. S. M. Vellakkaran, D. Banerjee, *Org. Lett.* **2019**, *21*, 7514.

[13] B. M. Ramalingam, I. Ramakrishna, M. Baidya, *J. Org. Chem.* **2019**, *84*, 9819.

[14] C. Zhang, Z. Li, Y. Fang, S. Jiang, M. Wang, G. Zhang, *Tetrahedron* **2020**, *76*, 130968.

[15] M. Rauch, S. Kar, A. Kumar, L. Avram, L. J. Shimon, D. Milstein, *J. Am. Chem. Soc.* **2020**, *142*, 14513.

[16] C. Gunanathan, D. Milstein, *Chem. Rev.* **2014**, *114*, 12024.

[17] H. A. Younus, N. Ahmad, W. Su, F. Verpoort, *Coord. Chem. Rev.* **2014**, *276*, 112.

[18] T. S. Manikandan, R. Ramesh, N. Shivalingegowda, L. N. Krishnappagowda, *ChemistrySelect* **2018**, *3*, 1561.

[19] M. Cao, L. V. Do, N. W. Hoffman, M. L. Kwan, J. K. Little, J. M. McGilvray, C. B. Morris, B. C. Söderberg, A. Wierzbicki, T. R. Cundari, C. H. Lake, *Organometallics* **2001**, *20*, 2270.

[20] E. Fogler, M. A. Iron, J. Zhang, Y. Ben-David, Y. Diskin-Posner, G. Leitus, L. J. Shimon, D. Milstein, *Inorg. Chem.* **2013**, *52*, 11469.

[21] R. Manikandan, G. Prakash, R. Kathirvel, P. Viswanathamurthi, *Spectrochim. Acta A Mol. Biomol. Spectrosc.* **2013**, *116*, 501.

[22] S. Balaji, G. Balamurugan, R. Ramesh, D. Semeril, *Organometallics* **2021**, *40*, 725.

[23] T. M. Aliyeu, D. V. Berdnikova, O. A. Fedorova, E. N. Gulakova, C. Stremmel, H. Ihmels, *J. Org. Chem.* **2016**, *81*, 9075.

SUPPORTING INFORMATION

Additional supporting information may be found in the online version of the article at the publisher's website.

How to cite this article: V. Tamilthendral, G. Balamurugan, R. Ramesh, J. G. Malecki, *Appl Organomet Chem* **2021**, e6561. https://doi.org/10.1002/aoc.6561